GEOLOGICAL SURVEY OF CANADA
COMMISSION GÉOLOGIQUE DU CANADA

CURRENT RESEARCH 1996-E

RECHERCHES EN COURS 1996-E

1996

Natural Resources Canada Ressources naturelles Canada

Canada

NOTICE TO LIBRARIANS AND INDEXERS

The Geological Survey's Current Research series contains many reports comparable in scope and subject matter to those appearing in scientific journals and other serials. Most contributions to Current Research include an abstract and bibliographic citation. It is hoped that these will assist you in cataloguing and indexing these reports and that this will result in a still wider dissemination of the results of the Geological Survey's research activities.

AVIS AUX BIBLIOTHÉCAIRES ET PRÉPARATEURS D'INDEX

La série Recherches en cours de la Commission géologique contient plusieurs rapports dont la portée et la nature sont comparables à ceux qui paraissent dans les revues scientifiques et autres périodiques. La plupart des articles publiés dans Recherches en cours sont accompagnés d'un résumé et d'une bibliographie, ce qui vous permettra, on l'espère, de cataloguer et d'indexer ces rapports, d'où une meilleure diffusion des résultats de recherche de la Commission géologique.

GEOLOGICAL SURVEY OF CANADA

COMMISSION GÉOLOGIQUE DU CANADA

CURRENT RESEARCH 1996-E

RECHERCHES EN COURS 1996-E

1996

Includes/comprend:

Cordillera and Pacific Margin
Cordillère et marge du Pacifique

Interior Plains and Arctic Canada
Plaines intérieures et région arctique du Canada

Canadian Shield
Bouclier canadien

Eastern Canada and National and General Programs
Est du Canada et programmes nationaux et généraux

Catalogue No. M44-1996/5E
ISBN 0-660-16519-8

Available in Canada from
Geological Survey of Canada offices:

601 Booth Street
Ottawa, Ontario K1A 0E8

3303-33rd Street N.W.,
Calgary, Alberta T2L 2A7

100 West Pender Street
Vancouver, B.C. V6B 1R8

or from

Canada Communication Group – Publishing
Ottawa, Ontario K1A 0S9

A deposit copy of this publication is also available for reference
in selected public libraries across Canada

Price subject to change without notice

Cover illustration

Shallow-dipping gabbro sills of the 0.72 Ga Franklin igneous events exposed in the Duke of York inlier of southern Victoria Island (see Rainbird et al., p. 125-134). View looks southwest along a fault coincident with the channel separating Victoria Island (right) and Richardson Islands (left). Strata on the islands are down-dropped at least 100 m and tilted to the southeast. Photo by R.H. Rainbird, 1995. GSC 1996-104

Photo en page couverture

Filons-couches de gabbro à pendage faible associés à l'épisode igné de Franklin (0,72 Ga); l'affleurement se trouve dans l'enclave de Duke of York de la partie sud de l'île Victoria (voir Rainbird et al., p. 125-134). Photo prise vers le sud-ouest, le long d'une faille qui correspond au chenal séparant l'île Victoria (à droite) des îles Richardson (à gauche). Les strates qui affleurent sur les îles Richardson sont affaissées d'au moins 100 m et montrent un basculement vers le sud-est. (Photo prise par R.H. Rainbird en 1995, GSC 1996-104).

Separates

A limited number of separates of the papers that appear in this volume are available by direct request to the individual authors. The addresses of the Geological Survey of Canada offices follow:

Geological Survey of Canada
601 Booth Street
OTTAWA, Ontario
K1A 0E8
(FAX: 613-996-9990)

Geological Survey of Canada (Calgary)
3303-33rd Street N.W.
CALGARY, Alberta
T2L 2A7
(FAX: 403-292-5377)

Geological Survey of Canada (Victoria)
100 West Pender Street
VANCOUVER, B.C.
V6B 1R8
(FAX: 604-666-1124)

Geological Survey of Canada (Victoria)
P.O. Box 6000
9860 Saanich Road
SIDNEY, B.C.
V8L 4B2
(Fax: 604-363-6565)

Geological Survey of Canada (Atlantic)
Bedford Institute of Oceanography
P.O. Box 1006
DARTMOUTH, N.S.
B2Y 4A2
(FAX: 902-426-2256)

Quebec Geoscience Centre/INRS
2535, boulevard Laurier
C.P. 7500
Sainte-Foy (Québec)
G1V 4C7
(FAX: 418-654-2615)

Tirés à part

On peut obtenir un nombre limité de «tirés à part» des articles qui paraissent dans cette publication en s'adressant directement à chaque auteur. Les adresses des différents bureaux de la Commission géologique du Canada sont les suivantes :

Commission géologique du Canada
601, rue Booth
OTTAWA, Ontario
K1A 0E8
(facsimilé : 613-996-9990)

Commission géologique du Canada (Calgary)
3303-33rd St. N.W.,
CALGARY, Alberta
T2L 2A7
(facsimilé : 403-292-5377)

Commission géologique du Canada (Victoria)
100 West Pender Street
VANCOUVER, British Columbia
V6B 1R8
(facsimilé : 604-666-1124)

Commission géologique du Canada (Victoria)
P.O. Box 6000
9860 Saanich Road
SIDNEY, British Columbia
V8L 4B2
(facsimilé : 604-363-6565)

Commission géologique du Canada (Atlantique)
Institut océanographique Bedford
P.O. Box 1006
DARTMOUTH, Nova Scotia
B2Y 4A2
(facsimilé : 902-426-2256)

Centre géoscientifique de Québec/INRS
2535, boulevard Laurier
C.P. 7500
Sainte-Foy (Québec)
G1V 4C7
(facsimilé : 418-654-2615)

CONTENTS

CORDILLERA AND PACIFIC MARGIN
CORDILLÈRE ET MARGE DU PACIFIQUE

INTERIOR PLAINS AND ARCTIC CANADA
PLAINES INTÉRIEURES ET RÉGION ARCTIQUE DU CANADA

CANADIAN SHIELD
BOUCLIER CNADIEN

EASTERN CANADA AND NATIONAL AND GENERAL PROGRAMS
EST DU CANADA ET PROGRAMMES NATIONAUX ET GÉNÉRAUX

CORDILLERA AND PACIFIC MARGIN

CORDILLÈRE ET MARGE DU PACIFIQUE

Sedimentary processes and surficial geology of the Pacific margin of the Queen Charlotte Islands, British Columbia

J. Vaughn Barrie and Kim W. Conway
GSC Pacific, Sidney

J.V. Barrie and K.W. Conway, 1996: Sedimentary processes and surficial geology of the Pacific margin of the Queen Charlotte Islands, British Columbia; in Current Research 1996-E; Geological Survey of Canada, p. 1-6.

Abstract: The active Pacific margin of the Queen Charlotte Islands has been subject to vigourous wave and tidal energy since glacial times resulting in a continental shelf and coastal zone that are almost devoid of sediment. After minimal glaciation of the narrow shelf, the region became emergent with sea level lowering of up to, and possibly greater, than 200 m due to a glacio-isostatic forebulge ending near 10 400 BP (^{14}C date) followed by a rapid transgression that reached approximately 15 m above present sea level. This transgression effectively removed all unconsolidated sediment along the coast except in a few protected basins, such as Rennell Sound.

Résumé : Là où se trouvent les îles de la Reine-Charlotte, la marge active du Pacifique a été, depuis les temps glaciaires, soumise à l'action vigoureuse des vagues et des marées; il en a résulté une plate-forme continentale et une zone littorale quasi dépourvues de sédiments. Après une glaciation minimale de l'étroite plate-forme, la région a émergé, l'abaissement du niveau marin atteignant, et peut-être dépassant, 200 mètres. Ce phénomène s'explique par un enfoncement périphérique d'origine glacio-isostatique qui s'est terminé il y a environ 10 400 ans (datation au ^{14}C). Cet enfoncement a été suivi d'une rapide transgression qui a atteint environ 15 mètres au-dessus du niveau marin actuel. Cette forte transgression du Pacifique à circulation libre a effectivement éliminé tous les sédiments non consolidés accumulés sur la côte, sauf dans quelques bassins protégés comme le détroit de Rennell.

INTRODUCTION

The western shores of the Queen Charlotte Islands are distinctly rugged with little refuge from the North Pacific Ocean. George Dawson describes this coast from his 1878 expedition as having steep rocky sides with little or no beach and bold water (Dawson, 1878). Consequently these shores have been, and are, relatively uninhabited and many marine areas are not yet completely charted. The most current charts of the area date from hydrographic surveys of 1935 to 1937.

The continental shelf off the Queen Charlotte Islands is extremely narrow extending offshore less than 5 km in the south and up to 30 km at 54°N latitude to the shelf break at roughly 200 m water depth. Bedrock geology of the onshore areas adjacent to the shelf and enclosing the inlets of the Queen Charlotte Islands is a diverse assemblage of Jurassic to Tertiary rocks. In the north the Masset Formation basalt predominates (Hickson, 1991) and in the south, plutonic Jurassic and Tertiary rocks occur (Anderson and Reichenbach, 1991).

The shelf physiography is controlled by the Queen Charlotte Fault which separates the North American and Pacific lithospheric plates. Throughout the Quaternary, motion on the fault has been mostly strike-slip with the Pacific plate moving northward relative to North America at an average rate of several centimetres per year (Riddihough, 1988). Consequently, this is a region of elevated seismicity with Canada's largest earthquake (magnitude 8.1) occurring adjacent to the northwestern shelf break of Graham Island in 1949.

In addition to being an exposed high energy environment and subject to the most severe tectonism in Canada, the area has also undergone dramatic sea level fluctuations. Josenhans et al. (1995) give evidence for relative fall of sea level of more than 100 m with large areas adjacent to the Queen Charlotte Islands being subaerially exposed. From these results and the earlier work of Luternauer et al. (1989) and Barrie et al. (1991) in Queen Charlotte Sound and Hecate Strait, there is conclusive evidence for regional sea level lowering at the end of the late Wisconsinan, of at least 100 m, and indirect evidence of up to 170 m of relative sea level lowering (Josenhans et al., 1993) at 10 400 BP (^{14}C date). Eustatic sea level rise, coupled with subsidence of a glacio-isostatic forebulge resulted in sea levels rising very rapidly, reaching the present shoreline on the Queen Charlotte Islands by about 9100 BP (^{14}C date). Sea levels reached a plateau at 15 to 13 m above current levels 8900 to 5500 BP (^{14}C date) and fell slowly until the present (Josenhans et al., 1995).

As an extension to the program of the Geological Survey of Canada to map the Quaternary geology of the Queen Charlotte Basin, a preliminary survey was undertaken of the western coastal areas of the Queen Charlotte Islands in co-operation with Parks Canada. The objectives were to: 1) undertake the first base level surficial geology mapping of the continental shelf of the western Queen Charlotte Islands; 2) confirm if the rapid late Quaternary to early Holocene environmental changes of the eastern Queen Charlotte Islands can be interpreted from Quaternary marine sediments of the western shelf; and, 3) corroborate the suggestion that a significant continental shelf tilt to the west existed in northern British Columbia at 10.5 ka due to a glacio-isostatic forebulge. Josenhans et al. (1995) suggest that the western continental shelf of the Queen Charlotte Islands could have emerged by as much as 200 m or more above present day sea level at the beginning of the Holocene.

DATA COLLECTION

An initial high resolution geophysical survey line was collected in September 1990 off northwestern Graham Island from the *CFAV Endeavour*. In June of 1995, aboard the

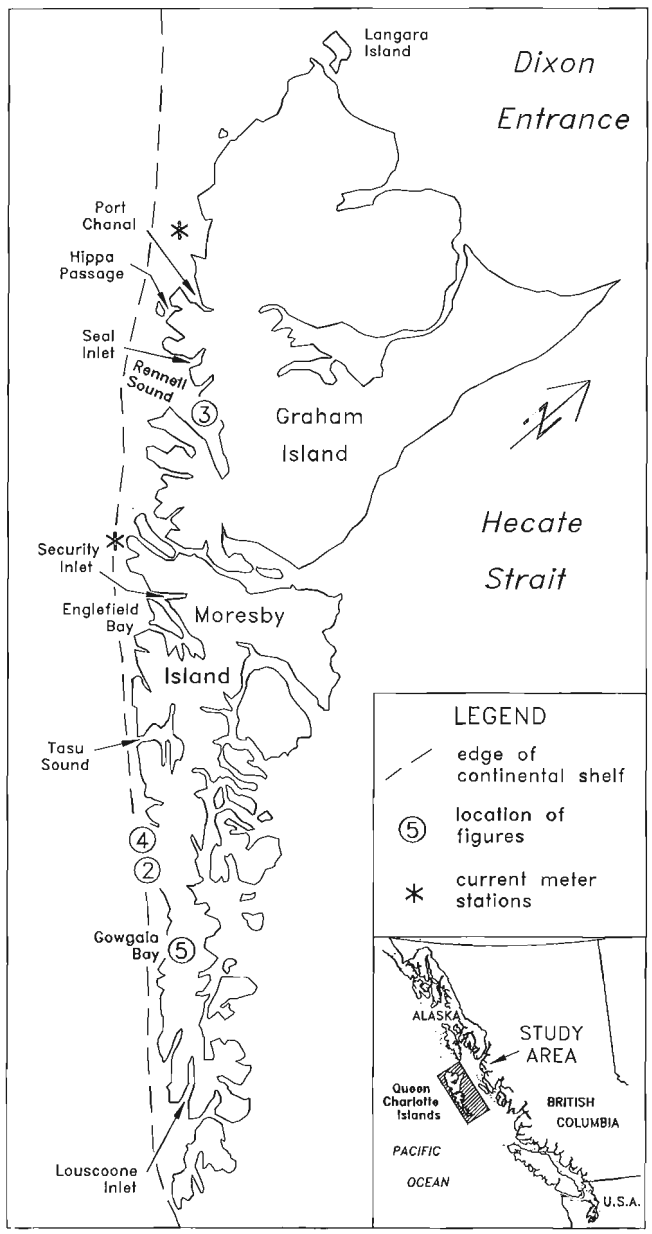

Figure 1. *The continental shelf and inland waters of the western Queen Charlotte Islands. Locations of areas studied, current meter stations, and figures presented are shown.*

CSS Tully, a preliminary survey was undertaken of a portion of the southern continental shelf and major inlets of the west coast of the Queen Charlotte Islands, again using a high resolution subbottom profiler and sidescan sonar. Inlets surveyed include, from south to north, Gowgaia Bay, Tasu Sound, Englefield Bay, Security Inlet, Rennell Sound, Seal Inlet, Hippa Passage, and Port Chanal (Fig. 1).

Five sediment cores were obtained from Security Inlet, Rennell Sound, and Seal Inlet during the survey. This is the first marine geological/geophysical survey of this region of the Canadian margin. In addition, a land-based coastal survey was undertaken in the Rennell Sound area to identify raised marine deposits in September, 1995.

OCEANOGRAPHIC SETTING

During the winter season when the strength, duration, and fetch of winds are greatest, seas off the Queen Charlottes exceed 1.5 m about sixty per cent of the time, 3.5 m twenty to thirty per cent of the time until January, while swell heights in excess of 1.5 m occur fifty per cent of the time (Thomson, 1989). While the swell is primarily from southwest and west during the winter period, the seas from cyclonic winds tend to be from the southeast and northwest due to alignment of the winds with the coastal terrain. From July 1984 to March 1985 a directional wave-rider buoy was deployed in 285 m of water approximately 30 km northwest of Langara Island (Fig. 1) at the western approaches of Dixon Entrance (Dobrocky Seatech Ltd., 1987). Typical wave periods were from 10 to 12 s and wave heights of 3.0 to 4.0 m during the winter months. During storm events the average significant wave period was 12.6 s with a mean significant wave height of 5.8 m coming from a west to southwesterly direction (225-270 degrees true).

The tidal currents on the west coast of the Queen Charlotte Islands are primarily rectilinear, parallel to the coastline of the islands (Thomson, 1981, 1989; Huggett et al., 1992a, b). Tidal range is typically 4.5 m. Current velocities have a mean range between 0.15 and 0.25 $m \cdot s^{-1}$ with maximum velocities reaching 0.80 $m \cdot s^{-1}$. At 51 m water depth off northwestern Graham Island, the mean current velocities were between 0.25 and 0.30 $m \cdot s^{-1}$, probably reflecting the effects of wind-driven circulation and combined unidirectional and oscillatory flow.

SURFICIAL GEOLOGY

The striking observation from all survey lines collected from the continental shelf off the western Queen Charlotte Islands is that there is little to no Quaternary sediment, only bedrock

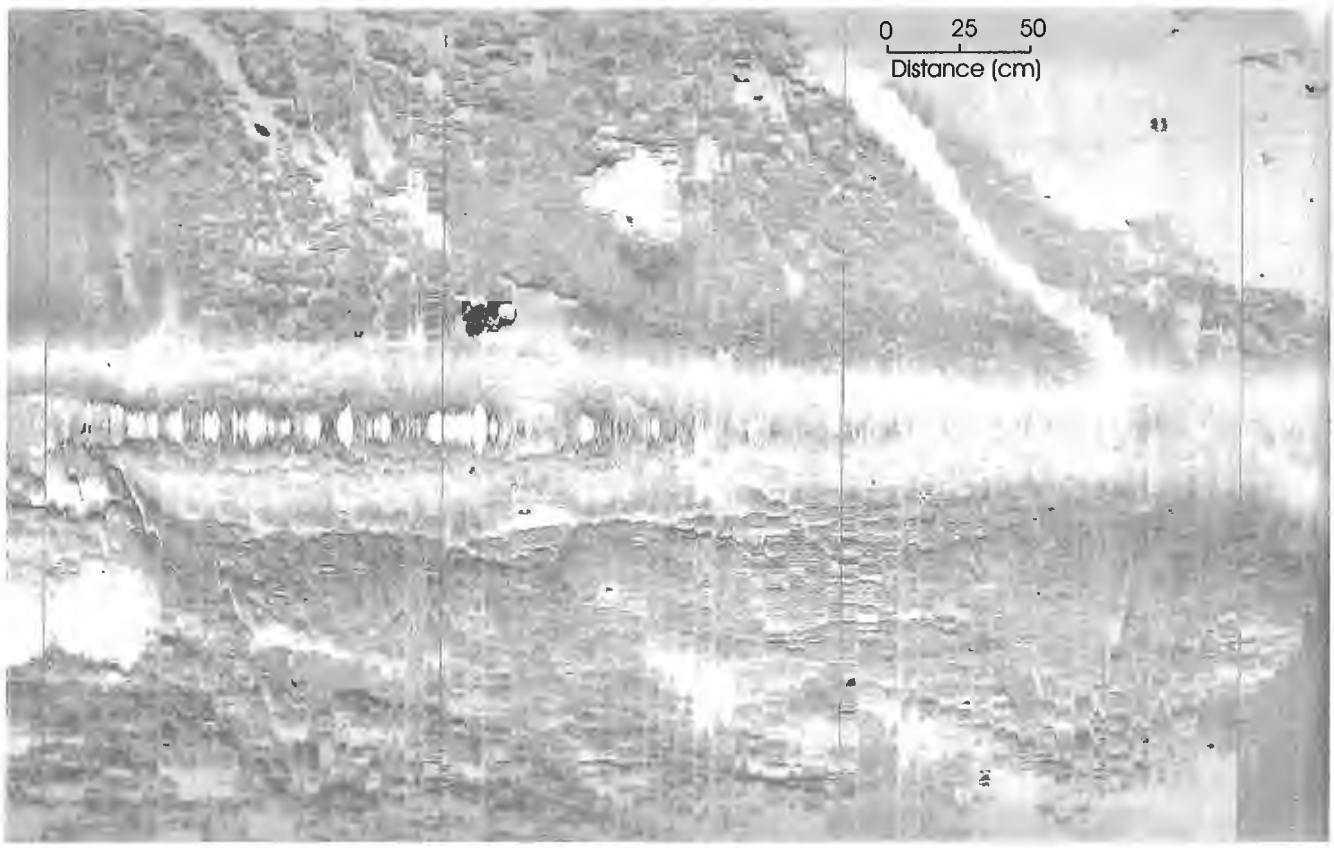

Figure 2. *Sidescan sonar image of the continental shelf off Moresby Island at approximately 200 m water depth showing the predominant bedrock seafloor with areas of thin mobile sand cover. Location is shown in Figure 1.*

(Fig. 2). This is true for all areas of the shelf surveyed except the northern portion of the shelf approaching Dixon Entrance where the shelf extends to 30 km offshore. Sparse mobile sand occurs in the small depressions formed by the rough bedrock seafloor (Fig. 2). Those inlets that are open to the Pacific Ocean with a muted or no sill at the entrance are also predominantly floored by bedrock. Where small streams enter these inlets, coarse grained fan deltas have developed, but are usually very limited in extent.

Those inlets or fiords that are constrained by a bedrock sill at the entrance, such as Gowgaia Bay, Port Chanal, and Tasu Sound, have fine grained, organic-rich, bottom sediments, typical fiord sedimentation for Canadian fiords (Syvitski et al., 1987). The seaward entrances to these fiords are usually very narrow (e.g. 550 m for Tasu Sound) and shallow. The sill height at the entrance of Gowgaia Bay is approximately 60 m, 40 m for Port Chanal, and 110 m for Tasu Sound. Consequently, Pacific Ocean wave energy does not penetrate any of these fiords to any appreciable degree. Inlets that are orientated such that they are not open to the Pacific swell, such as Seal Inlet (Fig. 1), also contain some fine grained Holocene sediments.

Only in the largest inlet, Rennell Sound, is there any appreciable pre-Holocene stratigraphy preserved in the inner basin (Fig. 3). The Huntec DTS high resolution subbottom profiler records show a stratified sand overlying a coarse grained unit with a cut-and-fill complex stratigraphy normally associated with drowned fluvial sediments. Channels can be seen on both the subbottom profiles and the sidescan sonar records within this lower unit. One core was obtained in Rennell Sound that penetrated this stratigraphy (Fig. 3). The overlying Holocene unit is a bioturbated, muddy sand with organic and shell material. At 2.45 m a sharp contact demarks the change to a well sorted, massive, fine grained sand (Fig. 3). Below this, at 4.05 m, are interbedded silt and sand units with minor gravel and wood fragments. One wood fragment selected from the base of this unit at 4.40 m was dated (^{14}C) at 12 340 BP (L26280 Fig. 3). Underlying this is a black massive sand unit that grades into a fine gravel that is devoid of any marine indicators or dateable fragments. The bottom coarse sand and gravel unit is probably alluvial material. With further microfaunal identification and radiocarbon dating we should be able to confirm this interpretation.

At two sites along the coast adjacent to the Quaternary section in Rennell Sound, raised marine beach deposits were mapped that stand approximately 15 m above present sea level. This deposit confirms that the early Holocene high stand (8900 to 5500 BP; ^{14}C date) observed elsewhere on the eastern Queen Charlotte Islands (Clague et al., 1982; Josenhans

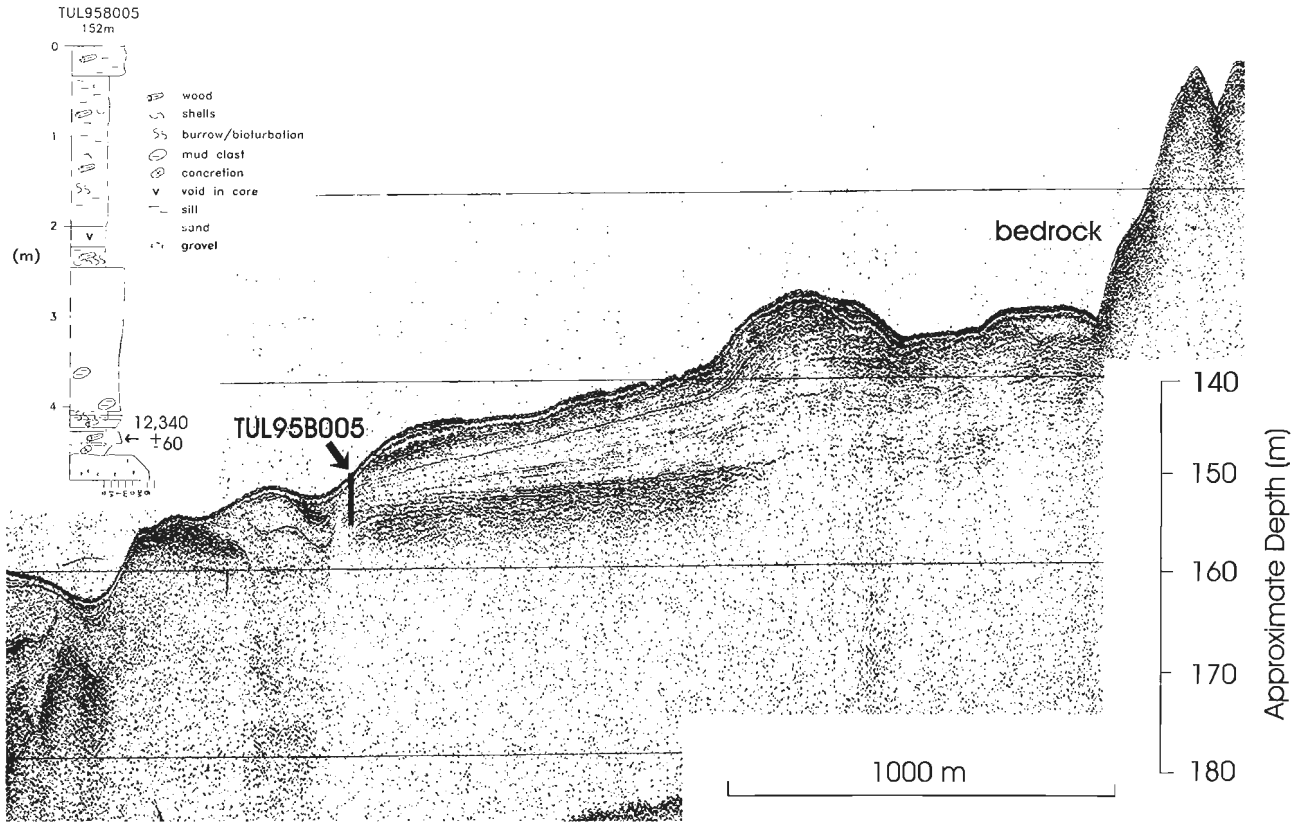

Figure 3. *Huntec DTS subbottom profile illustrating the late Quaternary stratigraphy of the inner basin of Rennell Sound (Fig. 1). The description and location of a sediment core obtained within the section are shown.*

et al., 1995) was a regional event ending a very rapid transgression of the continental shelf.

SEABED FEATURES AND SEDIMENTARY PROCESSES

A dominant feature of the continental shelf off the western Queen Charlotte Islands is the occurrence of deep (10-35 m) channels seaward of the inlets off the west coast of the Queen Charlotte Islands. For example, at approximately 200 m water depth our survey recorded deep channels (Fig. 4) near the shelf break adjacent to all the inlets south of Tasu Sound. These channels are cut into bedrock and characteristic of fluvial channels in shape, but are presently devoid of any sediment other than a thin layer of mobile sand.

Tectonism has resulted in disturbance of the limited Quaternary deposits, and bedrock faulting and folding at the seabed. In Gowgaia Bay a recent fault can be mapped that cuts through Holocene sediments to the seafloor (Fig. 5). Similar occurrences are seen in most areas where Quaternary sediments have been surveyed and not acoustically masked by shallow gas. Off northwestern Graham Island the bedrock surface has been folded, sheared, and faulted similar to areas mapped off Vancouver Island to the south (Yorath, 1980). This area is close to the epicentre of the 1949 magnitude 8.1 earthquake along the Queen Charlotte fault, where up to 7 m of movement would have occurred over several hundred kilometres during the rupture (G. Rogers, pers. comm., 1996). A tsunami was observed in Tasu Sound at the time of the 1949 earthquake, the result of a large submarine failure that occurred along the southern arm of inlet near the entrance.

DISCUSSION

Initial results indicate that the high energy regime of the western continental shelf of the Queen Charlotte Islands has resulted in most of the seabed remaining free of sediment and that only in the fiords where a shallow entrance sill occurs, such as Tasu Sound, does modern, organic-rich, fine grained sedimentation occur. The combined wave and tidal energy, particularly through the winter months, is strong enough to transport most material up to gravel size well offshore. Watersheds of the inlets and coastal waters of the western Queen Charlotte Islands are very limited and drain terrains largely barren of unconsolidated sediments. What sediment

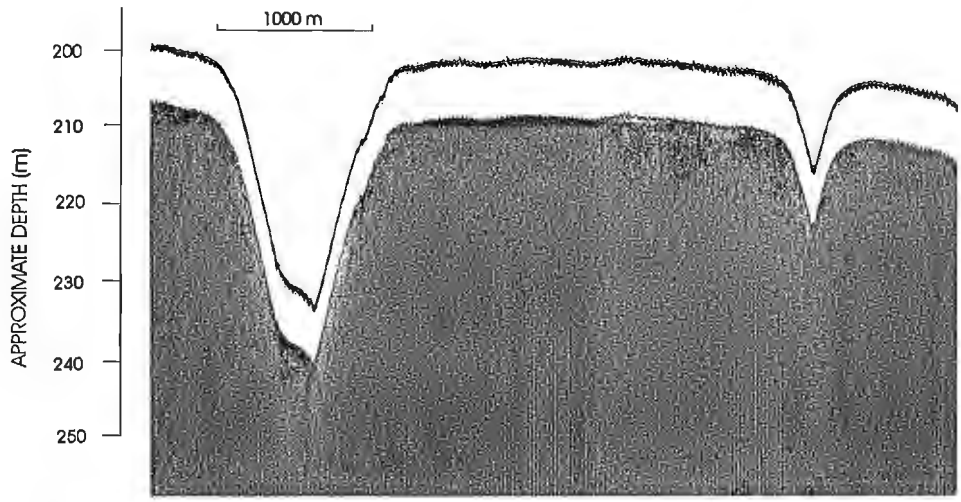

Figure 4.

Shelf-parallel, Huntec DTS profile near the shelfbreak off Moresby Island (Fig. 1) showing the characteristic morphology of fluvial channels crossing the shelf to the continental slope.

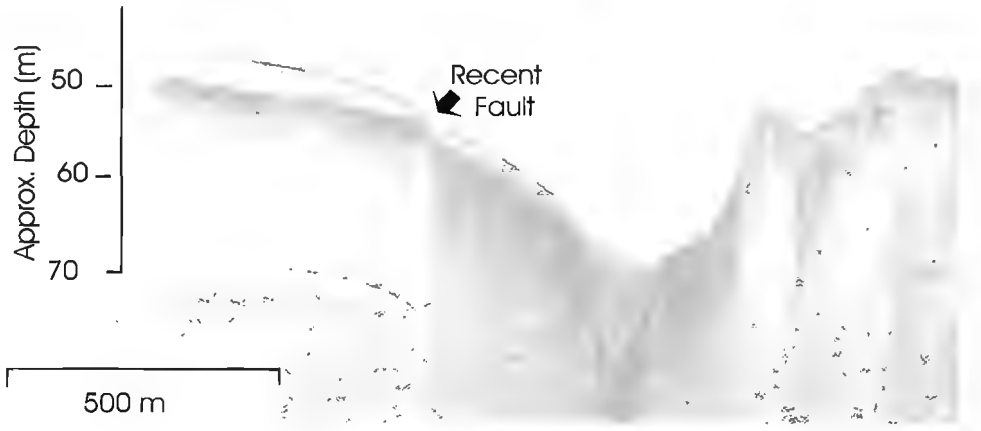

Figure 5.

High-resolution seismic profile of displaced Holocene sediments in a small basin within Gowgaia Bay (Fig. 1). Coincident sidescan sonar coverage indicates that this shallow fault can be traced across the entire basin.

that does reach the coast is remobilized and moved offshore unless trapped in one of the restricted inlets. The very coarse component is left as a lag near the point of initial deposition into the marine environment.

The existing occurrences of late Quaternary sediments contain Holocene muddy sands with prolific infauna overlying what appear to be fluvial outwash sediments. If this interpretation is correct, then the channels identified on the seismic profiles and sidescan sonar records most likely represent drainage features dating from sea level lowering at the end of the late Wisconsinan stage. The channels appear to make their way to the shelf break indicating that the shelf was emergent to approximately 200 m water depth and the coastline was situated at the present day shelf break before 12 400 BP (^{14}C date) until approximately 10 400 BP (^{14}C date), as predicted by Josenhans et al. (1995). This is consistent with the identification of channels crossing the shelf off all the inlets in the southern Queen Charlotte Islands. The subsequent rapid and dramatic early Holocene transgression has removed most of the alluvial postglacial sediment from the shelf, except for a few protected areas such as Rennell Sound.

From the mapping of all Quaternary sections seen on the high resolution seismic profiles, there is no evidence for till or any identifiable glacial features, such as iceberg scours. Clague (1989) suggested that ice moved out onto the shelf area of the western coast but implied that the ice extent was limited and that some areas of the shelf could have been free of ice during the last glaciation. The survey results from the western shelf also suggest that the Wisconsinan valley and outlet glaciers were restricted to the Queen Charlotte mountain areas and that if ice crossed the shelf, it was limited and retreat was very rapid.

SUMMARY

These preliminary results suggest that after a minimal glaciation of the western shelf of the Queen Charlotte Islands the area became emergent with relative sea level lowering of up to and possibly greater that 200 m, due to a glacioisostatic forebulge ending at 10 400 BP (^{14}C date), followed by a rapid transgression that reached approximately 15 m above present sea level. This transgression by the Pacific Ocean removed all sediments along the coast except in a few protected basins such as Rennell Sound. Subsequent wave and tidal current energy coupled with limited new sedimentation has left this dynamic coastline barren. The impact of periodic earthquakes on a precipitous coastline has further contributed to the instability of the coastal environment.

ACKNOWLEDGMENTS

We would like to thank the captains and crews of *CFAV Endeavour* and, particularly, the *CSS Tully*, for their support in geophysical surveying and collection of the cores in poorly charted and dangerous waters. B. Sawyer and R. Franklin produced the illustrations and the manuscript was critically reviewed by Brian Bornhold.

REFERENCES

Anderson, R.G. and Reichenbach, I.
1991: U-Pb and K-Ar framework for Middle to Late Jurassic (172-158) and Tertiary (46-27) plutons in Queen Charlotte Islands, British Columbia; in Evolution and Hydrocarbon Potential of the Queen Charlotte Basin, British Columbia, Geological Survey of Canada, Paper 90-10, p. 59-87.

Barrie, J.V., Bornhold, B.D., Conway, K.W., and Luternauer, J.L.
1991: Surficial geology of the northwestern Canadian continental shelf; Continental Shelf Research, v. 11, p. 701-715.

Clague, J.J.
1989: Quaternary geology of the Queen Charlotte Islands; in The Outer Shores, (ed.) G.G.E. Scudder and N. Gessler; Queen Charlotte Islands Museum Press, Skidegate, Q.C.I., p. 65-74.

Clague, J.J., Harper, J.R., Hebda, R.J., and Howes, D.E.
1982: Late Quaternary sea level and crustal movements, coastal British Columbia; Canadian Journal of Earth Sciences, v. 19, p. 597-618.

Dawson, G.M.
1878: George Dawson's 1878 Survey of the Queen Charlotte Islands; in To The Charlottes, (ed.) D. Cole and B. Lockner; University of British Columbia Press, Vancouver, British Columbia, 1993, p. 212.

Dobrocky Seatech Ltd.
1987: Wave Climate Study – Northern Coast of British Columbia; Environmental Studies Revolving Fund Report 59, Energy, Mines and Resources, Ottawa, p. 93.

Hickson, C.J.
1991: The Masset Formation on Graham Island, Queen Charlotte Islands, British Columbia; in Evolution and Hydrocarbon Potential of the Queen Charlotte Basin, British Columbia, Geological Survey of Canada, Paper 90-10, p. 305-324.

Josenhans, H.W., Barrie, J.V., Conway, K.W., Patterson, T., Mathewes, R.W., and Woodsworth, G.J.
1993: Surficial geology of the Queen Charlotte Basin: evidence of submerged proglacial lakes at 170 m on the continental shelf of western Canada; in Current Research, Part A; Geological Survey of Canada, Paper 93-1A, p. 119-127.

Josenhans, H.W., Fedje, D.W., Conway, K.W., and Barrie, J.V.
1995: Post glacial sea-levels on the western Canadian continental shelf: evidence for rapid change, extensive subaerial exposure, and early human habitation; Marine Geology, v. 125, p. 73-94.

Huggett, W.S., Thomson, R.E., and Woodward, M.J.
1992a: Dixon Entrance, Hecate Strait and the West Coast of the Queen Charlotte Islands; 1983, 1984, and 1985; Part 1: Introduction and Results from the West Coast (south), Stations QA1 to QC2. Data Record of Current Observations Volume XX, Department of Fisheries and Oceans, p. 301

Huggett, W.S., Thomson, R.E., and Woodward, M.J. (cont.)
1992b: Dixon Entrance, Hecate Strait and the West Coast of the Queen Charlotte Islands; 1983, 1984, and 1985; Part 2: Results from the central West Coast, Stations QC3 to QE3. Data Record of Current Observations Volume XX, Department of Fisheries and Oceans, p. 301.

Luternauer, J.L., Clague, J.J., Conway, K.W., Barrie, J.V., Blaise, B., and Mathewes, R.W.
1989: Late Pleistocene terrestrial deposits on the continental shelf of western Canada: evidence for rapid sea-level change at the end of the last glaciation; Geology, v. 17, p. 357-360.

Riddihough, R.P.
1988: The northeast Pacific Ocean and margin; in The Ocean Basins and Margins, Volume 7B, The Pacific Ocean; (ed.) A.E.M. Nairn, F.W. Stehli, and S. Uyeda; Plenum, New York, p. 85-118.

Syvitski, J.P.M., Burell, D.C., and Skei, J.M.
1987: Fjords: Processes and Products; Springer-Verlag, New York, New York, p. 379.

Thomson, R.E.
1981: Oceanography of the British Columbia Coast; Canada Special Publication of Fisheries and Aquatic Sciences, no. 56, p. 291.
1989: The Queen Charlotte Islands physical oceanography; in The Outer Shores, (ed.) G.G.E. Scudder and N. Gessler; Queen Charlotte Islands Museum Press, Skidegate, Q.C.I., p. 65-74.

Yorath, C.J.
1980: The Apollo structure in Tofino Basin, Canadian Pacific continental shelf; Canadian Journal of Earth Sciences, v. 17, p. 758-775.

Geological Survey of Canada Project 890052

Radiolarian biostratigraphy and implications, Cache Creek Group of Fort Fraser and Prince George map areas, central British Columbia[1]

F. Cordey[2] and L.C. Struik
GSC Pacific, Vancouver

Cordey, F. and Struik, L.C., 1996: Radiolarian biostratigraphy and implications, Cache Creek Group of Fort Fraser and Prince George map areas, central British Columbia; in Current Research 1996-E; Geological Survey of Canada, p. 7-18.

Abstract: As part of the new Nechako NATMAP project, radiolarian investigations from the Fort Fraser (93K) and Prince George (93G) map areas in central British Columbia provide control on the age and structures of the Cache Creek Group and related units. Twenty-five localities of radiolarian chert, siliceous mudstone, limestone, and chert-bearing conglomerate from the Cache Creek Group and the Sifton Formation range in age from late Pennsylvanian-early Permian to Early Jurassic (Pliensbachian). These results provide a new stratigraphic framework for the area. In central British Columbia, Cache Creek Group upper Paleozoic rocks include limestone, chert, and basalt, and may include gabbro and ultramafics, and Mesozoic rocks include greywacke, siltstone, argillite, limestone, and basalt tuff. Regionally, these results give new information for correlations within the Cache Creek Terrane as a whole, for instance about transitional intervals of sedimentation from carbonate to chert and chert to hemipelagics.

Résumé : Une étude de biostratigraphie des radiolaires menée dans le cadre du nouveau projet Nechako du CARTNAT (feuilles Fort Fraser, 93K, et Prince George, 93G; centre de la Colombie- Britannique) a permis d'établir un contrôle sur l'âge et les structures du Groupe Cache Creek et des unités associées. Les vingt-cinq localités de radiolarites, d'argilites siliceuses, de calcaires et de conglomérats à clastes de jaspes du Groupe de Cache Creek et de la Formation de Sifton ont fait ressortir un intervalle d'âge qui s'étend du Pennsylvanien supérieur-Permien inférieur au Jurassique inférieur (Pliensbachien). Ces résultats donnent la possibilité de poser de nouvelles bases stratigraphiques pour le groupe dans la région. Dans le centre de la Colombie-Britannique, les lithologies du Paléozoïque supérieur associées au Groupe de Cache Creek comprennent des roches carbonatées, des radiolarites et des basaltes, ainsi que potentiellement des gabbros et des roches ultrabasiques; les roches mésozoïques comprennent des greywackes, des argilites, des radiolarites, des calcaires et des tufs basaltiques. À l'échelle régionale, ces données fournissent des informations sur le Groupe de Cache Creek dans son ensemble, en particulier sur les intervalles marquant les deux transitions suivantes : d'une part, le passage d'une sédimentation carbonatée à une sédimentation siliceuse et, d'autre part, d'une sédimentation siliceuse à une sédimentation hémipélagique.

[1] Contribution to the Nechako NATMAP Project; a joint mapping project of the Geological Survey of Canada and British Columbia Geological Survey Branch.
[2] #311-1080 Pacific Street, Vancouver, British Columbia V6E 4C2

INTRODUCTION

As part of the Nechako NATMAP mapping project (Struik and McMillan, 1996), new bedrock geological mapping has started in the Fort Fraser map area (93K) (Struik et al., 1996), one of the least known areas of the Cache Creek Terrane. In conjunction with this new project, radiolarian biostratigraphic investigations have been undertaken in the area, and to a minor extent in Prince George map area (93G) (Fig. 1). Results from this work have improved our understanding of the stratigraphy and structure of the Cache Creek Group and related units in the region.

Radiolarian biostratigraphy has been applied to Paleozoic and Mesozoic oceanic strata of the Cache Creek Terrane of southern British Columbia and northern British Columbia/ southern Yukon Territory (Cordey et al., 1987, 1991; Cordey and Read, 1992). Biostratigraphic results from central British Columbia provide new information on paleogeographic and paleoenvironmental settings within the Cache Creek belt as a whole.

A recent report presented preliminary field and laboratory results from the 1995 field season (Cordey and Struik, 1996). The present paper completes the 1995-1996 work by reporting on results obtained on 25 selected productive localities from the Cache Creek Group and derived clastics where radiolarian fauna ranging in age from late Pennsylvanian-early Permian to Early Jurassic (Pliensbachian) were found.

Previous work

The Cache Creek Group in Fort St. James region is exposed along a zone that has been called the Stuart Lake belt by Armstrong (1949). In the belt, three main lithological divisions were identified: (1) limestone, (2) ribbon chert, and (3) greenstone. Within the ribbon chert division, Armstrong (1949) recognized occurrences of ribbon chert, slate, and argillaceous quartzite, in places interstratified with schistose greywacke and conglomerate, as well as intercalated bodies of greenstone. Ribbon chert strata was estimated at a minimum total thickness of 1500 m.

This work builds on the regional mapping of Armstrong (1949) and the detailed mapping of Paterson (1973) and Ash et al. (1993), which should be referred to for more complete descriptions and distributions of some of the rocks units described here.

The age of the Cache Creek Group in Fort Fraser has been determined by dating the limestone division with fusulinids and conodonts (Orchard and Struik, 1996, and references therein), but until recently, no age control was known from the ribbon chert division, interpreted as Paleozoic in age based on spatial associations with the limestone (Armstrong, 1949).

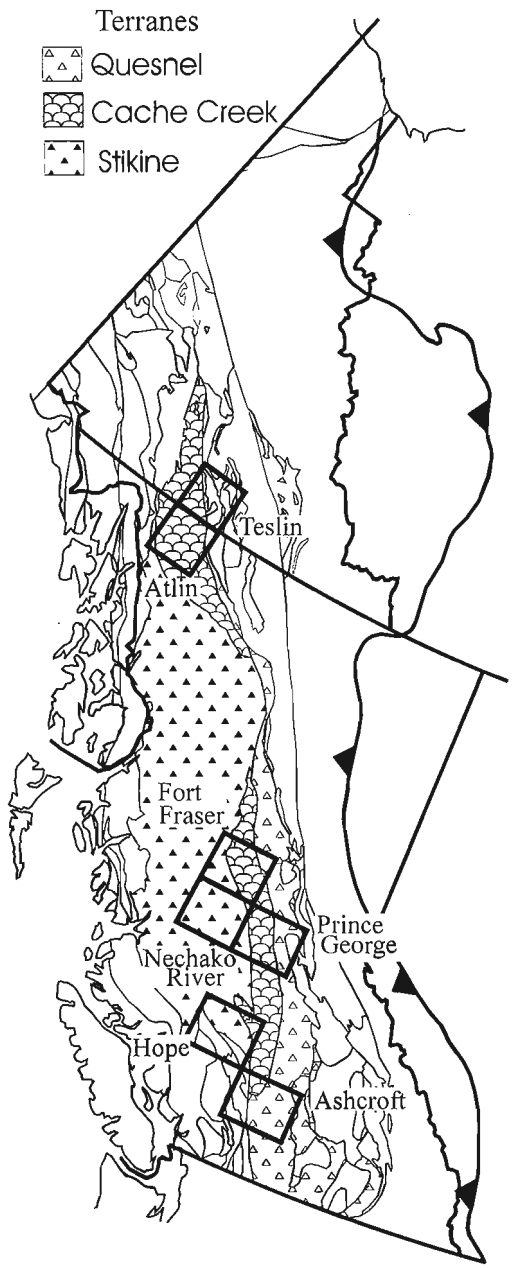

Figure 1. *Terrane map of the Canadian Cordillera with locations of 1:250 000 scale NTS map areas referred to in the text. Fieldwork reported here is from the Fort Fraser and Prince George map areas.*

SAMPLED UNITS AND RESULTS

In Fort St. James area, radiolarian-bearing rocks consist of four types: 1) ribbon chert, 2) siliceous mudstone, 3) limestone interbedded with chert, and 4) chert clasts. These rocks were sampled from various units within the Cache Creek Group, although they are primarily from units 5, and 6 of Ash et al. (1993) (Fig. 2). The chert clasts were mainly from unit 8 (Ash et al., 1993).

These strata types were collected applying field techniques of radiolarian detection and selection, as radiolarian preservation varies significantly from bed to bed. Samples were processed with 4 to 8% hydrofluoric acid (HF) solutions during 12 to 48 hours depending on the degree of matrix crystallinity.

Ribbon chert

Ribbon chert is the dominant rock type within the Stuart Lake belt of the Cache Creek Group (Armstrong, 1949). More recently, it has been established as characteristic of unit 5 of Ash et al. (1993). Consistent with these previous surveys, the principal areas of exposure of ribbon chert are: 1) Fort St. James area, 2) south-central side of Stuart Lake, and 3) north shore of the North Arm of Stuart Lake. Chert exposures near Fort St. James are referred to as the Sowchea sequence (Struik et al., 1996). In southern Fort Fraser map area, Cache Creek Group ribbon chert has been sampled on both sides of the Nechako River (Fig. 2).

Ribbon chert of the map area is dominantly grey or blue-grey, with local variations to light green, light grey, or black. Chert layers vary from 1 to 10 cm thick, and average 3 to 4 cm. They are separated by shale or schist partings of 0.2 to 5 cm thick. As is common elsewhere in the accreted terranes of the Cordillera, the chert sequences are folded and faulted (illustrations in Cordey and Struik, 1996), typically more so than adjacent lithologies. Such deformation may be due to stratigraphic unconformities and/or tectonic juxtaposition, or a distinct tectonic behaviour related to the incompetent, thinly bedded structure of ribbon chert.

Ribbon chert is locally interbedded with siliceous siltstone and chert breccias, as for example at the Sailing Club marina in Fort St. James (Fig. 2), a locality where Late Triassic conodonts and radiolarians (F. Cordey, unpub. report, 1990; Orchard and Struik, 1996) were previously found (K8.3,4). These clastic layers are characteristic of the Sowchea sequence (Struik et al., 1996). Ribbon chert sequences are locally found interlayered with basalt breccia and limestone, although stratigraphic relationships are unclear in many places.

On Battleship Island, the most southwesterly extension of the Mount Pope limestone unit (Fig. 2), thinly bedded limestone is interlayered with black and light brown chert. Radiolarians of late Pennsylvanian-early Permian age were released from one of the limestone beds on the top part of the section (K9.1, Table 1).

Table 1. Paleozoic radiolarian associations and ages from ribbon chert, siliceous mudstone, and carbonate from Fort Fraser (93K) map area. See Figure 2 for location.

Field No. GSC Loc.	Locality	Unit	Lithology	Radiolarian association	Age
95-SCB-2310 C-302768	K9-2	PTCCl	grey ribbon chert	*Latentifistula* sp., *Quinqueremis* sp.	Permian
95-FC-2-1 C-303005	K8-5	PTCCs	black cherty mudstone - (w.local beds of limy silt)	*Latentifistula texana* Nazarov and Ormiston, *Lat.* sp. cf. *pleniospongiosa* Nazarov and Ormiston, *Pseudoalbaillella* sp. cf. *globosa* Ishiga and Imoto, *Tormentum? Inflatum* Nazarov and Ormiston	Late Permian; Guadalupian
95-SCB-2707 C-3022707	K9-5	PTCCl	grey ribbon chert	*Entactinia* sp., *Follicucullus scholasticus* Ormiston and Babcock morphotype I Ishiga, *Follicucullus scholasticus* Ormiston and Babcock morphotype II Ishiga, fragments of Latentifistulidae	Late Permian; Guadalupian
95-SCB-2710 C-303779	K9-3	PTCCl	black ribbon chert	*Latentifistula texana* Nazarov and Ormiston, *Latentibifistula*(?) sp., *Nazarovella* sp. cf. *robusta* (De Wever and Caridroit), *Pseudoalbaillella* sp. cf. *globosa* Ishiga and Imoto, *Quadricaulis* sp. 1 Caridroit	Permian; Leonardian-Guadalupian
95-SCB-2708 C-302778	K9-4	PTCCl	grey ribbon chert	*Albaillella* sp., *Latentifistula* sp., *Pseudoalbaillella* sp. aff. *scalprata* Holdsworth and Jones, *Triactofenestrella*(?) sp.	Early Permian
95-SCB-1702 C-302755	K8-2	PTCCl	grey ribbon chert	*Pseudoalbaillella simplex* Ishiga et Imoto, *Pseudoalbaillella U-forma* Holdsworth and Jones morphotype II, *Pseudoalbaillella* sp. aff. *scalprata* Holdsworth and Jones	Early Permian; Wolfcampian
95-SCB-1709 C-302759	K8-1	PTCCl	grey ribbon chert	*Ishigaum* sp., *Latentifistula* sp. cf. *crux* Nazarov and Ormiston	Late Paleozoic (Pennsylvanian-Permian)
95FC-15-4 C-303016	K9-1	PTCCl	micritic limestone interb. w. chert	*Pseudoalbaillella U-forma* Group H and J, *Ps.* aff. *annulata* Ishiga	Late Pennsylvanian-Early Permian;

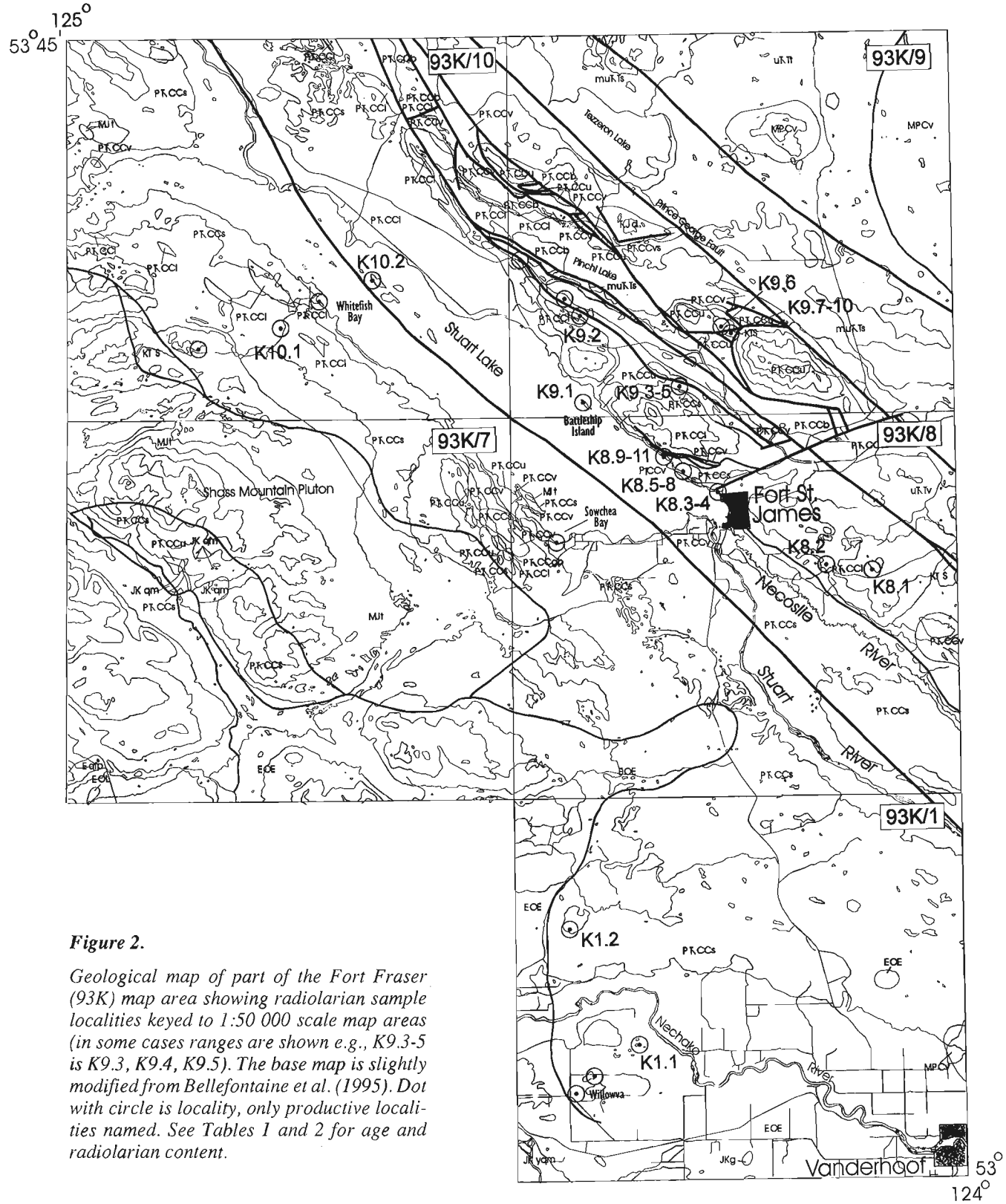

Figure 2.

Geological map of part of the Fort Fraser (93K) map area showing radiolarian sample localities keyed to 1:50 000 scale map areas (in some cases ranges are shown e.g., K9.3-5 is K9.3, K9.4, K9.5). The base map is slightly modified from Bellefontaine et al. (1995). Dot with circle is locality, only productive localities named. See Tables 1 and 2 for age and radiolarian content.

In Prince George east half (Struik et al., 1990) a section of grey radiolarian chert overlain by siliceous mudstone was sampled along the Blackwater River near the crossing of the Blackwater road (Punchaw Lake 93G/6). Middle Triassic (Ladinian) and Early Jurassic (Pliensbachian) radiolaria (respectively G6.1 and G6.2, Fig. 3, Table 2) were extracted from two beds of the section.

Siliceous mudstone

This rock characterizes the Sowchea sequence (Struik et al., 1996) which consists of siltstone and slate with minor amounts of chert, limestone, and greywacke. This unit, partly referred to as unit 6 by Ash et al. (1993), underlies a large area to the southwest of Stuart Lake (PTCCs, Fig. 2). No fossils was reported from the unit, and its age was based on association with the Mount Pope limestone (Armstrong, 1949). It may be in part Triassic as it is locally interlayered with Late Triassic ribbon cherts near the Fort St. James Sailing Club (Struik et al., 1996). Poorly preserved radiolarians from this unit suggests Late Triassic (K10.2, Table 2) and possibly Late Triassic-Early Jurassic (K10.1, Table 2) ages.

Miocene and Pliocene

MPCv — *Chilcotin Group:* olivine basalt

Eocene

EOE — *Endako Group:* basalt, andesite, minor gabbro

EOL — *Ootsa Lake Group:* rhyolite, dacite, andesite

Eqfp — rhyolite porphyry dykes

Cretaceous and Tertiary

KTS — *Sifton Formation:* conglomerate, sandstone siltstone, shale, coal (10)

Jurassic and Cretaceous

Francois Intrusions (JKqm - JKg)

JKqm — hornblende-biotite quartz monzonite

JKg — granite, granodiorite

Jurassic

MJt — tonalite, diorite (11)

Triassic and Jurassic

TRJd — diorite (11)

Triassic

Takla Group (uTRTt , muTRTs)

uTRTt — tuff, cherty tuff, siliceous argillite

uTRTv — basalt

muTRTs — argillite, greywacke, siltstone, shale, minor limestone, tuff, basalt

Cache Creek Group (TRCCsv - PTRCCvs)

TRCCsv — *Pinchi Sequence:* greywacke, siltstone, slate, basalt tuff, minor limestone, siliceous argillite (8)

upper Carboniferous to Triassic

Sowchea Sequence (PTRCCs - PTRCCsl)

PTRCCs — argillite, chert, siltstone, phyllite, sandstone, limestone, basalt (5,6)

PTRCCsl — limestone, greenstone, chert (7)

PTRCCl — *Pope formation:* limestone, greenstone, chert (7)

PTRCCv — basalt, minor limestone, argillite, chert (4)

PTRCCgb — *Railway Gabbro:* grabbro, diorite, peridotite, hornblendite, pyroxenite (3)

PTRCCu — *Trembleur Ultramafics:* serpentinite, harzburgite, dunite, peridotite, carbonatized equivalents (1,2)

PTRCCb — blueschist (chert, schist, greywacke, metabasalt, limestone)

Figure 2. *(cont.)*

Chert clasts

Chert clasts are found in three main units of the region: 1) intrasedimentary layers of chert breccia interbedded with ribbon cherts near Stuart Lake Lodge northwest of Fort St. James, 2) chert clasts of various sizes within sandstone and greywacke layers of Pinchi sequence sediments and basalts (Struik et al., 1996) (PTCCs between Stuart and Pinchi lakes, Fig. 2), and 3) chert pebbles within Cretaceous breccia and conglomerate (Sifton Formation KTS, Fig. 2) located to the southeast of Pinchi Lake (Fig. 2).

Within the Sifton Formation, clastic layers grade from breccia to conglomerate facies in a broad northwest to southeast direction. Chert clasts are dominantly grey or green and locally brown or black. Occurrence of small angular chert chips from breccia beds and large round pebbles from conglomerate favour the interpretation of a local origin for the clasts, for instance chert units of the Cache Creek Group visible to the southwest near Fort St. James. Six chert clasts removed from this unit (localities K9.7 to K9.10, Fig. 2) released radiolarian associations ranging in age from Middle Triassic to Late Triassic (Table 2). Identical ages were found in place in the chert sequence along the road to Stuart Lake Lodge in the Fort St. James area, supporting the interpretation of a local derivation from the Cache Creek Group.

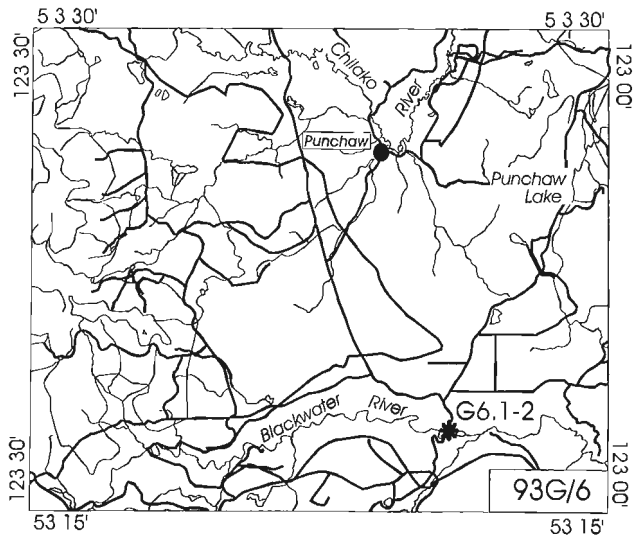

Figure 3. *Location map of Prince George (93G) localities (G6.1 and G6.2) displayed on Punchaw Lake (93G/6) 1:50 000 scale map area.*

Table 2. Mesozoic radiolarian associations and ages from ribbon chert, siliceous mudstone, and chert clasts from Fort Fraser (93K) and Prince George (93G) map areas. See Figures 2 and 3 for location.

Field No. GSC Loc.	Locality	Unit	Lithology	Radiolarian association	Age
95-FC-21-4 C-303032	G6-2	PTCCs	grey ribbon chert	*Atalanta* sp.; *Bipedis* sp.,*?Cantalum* sp.,*?Canutus* sp., *Lantus* sp.,*Orbiculiforma*(?) *trispina* Yeh, *Orbiculiforma argescens* Cordey, *Parahsuum simplum* Yao, *?Pleesus* sp., *Praeconocaryomma* spp., *Thurstonia* sp.	Early Jurassic (Pliensbachian)
95-FC-6-1 C-303012	K10-1	PTCCs	black cherty siltstone	*?Orbiculiforma* sp.	possibly Late Triassic - Early Jurassic
95-FC-8-2 C-303814	K10-2	PTCCs	black cherty mudstone	*?Capnuchosphaera* sp.	possibly Late Triassic
95-SCB-3903 C-302799	K1-1	PTCCs	grey ribbon chert	*Canoptum* sp., *? Katroma* sp., ? Nassellaria gen. et sp. Indet. X Hori, ? *Protopsium* sp.	Late Triassic or Early Jurassic
95-SCB-4108 C-302791	K1-2	PTCCs	grey ribbon chert	? *Livarella* sp., *Paronaella* sp., *Podobursa* sp.	Late Triassic, possibly late Norian/Rhaetian
95-SCB-3210 C-302789	K9-7	KTS	chert clast	*Canoptum* sp., *Risella* sp.	Late Triassic; late Norian/Rhaetian
95-FC-18-1 C-303025	K9-9	KTS	green chert pebble	*Livarella* sp., *Paratriassoastrum* sp.	Late Triassic; late Norian/Rhaetian
95-FC-19-3 C-303027	K9-10	KTS	green chert pebble	*Canesium lentum* Blome, *Capnodoce fragilis* Blome *C. traversi* Blome, *Latium* aff. *longulum* Blome, *Latium* spp., *Palaeosatumalis tenulspinosus* (Kozur and Mostler), *Sarla* sp., *Squinabolella* sp., *Syringocapsa* sp.	Late Triassic; early-middle Norian
95-SCB-3208 C-302788	K9-6	PTCCsv	chert clasts in basalt	*Capnodoce* sp.	Late Triassic; late Carnian-middle Norian
95-FC-1-3 C-303061	K8-4	PTCCs	brown ribbon chert	*Capnodoce* sp.	Late Triassic; late Carnian-middle Norian
95-FC-2-2 C-303063	K8-6	PTCCs	black cherty mudstone	*Capnodoce* sp., *Capnuchosphaera* sp., *Corum* sp., *Xipha pessagnoi* (Nakaseko and Nishimura)	Late Triassic; late Carnian-middle Norian
95-FC-2-4 C-303064	K8-8	PTCCs	green ribbon chert	*Capnodoce* sp., *Loffa* sp., *Paronaella* sp.	Late Triassic; late Carnian-middle Norian
95FC-16-1 C-303019	K8-9	PTCCs	black ribbon chert	*Capnuchosphaera* sp.	Late Triassic; Carnian-middle Norian
95-FC-16-4 C-303068	K8-10	PTCCs	grey ribbon chert	*Sarla* sp.	Late Triassic; Carnian-middle Norian
95-FC-17-3 C-303023	K9-8	KTS	black chert pebble	*Capnodoce* sp., *Capnuchosphaera* sp., *Pseudostylosphaera* sp.	Late Triassic; late Carnian
95-FC-1-1 C-303060	K8-3	PTCCs	grey ribbon chert	*Capnuchosphaera* sp., *Plafkerium* sp., *Pseudostylosphaera* sp. cf. *compacta* (Nazarov and Ormiston)	Late Triassic; Carnian
95-FC-21-1 C-303030	G6-1	PTCCs	grey ribbon chert	*Plafkerium cochleatum* (Nakaseko and Nishimura); *Pseudostylosphaera tenuis* (Nakasko and Nishimura); *Spongoserrula rarauana* Dumitrică; *Yeharaia* sp. cf. *lata* Kozur and Mostler	Middle Triassic; Ladinian
95-FC-17-2 C-303022	K9-8	KTS	black chert pebble	*Plafkerium* sp., *Pseudoeucyrtis*(?) sp., *Pseudostylosphaera magnispinosa* Yeh, *Ps.* aff. *tenuis* (Nakaseko and Nishimura), *Triassocampe* sp.	Middle Triassic;Ladinian
95-FC-19-4 C-303028	K9-10	KTS	green chert pebble	*Plafkerium cochleatum* (Nakaseko and Nishimura), *Pl. variabilis* (Nakaseko and Nishimura), *Poulpus* sp., *Praesarla* sp. cf. *integrita* Cordey et al., *Pseudoeucyrtis*(?) sp., *Silicarmiger latus* Kozur and Mostler, *Yeharaia elegans* Nakaseko and Nishimura	Middle Triassic; late Anisian-Ladinian
95-FC-2-3 C-303006	K8-7	PTCCs	grey ribbon chert	*Annulotriassocampe campanilis* Kozur and Mostler, *Pseudostylosphaera longispinosa* Kozur and Mostler, *Ps. tenuis* (Nakaseko and Nishimura)	Middle Triassic; late Anisian-early Ladinian
95-FC-16-5 C-303069	K8-11	PTCCs	grey ribbon chert	*Plafkerium* sp., *Pseudostylosphaera* sp., *Praesarla* sp., *Yeharaia* sp.	Middle Triassic

RADIOLARIAN FAUNA

Carboniferous-Permian

The oldest radiolarian association of the area was found in a thin limestone bed interlayered with chert at Battleship Island (K9.1, Fig. 2; Table 1), releasing a late Carboniferous-early Permian association correlative with *Pseudoalbaillella U. forma* assemblage zone, an uncommon association within the Cache Creek Group.

Five other localities released radiolarians correlative with Permian assemblage zones ranging in age from Wolfcampian to Guadalupian (Table 1). The Wolfcampian association (K8.1, Table 1) contains *Pseudoalbaillella simplex* Ishiga and Imoto and *Ps. U. forma* Holdsworth and Jones morphotype II Ishiga, a characteristic Early Permian assemblage described in Japan (Ishiga and Imoto, 1980). Two Guadalupian localities feature different associations (K8.5 and K9.3; Table 1): one contains a rich fauna of Albaillellaria, while the other is dominated by representatives of the Latentifistulidea superfamily.

A section featuring Permian and Triassic ribbon chert (localities K8.5 to K8.8, Fig. 2) released a rich sponge spicules fauna along with Guadalupian radiolarians. The interbedding of spiculitic and radiolarian cherts may indicate a local shallower water depth below high planktonic productivity radiolarian depocenter in the Late Permian.

Triassic

Four Middle Triassic radiolarian associations were recovered from ribbon chert near Fort St. James. Two occur in sections of the Cache Creek Group which also released Late Triassic fauna (K8.7, K8.11). The two others (K9.8, K9.10) were found within chert pebbles of the Sifton Formation, presumably derived from the Cache Creek Group.

One Middle Triassic fauna was found at Blackwater (G6.1) in a section that also features Early Jurassic ribbon chert. The association is Ladinian in age, and includes well-preserved representatives of *Spongoserrula rarauana* Dumitricà (Plate 1, fig. 5-6), which in Canada was only known within siliceous argillite of the Camp Cove Formation (Cordey et al., 1988). This species described in western Tethys (Dumitricà, 1982) is rather uncommon in North America.

Ribbon chert from Fort Fraser released twelve Late Triassic radiolarian associations correlative with *Capnuchosphaera*, *Capnodoce*, and *Betraccium* zones (Table 2). They range in age from Carnian to late Norian/Rhaetian, and include late Carnian, late Carnian-middle Norian and early-middle Norian associations. The ribbon chert localities of the Cache Creek Group and the chert pebbles of the Sifton Formation have similar ages (Carnian, late Carnian-middle Norian, late Norian/Rhaetian), consistent with a Cache Creek origin for the Sifton Formation clasts.

Early Jurassic

An Early Jurassic radiolarian association released from ribbon chert of the Blackwater section in Prince George map area (G6.2, Table 2) contains taxa whose common age range is confined to the Pliensbachian. Middle Triassic chert also occurs in the section, and we expect intermediate ages from future collecting. Across a minor fault, ribbon chert is conformably overlain by siliceous mudstone that has yet to be dated.

STRATIGRAPHY

Following Struik et al. (1996) and Cordey and Struik (1996), and using the cumulative age control provided by extracted fossils, the Cache Creek Group of central British Columbia is divided into six informal units (Fig. 4). They include: Mount Pope sequence, undifferentiated basalts, Trembleur ultramafics, Railway gabbro, and the Sowchea and Pinchi sequences. Contact and depositional relationships between the units are mainly unknown. Some relationships can be preliminarily interpreted from the distribution of the rocks and radiolarian ages.

Upper Paleozoic

Mount Pope sequence (PTCCl)

Mount Pope sequence consists mainly of light grey-weathering, light brown grey and grey micrite and bioclastic limestone. Thin basalt breccia and ribbon chert units are interlayered with the limestone in a few places. The best exposures are at Mount Pope where a nearly continuous section can be mapped from the shore of Stuart Lake to the top of the mountain (Fig. 2) (Struik et al., 1996; Orchard and Struik, 1996).

The age of the limestone has been previously determined as Middle Pennsylvanian and Early Permian from fusulinids and conodonts (Orchard and Struik, 1996, and references therein). Radiolaria extracted from chert and limestone of the unit (K8.1, K8.2, K9.1) are consistent with that age.

The ages of the limestone and the chert units within the Mount Pope sequence are consistent with a stratigraphic interlayering of the two units. The upper contact of the Mount Pope sequence is defined at the top of the thick limestone unit. North of Mount Pope, the contact is marked by a Leonardian chert unit containing a thin bed of volcaniclastic basalt (Fig. 2; K9.3, K9.4, K9.5, K9.2). From these relationships the upper contact of the Mount Pope sequence is tentatively interpreted as Early or Middle Permian.

Undifferentiated basalt

Cache Creek Group basalt near Fort St. James is mainly olive, aphanitic to finely crystalline, massive to breccia (Struik et al., 1996). The age of the basalts would be in part Pennsylvanian as basalt occurs within the Pennsylvanian

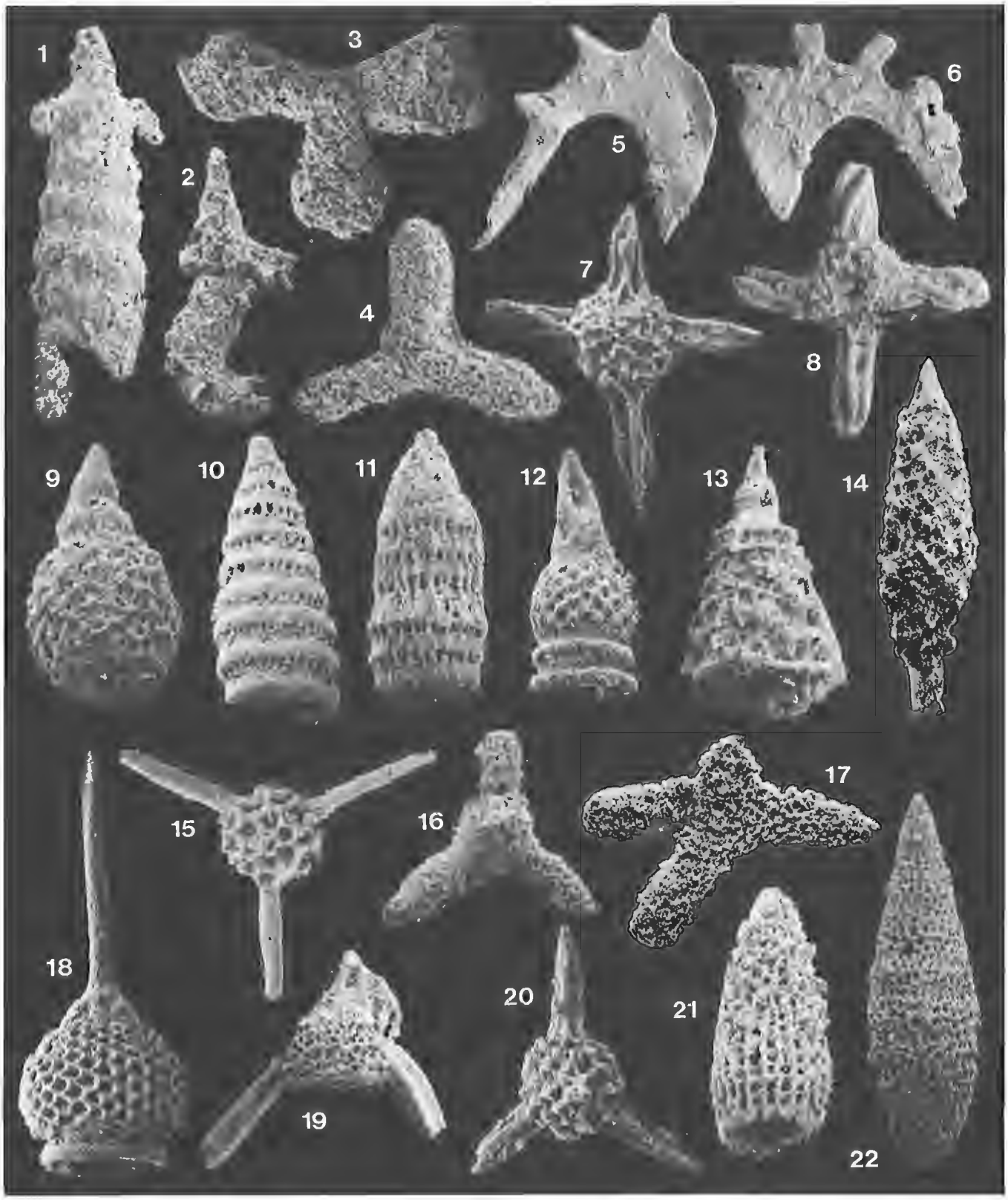
1
3
6
5
2
7
4
8
9
10
11
12
13
14
17
15
16
18
20
21
19
22

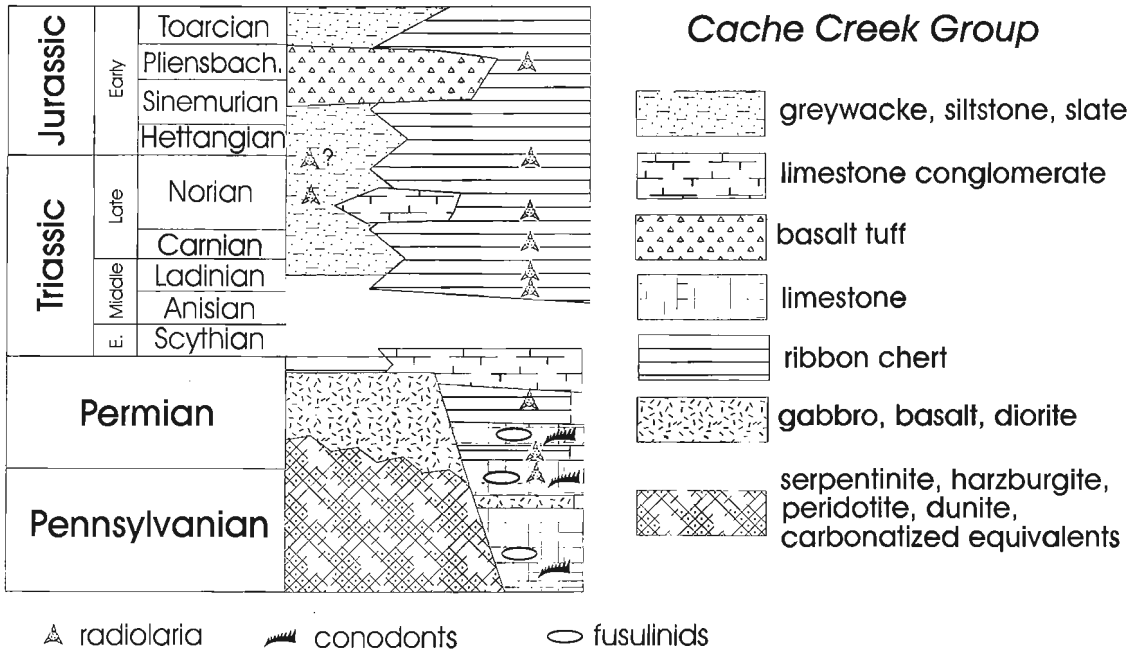

Figure 4. *Stratigraphy of the Cache Creek Group in Fort Fraser (93K) and Prince George (93G) map areas.*

PLATE 1

Scanning Electron micrographs of radiolarians of Paleozoic (fig. 1-4) and Mesozoic (fig. 5-22) ages from the Cache Creek Group, Fort Fraser and Prince George map areas, central British Columbia. The following are indicated: identification, locality, GSC locality no., field sample, GSC specimen number, and magnification.

1. *Pseudoalbaillella* sp. aff. *annulata* Ishiga, K9.1, GSC loc. C-303016, 95-FC-15-4, GSC 101481, x120.
2. *Pseudoalbaillella U-forma* Group, K9.1, GSC loc. C-303016, 95-FC-15-4, GSC 101482, x120.
3. *Latentifistula texana* Nazarov and Ormiston, K8.5, GSC loc. C-303005, 95-FC-2-1, GSC 101483, x100.
4. *Latentifistula* sp. cf. *pleniospongiosa* Nazarov and Ormiston, K8.5, GSC loc. C-303005, 95-FC-2-1, GSC 101484, x100.

5-6. *Spongoserrula rarauana* Dumitrică, G6.1, GSC loc. C-303030, 95-FC-21-1, GSC 101485 (fig. 5), GSC 101486 (fig. 6), x120.

7. *Plafkerium variabilis* (Nakaseko and Nishimura), K9.10, GSC loc. C-303028, 95-FC-19-4, GSC 101487, x140.
8. *Plafkerium cochleatum* (Nakaseko and Nishimura), G6.1, GSC loc. C-303030, 95-FC-21-1, GSC 101488, x120.
9. *Canesium lentum Blome*, K9.10, GSC loc. C-303027, 95-FC-19-3, GSC 101489, x190.
10. *Latium* sp. aff. *longulum* Blome, K9.10, GSC loc. C-303027, 95-FC-19-3, GSC 101490, x170.
11. *Latium* sp., K9.10, GSC loc. C-303027, 95-FC-19-3, GSC 101491, x190.
12. *Yeharaia elegans* Nakaseko and Nishimura, K9.10, GSC loc. C-303028, 95-FC-19-4, GSC 101492, x170.
13. *Silicarmiger latus* Kozur and Mostler, K9.10, GSC loc. C-303028, 95-FC-19-4, GSC 101493, x140.
14. *Pseudoeucyrtis*(?) sp., K9.10, GSC loc. C-303028, 95-FC-19-4, GSC 101494, x140.
15. *Capnodoce traversi* Blome, K9.10, GSC loc. C-303027, 95-FC-19-3, GSC 101495, x140.
16. *Livarella* sp., K9.9, GSC loc. C-303025, 95-FC-18-1, GSC 101496, x160.
17. *Paratriassoastrum* sp., K9.9, GSC loc. C-303025, 95-FC-18-1, GSC 101497, x140.
18. *Squinabolella* sp., K9.10, GSC loc. C-303027, 95-FC-19-3, GSC 101498, x165.
19. *Bipedis* sp., G6.2, GSC loc. C-303032, 95-FC-21-4, GSC 101499, x140.
20. ?*Cantalum* sp., G6.2, GSC loc. C-303032, 95-FC-21-4, GSC 101500, x140.
21. *Parahsuum simplum* Yao, G6.2, GSC loc. C-303032, 95-FC-21-4, GSC 101501, x200.
22. ?*Pleesus* sp. G6.2, GSC loc. C-303032, 95-FC-21-4, GSC 101502, x145.

limestone. From the association with the Late Permian ribbon chert at localities K9.2 to K9.5, some fragmental basalt would be Permian.

Trembleur ultramafics and Railway gabbro

These rock suites occur as fault bounded blocks and have no age constraints. Armstrong (1949) and Paterson (1973) mapped the Trembleur ultramafic rocks as harzburgites and peridotites. Locally they are layered cumulates, and invariably have been partly altered to serpentinite. Ash et al. (1993) divided these rocks into crustal and mantle representatives.

The Railway gabbro underlies a narrow belt along the south side of Pinchi Lake. The gabbro is intimately mixed with basalt and microgabbro, and all those rocks are crosscut by numerous veins and veinlets of plagioclase and cryptocrystalline quartz. Paterson (1973) suggested that the gabbro basalt sequence was unconformably overlain by upper Triassic limestone and volcaniclastics to the north, and possibly underlain by ultramafic rocks to the south.

Mesozoic (mainly Middle Triassic to Early Jurassic)

Sowchea sequence (PTCCs and PTCCsl)

This unit underlies a large area mainly to the southwest of Stuart Lake and may be the lateral equivalent of the Pinchi sequence (Struik et al., 1996). The rocks consist of siltstone, slate, chert, chert conglomerate, limestone, and lesser amounts of greywacke. Locally these rocks are interbedded with intraformational conglomerates and breccias. Most of the fine grained sediments range from cherty argillites and slates to muddy cherts. Rocks of the unit are grey to dark grey and thinly bedded, and are commonly disrupted by bedding parallel and nearly bedding parallel slip. Typical of these clastic rocks are the easily accessible outcrops at the west end of the Sowchea Bay Provincial Park and the Sailing Club marina on Stuart Lake. Disparate units of ribbon chert and siltstone of Upper Permian, Triassic, and Lower Jurassic age in Fort Fraser and Prince George map areas are included within this sequence.

The age of the Sowchea sequence ranges from Late Permian to Early Jurassic (Cordey and Struik, 1996; Orchard and Struik, 1996; this report).

Pinchi sequence (TCCsv)

These rocks are exposed on both sides of Pinchi Lake. They consist of greywacke, chert sandstone, siltstone, slate, basalt tuff, and minor limestone (Struik et al., 1996).

Good exposures of this sequence are found west of Murray Ridge and between the B.C. Rail line and Pinchi Lake (Fig. 3). This sequence was mapped by Armstrong (1949) and Paterson (1973) as Takla Group, and interpreted by Bellefontaine et al. (1995) as Cache Creek Group. Paterson interpreted the unit to unconformably overlie the Railway gabbro.

The age of the Pinchi sequence is determined from macrofossils (Armstrong, 1949; Paterson, 1973), and from radiolaria derived from chert pebbles in volcaniclastic basalt as Upper Triassic to Lower Jurassic. These rocks are correlated with the Sowchea sequence and other Triassic/Jurassic Cache Creek Group sedimentary sequences in the Cordillera.

Carnian and Norian radiolaria extracted from pebbles contained within the basalt tuff at the south end of Pinchi Lake (K9.6) constrain the age of the basalt to Upper Triassic or younger age. The basalt overlies Upper Triassic Monotis-bearing limestone. The age of the pebbles is consistent with this datum, and the basalt is likely uppermost Triassic or Early Jurassic in age.

Comparisons with other areas of the Cache Creek Terrane

All segments of the Cache Creek Terrane (Fig. 1) display intervals of radiolarian-bearing strata of Late Paleozoic to Early Mesozoic age: in the type locality of the Cache Creek Group in Ashcroft map area (92I), ribbon chert ranges in age from Early Permian to Late Triassic, along with Early or Middle Jurassic siliceous mudstone (Cordey et al., 1987); in Taseko Lakes map area (92O), chert of Early Permian to Early Jurassic age is conformably overlain by Early Jurassic siliceous mudstone (Cordey and Read, 1992, and unpub. data, 1993). In Atlin (104N) and Teslin (105C) map areas of northern British Columbia and southern Yukon, radiolarian cherts range in age from Pennsylvanian to Early Jurassic, including widely exposed Middle and Late Triassic ribbon chert interbedded with fine- and coarse-grained siliceous clastic rocks of Late Triassic and Early Jurassic age on Teslin Plateau (Cordey et al., 1991; Gordey and Stevens, 1994).

Although based on relatively preliminary exploration, we are able to identify within the stratigraphy of the Cache Creek Group of Fort Fraser and Prince George map areas: 1) features similar with these more thoroughly studied regions, and 2) new features.

Similar features

The Early Permian (Wolfcampian) to Late Triassic (Norian, possibly late Norian/Rhaetian) age range obtained on chert near Fort St. James bears the closest resemblance with the type locality of the Cache Creek Group in southern British Columbia (Cordey, in press). The local interbedding of clastic strata in the Late Triassic in Fort Fraser and the transition from chert to siliceous mudstone in Prince George resembles the Mesozoic stratigraphy of the Cache Creek Group in southern Yukon, although Paleozoic and Mesozoic chert are there rarely found in the same zones of the terrane.

The stratigraphic reconstruction of chert-bearing units from different tectonic slices of the Cache Creek Terrane in Fort Fraser-Prince George areas indicates that intervals of chert deposition in this region, as is in other areas of the terrane, have potentially been continuous over long periods of time: in Fort St. James area, some sections display Early or Late Permian chert overlying Mount Pope carbonate, this

Paleozoic chert being locally associated with Middle and Late Triassic chert. At Blackwater, an apparent conformable section features Middle Triassic (Ladinian) and Early Jurassic (Pliensbachian) ribbon chert devoid of major clastic input within this interval. The total age range of the sequence is probably more extended as the base of the sequence was not observed, and the top not yet dated.

New features

The Paleozoic transition from limestone to chert found at Battleship Island has never been observed before in the Cache Creek Terrane. At this locality (K9.1), radiolarians were observed in the chert, but have been better recovered from a limestone interbed. This transition seems to occur in the late Pennsylvanian or near the Pennsylvanian/Permian boundary. The Mount Pope limestone has been interpreted as shallow-water carbonate atoll material accumulated after downslope transportation (Orchard and Struik, 1996, and references therein). We can suggest the following hypotheses regarding the conditions of change from carbonate to chert deposition: 1) onset of chert deposition results from a progressive deepening of the corresponding pelagic basin. This transition is likely to be diachronous within the area, as fusulinid-bearing carbonate deposition persisted locally into the Early Permian (Orchard and Struik, 1996, and references therein); and 2) the initiation of chert deposition near the Pennsylvanian/Permian boundary may be linked to an increase of siliceous planktonic productivity which induced an uprise of the Carbonate Compensation Depth (CCD). The occurrence of Guadalupian radiolarians within spiculitic chert near Fort St. James suggests that this siliceous productivity was particularly high in the Late Permian. This is consistent with the "mid-Permian chert event" hypothesis of Murchey and Jones (1992).

In the Mesozoic, the depositional transition from ribbon chert (pelagic) to siliceous mudstone (hemipelagic) in the Early Jurassic is potentially one of the best exposed in the whole terrane and will be studied in more detail. In Taseko Lakes, the younger cherts are dated Sinemurian or Pliensbachian (Cordey and Read, unpub. data, 1993), and within the interval Sinemurian-Toarcian, possibly late Sinemurian, in Teslin area (Cordey et al., 1991). The Pliensbachian locality from Blackwater suggests that Prince George map area may yield among the youngest pelagic strata of the Cache Creek Terrane.

CONCLUSIONS

The Cache Creek Group in central British Columbia, previously considered confined to the Late Paleozoic has yielded late Carboniferous/early Permian to Jurassic radiolarians from ribbon chert, limestone, and siliceous mudstone strata. In addition, chert clasts from basalt, conglomerate and breccia have yielded a wide range of Triassic ages.

These results contribute to the understanding of the stratigraphy of the Cache Creek Group within the area, for instance the local Paleozoic transition from carbonate to chert deposition, Triassic clastic input within chert strata, and possible long intervals of chert deposition from Permian to Late Jurassic. From the distribution of rock units, the existing fossil information, and the radiolarian determinations presented here, it is possible to divide the Cache Creek Group of central British Columbia into six upper Paleozoic and Mesozoic units.

ACKNOWLEDGMENTS

Claire Floriet provided enthusiastic assistance in the field. We express our thanks to Steve Irwin for his review and Bev Vanlier for her help in the preparation of the manuscript.

REFERENCES

Armstrong, J.E.
1949: Fort St. James map-area, Cassiar and Coast Districts, British Columbia; Geological Survey of Canada, Memoir 252.

Ash, C., MacDonald, R.W.J., and Paterson, I.A.
1993: Geology of the Stuart and Pinchi Lakes area, central British Columbia (93K); British Columbia Ministry of Energy, Mines and Petroleum Resources, Open File 1993-9.

Bellefontaine, K.A., Legun, A., Massey, N., and Desjardins, P.
1995: Digital geological compilation of northeast B.C. – southern half (NTS 83D, E, 93F, G, H, I, J, K, N, O, P); British Columbia Ministry of Energy, Mines and Petroleum Resources, Open File 1995-24.

Cordey, F.
in press: Radiolaires des complexes d'accrétion cordillerains; Geological Survey of Canada, Bulletin 509.

Cordey, F. and Read, P.B.
1992: Permian and Triassic radiolarian ages from the Cache Creek Complex, Dog Creek and Alkali Lake, southwestern British Columbia; in Current Research, Part E; Geological Survey of Canada, Paper 92-1E, p. 41-51.

Cordey, F. and Struik, L.C.
1996: Scope and preliminary results of radiolarian biostratigraphic studies, Fort Fraser and Prince George map areas, central British Columbia; in Current Research 1996-A; Geological Survey of Canada, p. 83-90.

Cordey, F., DeWever, P., Dumitrică, P., Danelian, P., Kito, N., and Vrielynck, B.
1988: Description of some new Middle Triassic radiolarian species from the Camp Cove Formation, southern British Columbia, Canada; Revue de Micropaléontologie, v. 31, p. 30-37.

Cordey, F., Gordey, S.P., and Orchard, M.J.
1991: New biostratigraphic data for the northern Cache Creek Terrane, Teslin map area, southern Yukon; in Current Research, Part E; Geological Survey of Canada, Paper 91-1E, p. 67-76.

Cordey, F., Mortimer, N., DeWever, P., and Monger, J.W.H.
1987: Significance of Jurassic radiolarians from the Cache Creek terrane, British Columbia; Geology, v. 15, p. 1151-1154.

Dumitrică, P.
1982: Triassic Oertlisponginae (Radiolaria) from Eastern Carpathians and Southern Alps; Dari de Seama, Institutul de Geologie si Geofizică, Bucuresti, v. 67, p. 57-74.

Gordey, S.P. and Stevens, R.A.
1994: Tectonic framework of the Teslin region, southern Yukon Territory; in Current Research 1994-A; Geological Survey of Canada; p. 11-18.

Ishiga, H. and Imoto, N.
1980: Some Permian radiolarians in the Tamba district, Southwest Japan; Earth Sciences (Chikyu Kagaku), v. 34, p. 333-345.

Murchey, B.L. and Jones, D.L.
1992: A mid-Permian chert event: widespread deposition of biogenic siliceous sediments in coastal, island arc and oceanic basins; in The Significance and Application of Radiolaria to Terrane Analysis, (ed.) J. Aitchison and B. Murchey; Palaeogeography, Palaeoclimatology, Palaeoecology, v. 96, p. 161-174.

Orchard, M.J. and Struik, L.C.
1996: Conodont biostratigraphy, lithostratigraphy, and correlation of the Cache Creek Group near Fort St. James, British Columbia; in Current Research 1996-A; Geological Survey of Canada, p. 77-82.

Paterson, I.A.
1973: The geology of the Pinchi Lake area, central British Columbia; Ph.D. thesis, University of British Columbia, Vancouver, British Columbia, 263 p.

Struik, L.C. and McMillan, W.J.
1996: Nechako Project Overview, central British Columbia; in Current Research 1996-A; Geological Survey of Canada, p. 57-62.

Struik, L.C., Floriet, C., and Cordey, F.
1996: Geology near Fort St. James, central British Columbia; in Current Research 1996-A; Geological Survey of Canada, p. 71-76.

Struik, L.C., Fuller, E.A., and Lynch, T.
1990: Geology of Prince George (east half), British Columbia (93G east); Geological Survey of Canada, Open File 2172.

Geological Survey of Canada Project 950036

Electrical resistivity of rock samples from Vancouver Island, British Columbia

N. Scromeda, T.J. Katsube, and M. Best[1]
Mineral Resources Division, Ottawa

Scromeda, N., Katsube, T.J., and Best, M., 1996: Electrical resistivity of rock samples from Vancouver Island, British Columbia; in Current Research 1996-E; Geological Survey of Canada, p. 19-22.

Abstract: Bulk electrical resistivity (ρ_r) has been measured on 16 rock samples (volcanic, plutonic, and sedimentary) from northern Vancouver Island to assist in the interpretation of ground electromagnetic surveys. Effective porosity (ϕ_E) and bulk density (δ_B) have also been measured to provide additional information on the rocks.

Results indicate that ρ_r values of these rocks are generally outside the reported range for similar rocks. The ρ_r values for the sandstones (110-6700 Ω·m) resemble Precambrian terrestrial sandstones (300-5000 Ω·m). The larger ρ_r values for the volcanic rocks (230-26 000 Ω·m) are considerably larger than the generally accepted values (10-5000 Ω·m). The ρ_r values (230-290 Ω·m) for the diorites have little resemblance to those of crystalline rocks (47 000-280 000 Ω·m). These results, including the ϕ_E and δ_B data, suggest that some of these rocks are extremely tight with the majority of the pores being blocked, and that the diorites are unusually porous.

Résumé : La résistivité électrique apparente (ρ_r) a été mesurée sur 16 échantillons de roches volcaniques, plutoniques et sédimentaires provenant de la partie nord de l'île de Vancouver, dans le but de faciliter l'interprétation des levés électromagnétiques terrestres. La porosité efficace (ϕ_E) et la masse volumique apparente (δ_B) ont également été calculées pour en savoir encore plus sur ces roches.

Les résultats indiquent que les valeurs de ρ_r de ces échantillons se situent généralement à l'extérieur de l'intervalle obtenu pour des roches semblables. Les valeurs de p_r des grès (110-6 700 Ω·m) sont proches de celles des grès terrestres précambriens (300-5 000 Ω·m). Les valeurs de ρ_r des roches volcaniques (230-26 000 Ω·m) sont considérablement plus élevées que les valeurs généralement acceptées (10-5 000 Ω·m). Quant aux valeurs de ρ_r des diorites (230-290 Ω·m), elles diffèrent beaucoup de celles des roches cristallines (47 000-280 000 Ω·m). Ces résultats, incluant les données de ϕ_E et de δ_B, indiquent que certaines de ces roches sont très étanches, la majorité des pores étant bloqués, et que les diorites sont inhabituellement poreuses.

[1] GSC Pacific, Sidney

INTRODUCTION

Bulk electrical resistivity, ρ_r, measurements have been carried out on 16 rock samples collected from northern Vancouver Island (British Columbia), for the purpose of assisting in the interpretation of ground electromagnetic surveys. Effective porosity, ϕ_E, and bulk density, δ_B, measurements have also been carried out on these samples, in order to provide additional information on their petrophysical characteristics.

METHOD OF INVESTIGATION

Samples and sample preparation

The 16 rock samples were drill cores, of 2.44-2.49 cm (1") in diameter and about 5 cm in length, collected from northern Vancouver Island. They are a mixture of volcanic (basalt, tuff), plutonic (diorite), and sedimentary (sandstone) rocks. Sample information, including field identification numbers, rock type and lithologies, is listed in Table 1. At least two specimens were cut from each of these core samples, one for bulk electrical resistivity (ρ_r) and bulk density (δ_B) measurements, and another for effective porosity (ϕ_E) measurements. The geometric characteristics of the specimens used for electrical and bulk density measurements are listed in Table 2. Their specimen thicknesses are in the range of 0.53-0.66 cm. The geometric factor (K_G), listed in Table 2, is a parameter derived from the specimen dimensions, and is used in the bulk electrical resistivity (ρ_r) determination.

Bulk density and effective porosity measurements

The caliper method (API, 1960) has been used to determine the bulk density, δ_B, of the samples, by measuring the dimensions and weight of the disk-shaped specimens. This measurement constitutes part of the porosity determining procedure. Effective porosity, ϕ_E, in principle represents the pore volume of all interconnected pores. In this study, it is determined from the difference in weight between the oven-dried and water-saturated rock specimens. The API Recommended Practice for Core-Analysis Procedures (API, 1960) has generally been followed in these measurements. The procedures routinely used in our measurements are described in the literature (Katsube and Scromeda, 1991; Katsube et al., 1992a; Scromeda and Katsube, 1994).

Bulk electrical resistivity measurements

The bulk electrical resistivity, ρ_r, is determined from the complex electrical resistivity, ρ^*, measurements made on the disc-shaped specimens by methods described in recent publications (e.g. Katsube et al., 1991; Katsube and Salisbury, 1991; Katsube and Scromeda, 1994). The complex electrical resistivity (ρ^*) is measured over a frequency range of 1-10^6 Hz, with ρ_r representing a bulk electrical resistivity at frequencies of about 10^2-10^3 Hz. It is a function of the pore structure and pore fluid resistivity, and is considered to exclude any other effects, such as pore surface, dielectric or any other polarizations (e.g. Katsube, 1975; Katsube and Walsh, 1987).

Table 1. Sample information for samples from north Vancouver Island (British Columbia).

Sample No.	Sample I.D.	Lithology	Formation
MP-1	93GNX 4-4	Basalt	Karmutsen
MP-2	93GNX 4-8	Basalt	Karmutsen
MP-3	93GNX 6-5	Basalt	Karmutsen
MP-4	93GNX 15-1-1	Volcanic	Bonanza
MP-5	93GNX 17-8	Basalt	Bonanza
MP-6	93GNX 17-10-2	Basalt	Bonanza
MP-7	93GNX 18-5	Basalt	Bonanza
MP-8	93GNX 15-11	Volcanic	Bonanza
MP-9	93GNX 20-1	Tuff	Bonanza
MP-10	93GNX 22-5	Volcanic	Bonanza
MP-11	JHA 4-2-3	SS-CG	PB-Lr Jurasic
MP-12	JHA 13-7	SS-Tuff	PB-Lr Jurasic
MP-13	JHA 17-5	SS	Cretaceous
MP-14	LSN 21-2	SS-CG	Cretaceous
MP-15	LSN 6-4	Diorite	Bonanza Plutonic
MP-16	LSN 20-1	Diorite	Bonanza Plutonic

I.D. = Field Identification Number
SS = Sandstone
CG = Conglomerate
PB = Parsons Bay

Table 2. Dimensions of specimens cut out from the samples.

Samples	r_D (cm)	ℓ (cm)	W (g)	V (cm^3)	K_G (m)	δ_B (g/mL)
MP-1a	2.488	0.568	8.2830	2.76	8.56	3.00
MP-2a	2.457	0.631	9.4452	2.99	7.51	3.16
MP-3a	2.455	0.566	8.4663	2.68	8.36	3.16
MP-4a	2.454	0.590	7.9015	2.79	8.02	2.83
MP-5a	2.457	0.637	8.7493	3.02	7.44	2.90
MP-6a	2.456	0.533	7.0741	2.53	8.89	2.80
MP-7a	2.445	0.662	8.4863	3.11	7.09	2.73
MP-8a	2.451	0.548	6.9510	2.59	8.61	2.69
MP-9a	2.451	0.622	7.9902	2.93	7.59	2.72
MP-10a	2.457	0.568	7.4339	2.69	8.35	2.76
MP-11a	2.444	0.552	6.9617	2.59	8.50	2.69
MP-12a	2.459	0.645	8.5240	3.06	7.36	2.78
MP-13a	2.442	0.585	7.1278	2.74	8.01	2.60
MP-14a	2.454	0.644	8.2835	3.05	7.34	2.72
MP-15a	2.455	0.596	8.3611	2.82	7.94	2.96
MP-16a	2.455	0.570	7.7171	2.70	8.30	2.86

r_D = diameter
ℓ = thickness
W = weight*
* = measured under room-dry (humidity: 40 %) conditions
V = volume
K_G = geometric factor
δ_B = bulk density

EXPERIMENTAL RESULTS

The results of the bulk density (δ_B) determinations are listed in Tables 2 and 3. The δ_B values are in the range of 2.7-3.2 g/mL for the basalts, 2.6-2.8 g/mL for the sandstones and those represented by the term "volcanic rocks", and 2.9-3.0 g/mL for the diorites. The results of the effective porosity (ϕ_E) measurements are listed in Table 3. The ϕ_E values for these rocks are in the range of 1.9-9.8%, with no distinct trends related to lithology or rock type.

The results of the bulk electrical resistivity (ρ_r) measurements are listed in Table 4. Determinations have been made at 24 and 48 hours after water saturation, to ensure that they represent ρ_r values stable with time. The complex resistivity plots used to determine ρ_r all showed normal arcs with no distortions, for this set of samples. They resemble those displayed in Figures 2, 3, and 4b in the publication by Katsube et al. (1992b). The ρ_r values for these rocks are generally in the range of 100-7000 Ω·m, with exceptions for some of the basalts and volcanic rocks that are in the range of 10 000-26 000 Ω·m.

DISCUSSIONS AND CONCLUSIONS

The results for all three parameters, bulk density (δ_B), effective porosity (ϕ_E), and bulk electrical resistivity (ρ_r) are compiled in Table 5 for all of the 16 samples. The δ_B values for the basalts (2.7-3.2 g/mL), volcanic rocks (2.7-2.8 g/mL), and diorites (2.9-3.0 g/mL) are within the reported range of values, 2.27-3.21 g/mL (Johnson and Olhoeft, 1984), 2.33-3.15 g/mL (Daly et al., 1966) and 2.27-2.96 g/mL (Johnson and Olhoeft, 1984), respectively, for these three rock types.

Table 4. Results of electrical resistivity measurements.

Sample No.	Meas. #1	ρ_r, (10^3 Ω·m) Meas. #2	Mean*
MP-1a	4.33	4.14	4.24 ± 0.10
MP-2a	10.6	9.66	10.1 ± 0.50
MP-3a	2.76	2.58	2.67 ± 0.09
MP-4a	0.64	0.65	0.65 ± 0.01
MP-5a	0.63	0.63	0.63 ± 0.0
MP-6a	0.35	0.37	0.36 ± 0.10
MP-7a	2.16	1.92	2.04 ± 0.12
MP-8a	12.9	23.7	18.3 ± 5.4
MP-9a	0.23	0.22	0.23 ± 0.01
MP-10a	19.8	32.5	26.1 ± 6.4
MP-11a	0.11	0.11	0.11 ± 0.0
MP-12a	0.31	0.32	0.32 ± 0.01
MP-13a	6.21	7.13	6.67 ± 0.46
MP-14a	0.17	0.18	0.18 ± 0.01
MP-15a	0.28	0.30	0.29 ± 0.01
MP-16a	0.23	0.23	0.23 ± 0.01

ρ_r = Bulk Electrical Resistivity
Meas. (#1) = Measurement after 24 hours of saturation.
Meas. (#2) = Measurement after 48 hours of saturation.
*: The values following the ± sign represent the larger of the two differences between the Mean and the two Measurement (#1 and #2) values. Since the ρ_r values decrease immediately after saturation, it is necessary to make at least two measurements, a reasonable time apart, to ensure a stable value has been reached. Equal, or a larger value for the second ρ_r measurement, most likely, implies that stability has been reached.

Table 3. Results of the effective porosity measurements.

Sample	δ_B* (g/mL)	W_W (g)	W_D (g)	S_{ir} (%)	ϕ_E (%)
MP-1b	3.00	9.2003	9.1382	44.1	2.04
MP-2b	3.16	10.4733	10.3958	69.0	2.36
MP-3b	3.16	8.7668	8.7142	51.5	1.91
MP-4b	2.83	8.3575	8.2503	28.4	3.68
MP-5b	2.90	6.5568	6.4465	42.8	4.96
MP-6b	2.80	7.8382	7.6387	37.1	7.31
MP-7b	2.73	7.8937	7.7770	52.5	4.10
MP-8b	2.69	8.4350	8.2442	6.8	6.23
MP-9b	2.72	6.5288	6.4065	59.9	5.19
MP-10b	2.76	7.2954	7.2170	4.0	3.00
MP-11b	2.69	6.7196	6.4841	36.1	9.77
MP-12b	2.78	7.5493	7.4160	34.4	5.00
MP-13b	2.60	5.1448	4.9571	32.3	9.84
MP-14b	2.72	7.2563	7.0932	51.7	6.25
MP-15b	2.96	7.4623	7.3567	57.0	4.25
MP-16b	2.86	5.6262	5.4522	66.2	9.13

δ_B = bulk density
* = values from Table 2
W_w = wet weight
W_D = dry weight
S_{ir}= irreducible water saturation
ϕ_E = effective porosity

Table 5. Summary of petrophysical properties.

Sample No.	Lithology	δ_B (g/mL)	ϕ_E (%)	ρ_r (10^3 Ω·m)
MP-1	Basalt	3.00	2.04	4.24
MP-2	Basalt	3.16	2.36	10.1
MP-3	Basalt	3.16	1.91	2.67
MP-4	Volcanic	2.83	3.68	0.65
MP-5	Basalt	2.90	4.96	0.63
MP-6	Basalt	2.80	7.31	0.36
MP-7	Basalt	2.73	4.10	2.04
MP-8	Volcanic	2.69	6.23	18.3
MP-9	Tuff	2.72	5.19	0.23
MP-10	Volcanic	2.76	3.00	26.1
MP-11	SS-CG	2.69	9.77	0.11
MP-12	SS-Tuff	2.78	5.00	0.32
MP-13	SS	2.60	9.84	6.67
MP-14	SS-CG	2.72	6.25	0.18
MP-15	Diorite	2.96	4.25	0.29
MP-16	Diorite	2.86	9.13	0.23

δ_B = Bulk Density
ϕ_E = Effective Porosity
ρ_r = Bulk Electrical Resistivity

The δ_B values for sandstones (2.6-2.8 g/mL) are rather high compared to the commonly accepted range of 1.99-2.45 g/mL (Johnson and Olhoeft, 1984) for this rock type, probably due to high concentration of volcanic clasts.

There is a limited amount of information in the literature on the porosity for volcanic rocks including basalts. The range of ϕ_E values for sandstones (5.0-9.8%) is at the lower end of the accepted range of 8.8-38.3% (Daly et al., 1966). On the other hand, the range of ϕ_E values for the diorites (4.3-9.1%) is considerably higher than the previously reported values of 0.51-0.55% (Hume and Katsube, 1987) for this rock type, or for those of 0.07-0.43% (Katsube and Mareschal, 1993) for crystalline rocks in general.

The ρ_r values of these rocks are generally outside the reported range of values for similar rock types. The ρ_r values for the sandstones (110-6700 Ω·m) resemble those of Precambrian terrestrial sandstones with known values between 300-5000 Ω·m (Keller, 1966). The larger ρ_r values (230-26 000 Ω·m) for the volcanic rocks, including basalts, are considerably higher than the published values of 10-5000 Ω·m (Keller, 1966). The ρ_r values (230-290 Ω·m) for the diorites have no resemblance to the previously reported values of 47 000-280 000 Ω·m (Katsube and Mareschal, 1993) for crystalline rocks.

These results suggest that the sandstones and some of the volcanic rocks (including the basalts) are extremely tight with the majority of the pores being blocked. These results also suggest that the diorites are unusually porous, and could have been subject to extensive weathering.

ACKNOWLEDGMENTS

The authors are grateful to L. Diakow from the British Columbia Geological Survey Branch for providing the samples used in this study. The authors express their appreciation for the critical review of this paper by Q. Bristow (Geological Survey of Canada).

REFERENCES

API (American Petroleum Institute)
1960: Recommended practices for core-analysis procedure; API Recommended Practice 40 (RP 40) First Edition, American Petroleum Institute, Washington, D.C., p. 55.

Daly, R.A., Manger, E.G., and Clark, S.P. Jr.
1966: Density of rocks: Section 4; in Handbook of Physical Constants; Geological Society of America, Memoir 97, p. 19-26.

Hume, J.P. and Katsube, T.J.
1987: Pore structure characteristics; in Geotechnical Studies at East Bull Lake Research Area, (ed.) A.G. Latham; Canada Centre for Mineral and Energy Technology, CANMET Report MRL 87-94, p. 39-66.

Johnson, G.R. and Olhoeft, G.R.
1984: Density of rocks and minerals; in CRC Handbook of Physical Properties of Rocks, Vol 3; CRC Press, Inc. Florida, p. 2-38.

Katsube, T.J.
1975: The electrical polarization mechanism model for moist rocks; in Report of Activities, Part C; Geological Survey of Canada, Paper 75-1C, p. 353-360.

Katsube, T.J. and Mareschal, M.
1993: Petrophysical model of deep electrical conductors; Graphite lining as a source and its disconnection due to uplift; Journal of Geophysical Research, v. 98, B5, p. 8019-8030.

Katsube, T.J. and Salisbury, M.
1991: Petrophysical characteristics of surface core samples from the Sudbury structure; in Current Research, Part E; Geological Survey of Canada, Paper 91-1E, p. 265-271.

Katsube, T.J. and Scromeda, N.
1991: Effective porosity measuring procedure for low porosity rocks; in Current Research, Part E; Geological Survey of Canada, Paper 91-1E, p. 291 -297.
1994: Physical properties of Canadian kimberlites; Somerset Island and Saskatchewan; in Current Research, 1994-B, Geological Survey of Canada, p. 35-42.

Katsube, T.J. and Walsh, J.B.
1987: Effective aperture for fluid flow in microcracks; International Journal of Rock Mechanics and Mining Sciences and Geomechanics Abstracts, v. 24, p. 175-183.

Katsube, T.J., Best, M.E., and Mudford, B.S.
1991: Petrophysical characteristics of shales from the Scotian Shelf; Geophysics, v. 56, p. 1681-1689.

Katsube, T.J., Scromeda, N., and Williamson, M.
1992a: Effective porosity of tight shales from the Venture Gas Field, offshore Nova Scotia; in Current Research, Part D; Geological Survey of Canada, Paper 92-1D, p. 111-119.

Katsube, T.J., Scromeda, N., Mareschal, M., and Bailey, R.C.
1992b: Electrical resistivity and porosity of crystalline rock samples from the Kapuskasing Structural Zone, Ontario; in Current Research, Part E; Geological Survey of Canada, Paper 92-1E, p. 225-236.

Keller, G.V.
1966: Electrical properties of rocks and minerals; in Handbook of Physical Constants, (ed.) S.P. Clark, Jr.; Geological Society of America, Memoir 97, p. 553-577.

Scromeda, N. and Katsube, T.J.
1994: Effect of temperature on drying procedures used in porosity measurements of tight rocks; in Current Research 1994-E, Geological Survey of Canada, p. 283-289.

Geological Survey of Canada Project 870057

Surficial geology and sedimentary processes, Skeena River delta, British Columbia

K.W. Conway, B.D. Bornhold, and J.V. Barrie
GSC Pacific, Sidney

Conway, K.W., Bornhold, B.D., and Barrie, J.V., 1996: Surficial geology and sedimentary processes, Skeena River delta, British Columbia; in Current Research 1996-E; Geological Survey of Canada, p. 23-32.

Abstract: The delta of the Skeena River has developed within a constricted, subdivided coastal setting strongly influenced by tides. The delta progrades into deep water at several discrete depocentres, separated by islands and shoals. Delivery of sand to the delta front by tractive transport as bedload occurs to the north and south of Kennedy Island. Sediment moving as intertidal sand ridges and subtidal dunes is transported from river mouth bars to tidal flats and channels, and to the delta front proper. Slope failure of sediments from the delta front onto and down the delta slope has resulted in the development of a 30-40 m thick, stacked sequence of channelized failure deposits. Interstitial gas is ubiquitous in both muddy prodelta and delta sediments and pockmarks are found in the southern part of the study area.

Résumé : Le delta de la rivière Skeena s'est formé dans un milieu littoral restreint fortement modifié par les marées. En eaux profondes, le delta présente plusieurs dépocentres distincts, séparés par des îles et des récifs. Au nord et au sud de l'île Kennedy, le sable est transporté par traction sous forme de charge de fond vers le front du delta. Des barres de l'embouchure jusqu'aux estrans et aux chenaux, et par la suite jusqu'au front deltaïque proprement dit, les sédiments se déplacent sous forme de crêtes de sable intertidales et de dunes infratidales. La rupture de pente du front deltaïque a donné lieu au transport de sédiments jusqu'au bas de sa pente et a créé un empilement de matériaux chenalisés de 30 à 40 m d'épaisseur. Le gaz interstitiel est omniprésent dans les sédiments boueux tant prodeltaïques que deltaïques; il est à l'origine de dépressions à la surface des sédiments dans la partie méridionale de la zone à l'étude.

INTRODUCTION

The Skeena River, draining an area of 52 000 km^2, is the second largest river, in terms of discharge, to debouch into the Pacific Ocean along the British Columbia coast (Fig. 1). The bed of the Skeena, near its mouth, occupies the floor of a steep walled fiord valley which was a major conduit for ice flowing out of the Coast Range during the last (Fraser) glaciation (Clague, 1984). The modern soils near the mouth of the river are underlain by up to 40 m of glaciomarine mud, the river valley having been inundated by the sea at the end of the last glaciation between 10.9 and 10 ka BP.

The delta of the Skeena is unique in that the basin receiving the sediment load is a complex of islands and channels (Fig. 1). The delta is essentially "wrapped around" several islands, Kennedy, Smith, Marrack and De Horesy, adjacent to the mainland (Hoos, 1975).

The river was a transportation corridor between 1891 and 1912 with riverboats travelling as far as 210 km upstream, despite shifting gravel and sandbars and several canyons (Large, 1981). The Port of Prince Rupert at the northern edge of the Skeena estuary is an important maritime shipping hub and railway terminus. The Skeena River is the largest producing salmon river after the Fraser River, in British Columbia and its estuary is an important habitat for young salmon as well as other species.

Luternauer (1976, 1984) examined the surficial geology of the Skeena Delta using grab sampling, gravity coring, and airgun seismic profiling. Technological improvements in underwater acoustic geophysical systems, especially high resolution seismic profiling instruments, allow more detailed inferences about processes and seafloor dynamics at the delta front to be made. In August 1994, the *CSS Vector* surveyed the offshore portions of the Skeena Delta to examine the processes of sedimentation along the delta front. Since a great deal more is known about the Fraser River deltaic system than about the Skeena, the Fraser River is used as a point of comparison in several instances.

HYDROLOGY AND OCEANOGRAPHY

Flow rates in the Skeena 105 km upstream of the rivermouth vary from 300 to 500 $m^3 \cdot s^{-1}$ during low runoff stage in winter, to a high of 4200 $m^3 \cdot s^{-1}$ during the freshet. This compares to the Fraser River about 1000 $m^3 \cdot s^{-1}$ at a low in March to over 11 000 $m^3 \cdot s^{-1}$ in the mid-June to July freshet (Thomson, 1981). The Skeena River occupies the floor of a steep sided fiord valley and has developed a series of established bars in the lower portion of the watershed. The outflow is divided through three passages, with roughly 25% flowing through Inverness Passage and the remainder divided equally between Telegraph and Marcus passages (Hoos, 1975). The tidal range is more than 7 m, and generates significant currents and eddies in the passages and channels. Tidal currents measured in the Telegraph and Marcus passages are up to 200 $cm \cdot s^{-1}$ (4 knots) on the ebb when the river effluent combines with the tide to produce slightly stronger currents than are measured at the flood (Hoos, 1975; Ages, 1995).

METHODS

The surficial marine geology and seafloor morphology were mapped from 215 line km of sidescan sonar (330 and 120 kHz frequencies) and high resolution seismic data collected in August 1994 from the *CSS Vector* (Conway et al., 1996) with a nominal line spacing of 150 m (Fig. 2a, b). Cores were collected using a 1000 kg Benthos piston coring system, then split, photographed, and described prior to subsampling for grain size and other analyses. A settling tube and a Sedigraph were used to analyze the sand and mud fractions. Radiocarbon dating of selected wood samples from cores was done at the IsoTrace Laboratory, University of Toronto.

RESULTS AND DISCUSSION

Sedimentary processes

Sand is transported towards the delta front as bedload. Evidence for this includes small to medium dunes visible on sidescan sonargraphs as well as large sand ridges, visible on aerial photographs, forming the surface of part of the "Base Sand", the tidal bank on the north side of Kennedy Island. Luternauer (1976) noted areas of megaripples (medium dunes) at the perimeter of Marcus Passage. The river mouth and delta platform form a discontinous set of sand and gravel bars with intervening channels for a distance of 15 to 20 km from Mowitch Point to the delta front (Luternauer, 1976; Bornhold, 1978). The margins of the channels are floored by organic-rich muddy sediments (Luternauer, 1976).

In other British Columbia estuaries such as the Fraser River (Hart, 1995), and Campbell River (Hoos, 1975) a salt wedge moves up the river with flood tides. The salt water, being more dense than the fresh displaces the river water on the floor of the river, especially during low discharge periods. The salt wedge has significant implications for sedimentary processes in that bedload transport of sediments can only continue downstream to the limit of intrusion of the salt wedge (Hart, 1995). In the Skeena River no salt wedge forms within the river (Ages, 1995) probably due to turbulent flow across the irregular shallow bottom which results in a well mixed water column. There is some evidence of stratification occurring during periods of high runoff and low tidal range, however (Hoos, 1975).

Two areas of mass wasting on the delta front have been identified to the north and south of Kennedy Island (Fig. 2a, b). The stacked failures, up to 40 m thick, form lense-shaped accumulations that have been channelized as turbidity currents flow down the surface of the deposit. Areas of the failure unit on the lower delta front (below 70 m), appear to be draped with mud deposited from suspension (Fig. 3). One core (VEC94A020) sampled part of the failure

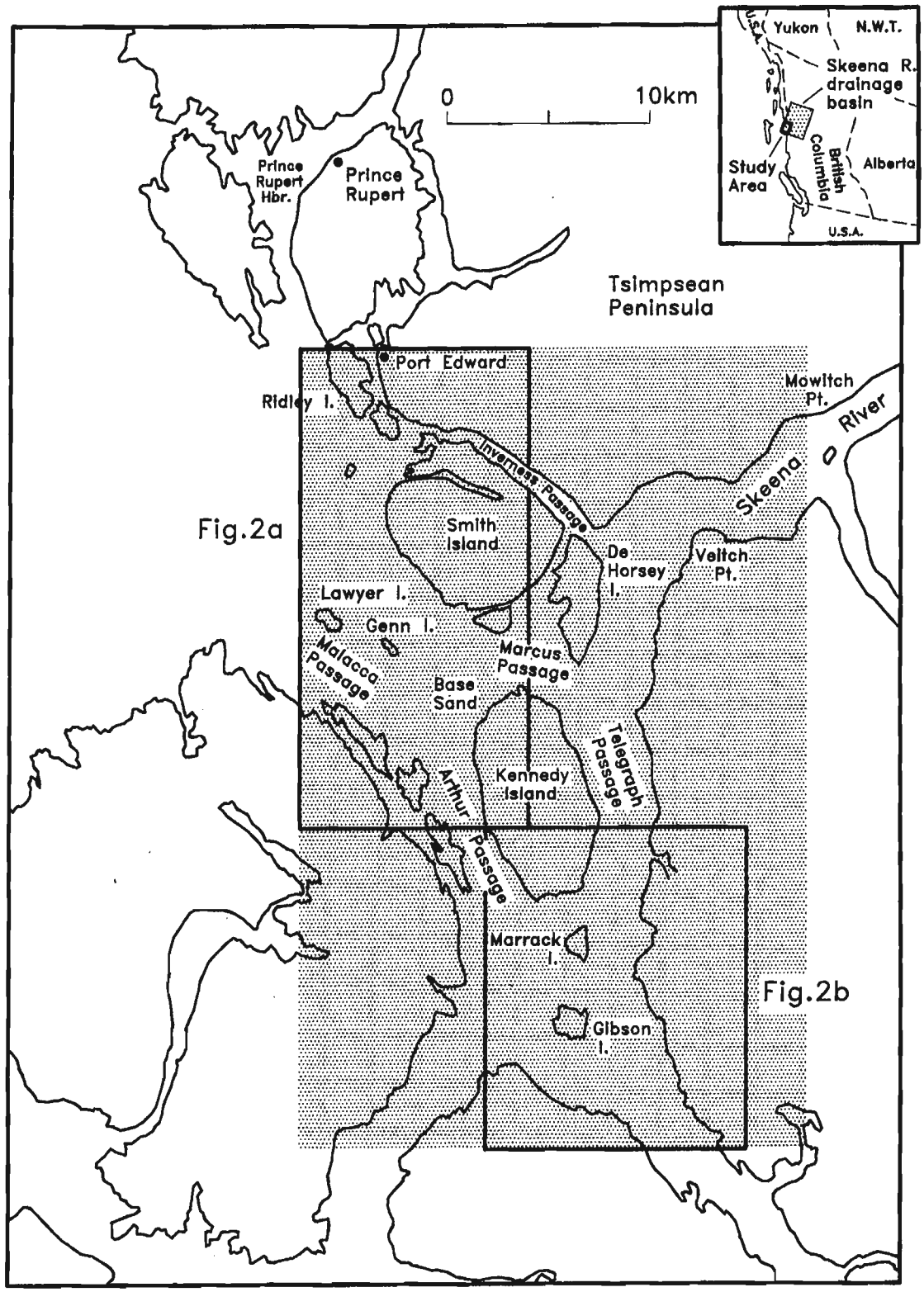

Figure 1. *Location of the Skeena River delta study area. Drainage area of the Skeena is indicated by shaded box on the inset map (from Hoos, 1975).*

a

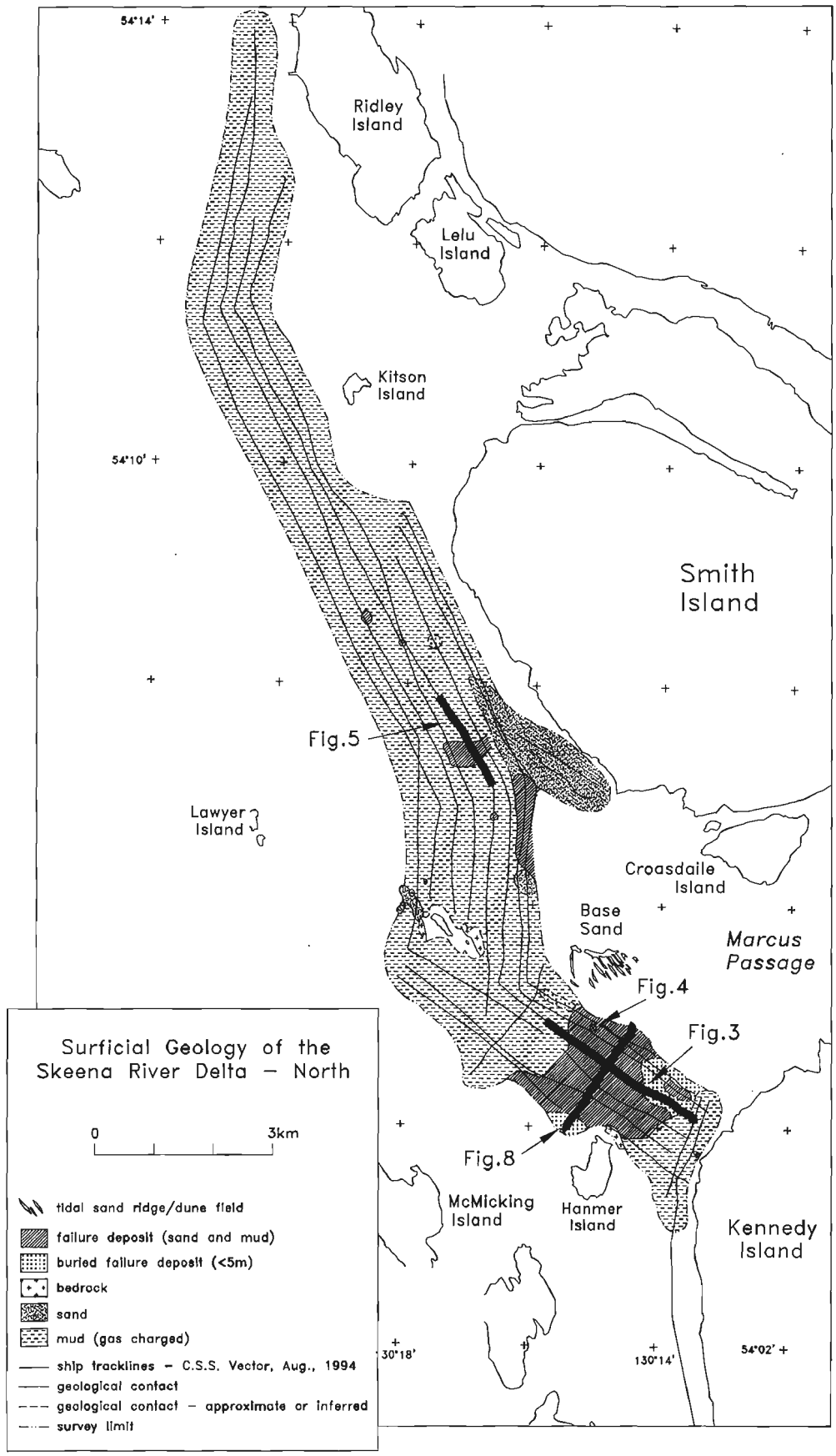

Figure 2a and 2b. *North and south portions of the Skeena Delta showing the distribution of sediments and morphological features on the Skeena River delta. Debris flow deposits have accumulated predominately north and south of Kennedy Island.*

b

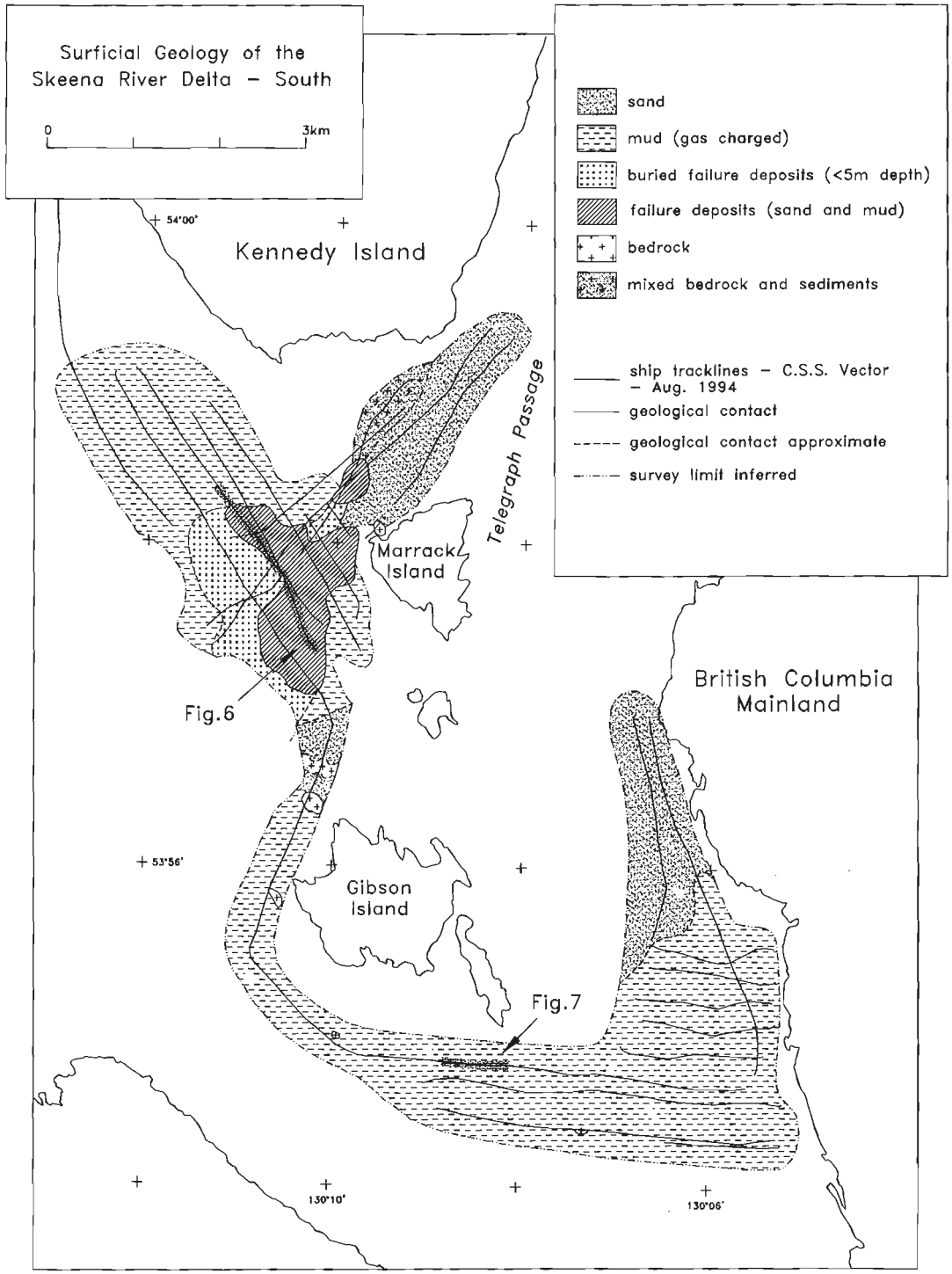
Surficial Geology of the
Skeena River Delta – South
0
3km
sand
mud (gas charged)
buried failure deposits (<5m depth)
failure deposits (sand and mud)
bedrock
mixed bedrock and sediments
ship tracklines – C.S.S. Vector – Aug. 1994
geological contact
geological contact approximate
survey limit inferred
54°00'
Kennedy Island
Telegraph Passage
Marrack Island
British Columbia Mainland
Fig.6
53°56'
Gibson Island
Fig.7
130°10'
130°06'

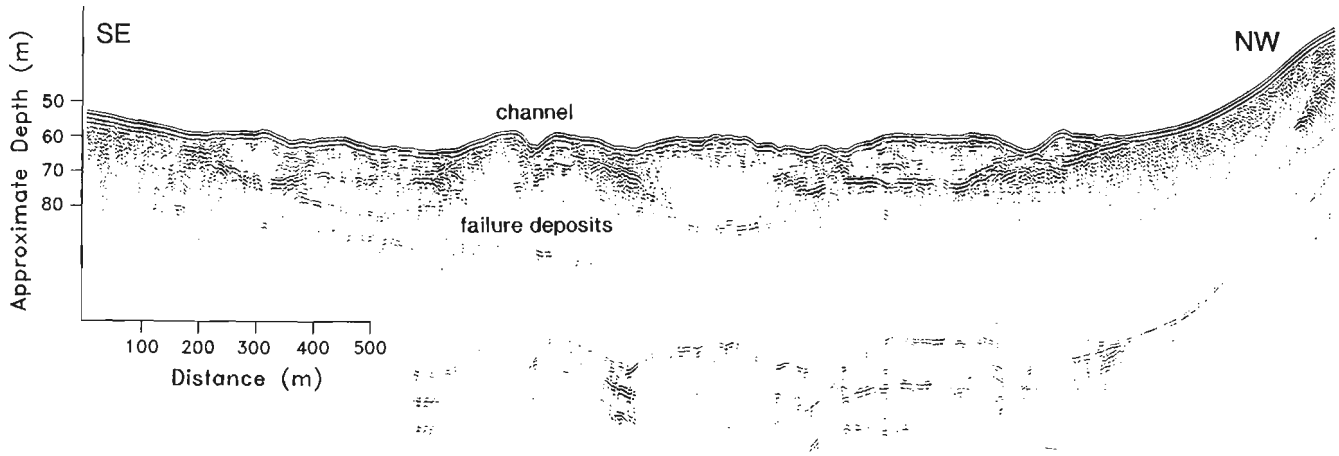

Figure 3. The discontinuous failure deposits can be seen in this seismic profile. They are more than 30 m thick in this area (Fig. 2a shows profile location).

sequence (Fig. 4) and shows a massive sand interbedded with bioturbated mud. The sand units are deposited as mass flow events from the delta slope and the bioturbated muds indicate ongoing sedimentation occurs on the delta front between events. The thickest sand bed is 85 cm thick, while the maximum thickness of failure units seen in the stacked failure sequence is about 5 m. Abundant wood debris and terrestrial organic matter, contribute to the gassy nature of the sediments on the prodelta. Bioturbation and contained molluscan macrofauna indicate that deposition is slow enough, between debris flow and turbidity current events for infauna to survive. The radiocarbon ages on contained wood material indicate that failures on the delta front occur frequently. The inverted radiocarbon chronology (dates are younger downcore) suggest that material from the delta front may be failing in a retrogressive fashion, burying younger deposits with older. West of Smith Island some limited areas of both buried and surficial debris flow deposits are seen (Fig. 2a) indicating that failure of the Smith Island portion of the delta front was ongoing in the recent past and that these failure sediments have been buried by suspension deposits.

Fine-grained sedimentation occurs over a wide area as a buoyant plume, visible on air photos, disperses the suspended fine fraction over the several basins, passages, and tidal flats in the vicinity of the river mouth. Interstitial, biogenic gas is abundant within these muddy sediments (Fig. 5). The delta system is atypical of most deltas in that the development of the "normal" delta shape and sequence of foreset and topset beds are greatly constrained by the shoals, channels, and islands in the path of the expanding delta. The delta front extends about 12 km south and about 18 km to the north of Kennedy Island. The delta appears to have partially incorporated the Gen Islands (Fig. 2) offshore of the "Base Sand", where a series of flat-topped mounds occur, roughly connecting the base sand platform to the island. The sediments capping the broad mounds are gassy and the mounds are divided by channels. The surficial sediments probably mantle bedrock protrusions, on strike with the Gen and Lawyer islands.

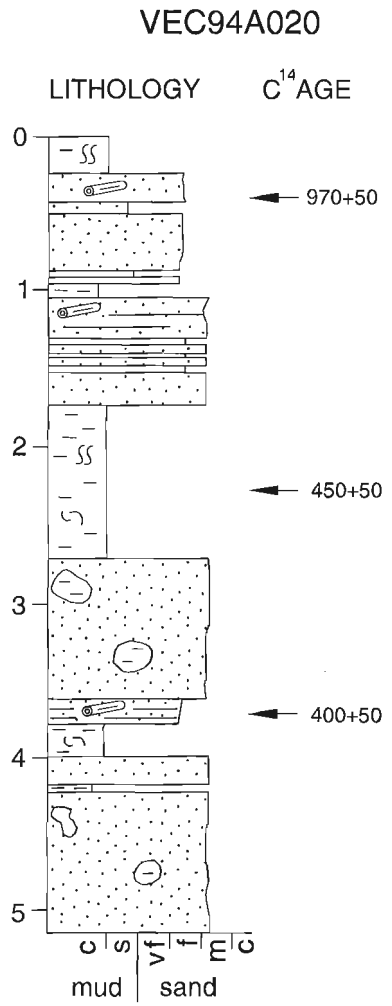

Figure 4. Core Vec94A020 shows interbedding of massive sand units and bioturbated muds. The radiocarbon chronology indicates a rapid rate of deposition (1 cm·a^{-1}). The thick sand beds represent failure deposits while the muds represent relatively quiescent periods between failures.

Channels

Channels are found both north and south of Kennedy Island. Those north of Kennedy, offshore of the "Base Sand", appear to be buried in places and are thus discontinuous features. These channels are up to about 8 m deep starting at the break in slope and continuing down to the 65 m water depth. Levees, or spill-over lobes of turbidity currents, are observed in some sections of the channel.

The channel seen in the southern portion of the delta front adjacent to Marrack Island (Fig. 6) is continuous for about 1 km and is up to 11 m deep. The channel has developed as a conduit for debris flows and turbidity currents derived from upslope failures. Levees, or spill-over lobes of turbidity currents, are present, as in the northern example. The source of material for the progradation of the delta front is the bedload carried from the river mouth to the top of the delta slope by ebb tidal currents. A trough is apparent where the failure unit begins between Kennedy and Marrack islands, suggesting mass wasting processes affect the morphology of the delta break in slope at this site. Luternauer (1984) noted the sandy nature of surficial sediments farther offshore in this area indicating that delivery of sediments to the seafloor is by mass wasting events and possibly turbidity currents.

Many deltas undergo avulsion, or channel switching as one route to the ocean in time becomes less efficient than others (Hart, 1995). In the case of the Skeena River, channel switching and other fluvial processes are not observed or are complicated by the basin geometry to the extent that these processes are not recognizable. One area of buried channels, possibly reflecting avulsion events occurs north of the "Base Sand" adjacent to Smith Island (Fig. 2). The buried and small surficial failure deposits in the same area may also be an indication of a former position of delta front progradation.

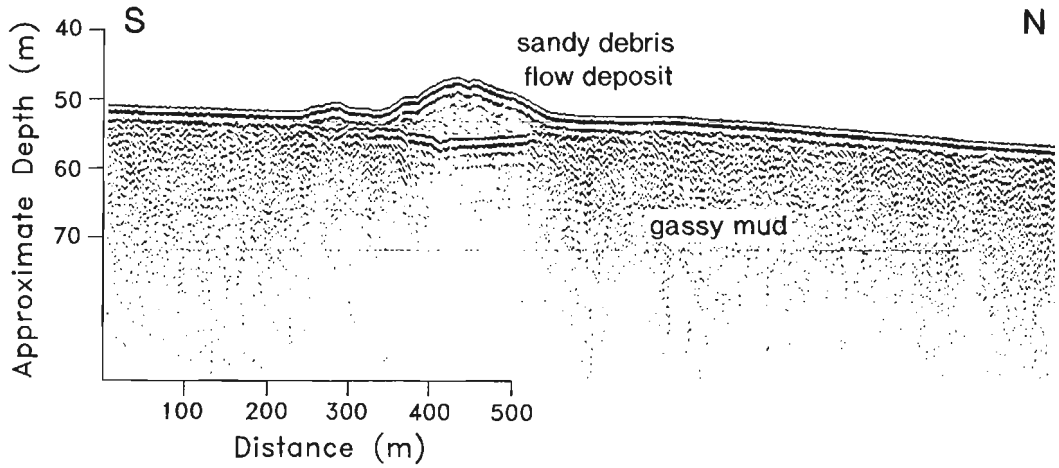

Figure 5. *A 9 m thick debris flow deposit, the result of a single event, rests on the otherwise undisturbed gassy delta sediments.*

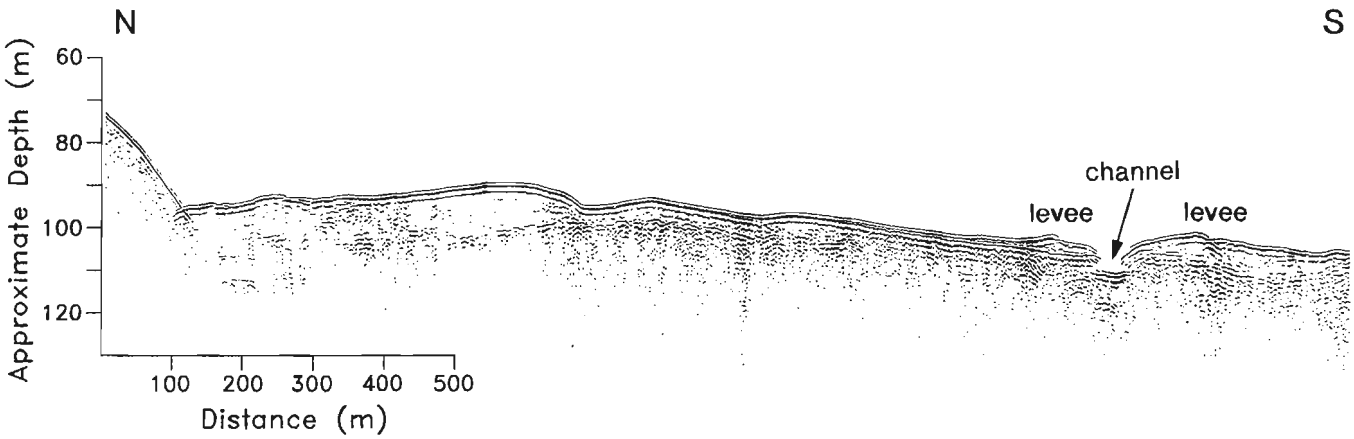

Figure 6. *A channel up to 11 m deep, with adjacent levees has developed near Marrack Island. Delivery of sediment to the upper end of the channel is facilitated by ebb tidal currrents moving sand as bedload to the top of the slope.*

Shallow Gas

Shallow gas obscurs the seismic data collected in areas of mud accumulation; penetration is normally less than 10 m, and commonly only 1-2 m. Where sediments are predominatly sand, more acoustic penetration is achieved. Figure 5, a sandy failure superimposed on muddy, gassy prodelta sediments, illustrates the difference in the acoustic properties of the two dominant lithologies.

Pockmarks occur in the southernmost part of the study area (Fig. 7). These features, which are up to 25 m wide and 1-3 m deep, are caused by shallow gas venting at the seafloor. Bornhold (1978) noted that the terrestrial organic matter content of Skeena delta sediments was high relative to many other British Columbia shelf and nearshore sediments. Incomplete biological oxidation of this organic matter is the likley source of the gas in the surficial sediments.

Delta front processes – comparison to Fraser River delta

The Fraser River delta has been the subject of intensive study by the Geological Survey of Canada over the past 6 years (e.g. Hart et al., 1992). Natural fluvial and deltaic developments have been significantly impacted by human activities; the river formerly underwent significant episodes of channel switching (Clague et al., 1983) prior to construction of a training wall to fix the main arm of the Fraser in place. In addition, considerable dredging of river sand for navigational purposes as well as for construction material is carried out. The fixed arm of the river now ensures a large proportion of the bedload bypasses the delta slope by delivering sand directly to the basin floor through a well developed submarine channel system (Hart et al., 1992).

Acoustic data indicate that large areas of the Fraser delta slope are underlain by failure deposits, especially the Roberts Bank area, an important coal, ferry and container port (Hart et al., 1992; Hart and Olynyk, unpublished report, 1994). This

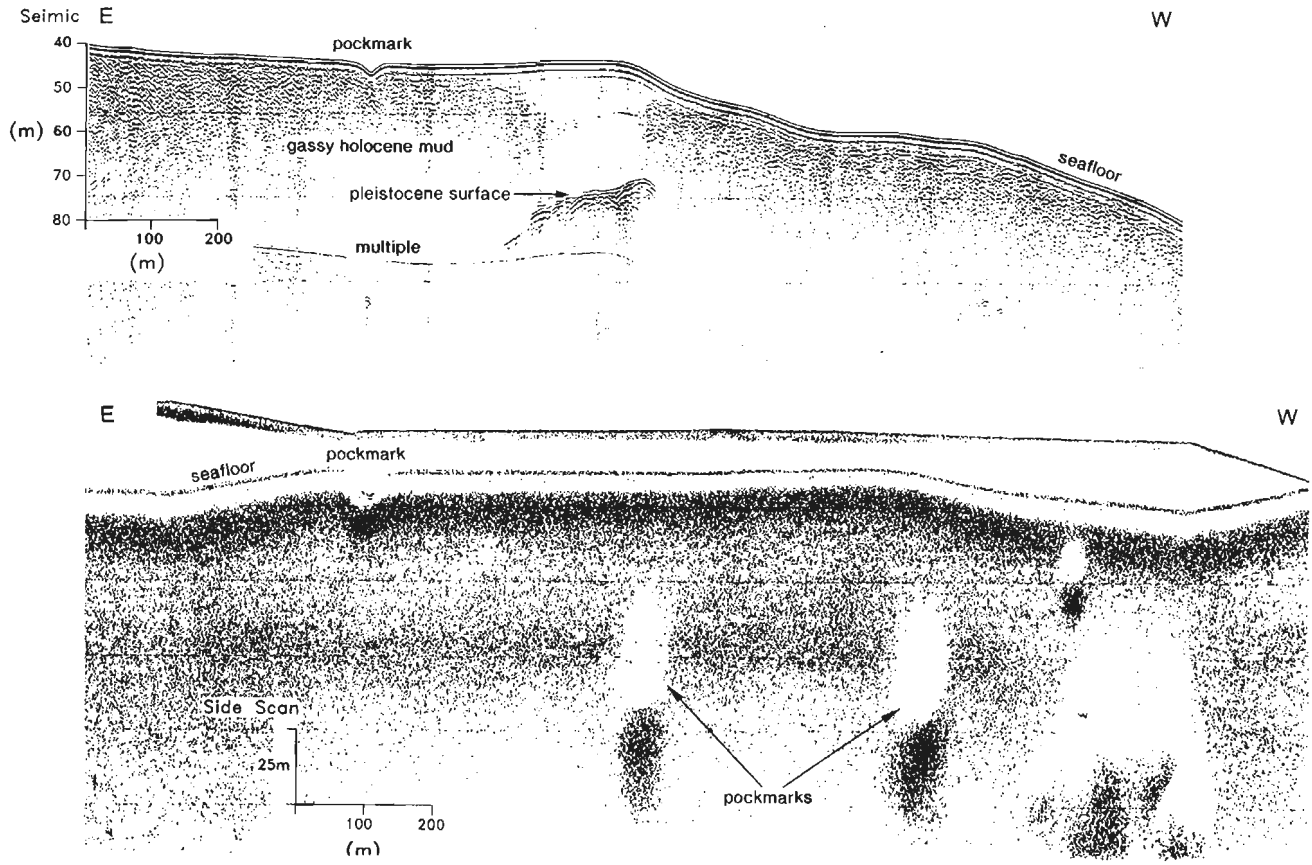

Figure 7. *Pock marks, gas escape features, are found in the southern part of the study area in the prodelta mud. Shown is a seismic profile crossing one pockmark and the starboard channel of the corresponding sonograph which crosses the same pockmark and shows about 10 others.*

failure unit forms a wedge-shaped deposit extending to about the 180 m isobath. Concern has been raised whether this unit is evidence of a serious, ongoing landslide hazard to existing and planned installations at the Roberts Bank port site or normal river mouth sediments deposited when the main channel entered the sea at Roberts Bank.

The acoustic signature of slide debris underlying the channelized surficial deposits north and south of Kennedy Island are very similar to those imaged at Roberts Bank (Fig. 8). The seismic and core data suggest that the deposits on the Skeena Delta slope are the result of ongoing fluvial discharge both north and south of Kennedy Island and periodic failure of portions of the delta front. The failures relate to the present position of accumulation of sediments on the delta front and do not appear to represent a single massive event. Core VEC94A020 indicates ongoing fine-grained sedimentation between episodes of mass wasting of the delta front.

CONCLUSIONS

1. Debris flow deposits have accumulated on the Skeena River delta front at loci of rapid sedimentation associated with progradation of the delta front. The composite thickness of failure deposits is up to 40 m. Channels, up to 11 m deep, are associated with the stacked debris flow sequence and levees occur along some channel segments.
2. Surficial sediments contain gas in sufficient quantity to obscure seismic records in muddy sediments of the delta and to have generated pockmarks in the southern part of the prodelta.
3. Tractive transport of bedload in the main channels of the river results in delivery of coarse grained materials to the delta front. Bedforms including dunes and sand ridges occur.
4. Radiocarbon dating of wood material indicates a sedimentation rate of about 1 cm per annum, in one area of debris flow activity.

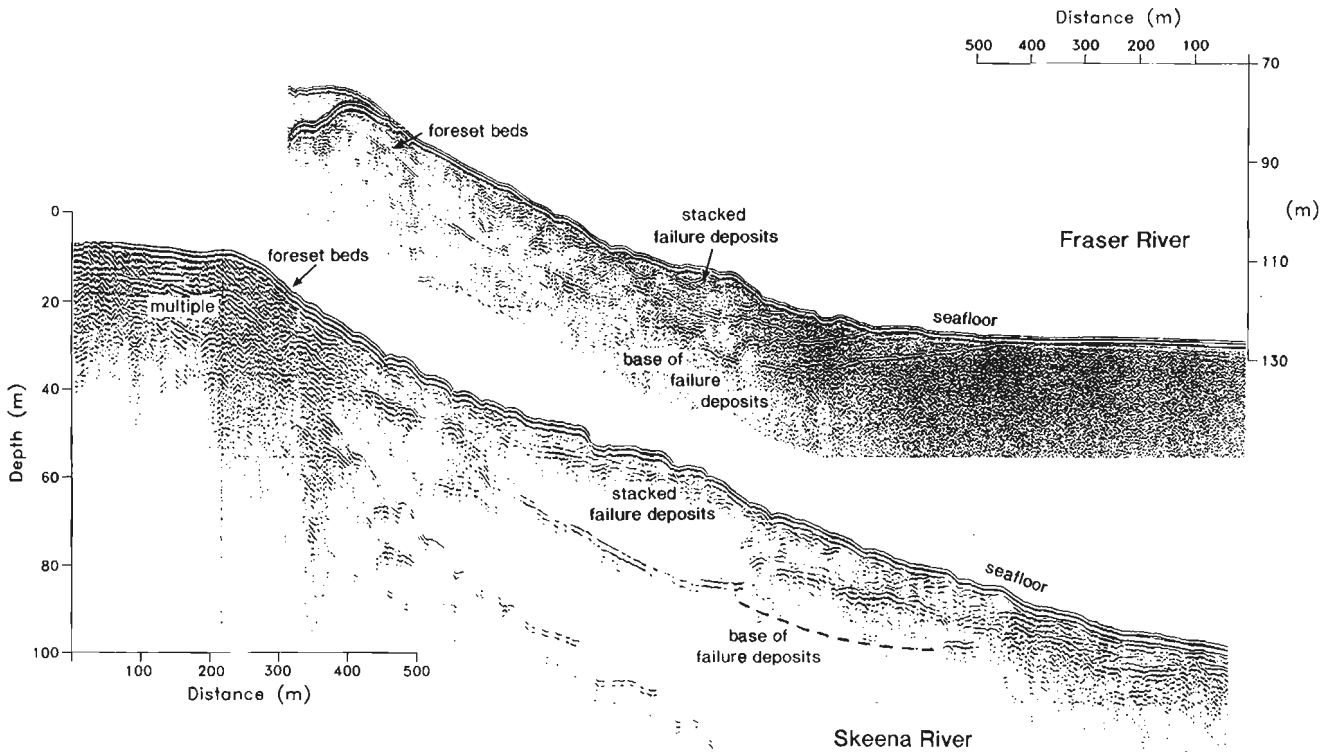

Figure 8. *Shore-normal seismic section showing the wedge-shaped complex of failure deposits accumulating on the delta slope. At the top of the slope what appear to be topset and prograding foreset beds give way to the discontinuous failure deposits on the delta slope (see Fig. 2 for location). The Huntec sparker record on Fraser Delta at Roberts Bank displays a similar wedge-shaped accumulation of failed material on the delta slope.*

ACKNOWLEDGMENTS

Thanks are due Ivan Frydecky, Tsumoru Sagayama, and Jan Schuh, and the officers and crew of the *CSS Vector* for assistance with data collection. Kudos to Richard Franklin and Brian Sawyer for careful preparation of the figures. Dave Mosher kindly offered the seismic section of Roberts Bank and Ralph Currie provided a very helpful review of an earlier version of this paper.

REFERENCES

Ages, A.B.
1995: The salinity intrusion in the Skeena River: observations of salinities, temperatures and currents 1979, 1984; Canadian Data Report of Hydrography and Ocean Sciences, no. 138, 28 p.

Bornhold, B.D.
1978: Carbon/nitrogen (C/N) ratios in surficial marine sediments of British Columbia; in Current Research, Part C; Geological Survey of Canada, Paper 78-1C, p. 108-112.

Clague, J.J.
1984: Quaternary Geology and Geomorphology, Smithers-Terrace-Prince Rupert area, British Columbia; Geological Survey of Canada, Memoir 413, 71 p.

Clague, J.J., Luternauer,J.L., and Hebda, R.J.
1983: Sedimentary environments and postglacial history of the Fraser River and lower Fraser valley, British Columbia; Canadian Journal of Earth Sciences, v. 20, p. 1314-1320.

Conway, K.W., Bornhold, B.D., and Barrie, J.V.
1996: Surficial geology of the Skeena River delta; Geological Survey of Canada Open File 3307.

Hart, B.S.
1995: Delta front estuaries; in Geomorphology and Sedimentology of Estuaries; Developments in Sedimentology, v. 53, p. 207-226.

Hart, B.S., Prior, D.B., Barrie, J.V., Currie, R.G., and Luternauer, J.L.
1992: A river mouth submarine channel and failure complex, Fraser delta, Canada, Sedimentary Geology, v. 81, p. 73-87.

Hoos, L.M.
1975: The Skeena River estuary - status of environmental knowledge to 1975; Environment Canada, Special Estuary Series, no. 3, 418 p.

Large, R.G.
1981: The Skeena, River of Destiny; Gray's Publishing, Sidney, British Columbia.

Luternauer, J.L.
1976: Skeena Delta sedimentation, British Columbia; in Report of Activities, Part A; Geological Survey of Canada, Paper 76-1A, p. 239-242.
1984: Skeena, Nanaimo and Cowichan River deltas and offshore environs, British Columbia; Geological Survey of Canada, Open File 1112.

Thomson, R.E.
1981: Oceanography of the British Columbia Coast; Canadian Special Publication of Fisheries and Aquatic Sciences, no. 56, 291 p.

Geological Survey of Canada Project 940005

Swath bathymetric surveys in the Strait of Georgia, British Columbia

Ralph G. Currie and David C. Mosher
GSC Pacific, Sidney

Currie, R.G. and Mosher, D.C., 1996: Swath bathymetric surveys in the Strait of Georgia, British Columbia; in Current Research 1996-E; Geological Survey of Canada, p. 33-40.

Abstract: During October and November, 1994, a joint venture between three federal departments and private industry conducted swath bathymetric surveys over selected areas in the Strait of Georgia. This project was the first time this technology had been employed on the west coast of Canada. Approximately 240 km^2 of data were collected over five areas. Most areas surveyed were known from previous geophysical and geological investigations to contain significant evidence of sediment mass failures and other complex sedimentological features. Three of these areas (Malaspina Strait, Sabine Channel, and southern Roberts Bank) are important electrical transmission cable corridors, through which power is brought to Vancouver Island from the mainland. Seafloor images based on swath bathymetric data provide an invaluable asset for geological interpretation, as well as providing accurate and detailed slope angle and other morphological information for geotechnical assessments.

Résumé : En octobre et en novembre 1994, une entreprise réunissant trois ministères fédéraux et l'industrie privée a permis de réaliser des levés bathymétriques par secteurs dans des régions choisies du détroit de Géorgie. C'était la première fois que cette technologie était utilisée sur la côte ouest du pays. Les données recueillies proviennent de cinq régions couvrant une superficie de 240 kilomètres carrés. Des études géophysiques et géologiques antérieures avaient révélé que toutes ces régions présentaient des indices significatifs de ruptures de masse de sédiments et d'autres structures sédimentaires complexes. Trois de ces régions (détroit de Malaspina, chenal Sabine et partie sud du banc Roberts) sont d'importants corridors empruntés pour le passage de câbles de transport d'hydro-électricité entre le continent et l'île de Vancouver. Une réduction appropriée des données et les images produites à partir des résultats des levés bathymétriques par secteurs constituent un atout inestimable pour l'interprétation géologique, en plus de fournir des informations exactes et détaillées sur l'angle des talus et d'autres caractéristiques morphologiques qui servent aux évaluations géotechniques.

INTRODUCTION

Multibeam swath bathymetric data sets produce high-resolution images of the morphology of the seafloor. This new perspective is proving valuable to hydrographers, engineers and geologists, providing both quantitative and qualitative information about the surface of the ocean floor. Over the past few years several surveys have taken place off the east coast of Canada but because a system with swath capabilities has not been available on the West Coast, surveys in this region have been delayed. A cooperative program between several organizations was therefore developed to offset the costs of mobilization and to bring this technology to the West Coast.

During October and November, 1994 a joint venture between the Canadian Hydrographic Service (CHS) – Pacific, the Department of Fisheries and Oceans, acting on behalf of the National Action Committee on Ocean Mapping (NACOM), Natural Resources Canada (GSC Pacific, Sidney), the Department of National Defence (Maritime Forces Pacific – Plans and Operations) in co-operation with Terra Surveys Ltd. and Geo-Resources Inc. conducted swath bathymetric surveys over selected areas of interest in the Strait of Georgia. Five areas were surveyed: (1) Whiskey Foxtrot, a naval testing area off Nanoose Bay; (2) Sabine Channel and (3) Malaspina Strait, both part of an electrical transmission cable corridor between Vancouver Island and the mainland; (4) Sand Heads, at the mouth of the Fraser River, and the Foreslope Hills, a region of complex hill and trough topography of unknown origin; and (5) southern Roberts Bank, the second electrical transmission cable corridor providing power to Vancouver Island and site of the Roberts Bank failure complex.

DATA ACQUISITION

Geo-Resources Inc., the prime contractor for this survey, operated a SIMRAD EM100 multibeam sounder mounted in a 'DOLPHIN'. The SIMRAD EM100 system is a 95 kHz, 32-beam sounder with a beam size of 2.5° by 3.0°. These angles translate to a swath width of 0.7 to 2.4 times water depth, depending upon the mode chosen. The minimum useful depth is approximately 10 m with a maximum depth of 600-700 m depending upon bottom type. The ping rate is depth dependent with a maximum of 4 kHz.

DOLPHIN (Deep Ocean Logging Platform with Hydrographic Instrumentation and Navigation) is a semi-submersible, torpedo-shaped remotely operated vehicle approximately 8 m long and 1 m in diameter. In addition to the sounder, it carries a Magnavox 4200D differential GPS receiver, a Robertson RG3 gyro, a TSS335B motion sensor and appropriate electronics to provide data transmission to and from the mother vessel (*CSS Revisor*). This data link allows survey results and systems on DOLPHIN to be monitored on the *Revisor* as well as operator intervention in cases were there are problems with the semi-autonomous line keeping.

Navigation data were recorded in real time as differential GPS (DGPS). Differential corrections were provided from the marine radio beacon at Point Atkinson for all areas surveyed except Malaspina Strait. A temporary differential reference was set up over a CHS survey monument on McRae Islet for the Malaspina survey.

The entire system generates between 0.7-2.0 Mbytes of digital data per hour of survey, depending on water depth. As water depth increases, firing rate is reduced and the number of active channels is reduced to those with narrower beam angles. In this survey, 100 Mbytes of digital data were collected.

Depth soundings are recorded as traveltime, i.e. the time it takes for sound to travel from the transducer to the seafloor and return. To convert traveltime to depth in some length scale, it is necessary to know the velocity with which sound travels in the water column. Sound velocity is largely a function of salinity and temperature of the water, properties which may change with depth, depending on the structure of the water column. Sound velocity profiles were obtained in all survey areas as part of the survey procedure. Sound velocity profiles cast were performed daily as part of the Roberts Bank survey due to its proximity to the Fraser River. These sound velocity profile data were used by the SIMRAD EM100 to create a look-up table which allowed the system to convert beam angle and travel time to depth and crosstrack distance. Other errors, such as heave, roll and pitch were compensated for in real-time.

Post-processing involved tidal correction and review of all navigation and sounding data to ensure accuracy and consistency within the data, and verification that the data met hydrographic standards. For the most part, post-processing was conducted by Geo-Resources Inc. Processing was conducted in the Hydrographic Information Processing System (HIPS) environment, a suite of specialized programs running in a Unix environment developed by Universal Systems Ltd.

The Hydrographic Information Processing System includes an extensive collection of programs to both automatically and interactively 'clean' the logged data, both navigation and depth, and apply tidal corrections. This system also calculates the final position and depth for all soundings based on inputs such as observed depth, navigation, vessel dynamics such as gyro, heave, pitch and roll and tide. This merge takes place after all inputs have been reviewed and edited.

Tidal corrections were provided from a gauge at CFMETR in Nanoose Bay for the Whiskey Foxtrot area. At all other sites, corrections were provided from temporary installations of low power tide gauges (LPTG) in each region during the survey period. Zero offset corrections for the low power tide gauges were made in Sabine Channel with the False Bay gauge, in the Malaspina Strait area with local shorebased benchmarks, and in the southern Strait of Georgia with a permanent installation at Point Atkinson.

Final data processing was conducted with in-house developed software and with geographic information system (GIS) software GRASS (Geographic Resource Analysis and Support System), designed and developed by researchers in the US Army Construction Engineering Research Laboratory. The x-y-z data generated by the Hydrographic Information

Processing System were downloaded onto a Unix workstation and converted to a 10 x 10 m grid to produce a regular lattice. All subsequent operations were performed on this regular lattice. Within a GIS, a number of options are available to map and display data, including depth or bathymetric contouring, slope angles, hydrologic flow trajectories (flowlines), and oblique illumination. All figures of the data shown in this paper are oblique illumination.

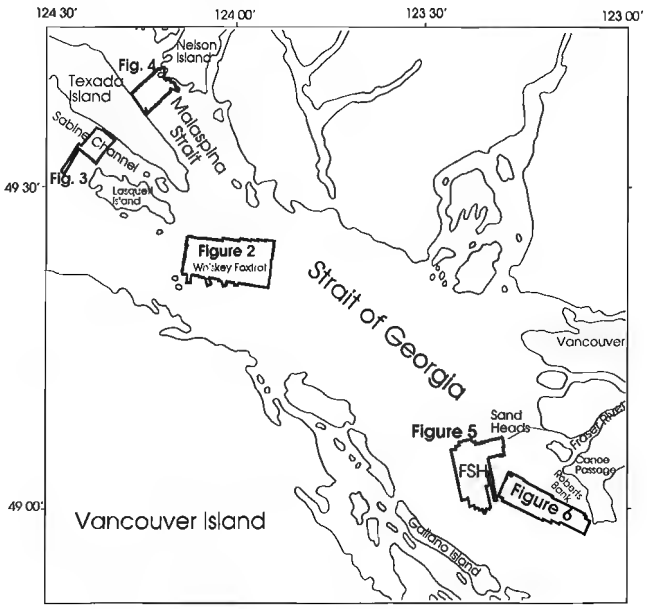

Figure 1. *Location diagram of the Strait of Georgia, showing the locations of the five swath bathymetric survey sites in bold outline. Locations of Figures 2 to 6 are shown. FSH stands for Foreslope Hills.*

Oblique Illumination, also known as analytic hillshading or shaded-relief imaging, assumes an illumination source at an infinite distance from the surface, positioned at a specified azimuth and altitude with respect to the surface. The resulting distribution of shade or reflectance values for the surface is then calculated. The value is determined by the local shape not the absolute depth. The images have few quantifiable uses, but are evocative for qualitative interpretation.

RESULTS AND PRELIMINARY INTERPRETATIONS

Whiskey Foxtrot

The Whiskey Foxtrot (WF) site lies in the southwest corner of the Whiskey Foxtrot military exercise area in the central Strait of Georgia (Fig. 1). The survey area covers about 117 km^2 and lies just northeast of Ballenas Islands. The site was chosen by the Department of National Defence. Little previous geological or geophysical information had been collected in the Whiskey Foxtrot survey area. Water depths range from 132 to 441 m, being deepest in the central area (the area with a smooth surface in Fig. 2), and shallowest to the south and in the extreme northeast corner.

Most obvious from the hillshaded image of bathymetry (Fig. 2) are the roughly east-west trending ridges. The image shows two ridge systems with a central deep channel between them. The largest ridge, which forms the southern half of the image, rises from about 400 m on its flanks to about 190 m at its crest. There appears to be a dramatic drop in elevation at the northern edge of this ridge where it drops suddenly to 400 m water depth. At each crest, smaller ridges or lineations appear, oriented in the same direction as the larger ridges.

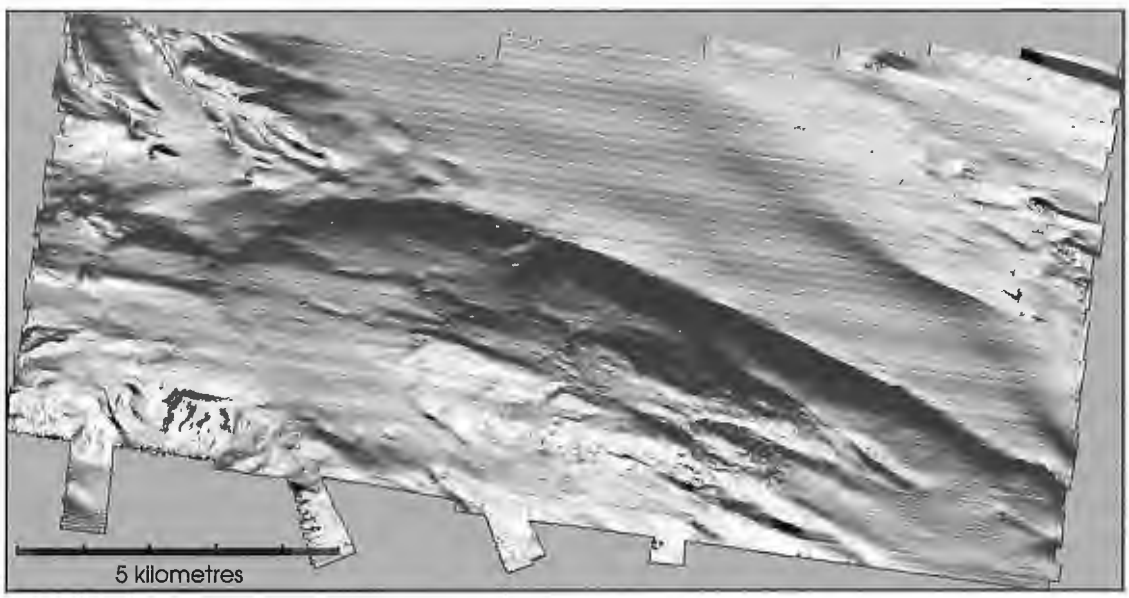

Figure 2. *Computer-generated oblique illumination or hillshaded image of swath bathymetric data from the Whisky Foxtrot area (see Fig. 1 for location). The top of the image is north. The angle of false-sun illumination (altitude) is 45° above horizontal and the azimuth is 180°.*

Without subbottom information or geological groundtruth it is impossible to confirm the interpretation of this morphology. Similar ridges are seen farther south within the Strait of Georgia, especially on the western side of the strait. These ridges are interpreted as reflecting basement topography, possibly thinly covered by post-glacial sediment derived from the Fraser River plume. The basement is likely Nanaimo Group Tertiary sedimentary rock which has been compressed north to south, yielding folds and thrust faults which strike roughly east to west (Hamilton, 1991). Some sedimentary features are likely overprinted on the general morphology, resulting from strong tidal currents in the region, and downslope sediment movement. Subbottom acoustic (seismic reflection) data are required to separate sedimentary from bedrock controlled features.

Sabine Channel

The Sabine Channel survey area represents a section of an electrical transmission cable corridor from the west side of Texada Island to Vancouver Island (Fig. 1). Five high-voltage transmission cables lie within this corridor. The survey area covers only the eastern portion of this corridor, on the west side of Texada Island to just north of Lasqueti Island. The site was chosen to map the distribution and morphology of sediment masses and topography and assess their potential impact on the power cables. Total survey area is about 21 km^2 and water depths in the area range from 6 to 360 m.

The hillshaded image of the swath bathymetry data (Fig. 3) shows a complex bottom morphology. The terrain is steep and rugged adjacent to Texada Island, largely reflecting basement topography. Bedrock outcrops are common, as observed during submersible operations conducted a number of years ago. There are a few gullies or valleys through this rough terrain. The central portion of Sabine Channel is the deepest in terms of water depth. It shows what is likely a thick sediment cover, producing a smooth seafloor. This sediment cover is probably derived from the Fraser River plume. The presence of what appear to be northwest-southeast trending seafloor lineations may be related to bedrock topography or may be erosional channels cut into the seafloor sediment, in which case bottom currents would be strong and active. The seafloor morphology becomes somewhat rugged again as the corridor crosses to the north of Lasqueti Island, reflecting the underlying basement topography and thinning sediment cover.

Malaspina Strait

The Malaspina Strait survey site represents the eastern part of the same electrical power transmission cable corridor that crosses Sabine Channel. The site runs from Nelson Island (Cape Cockburn) in the east, across Malaspina Strait to Texada Island in the west (Fig. 1). Total survey area is 40 km^2 and water depths range from 7 to 375 m, with the deepest portion in the central strait and rising to the southwest and northeast near the coastlines. The site was chosen in order to map the distribution and morphology of sediment masses and topography to assess their potential impact on the power cables.

Previous geophysical investigations in this area (Bornhold et al., unpublished report to BC Hydro, 1994) provide subbottom and sidescan sonar data to complement the swath bathymetry. The central part of Malaspina Strait is underlain by a thick sequence (up to 100 m) of sediment, mostly derived from the Fraser Delta plume. The high degree of acoustic transparency evident in high-resolution seismic profiles of these sediments suggests they are fine grained with a very high water content. The morphological expression of this sequence is flat and relatively featureless (Fig. 4). On both flanks, however, these sediments thin and the bottom morphology becomes far more complex. The seafloor of the eastern portion of the corridor, where the slope rises to Nelson Island, is rugged, largely controlled by bedrock. The seafloor of the western side, where the cables approach Texada Island, is not as rugged, but many channels and chutes crossing the slope are evident. These features are related to debris flow and turbidity current activity as unconsolidated sediment fails downslope. Seismic reflection and sidescan records from this area show debris lobes, chutes, flute marks, slide blocks and masses of unconsolidated sediment "perched" precariously on steep slopes (Bornhold et al., unpublished report to BC Hydro, 1994).

Sand Heads and Foreslope Hills

The Sand Heads and Foreslope Hills survey area encompasses about 60 km^2 of seafloor. The area was surveyed with two objectives: 1) to study the morphology of the sea valleys which cut into the foreslope of the Fraser Delta by sediment discharge from the main channel of the Fraser River, and 2) to visualize in detail the morphology of the Foreslope Hills, an anomalous set of hills and valleys in the south-central portion of the Strait of Georgia, the origins of which have yet to be convincingly explained. Water depths at this site range from 10 m to 317 m with depth increasing to the west.

Sand Heads is at the western terminus of the training wall which restrains the main channel of the Fraser River as it crosses the delta plain and intertidal zone to the break in slope. Eighty per cent of the sediment supplied to the delta flushes through Sand Heads within the main channel. Sand constitutes about 35% of the 17.3 million tonnes of sediment discharged annually. The hillshaded image of the Sand Heads area shows five channels or gullies coalescing into one main valley downslope (Fig. 5). This curvilinear feature is up to 60 m deep, 100 m wide and 6000 m long. There are several minor gullies adjacent to the upslope main gullies that appear subdued or faded in the image. This subdued character probably means they are relict, or at least inactive at present. Hart et al. (1992) identified basal debris flow deposits within the main valley. They deduced that debris flows, constrained by the valley walls, are the major mechanism by which bedload is able to bypass the foreslope and travel to the floor of the Strait of Georgia. Recurrent sediment failures and break-in-slope regressions have been documented at Sand Heads (McKenna et al., 1992; Chillarige et al., 1994). On the foreslope south of this valley system is an area with a series of semi-parallel ridge-like features where the orientation of the ridges is roughly perpendicular to the slope (Fig. 5). These

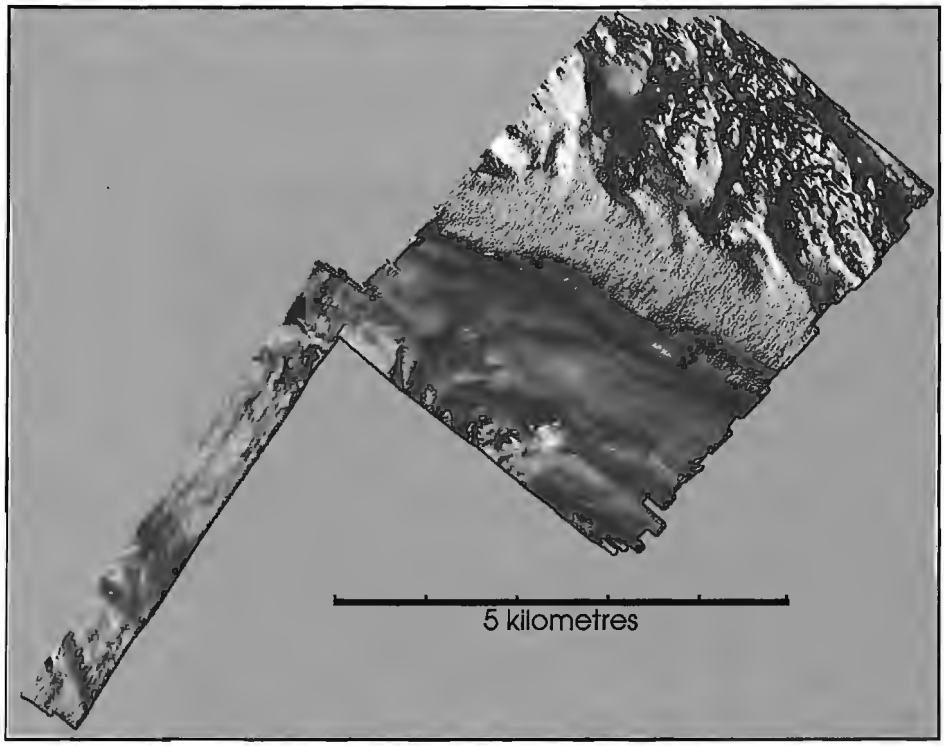

Figure 3.

Hillshaded image of swath bathymetric data from the Sabine Channel survey site (see Fig. 1 for location). The top of the image is north. The coast of the west side of Texada Island is to the northeast. The altitude of illumination is 45° above horizontal and the azimuth of illumination is 120°.

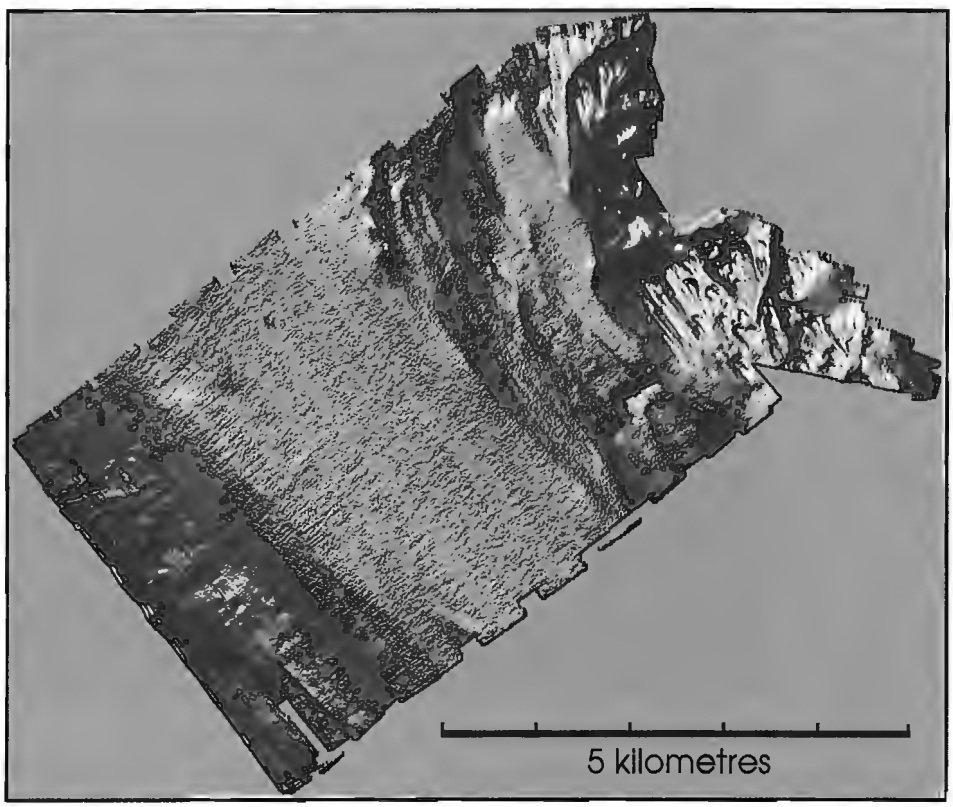

Figure 4.

Hillshaded image of the swath bathymetric data from the Malaspina Strait survey site (see Fig. 1 for location). The top of the image is north and Nelson Island is to the northeast and Texada Island is to the southwest. The altitude of illumination is 45° above horizontal and the azimuth of illumination is 150°.

sinusoidal ridges measure 60 to 100 m from crest to crest and several metres in amplitude. They are interpreted to result from rotational deformation by creep failure.

The Foreslope Hills (FSH) are a series of ridges and troughs within the central part of the Strait of Georgia, west of Sand Heads, in water depths between 230 and 320 m. They cover an area more than 60 km^2 and are clearly visible on bathymetric charts dating as far back as 1938. They are formed of the youngest Upper Post-Glacial sediment sequence of Hamilton (1991). Turbidites from the Sand Heads sea valley appear to be ponding within the troughs. Swath bathymetric data (Fig. 5) delineate the Foreslope Hills rather distinctly, showing them as ridges with wavelengths of 500-600 m, heights of about 20 m, and crestlines in the order

Figure 5. *Hillshaded image of bathymetric data from the Foreslope Hills – Sand Heads survey site (see Fig. 1 for location). The top of the image is north and Sand Heads is off the upper, northeast corner of the image. The altitude of illumination is 45° above horizontal and the azimuth of illumination is 320°.*

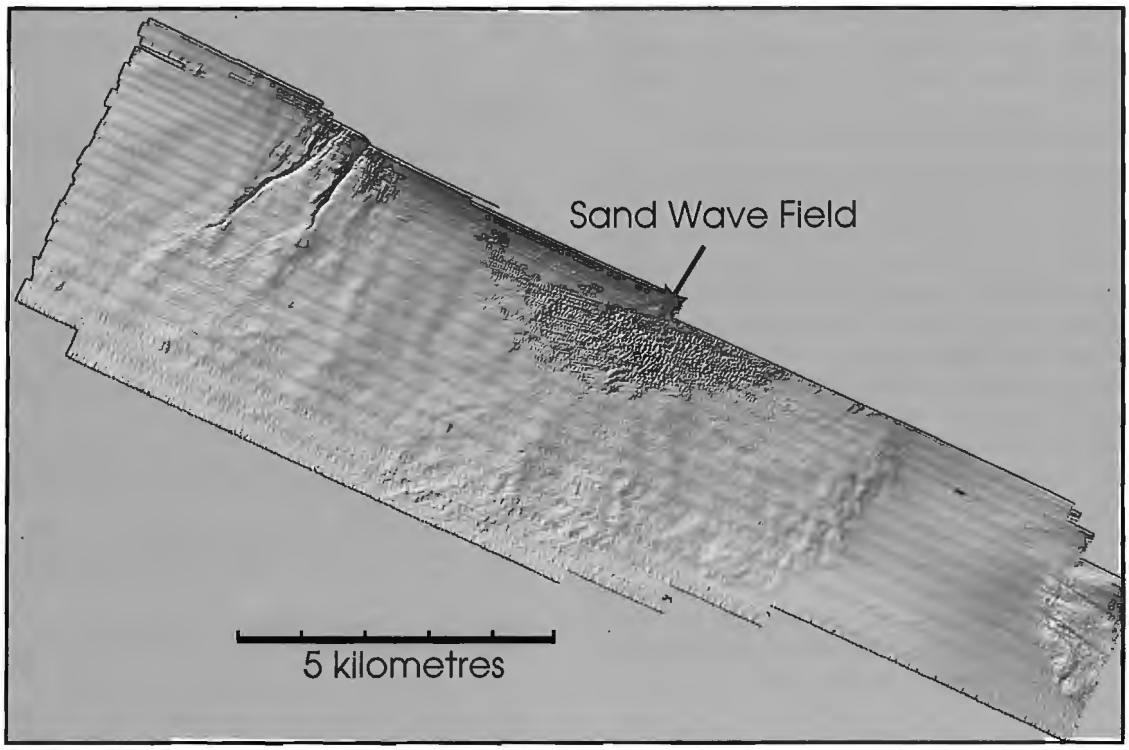

Figure 6. *Hillshaded image of swath bathymetric data from the southern Roberts Bank survey site (see Fig. 1 for location). The top of the image is north The Vancouver DeltaPort (Coal Port) and BC Ferry Terminals at Tsawwassen lie adjacent to and just northeast of the sand wave field. The angle of illumination is 45° above horizontal and the azimuth of illumination is 345°.*

of 5000 m long. The orientation of the ridges changes from a west-northwest direction in the north to north in the southern portion of the area.

The morphology of the Foreslope Hills is unique in the Strait of Georgia. Their position off the Fraser Delta suggests a genetic relationship with the delta. A number of hypotheses have been forwarded as to their origin. Mathews and Shepard (1962) and Terzaghi (1962) postulated they resulted from a large slope failure from the foreslope of the Fraser Delta. Shepard (1967) speculated that they may actually be mud diapirs, similar in evolution to those later described on the Mississippi delta by Prior and Coleman (1984). Tiffin et al. (1971) and Lutemauer and Finn (1983) concluded the Foreslope Hills were compressional folds of weaker deposits, caused by instability farther upslope. Hamilton and Wigen (1987) attributed their origin to a large slide deposit from the foreslope of the delta. They suggested that if a major slide had occurred, then there may have been an associated tsunamis. Hart (1993) reviewed available geophysical data and concluded that the asymmetry in the internal structure were landward dipping shear planes caused by in-place rotational displacement in a downslope direction. Seismic reflection data over the Foreslope Hills show an internal architecture similar to what might be expected of migrating sediment waves, implying that bedforms could be another explanation for their origin (Mosher et al., 1995).

Southern Roberts Bank

The final site surveyed is an area on the foreslope off southern Roberts Bank. It not only has an electrical transmission cable corridor crossing it, but also is the site of a sediment failure complex of undetermined origin. The area surveyed, which approximates the areal extent of the failure complex, is 75 km^2. Water depths at the site range from 10 to 201 m, with the shallowest depths being along the northeast side of the area and the deepest in the southwest corner.

A hillshaded image of swath bathymetry data from this site (Fig. 6) shows several distinctive features: 1) on the northeastern side of the image, two downslope trending gullies related to discharge of water and sediment through Canoe Passage, 2) a patchy area in the north-central portion of the image is a sandwave field and dredge-spoils dump, and 3) in the southeasternmost portion of the image, a slightly rougher seafloor is related to a Pleistocene outcrop. This Pleistocene material eventually surfaces to form Point Roberts. The general nature of this image, however, is such that it clearly defines the failure complex as distinct from the surrounding delta foreslope by its hummocky, rougher topographic nature. In seismic reflection records, the failure complex is shown as a zone with a hummocky surface and incoherent reflections in the subsurface, but with some semi-coherent internal impedance contrasts. The toe of the complex forms a distinctive wedge-shape against "normal" delta sediment at the base

of the foreslope, demonstrating sediment runout on top of the existing seafloor. The whole complex appears to be buried by 1-2 m of recent sediment, mostly sand. In the swath imagery, the hummocky nature of the surface of the failure complex appears to form subdued, downslope-trending gullies.

Interpretations of the failure complex range from: 1) a single massive slope failure event, 2) a series of failure events occurring in close succession, 3) a river mouth failure complex built up over a period of time, and 4) simply a change in sediment type and facies, unrelated to slope failure (Mosher, unpublished report to BC Hydro, 1994; Mosher et al., 1994; Terra Surveys, unpublished report to BC Hydro, 1994). Seismic reflection evidence clearly indicates that some slope failure process is likely involved, due to the incoherent nature of the reflections. The downslope fabric of the feature, as shown in the swath image, is suggestive of a river mouth failure complex, where gullies, similar to the two at Canoe Passage were formed associated with river discharge. As the river mouth changed locations across the delta plain, these gullies migrated. The result is a failure complex comprising debris flows, lobes, channels, and gullies built up over a period of time when the river mouth discharged in this region and was free to migrate across the delta plain.

CONCLUSIONS

A co-operative program between three federal government departments and two private companies to acquire swath bathymetry data from selected areas off the British Columbia coast has been highly successful. Five areas were surveyed yielding 100% coverage within each area. Resulting data were post-processed to provide highly effective and informative data sets and images. These data are appropriate for GIS analysis and can be effectively used for engineering and geological assessments.

REFERENCES

Chillarige, A.R.V., Robertson, P.K., Morgenstern, N.R., Christian, H.A., and Woeller, D.J.
1994: Evaluation of wave effects on seabed instability in the Fraser River delta; Proceedings 47th Canadian Geotechnical Conference, 21-23 September, Halifax, p.186a-186j.

Hamilton, T.S.
1991: Seismic stratigraphy of unconsolidated sediments in the central Strait of Georgia: Hornby Island to Roberts Bank; Geological Survey of Canada, Open File 2350.

Hamilton T.S. and Wigen S.O.
1987: The Foreslope Hills of the Fraser Delta: Implications for tsunamis in Georgia Strait; International Journal of the Tsunami Society, v. 5, p. 15-33.

Hart, B.S.
1993: Large scale in-situ rotational failure on a low angle delta slope, Fraser Delta, Canada; Geo-Marine Letters, v. 13, p. 219-226.

Hart, B.S., Prior, D.B., Barrie, J.V., Currie, R.G., and Luternauer, J.L.
1992: A river mouth submarine channel and failure complex, Fraser Delta, Canada; Sedimentary Geology, v. 81, p. 73-87.

Luternauer, J. and Finn, W.D.L.
1983: Stability of the Fraser River Delta front; Canadian Geotechnical Journal, v. 20(4), p. 603-616.

Mathews, W.H. and Shepard, F.P.
1962: Sedimentation of the Fraser River delta, British Columbia; American Association of Petroleum Geologists Bulletin, v. 46, p. 1416-1438.

McKenna, G.T., Luternauer, J.L., and Kostaschuk, R.A.
1992: Large-scale mass-wasting events on the Fraser River delta near Sand Heads, British Columbia; Canadian Geotechnical Journal, v. 29, p. 151-156.

Mosher, D.C., Christian, H.A., and Barrie, J.V.
1994: Hazards to development in the offshore of the Fraser River Delta; Geological Society of America, 1994 Annual Meeting, Seattle, Washington, Program with Abstracts, p. A469.

Mosher, D.C., Nichols, B., and Scientific Party of PGC95001
1995: Multichannel seismic reflection survey of the marine Fraser River Delta, Vancouver, British Columbia: Tully PGC95001; in Current Research, Part E; Geological Survey of Canada, p. 37-45.

Prior, D.B., Bornhold, B.D., and Johns, M.W.
1984: Depositional characteristics of a submarine debris flow; Journal of Geology, v. 92, p. 707-727.

Shepard, F.P.
1967: Delta-front diapirs of Magdalena River, Columbia, compared with hills of other large deltas; Transactions, Gulf Coast Association of Geological Societies, v. 17, p. 316-325.

Terzaghi, K.
1962: Discussion, on Sedimentation of Fraser River Delta, British Columbia by W.H. Mathews and F.P. Shepard; Bulletin of the American Association of Petroleum Geologists, v. 46(8), p. 1438-1443.

Tiffin, D.L., Murray, J.W., Mayers, I.R., and Garrison, R.E.
1971: Structure and origin of Foreslope Hills, Fraser Delta, British Columbia; Bulletin Canadian Petroleum Geology, v. 19, p. 589-600.

Geological Survey of Canada Project 890052

Mapping Pleistocene deposits beneath the Fraser River delta: preliminary geological and geophysical results

J.L. Luternauer and James A. Hunter[1]
GSC Pacific, Vancouver

Luternauer, J.L. and Hunter, J.A., 1996: Mapping Pleistocene deposits beneath the Fraser River delta: preliminary geological and geophysical results; in Current Research 1996-E; Geological Survey of Canada, p. 41-48.

Abstract: Direct sampling, chronological analysis, and remote geophysical techniques have identified Pleistocene deposits beneath the Fraser River delta sediments. Relief on the surface of documented Pleistocene deposits is high; depth beneath ground surface to these deposits ranges from 8 to 305 m. Known Pleistocene sequences are highly variable in grain size but gravel, diamicton, or till constitute <20% of the total deposits. Pronounced changes in geophysical properties are associated with the Holocene-Pleistocene boundary. Information acquired to date emphasizes the complexity of the region's geological architecture and suggests that a map of subsurface Pleistocene deposits will contribute to geotechnical assessments of local earthquake hazards.

Résumé : Un échantillonnage direct, des analyses chronologiques et des levés géophysiques à distance ont révélé la présence de dépôts pléistocènes sous les sédiments du delta du Fraser. Il existe un relief prononcé à la surface de sédiments pléistocènes qui ont fait l'objet de publications; la profondeur de ces dépôts (à partir de la surface) varie de 8 à 305 mètres. La granulométrie des séquences pléistocènes connues est très variable, mais le gravier, le diamicton ou le till constituent moins de 20 % de la totalité des sédiments. Les changements marqués des propriétés géophysiques sont associés à la limite entre l'Holocène et le Pléistocène. Les informations acquises à ce jour soulignent la complexité de l'architecture géologique de la région et indiquent qu'une carte des dépôts pléistocènes de subsurface contribuera aux évaluations géotechniques des risques sismiques locaux.

[1] Terrain Sciences Division, Ottawa

INTRODUCTION

As part of multidisciplinary investigations of the Fraser River delta, the Geological Survey of Canada is collecting, interpreting, and compiling information on local subsurface Pleistocene deposits. These studies have improved understanding of the geological evolution of this area, are helping develop and refine field and analytical techniques for characterizing subsurface Quaternary deposits, and will permit more reliable 2- and 3-dimensional geotechnical modeling of potential ground motion amplification during a strong earthquake.

The purpose of this interim report is to identify and describe the techniques that have been successfully applied to sample and identify Pleistocene deposits, to summarize the status of knowledge of subsurface Pleistocene deposits in the area, and to provide information on regional variations of geophysical properties to help refine geotechnical assessments of potential seismic response of the delta.

The location of the geological-geophysical sites discussed in this report are shown in Figure 1.

METHODS

The primary tool for directly observing Pleistocene deposits is the industrial drill rig. We have sampled these deposits using conventional rotary drilling and the Standard Penetration Test split-tube with either a hydraulic piston sampler or a fixed piston sampler, a 3 m long spring loaded core barrel with a retracting inner tube assembly, and a conventional PQ-3 wire-line core barrel (Luternauer et al., 1991; Christian et al., 1994, 1995; Dallimore et al., 1995). Continuous coring up to depths of 60 m also has been done with a vibro-sonic/rotary device. As Fraser River delta sediments consist mainly of clay, silt, and sand (Clague et al., 1991) and have not been observed to contain clasts any coarser than pebble size (<64 mm), abrupt slowing of drilling penetration rate or refusal, suggesting the presence of medium to coarse gravel (>64 mm), also has served as an indication of the presence of Pleistocene deposits. Boreholes are cased with 2.00-2.50" (5.08-6.35 cm) I.D. PVC pipe to permit downhole geophysical logging. Age of sediments based on radiocarbon analysis was determined by accelerator mass spectrometry at IsoTrace Laboratory, University of Toronto (Clague et al., 1991; Luternauer et al., 1991, 1994).

The geophysical characteristics which are associated with the Holocene-Pleistocene boundary include electrical conductivity, magnetic susceptibility, and shear wave velocity contrasts. Example borehole logs which demonstrate these variations are shown in Figure 2 along with the generalized geology, for GSC borehole FD94-4 (map site J) (after Dallimore et al., 1995).

Most of the Holocene section contains saline porewater (Dallimore et al., 1995) which is reflected in high values of measured formation electrical conductivities, in the order of

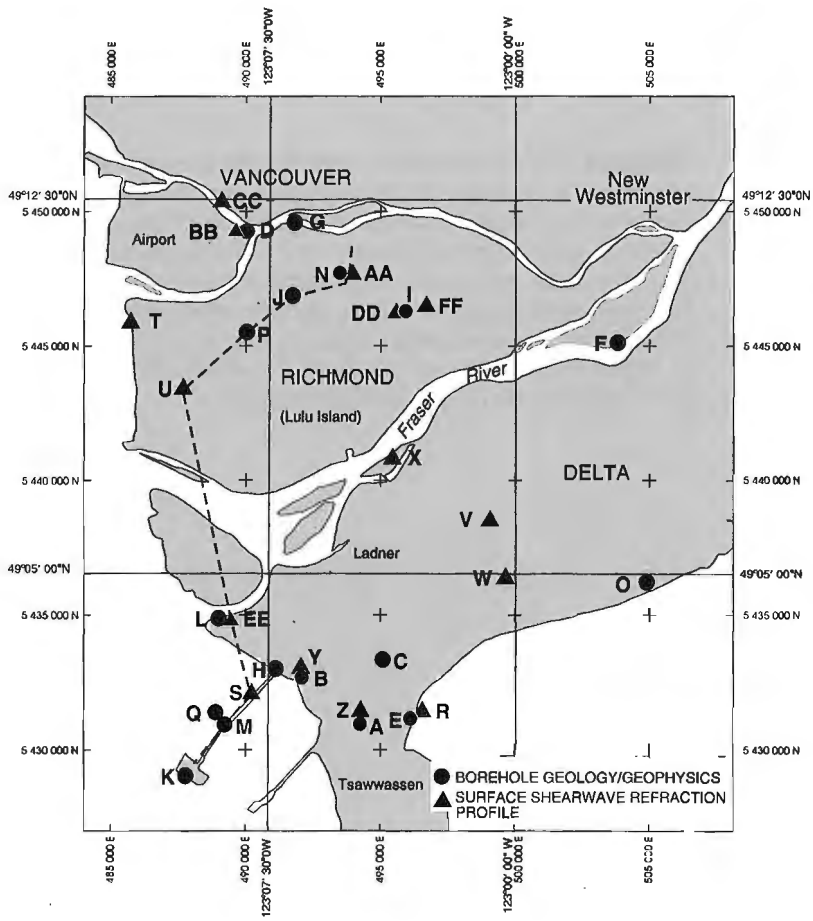

Figure 1.

Location and letter designation of borehole geology-geophysics survey sites and surface shear wave refraction seismic survey sites used in this study. Dashed line represents location of composite section displayed in Figure 4.

600-1000 milliSiemens/metre. In the borehole at site J, as well as at eight other boreholes in the study area which encountered Pleistocene sediments at depth (map sites B, D, G, H, K, L, M, O), a distinct decreasing conductivity gradient with depth is associated with the basal Holocene (distal) deltaic sediments. Laboratory measurements (Dallimore et al., 1995; Christian et al., 1995) have confirmed the conductivity gradient to be associated with a decreasing salinity gradient with depth, the geological origin of which has not yet been determined. The Holocene-Pleistocene boundary is associated with the base of the gradient layer where fresh water fills the sediment pore-spaces. An empirical relationship between electrical conductivity and porewater salinity for Fraser River delta Quaternary sediments (J.A. Hunter, unpub. data, 1996) is used to estimate porewater salinity from geophysical borehole or surface conductivity measurements.

The magnetic susceptibility log responds primarily to ferrimagnetic material content in sediments (McNeil et al., 1996); the largest response is attributed to the presence of magnetite. In Holocene deltaic sediments in the survey area, the measured magnetic susceptibility is low; however, in six boreholes where geological interpretations in boreholes have indicated the presence of the Holocene and Pleistocene sediments, this boundary is typified by an abrupt increase in magnetic susceptibility response (identified at map sites B, D, G, H, J, K, L, M). Such variations have been confirmed by Hunter et al. (1995) through correlation with laboratory measurements on core samples at map sites I and J. This characteristic has been utilized to support the identification of the boundary in three other holes where geological information was incomplete (map sites B, L, M).

Shear wave velocities of near-surface Holocene sediments (0-100 m depth) in the study area are in the range of 80-350 m/s (Hunter et al., 1990; Hunter, 1995) with velocity increasing uniformly with depth of burial. In areas where Holocene sediments are thicker (200 m depth or more), velocities can reach 400 m/s (Dallimore et al., 1995). In six boreholes where geological interpretations of the Holocene-Pleistocene boundary have been made (map sites D, G, I, J, K, L), there is an abrupt increase in the shear wave velocity which deviates markedly from the uniform increase in velocity (due to load pressure) within the Holocene section. The shear wave velocities associated with Pleistocene sediments may be as low as 350 m/s where the materials are near surface and fine grained, or as high as 750 m/s at depth, where the materials are coarse-grained gravel or diamicton. Invariably, however, there is a distinct velocity discontinuity associated with the Holocene-Pleistocene boundary. This attribute has been utilized in support of the identification of the boundary in boreholes where geological data was incomplete (map sites B, L, M).

Surface shear wave refraction techniques have been carried out in a routine reconnaissance manner throughout the survey area in order to provide regional shear wave velocity-depth information of near surface sediments (0-50 m depth range). Over 100 such sites have been occupied in the Fraser River delta using a "true-reversal" shear refraction field procedure which employs a horizontally polarized (SH) geophone array and recording techniques (Hunter et al., 1992). A few sites have yielded anomalously high shear wave velocity layers at relatively shallow depths, some of which have been subsequently drilled and interpreted to contain Pleistocene deposits (sites AA, DD, EE).

In the application of the seismic refraction technique, the tacit assumption is that shear wave velocities increase with depth, either as a gradient or step-wise. From our borehole experience, this assumption is valid for the Holocene deltaic sediments (to within the wavelength resolution of the technique when compared to borehole shear wave velocity logs), and can identify the abrupt velocity discontinuity associated with the top of the Pleistocene. However, our borehole shear wave data, indicates that shear wave velocity reversals occur within the Pleistocene sequence; hence, the shear wave refraction technique may not detect velocity reversals within the Pleistocene sequence (e.g., see Fig. 2), and can only reliably estimate the velocity associated with the top of the Pleistocene, the depth to this velocity discontinuity, and its apparent dip, within this survey area.

Several "deep sounding" sites were also occupied in the survey area. These were established to probe to considerable depth in areas where thick Holocene sediments were suspected. These sites required ambient noise-free areas with

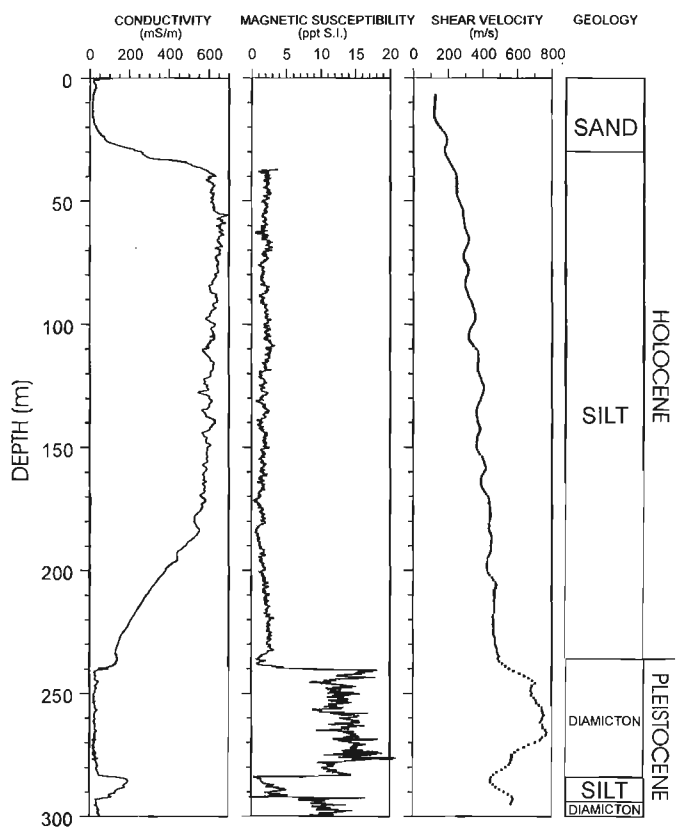

Figure 2. Borehole geophysical measurements and generalized geology for site J (FD94-4). Electrical conductivity and magnetic susceptibility logging was done at 0.1 m depth intervals. Down-hole shear wave travel-time logging was done at 1 m depth intervals and 11-point running least-squares velocity fit has been applied to the data.

Table 1. Geological and geophysical borehole data summary.

MAP LETTER (data source)	HOLE	DEPTH (m) TO PLEISTOCENE DEPOSITS (based on first occurrence of gravel or diamicton and/or geophysical anomalies)	THICKNESS (m) AND LITHOLOGY OF CORED INTERVAL OF PLEISTOCENE DEPOSITS (selectively or continuously sampled)	BOREHOLE GEOPHYSICAL DETECTION METHOD(S)
A (Clague et al., 1991)	FD86-1	8	8-85 DIAMICTON	N/A, see also adjacent site Z in Table 2
B (Clague et al., 1991)	FD86-5	51 (based on geology) 33 (based on geophysical anomalies)	51-88 interlayered sandy GRAVEL, CLAY and DIAMICTON	SHEAR VELOCITY, MAGNETIC SUSCEPTIBILITY, CONDUCTIVITY see also adjacent site YY in Table 2
C (Luternauer et al., 1991, 1994)	FD87-1A	185	185-367 mainly CLAY, SILT and SAND with minor (ca. 10%) DIAMICTON	N/A
D (Hunter et al., 1994)	FD90-1	35	35-43 DIAMICTON	SHEAR VELOCITY, MAGNETIC SUSCEPTIBILITY, CONDUCTIVITY
E (M.C. Roberts, pers. comm., 1996)	SFU90-3	53	drilled and cased hole no sampling stiff drilling below 53 m	N/A, see also adjacent site R in Table 2
F (Bazett and McCammon, 1986)	GA-111	66	66.2-80.9 stiff to hard, stony, silty CLAY (DIAMICTON) 80.9-114.9 generally very dense, layered SILT and SAND with occasional thin layers of silty CLAY at base 114.9-122.4 very stiff to hard stony silty CLAY (DIAMICTON) 122.4-145.3 very stiff to hard CLAY	N/A
G (Hunter et al., 1994)	FD92-2	32	32-35 DIAMICTON	SHEAR VELOCITY MAGNETIC SUSCEPTIBILITY, CONDUCTIVITY
H (Christian et al., 1994)	FD92-11	100	100-101 interbedded clay, silt and very fine sand 101 refusal (inferred DIAMICTON)	MAGNETIC SUSCEPTIBILITY, CONDUCTIVITY
I (Dallimore et al., 1995)	FD94-3	19	19-305 below capping gravel core consists mainly of alternating very stiff to very hard silty CLAY and very dense SAND	SHEAR VELOCITY, MAGNETIC SUSCEPTIBILITY, see also adjacent site DD in Table 2
J (Dallimore et al., 1995)	FD94-4	236	236-301 mainly DIAMICTON with ca. 20% hard to vey hard silty CLAY intervals centered at 280-289	SHEAR VELOCITY, MAGNETIC SUSCEPTIBILITY, CONDUCTIVITY
K (Christian et al., 1995)	FD95-S1	109	109-122 DIAMICTON 122-124 sandy SILT 124-144 clayey and sandy SILT 144-150 SAND and SILT 150-152 DIAMICTON/ CLAY	SHEAR VELOCITY, MAGNETIC SUSCEPTIBILITY, CONDUCTIVITY
L	FD95-2	52	drilled and cased hole no sampling stiff drilling below 52 m	SHEAR VELOCITY, MAGNETIC SUSCEPTIBILITY, CONDUCTIVITY see also adjacent site EE in Table 2
M	FD95-4	91	no-sampling stiff drilling below 91 m	MAGNETIC SUSCEPTIBILITY, CONDUCTIVITY
N	FD95-8	50	stiff drilling below 50 m	see adjacent site AA in Table 2
O (J. Britton, Dynamic Oil Co. Ltd., pers. comm., 1996)	MUD BAY d-95-D	186	186-266 SAND (pebbly and coarse at top grading to very fine at bottom) 266-447 interlayered CLAY and SILTSTONE	conventional industry electrical and sonic logs indicating a decreasing conductivity gradient and a sonic (P- wave) discontinuity
P	FD96-1	305	305-328 DIAMICTON	N/A
Q (Swan Wooster Engineering, 1968, Roberts Bank Soil Information for National Harbours Board) (Unpublished)	DH-10	78	78-80 (est.) TILL (DIAMICTON)	N/A

relatively undisturbed surface soil conditions over linear distances of up to 800 m. Such sites are rare in an urban environment, and often site conditions and logistics dictated only "single-ended" (seismic energy source at one end of the array only) rather than "true-reversal" (seismic energy source at both ends of the array) soundings. This restriction had little consequence in defining the Holocene velocity sequence; however, if an abrupt (Pleistocene) velocity increase was encountered, estimates of the true shear velocity and apparent dip may be limited. Some of the "deep sounding" sites encountered no abrupt velocity discontinuities at depth, despite long-offset geophone arrays and good signal-to-noise conditions. In these circumstances, a minimum depth estimate to the top of Pleistocene materials was computed by assuming a refraction velocity model with an abrupt increase to a 700 m/s velocity layer immediately below the velocity-depth profile measured for the site. Such locations (map sites T, U, V, W, X) have been included in the geophysical data set, in order to indicate areas where the Holocene deltaic sequence is unusually thick, and where future geological-geophysical work may be required to define the Holocene-Pleistocene structure.

RESULTS

The database and interpretation techniques for the Holocene-Pleistocene boundary are summarized in Table 1 for geological-geophysical borehole investigations and in Table 2 for the surface shear-wave refraction sites. As well, the interpreted depth below surface to the boundary are given for all sites in Figure 3; where the boundary has been interpreted to be dipping, from geophysical studies, the average depth value is given on the map.

Medium to coarse gravel and diamicton have been recovered from cores in the Fraser River delta area (Table 1). These types of deposits are considered to be of Pleistocene age because they are not characteristic of immediately overlying Fraser River delta sediments, and their Pleistocene age is confirmed at sites C and J. At site H the oldest corrected radiocarbon age yielded from an analyzed shell, extracted 1 m above the diamicton at the base of the core, is 9600 ± 70 BP (IsoTrace Lab #TO-4894; P. Monahan, pers. comm., 1996). Sharply reduced penetration rates during the course of drilling suggests coarse Pleistocene age gravel beds also occur at four other unsampled borehole sites.

Capilano Sediments (Armstrong, 1984) of Late Pleistocene age, having a generally high proportion of fine matrix to gravel (dropstone?) content, may overlie gravel-rich drift-derived sediments in the area (Luternauer et al., 1991, 1994). The relative paucity of medium to coarse gravel in these deposits, relative to a diamicton or gravel bed, may obscure their Pleistocene glacial origin. In those cores where these sediments are present, but their Pleistocene age is not recognized, depth to Pleistocene sediments may be overestimated. However, Capilano Sediments appear to be thin over the main part of the delta (Luternauer et al., 1991, 1994; Dallimore et al., 1995), and it is likely that the shallowest medium to coarse gravel beds or diamicton lie at or near the top of the Pleistocene sequence in this area.

Where complete geological and geophysical data were available in boreholes, the interpretations of the depth position of the Pleistocene surface correlated well, and the values given in Table 1 (sites D, G, H, I, J, K) represent a match of both types of data (to within 1 m).

At site B, two depths are given. In this borehole, continuous core sampling was not available in the immediate vicinity of 33 m depth where prominent geophysical anomalies were observed. Immediately below this depth, the sampled materials are sand, and from the conservative geological criteria established above, the Pleistocene surface was interpreted at 51 m depth where the first gravel was encountered. The greater depth value has been shown on the map in Figure 3. At all other sites where geological information was limited or lacking, but where geophysical logging was done, changes in drilling characteristics correlated well with the interpreted depth to Pleistocene deposits (to within ±2 m from the driller's log).

Figure 4 shows a north-south composite section of shear wave velocity-depth distribution and the interpreted Pleistocene surface across the survey area, from the data used in this study (see Fig. 1 for the location). It can be seen that the vertical velocity-depth variation within the Holocene deltaic sediments is relatively uniform. A concentration of iso-velocity contours is associated with the interpreted Pleistocene surface and is indicative of an abrupt shear wave velocity discontinuity.

It is obvious that the Holocene-Pleistocene boundary is not flat-lying beneath the Fraser River delta. Despite the paucity of data in some areas, there appears to be a definite trend towards a thick Holocene sequence in the central portion of the area; it is not yet certain whether this "trough" displays a directional trend, although there is an indication of a northwest-southeast linearity. A similar trend is displayed by ridges within the adjacent Strait of Georgia, which are underlain by Pleistocene deposits (Clague, 1977; Hart et al., 1995), and by the topography of the Tertiary bedrock surface underlying the delta (Britton et al., 1995).

SUMMARY

The surface of the Pleistocene sequence under the delta has a high relief and, based on available information, ranges from 8 to 305 m beneath the delta surface. Observed Pleistocene deposits range in grain size from medium to coarse gravel to clay, but diamicton or till appears to constitute less than 20% of the sediments. This information, along with newly acquired data on the shear wave velocity variations in these deposits can be used to refine geotechnical assessments of local potential ground motion amplification during a severe earthquake (Luternauer et al., 1995).

It is apparent that the existing database is not yet sufficient to characterize the spacial distribution of the Holocene-Pleistocene boundary in many areas of the Fraser River delta to the degree required for 2-dimensional or 3-dimensional ground-motion amplification studies of earthquake shaking. The existing database, in conjunction with previously published studies of

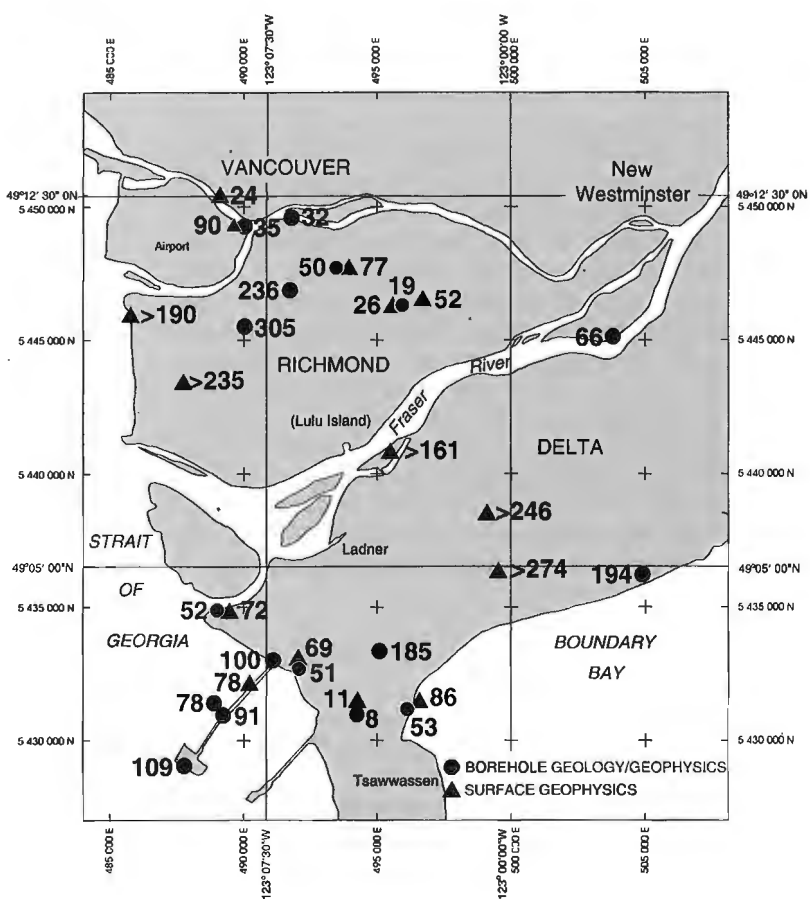

Figure 3.

Depth to surface of Pleistocene deposits (m below ground surface) from geological and geophysical interpretations. At sites of surface geophysical surveys, where an apparent dip of the deposit surface was detected, the value shown is the arithmetic average to the top of Pleistocene deposits. Specific depth variations are displayed in Table 2.

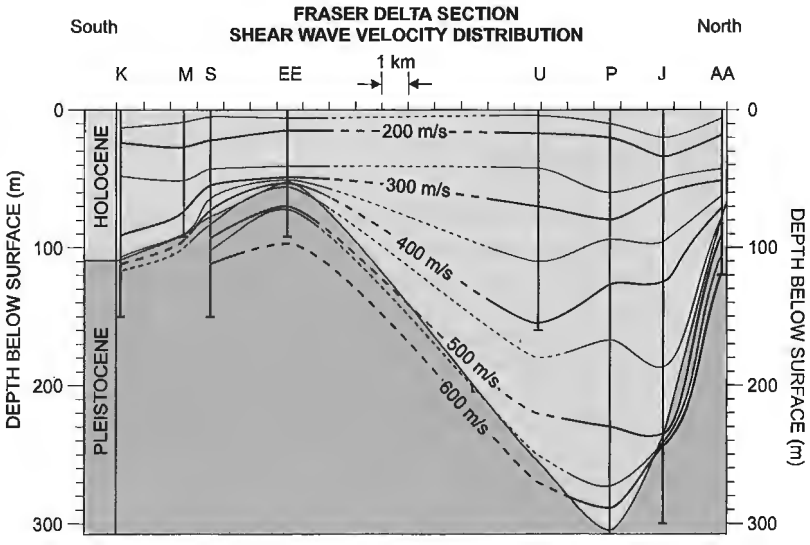

Figure 4.

A composite section of the distribution of shear wave velocity vs depth indicating the surface of Pleistocene deposits beneath the Fraser River delta. Refer to Figure 1 for location of cross-section.

the subsurface bedrock topography (Britton et al., 1995; Harris et al., 1995), indicates the subsurface architecture of the delta is complex, raising the possibility that ground surface response during a severe earthquake may be more difficult to predict than previously considered.

The data presented here, form a basis for, and help focus, future research into the architecture of subsurface Quaternary deposits in the Fraser River delta area. New technologies have been tested and applied to define fundamental geological and geophysical properties of these deposits. The results of this research point the way to the future development and application of cost-effective survey techniques for this survey area as well as many other similar settings in Canada.

ACKNOWLEDGMENTS

We wish to thank L. Jackson for critically reviewing the final draft of the manuscript, P. Monahan for offering a number of helpful suggestions for improving an earlier draft, and B. Vanlier for the final formatting of the manuscript.

Table 2. Surface shear wave refraction data summary.

MAP LETTER (data source)	DEPTH TO TOP OF PLEISTOCENE DEPOSITS (m) mean, range and apparent dip direction or minimum depth	HOLOCENE SHEAR WAVE VELOCITY RANGE (m/s)	PLEISTOCENE DEPOSIT SHEAR WAVE VELOCITY RANGE (m/s)	SITE SURVEY DESCRIPTION
R	86 (70 to 110) N	120-340	450-550	– reversed refraction – array length 480 m
S	78 (77-79) N	80-300	450-730	– reversed refraction – array length 480 m
T	>190	180-350	N/A	– single ended refraction – array length 490 m
U	>235	100-420	N/A	– reversed refraction – array length 600 m
V	>246	135-400	N/A	– single-ended refraction – array length 650 m
W	>274	140-390	N/A	– single ended refraction – array length 790 m
X	>161	90-350	N/A	– single ended refraction – array length 540 m
Y (site #5 of Hunter et al., 1992)	69 (50-87) NE	110-270	550	– reversed refraction – array length 300 m
Z (site #9 of Hunter et al., 1992)	11 (4-18) S	130-200	400-650	– reversed refraction – array length 270 m
AA (site #30 of Hunter et al., 1992)	77 (70-84) NE	80-300	450-550	– reversed refraction – array length 270 m
BB (site #36 of Hunter et al., 1992)	90 (50-130) NW	50-250	750	– reversed refraction – array length 330 m
CC (site #38 of Hunter et al., 1992)	24 (16-32) S	100-270	600-740	– reversed refraction – array length 100 m
DD (site #70 of Hunter et al., 1992)	26 (19-33) S	120-210	320-460	– reversed refraction – array length 270 m
EE	72 (69-75) NE	85-260	395-545	– reversed refraction – array length 270 m
FF	52 (50-54) N	75-322	375-660	– reversed refraction – array length 330 m

REFERENCES

Armstrong, J.E.
1984: Environmental and engineering applications of the surficial geology of the Fraser Lowland, British Columbia; Geological Survey of Canada, Paper 83-23, 54 p.

Bazett, D.J. and McCammon, N.R.
1986: Foundations of the Annacis cable-stayed bridge; Canadian Geotechnical Journal, v. 23, p. 458-471.

Britton, J.R., Harris, J.B., Hunter, J.A., and Luternauer, J.L.
1995: The bedrock surface beneath the Fraser River delta in British Columbia based on seismic measurements; in Current Research 1995-E; Geological Survey of Canada, p. 83-89.

Christian, H.A., Barrie, J.V., MacDonald, R., Monahan, P.A., Hunter, J.A., and Luternauer, J.L.
1995: Slope instability on Roberts Bank, Fraser River delta, Vancouver, British Columbia; 48th Annual Canadian Geotechnical Conference, September 25-27, 1995, Vancouver, British Columbia, Preprint Volume 2, p. 937-946.

Christian, H.A., Monahan, P.A., and Barrie, J.V.
1994: Deep hole geotechnical investigation adjacent to the B.C. Hydro Canoe Pass Submarine Cable Terminal, Fraser River delta, British Columbia; Geological Survey of Canada, Open File 2861.

Clague, J.J.
1977: Quadra Sand: a study of the Late Pleistocene geology and geomorphic history of coastal southwest British Columbia; Geological Survey of Canada, Paper 77-17, 24 p.

Clague, J.J., Luternauer, J.L., Pullan, S.E., and Hunter, J.E.
1991: Postglacial deltaic sediments, southern Fraser River delta, B.C.; Canadian Journal of Earth Sciences, v. 28, no. 9, p. 1386-1393.

Dallimore, S.R., Edwardson, K.A., Hunter, J.A., Clague, J.J., and Luternauer, J.L.
1995: Composite geotechnical logs for two deep boreholes in the Fraser River delta, British Columbia; Geological Survey of Canada, Open File 3018.

Harris, J.B., Hunter, J.A., Luternauer, J.L., and Finn, W.D.
1995: Site response modelling of the Fraser River delta, British Columbia; in Current Research 1995-E; Geological Survey of Canada, p. 69-75.

Hart, B.S., Hamilton, T.S., Barrie, J.V., and Prior, D.B.
1995: Chapter 8: Seismic stratigraphy and sedimentary framework of a deep-water Holocene delta: The Fraser delta, Canada; in Geology of Deltas, (ed.) M.N. Oti and G. Postma; A.A. Balkema, Rotterdam, Brookfield, p. 167-178.

Hunter, J.A.
1995: Shear wave velocities of Holocene sediments, Fraser River delta, British Columbia; in Current Research 1995-A; Geological Survey of Canada, p. 29-32.

Hunter, J.A., Burns, R.A., and Good, R.L.
1990: Borehole shear wave velocity measurements, Fraser delta; Geological Survey of Canada, Open File 2229.

Hunter, J.A., Burns, R.A., Good, R.L., Wang, Y., and Evans, M.E.
1995: Borehole magnetic susceptibility measurements in unconsolidated overburden of the Fraser River delta, British Columbia; in Current Research 1995-E; Geological Survey of Canada, p. 77-82.

Hunter, J.A., Luternauer, J.L., Neave, K.G., Pullan, S.E., Good, R.L., Burns, R.A., and Douma, M.
1992: Shallow shear-wave velocity-depth data in the Fraser delta, from surface refraction measurements, 1989, 1990, 1991; Geological Survey of Canada, Open File 2504.

Hunter, J.A., Luternauer, J.L., Roberts, M.C., Monahan, P.A., and Douma, M.
1994: Borehole geophysics logs, Fraser River delta (92G), British Columbia; Geological Survey of Canada, Open File 2841, 30 p. and 2 diskettes.

Luternauer, J.L., Barrie, J.V., Christian, H.A., Clague, J.J., Evoy, R.W., Hart, B.S., Hunter, J.A., Killeen, P.G., Kostaschuk, R.A., Mathewes, R.W., Monahan, P.A., Moslow, T.F., Mwenifumbo, C.J., Olynyk, H.W., Patterson, R.T., Pullan, S.E., Roberts, M.C., Robertson, P.K., Tarbotton, M.R., and Woeller, D.J.
1994: Fraser River delta: geology, geohazards and human impact; in Geology and Geological Hazards of the Vancouver Region, (ed.) J.W.H. Monger; Geological Survey of Canada, Bulletin 481, p. 197-220.

Luternauer, J.L., Clague, J.J., and Feeney, T.D.
1991: A 367 m core from southwestern Fraser River delta, British Columbia; in Current Research, Part E; Geological Survey of Canada, Paper 91-1E, p. 127-134.

Luternauer, J.L., Harris, J.B., Hunter, J.A., and Finn, W.D.L.
1995: Fraser River delta geology: modelling for seismic hazard assessment; Association of Professional Engineers and Geoscientists of BC Magazine, v. 46, p. 10-14.

McNeil, J.D., Hunter, J.A., and Bosnar, M.
1996: Application of a borehole induction magnetic susceptibility logger to shallow lithological logging; Journal of Environmental and Engineering Geophysics, v. 0, no. 2, p. 77-90.

Geological Survey of Canada Projects 860022, 950029

Paleozoic conodont/radiolarian calibration in the Canadian Cordillera

F. Cordey[1], M.J. Orchard, and S.E.B. Irwin
GSC Pacific, Vancouver

Cordey, F., Orchard, M.J., and Irwin, S.E.B., 1996: Paleozoic conodont/radiolarian calibration in the Canadian Cordillera; in Current Research 1996-E; Geological Survey of Canada, p. 49-54.

Abstract: In contrast with the Mesozoic where substantial progress has been made in recent years in developing zonations within the Canadian Cordillera, there has been relatively little study of Paleozoic radiolarian fauna. As a result of previous and current Cordilleran mapping, Paleozoic conodont and radiolarian assemblages were found co-occurring at forty-five localities of chert and carbonate strata from southern British Columbia to northern Yukon, ranging in age from Ordovician to Permian. Conodont occurrences provide a mean for calibrating the radiolarian assemblages. This project focuses on developing this Paleozoic calibration in order to improve the geochronological tool available to mapping in the Canadian Cordillera, in particular in areas of active mining exploration like the Selwyn and Kechika basins.

Résumé : Le Paléozoïque et ses faunes de radiolaires ont fait l'objet de relativement peu d'études, à la différence du Mésozoïque pour lequel des progrès substantiels ont été accomplis ces dernières années en ce qui a trait au développement de biozonations au sein de la Cordillère canadienne. Des échantillons récoltés lors de travaux de cartographie ont permis d'identifier divers assemblages de radiolaires et de conodontes d'âge ordovicien à permien, lesquels coexistent à 45 localités de jaspes et roches carbonatées de la partie sud de la Colombie-Britannique à la partie nord du Yukon. Les conodontes permettent de calibrer les assemblages de radiolaires. Le présent projet s'attache à définir une calibration paléozoïque, afin d'améliorer les outils géochronologiques disponibles pour la cartographie de la Cordillère canadienne et, en particulier, des régions où se fait de l'exploration minière (comme par exemple les bassins de Selwyn et de Kechika).

[1] 311-1080 Pacific Street, Vancouver, British Columbia V6E 4C2

INTRODUCTION

In contrast with the substantial progress that has been made recently in describing Mesozoic collections and developing radiolarian zonations within the Canadian Cordillera, there has been relatively little study of Paleozoic radiolarian faunas.

Because of the relatively recent discovery and development of radiolarian extraction techniques (Dumitricà, 1970; Pessagno and Newport, 1972), Paleozoic radiolarian zonation lacks the precision provided by conodonts, particularly for the Lower and Middle Paleozoic.

Conodont processing linked to Cordilleran mapping has revealed the co-occurrence of conodonts and radiolarians at an increasing number of localities, some of which are in areas of mining interest. These localities are scattered throughout the Cordillera from southern British Columbia to northern Yukon Territory, from the Insular belt in the west to the outboard cratonic margin (Fig. 1). They are found within the interval Ordovician to Permian, a time span encountered in few regions in the world.

These co-occurrences provide a means for improving Cordilleran and worldwide Paleozoic radiolarian zonation by intercalibrating it with conodont zonation. Conodont-radiolarian associations also enhance the value of both microfossil groups in paleobiogeographic analysis.

The goal of this Cordilleran project is to develop and improve this intercalibration. This paper presents the record of available collections, and assesses their potential for contributing to Cordilleran geoscience.

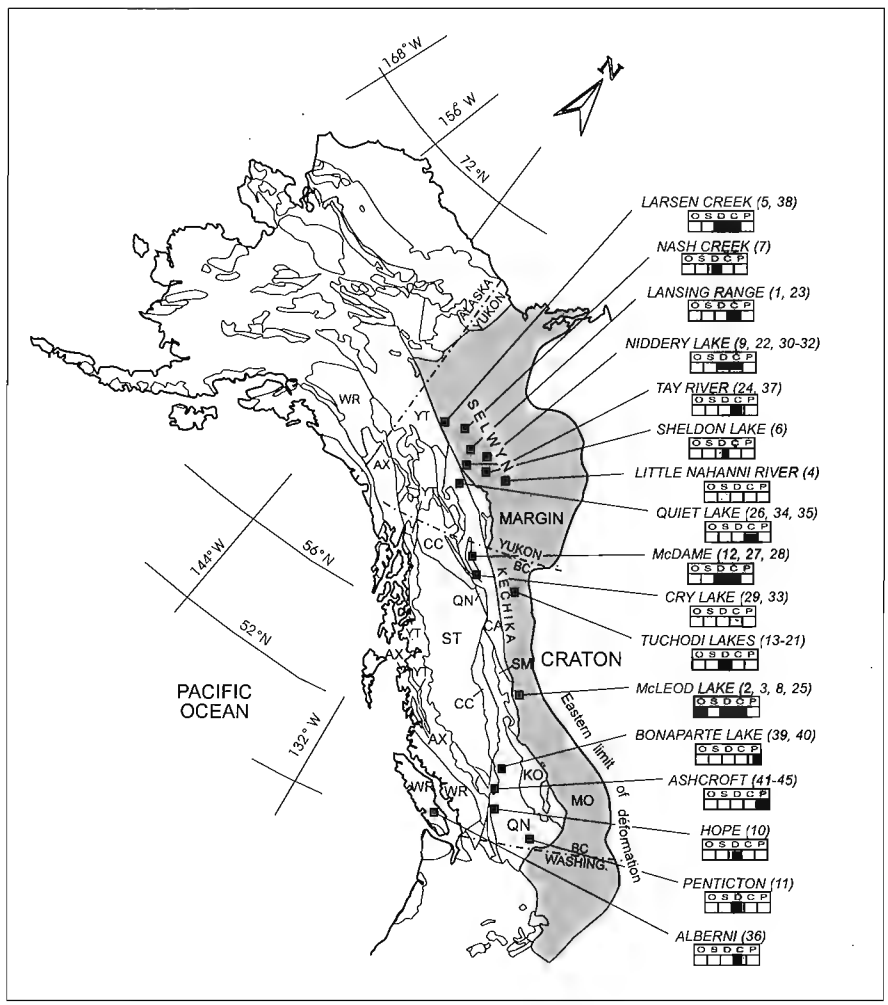

Figure 1. *Location of map areas where Paleozoic conodont/radiolarian co-occurring associations are known within the Canadian Cordillera. Shaded zone: continental margin units. Terranes abbreviations: WR, Wrangellia; AX, Alexander; ST, Stikinia; CC, Cache Creek; QN, Quesnellia; YT, Yukon-Tanana; SM, Slide Mountain; KO, Kootenay; MO, Monashee. Numbers refer to localities from Table 1 and cited in text. Age of localities within a given map area: O: Ordovician, S: Silurian, C: Carboniferous, D: Devonian, P: Permian.*

The first author is responsible for assessing the radiolarian collections from samples previously dated with conodonts by M.J. Orchard, or in the case of those from the Late Devonian strata of Selwyn and Kechika basins, by S.E.B. Irwin.

SOURCE OF COLLECTIONS

Cordilleran mapping programs by government agencies such as the Geological Survey of Canada (Vancouver) and the B.C. Geological Survey Branch (Victoria) generate each year a number of microfossil collections from various Cordilleran regions. The productive strata are lithologically diverse, represent various geological settings, and are wide ranging in age.

Conodonts are usually sought in, and recovered from carbonate samples, whereas radiolarians are more commonly extracted from siliceous rocks such as ribbon chert or cherty mudstones. Because chert requires slow etching and dissolution of a relatively small amount of rock, conodonts are infrequently recovered as a biproduct. Both radiolarians and conodonts are less well preserved in chert compared with limestone, but they are nevertheless extremely useful index fossils in these domains.

Limestone samples that are commonly processed for conodonts are much larger than chert samples, but of the often large insoluble residue, only a heavy concentrate (density >2.85) is systematically searched for microfossils. Radiolarians may occur in these fractions when they are pyritized, which is the case with many assemblages reported here. There is considerable potential for recovering much larger radiolarian collections from light fractions of limestone residues, as has been shown with Triassic samples from the Queen Charlotte Islands (Carter et al., 1989). Similarly, more voluminous chert processing has the potential to yield additional conodont collections.

The details about location, geological unit, age, and state of preservation of forty-five Paleozoic radiolarian-conodont assemblages are presented in Table 1.

Table 1. Localities of Paleozoic conodont/radiolaria co-occurrences within the Canadian Cordillera. Localities numbers on the left side of the table refer to localities cited in text and in Figure 1.

Loc. No.	Map Area	GSC Locality	Field Sample	Geological Unit	Conodont Age	Lithology	Radiolarian preservation
45	Ashcroft (92I/14)	C-102500	80-MJOS-Loon3	Cache Creek Group, Eastern Belt	Late Permian, (Guadalupian)	Chert	moderate
44	Ashcroft (92I/11)	C-087649	80-MVS-65C	Cache Creek Group, Eastern Belt	Permian	Chert	moderate
43	Ashcroft (92I/13)	C-102552	80-MVS-191	Cache Creek Gp, Marble Canyon	Permian	Chert	moderate
42	Ashcroft (92I/14)	C-087650	80-MV-182	Cache Creek Gp, Eastern Belt	Permian	Chert	moderate
41	Ashcroft (92I/14)	C-087651	80-MV-296g	Cache Creek Gp, Marble Canyon	Permian	Chert	good
40	Bonaparte Lake (92P/8)	C-102432	81-Preto-S-140	Fennell Formation	Permian	Chert	moderate
39	Bonaparte Lake (92P/1)	C-102412	81-MC-4	Fennell Formation	Early(?) Permian; (?)Leonardian	Chert	moderate
38	Larsen Creek (116A/14)	C-108186	92-TOA-22-5	unnamed	Late Carbonif.; late Namurian	Carbonate	moderate
37	Tay River (105K/11)	C-118137	85-GGA-33-G1	Mount Christie Fm	Late Carboniferous	Chert	good
36	Albemi (92F/7)	C-127720	85-YB-80	Buttle Lake Group	Carboniferous	Chert	good
35	Quiet Lake (105F/14)	C-081657	82-DY-2170	Earn Group	Mid-Late Carboniferous	Carbonate	poor
34	Quiet Lake (105F/14)	C-081658	82-DY-2171	Earn Group	Mid-Late Carboniferous	Carbonate	poor
33	Cry Lake (104I/16)	C-103233	83-GAH-81aF	Earn Group	Early Carboniferous	Carbonate	poor
32	Niddery Lake (105O/1)	C-108152	83-TOA-4-5-343	Earn Group, Portrait Lake Fm	Early Carboniferous	Carbonate	moderate
31	Niddery Lake (105O/2)	C-108154	83-TOA-7-3	Earn Group, Tsichu Fm	Early Carboniferous	Carbonate	poor
30	Niddery Lake (105O/7)	C-108161	83-TOA-17-2	Earn Group, Tsichu Fm	Early Carboniferous	Carbonate	moderate
29	Cry Lake (104I/15)	C-116039	84-GAH-321r	Sylvester Group	Early Carboniferous	Chert	poor
28	McDame (104P/13)	C-153818	87-JN-39-11	Sylvester Group	Early Carboniferous	Carbonate	poor
27	McDame (104P/12)	C-159221	87-KG-38-10	Sylvester Group	Early Carboniferous	Carbonate	poor
26	Quiet Lake (105F/15)	O-093428	75-TO-201	unnamed	Early Carboniferous; Visean	Carbonate	moderate
25	McLeod Lake (93J/9)	C-159747	88-SCB-513	unnamed	Early Carbonif.; Tournaisian	Carbonate	poor
24	Tay River (105K/11)	O-093483	76-TO-3-1	unit 5b Roddick/Green	Early Carbonif.; Tournaisian	Carbonate	poor
23	Lansing Range (105N/9)	C-302367	93-RAS-316	Earn Group	Early Carbonif.; Tournaisian	Chert	moderate
22	Niddery Lake (105O/8)	C-108159	83-TOA-15-2	Earn Group, Portrait Lake Fm	Late Devonian; mid. Famennian	Carbonate	moderate
21	Tuchodi Lake (94K/40	C-209161	94-SP-GH-93-66-4	Earn Group, Gunsteel Fm	Late Devonian, Famennian	Crbonate	good
20	Tuchodi Lakes (94K/4)	C-116730	86-OF-M-G143	Earn Group, Gunsteel Fm	Late Devonian; Famennian	Carbonate	good
19	Tuchodi Lakes (94K/4)	C-116957	86-OF-M-G7	Earn Group, Gunsteel Fm	Late Devonian; Famennian	Carbonate	poor
18	Tuchodi Lakes (94K/4)	C-116958	86-OF-M-G8	Earn Group, Gunsteel Fm	Late Devonian; Famennian	Carbonate	good
17	Tuchodi Lakes (94K/4)	C-116965	86-OF-M-G15	Earn Group, Gunsteel Fm	Late Devonian; Famennian	Carbonate	poor
16	Tuchodi Lakes (94K/4)	C-116969	86-OF-M-G19	Earn Group, Gunsteel Fm	Late Devonian; Famennian	Carbonate	good
15	Tuchodi Lakes (94K/4)	C-116992	86-OF-M-G42	Earn Group, Gunsteel Fm	Late Devonian; Famennian	Carbonate	good
14	Tuchodi Lakes (94K/4)	C-118548	85-OF-M-16	Earn Group	Late Devonian; Famennian	Carbonate	moderate
13	Tuchodi Lakes (94K/4)	C-116914	86-OF-M-32	Earn Group, Gunsteel Fm	Late Devonian; Famennian	Carbonate	poor
12	McDame (104P/12)	C-153835	87-JN-4-8	Earn Group	Late Devon.; mid-late Fam.	Carbonate	good
11	Penticton (82E/4)	C-117751	84-FC-CKO	Apex Mtn Cx., Old Tom Fm	Late Devonian; Famennian	Chert	poor
10	Hope (92I/5)	C-301414	85-FC-LY1-04	Spences Bridge Group	Late Devonian; Famennian	Chert	good
9	Niddery Lake (105O/1)	C-118032	84-MJO-MM3	Earn Group	Late Devonian; Frasnian	Carbonate	moderate
8	McLeod Lake (93J/10)	C-159577	88-SCB-247	Sandpile Group	Middle Devonian	Carbonate	moderate
7	Nash Creek (106D/11)	C-176304	89-TDA-N8932	Unit 13 Green	Middle Devonian; Eifelian	Carbonate	poor
6	Sheldon Lake (105J/8)	C-087614	80-GGA-68B2	Sapper Formation	Early Devonian; Emsian	Carbonate	moderate
5	Larsen Creek (116A/11)	C-202421	93-TOA-26-5	Ogilvie Formation	Early Devonian; Emsian	Carbonate	moderate
4	Little Nahanni R (105I/6)	C-116206	84-IRJ-DDH-88-15	Road River Group	Early? Silurian	Carbonate	?mazuelloids
3	McLeod Lake (93J/10)	C-159708	88-SCBC-232	unnamed	Middle to Late Ordovician	Carbonate	poor
2	McLeod Lake (93J/15)	C-159733	88-SCBO-8A	unnamed	Ordovician	Carbonate	poor
1	Lansing Range (105N/9)	C-302368	93-RAS-326	Road River Group	Ordovician	Chert	good

FAUNAL ASSEMBLAGES

Ordovician

Radiolarians co-occur with Middle-Late Ordovician conodonts within an unnamed limestone unit of the Kechika basin in McLeod Lake (93J) area (localities 2, 3; Table 1). Those recovered to date are relatively poorly preserved. More recent mapping in the Selwyn Basin has revealed the occurrence of radiolarians from chert of the Road River Group (F. Cordey and C. Roots, unpub. data, 1995). Some of these associations are pyritized and very well preserved. One association (locality 1, Table 1) is correlative with the Middle Ordovician *Haplentactinia juncta-Inanigutta unica* Assemblage (Nazarov and Ormiston, 1993), which is one of the oldest known radiolarian faunas in North America. The fauna comprises specimens of *Inanigutta* and *Inanibigutta* (Fig. 2, no. 1-3), including *Inanibigutta* sp. aff. *aksakensis* Nazarov (Fig. 2, no. 1). Conodonts of Middle Ordovician age have also been reported from chert strata of the Road River Group (Orchard, 1986), which have excellent potential for improving our knowledge of Ordovician radiolarian taxa and biochronology.

Silurian

Silurian radiolarians have also been found within chert of the Road River Group in Lansing Range (105N) map area (F. Cordey, unpub. data, 1995), but no conodonts have yet been found within the chert. Collections from the Road River Group in both Selwyn and Kechika basins (locality 4; Table 1) contain radiolarian-like mazuelloids (Norford and Orchard, 1985),

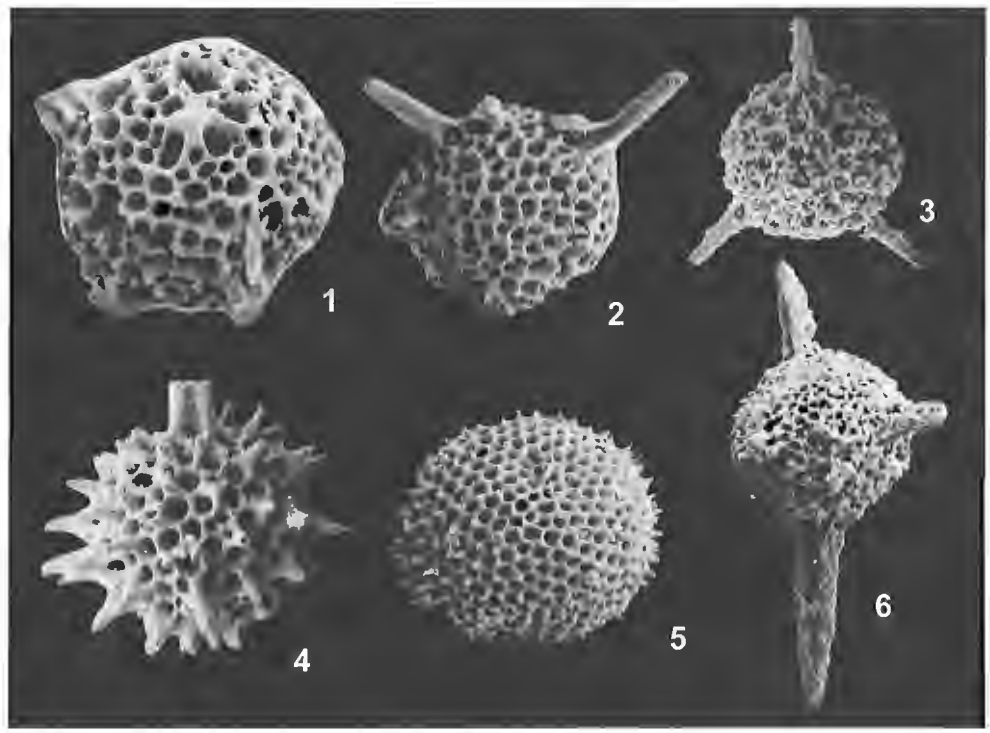

1. *Inanibigutta* sp. aff. *aksakensis* (Nazarov), Ordovician, Road River Group, Lansing Range 105N, loc. C-302368, GSC 101503, x180.
2. *Inanigutta* sp. aff. *complanata* (Nazarov), Ordovician, Road River Group, Lansing Range 105N, loc. C-302368, GSC 101504, x160.
3. *Inanibigutta* sp. aff. *excurrens* (Nazarov), Ordovician, Road River Group, Lansing Range 105N, loc. C-302368, GSC 101505, x140.
4. ?*Entactinia* sp., Late Carboniferous, Mount Christie Formation, Tay River 105K, loc. C-118137, GSC 101506, x150.
5. Spumellaria gen. sp. indet., Late Carboniferous, Mount Christie Formation, Tay River 105K, loc. C-118137, GSC 101507, x125.
6. *Entactinosphaera palimbola* (Foreman); Late Devonian (Famennian), Eam Group, Gunsteel Formation, loc. C-209161, GSC 101508, x140.

Figure 2. *Selection of Paleozoic radiolarians from the Canadian Cordillera occurring with conodonts. The following are indicated for each figure: identification, age, unit, map area, GSC locality no., GSC specimen no., and magnification.*

spherical phosphatic microfossils first reported from Silurian strata of North Greenland (Aldridge and Armstrong, 1981). The affinity of these peculiar microfossils remains undetermined.

Devonian

Early Devonian carbonates of the Ogilvie and Sapper formations (respectively Larsen Creek 116A and Sheldon Lake 105J map areas) contains conodonts dated as Emsian and moderately preserved radiolarians (localities 5, 6; Table 1).

Middle Devonian (Eifelian) conodonts co-occur with poorly preserved radiolarians in an unnamed unit of Nash Creek (106D) map area (locality 7; Table 1). This association is tentatively correlated with the *Spondentactinella windjanensis-Entactinosphaera nigra* Assemblage of Nazarov (1984).

In the allochthonous terranes of the Cordillera, radiolarians and conodonts of Late Devonian age co-occur at two localities: (1) in ribbon chert of the Old Tom Formation from Apex Mountain Complex (Quesnellia terrane) where specimens of *Entactinia* occur with *Palmatolepis minuta* (locality 11; Table 1) (Orchard, 1991); (2) in a chert pebble of the Spences Bridge Group where *Entactinia* sp. aff. *vulgaris* (Cordey, in press) occur with *Palmatolepis glabra* Ulrich and Bassler (locality 10; Table 1).

A more promising region for improving the Late Devonian radiolarian zonation is represented by the Selwyn and Kechika basins of northern British Columbia and Yukon (Tuchodi Lake 94K and Niddery Lake 105O map areas), where many carbonate samples from the Earn Group (localities 9, 12 to 22) contain rich and commonly well dated conodont fauna of Frasnian and Famennian age. Radiolarians are present in many samples, and are commonly abundant and well preserved. A preliminary assessment of these radiolarian faunas indicates that they are correlative with both the *Polyentactinia circumretia-Entactinosphaera egindyensis* and the *Tetrentactinia barysphaera-Ceratoikiscum famennium* assemblages of Nazarov and Ormiston (1993), respectively Frasnian and Famennian in age.

For example, the collection from locality 21 includes the Famennian radiolarian *Entactinosphaera palimbola* Foreman (Fig. 2, no. 6) along with conodonts correlative with the uppermost *marginifera* through Lower *trachytera* zones. Several other Famennian conodont zones are recognized in the radiolarian-bearing Earn Group (Irwin and Orchard, 1991; Paradis et al., 1996). The precision provided by these conodont associations and the good preservation of many radiolarians indicate good potential to improve the Late Devonian radiolarian zonation.

The utility of the Earn Group radiolarian assemblages is enhanced because, within the structurally complex and metalliferous Earn Group of the Selwyn and Kechika basins, they locally occur in both siliceous and carbonate facies that lack conodonts (F. Cordey and S. Paradis, unpub. data, 1994). Some of these radiolarian faunas, which may be pyritized and well preserved, have been recovered from siliceous mudstones from drill cores. Conodont faunas have also been extracted from drill core in the region, which emphasizes the general utility of both fossil groups in subsurface exploration.

Furthermore, although radiolarians of Late Devonian age are known in North America, most have been recovered from more southerly latitudes (Nazarov and Ormiston, 1993). The occurrences of well dated radiolarian associations from northern British Columbia and Yukon Territory, also have potential to provide useful biogeographic data.

Carboniferous

Sixteen localities where radiolarian-conodont associations of Early and Late Carboniferous age are known are widespread in the Cordillera. Lower Carboniferous assemblages from chert and carbonate of the Sylvester Group (localities 27 to 29) did not yield well preserved fauna so far. Moderately or well preserved radiolarian associations co-occurring with Lower Carboniferous conodonts are reported from the Earn Group (Lansing Range 105N and Niddery Lake 105O map areas) and an unnamed unit (Quiet Lake 105F map area). The associations, dated as Tournaisian or Visean (localities 23, 26), provide good potential for calibration, as well as comparison with more southerly radiolarian assemblages. One occurs in the oldest chert recovered from the Bridge River terrane (Cordey, in press), which correlates with the pre-*Albaillella pennata* 2 Zone of Holdsworth and Jones (1980), Zone Ab-4B of Cheng (1986), and the *Albaillella cartalla* and *Latentifistula concentrica* zones of Braun and Schmidt-Effing (1993).

Late Carboniferous radiolarians occur with conodonts in laminated chert of the Buttle Lake Group on Vancouver Island (locality 36, Alberni 92F map area). In Yukon Territory, associations are found within Mount Christie Formation (locality 37, Tay River 105K map area) and an unnamed unit (Larsen Creek 116A map area). More recently, radiolarians of Late Carboniferous or Early Permian age were recovered from limestone interbedded with chert within the Mount Pope sequence of the Cache Creek Group near Fort St. James (Cordey and Struik, 1996). Conodont processing from the same section is in progress.

Permian

Although Permian localities from chert of the Canadian accreted terranes are abundant (Cordey and Struik, 1996, and references therein), co-occurrences of radiolarian and conodonts within this time period are relatively uncommon. Recent progress in Paleozoic radiolarian biostratigraphy has been focused on the Permian (Ishiga, 1990; Blome and Reed, 1992; Nazarov and Ormiston, 1993, and references therein), which therefore has the most refined biostratigraphy for Paleozoic radiolarians.

We report six localities from chert of the Fennell Formation (localities 39, 40) (Orchard, 1986), and the Cache Creek Group (localities 41 to 45). Among them, locality 41 from the Marble Canyon Formation contains a very rich and well preserved fauna of Latentifistulidae, some of which remain undescribed.

FUTURE WORK

As outlined in the introduction, this report represents a preliminary assessment of the potential for Paleozoic conodont/radiolarian intercalibration in the Canadian Cordillera. Most of the radiolarian collections thus far studied have been recovered from fractions resulting from conodont processing, and therefore have not been adequately targeted for radiolarian extraction and recovery.

Future study should focus on: (1) selectively reprocessing productive chert samples, adapting the chemical extraction to optimize radiolarian recovery; and (2) examination of light fractions from carbonate samples which released conodonts and radiolarians in the heavy concentrate.

The most promising aspect of the study so far concerns the Late Devonian conodont/radiolarian collections from the Earn Group. There is clearly good potential for developing a refined Late Devonian radiolarian biozonation for the Canadian Cordillera, and applying it to exploration in the region. The discovery of well-preserved radiolarians in the Lower Paleozoic is also of particular interest for paleontological studies, *a fortiori* when these fauna are calibrated with conodonts.

ACKNOWLEDGMENTS

We thank Cordilleran geologists who collected Paleozoic microfossil samples that contributed to this study: Grant Abbott, Ken Dawson, Tekla Harms, Steve Gordey, Kim Green, Ian Jonasson, Ken McClay, Jim Monger, JoAnne Nelson, Suzanne Paradis, Vic Preto, Charlie Roots, Paul Schiarizza, Ken Shannon, Bert Struik, Dirk Tempelman-Kluit, Bob Turner, and Chris Yorath. We also thank Howard Tipper who reviewed and Bev Vanlier who edited the manuscript.

REFERENCES

Aldridge, R.J. and Armstrong, H.A.
1981: Spherical phosphatic microfossils from the Silurian of North Greenland; Nature, v. 292, p. 531-533.

Blome, C.D. and Reed, K.M.
1992: Permian and Early(?) Triassic radiolarian faunas from the Grindstone terrane, Central Oregon; Journal of Paleontology, v. 66, no. 3, p. 351-383.

Braun, A. and Schmidt-Effing, R.
1993: Biozonation, diagenesis and evolution of radiolarians in the Lower Carboniferous of Germany; in Interrad VI, (ed.) D. Lazarus and P. De Wever; Marine Micropaleontology, v. 21, p. 369-383.

Carter, E.S., Orchard, M.J., and Tozer, E.T.
1989: Integrated ammonoid-conodont-radiolarian biostratigraphy, Late Triassic Kunga Group, Queen Charlotte Islands, British Columbia; in Current Research, Part H; Geological Survey of Canada, Paper 89-1H, p. 23-30.

Cheng, Y.N.
1986: Taxonomic Studies on Upper Paleozoic Radiolaria; National Museum of Natural Science, Special Publication no. 1, Taichung-Taiwan, 311 p.

Cordey, F.
in press: Radiolaires des complexes d'accrétion cordillérains; Geological Survey of Canada, Bulletin 509.

Cordey, F. and Struik, L.C.
1996: Radiolarian biostratigraphy and implications, Cache Creek Group of Fort Fraser and Prince George map areas, central British Columbia; in Current Research 1996-E; Geological Survey of Canada.

Dumitricà, P.
1970: Cryptocephalic and cryptothoracic Nassellaria in some Mesozoic deposits of Romania; Revue roumaine de Géologie, Géophysique et Géographie, Série Géologie, Bucuresti, v. 14, p. 45-124.

Holdsworth, B.K. and Jones, D.L.
1980: Preliminary radiolarian zonation for Late Devonian through Permian time; Geology, v. 8, p. 281-285.

Irwin, S.E.B. and Orchard, M.J.
1991: Upper Devonian-Lower Carboniferous conodont biostratigraphy of the Earn Group and overlying units, northern Canadian Cordillera; in Ordovician to Triassic Conodont Paleontology of the Canadian Cordillera, (ed.) M.J. Orchard and A.D. McCracken; Geological Survey of Canada, Bulletin 417, p. 185-213.

Ishiga, H.
1990: Paleozoic Radiolarians; in Pre-Cretaceous Terranes of Japan, (ed.) K. Ichikawa, S. Mizutani, I. Hara, and A. Yao; International Geological Correlation Program Project, no. 224, Osaka, p. 285-295.

Nazarov, B.B.
1984: Radiolaria of the Paleozoic; Geological Institute Akademia Nauka, Moscow, p. 1-56.

Nazarov, B.B. and Ormiston, A.R.
1993: New biostratigraphically important Paleozoic Radiolaria of Eurasia and North America; Micropaleontology, Special Publication, no. 6, p. 22-60.

Norford, B.S. and Orchard, M.J.
1985: Early Silurian age of rocks hosting lead-zinc mineralization at Howards Pass, Yukon Territory and the District of Mackenzie and local biostratigraphy of the Road River Formation and Earn Group; Geological Survey of Canada, Paper 83-18, 35 p.

Orchard, M.J.
1986: Conodonts from western Canadian chert: their nature, distribution and stratigraphic application; in Investigative Techniques and Applications, (ed.) R.H. Austin; Ellis Horwood Limited, Chichester, p. 94-119.
1991: Conodonts, time and terranes: an overview of the biostratigraphic record in the western Canadian Cordillera; in Ordovician to Triassic Conodont Paleontology of the Canadian Cordillera, (ed.) M.J. Orchard and A.D. McCracken; Geological Survey of Canada, Bulletin 417, p. 1-26.

Paradis, S., Nelson, J.L., and Irwin, S.E.B.
1996: Conodont biostratigraphy of the Driftpile stratiform Ba-Zn-Pb deposit, Gataga district, northeastern British Columbia; in Current Research 1996-E; Geological Survey of Canada.

Pessagno, E.A., Jr. and Newport, R.L.
1972: A new technique for extracting Radiolaria from radiolarian chert; Micropaleontology, v. 2, p. 231-234.

Geological Survey of Canada Project 810028

Conodont biostratigraphy of the Driftpile stratiform Ba-Zn-Pb deposit, Gataga district, northeastern British Columbia

S. Paradis, J.L. Nelson[1], and S.E.B. Irwin[2]
Mineral Resources Division, Vancouver

Paradis, S., Nelson, J.L., and Irwin, S.E.B., 1996: Conodont biostratigraphy of the Driftpile stratiform Ba-Zn-Pb deposit, Gataga district, northeastern British Columbia; in Current Research 1996-E; Geological Survey of Canada, p. 55-64.

Abstract: The Driftpile deposit is hosted by fine-grained siliciclastic rocks of the Upper Devonian Gunsteel formation, in a series of imbricate northeastward-verging thrust panels. Mineralized units consist of two facies – localized pyrite (±sphalerite, galena), and laterally extensive barite-pyrite (±sphalerite, galena) facies. Both have a siliceous, poorly bedded, locally radiolarian-bearing shale/mudstone footwall and a concretionary and nodular shale/mudstone turbidite hanging wall.

Conodont biostratigraphy indicates that all mineralized units are mid-Famennian. The pyrite (±sphalerite, galena) unit of the "Main Zone" is *trachytera* Zone, the barite-pyrite (±sphalerite, galena) unit of the "East Zone" is early Upper *marginifera*, and the mineralized unit of the "North Trench Zone" is Lower *marginifera* Zone. The Driftpile deposit thus comprises several distinct sulphide (±barite) lenses. Centres of exhalative activity shifted from sub-basin to sub-basin through mid-Famennian time. The present deposit morphology is due to Jura-Cretaceous thrusting.

Résumé : Le gîte de Driftpile est encaissé dans des roches silicoclastiques à grains fins de la formation de Gunsteel (Dévonien moyen à supérieur) et dans une série de panneaux de charriage à vergence vers le nord-est. La minéralisation se présente sous deux formes, d'abord un faciès à pyrite (± sphalérite, galène) en amas localisés, mais aussi un faciès à barytine et pyrite (± sphalérite, galène) à grande étendue latérale. Dans les deux cas, l'éponte inférieure consiste en de l'argilite et du mudstone siliceux mal lité à radiolaires (localement), et l'éponte supérieure en de l'argilite nodulaire et du mudstone turbiditique.

La biostratigraphie des conodontes indiquent que toutes les minéralisations sont du Famennien moyen. L'unité à pyrite (± sphalérite, galène) de la «Main Zone» (secteur principal) est la zone à *trachytera*, l'unité à barytine et pyrite (± sphalérite, galène) de la «East Zone» (secteur oriental) est la zone à *marginifera* supérieur et l'unité minéralisée de la «North Trench Zone» (fosse septentrionale) est la zone à *marginifera* inférieur. Le gîte de Driftpile comprend donc plusieurs lentilles de sulfures (± barytine). Les centres d'activité exhalative se sont déplacés d'un sous-basin à l'autre durant le Famennien moyen. La morphologie actuelle du gîte découle du charriage au Jura-Crétacé.

[1] British Columbia, Ministry of Energy, Mines and Petroleum Resources, Geological Survey Branch, 1810 Blanshard Street, Victoria, British Columbia V8V 1X4
[2] GSC Pacific, Vancouver

INTRODUCTION

The Kechika Trough of northeastern British Columbia hosts one of the world's largest concentrations of sediment-hosted, stratiform lead-zinc-silver-barite and barite deposits. One of them, the Driftpile deposit, is located in the Gataga district (Fig. 1). It consists of stratiform Ba-Zn-Pb minerals interbedded with fine-grained carbonaceous and siliciclastic marine strata of the Upper Devonian Earn Group.

This paper summarizes new conodont biostratigraphic ages for the Driftpile deposit. The objectives of this project are to constrain the timing and duration of the mineralizing events at Driftpile. Due to complexly interfingering lithofacies and the intense deformation in the deposit area, it is difficult to constrain the stratigraphic position of the stratiform pyrite (±sphalerite, galena) and barite-pyrite (±sphalerite, galena) units without fossil control. Conodont biostratigraphy has been applied to

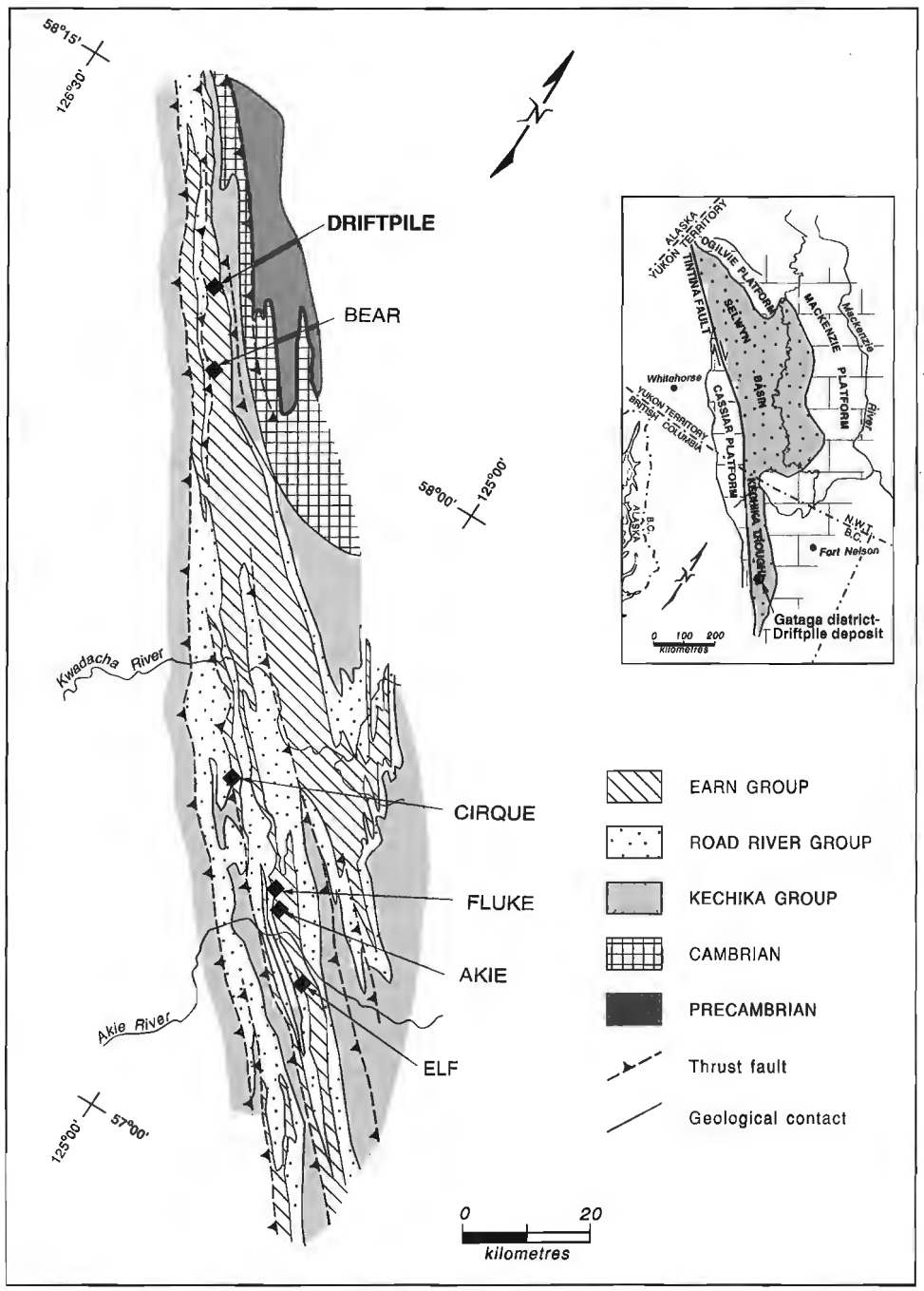

Figure 1. *Regional geology of the central and southern Kechika Trough. Geology by MacIntyre (1992) and McClay et al. (1989) for the area around the Driftpile deposit.*

determine the ages of similar deposits at Macmillan Pass, Midway, and other Gataga areas (Irwin, 1990; Irwin and Orchard, 1991).

This study forms part of a two-year multidisciplinary program in the Gataga district which began in 1994, which also includes regional mapping and geochemical studies (see Paradis et al., 1995a,b; Nelson et al., 1995; Ferri et al., 1995, 1996; Lett and Jackaman, 1995; Jackaman et al., 1996) in cooperation with the Geological Survey Branch of the British Columbia Ministry of Energy, Mines and Petroleum Resources.

METHODOLOGY

In 1994 and 1995, field logging and sampling of core was completed from 25 drillholes from mineralized zones, such as the "Main", "Camp", "East", "North Trench", and "Canyon Zone" of the Driftpile deposit (Fig. 2). Geological mapping along the Driftpile Creek was done at the scale of 1:2000 (Fig. 2B).

Over 100 samples of calcareous and carbonaceous shale, mudstone, and siltstone from drill core material of the 1980, 1993 and 1994 holes were collected and submitted to S.E.B. Irwin and M.J. Orchard (GSC) for conodont biostratigraphic and taxonomic studies. Samples weights ranged from 1 to 4 kg. The standard techniques of acetic acid dissolution, wet sieving, and heavy liquid separation were used to extract and concentrate the conodonts from the host rock (Stone, 1986). Many samples contained large amounts of barite and framboidal pyrite.

REGIONAL GEOLOGY

The Gataga district lies within the Muskwa Range of the northern Rocky Mountains, directly east of the Northern Rocky Mountain Trench strike slip fault (Gabrielse, 1985; Gabrielse et al., 1992). It includes part of the Kechika Trough, which forms the southern extension of the Lower to Mid-Paleozoic Selwyn Basin (Fig. 1). The geometry of the Kechika Trough has been interpreted either as a two-sided trough surrounded on three sides by shallower water facies (McClay et al., 1989; MacIntyre, 1992) or as a west-facing open continental slope (Gabrielse, 1985; pers. comm., 1994). It is delineated by "shale-outs" of early to mid-Paleozoic shelf and platformal successions. The stratigraphy is characterized by dark, fine-grained siliciclastic rock and chert, representing quiet, deep water deposition. This environment of slow sedimentation coupled with tectonism was conducive to the formation of sedimentary exhalative deposits at various times within the basin. Several episodes of sedimentary exhalative barite and barite-sulphide mineralization occurred in the Kechika Trough: Middle Ordovician, Early Silurian, and Late Devonian. Clastic rocks of the Upper Devonian lower Earn Group host regionally extensive stratiform SEDEX barite-sulphide deposits, including Driftpile, Bear, Cirque, Akie, and Fluke (Fig. 1).

The Earn Group lithologies and their tectonic setting represent a tensional regime that resulted either from continental rifting and strike-slip faulting (Abbott et al., 1986), or from flexural extension during foreland deformation related to the Antler orogeny (Smith et al., 1993). The Earn Group has been subdivided into three informal formations, Gunsteel, Akie, and Warneford, by Jefferson et al. (1983), Pigage (1986) and MacIntyre (1992). The Gunsteel formation of Middle to Late Devonian age is equivalent to the lower Earn Group which hosts Driftpile, Bear, Akie, Fluke, and Cirque in the Gataga district, and Tom and Jason in the Macmillan Pass area of eastern Yukon. The lower Earn Group is typically carbonaceous and siliceous, and includes cherty argillite, radiolarian chert, siliceous carbonaceous shale, carbonaceous chert, and fine-grained turbidite sandstone, siltstone, and mudstone.

Jura-Cretaceous crustal shortening of the ancestral North America continental margin deformed the Paleozoic to Mississippian strata of the Gataga district into a complex, mainly northeast-verging fold and thrust belt. McClay et al. (1989) recognized five major thrust panels, defined by rocks of different stratigraphic levels and/or contrasting lithofacies. Within each major panel, the strata are folded and stacked in duplexes. The thrust faults that bound the major panels may be reactivated Paleozoic growth faults. The Upper Devonian sediment-hosted stratiform barite-sulphide units occur in the central thrust panel. A stack of upper Road River and Earn Group horsts is exposed within this panel, bounded by décollements at the base of the upper Road River Group and within the Earn Group.

The geology of the Gataga district is more thoroughly described by MacIntyre (1992) and Ferri et al. (1995, 1996).

GEOLOGY OF THE DRIFTPILE DEPOSIT

Overview

The Driftpile property is underlain by northwest-trending variably carbonaceous and siliceous black shale and argillite, silty shale, siltstone, and chert of the Upper Devonian Gunsteel formation (Fig. 2). Gunsteel exposures are bounded to the west by the Mount Waldemar fault, which carries Middle Devonian to Ordovician rocks of the Road River Group in its hanging wall, and to the east by Paleozoic carbonates of the MacDonald Platform.

Barite and/or pyritic shale with local concentrations of sphalerite and galena are interbedded with the carbonaceous and siliceous fine-grained siliciclastic rocks of the lower Earn Group in several thrust-bounded panels (Fig. 2).

Conodont faunas collected within the barite-sulphide units and their host rocks range from the Upper *triangularis* Zone to the Upper *trachytera* Zone, indicating an early to mid-Famennian age.

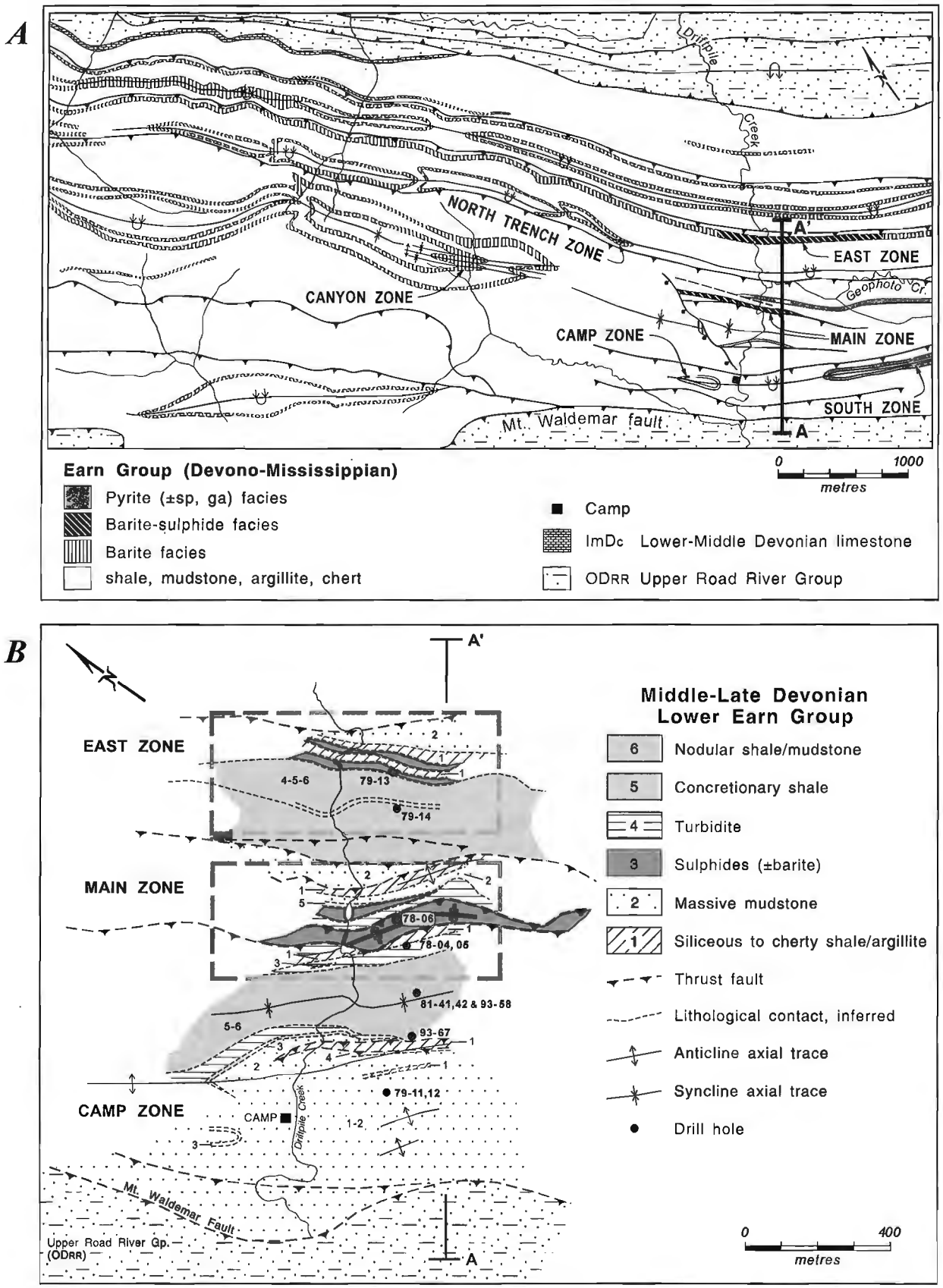

Figure 2. *A) Simplified geology of the Driftpile property. After Insley (1990), with modifications in the southeast corner from drilling and mapping by Teck Exploration Ltd. in 1993 and 1994. The A-A' is also located in Figure 2B, and the cross-section A-A' is Figure 3.* ***B)*** *Detailed geology of the Driftpile Creek area and location of drillholes.*

Stratigraphy and mineralization

The stratigraphy and the mineralization of the Driftpile deposit area has been described in detail by Farmer et al. (1994), Paradis et al. (1995a), and Farmer and Stewart (unpublished report to Teck Exploration, 1995). Only a summary is presented here.

Footwall rocks to the mineralized units 3A and 3B consist of variably siliceous and carbonaceous shale, argillite, and mudstone (Fig. 3). They include massive, homogeneous, in part siliceous black shale and mudstone (unit 2), well-laminated siliceous to cherty carbonaceous radiolarian-bearing shale and argillite (unit 1), and locally a concretionary shale (unit 5). A cryptic pyrite laminated mudstone, characterized by distinctive millimetre-scale pyrite laminations, is commonly present as metre-thick interbeds in units 1 and 2. Farmer and Stewart (unpublished report to Teck Exploration, 1995) suggested that it may represent a distal expression of the mineralized units, as it tends to occur below or lateral to the mineralized units. Contact between footwall and mineralized rocks is sharp and conformable where not faulted.

Mineralized units consist of a pyrite (±sphalerite, galena) facies (unit 3A) and a barite-pyrite (±sphalerite, galena) facies (unit 3B) (Fig. 3). This bimodal occurrence is also observed elsewhere in the Kechika Trough and the Selwyn Basin (Dawson and Orchard, 1982).

Unit 3A consists of massive to laminated spheroidal and framboidal pyrite (30-75 volume per cent) associated with subordinate amounts of fine-grained sphalerite and galena, and recrystallized carbonate concretions and fragments interbedded with carbonaceous siliceous shale/mudstone and chert. The abundance of recrystallized carbonate concretions are a distinctive feature of this unit. The laminations are strongly deformed, microfolded and deflected around the carbonate concretions. The lowest beds of unit 3A tend to be more thickly laminated, banded or massive and may include fine-grained galena and finely laminated sphalerite. Pyrite occurs either as euhedral grains and aggregates of grains or, most commonly, as framboidal/spheroidal recrystallized clusters. The latter forms the massive pyritic ore facies. Sphalerite occurs as intergrowths and interstitial grains and as fine-grained laminations. Galena occurs principally as coarse-grained recrystallized aggregates and as remobilized fracture and veinlet infillings. Laminae of black cherty mudstone/shale are scarce within the massive section of the mineralized units but increase upwards. Unit 3A is commonly gradational upwards into a "transitional unit" that consists of alternating beds of mudstone/shale (50-70 volume per cent) and pyrite (±sphalerite, galena) facies.

Unit 3B is regionally extensive. Some units can be followed more or less continuously over a strike length of 50 km, complexly repeated by folding and thrust faulting (McClay et al., 1988; McClay, 1991). In the "Main Zone", unit 3B has

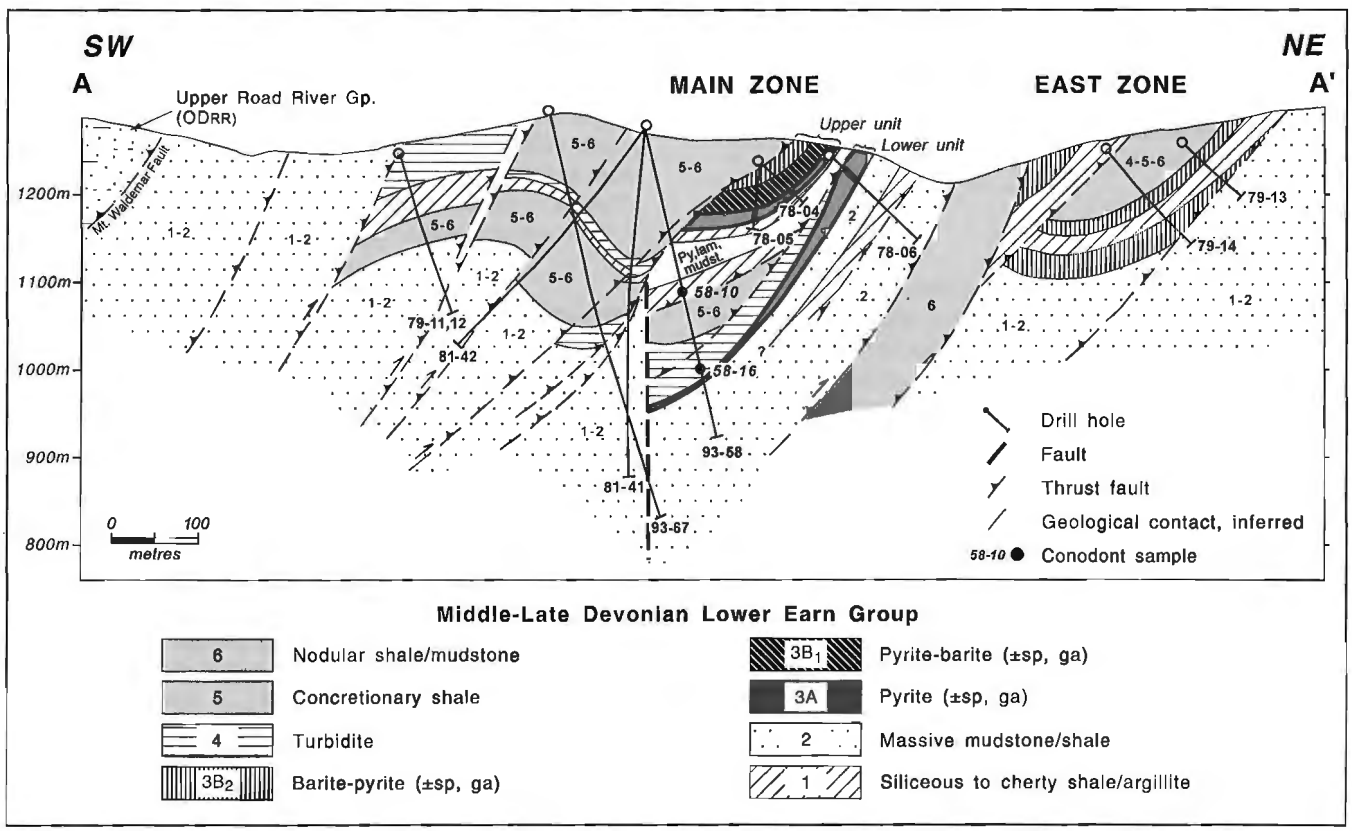

Figure 3. *Stratigraphic section along the Driftpile Creek area (location see Fig. 2A, B). Abbreviations: py = pyrite, lam = laminated, mudst = mudstone.*

been divided into 2 subfacies - a lower pyrite-rich (3B1) and an upper barite-rich (3B2) facies (Fig. 3). Both consist of variable proportions of rhythmically interbedded laminated pyrite, massive, laminated, and blebby barite, siliceous argillite and chert, and subordinate amounts of sphalerite and galena. Unit 3B1 consists of up to 70 volume per cent of pyrite laminae interbedded with beds of blebby barite and siliceous black argillite. Massive, poorly laminated pyrite (and minor sphalerite and galena) occurs at the base of this unit. Unit 3B1 grades upwards into unit 3B2. The latter consists of beds of blebby and laminated barite (up to 60 volume per cent) and variable amounts of laminated pyrite (minor sphalerite and galena) interbedded with massive siliceous black argillite. One surface expression of this unit at Driftpile is an orange to pale brown weathering gossan called the "barite kill-zone".

Contacts between the mineralized and the hanging wall units are gradational over tens of metres. The hanging wall to both mineralized facies consists of a laminated turbidite lithofacies (unit 4) overlain by a concretionary shale/mudstone (unit 5) and a nodular shale/mudstone (unit 6), all in gradational contact as the frequency of the laminae (pyrite and/or barite, siltite, and shale) diminishes and bedding thickness increases up-section. Unit 4 includes a lower, well laminated pyrite-rich mudstone grading upward into a well laminated but pyrite-poor mudstone. Carbonate concretions are common. They increase in size but diminish in frequency up-section, and their degree of recrystallization diminishes away from the mineralized units. Unit 5 consists of a moderately laminated, medium-bedded grey to black shale/mudstone with abundant (10-30 volume per cent) carbonate concretions. Unit 6 is a grey to black, thick bedded, poorly to moderately laminated lithofacies which contains millimetre-sized mudstone (±calcite, barite, pyrite) nodules, and sporadically distributed carbonate concretions (<1 volume per cent). It is the most common lithology in the Driftpile Creek area.

Structure

The structure at Driftpile is dominated by northeastward-vergent thrust panels, and related folds that trend northwest and plunge gently (10-20°) northwest (see Fig. 2, 3). The fold and thrust patterns result in intense imbrication and repetition of strata in a northeast direction, whereas units, notably the barite-sulphide units, tend to be laterally continuous in a northwest direction, parallel to the structural grain. Thrust faults dip moderately southwest. The most notable thrust fault in the Driftpile deposit area is the Mount Waldemar, which places Ordovician to Middle Devonian Road River rocks over Gunsteel stratigraphy.

Within the thrust panels, strata are folded with moderately southwest-dipping to vertical axial planes and gently northwest-plunging fold axes. Folds are open, upright and somewhat symmetrical away from the thrust faults, and tight and asymmetric (commonly overturned) adjacent to them. Small-scale upright chevron folds are developed in the cores of larger folds. This feature renders vergence data from the sparse outcrops in the Driftpile Creek valley of equivocal value in interpretation of large-scale structures. In the central part of the section, a southwest-dipping reverse fault offsets the western limb of a syncline and also truncates a possible syn-sedimentary fault in its footwall (Fig. 3). In drill core, this fault and others with demonstrable offsets are expressed as crush zones several metres wide. In addition to these obvious brittle shears, conodont data have helped to identify a cryptic bedding-parallel thrust fault within the "Main Zone" (see below), which duplicates the mineralized units of the "Main Zone" (Fig. 3).

Axial planar cleavage is penetrative in argillaceous lithologies; cleavage-bedding angles are typically moderate to large, in keeping with the open nature of the folds. The mineralized units have undergone intense deformation due to folding, cleavage development, and imbrication (McClay and Insley, 1986; McClay, 1991; Insley, 1990, 1991). In their vicinity, bedding is transposed into cleavage and mesoscopic folds are abundant. It is likely that the more ductile sulphides folded disharmonically and were thickened in fold hinges to a greater extent that their host argillaceous rocks.

BIOSTRATIGRAPHY

Introduction

Samples were collected from the footwall rocks, mineralized units, and hanging wall rocks of the "Main", "South", "Camp", "North Trench", and "East" zones of the Driftpile deposit. So far, of the 118 samples collected, 24 produced conodonts of Late Devonian age, i.e. early to mid-Famennian *triangularis to trachytera* zones (Fig. 4).

Conodonts undergo sequential colour changes with increasing temperature. The colour changes are produced by progressive carbonization and eventual distillation of organic matter within the conodont skeletal tissue. All of the conodonts collected at Driftpile had a colour alteration index (CAI) value of 5, indicative of temperatures of 300°C+. Proximity to the mineralized units does not affect this value.

General remarks

In this paper, we employ a form taxonomy in describing the platform conodonts of the Earn Group. This reflects the current state of knowledge, the basis of the standard zonation, and the fact that Earn Group conodont collections include few well preserved non-platform elements. Recent revisions to Upper Devonian zonation by Ziegler and Sandberg (1990) have used conodonts entirely from the *Palmatolepis* biofacies. We have adopted a modified form of that standard for the Earn Group.

Results of preliminary conodont biostratigraphic studies within the Earn Group have been presented by Dawson and Orchard (1982), Gordey et al. (1982), Orchard and Irwin (1988), Orchard (1989), Irwin and Orchard (1989), Irwin (1990), Irwin and Orchard (1991), and Paradis et al. (1995b). Prior to these studies, the stratigraphy of the Earn Group was very poorly understood, partly due to the structural complexity, the monotony of the lithologies, the lack of diagnostic macrofossils, and the lack of reliable marker horizons. The

conodonts provide important age constraints on the lithofacies variation, the intra-Earn Group discontinuities, and the sedimentary exhalative barite-sulphide units.

Results

The Driftpile deposit area is dominated by the offshore and deep water *Palmatolepis* faunas characteristic of the Upper Devonian (Ziegler and Sandberg, 1990) (Plate 1). Conodont faunas range from the lowermost Famennian Upper *triangularis* Zone to the middle Famennian Upper *trachytera* Zone (Fig. 4). The whole Famennian is about 7 million years in duration, from 367 to 360 million years, therefore one conodont zone is approximately 1 million year in duration.

The pyrite (±sphalerite, galena) unit (3A) of the "Main Zone" is dated by conodont faunas as Uppermost *marginifera* through *trachytera* Zone, the youngest event that we have documented at Driftpile (Fig. 5). The barite-pyrite unit (3B) of the "East Zone" is well constrained in the lower part of the Upper *marginifera* Zone. The pyrite (±sphalerite, galena) unit (3A) of the "North Trench Zone" is also tightly constrained in the Lower *marginifera* Zone, the oldest event so far recognized. These results suggest that the mineralization at the "North Trench" and at the "East" zones were less than 0.5 million year in duration.

The pyrite (±sphalerite, galena) unit of the "South Zone" is less tightly constrained by conodont faunas, which indicate a broad range of Lower *marginifera* through Upper *trachytera* zones (Fig. 4). The pyrite (±sphalerite, galena) unit of the "Camp Zone" has also a fairly broad range of Upper *marginifera* through Upper *trachytera* zones. Mineralization of these two zones could be of the same age as the "Main Zone" or as the "East Zone". A better resolution of these time ranges is required to solve this problem.

Samples 66-4, 59-10, and 62-10 of the "Main Zone" (see Fig. 3) indicate that footwall rocks to the "lower unit" (3A) range in age from Upper *triangularis* up through the lower part of the Lower *trachytera* zones. The uppermost *marginifera* through Lower *trachytera* sample lies structurally below sample 58-10 (Upper *triangularis* to Upper *crepida*) from the footwall to the structurally higher "upper unit" (3A, 3B2, 3B1) of the "Main Zone". This structural age reversal implies the presence of a cryptic bedding-parallel thrust fault that duplicates the mineralized units, and that puts older on younger rocks.

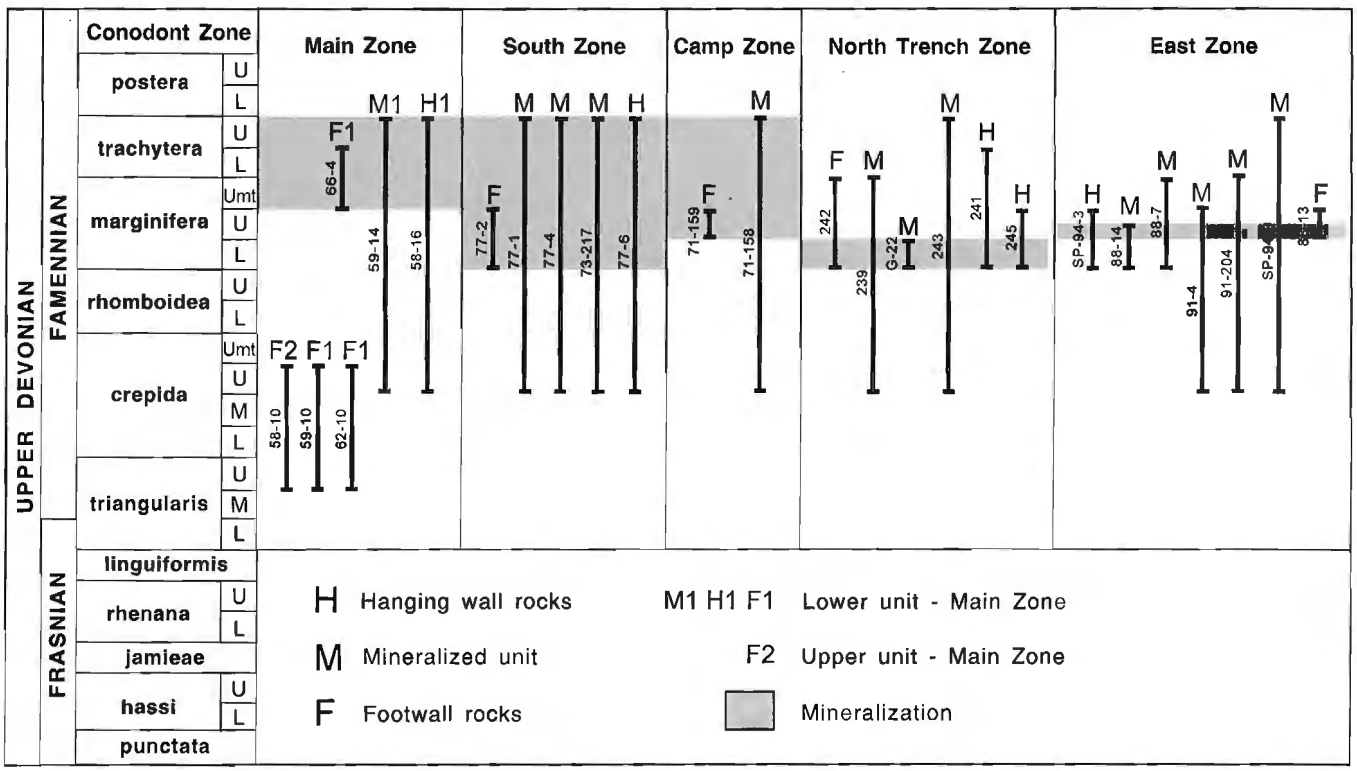

Figure 4. *Range for Famennian faunas recognized at Driftpile using the revised international standard Upper Devonian conodont zonation of Ziegler and Sandberg (1990). Abbreviations: Umt = Uppermost, U = Upper, M = Middle, and L = Lower.*

PLATE 1
(Localities are described in Table 1).

1. *Palmatolepis glabra acuta* Helms 1963. GSC 101681, x70, GSC Loc. No. C-209198.
2. *Palmatolepis glabra distorta* Branson & Mehl 1934. GSC 101682, x70, GSC Loc. No. C-209192.
3. *Palmatolepis rugosa trachytera* Ziegler 1960. GSC 101683, x70, GSC Loc. No. C-209161.
4. *Palmatolepis glabra prima* Ziegler & Huddle 1969. GSC 101684, x70, GSC Loc. No. C-209192.
5. *Palmatolepis glabra pectinata* Ziegler 1962. GSC 101685, x70, GSC Loc. No. C-209198.
6. *Palmatolepis marginifera utahensis* Ziegler & Sandberg 1984. GSC 101686, x70, GSC Loc. No. C-302197.
7. *Palmatolepis marginifera marginifera* Helms 1959. GSC 101687, x70, GSC Loc. No. C-209165.
8. *Palmatolepis glabra lepta* Zeigler & Huddle 1969. GSC 101688, x70, GSC Loc. No. C-302197.

DISCUSSION

Geological mapping in the Driftpile Creek area (Fig. 2), core logging, construction of an east-west stratigraphic section (Fig. 3), and conodont age dating (Fig. 4) provide a preliminary stratigraphic and structural framework for the stratiform pyrite (±sphalerite, galena) and barite-pyrite (±sphalerite, galena) mineralization at Driftpile (Nelson et al., 1995; Paradis et al., 1995a). Imbricated, internally folded thrust panels host separate mineralized bodies, such as the "Main", "East", "North Trench", "Camp", and the "South" zones.

A key problem in the interpretation of the Driftpile deposit is: do these thrust-bounded mineralized zones represent stratigraphically distinct bodies, or are they lateral facies variation with the barite-pyrite (±sphalerite, galena) facies (unit 3B) forming an apron outboard to the pyrite (±sphalerite, galena) facies (unit 3A)? For instance, according to Insley (1990), unit 3B occurs in all cases either stratigraphically above unit 3A, or flanking it. In this model the baritic unit should be either coeval with or younger than the pyrite-dominated unit.

Conodont age dating has established the beginnings of a biostratigraphic framework at Driftpile. Unit 3A has returned both the oldest and the youngest ages for mineralizing events: the oldest in the "North Trench Zone" within the Lower *marginifera* Zone, and the youngest event in the lower unit of the "Main Zone" in the upper *marginifera* through *trachytera* zones. Unit 3B in the "East Zone" (Upper *marginifera* Zone) is intermediate in age between these two 3A occurrences. Therefore the stratigraphy of mineralized units at Driftpile is much more complex than previously understood. There is no fixed sequence of pyrite-dominated and barite-dominated units. Moreover, each well-dated mineralized unit is different in age from the others, suggesting that the centres of mineralization may have shifted from sub-basin to sub-basin through time. Finally, the apparent stratigraphic sequence within the "Main" Zone, with a barite-dominated unit above a pyrite-dominated unit (Fig. 3), is shown to be the result of bedding-parallel thrust imbrication prior to the development of the steep thrust faults.

Table 1. Locality Registry

GSC Loc. No. C-209198. Sample no. 94-SP-GH-93-88-14, Tuchodi Lakes Map Area (94K/4), 58°4'6", 125°54'35". Limestone in the Earn Group.

GSC Loc. No. C-209192. Sample no. 94-SP-GH-SP-94-3, Tuchodi Lakes Map Area (94K/4), 58°4'12", 125°54'12". Limestone in the Earn Group.

GSC Loc. No. C-209161. Sample no. 94-SP-GH-93-66-4, Tuchodi Lakes Map Area (94K/4), 58°4', 125°54'50". Limestone in the Earn Group.

GSC Loc. No. C-209165. Sample no. 94-SP-GH-94-77-2, Tuchodi Lakes Map Area (94K/4), 58°4', 125°54'50". Limestone in the Earn Group.

GSC Loc. No. C-302197. Sample no. 94-SP-GH-94-88-13, Tuchodi Lakes Map Area (94K/4), 58°4',125°54'50". Calcareous, laminated siltite in the Earn Group.

SUMMARY

Biostratigraphy of the lower Earn Group at Driftpile defines at least three cycles of mineralization during mid-Famennian time, each preceded by a period of anoxic, starved sedimentation (as evidenced by the footwall siliceous shale and radiolarian chert; unit 1) and succeeded by an influx of fine-grained distal mud turbidites (unit 4) and concretionary shale and nodular shale/mudstone (units 5 and 6). The footwall rocks represent a period of anoxic, starved sedimentation and tectonic quiescence, whereas the mineralizing events and the onset of the turbidite accumulation represent a period of tectonic activity. Each episode of mineralization seems to have been of short duration, as demonstrated for the "North Trench Zone" and the "East Zone". The centres of exhalative activity shifted from place to place within the Driftpile area through the mid-Famennian time. The present deposit morphology is due to polyphase Jura-Cretaceous thrusting superimposed on an already-complex stratigraphy.

ACKNOWLEDGMENTS

The authors are very grateful to R. Farmer and H. Stewart of Teck Exploration Ltd., and to K. Thorsen of Teck Corporation for lively exchange of ideas, for technical support in the field, and for providing access to property and data.

We are extremely grateful to Carole Augereau for her assistance in the field. Drafting was done by Verna Vilkos and Tonia Williams. M.J. Orchard (GSC) reviewed the manuscript.

REFERENCES

Abbott J.G., Gordey, S.P., and Tempelman-Kluit, D.J.
1986: Setting of stratiform, sediment-hosted Pb-Zn deposits in Yukon and northeastern British Columbia; Canadian Mining and Metallurgical Bulletin, Special Volume 37, p. 1-18.

Dawson, K.M. and Orchard, M.J.
1982: Regional metallogeny of the Northern Cordillera: biostratigraphy, correlation and metallogenic significance of bedded barite occurrences in eastern Yukon and western District of Mackenzie; in Current Research, Part C; Geological Survey of Canada, Paper 82-1C, p. 31-35.

Farmer, R., Oliver, J., and Evans, G.
1994: Diamond Drilling on the Driftpile Creek Property (P, D, Goof and Pook Claims), Liard Mining Division NTS 94K/4W, 58°04' North, 125°55' West; British Columbia Ministry of Energy, Mines and Petroleum Resources, Assessment Report.

Ferri, P.F., Nelson J.L., and Rees, C.
1995: Geology and mineralization of the Gataga river area, Northern Rocky Mountains (94L/7, 8, 9, and 10); in Geological Fieldwork 1994, (ed.) B. Grant, and J.M. Newell; British Columbia Ministry of Energy, Mines and Petroleum Resources, Geological Survey Branch, Paper 1995-1, p. 277-298.

Ferri, P.F., Rees, C., and Nelson, J.L.
1996: Geology and mineralization of the Gataga mountain area, Northern Rocky Mountains (94L/10, 11, 14 and 15); in Geological Fieldwork 1995, (ed.) B. Grant, and J.M. Newell; British Columbia Ministry of Energy, Mines and Petroleum Resources, Geological Survey Branch, Paper 1996-1, p. 137-154.

Gabrielse, H.
1985: Major dextral transcurrent displacements along the northern Rocky Mountain trench and related lineaments in north-central British Columbia; Geological Society of America Bulletin, v. 96, p. 1-24.

Gabrielse, H., Monger, J.W.H., Wheeler, J.O., and Yorath, C.J.
1992: Part A. Morphogeological belts, tectonic assemblages and terranes; in Chapter 2 of Geology of the Cordilleran Orogen in Canada, (ed.) H. Gabrielse and C.J. Yorath; Geological Survey of Canada, Geology of Canada, no. 4, p. 15-28.

Gordey, S.P., Abbott, J.G., and Orchard, M.J.
1982: Devono-Mississippian (Earn Group) and younger strata in east-central Yukon; in Current Research, Part B; Geological Survey of Canada, Paper 82-1B, p. 93-100.

Insley, M.W.
1990: Sedimentology and geochemistry of the Driftpile Ba-Fe-Zn-Pb mineralization, northeastern British Columbia; Ph.D. thesis, Royal Holloway and Bedford New College, University of London, 377 p.
1991: Modification of sedimentary barite textures during deformation, Gataga District, NE British Columbia; Ore Geology Reviews, v. 6, p. 463-473.

Irwin, S.E.B.
1990: Late Devonian conodont biostratigraphy of the Earn Group with age constraints for stratiform mineral deposits, Selwyn and Kechika basins, northern British Columbia; M.Sc. thesis, University of British Columbia, Vancouver, British Columbia, 311 p.

Irwin, S.E.B. and Orchard, M.J.
1989: Conodont biostratigraphy and constraints on Upper Devonian mineral deposits in the Earn Group, northern British Columbia and Yukon; in Current Research, Part E; Geological Survey of Canada, Paper 89-1E, p. 13-19.
1991: Upper Devonian – Lower Carboniferous conodont biostratigraphy of the Earn Group and overlying units, northern Canadian Cordilleran; in Ordovician to Triassic Conodont Paleontology of the Canadian Cordillera, (ed.) M.J. Orchard and A.D. McCracken; Geological Survey of Canada, Bulletin 417, p. 185-203.

Jackaman, W., Cook, S., Lett, R., Sibbick, S., and Matysek, P.
1996: 1995 Regional geochemical survey program: review of activities; in Geological Fieldwork 1995, (ed.) B. Grant, and J.M. Newell; British Columbia Ministry of Energy, Mines and Petroleum Resources, Geological Survey Branch, Paper 1996-1, p. 181-183.

Jefferson, C.W., Kilby, D.B., Pigage, L.C., and Roberts, W.J.
1983: The Cirque barite-lead-zinc deposits, northeast British Columbia; in Sediment-hosted Stratiform Lead-zinc Deposits, (ed.) D.F. Sangster; Mineralogical Association of Canada, Short Course Handbook, v. 8, p. 121-140.

Lett, R.E. and Jackaman, W.
1995: Geochemical orientation survey in the Driftpile Creek area, northeastern, B.C. (94K, L); in Geological Fieldwork 1994, (ed.) B. Grant, and J.M. Newell; British Columbia Ministry of Energy, Mines and Petroleum Resources, Geological Survey Branch, Paper 1995-1, p. 269-275.

MacIntyre, D.G.
1992: Geological setting and genesis of sedimentary exhalative barite and barite-sulphide deposits, Gataga district, northeastern British Columbia; Canadian Mining and Metallurgical Bulletin, Exploration and Mining Geology, v. 1, no. 1, p. 1-20.

McClay, K.R.
1991: Deformation of stratiform Zn-Pb (-barite) deposits in the northern Canadian Cordillera; Ore Geology Reviews, v. 6, p. 435-462.

McClay, K.R. and Insley, M.W.
1986: Structure and mineralization of the Driftpile Creek area, northeastern British Columbia (94E/16, 94F/14, 94K/4, 94L/1); in Geological Fieldwork 1985; British Columbia Ministry of Energy, Mines and Petroleum Resources, Geological Survey Branch, Paper 1986-1, p. 343-350.

McClay, K.R., Insley, M.W., Way, N.A., and Anderton, R.
1988: Tectonics and mineralization of the Kechika Trough, Gataga area, northeastern British Columbia; in Current Research, Part E; Geological Survey of Canada, Paper 88-1E, p. 1-12.

McClay, K.R., Insley, M.W., and Anderton, R.
1989: Inversion of the Kechika Trough, northeastern British Columbia, Canada; in Inversion and Tectonics, (ed.) M.A. Cooper and G.D. Williams; Geological Society of London, Special Publication No. 44, p. 235-257.

Nelson, J.L., Paradis, S., and Farmer, R.
1995: Geology of the Driftpile stratiform Ba-Fe-Zn-Pb deposit, north-central British Columbia; in Geological Fieldwork 1994, (ed.) B. Grant, and J.M. Newell, British Columbia Ministry of Energy, Mines and Petroleum Resources, Geological Survey Branch, Paper 1995-1, p. 261-268.

Orchard, M.J.
1989: Conodonts from the Frasnian-Famennian boundary interval in western Canada; in Devonian of the world, (ed.) N.J. McMillan, A.F. Embry, and D.J. Glass; Canadian Society of Petroleum Geologists, Memoir 14, p. 35-52.

Orchard, M.J. and Irwin, S.E.B.
1988: Conodont biostratigraphy, Midway property, northern British Columbia (104/O16); in Geological Fieldwork 1987; British Columbia Ministry of Energy, Mines and Petroleum Resources, Geological Survey Branch, Paper 1988-1, p. 249-253.

Paradis, S., Nelson, J.L., and Farmer, R.
1995a: Stratigraphy and structure of the Driftpile stratiform Ba-Zn-Pb deposit, Gataga area, northeastern British Columbia; in Current Research 1995-A; Geological Survey of Canada, p. 149-157.

Paradis, S., Nelson, J.L., and Farmer, R.
1995b: Stratigraphy and mineralization of the Driftpile stratiform Ba-Zn-Pb Sedex deposit, northeastern British Columbia; abstract in Geological Association of Canada, annual meeting, Victoria'95, v. 20, p. A-80.

Pigage, L.C.
1986: Geology of the Cirque barite-zinc-lead-silver deposits, northeastern British Columbia; in Mineral Deposits of Northern Cordillera, (ed.) J. Morin; Canadian Mining and Metallurgical Bulletin, Special Volume 37, p. 71-86.

Smith, M.T., Dickinson, W.R., and Gehrels, G.E.
1993: Contractional nature of Devonian-Mississippian Antler tectonism along the North American continental margin; Geology, v. 21, p. 21-24.

Stone, J.
1986: Review of investigative techniques used in the study of conodonts; in Conodonts: Investigative Techniques and Applications, (ed.) R.L. Austin; The British Micropalaeontological Society, Ellis Horwood Ltd., p. 19-34.

Ziegler, W. and Sandberg, C.A.
1990: The Late Devonian standard conodont zonation; Courier Forschungsinstitut Senckenberg, no. 121, 115 p.

Geological Survey of Canada Project 740098

An overview of xenolith-bearing Neogene to Recent volcanics in the northern Cordillera

T.S. Hamilton, J. Dostal[1], and J.M. Shaw[2]
GSC Pacific, Sidney

Hamilton, T.S., Dostal, J., and Shaw, J.M., 1996: An overview of xenolith-bearing Neogene to Recent volcanics in the northern Cordillera; in Current Research 1996-E; Geological Survey of Canada, p. 65-75.

Abstract: During August 1994 and July 1995 xenoliths were collected from 19 Neogene to Recent volcanic centres in the northern Cordillera including: Prindle (Alaska); 60 Mile, Clinton Creek, 40 Mile, Ne Che Dhawa, Alligator Lake (Yukon); Ruby Mountain, Cracker Creek, Volcano Creek, Chikoida Mountain, Llangorse, Ash Mountain, 3 Caribou Tuya, South Tuya, Matthews Tuya, Castle Rock, Maitland Creek, Aiyansh/Tseax River, and Summit Lake (British Columbia). This report presents the locations, xenolith types, and preliminary descriptions. Xenoliths types include: depleted and undepleted spinel lherzolite, clinopyroxene megacrysts, clinopyroxenite, gabbro, and granitic and metamorphic rocks (including granulite facies banded gneiss). Microprobe analyses for olivine, orthopyroxene, and clinopyroxene from peridotite xenoliths in three of the centres are consistent with a mantle paragenesis.

The xenoliths are the foundation for ongoing petrological studies of the Cordilleran crust and upper mantle. They represent the only physical samples of the northern Cordilleran subsurface geology available to constrain the geophysics from the Lithoprobe SNORCLE transects.

Résumé : En août 1994 et en juillet 1995, des xénolites ont été échantillonnés dans dix-neuf centres volcaniques datant du Néogène à l'Holocène dans la partie nord de la Cordillère; les centres sont les suivants : Prindle (Alaska); 60 Mile, Clinton Creek, 40 Mile, Ne Che Dhawa et Alligator Lake (Yukon); Ruby Mountain, Cracker Creek, Volcano Creek, Chikoida Mountain, Llangorse, Ash Mountain, 3 Caribou Tuya, South Tuya, Mathew's Tuya, Castle Rock, Maitland Creek, Aiyansh/Tseax River et Summit Lake (Colombie-Britannique). Dans le présent rapport, les auteurs précisent l'emplacement des centres volcaniques, citent les divers types de xénolites et en donnent une description provisoire. Les types de xénolites observés sont les suivants : lherzolite à spinelle (appauvrie et non appauvrie), mégacristaux de clinopyroxène, clinopyroxénite, gabbro, roches granitiques et roches métamorphiques (incluant des gneiss rubanés métamorphisés au faciès des granulites). Des analyses à la microsonde de cristaux d'olivine, d'orthopyroxène et de clinopyroxène provenant de xénolites de péridotite échantillonnés dans trois des centres mettent en évidence une paragenèse mantellique.

Les xénolites sont le fondement d'études pétrologiques actuellement menées sur la croûte et le manteau supérieur de la Cordillère. Ils représentent les seuls exemples physiques donnant une idée de la géologie en subsurface dans la partie nord de la Cordillère et permettant de corroborer les caractéristiques géophysiques établies dans le cadre des travaux associés au transect SNORCLE du Lithoprobe.

[1] Department of Geology, St. Mary's University, Halifax, Nova Scotia B3H 3C3
[2]Mineral Resources Division, Ottawa

INTRODUCTION

Upper mantle xenoliths occur in many of the Neogene to Recent basaltic volcanic centres in the northern Cordillera (Fig. 1; Littlejohn and Greenwood, 1974; Nicholls et al., 1982). Some of the volcanic centres are large and long-lived (Mount Edziza; Hamilton, 1990; Souther, 1992), while others are monogenetic cinder cones and isolated flows. All of the centres numbered on Figure 1 are characterized briefly in Table 1 with references to previous work.

New xenolith lithologies include: mantle derived ultramafic rocks of the spinel lherzolite suite, granulites and gabbros from deep in the crust, and rocks resembling the upper crustal geology adjacent to the volcanic vents. An attempt was made to sample the available xenolith diversity and the largest and freshest samples available. This paper provides an index to the xenolith localities sampled during the 1994-1995 field seasons and a brief description of each site.

In Alaska, Yukon, and northern British Columbia the Tertiary volcanics sample deep crustal xenoliths from beneath the pericratonic Yukon-Tanana terrane and oceanic Stikinia. These samples address the basement to the accreted terranes of the northern Cordillera. Granulites, collected at Prindle (Foster et al., 1966), Alligator Lake (Eiche et al., 1987), and Castle Rock (Littlejohn and Greenwood, 1974), will afford a look at the lower crustal composition and formation; and provide important ground truth apropos lithology, age, and physical properties.

DESCRIPTION OF CENTRES SAMPLED IN 1994 AND 1995

Xenoliths were collected from nineteen Neogene to Recent volcanic centres in the northern Cordillera including: Prindle (Alaska); 60 Mile, Clinton Creek, 40 Mile, Ne Che Dhawa, Alligator Lake (Yukon); and Ruby Mountain, Cracker Creek, Volcano Creek, Chikoida Mountain, Llangorse, Ash Mountain, 3 Caribou Tuya, South Tuya, Mathews Tuya, Castle Rock, Maitland Creek, Aiyansh/Tseax River, and Summit Lake (British Columbia). Locations are shown on Figure 1. Brief descriptions of the geology and xenolith suite at each of the sites is listed below, wherein numbers in parentheses correspond to Table 1.

Alaska/Yukon Territory

Prindle Volcano (1)

Prindle Volcano (Fig. 1, 2a) is a breached basanite cinder cone (1 km by 150 m) and flow built on the Yukon-Tanana upland and allochthonous terrane (Foster, 1990) . Situated 30 km west of the Yukon-Alaska border, helicopters offer the only access (Foster, 1981). Local geology has been mapped and described by Foster (1970) and Foster et al. (1994). Prindle contains a varied xenolith suite up to a few per cent of the scoria, including banded fertile peridotites (spinel lherzolite, harzburgite, and wehrlite) and both leucocratic and melanocratic granulites (Foster et al., 1966) with subordinate crustal rocks. The bedrock geology includes serpentinized peridotites (Foster et al., 1994) that are considerably more structurally deformed and retrograded to serpentine than the fresh peridotites carried in the Prindle scoria and flow. Most metamorphic rocks of this region are of greenschist or amphibolite grade, unlike the granulite facies xenoliths occurring at Prindle. Apparently the majority of the xenoliths at Prindle derive from the lower crust and upper mantle and do not relate to the upper crustal geology (Foster et al., 1966). Black resorbed megacrysts of augite and pyroxenite clasts may relate to deep or early crystallization of this basanite cone and flow. This cinder cone shows little erosion and Foster assigned a minimum age of Late Pleistocene to Holocene. While there has been a long history of glaciation in this part of Alaska beginning in upper Tertiary (Foster et al., 1994), for Prindle to have been older than a few thousand years would require that it survived erosion in an ice free region. Studies of the xenoliths from Prindle should constrain the basement of the Yukon-Tanana terrane and describe the underlying upper mantle.

60 mile occurrence (2)

The 60 Mile occurrence is a xenolith laden, basaltic breccia pipe in the Yukon west of Dawson City (Fig. 1, Table 1). This locality, north of confluence of Big Gold Creek with the 60 Mile River, sits on the pericratonic Nisling terrane. The outcrop has been exposed by bulldozing cuts in the course of mining exploration (A. Downes, pers. comm., 1995), and has been reported by Mortensen and Roddick (1989) as a xenolith locality and part of the Miocene volcanic succession in the northern Cordillera. Cretaceous or Tertiary volcanic ash beds and thin coals, are exposed nearby on Big Gold Creek. Mortensen (1992) confidently reported a $^{39}Ar/^{40}Ar$ age on the host basalt of 17.2 Ma, despite the vesicular, rubbly, and extremely xenolith laden nature of the outcrop (>20%). Unpublished petrographic analysis (A. Downes, pers. comm., 1995) report the host volcanic matrix to be a lamproite. The xenoliths include friable coarse protogranular peridotites, igneous and metamorphic rock, and sandstones.

Clinton Creek (3)

The Clinton Creek xenolith occurrence (Fig. 1, Table 1) consists of rubbly outcrop and locally derived float in roadcuts and quarries west of the Clinton Creek townsite and the junction of Clinton Creek with 40 Mile River (Mortensen and Roddick, 1989). While no basalt from this locality was dated, the geology and lithologies are similar to nearby sites with Lower Miocene dates. The xenolith material consisted of fresh to friable, variably banded, fertile spinel lherzolites up to a few tens of centimetres across with smaller, partially melted and reacted, granitic and metamorphosed pelitic and siliciclastic rocks. Nearby outcrops of the underlying pericratonic Slide Mountain terrane include serpentinized peridotites, and the Clinton Creek asbestos deposit. There is abundant bedrock-derived float of chromite-bearing dunite.

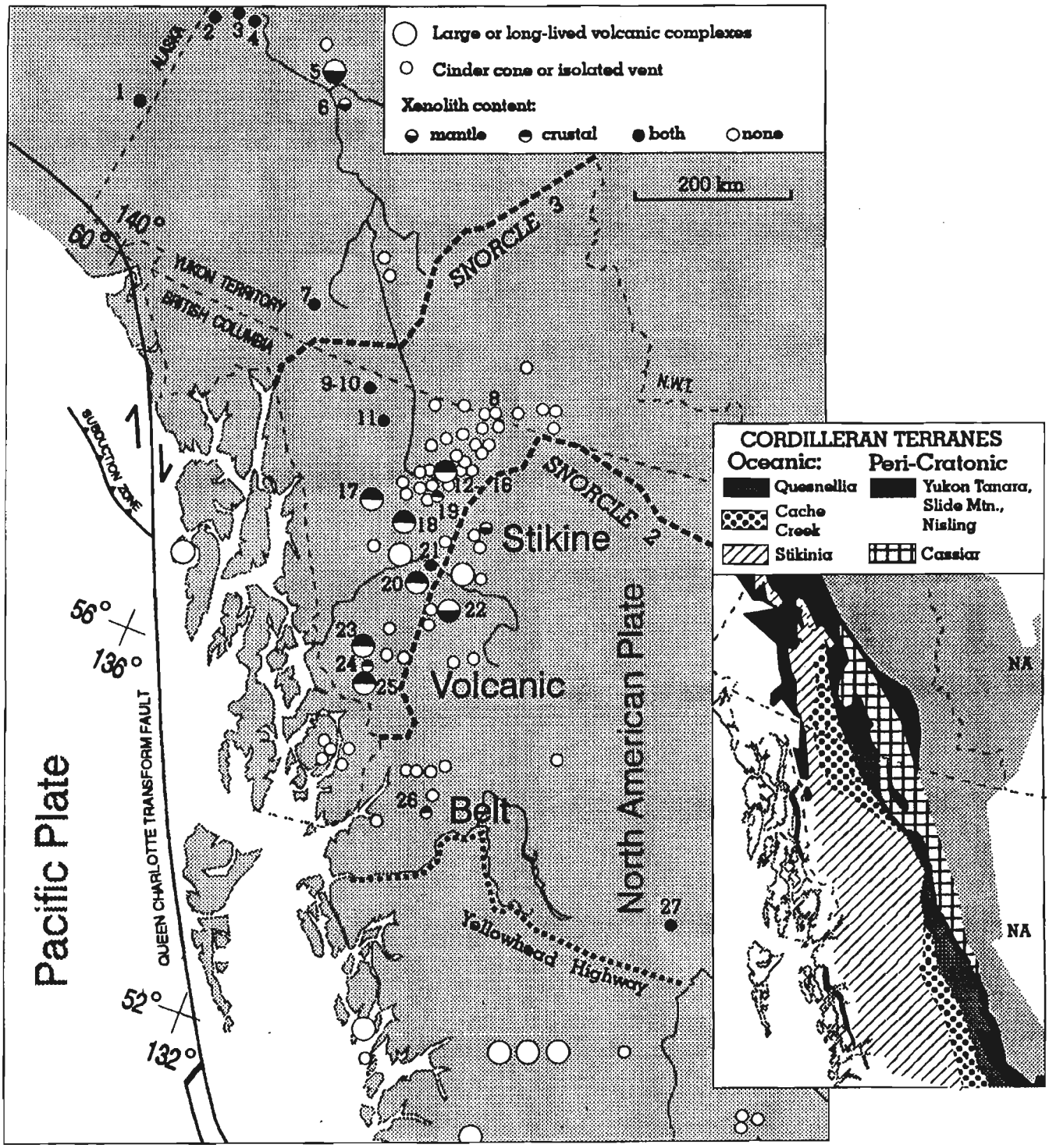

Figure 1. *The distribution of Neogene volcanic centres and xenolith localities for the northern Cordillera are shown with respect to political boundaries, large rivers and the two proposed transects for Lithoprobe's SNORCLE Project. Neogene volcanic centres are shown with circles (after Hickson, 1990). Larger circles refer to long-lived or large central volcanoes, while small circles refer to isolated cinder cones, flows or smaller volcanic centres. The xenolith occurrences are coded as per the legend. Numbers refer to brief descriptions of volcanos or xenolith localities in Table 1, and in the text. The inset simplified terrane map suggests what material may be sampled at each site.*

40 Mile River-Yukon River (4)

The 40 Mile site (Fig. 1, Table 1) on the pericratonic Nisling terrane, is a columnar jointed volcanic plug or thick flow, approximately 5 km upstream on the Yukon River from the mouth of 40 Mile River. This occurrence, dated by Mortensen and Roddick (1989) at 19.9 Ma, is perched on the flank of the Yukon River valley, and accessible by boat and a steep climb from the Yukon River, or on foot from the Clinton Creek road. Apparently this basalt erupted before the downcutting of the Yukon River. Both it and the Clinton Creek site occur on the plateau surface. Angular unreacted schist occurs at the lowest level of basalt outcrop. Higher up and on the south face of the vertical flaring, polygonal jointed basalt, both spinel lherzolite and schist xenoliths occur to a few centimetres in size.

Table 1. Locations of young volcanics and xenolith collection sites in the northern Cordillera.

Locality	Long.	Lat.	Elev.	Age	Xeno	Reference
1 Prindle Volcano	141.633	63.880	1222	Pleistocene	Both	Foster et al., 1966, 1994
2 60 Mile	140.767	64.050	914	17.2	Both	Mortensen, 1992
3 Clinton Creek	140.525	64.378	457	Miocene	Both	Mortensen, 1992
4 40 Mile	140.625	64.396	457	19.9	Both	Mortensen, 1992
5 Volcano Mountain	137.383	62.932	1238	Holocene	Mantle	Trupia and Nicholls, 1996; Francis and Ludden, 1990; Jackson and Stevens, 1992
6 Ne Che Dhawa	137.267	62.750	671	Pleistocene	Mantle	Jackson and Stevens, 1992; Sinclair et al., 1977
7 Alligator Lake	135.417	60.377	1981	Pleistocene	Both	Eiche et al., 1987; Francis, 1975
8 Rancheria	128.817	60.233	853	0.232-0.765	None	Klassen, 1987
9 Ruby Mountain	133.320	59.680	1835	Holocene	Both	Aitken, 1959; Nicholls et al., 1982; Edwards et al., 1996
10 Chikoidea	133.025	59.188	1875	Cretaceous-Quaternary	Both	Mihalynuk et al., 1996; Edwards et al., 1996
11 Llangorse	132.771	59.333	1690	Quaternary	Both	Aitken, 1959; Edwards et al., 1996
12 Ash Mountain	130.518	59.277	2125	Pleistocene	Crustal	Moore et al., 1995; Allen, 1990
13 Three Cariboo Tuya	130.560	59.242	1680	Pleistocene	Crustal	Moore et al., 1995; Allen, 1990
14 South Tuya	130.508	59.208	1830	Pleistocene	Crustal	Moore et al., 1995; Allen, 1990
15 Mathews Tuya	130.430	59.200	1670	Pleistocene	Crustal	Moore et al., 1995; Allen, 1990
16 Tuya Butte	130.550	59.100	1525	Pleistocene	Crustal	Moore et al., 1995; Mathews, 1947; Allen, 1990
17 Heart Peaks	131.963	58.598	2010	Miocene-Quaternary	Crustal	Casey, 1980
18 Level Mountain	131.350	58.420	2190	Miocene-Quaternary	Crustal	Hamilton, 1990
19 Kawdy Mountain	131.235	58.877	1920	Quaternary	Crustal	Hamilton and Evans, 1983
20 Mount Edziza	130.700	57.700	2786	Miocene-Holocene	Crustal	Souther, 1992
21 Castle Rock	130.217	57.837	1890	Quaternary	Both	Littlejohn and Greenwood, 1974; Souther, 1977
22 Maitland Creek	129.467	57.444	1551	Pliocene	Mantle	Evenchick and Thorkelson, 1993; Souther, 1990
23 Hoodoo Mountain	131.290	56.770	1700	Quaternary	Crustal	Edwards and Russell, 1994
24 Little Bear Mountain	131.300	56.815	1067	Quaternary	Crustal	Edwards and Russell, 1994
25 Iskut-Unuk Cones	130.600	56.710	914	Quaternary-Holocene	Crustal	Grove, 1986; Hauksdottir, 1994
26 Aiyansh-Tseax River	128.900	55.117	198	Holocene	Crustal	Sutherland Brown, 1969
27 Summit Lake	122.525	54.260	756	Miocene	Both	Brearley et al., 1984; Ross, 1983

Ne Che Dhawa (6)

Ne Che Dhawa (Fig. 1, Table 1) also referred to as Fort Selkirk Volcanics and Wooten cone (Francis, 1990), is a mid-Quaternary subglacial volcano (Jackson, 1989) on the east shore of the Yukon River just south of Pelly Crossing. This vent, and Volcano Mountain just to the north, sit on a narrow sliver of Cache Creek Terrane sandwiched between Stikinia to the west and the pericratonic Nisutlin terrane to the east. The 200 m high, eroded volcanic edifice comprises bedded palagonite tuff with small and weathered, refractory, coarse grained protogranular peridotites. Many large, fractured olivine xenocrysts also occur in the tuff. Xenoliths from here have been analyzed and discussed by Littlejohn and Greenwood (1974) and Sinclair et al. (1977) who confirmed the refractory nature of the peridotite mineralogy and Ross (1983) who calculated an pyroxene geotherm for this site resembling that for ocean crust. Mitchell (1987) described the peridotites from this site as being the most refractory in the whole Cordillera.

Alligator Lake (7)

Alligator Lake (Fig. 1, Table 1) 30 km southwest of Whitehorse, is a pair of glacially modified basaltic cinder cones which sit on a platform of flat lying, columnar jointed, alkali olivine basalt flows (Eiche et al., 1987). These vents sit on the western edge of Stikinia against the Coast Plutonic Complex and the pericratonic Nisling terrane. Collections

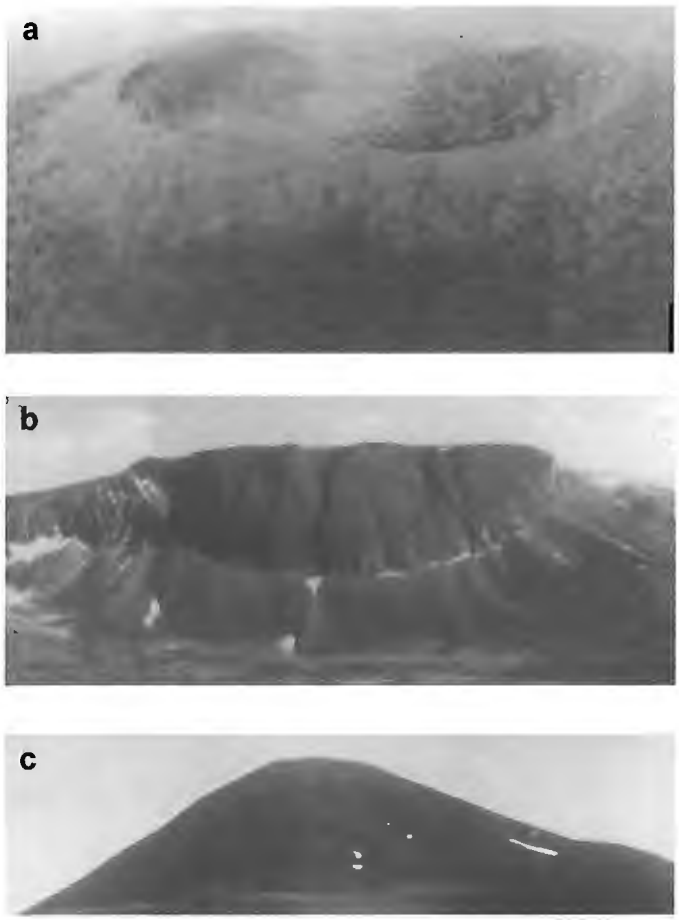

a) Aerial view to the southeast of Prindle volcano.

b) Aerial view to the south of Llangorse, an eroded volcanic plug southeast of Atlin, British Columbia (Aitken, 1959). The prominent dark cliff outcrop, approximately 60 m high, is of vertical columnar jointed aphyric basanite with minor crosscutting gabbroic dykes and apophyses. The irregular rocks to the left are granodiorite. The gentler slope to the right has steeply dipping volcanic breccias, likely crater fill facies (Edwards et al., 1996).

c) View to the south of South Tuya volcano (Moore et al., 1995), a subglacial basaltic scoria cone located in the southern Cassiar Mountains. The edifice is approximately 400 m high and 2 km wide, extending beyond the field of view.

d) Maitland volcanics atop Spatsizi Plateau, view to southwest. Foreground has rubbly outcrop of basaltic dyke with peridotite xenoliths. Background shows the largest volcanic plug and dyke which fed the Maitland volcanics.

Figure 2.

comprise xenoliths of spinel lherzolite, harzburgite, rare wehrlite, partially melted quartzofeldspathic crustal rocks, and resorbed black clinopyroxene megacrysts which all occur in large scoria bombs and in eroded and weathered dykes along the edge of the alpine valley which separates the two cinder cones. Phlogopite occurs in a reaction texture armouring pyroxene but not as an equilibrium part of the mantle assemblage. The peridotite suite contains both enriched spinel lherzolites and depleted harzburgites (Francis, 1987) and the crustal xenoliths include garnet-bearing granulite facies metapelites, which have not previously been reported from this site.

Atlin area

Ruby Mountain/Cracker Creek/Volcanic Creek (9)

Ruby Mountain (Aitken, 1959; Nicholls et al., 1982; Edwards et al., 1996) is a Quaternary basaltic cinder cone near Surprise Lake in the Cache Creek terrane of northwestern British Columbia (Fig. 1, Table 1). This large cinder cone is built against the flank of an alpine glacial valley and has flows and pyroclastic deposits which are interlayered with glacial deposits. The edifice postdates the cutting of the alpine valley, and nearby satellitic cones (Cracker Cone, Volcano Creek) are little modified and may be Holocene. Crustal xenoliths and feldspar xenocrysts are common and may be derived from

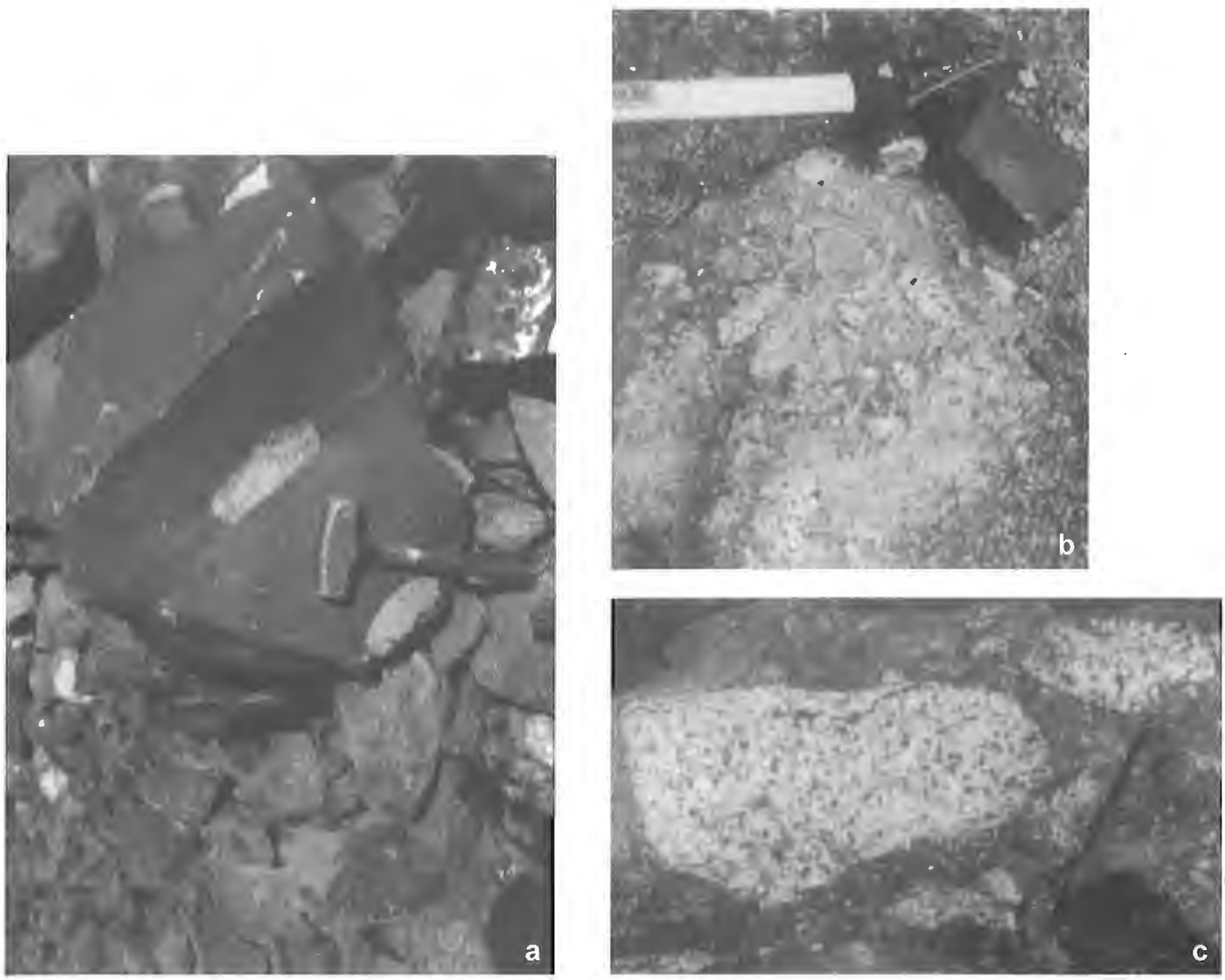

Figure 3. a) *Tabular lherzolite inclusion 16 cm by 5 cm in basaltic talus, Llangorse volcano. Note sledge for scale. In this vent, some lherzolite xenoliths exceed 50 cm across.* ***b)*** *Angular granodiorite xenoliths to 20 cm and sparse lherzolites to 5 cm in poorly sorted volcanic breccia at western side of Llangorse volcano (Edwards et al., 1996). This combination of crustal- and mantle-derived xenoliths is a common feature of many volcanic vents in the northern Cordillera. Digested Lherzolite has been outlined in black.* ***c)*** *Angular granitic xenoliths to 65 cm, contained in plagioclase phyric basaltic breccia South Tuya volcano (see Fig. 2c). Crustal xenoliths of igneous like these and metamorphic rocks are present throughout the subglacial volcanoes of the Southern Cassiar Mountains.*

the Surprise Lake Batholith (Aitken, 1959). Spinel peridotites to a few centimetres across are rarer but can be found both near the summit of Ruby Mountain and in the columnar jointed flow which lies along Ruby Creek.

Chikoida Mountain (10)

Chikoida Mountain (Edwards et al., 1996) is underlain by a granitic stock which intrudes both the Cache Creek Group and Atlin peridotites (Aitken, 1959). Crosscutting the granite, on the southeast side of the granitic summit, are a series of small (<10 m) basaltic pipes of elliptical cross-section which intrude the Chikoida Mountain Stock (Mihalynuk et al., 1996). The basalt pipes are arranged southwest-northeast, parallel to the local structural grain and the glacial valley now occupied by Katrina Creek. The basalt is intensely weathered and devitrified to a dull black or chocolate brown appearance. Within the basalt pipes are irregular, friable and dissaggregated protogranular and layered spinel lherzolites and granitic xenoliths. Most spinel peridotites are depleted, and appear less hydrous, less strained, and fresher than the local alpine peridotite suite. The granitic xenoliths resemble the local country rock of the Chikoida Mountain Stock in texture and mineralogy. The basalt pipes were conduits for an eroded volcano.

Llangorse (11)

Llangorse (Fig. 1, Table 1) in the Cache Creek terrane is a thick columnar jointed plug (Fig. 2b) with crosscutting pegmatitic gabbro dykes and having a steeply dipping crater facies of unconsolidated volcanic breccia under both sides. The steeply dipping breccias, first reported by Aitken (1959), contain both basaltic bombs and granitic clasts. Local bedrock is the Mount Llangorse quartz diorite. Both the basanite body (Fig. 3a) and the breccia (Fig. 3b) contain peridotite xenoliths to several tens of centimetres across, such as only occur in or near volcanic vents. Abundant and fresh peridotites are depleted spinel lherzolites and harzburgites. The large plutonic fragments in the breccia (Fig. 2b), were likely derived from the Mount Llangorse stock. Higgins and Allen (1985) reported peridotite inclusions in nephelinite dykes nearby.

Southern Cassiar Mountains

Ash Mountain (12)

Ash Mountain (Fig. 1, Table 1) is a large subglacial mound (Allen, 1990; Moore et al., 1995), with coarse basaltic block and pillow breccias around the lower flanks and reworked bedded hyaloclastite with crosscutting dykes in the uppermost portion of the edifice. Samples of plutonic and metamorphic rock up to several centimetres across are apparently all upper crustal xenoliths derived from local bedrock. The location of this volcanic vent, along with South Tuya, Mathews Tuya, and Tuya Butte, appear to be controlled by local bedrock structure. All intrude pericratonic metamorphic rocks of the Nisling terrane along the edge of a Cretaceous pluton, parallel to the contact with Slide Mountain terrane to the southwest.

Three Caribou Tuya (13)

Three Caribou Tuya (Fig. 1, Table 1) is a subglacial mound (Moore et al., 1995) with fresh basaltic scoria containing abundant small crustal xenoliths on the flanks, and bedded hyaloclastite, pillow basalt, and pillow breccia all cut by dykes along the summit ridge. The xenoliths collected were the same lithologies described for Ash Mountain. All xenoliths were smaller than a few centimetres and plutonic types dominate over metamorphic rocks.

South Tuya (14)

South Tuya (Fig. 1, Table 1, Fig. 2c) is a large subglacial mound (Moore et al., 1995) with bedded hyaloclastites and dykes in the upper portions, a terrace along its western side, and pipes with abundant crustal xenoliths to several tens of centimetres across (Fig. 3c) resembling a breccia. This volcanic vent is situated on an intrusive contact between a Cretaceous pluton and Nisling terrane pericratonic metamorphic rocks. Xenoliths here are all crustal, representing the same local plutonic and metamorphic lithologies described for Ash Mountain.

Mathews Tuya (15)

Mathews Tuya (Fig. 1, Table 1) like the others in the area near High Tuya Lake, is a subglacial volcano (Allen et al., 1982; Moore et al., 1995) with a flat top. Bedded hyaloclastite crosscut by feeder pipes forms the north face. Crustal xenoliths, dominantly of plutonic rock, occur both low down in the flank strata and up in the feeder dykes.

Stikine Plateau

Castle Rock (21)

Castle Rock (Fig. 1, Table 1), on the northernmost edge of the Klastline Plateau within Stikinia, is an overlapping complex of Quaternary volcanic cinder cones containing some of the largest, freshest, most fertile and most variable xenoliths in the Cordillera (Mitchell, 1987). Littlejohn and Greenwood (1974) reported mineral analyses on the spinel peridotites and Hamilton (1981) found some of these also to contain anorthite-rich plagioclase in addition to spinel, and iron-nickel monosulphide. Collections from several of the pipes and dykes yielded both depleted and enriched peridotites, mafic gabbros and granulite gneisses, black augite megacrysts, and plutonic, metamorphic, and sedimentary rocks resembling units mapped nearby. Granulites were previously unknown from this site. Xenoliths are large (peridotite to 25 cm and granulite to 35 cm) and abundant (greater than 10%) in pipes and dykes and downhill from them, while in the scoria, they are small and rare.

Spatsizi Plateau

Maitland Volcano (22)

Maitland Volcano (Fig. 1, 2d; Table 1) consists of horizontal Tertiary basalt flows and pyroclastics, and the dykes and necks which fed them, outcropping near Maitland Creek and Klappan River (Souther, 1990). The Pliocene Maitland Volcanics are the remnants of a formerly more extensive volcanic complex capping the uplifted Spatsizi Plateau (Evenchick and Thorkelson, 1993) within Stikinia. Two eroded pipes (10-20 m across) and two thin dykes (1-3 m) carry banded fertile spinel lherzolite, wehrlite, and olivine websterite xenoliths to several decimetres, although most are friable from alpine weathering. C.A. Evenchick (pers. comm., 1995) reported other xenolith localities containing crustal samples on the plateau east-southeast of Tumeka Lake and further to the east in the Klappan valley.

Boundary Ranges

Little Bear Mountain (24)

Little Bear Mountain (Edwards and Russell, 1995) on Stikinia, is a subglacial, basaltic volcano north of Hoodoo Mountain (Edwards and Russell, 1994). Little Bear Mountain comprises olivine-plagioclase phyric alkali olivine basalt which occurs as pillowed lavas, dykes, and hyaloclastite. All rock types contain resorbed black clinopyroxene megacrysts and partly melted granite to syenites and some of the felsic xenoliths contain pyroxene (Edwards and Russell, 1995). This occurrence resembles those for the nearby Iskut and Unuk river centres (Hauksdottir, 1994).

North of the Yellowhead Highway

Aiyansh Flow/Tseax River Cone (26)

The Aiyansh flow (Fig. 1, Table 1) (Sutherland Brown, 1969) and Tseax River cone from which this ferrobasalt issued constitute a recent historical eruption through the western edge of Stikinia. The flow contains resorbed and disaggregated plagioclase megacrysts and rare quartzite xenoliths to 5 cm.

Summit Lake (27)

Summit Lake is an eroded Miocene basaltic neck which occurs in an abandoned railroad quarry northwest of Prince George (Fig. 1, Table 1). Fresh spinel lherzolite, dunite, harzburgite, and wehrlite xenoliths to 20 cm are present in blasted faces and as smaller fragments among the material crushed for roadbase. A variety of crustal xenoliths are present, as are gabbros and resorbed megacrysts of plagioclase and black augite. Peridotite mineralogy and a pyroxene geotherm were previously reported by Brearley et al. (1984). Xenoliths from this location on the eastern edge of Quesnellia against the Slide Mountain terrane, may help locate western edge of cratonic basement.

PETROGRAPHY AND MINERALOGY OF XENOLITHS

Preliminary petrography for three sites (Alligator Lake, Castle Rock, and Summit Lake) revealed four distinct xenolith assemblages: upper mantle peridotites, lower crustal mafic and felsic metamorphic and plutonic rocks, large xenocrysts and cognate inclusions, and upper crustal unreacted or partly melted plutonic and metamorphic rocks. Although upper crustal xenoliths are present in many instances, because they represent mapped units reported on elsewhere, they are not discussed. Only the first group representing the upper mantle is discussed in detail in this paper.

Ultramafic xenoliths are present in a variety of lithologies and textures. The two most common lithologies are spinel lherzolite and harzburgite, while lesser amounts of dunite, olivine websterite, and wehrlite occur. The most common textures in order of decreasing abundance are protogranular, granuloblastic, and strained. Textures range from unstrained equigranular with triple junctions, to larger tabular crystals of olivine showing parallel orientation, to olivines that display undulatory extinction and weak kink bands.

The four common mineral phases are forsteritic olivine (Fo_{90-92}, Table 2a), enstatite-rich orthopyroxene (Table 2b), diopside-rich clinopyroxene (Table 2c), and brown or green spinel, and all are universally present, suggesting the varied peridotite lithologies are mineral segregations. Although compositions are refractory and in the realm for mantle derived peridotites, there is some compositional variation both within sites and between sites. The enriched peridotites are mineralogically banded having bands richer in chrome diopside and spinel, and the other ultramafic xenoliths like wehrlite and olivine websterite are often tabular, resembling the enriched bands within the ubiquitous lherzolite. In some samples from Summit Lake, clinopyroxene grains exhibit a reaction texture wherein the diopside has spongy poikiloblastic rims consisting of glass and small clinopyroxene grains. Spinel commonly occurs as a brown interstitial phase with highly variable grain size. In some samples, rounded spinels are included in other minerals or are rimmed by black spinel. In partially disaggregated or melted xenoliths, spinel is sometimes greenish-brown. Spinel shows the largest variations of any ultramafic phase. They show significant variations in Al, Mg, Cr, and Fe. Because of the mineralogical and textural variation in ultramafic xenoliths, even from single volcanoes, it is likely that a substantial thickness the sub-Cordilleran upper mantle is sampled by the volcanic process or that the portion of mantle sampled is heterogeneous or has a complex history.

GENERAL OBSERVATIONS ON XENOLITH DISTRIBUTION AND IMPORTANCE

There are two apparent trends for the xenolith occurrences (Fig. 1). Crustal xenolith sites lie in a northerly trend along the Stikine Volcanic Belt (Souther, 1977), sampling both the allochthonous Intermontane Superterrane (Stikinia, Cache Creek, Quesnellia) and the peri-cratonic Slide Mountain,

Table 2a. Olivine analyses and structure formulae.

	1	2	3
SiO_2	40.66	40.92	41.12
TiO_2	nd	nd	nd
Al_2O_3	nd	nd	nd
FeO	9.20	8.81	9.25
MnO	0.20	0.29	0.16
MgO	49.03	50.28	49.43
CaO	0.07	0.05	0.10
NiO	0.38	nd	nd
TOTAL	99.54	100.35	100.06
Si	1.00	0.9954	1.00
Ti			
Al			
Fe_2+	0.1892	0.1792	0.1888
Mn	0.0042	0.006	0.0033
Mg	1.80	1.82	1.80
Ca	0.0018	0.0013	0.0026
Ni	0.0075		
Mg/Mg+Fe	0.9048	0.9105	0.9050

1) Alligator Lake: ALG-10, spinel lherzolite
2) Summit Lake: SLG-07, spinel lherzolite
3) Castle Rock: CRG11-10, spinel lherzolite
nd – not determined

Table 2b. Orthopyroxene analyses.

	4	5	6
SiO_2	54.27	54.87	53.93
TiO_2	0.09	nd	0.11
Al_2O_3	5.35	3.55	3.13
FeO	5.76	6.03	6.16
MnO	0.16	nd	0.13
MgO	32.88	33.21	32.00
CaO	1.02	1.05	1.11
Na_2O	0.13	0.12	0.14
NiO	0.08	nd	nd
Cr_2O_3	0.54	0.62	0.79
TOTAL	100.28	99.45	99.30

4) Alligator Lake: ALG-10, spinel lherzolite
5) Summit Lake: SLG-07, spinel lherzolite
6) Castle Rock: CRG11-10, Spinel lherzolite
nd: not determined

Table 2c. Clinopyroxene analyses.

	7	8	9
SiO_2	51.49	52.36	51.47
TiO_2	0.26	0.07	0.27
Al_2O_3	6.42	4.07	6.00
FeO	2.97	3.31	3.28
MnO	0.17	nd	0.15
MgO	16.28	16.79	16.25
CaO	20.28	20.55	19.49
Na_2O	1.41	1.38	1.35
Cr_2O_3	0.92	1.51	1.14
TOTAL	100.20	100.04	99.40

7) Alligator Lake: ALG-10, spinel lherzolite
8) Summit Lake: SLG-07, spinel lherzolite
9) Castle Rock: CRG11-10, spinel lherzolite
nd: not determined

Nisling, Yukon Tanana, Nisutlin, and Cassiar terranes (Wheeler et al., 1991). Mantle xenoliths lie along a northwesterly trend between 200 and 350 km inland from the Queen Charlotte-Fairweather transform fault at the North American continental margin. Differences among mantle xenoliths (their compositions, textures, physical properties, and geothermal gradients) may provide insight into the mechanisms for continental growth. For example, contrasts between mantle xenolith compositions or properties from Prindle (overlying the Yukon-Tanana terrane) and Alligator Lake or Castle Rock (which both lie on Stikinia) could reflect differences for the emplacement of those two terranes.

Three sites sample granulite facies lower crustal rocks indicated by refractory mineral assemblages. Garnet occurs in metamorphosed siliciclastic xenoliths from Alligator Lake and Castle Rock along with high temperature aluminosilicates. Similar granulite xenoliths that were previously reported for the Prindle volcano (Foster et al., 1966) were collected in 1995.

DISCUSSION

The principle intent of these new xenolith collections and the laboratory studies to follow is to provide ground truth for the Lithoprobe SNORCLE Transect. Essentially, these xenoliths provide samples across the crust and upper mantle beneath the allochthonous terranes of the northern Cordillera. As Figure 1 shows, some centres carry only a mantle sample, while others carry only a crustal sample. Not all centres carry the cognate gabbros or aluminous augite megacrysts. Some sites like Prindle, Alligator Lake, Castle Rock, and Summit Lake have all three types of material. Perhaps the variation in xenolith content relates to the local state of stress in the lithosphere and its controls on magma derivation and transport.

It is significant to point out that all of the xenolith samples arise from extensional volcanics (Souther, 1992) in a postaccretionary, nonconvergent tectonic regime inboard of Queen Charlotte/Fairweather fault. Essentially there are no arcs in this region nor have there been since early Tertiary.

Other investigations into the texture and petrology of the xenoliths will contribute to our understanding of assimilation and magma contamination (Edwards and Russell, 1994; Hauksdottir, 1994), past geothermal gradients (Ross, 1983), magma rise times, and the nature and evolution of the sub-Cordilleran upper mantle. Chrome diopside-spinel-glass symplectite textures which have been reported previously (Ross, 1983) and encountered in newly collected material from Alligator Lake and Summit Lake could relate to basalt genesis as in decompression melting associated with the garnet to spinel transition (McKenzie and O'Nions, 1991). Finally, for xenoliths whose depth of origin can be well constrained, petrophysical measurements are essential to provide groundtruth for the geophysics.

ACKNOWLEDGMENTS

This work was conducted with Geological Survey of Canada A-base funding to T.S. Hamilton. The 1994 fieldwork was conducted with the able assistance of Jennifer Shaw of MRD. Fieldwork in 1995 was assisted by Ben Edwards and Kirsty Simpson of the University of British Columbia under the Geological Survey of Canada Volunteers Program. Chemical analyses were funded by an NSERC grant to J. Dostal (OPG3782). The crustal xenoliths reside at the Department of Geological Sciences, University of British Columbia while the mantle xenoliths reside at Pacific Geoscience Centre.

REFERENCES

Aitken, J.D.
1959: Atlin map-area, British Columbia (104 N); Geological Survey of Canada, Memoir 307, 89 p.

Allen, C.
1990: Tuya Butte, Canada; in Volcanoes of North America, (ed.) C.A. Wood and J. Kienle; Cambridge University Press, p. 119-121.

Allen, C.C., Jercinovic, M.J., and Allen, J.S.B.
1982: Subglacial volcanism in north-central British Columbia and Iceland; Journal of Geology, v. 90, p. 699-715.

Brearley, M., Scarfe, C.M., and Fujii, T.
1984: Petrology of ultramafic xenoliths from Summit Lake, near Prince George, British Columbia; Contributions to Mineralogy and Petrology, v. 88, p. 53-63.

Casey, J.
1980: Geology of the Heart Peaks volcanic centre; M.Sc. thesis, Geology Department, University of Alberta, Edmonton, Alberta, 186 p.

Edwards, B.R. and Russell, J.K.
1994: Preliminary stratigraphy of Hoodoo Mountain volcanic centre, northwestern British Columbia; in Current Research 1994-A; Geological Survey of Canada, p. 69-76.
1995: An overview of the nature, distribution and tectonic significance of xenoliths from the Stikine Volcanic Belt, northern Cordillera; in Slave Northern Cordillera Lithospheric Evolution, (comp.) F. Cook and P. Erdmer; (SNORCLE) and Cordilleran Tectonics Workshop, Lithoprobe Report #50, p. 96-107.

Edwards, B.R., Hamilton, T.S., Nicholls, J., Stout, M.Z., Simpson, K., and Russell, J.K.
1996: Quaternary volcanism in the Atlin area, northwestern British Columbia; in Current Research 1996-A; Geological Survey of Canada, p. 29-36.

Eiche, G., Francis, D., and Ludden, J.
1987: Primary alkaline magmas associated with the Quaternary Alligator Lake volcanic complex, Yukon Territory, Canada; Contributions to Mineralogy and Petrology, v. 95, p. 191-201.

Evenchick, C.A. and Thorkelson, D.J.
1993: Geology, Spatsizi River; Geological Survey of Canada, Open File 2719, scale 1:250 000.

Foster, H.D.
1970: Reconnaissance geologic map of the Tanacross quadrangle, Alaska; United States Geological Survey, Miscellaneous Geologic Investigations Map I-593, scale 1:250 000.
1981: A minimum age for Prindle volcano, Yukon-Tanana upland; in The United States Geological Survey in Alaska: Accomplishments During 1979, (ed.) N.R.D. Albert and T. Hudson; United States Geological Survey, Circular 823-B, p. B37-B38.
1990: Prindle, Eastern Alaska; in Volcanoes of North America, (ed.) C.A. Wood and J. Kienle; Cambridge University Press, p. 108-109.

Foster, H.D., Forbes, R.B., and Ragan, D.M.
1966: Granulite and peridotite inclusions from Prindle volcano, Yukon-Tanana upland, Alaska; United States Geological Survey, Professional Paper 550-B, p. B115-B119.

Foster, H.D., Kieth, T.E.C., and Menzie, W.D.
1994: Geology of the Yukon-Tanana area of east-central Alaska. Chapter 6; in The Geology of North America, Vol. G-1: The Geology of Alaska; The Geological Society of America, p. 205-240.

Francis, D.
1975: The origin of amphibole in lherzolite xenoliths from Nunivak Island, Alaska; Journal of Petrology, v. 17, p. 357-378.
1987: Mantle-melt interaction recorded in spinel lherzolite xenoliths from the Alligator Lake volcanic complex, Yukon, Canada; Journal of Petrology, v. 28, p. 569-597.
1990: Volcano Mountain; in Volcanoes of North America, (ed.) C.A. Wood and J. Kienle; Cambridge University Press, p. 118-119.

Francis, D. and Ludden, J.
1990: The mantle source for olivine nephelinite, basanite and alkaline olivine basalts at Fort Selkirk, Yukon, Canada; Journal of Petrology, v. 31.

Grove, E.W.
1986: Geology and mineral deposits of the Unuk River-Salmon River-Anyox Area; British Columbia Ministry of Energy, Mines and Petroleum Resources, Bulletin 63, 152 p.

Hamilton, T.S.
1981: Late Cenozoic alkaline volcanics of the Level Mountain Range, northwestern British Columbia: geology, petrology and paleomagnetism; Ph.D. thesis, Geology Department, University of Alberta, Edmonton, Alberta, 490 p.
1990: Level Mountain, Canada; in Volcanoes of North America, (ed.) C.A. Wood and J. Kienle; Cambridge University Press, p. 121-123.

Hamilton, T.S. and Evans, M.E.
1983: A magnetostratigraphic and secular variation study of Level Mountain, northern British Columbia; Geophysical Journal of the Royal Astronomical Society, v. 73, p. 39-49.

Hauksdottir, S.
1994: Petrography, geochemistry and petrogenesis of the Iskut-Unuk Rivers volcanic centres, northwestern British Columbia; MSc. thesis, Department of Geological Sciences, University of British Columbia, Vancouver, British Columbia, 253 p.

Hickson, C.J.
1990: Canadian Cordillera vent map and table; in Volcanoes of North America, (ed.) C.A. Wood and J. Kienle; Cambridge University Press, p. 110-117.

Higgins, M.D. and Allen, J.M.
1985: A new locality for primary xenolith-bearing nephelinites in northwestern British Columbia; Canadian Journal of Earth Sciences, v. 22, p. 1556-1559.

Jackson, L.E., Jr.
1989: Pleistocene subglacial volcanism near Forth Selkirk, Yukon Territory; in Current Research, Part E; Geological Survey of Canada, Paper 89-1E, p. 251-256.
Jackson, L.E. Jr. and Stevens, W.
1992: A recent eruptive history of Volcano Mountain, Yukon Territory; in Current Research, Part A; Geological Survey of Canada, Paper 92-1A, p. 33-39.

Klassen, R.W.
1987: The Tertiary-Pleistocene stratigraphy of the Liard Plain, southeastern Yukon Territory; Geological Survey of Canada, Paper 86-17, p. 1-16.

Littlejohn, A.L. and Greenwood, H.J.
1974: Lherzolite nodules in basalts from British Columbia; Canadian Journal of Earth Sciences, v. 11, p. 1288-1308.

Mathews, W.H.
1947: "Tuyas", flat topped volcanoes in northern British Columbia; American Journal of Science, v. 245, p. 560-570.

McKenzie, D. and O'Nions, R.K.
1991: Partial melt distributions from inversion of rare earth element concentrations; Journal of Petrology, v. 32, p. 1021-1091.

Mihalynuk, M.G., Bellefontaine, K.A., Brown, D.A., Logan, J.M., Nelson, J.L., Legun, A.S., and Diakow, L.J.
1996: Geological compilation, northwest British Columbia (NTS 94E, L, M; 104F, G, H, I, J, K, L, M, N, O, P; 114J,O, P); British Columbia Ministry of Energy, Mines and Petroleum Resources, Open File 1996-11.

Mitchell, R.H.
1987: Mantle derived xenoliths in Canada; in Mantle Xenoliths, P.H. Nixon (ed.); Wiley & Sons Ltd., p. 33-40.

Moore, J.G., Hickson, C.J., and Calk, L.C.
1995: Tholeiitic-alkalic transition at subglacial volcanoes, Tuya region, British Columbia; Journal of Geophysical Research, Solid Earth, v. 100, B12, p. 24 577-24 592.

Mortensen, J.K.
1992: British Columbia, GSC 92-29; in Radiogenic Age and Isotopic Studies: Report 6; Geological Survey of Canada, Paper 92-2, p. 192.
Mortensen, J.K. and Roddick, J.C.
1989: Miocene ^{40}Ar-^{39}Ar and K-Ar ages for basaltic volcanic rocks in southwestern Dawson map area, western Yukon Territory; in Radiogenic Age and Isotopic Studies: Report 3; Geological Survey of Canada, Paper 89-2, p. 17-22.
Nicholls, J., Stout, M.Z., and Fiesenger, D.W.
1982: Petrologic variations in Quaternary volcanic rocks, British Columbia, and the nature of the underlying upper mantle; Contributions to Mineralogy and Petrology, v. 79, p. 201-218.
Ross, J.V.
1983: The nature and rheology of the cordilleran upper mantle of British Columbia: inferences from peridotite xenoliths; Tectonophysics, v. 100, p. 321-357.
Sinclair, P.D., Tempelman-Kluit, D.J., and Medaris, L.G., Jr.
1977: Lherzolite nodules from a Pleistocene cinder cone in central Yukon; Canadian Journal of Earth Sciences, v. 15, p. 220-226.
Souther, J.G.
1977: Volcanism and tectonic environments in the Canadian Cordillera, a second look; in Volcanic Regimes in Canada, (ed.) W.R.A. Baragar, L.C. Coleman, and J.M. Hall; Geological Association of Canada, Special Paper 16, p. 3-24.
1990: Maitland, Canada; in Volcanoes of North America, (ed.) C.A. Wood and J. Kienle; Cambridge University Press, p. 126-127.
1992: The late Cenozoic Mt. Edziza Volcanic Complex, British Columbia; Geological Survey of Canada, Memoir 420, 320 p.
Sutherland Brown, A.
1969: Aiyansh lava flow British Columbia; Canadian Journal of Earth Sciences, v. 6, p. 1460-1468.
Trupia, S. and Nicholls, J.
1996: Petrology of Recent lava flows, Volcano Mountain, Yukon Territory, Canada; Lithos, v. 37, p. 61-78.
Wheeler, J.O., Brookfield, A.J., Gabrielse, H., Monger, J.W.H., Tipper, H.W., and Woodsworth, G.J. (comp.)
1991: Terrane Map of the Canadian Cordillera; Geological Survey of Canada, Map 1713A, scale 1:2 000 000.

Geological Survey of Canada Project 820018

Geology of the northeastern end of the Juneau Icefield Research Program Camp 26 nunatak, northwestern British Columbia

L.D. Currie, D.T. Carter[1], J. Cooper[2], M.E. Gunter[3], and C.L. Connor[4]
GSC Pacific, Vancouver

Currie, L.D., Carter, D.T., Cooper, J., Gunter, M.E., and Connor, C.L., 1996: Geology of the northeastern end of the Juneau Icefield Research Program Camp 26 nunatak, northwestern British Columbia; in Current Research 1996-E; Geological Survey of Canada, p. 77-86.

Abstract: The northeastern end of the Juneau Icefield Research Program's Camp 26 nunatak is underlain by metamorphic rocks (pelitic rocks, semi-pelitic rocks, marble, and minor hornblende amphibolite and quartzite), granitic-dioritic plutonic rocks, andesite, and volcaniclastic rocks. Correlation of the metamorphic rocks with the Jurassic or older Florence Range suite of Tracy Arm terrane (in part equivalent to Nisling terrane) increases the known extent of the Tracy Arm terrane in this area. The volcanic rocks are correlated with the Eocene Sloko Group, and may be coeval with the plutonic rocks.

A steep, east-west striking, south side-down fault cuts Florence Range suite and Sloko Group rocks exposed on the nunatak. East of the nunatak, the projected trace of the Llewellyn Fault Zone lies beneath the Llewellyn Glacier, and appears to be imaged by side-aperture-radar data. The relationship between these structures is not clear because they intersect beneath the glacier.

Résumé : L'extrémité nord-est du nunatak du camp 26, cartographié dans le cadre du Programme de recherche sur le champ glaciaire de Juneau, est caractérisée par des roches métamorphiques (roches pélitiques, roches semi-pélitiques, marbre et un peu d'amphibolite à hornblende et de quartzite), des roches plutoniques (de composition granitique à dioritique), des andésites et des roches volcanoclastiques. Les roches métamorphiques sont associées à la suite de Florence Range du terrane de Tracy Arm, ce qui accroît la superficie connue de ce terrane dans le secteur à l'étude. La suite de Florence Range remonte au Jurassique (ou à une époque plus ancienne) et le terrane de Tracy Arm est en partie équivalent au terrane de Nisling. Les roches volcaniques sont assignées au Groupe de Sloko de l'Éocène et sont peut-être contemporaines des roches plutoniques.

Une faille abrupte à compartiment sud affaissé et d'orientation est-ouest recoupe la suite de Florence Range et les roches du Groupe de Sloko affleurant sur le nunatak. À l'est du nunatak, la trace projetée de la zone de faille de Llewellyn est cachée par le glacier du même nom, mais semble ressortir sur les images obtenues par radar à visée latérale. Le lien qui existe entre ces structures n'est pas clair, du fait qu'elles s'entrecoupent sous le glacier.

[1] Department of Geology, Whitman College, Walla Walla, Washington, U.S.A. 99362
[2] Department of Geology, Southern Appalachian State University, Boone, North Carolina, U.S.A. 28608
[3] Department of Geology and Geological Engineering, University of Idaho, Moscow, Idaho, U.S.A. 83844-3022
[4] School of Education, University of Alaska Southeast, Juneau, Alaska, U.S.A. 99801

INTRODUCTION

Southeast Alaska and northwest British Columbia comprise allochthonous terranes accreted to the western margin of North America during Mesozoic and Tertiary time (e.g., Coney et al., 1980; Fig. 1). These include metamorphic rocks with inferred continental affinity that have been correlated across the Juneau Icefield, from southeast Alaska to the east side of the Coast Mountains of northern British Columbia. Silberling et al. (1994) included them in Tracy Arm terrane, Wheeler et al. (1991) considered them part of Nisling terrane, and Gehrels et al. (1990) referred to them as part of Yukon-Tanana terrane. Correlations have been made on the basis of lithological similarities because the metamorphic rocks cannot be followed continuously across the icefield; they have been extensively intruded by plutons, and are in large part concealed by ice, Quaternary glacial drift, and Tertiary volcanic rocks (Fig. 2).

Brew and Ford (1986, and references therein) have conducted reconnaissance mapping of many of the nunataks within the icefield, and during the 1995 field season, researchers and students of the Juneau Icefield Research Program (JIRP) and Geological Survey of Canada conducted geological mapping to determine the lithological and structural relationships of rocks exposed on the northeastern end of a nunatak that lies within the Llewellyn Glacier of the Juneau Icefield, just north of 59° north latitude, in the northeastern Coast Mountains of northwestern British Columbia. The nunatak is a base camp for the JIRP, and is informally referred to as the JIRP Camp 26 nunatak (Fig. 1, 2, 3). Its remoteness, difficult access and distance from other exposed outcrops has limited geological study of the area in the past, with the exception of unpublished JIRP Open File Reports by P.B. Skidmore (1987), A. Vrooman (1990) and M. Abolins (1991).

REGIONAL GEOLOGY

The area northeast of the Llewellyn Glacier is underlain by metamorphic rocks, the Cretaceous and younger plutonic rocks that intruded the metamorphic rocks, and the Tertiary Sloko Group volcanic rocks that overlie them (Fig. 2; Mihalynuk et al., 1989a,b, 1990; Currie, 1990, 1991, 1992a, b). The metamorphic rocks include the Florence Range and Boundary Ranges suites, and variably deformed plutonic rocks of the Tagish Lake suite. The Florence Range suite primarily comprises multiple deformed, amphibolite facies, muscovite-biotite schists (>20% micaceous minerals, ±garnet±kyanite±sillimanite± andalusite±staurolite), semipelitic rocks (10 to 20% micaceous minerals), and marble. It also includes minor quartzite (>90% quartz), calc-silicate layers, and hornblende amphibolite layers (Currie, 1994). On the basis of these rock-types, their relative abundances, and the lack of a significant igneous component, the Florence Range suite is considered part of Tracy Arm terrane, a continental margin assemblage of poorly constrained age (>175 Ma; Currie, 1990, 1991, 1992a).

In contrast, the Boundary Ranges suite is composed of: felsic and mafic metavolcanic rocks, metapelitic rocks and minor marble layers that are at least in part Mississippian or older; Devono-Mississippian orthogneisses; and a metamorphosed Permian volcanic rock. Together with the Early to Middle Jurassic Tagish Lake suite plutons that intruded it, the Boundary Ranges suite is included in Stikinia, a mid-Paleozoic to Mesozoic volcanic arc assemblage (Fig. 2; Currie, 1992a; Currie and Parrish, 1993).

The Middle Jurassic contact between Tracy Arm terrane and Stikinia is exposed along the northern boundary of the Llewellyn Glacier about 9 km north of the Camp 26 nunatak (Fig. 2). About 3.5 km east of this terrane boundary, beneath the Hoboe Glacier, lies the inferred trace of a younger structure, the Llewellyn Fault Zone, a steep, north-northwest-striking fault zone that was active after ~100 Ma, and possibly earlier (Currie, 1992b). It is exposed farther north, near the bottom of the Hoboe Creek valley (Fig. 1; Currie and Parrish, 1993). Metamorphic rocks belonging to Stikinia are exposed on both sides of this fault zone, whereas Tracy Arm terrane rocks have only been recognized west of the fault zone.

The Stikinia-Tracy Arm terrane boundary has been tentatively extrapolated from the northern margin of the Llewellyn Glacier to a nunatak that lies ~3.5 km to the south on the basis of well exposed marble layers that appear to be continuous (Fig. 2; Currie, 1994). Because these marble layers are so prominent, this nunatak is informally referred to as the "marble mountain" nunatak (Fig. 2). The northeastern end of the next nunatak to the south, the JIRP Camp 26 nunatak, was mapped at 1:20 000 scale during the 1995 field season to determine whether geological units continue from the Marble Mountain nunatak to the Camp 26 nunatak. The lithological and structural relationships of rocks exposed there are the subject of this paper.

GEOLOGY OF THE NORTHEASTERN END OF THE JIRP CAMP 26 NUNATAK

The western half of the north end of the JIRP Camp 26 nunatak is underlain by metamorphic rocks, whereas the eastern side is dominated by volcaniclastic rocks and felsic-intermediate plutonic rocks (Fig. 2, 3). Both the metamorphic and igneous assemblages are crosscut by felsic and mafic dykes.

Figure 1. Terrane map of northwestern British Columbia, southwest Yukon and southeast Alaska (modified from Wheeler and McFeely, 1991 and Wheeler et al., 1991). Paleozoic rocks and Late Triassic to Middle Jurassic plutons of Stikinia, Cretaceous to Tertiary plutons and the location of Figure 2 are also shown. CF = Chief Fault; KSF = King Salmon Fault; LFZ = Llewellyn Fault Zone. Inset: AK = Alaska; BC = British Columbia; YT = Yukon Territory. Terrane map of northwestern British Columbia and adjacent southeastern Alaska (modified from Wheeler et al., 1991).

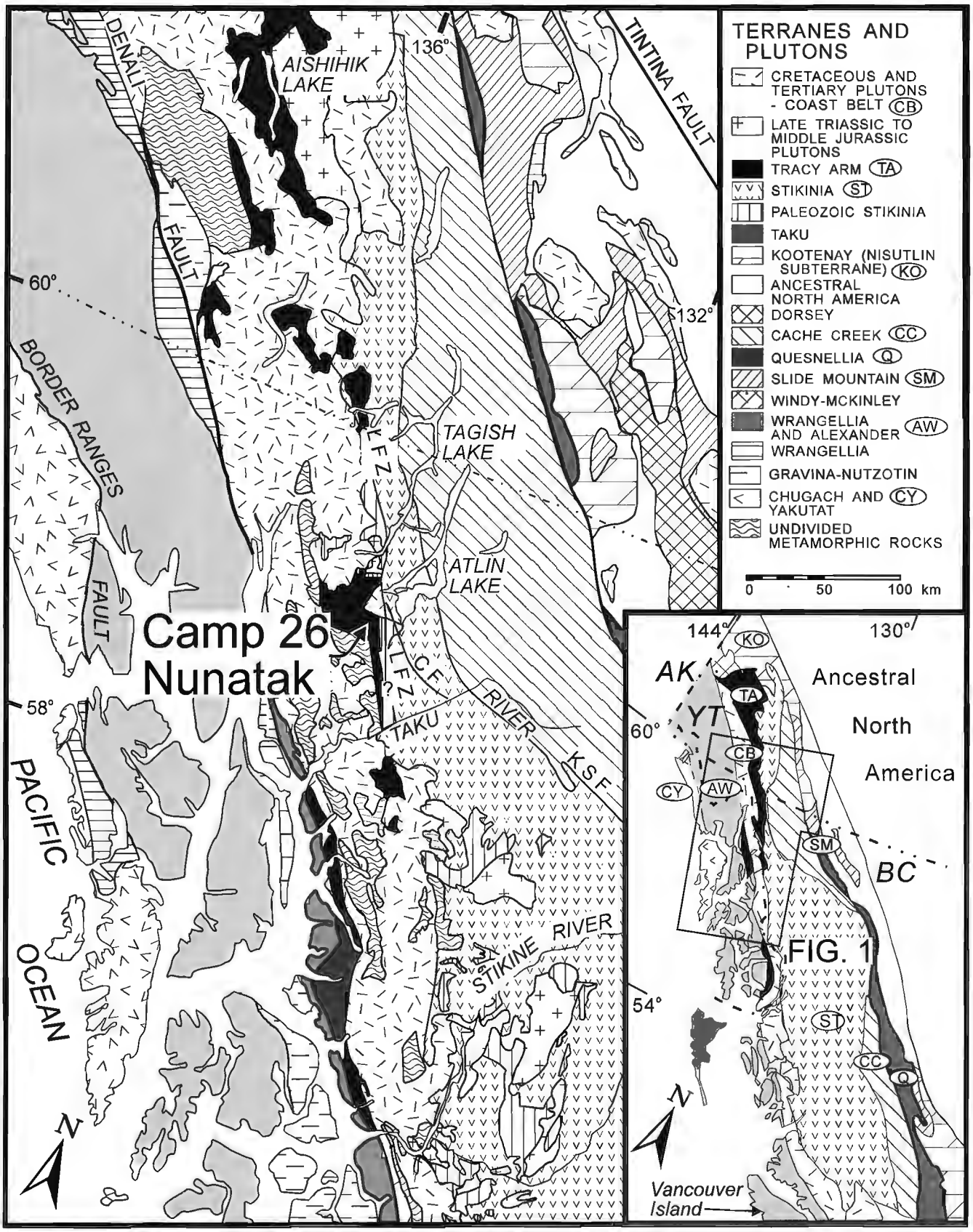
TERRANES AND PLUTONS
CRETACEOUS AND TERTIARY PLUTONS - COAST BELT (CB)
LATE TRIASSIC TO MIDDLE JURASSIC PLUTONS
TRACY ARM (TA)
STIKINIA (ST)
PALEOZOIC STIKINIA
TAKU
KOOTENAY (NISUTLIN SUBTERRANE) (KO)
ANCESTRAL NORTH AMERICA
DORSEY
CACHE CREEK (CC)
QUESNELLIA (Q)
SLIDE MOUNTAIN (SM)
WINDY-MCKINLEY
WRANGELLIA AND ALEXANDER (AW)
WRANGELLIA
GRAVINA-NUTZOTIN
CHUGACH AND YAKUTAT (CY)
UNDIVIDED METAMORPHIC ROCKS
0 50 100 km
DENALI FAULT
AISHIHIK LAKE
136°
TINTINA FAULT
132°
60°
BORDER RANGES FAULT
TAGISH LAKE
LFZ
ATLIN LAKE
Camp 26 Nunatak
CF
LFZ
58°
TAKU RIVER
KSF
PACIFIC OCEAN
STIKINE RIVER
54°
144°
130°
KO
AK
YT
TA
60°
CB
CY
AW
SM
BC
Ancestral North America
FIG. 1
ST
CC
Q
Vancouver Island

Metamorphic rocks

Metamorphic rocks are exposed on the northwest side of the Camp 26 nunatak and appear to continue to the south (Fig. 2). They comprise pelitic and semipelitic rocks and marble, with minor hornblende amphibolite and quartzite. The pelitic rocks and bedded quartzites range in texture from schistose to gneissic, with increasing quartz content. Pelitic rocks are muscovite or biotite rich, with interstitial plagioclase and quartz; some plagioclase is altering to sericite. Garnets up to 0.5 cm in diameter, and centimetre-scale leucosome pods occur locally within the pelitic rocks. On the north side of the mapped area, biotite is intergrown with chlorite and hornblende is associated with actinolite. Minerals in the semi-pelitic rocks include plagioclase, quartz and muscovite, with minor orthoclase, sericite, biotite and opaques. Quartz is interstitial, and also forms poikiloblasts within plagioclase grains. Quartzites contain at least 90% quartz, have interstitial muscovite, and are commonly bedded.

The easternmost metamorphic rocks comprise a 400 m wide band of strongly foliated marble layers that is bounded by volcanic(?) rocks along its southern boundary and is in

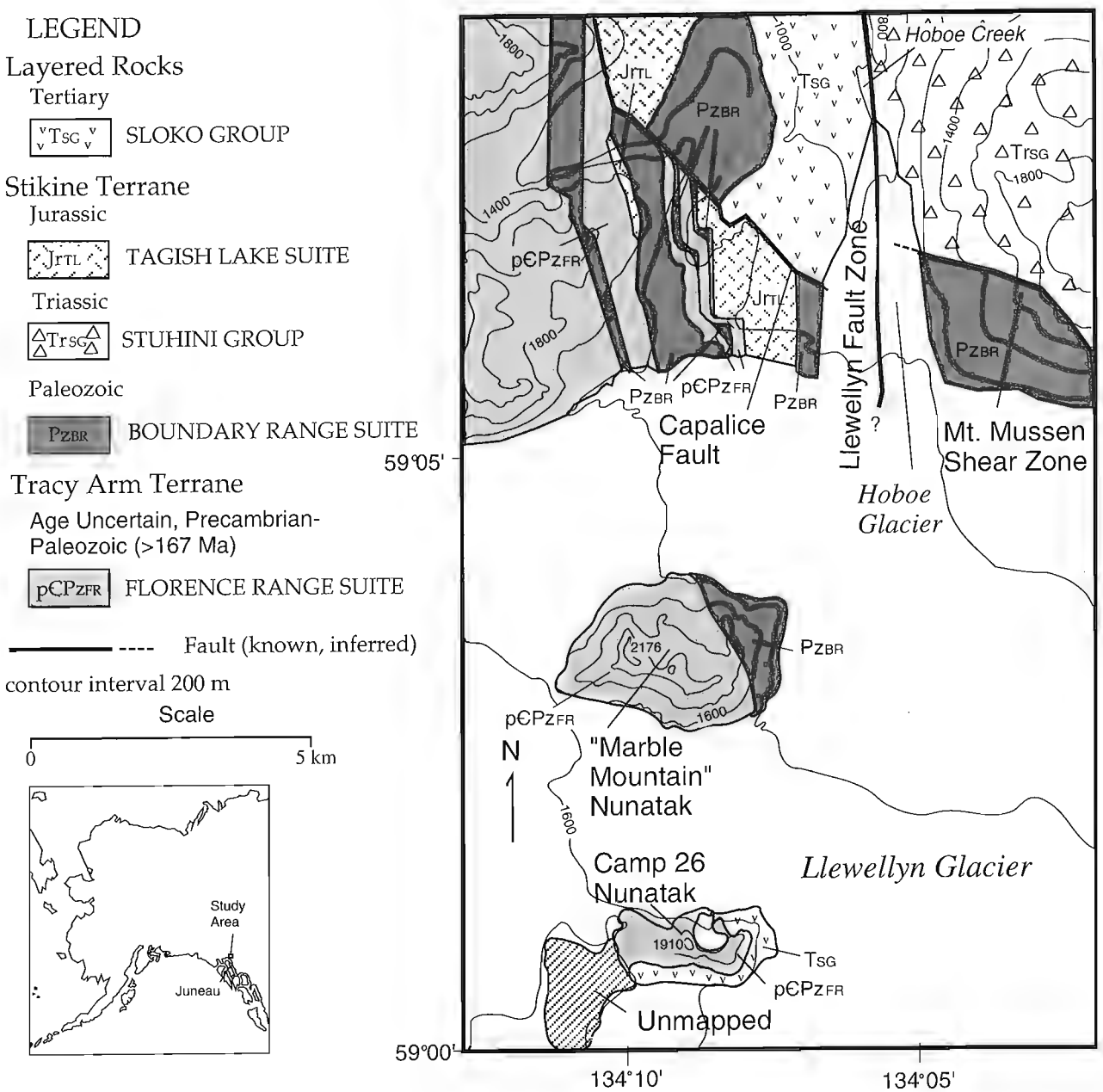

Figure 2. *Geological map of the northeast margin of the Juneau Icefield (based on Currie, 1990, 1991, 1992a, 1994).*

contact with pelitic rocks to the west. Individual marble layers are up to 1 m thick and are separated by thin (<1 cm) pelitic layers and, locally, diopside-bearing calcsilicate layers.

Hornblende amphibolite layers are generally associated with the pelitic rocks on the west side of the mapped area. They contain up to 90% hornblende and commonly include minor augite, garnet, plagioclase, sericite, and biotite.

Volcanic rocks

Volcanic rocks are exposed on the east and south sides of the study area. They are primarily orange-weathering, greenish-grey andesite, volcaniclastic rocks, and minor ignimbrite. In thin section the andesite contains a fine-grained groundmass with phenocrysts of plagioclase, hornblende, and biotite. Minor chloritization of hornblende is common. The andesite appears to grade into a more coarse-grained diorite toward the west.

Depositionally overlying the andesite are pyroclastic rocks. These are dominantly white-weathering, greenish-grey, matrix-supported, polylithic, lapilli tuffs. Clasts are angular, generally range from 1 to 10 cm (Fig. 4). Both volcanic (andesite, well layered cannibalized (?) volcaniclastic clasts, and flattened pumice fragments) and intrusive clasts (diorite) occur within the lapilli tuffs. Rare, white weathering, well layered ignimbrite layers, up to 10 cm thick have also been observed (Fig. 3). Locally, the andesite exhibits centimetre-scale bands interpreted as flow-banding, that at least locally dip steeply toward the east-northeast. Bedding planes in the ignimbrite generally dip toward the north, as do the flattening planes of pumice clasts in the lapilli tuff, which are also interpreted to reflecting bedding (Fig. 3).

Plutonic rocks

On the northeast side of the nunatak, an extensive plutonic outcrop is surrounded by andesitic country rock (Fig. 3). The plutonic rock varies in composition from a grey granite on the eastern side of the outcrop to a coarse-grained diorite on the western end of the outcrop. This very distinctive diorite contains twinned laths of actinolite that are up to 2 cm in length. Within the centre of outcrop granitoid material is interlayered with inclusions of fine-grained mafic material (Fig. 5). The mafic inclusions appear to be discontinuous, and are approximately 10 to 30 cm long and 10 cm thick (Fig. 5).

A small pluton and an independent vein of pink, medium-grained granite are located on the east-central side of the nunatak (Fig. 3). The pluton is several tens of metres wide and the vein is about 3 m wide and trends 312°. The andesite has a baked margin along its contact with the pink granite, and the granite contains inclusions of andesite; both relationships provide clear evidence that the granite is younger than the andesite.

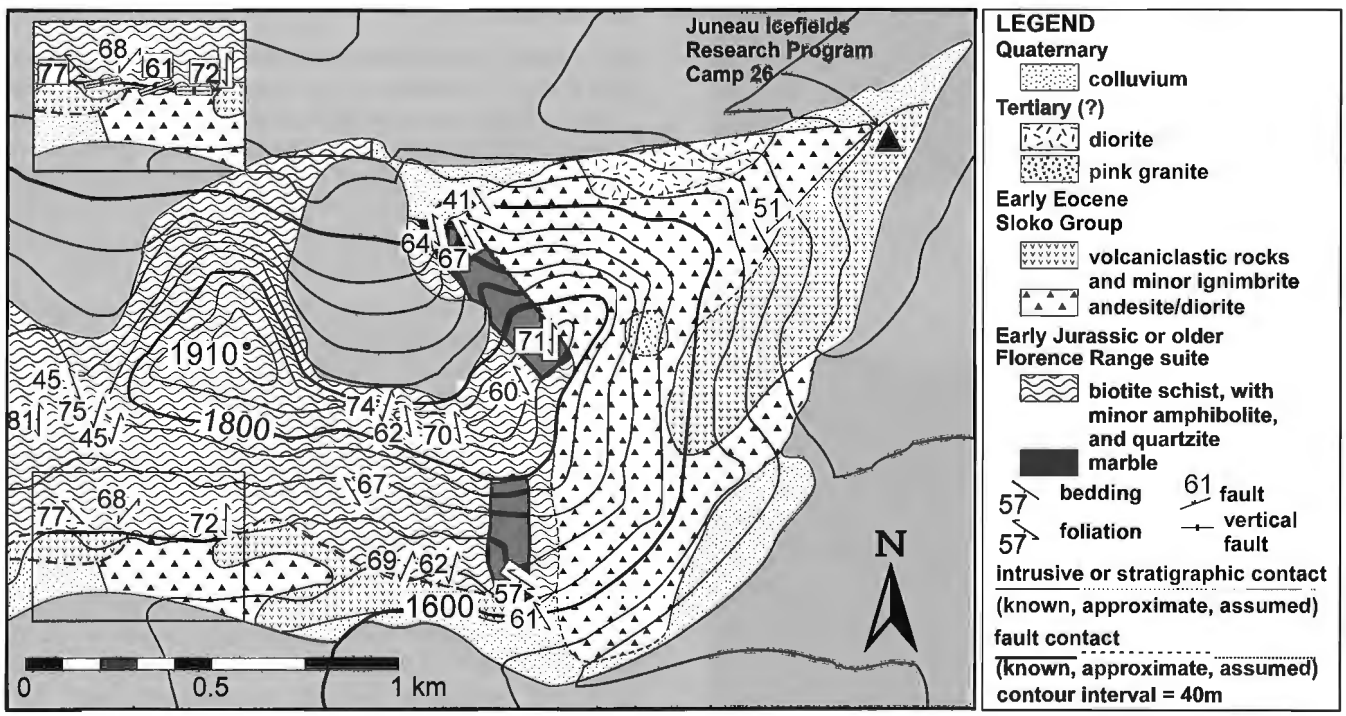

Figure 3. *Geological map of the north end of the Juneau Icefield Research Program Camp 26 nunatak. Contour interval is 40 m. Inset shows measured fault planes for the near-vertical, east-striking fault exposed on the nunatak.*

The mafic and felsic dykes generally strike between 060° and 070° and may comprise as much as 20% of an individual outcrop. The mafic dykes are commonly hornblende and/or plagioclase phyric, and crosscut the much less common felsic dykes.

Interpretation

Metamorphic rocks

Based on mineral abundances and textures, the protoliths for metapelitic rocks include shale and mudstone. More quartz-rich rocks are interpreted to be metamorphosed arkosic sandstone and sandstone. Marbles and calcsilicate layers are presumed to represent metamorphosed limestone and silicious limestone beds. Hornblende amphibolite layers comprise only a minor component of the metamorphic assemblage and are interpreted as metamorphosed mafic flows, dykes, sills, tuffs and/or reworked tuffs. Lithological contacts parallel foliation in the metamorphic rocks and are interpreted as transposed bedding surfaces, with the exception of contacts bounding the amphibolite layers, which may be transposed intrusive contacts.

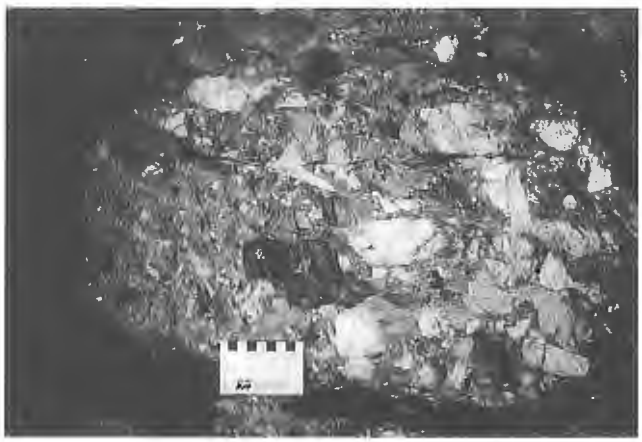

Figure 4. *Volcaniclastic rock interpreted as part of the Eocene Sloko Group.*

Figure 5. *Plutonic rock with inclusions of dark igneous material. Hammer head is 16 cm long.*

The metamorphic rock preserved on the JIRP Camp 26 nunatak are considered part of the Florence Range suite on the basis of rock-type and relative abundances. The dominantly sedimentary protoliths of the metamorphic assemblage, the presence of quartzite, and the apparent continuous nature of the marble layers are consistent with a continental margin origin for these rocks. The scarcity of metamorphosed igneous rocks common to the Boundary Range suite precludes inclusion of these rocks in Stikinia. Thus, the metamorphic rocks exposed on the northern end of the JIRP Camp 26 nunatak belong only to Tracy Arm terrane, and it is reasonable to assume that at least the west side of the "marble mountain" nunatak is also underlain by Tracy Arm terrane rocks. The Stikinia-Tracy Arm terrane boundary that outcrops north of the Llewellyn Glacier, and possibly on "Marble Mountain" nunatak, is not exposed on the JIRP Camp 26 nunatak.

The apparent stable association of garnet and biotite in the pelitic rocks, and the presence of stable hornblende indicate these metamorphic rocks experienced amphibolite facies pressure and temperature conditions. Local alteration to chlorite and actinolite may reflect subsequent greenschist facies conditions, possibly related to subsequent igneous activity (see below).

Igneous rocks

The volcanic rocks preserved on the northeast corner of the JIRP Camp 26 nunatak are not considered correlative with Triassic volcanic rocks of the Stuhini Group, as suggested by Werner (1978), because they lack the augite porphyry flows, conglomerates, folding, and epidote-chlorite alteration that are common in the Stuhini Group. Instead, they are considered part of the Sloko Group, which is characterized by pyroclastic rocks, with subordinate andesite flows (Souther, 1971).

Elsewhere, bedding planes in the Sloko Group are generally flat lying, but may dip as much as 40° (Souther, 1971). Sloko Group volcanic rocks unconformably rest atop older rocks, or are bounded by normal faults. The faults are considered syndepositional on the basis of andesite and trachyte dykes that parallel the faults, and are thought to be coeval with the volcanic rocks (Souther, 1971). The age of the Sloko Group is well documented isotopically, and is from 56 to 53 Ma (M.G. Mihalynuk, pers. comm., 1996). The volcanic rocks are commonly associated with Eocene plutons that are also considered contemporaneous with volcanism (e.g., massive quartz monzonite and a diorite bodies exposed ~35 km north of the JIRP Camp 26 nunatak that are associated with pyroclastic rocks (Mt. Switzer volcanic suite) have U-Pb zircon ages of 55.7 ± 0.2 Ma and 55.9 ± 0.2 Ma, respectively; Currie, 1992b).

Volcanic flows were only observed on the east side of the nunatak, suggesting that the gradual westward transition from andesite to diorite may reflect an undetected change from extrusive to intrusive rocks toward the west. It is clear that the

coarse-grained diorite exposed on the north side of the nunatak and the pink granite intruded the Sloko Group volcanic rocks, and are therefore younger than the volcanic rocks, but how much younger they are is not evident. The relative ages of the granite and the diorite are not known. The dykes are at least in part younger than all of the other rocks exposed on the nunatak, but their absolute ages are not known.

Structure

Metamorphic rocks

Lithological contacts and foliation in the Florence Range suite generally trend roughly north-northwest (Fig. 6). Locally, lithological contacts and foliation are folded by centimetre to outcrop-scale folds that plunge steeply toward the northwest. Micro-structural analysis of quartz-rich gneisses indicates that these rocks have been affected by both ductile shearing (e.g., sheared mica fish and drag folds), and local brittle deformation (offset quartz and feldspar grains).

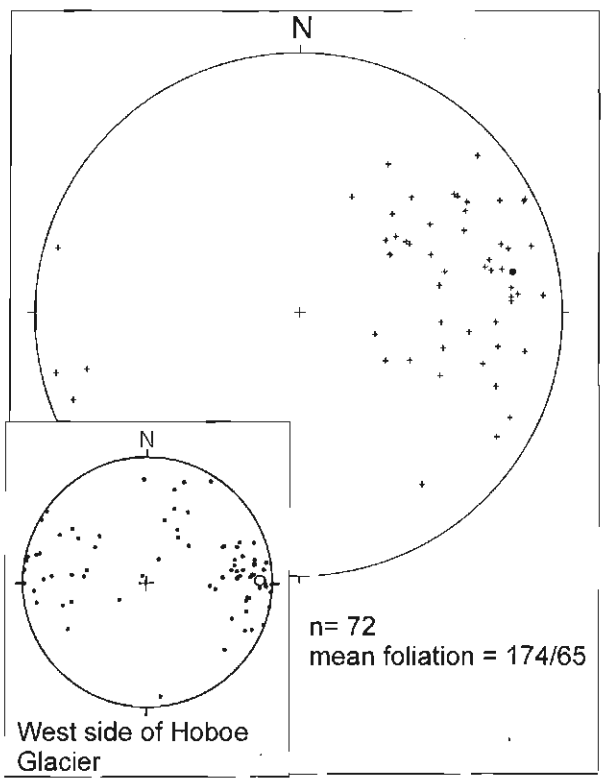

Figure 6. Stereonet showing poles to foliation planes in metamorphic rocks exposed on the JIRP Camp 26 nunatak. Inset stereonet shows poles to foliation planes in metamorphic rocks exposed west of Hoboe Glacier for comparison (from Currie, 1994).

Contact relationships

The contact between the Florence Range suite and the Sloko Group rocks to the east appears to dip steeply toward the west (Fig. 3), but its original contact relations are not clear. Because the contact has not been observed, and it is not clear whether the Sloko Group rocks are intrusive or extrusive, it is not known whether this contact is an intrusive, depositional, or faulted contact.

The Florence Range suite and Sloko Group are also juxtaposed along a steep, east-striking fault zone that outcrops on the south side of the northern portion of the Camp 26 nunatak (Fig. 3). Locally, the fault zone is well exposed, but elsewhere it is covered by Quaternary colluvium. It has a south-side-down sense of motion, based on exposure of metamorphic rocks (they were presumably originally deeper than the Sloko Group) on the north side of the nunatak, and an unknown component of strike-slip motion. The fault cuts lithological contacts and foliation in the Florence Range suite, rocks of the Sloko Group, and dykes that intruded the Sloko Group and Florence Range suite.

The fault zone ranges from centimetres to tens of metres in width, and includes a brecciated quartz matrix with angular inclusions of an east-trending green mafic dyke. If the correlation between the volcanic rocks exposed on JIRP Camp 26 nunatak and the Sloko volcanic rocks is correct, then the truncation of the volcanic rocks and the offset of dykes that intruded the volcanic rocks, by the fault zone, indicates that at least some of the movement on the fault zone is Early Eocene (~56 Ma) or younger. It is certainly plausible that this structure is syndepositional with the volcanic rocks, similar to faults that bound Sloko Group volcanic rocks elsewhere.

The relationship between the fault zone exposed on the nunatak and the Llewellyn fault zone is not clear. They are nearly perpendicular to one another and presumably intersect beneath the Llewellyn Glacier (Fig. 2).

The Llewellyn Fault Zone

The Llewellyn Fault Zone is a steep, north-northwest-striking, fault zone that has been traced over 150 km, from near the British Columbia-Yukon border to the toe of the Hoboe Glacier. Throughout much of its length, it forms significant topographic features (e.g., the southeast end of Tagish Lake; the Hoboe Creek valley). It was active after about 100 Ma, and possibly earlier (Currie, 1992b; Fig. 1, 2). South of the toe of the Hoboe Glacier, the Llewellyn Fault Zone disappears beneath the Hoboe and Llewellyn glaciers, making the location of its southern continuation uncertain (Fig. 2, 3). Mihalynuk et al. (1994) have suggested that the Chief Fault of the Tulsequah River area to the southwest (first described by Payne and Sisson, 1988) could be the southern continuation of the Llewellyn Fault Zone (Fig. 1), but this interpretation requires that the Llewellyn Fault Zone change direction by about 30° near Hoboe Glacier. Such a change

in strike could be accommodated by the Mt. Mussen shear zone (Fig. 2). Both the Mt. Mussen shear zone and the Chief Fault separate metamorphosed rocks of presumed Paleozoic age on the south and west from weakly metamorphosed upper Paleozoic and Mesozoic rocks, which underlie the areas to the east. However, a link between the Mt. Mussen shear zone and the Llewellyn Fault Zone has not been demonstrated (Fig. 2).

An alternative interpretation is supported by Band 4 Side aperture radar (SAR) data, which suggest that the Llewellyn Fault Zone continues with the same strike orientation toward the south-southeast (Fig. 7). Glaciers with little debris and crevassing are expressed as white areas in Figure 7 because they reflect the wavelengths in Band 4 well, whereas glaciers with extreme crevassing or significant rock cover absorb

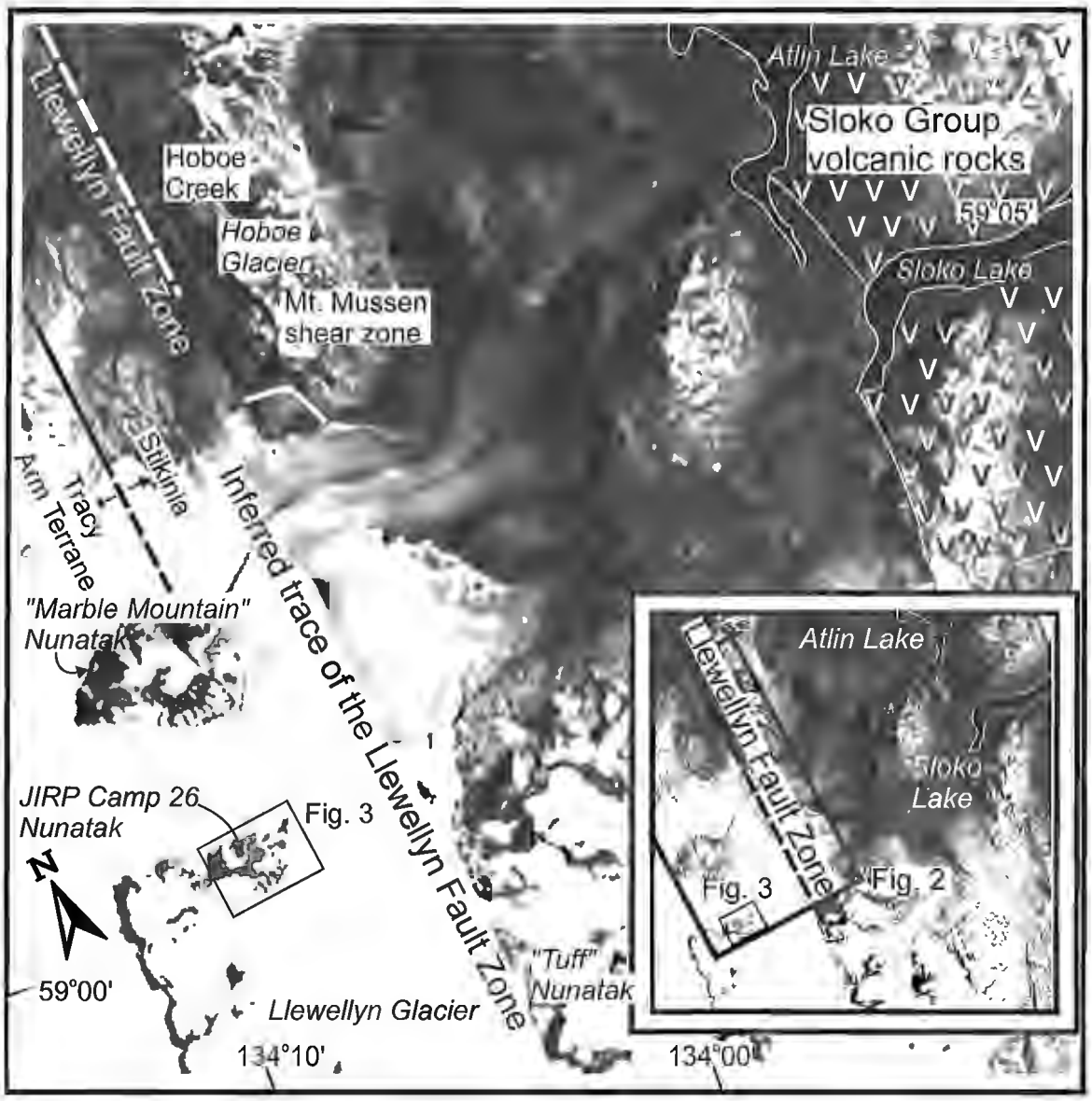

Figure 7. *The inferred trace of the Llewellyn Fault Zone is imaged by side aperture radar data (the multispectral scanner data have 128 brightness levels; this image was prepared using a linear stretch from 16 to 88). The south-southeast-trending strip of grey in the Llewellyn Glacier that is continuous with the Llewellyn Fault Zone is thought to reflect extreme crevassing caused by warping of the ice as it flows over an escarpment in the bedrock below the glacier. The location and orientation of the crevassed area suggest that an escarpment could be related to the Llewellyn Fault Zone, presumably having formed in response to a difference in the resistance to erosion of the rocks on either side fault zone. Rock and vegetation are medium to dark grey, and lakes are black. Glaciers with little debris and crevassing are expressed as white areas because they reflect all colour bands well. Glaciers with extreme crevassing or significant rock cover are light to medium grey. Inset shows the relative locations of Figures 2 and 3.*

some of the wavelengths, and are light to medium grey. The south-southeast-trending strip of grey in the Llewellyn Glacier that is continuous with the Llewellyn Fault Zone is thought to reflect extreme crevassing caused by warping of the ice as it flows over an escarpment in the bedrock below the glacier. The location and orientation of the crevassed area suggest that an escarpment could be related to the Llewellyn Fault Zone, presumably having formed in response to a difference in the resistance to erosion of the rocks on either side of the fault zone. If this interpretation is correct, the Llewellyn Fault Zone does not appear to be offset by any major structures, and the Mt. Mussen shear zone and Chief Fault could be splays of, or older and unrelated to, the Llewellyn Fault Zone.

CONCLUSIONS

Although rocks exposed on nunataks in the Juneau icefield are isolated from areas of more continuous outcrop on the northeast (northwestern British Columbia) and southwest (southeastern Alaska) sides of the Juneau Icefield, geological investigation of nunataks from within the glacier can contribute to the understanding of the complex geology of this area by providing information useful for correlations across the icefield. It may also advance our comprehension of the Tertiary and younger structural history of the northern Coast Mountains, and specifically, the possible relationship between Sloko Group volcanism and Eocene Coast Mountains Batholith plutonism. This investigation has expanded the known extent of the Florence Range suite (Tracy Arm Terrane) and Sloko Group, and has raised the possibility that the Llewellyn Fault Zone continues, along strike, south of the toe of Hoboe Glacier, beneath the Hoboe and Llewellyn glaciers.

ACKNOWLEDGMENTS

This research was made possible by scholarships from the Foundation for Glacier and Environmental Research to Carter and Cooper, logistical support of the Juneau Icefield Research Program, and the directorship of Maynard M. Miller. The authors wish to express their appreciation to Gregg Lamorey, who contributed to satellite data interpretation and Scott Richards, Kerri Rainville, and Riel J. Gagnon for assistance while mapping. Loren Powell did an outstanding job as camp manager of Camp 26. James Cooper would like to acknowledge Loren A. Raymond for assisting with thin section identification and Marjorie McKinney for helping with thin section preparation. Deron Carter would like to thank Kevin Pogue, his thesis adviser and John Winter, who helped with petrographic interpretation of the Florence Range Suite. Glenn Woodsworth is thanked for a thoughtful review of an earlier version of this paper.

REFERENCES

Abolins, M.
1991: Accretion of the Eastern Metamorphic Zone to Stikine Terrane, northern Boundary Range, Atlin Wilderness Park, Juneau Icefield, Alaska - B.C.; Senior thesis, University of California, Berkeley, California, 33 p.

Brew, D.A. and Ford, A.B.
1986: Preliminary reconnaissance geologic map of the Juneau, Taku River, Atlin and part of Skagway 1:250 000 quadrangles, southeastern Alaska; United States Geological Survey, Open File Report 85-395, 23 p.

Coney, P.J., Jones, D.L., and Monger, J.W.H.
1980: Cordilleran suspect terranes; Nature, v. 288, p. 329-333.

Currie, L.D.
1990: Metamorphic rocks in the Florence Range, Coast Mountains, northwestern British Columbia; in Current Research, Part E; Geological Survey of Canada, Paper 90-1E, p. 113-119.
1991: Geology of the Tagish Lake area, northern Coast Mountains, northwestern British Columbia; in Current Research, Part A; Geological Survey of Canada, Paper 91-1A, p. 147-153.
1992a: Metamorphic rocks in the Tagish Lake area, northern Coast Mountains, British Columbia: a possible link between Stikinia and parts of the Yukon-Tanana Terrane; in Current Research, Part E; Geological Survey of Canada, Paper 92-1E, p. 199-208.
1992b: U-Pb geochronology of Cretaceous and Tertiary plutonic rocks of the Tagish Lake area, northeastern Coast Mountains, British Columbia; in Radiogenic Age and Isotopic Studies: Report 6; Geological Survey of Canada, Paper 92-2, p. 163-170.
1994: The geology and mid-Jurassic amalgamation of Tracy Arm terrane and Stikinia of northwestern British Columbia; Ph.D. thesis, Carleton University, Ottawa, Ontario, 385 p.

Currie, L.D. and Parrish, R.R.
1993: Jurassic accretion of Nisling terrane along the western margin of Stikinia, Coast Mountains, northwestern British Columbia; Geology, v. 21, p. 235-238.

Gehrels, G.E., McClelland, W.C., Samson, S.D., Patchett, P.J., and Jackson, J.L.
1990: Ancient continental margin assemblage in the Coast Mountains, southeast Alaska and northwest Canada; Geology, v. 18, p. 208-211.

Mihalynuk, M.G., Currie, L.D., and Arksey, R.L.
1989a: Geology of the Tagish Lake area (Fantail Lake and Warm Creek) (104M/9W and 10E); in Geological Fieldwork 1987; British Columbia Ministry of Energy, Mines and Petroleum Resources, Paper 1989-1, p. 293-310.

Mihalynuk, M.G., Currie, L.D., Mountjoy, K.J., and Wallace, C.A.
1989b: Geology of the Fantail Lake (West) and Warm Creek (East) map area (104M/9W and 10E); British Columbia Geological Survey, Open File Map 1989-13 (1:50 000).

Mihalynuk, M.G., Mountjoy, K.J., Currie, L.D., Lofthouse, D.L., and Winder, N.
1990: Geology and geochemistry of the Edgar Lake and Fantail Lake map area (104M/8,9E); British Columbia Ministry of Energy, Mines and Petroleum Resources, Open File Map 1990-4 (1:50 000).

Mihalynuk, M.G., Smith, M.T., Hancock, K.D., and Dudka, S.
1994: Regional and economic geology of the Tulsequah River and Glacier areas (104K/12 & 13); in Exploration in British Columbia 1991; British Columbia Ministry of Energy, Mines and Petroleum Resources, Paper 1994-1, p. 171-205.

Payne, J.G. and Sisson, J.G.
1988: Geological report on the Tulsequah Property; British Columbia Ministry of Energy, Mines and Petroleum Resources, Assessment Report 17054.

Silberling, N.J., Jones, D.L., Monger, J.W.H., Coney, P.J., Berg, H.C., and Plafker, G.
1994: Lithotectonic terrane map of Alaska and adjacent parts of Canada; in Geology of Alaska, (ed.) H.C. Berg and G. Plafker; Geological Society of America, The Geology of North America, v. G-1.

Souther, J.G.
1971: Geology and mineral deposits of Tulsequah map-area, British Columbia; Geological Survey of Canada, Memoir 362, 84 p.

Werner, L.J.
1978: Metamorphic terrane, Northern Coast Mountains west of Atlin Lake, British Columbia; in Current Research, Part A; Geological Survey of Canada, Paper 78-1A, p. 69-70.

Wheeler, J.O. and McFeely, P.
1991: Tectonic assemblage map of the Canadian Cordillera and adjacent parts of the United States of America; Geological Survey of Canada, Map 1712A, 1:2 000 000.

Wheeler, J.O., Brookfield, A.J., Gabrielse, H., Monger, J.W.H., Tipper, H.W., and Woodsworth, G.J.
1991: Terrane map of the Canadian Cordillera; Geological Survey of Canada, Map 1713, scale 1:2 000 000.

Geological Survey of Canada Project 930038

A progress report on Mississippi Valley-type deposits of the Mackenzie Platform: fluid inclusion studies in sphalerite, quartz, and dolomite from the Bear deposit, Northwest Territories

J.J. Carrière and D.F. Sangster
Mineral Resources Division, Ottawa

Carrière, J.J. and Sangster, D.F., 1996: A progress report on Mississippi Valley-type deposits of the Mackenzie Platform: fluid inclusion studies in sphalerite, quartz, and dolomite from the Bear deposit, Northwest Territories; in Current Research 1996-E, Geological Survey of Canada, p. 87-96.

Abstract: Fluid inclusion, petrographic, cathodoluminescence, and microprobe studies were conducted on gangue and sulphide minerals. Primary inclusions in dolomite contain a fluid representative of the original hot, moderately high saline brine (20.7 to 25 equivalent wt.% NaCl, 210°C average homogenization temperature (Th)). In sphalerite, fluid trapped in pseudosecondary inclusions is probably a sample of the mineralizing fluid (14.2 to 19.4 equivalent wt.% NaCl, average Th 188°C), which was diluted and/or reset by later tectonic events. Temperatures of the first recognized liquid + ice + vapour in fluid inclusions range from -35° to -52°C, indicating the presence of salt(s) other than NaCl. The presence of CO_2 is confirmed in single phase inclusions in quartz and dolomite, and the presence of CH_4 is suggested through indirect evidence in the single phase inclusions. Cathodoluminescence revealed three textural varieties of dolomite. Microprobe analyses identified dolomite and calcite, and characterized the cathodoluminescence zonation in the saddle dolomite.

Résumé : La gangue et les minéraux sulfurés du gisement de Bear ont fait l'objet de diverses études (analyse des inclusions fluides, détermination de la pétrographie, cathodoluminescence et observation à la microsonde). Les inclusions primaires dans la dolomite contiennent un fluide représentatif de la saumure initiale à salinité moyennement élevée et chaude (entre 20,7 et 25,0 % en poids de NaCl, température moyenne d'homogénéisation de 210 °C). Dans la sphalérite, le fluide piégé dans des inclusions pseudosecondaires est probablement un échantillon du fluide minéralisateur (entre 14,2 et 19,4 % en poids de NaCl, température moyenne d'homogénéisation de 188 °C), qui a été dilué ou a été soumis à nouveau aux conditions initiales par des épisodes tectoniques ultérieurs. Les températures du premier mélange «liquide + glace + vapeur» déterminé dans les inclusions fluides varient de -35 °C à - 52 °C, ce qui signale la présence de sel(s) autre(s) que NaCl. La présence de CO_2 est confirmée dans des inclusions de phase unique dans le quartz et la dolomite; quant à la présence de CH_4, elle est révélée par des indices indirects dans les inclusions de phase unique. La cathodoluminescence a mis en évidence trois variétés texturales de dolomite. Les analyses par microsonde ont permis d'identifier la dolomite et la calcite et de caractériser la zonation (observée par cathodoluminescence) de la dolomite d'anticlinal.

INTRODUCTION

The Mackenzie Platform area (Fig. 1) is a sub-district of the much larger Mackenzie Valley lead-zinc district proposed by Sangster and Lancaster (1976). The sub-district is located in a remote region of the northern Canadian Cordillera, along the border between central Yukon Territory and western Northwest Territories. Here, platform carbonate rocks, containing dozens of lead-zinc deposits and occurrences, flank the eastern margin of Selwyn Basin. All lead-zinc occurrences and deposits are located in strata older than Late Devonian. A majority of deposits occur in Early Cambrian or older rocks, but a significant number of deposits, including the Bear deposit, occurs in younger rocks. The deposits, which follow the trend of Lower Paleozoic strata for 360 km along the Mackenzie Fold Belt, appear to be of classic Mississippi Valley-type (MVT). Zinc commonly predominates over lead by at least 10:1 (Gibbins, 1983).

Many deposits in the study area occur in platform carbonate rocks located around the northwest-trending Misty Creek Embayment. The embayment is defined by the change from Upper Cambrian-Lower Ordovician and Upper Ordovician-Lower Silurian platformal carbonate sequences, into correlative transitional and deeper water limestone, shale and chert; and by the presence of Middle Cambrian and Middle Ordovician basinal shales and transitional units (Cecile, 1982). The embayment is best defined by the transition from platform to basin facies, because these strata are extensively preserved within and around it. In the embayment area Late Mesozoic-Tertiary compression produced typical Mackenzie Mountain structures dominated by thrusts and open folds. However, northeasterly directed shortening is not considered to have been sufficient to affect the concept of the embayment geometry (Cecile, 1982).

This study is based on hand samples representative of the host rocks and mineralization of the Bear deposit. The study involved integration of standard petrography, cathodoluminescence microscopy (CL), fluid inclusion petrography (Roedder, 1984), microthermometric data, and electron microprobe analyses.

Deposit geology

The Bear lead-zinc deposit is located at 64°02′N and 129°19′W. It is hosted within breccias of Ordovician shale-carbonate transitional facies of the Mount Kindle Formation, and the overlying Delorme Formation. The Mount Kindle Formation occurs in the northern Mackenzie Mountains and

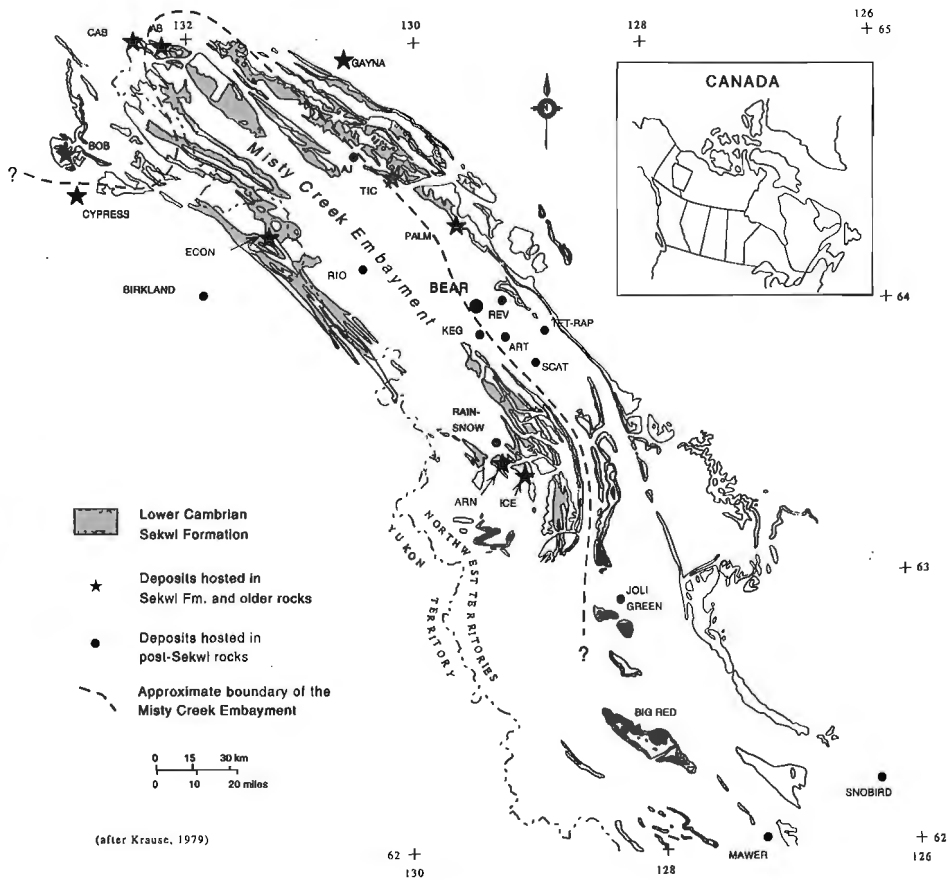

Figure 1. *Map of study area showing distribution of Sekwi Formation, location of zinc-lead deposits included in the Mackenzie Platform study, and the location of the Bear deposit. The boundary of the Misty Creek Embayment is outlined.*

is correlative with the Whittaker Formation to the south. The Mount Kindle Formation comprises up to 570 m of thick-bedded massive dark grey dolostone and minor limestone that are commonly vuggy, medium to coarsely crystalline, locally silicified, and contain some chert nodules and beds. In the Misty Creek Embayment area, and regionally, the Mount Kindle strata unconformably overlie the Franklin Mountain Formation and are unconformably overlain by Siluro-Devonian carbonate rocks. Mount Kindle transition facies host dolomite overlies the Duo Lake Formation. All macro fauna in the Mount Kindle Formation range from Late Ordovician to Early Silurian (Cecile, 1982). Brock (1976) noted that Lower and Middle Devonian carbonate strata are characterized by widespread evaporitic sequences, dolomite and limestone breccia.

The Bear deposit has two zones, a lead-rich one and a zinc-rich one. The lead-rich zone occurs as lenses of barite, with sphalerite, galena, quartz, calcite, and tetrahedrite in Delorme Formation breccia (K.M. Dawson, pers. comm., 1992); this zone, however, has not been examined in the present study.

Samples used in this study came from the zinc-rich breccia zone that is hosted in the Mount Kindle Formation and composed of host dolomite, pyrite, quartz, dolomite cement, sphalerite, and calcite. Neither barite nor tetrahedrite was identified in this study. Reserves at the Bear deposit have been estimated at 18.14 million tonnes grading 7% to 8% combined lead-zinc and 17 to 34 g/t silver (Brock, 1976). The breccia hosting the mineralization was described as a tectonic breccia by Dawson et al. (1991), but as intra-formational breccia by Brock (1976). Dawson also noted the presence of stylolites.

PETROGRAPHY AND CATHODOLUMINESCENCE

Petrographic studies were conducted on two doubly polished thin sections (Fig. 2a, b) and four fluid inclusion plates (Fig. 2c-f). The paragenetic sequence, as observed in this study, consists of host dolomite, pyrite, vein cement dolomite, quartz, saddle dolomite, quartz, sphalerite, and calcite. The successive coatings of breccia cavities by dolomite, quartz and sphalerite are illustrated in Figure 2(c, e, f). Within the pyrite a darker, grey phase (under reflected light) is evident and has been identified by SEM as an Fe oxide that contains minor Zn. The paragenetic position and composition of this mineral are not clear. Another unidentified dark mineral, non-reflective, with a feathery texture, was observed filling the last available cavities.

Dolomite from the study area exhibits three textural varieties according to criteria defined by Sibley and Gregg (1987): 1) non-planar mosaic replacement dolomite, 2) non-planar dolomite vein cement, and 3) saddle dolomite. The host dolomite of the Mount Kindle Formation is of the non-planar mosaic replacement type, and has a grain size ranging from 30 to 300 μm. Pyrite (Fig. 3a, b), euhedral to subhedral, is disseminated throughout the host dolomite. The host dolomite is mainly non-luminescent with a mottling of red, and is veined by a uniform orange-red luminescent calcite. These veins are commonly bordered by dolomite cement. As no planar dolomite was recognized at the Bear deposit, the host dolomite is likely to have formed in a burial environment at >50°C either by dolomitization of limestone or neomorphic recrystallization of pre-existing dolomite (Mazzullo, 1992; Woody et al., 1996).

Dolomite vein cement consists of anhedral to subhedral grains ranging from 60-960 μm in diameter and displaying a sweeping extinction, parts of which were luminescent red and other parts were non-luminescent. This cement occupies narrow veinlets, or borders the host dolomite (Fig. 2a, c, d).

Saddle dolomite fills open spaces in the ore breccias (Fig. 2b, e, f). Coarsely to very coarsely crystalline grains measuring 300-2400 μm have lobate crystal faces, are clear, and display undulatory extinction. Euhedral to subhedral, highly fractured, sphalerite appears to replace the saddle dolomite (Fig. 2b, e, f). Sphalerite has non-luminescent cores bordered by broad bands of bright yellow luminescent sphalerite.

The quartz is euhedral to subhedral and in places has replaced host dolomite. It also occurs in the centre of veins of dolomite cement, and has been partially replaced by saddle dolomite (Fig. 2e, f). The quartz in many cases contains fluid inclusion trails criss-crossing the grains (Fig. 4a, b). These trails (actually planes) of fluid inclusions are healed microcracks and indicate that the quartz was subject to deformation.

Stylolites at Bear are sutured and cut the saddle dolomite (Fig. 2f). In addition, veins of dolomite are offset by stylolites (Fig. 2a), suggesting that the stylolites post-date the vein dolomite. This indicates that deformation has overprinted ore-related minerals, and is consistent with the presence of fluid inclusion trails in quartz. The many healed fractures in Bear sphalerite (Fig. 6a, b) and quartz also indicate these minerals have been subjected to brittle deformation.

MICROPROBE DATA

Carbonate minerals showed end-member compositions for all dolomite types. $CaCO_3$ ranged from 53.96 to 55.69 wt.% (49.49 to 51.83 mol%) and $MgCO_3$ ranged from 43.60 to 45.63 wt.% (47.91 to 49.88 mol%). The $FeCO_3$ content of the three dolomite varieties all averaged below the detection limit of the microprobe (0.25 wt.% or 0.20 mol%). $FeCO_3$ content in dolomite ranged from 0 to 0.58 mol%. The average for 98 readings was 0.07 mol% $FeCO_3$. For dolomite (host rock) the range was 0 to 0.4 mol%, and the average for 62 readings was 0.09 mol% $FeCO_3$. The $MnCO_3$ content of the dolomite varieties averaged at or just above the detection limit of the microprobe (0.175 wt.% or 0.14 mol%). For dolomite, $MnCO_3$ content averaged 0.19 mol% for 98 values that ranged from 0 to 1.12 mol% $MnCO_3$. For host dolomite, the average $MnCO_3$ content for 62 values was 0.14 mol%, and these values ranged from 0 to 0.88 mol%.

FLUID INCLUSION PETROGRAPHY

Two types of inclusions were observed: Type 1, two-phase aqueous, and Type 2, one-phase CO_2. Type 1 inclusions were observed in quartz, dolomite, and sphalerite. The size of the

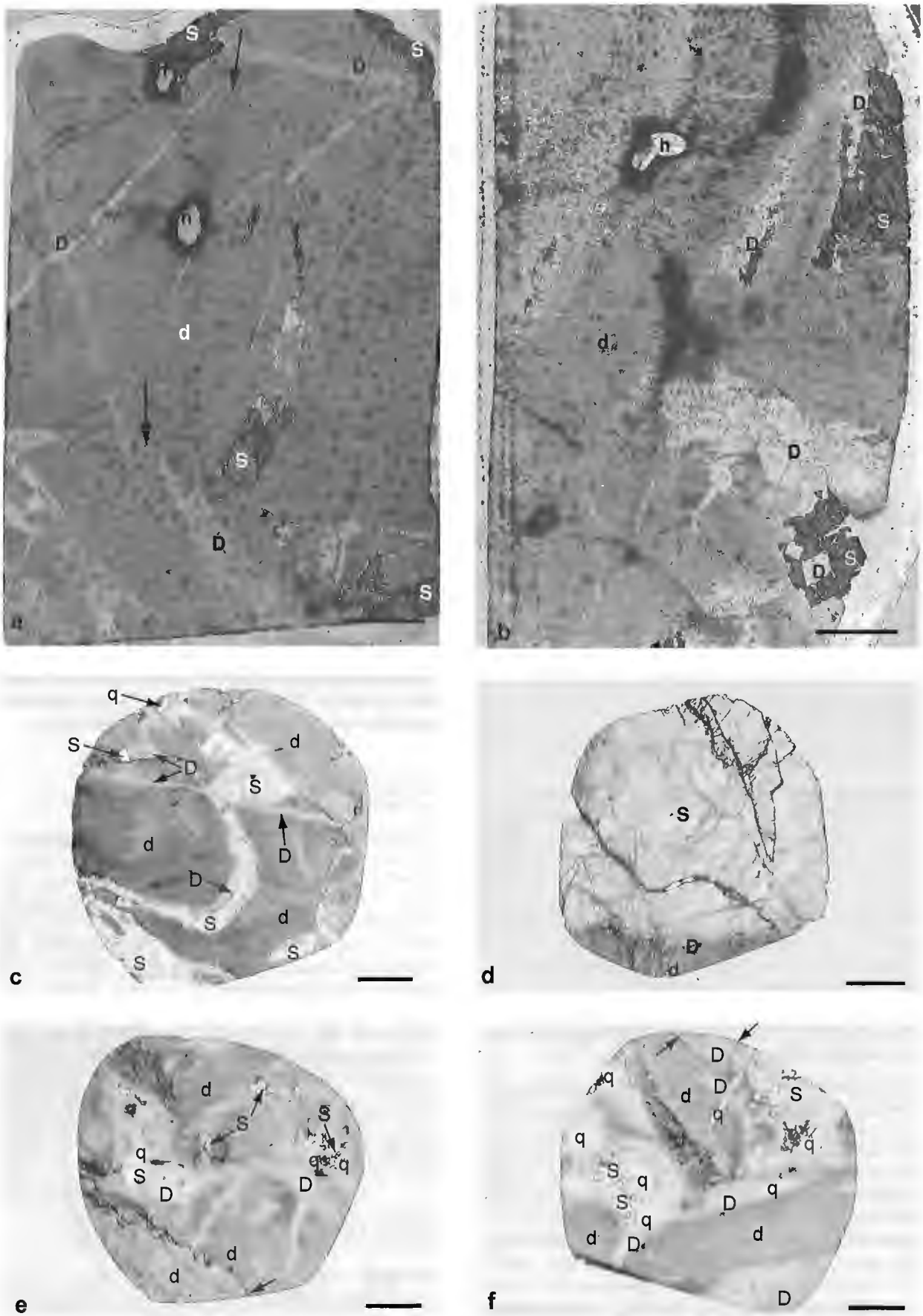
a
S
D
d
b
h
c
q
d
e
f

inclusions in quartz ranged from 4 µm to 40 µm, with 95% > 5 µm. The shapes varied from rounded to oval to completely irregular. The inclusions in dolomite ranged from 2 µm to 7 µm, with 85% measuring 5 µm or less, and were usually square or rhombohedral. The inclusions in sphalerite ranged from 3 µm to 26 µm, with 70% >5 µm. The shape of these inclusions was commonly tubular, but varied from oval to rounded to completely irregular. Both types of inclusions were observed co-existing in quartz in the same plane (Fig. 5a, b), and also in distinct planes. Type 2 inclusions were also observed in a plane in dolomite. Type 2 inclusions were all well rounded as ovals, triangles or elongated. They measured from 4 to 9 µm in diameter. Type 1 inclusions in dolomite are considered to be primary or pseudosecondary based on three modes of occurrence: isolated, in 3-D clusters, or distributed in planes, within a single grain. Criteria used to identify the fluid inclusions as primary, pseudosecondary, or secondary were based on Roedder (1984). Only a few inclusions in quartz and sphalerite met the criteria for primary, the remainder are regarded as pseudosecondary/secondary because most commonly a definite distinction cannot be made.

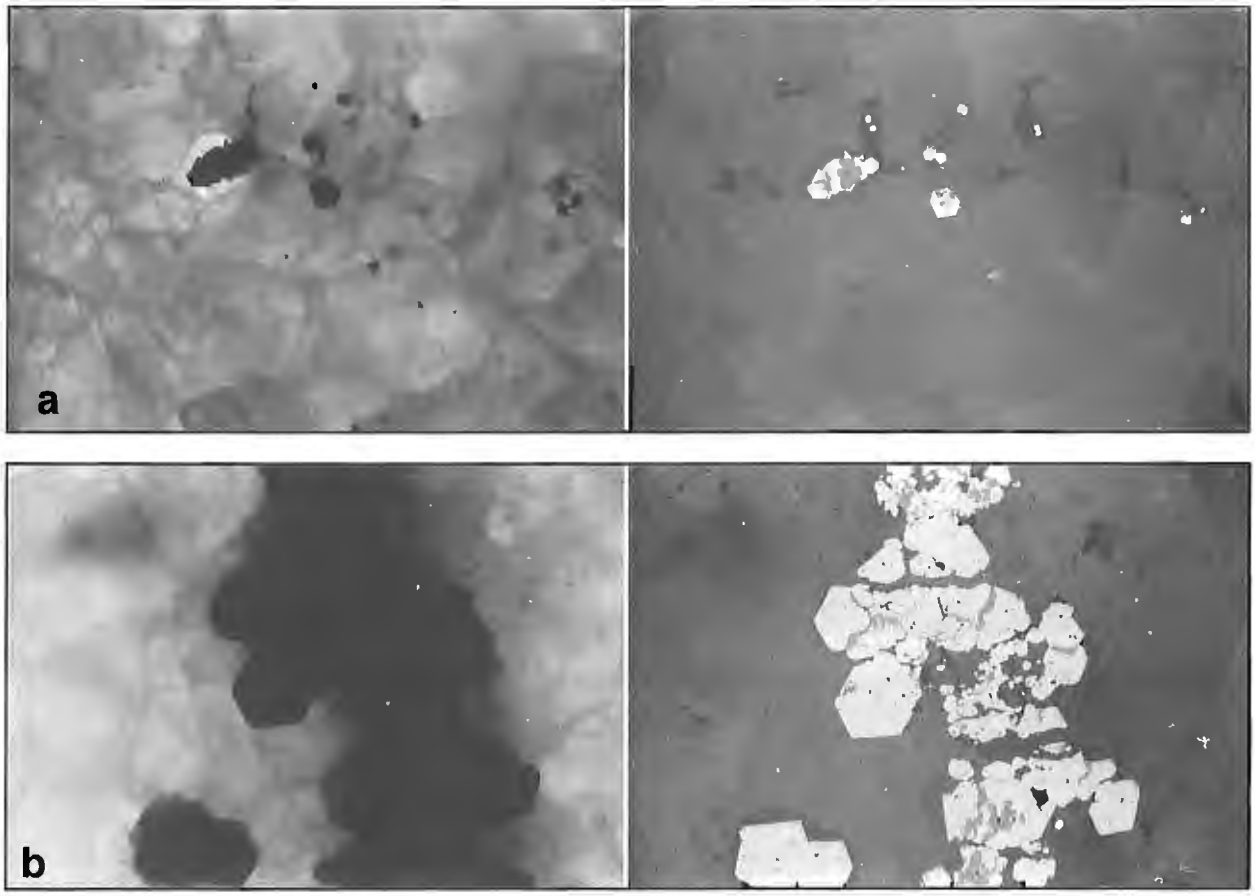

Figure 3. *Photomicrographs showing euhedral pyrite (light grey, reflected light) and the Fe oxide mineral (darker grey within the pyrite, reflected light) disseminated in host dolomite, both* ***a)*** *and* ***b)*** *from sample SP5489(2), transmitted light, uncrossed polars on the left, and reflected light on right. Width of view equals 0.7 mm.*

Figure 2. *Photographs of doubly polished thin sections and fluid inclusion plates illustrating mineral textures and paragenesis. Sample numbers as follow (see also Table 1):* ***a)*** *SP5487, showing dolomite vein cement (D) cutting dolomite host rock (d), with sphalerite (S) in cavities;* ***b)*** *SP5489, showing saddle dolomite (D) growing in open cavities within the host dolomite (d), and sphalerite (S) replacing the saddle dolomite; and fluid inclusion plates;* ***c)*** *SP5487, showing dolostone host rock;* ***d)*** *followed by vein dolomite (D) and sphalerite; (d) BEAR, ore sample showing dolomite host rock (d), with a thin coating of dolomite cement (D), followed by sphalerite (S);* ***e)*** *SP5489(1), showing dolomite host rock (d) cut by stylolite, saddle dolomite (D), followed by quartz (q) and sphalerite (S); and* ***f)*** *SP5489(2), showing dolomite cement (D) cut by stylolite, saddle dolomite (D) followed by quartz (q) and sphalerite (S). Letter (h) indicates hole. Stylolites are indicated by unlabeled*

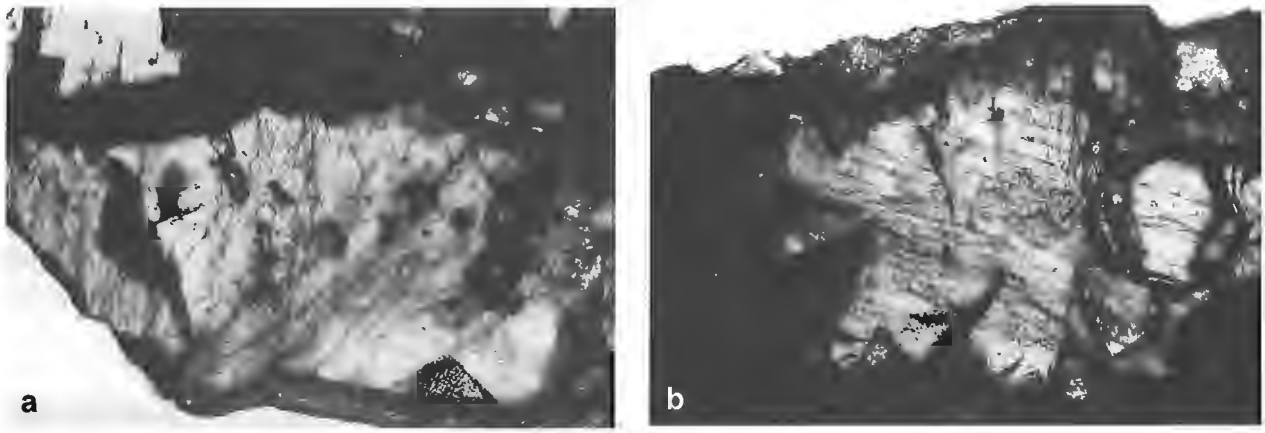

Figure 4. *Photomicrographs of quartz, both* ***a)*** *and* ***b)*** *from sample SP5489(2) displaying wispy texture created by the many fluid inclusion trails criss-crossing the grains (transmitted light, uncrossed polars). Width of view equals 1.4 mm.*

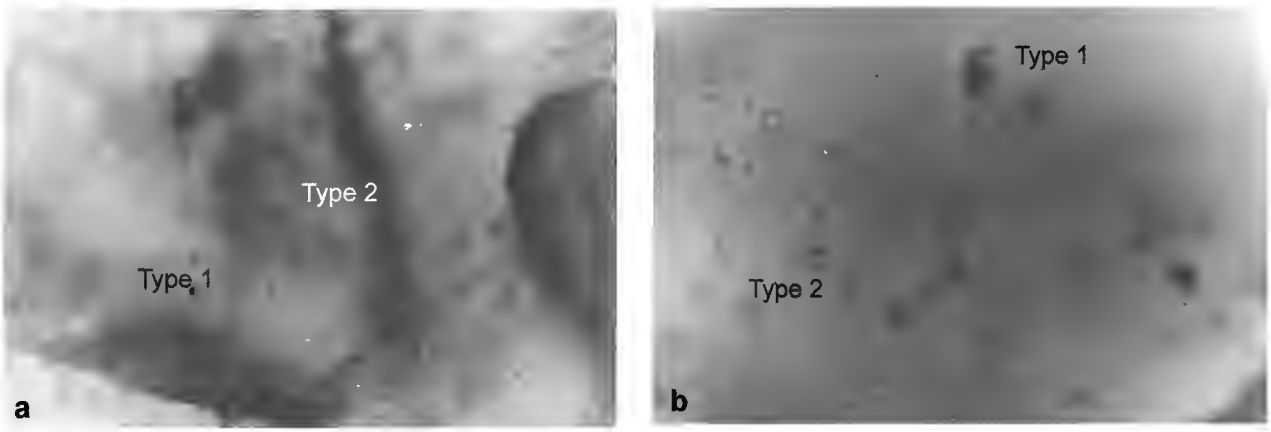

Figure 5. *Photomicrographs showing Type 1, two phase aqueous, and Type 2, one phase CO_2 fluid inclusions in quartz (transmitted light, uncrossed polars), both* ***a)*** *and* ***b)*** *from sample SP5489(2). Width of view equals 300 μm.*

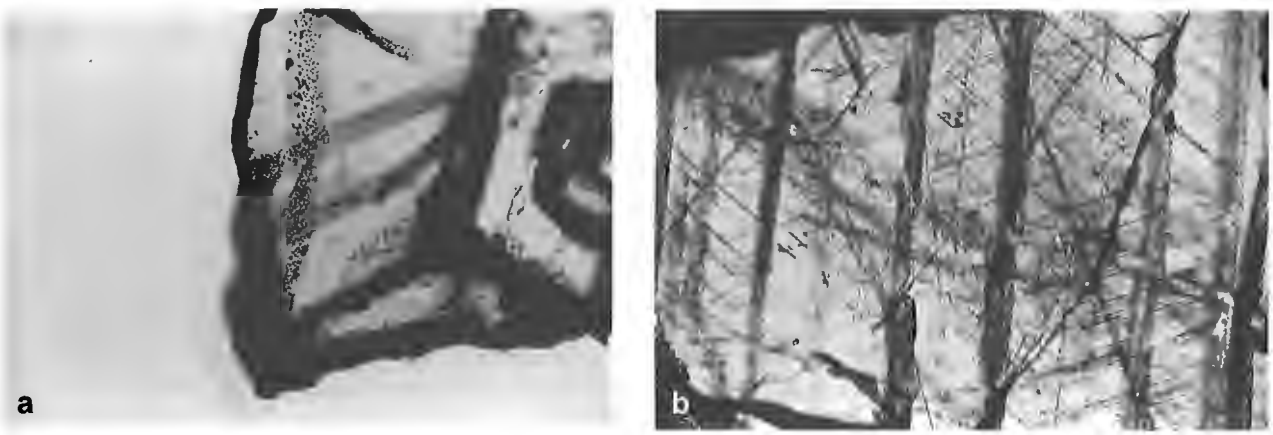

Figure 6. *Photomicrographs showing healed fractures in sphalerite (transmitted light, uncrossed polars):* ***a)*** *SP5489(2), width of chip is 0.8 mm, and* ***b)*** *BEAR, width of view equals 1.4 mm.*

Planes of inclusions are both secondary, in cases of clear fractures, or pseudo-secondary. Where trails are parallel to cleavage planes, as illustrated in sphalerite in Figure 7, inclusions are considered pseudosecondary. Commonly, the healing process following brittle deformation results in rows of inclusions that have a regular spacing within the plane, from cleavage steps in the original fracture surface. Slight movements of the two sides of such a stepped fracture relative to each other can yield tubular secondary and secondary-looking inclusions. Roedder (1984) concluded that, although sample material which presents positive proof of pseudosecondary origin is rare, many of the large healed cleavage or curving fracture planes, now delineated by planes of inclusions in most euhedral crystals from vugs, are probably pseudosecondary rather than secondary. Many examples of tubular inclusions were observed in Bear sphalerite (Fig. 7a, b).

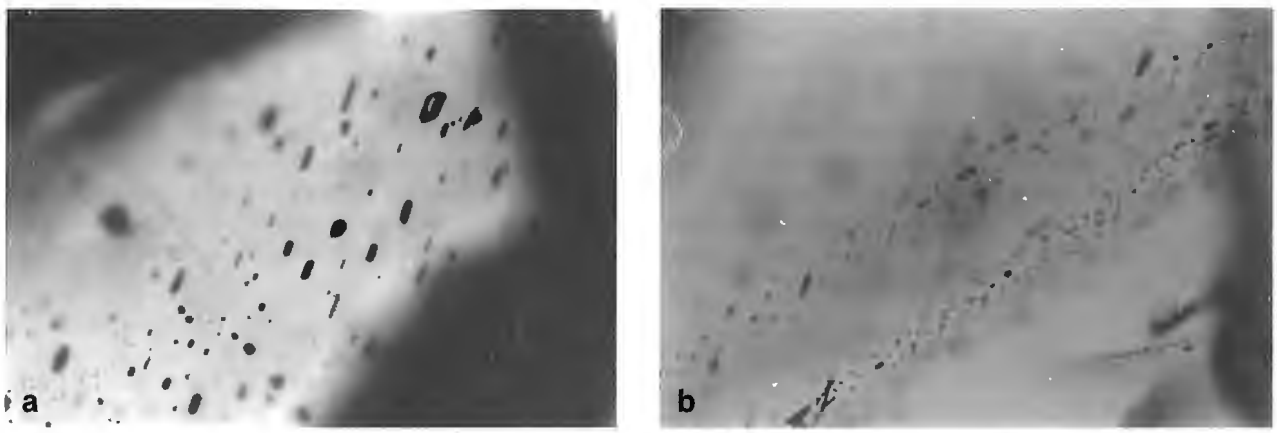

Figure 7. *Photomicrographs showing trails of tubular pseudosecondary fluid inclusions in sphalerite (transmitted light, uncrossed polars), both* ***a)*** *and* ***b)*** *from sample SP5489(2). Width of view equals 300 μm.*

Table 1. Sample I.D. number, type (primary = P, pseudosecondary = PS, secondary = S), number of inclusions (N), homogenization (Th) and melting (Tm) temperatures, number of inclusions (N), temperature of nucleation of ice (Tn), and salinity (equiv. wt. % NaCl) for sphalerite, dolomite, and quartz from the Bear deposit.

Sample I.D. Number	Type	N	Th °C	Tm (ice) °C	N	Tn (ice)°C	Salinity
Sphalerite							
BEAR	P	2	203-213°	-22.9°	1		23-25
	PS	8	142-171°	-14.1 to -16.0°	7		17.8-19.4
	S	14	94-124°		7	-44.8°to -50.2°	(low)
SP5489(1)	PS	11	177-199°	-12.5 to -15.6°	7	-64 to -68	16.4-19.1
SP5489(2)	PS	64	168-204°	-10.3 to -15.5°	56	-56.3 to -66.4°	14.3-19.1
Dolomite							
SP5489(1)	P/PS	31	161-249°	-19.3 to -24.4°	17	-40.2 to -86.4°	21.9-25
SP5489(2)	P/PS	12	176-248°	-17.6 to -25.0°	6	-34.9 to -81.8°	20.7-25
Quartz							
SP5489(1)	P(?)	4	225-255°	-21.2 to -24.2°	4	-63.7 to -82.4°	23.2-25
	PS/S	15	189-236°	-13.3 to -16.4°	3	-56 to -65°	17.2-19.8
	S	6	217-265°	-0.4 to -4.4°	5	-44.1 to -48.3°	0.7-7.0
SP5489(2)	P(?)	1	216°	-23.7°	3	-23.7	23-25
	PS/S	6	192-227°	-10.4 to -15.7°	6	-46.7 to -60°	14.4-19.2
	S	3	220-251°	-1.9 to -5.1°	5	-45.1 to -49.5°	3.23-8.00
SP5487	PS/S	7	158-189°	-10.7 to -12.8°	7	-46.4 to -49.1°	14.7-16.7

ANALYTICAL METHODS

Three hundred and fifty-five microthermometric determinations (Th = 208 and Tm = 147) were carried out on inclusions in sphalerite, quartz, and dolomite in four doubly polished sections (100 μm thick) using a Linkam heating/freezing stage. The stage was calibrated both before and after measurements using SYNFLINC Synthetic Standards and an additional four compounds of known melting points ranging from -56.6° to 200°C. A calibration curve was contructed from the results and all temperatures were corrected accordingly. Poor optical characteristics of many inclusions and their small size combined to give an average estimated precision of ±2°C on readings above, and ±0.5°C on readings below 0°C. All homogenization runs were repeated and results were either duplicated within 4°C or they were not included in Table 1. Freezing runs were also repeated and results were duplicated within 0.5°C. This indicates that minimal, if any, stretching took place during microthermometric experiments.

Aqueous fluid inclusions

Table 1 and Figure 8 summarize the microthermometric results. Pseudosecondary/secondary inclusions in sphalerite homogenize between 142° and 213°C, and average 188°C. Melting temperatures of ice (Tmi) range from -11.1° to -17.1°C, with one exception of -24.5°C. Excluding this value, salinity ranges from 14.2 to 19.4 equiv. wt.% NaCl. Vapour bubbles, at room temperature, occupy between 5 and 10% of the inclusion volume. Definitely secondary inclusions homogenize between 94° and 124°C, and gave an indication of low salinity "behaviour", which includes temperatures warmer than -47.8°C for the nucleation of ice on cooling, metastability, and vapour bubbles popping back between -5° and -1°C upon heating. The Tm of ice could not be measured directly for most secondary inclusions in sphalerite.

Inclusions in dolomite homogenize from 161° to 249°C, and average 210°C. Melting temperatures of ice fell in the range of -17.6° to -25.3°C. Melting temperatures less than -21.2°C cannot be converted to wt.% NaCl because they exceed the room temperature eutectic for the pure NaCl-H_2O system. No daughter crystals of halite were observed. The presence of divalent metal cations, probably calcium, is indicated as solutions containing these have lower melting points.

Inclusions in quartz showed the widest range in Tm of ice, with three distinct groups: low salinity (Tmi = -1.4° to -5.1°C), moderate salinity (Tmi = -10.4° to -15.7°C), and moderate-high salinity (Tmi = -21.2° to -24.2°C). The moderate-high salinity inclusions are primary/pseudosecondary inclusions and have homogenization temperatures ranging from 216° to 255°C; the moderate salinity inclusions are

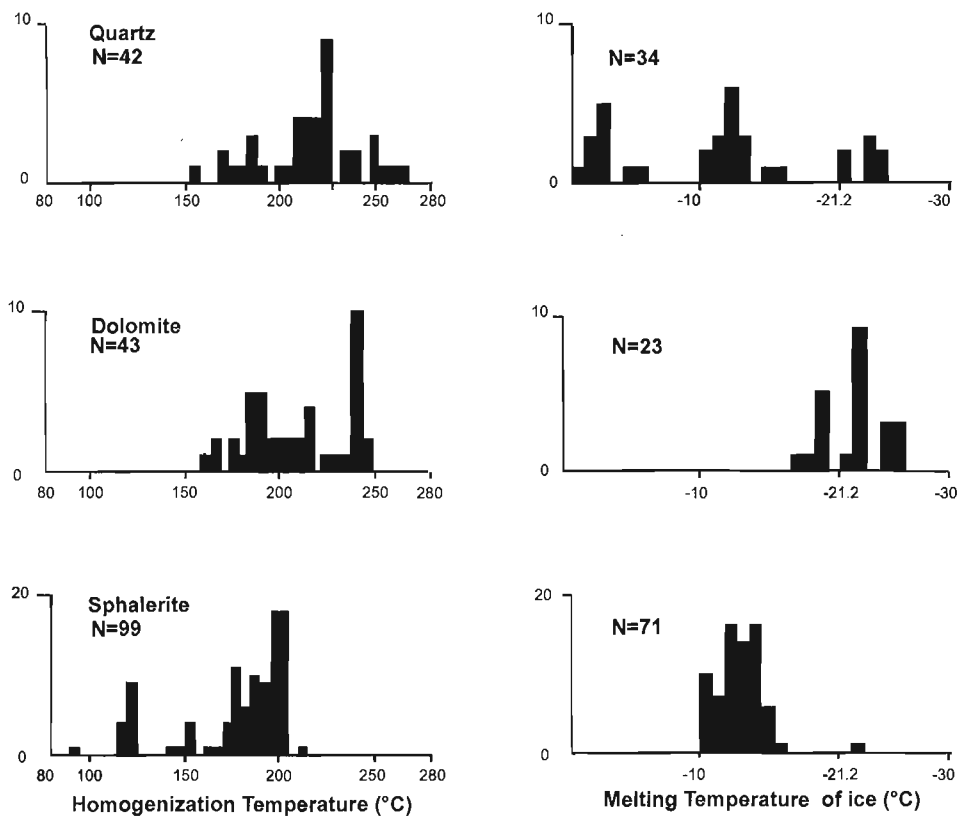

Figure 8. Frequency distribution of homogenization temperatures and melting temperatures of ice for fluid inclusions in quartz, dolomite, and sphalerite from the Bear deposit.

Table 2. Sample I.D. number, number of inclusions, melting (Tm) and homogenization (Th) temperatures, temperature of nucleation of ice (Tn) for CO_2 inclusions in dolomite (Chip #11) and quartz (Chips #16 and #7) from the Bear deposit.

Sample I.D. Number	No. of inclusions	Tm CO_2	Th CO_2	Tn °C
SP5487 Chip #11	6	-60.2 to -60.4°	4.8° to 6.9°	-101 to 103.9°
SP5489(1) Chip #16	8	-60.4°	2.6 to 11.3°	-101 to -103.9°
SP5489(2) Chip #7	7	-58.7 to -58.9°	4.0 to 13.8°	-100.4 to -102.9°

pseudosecondary/secondary and have Th ranging from 158° to 226°; and the low salinity inclusions are secondary and have Th ranging from 220° to 254°C. The frequency distribution plots in Figure 8 illustrate the results.

The presence of $CaCl_2$ in fluid inclusions was also indicated by the first melting temperatures. The aqueous inclusions from sphalerite, dolomite, and quartz showed similar first melting temperatures ranging from -35° to -50°C for sphalerite, -40° to -49°C for dolomite, and -35° to -52°C for quartz. These first melting temperatures are not exact true first melting or eutectic temperatures (Te) (-52°C for the H_2O-NaCl-$CaCl_2$ system), but represent the first temperatures at which liquid+ice+vapour was recognized. The fact that these temperatures are well below the eutectic temperature for the H_2O-NaCl system (-21.2°C), indicates the presence of other salts, probably $CaCl_2$.

CO_2 inclusions

Microthermometric results for CO_2 inclusions from Bear quartz and dolomite are listed in Table 2. CO_2 at room temperature that is present as a single phase at greater than critical density will, upon cooling, nucleate a vapour bubble (Roedder, 1984). The CO_2 inclusions within the samples from the Bear deposit nucleated a bubble on cooling before the temperature reached 0°C. Other characteristic behaviour included the fact that ice nucleated upon cooling at around -103°C, melted between -58.7° and -60.4°C. CO_2 homogenized between 2.6° and 13.8°C. The "low" melting temperature of CO_2 indicates the presence of additional volatile phases, probably CH_4 (Roedder,1984).

INTERPRETATION OF MICROTHERMOMETIC DATA

As shown in the temperature-salinity plot in Figure 9, three types of fluids were trapped at Bear: A) high temperature-moderately high saline fluid in the primary inclusions in dolomite, in one inclusion in sphalerite, and in a few inclusions in quartz; B) high temperature-moderately saline fluid in pseudosecondary inclusions in sphalerite, and in a few inclusions in quartz; and C) higher temperature-low salinity fluid in secondary inclusions in quartz. In sphalerite, the inclusions have been interpreted as pseudosecondary and contain a fluid which evolved over time, or by mixing with a cooler, less saline fluid, such as the low

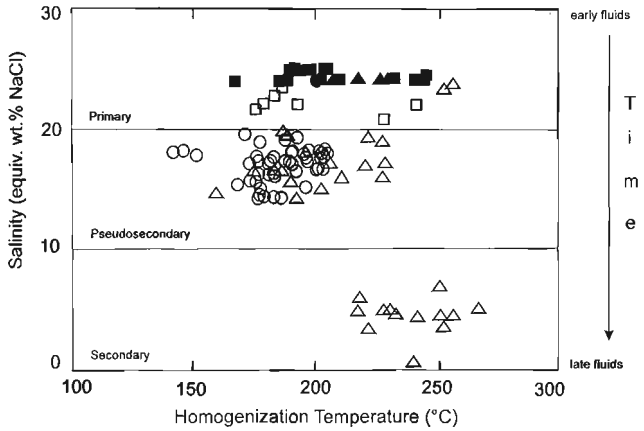

Figure 9. Temperature-salinity plot for fluid inclusions from the Bear deposit; squares = dolomite, triangles = quartz, and circles = sphalerite. Solid symbols represent inclusions with salinity ranging from 23 to 25 equiv. wt.% NaCl.

temperature-low salinity fluid found in the secondary inclusions in sphalerite. The hot, less saline, fluid in secondary inclusions in quartz is later, and unrelated to mineralization.

For plotting purposes, when Tmi was less than -21.2°C and the salinity, therefore, greater than 23.18 wt.% NaCl (the maximum value provided in Table 1 of Bodnar, 1993), the phase diagram for the NaCl-$CaCl_2$-H_2O system, Figure 3 from Vanko et al. (1988) was used. Although the exact position along the composition line on the phase diagram (Fig. 3, Vanko et al., 1988) is not known, the range of possible salinity can be determined. A minimum of 23 equiv. wt.% NaCl and a maximum of 25 equiv. wt.% NaCl based on Tm of ice ranging from -22.9° to -25.0°C was determined. Inferred salinities of this magnitude are significant because they constrain the characteristics of the dolomitizing fluid, which was likely also the mineralizing fluid.

The fact that inclusions in quartz display the full range of salinities suggests that these inclusions reflect the changing history, including the post-ore history, of the deposit. Quartz is easily affected tectonically and this may explain the repeated generation of fluid inclusion trails which sweep back and forth across the grains. Each progressive influx of fluid was recorded in the fluid inclusions in the healed fractures. Some inclusions remained sealed which protected their original contents from any change.

Homogenization temperatures in (hydrothermal) saddle dolomite range between 161° and 249°C. Because the exact timing of the flow of the hydrothermal (mineralizing) fluid is not known, it is possible that the homogenization temperatures of inclusions in the dolomite (and quartz and sphalerite) may have been affected by post-entrapment heating. Anderson (1988) described Mesozoic plutonic suites within the area which could have influenced the temperature of the mineralizing fluids. Hence, the results should be regarded as maximum values (Nesbitt and Muehlenbachs, 1994).

CONODONTS

Conodont colour alteration index (CAI) values (Read et al., 1991) suggest that the Bear host Mount Kindle Formation has been buried to significant depths, and therefore the host rock dolomite is referred to as burial dolomite. The CAI values average around 4, which suggest temperatures between 190° and 300°C. As the fluid inclusion temperatures are within the same range, either ore temperature equalled host rock temperature or the inclusions were reset to these higher temperatures by a post-ore heating event. It is, therefore, important to know the timing of the mineralization to determine if post-entrapment heating should be expected (Sangster et al., 1994).

CONCLUSIONS

The mineralizing fluid(s) at the Bear deposit were moderately saline, and contained $CaCl_2$ in addition to NaCl. The temperature of the fluids represented in primary and pseudosecondary inclusions ranged from 142° to 249°C, secondary inclusions hosted in quartz ranged from 217°-269°C with low salinity, and in sphalerite ranged from 94° to 124°C, with an indication of low salinity. There is a possibility that post-entrapment heating occurred.

The presence of CO_2 has been confirmed and the presence of CH_4 suggested by indirect evidence, which could be significant when considering the genesis of the deposit (Spirakis and Heyl, 1993).

ACKNOWLEDGMENTS

François Robert (GSC) and Ralph Thorpe (GSC) kindly reviewed the manuscript and made many useful suggestions. John Stirling and Dave Walker (GSC, Mineralogy Section) provided the microprobe and SEM analyses respectively. Samples were generously donated by K.M. Dawson (GSC, Vancouver) and J.S. Brock (American Bullion Minerals Ltd.). K.M. Dawson also supplied his field notes on the Bear deposit. Sections were prepared by Vancouver Petrographics Ltd.

REFERENCES

Anderson, R.G.
1988: An overview of some Mesozoic and Tertiary plutonic suites and their associated mineralization in the northern Canadian Cordillera; in Recent Advances in the Geology of Granite-related Mineral Deposits; Canadian Institute of Mining and Metallurgy, Special Volume 39, p. 96-113.

Bodnar, R.J.
1993: Revised equation and table for determining the freezing point depression of H O-NaCl solutions; Geochimica et Cosmochimica Acta, v. 57, p. 683-684.

Brock, J.S.
1976: Recent developments in the Selwyn-Mackenzie Zinc-Lead Province Yukon and Northwest Territories; Western Miner, March, p. 9-16.

Cecile, M.P.
1982: The Lower Paleozoic Misty Creek Embayment, Selwyn Basin, Yukon and Northwest Territories; Geological Survey of Canada, Bulletin 335, 78 p.

Dawson, K.M., Panteleyev, A., Sutherland Brown, A., and Woodsworth, G.J.
1991: Regional metallogeny, Chapter 19 in Geology of the Cordilleran Orogen in Canada, (ed.) H. Gabrielse and C.J. Yorath; Geological Survey of Canada, Geology of Canada, no. 4, p. 707-768.

Gibbins, W.A.
1983: Mississippi Valley Type lead-zinc district of northern Canada; in International Conference on Mississippi Valley-type lead-zinc deposits; Proceedings Volume, University of Missouri-Rolla, Rolla, Missouri, p. 403-414.

Krause, F.F.
1979: Sedimentology and stratigraphy of a continental terrace wedge: the Lower Cambrian Sekwi and June Lake Formations (Godlin River Group), Mackenzie Mountains, Northwest Territories, Canada; Ph.D. thesis, University of Calgary, Calgary, Alberta, 252 p.

Mazzullo, S.J.
1992: Geochemical and neomorphic alteration of dolomite: a review; Carbonates and Evaporites, v. 7, p. 21-37.

Nesbitt, B.E. and Muehlenbachs, K.
1994: Paleohydrogeology of the Canadian Rockies and origins of brines, Pb-Zn deposits and dolomitization in the Western Canada Sedimentary Basin; Geology, v. 22, p. 243-246.

Read, P.B., Psutka, J.F., and Fillipone, J.
1991: Organic maturity data for the Canadian Cordillera; Geological Survey of Canada, Open File 2341, 140 p.

Roedder, E.
1984: Fluid Inclusions; Reviews in Mineralogy, v. 12, Mineralogical Society of America, 646 p.

Sangster, D.F. and Lancaster, R.D.
1976: Geology of Canadian lead and zinc deposits; in Report of Activities, Part A; Geological Survey of Canada, Paper 76-1A, p. 301-310.

Sangster, D.F., Nowlan, G.S., and McCracken, A.D.
1994: Thermal comparison of Mississippi Valley-type lead-zinc deposits and their host rocks using fluid inclusion and conodont color alteration index data; Economic Geology, v. 89, p. 493-514.

Sibley, D.F. and Gregg, J.M.
1987: Classification of dolomite rock textures; Journal of Sedimentary Petrology, v. 57, p. 967-975.

Spirakis, C.S. and Heyl, A.V.
1993: Organic matter (bitumen and other forms) as the key to localization of Mississippi Valley-type ores; in Bitumens in Ore Deposits, (ed.) J. Parnell, H. Kucha, and P. Landais; Springer-Verlag, New York, p. 381-398.

Vanko, D.A., Bodnar, R.J., and Sterner, S.M.
1988: Synthetic fluid inclusions: VIII. Vapor-saturated halite solubility in part of the system NaCl-CaCl2-H2O, with application to fluid inclusions from oceanic hydrothermal systems; Geochimica et Cosmochimica Acta, v. 52, p. 2451-2456.

Woody, R.E., Gregg, J.M., and Koederitz, L.F.
1996: Effect of texture on petrophysical properties of dolomite: evidence from the Cambro-Ordovician of southeastern Missouri; American Association of Petroleum Geologists Bulletin, v. 80, p. 119-132.

Geological Survey of Canada Project 860018

Baculites compressus robinsoni Cobban from the Crowsnest River section at Lundbreck, Alberta: an implication for the timing of the late Cretaceous Bearpaw transgression into the southern Foothills of Alberta[1]

T. Jerzykiewicz
GSC Calgary, Calgary

Jerzykiewicz, T., 1996: Baculites compressus robinsoni *Cobban from the Crowsnest River section at Lundbreck, Alberta: an implication for the timing of the late Cretaceous Bearpaw transgression into the southern Foothills of Alberta; in Current Research 1996-E; Geological Survey of Canada, p. 97-100.*

Abstract: The occurrence of *Baculites compressus robinsoni* Cobban in the Bearpaw shale near Lundbreck, Alberta, indicates that during the time of the *Baculites compressus* Zone (i.e., at approximately 73.4 Ma), the Bearpaw marine transgression extended into the area now occupied by the Rocky Mountain Foothills. At that time, the Bearpaw transgression attained its maximum extent and covered both the southern plains and Rocky Mountain Foothills, and probably extended as far west as the footwall of the Lewis Thrust. The record of Bearpaw deposition in the southern Foothills is correlative with that of the southern plains. It consists of a lower shaly part, and an upper sandy part containing regressive, eastward prograding shelf-shoreface cycles, below the contact with the Blood Reserve Formation.

Résumé : La présence de *Baculites compressus robinsoni* Cobban dans le shale de Bearpaw, près de Lundbreck (Alberta), indique que durant la formation de la Zone à *Baculites compressus* (soit vers 73,4 Ma), la transgression marine de Bearpaw s'étendait jusqu'à la région maintenant occupée par les contreforts des Rocheuses. Pendant cet intervalle de temps, la transgression atteignait son maximum et couvrait tant les plaines méridionales que les contreforts des Rocheuses, allant peut-être même jusqu'au compartiment inférieur du chevauchement de Lewis. Les données sur la sédimentation des unités de Bearpaw dans la partie sud des contreforts peuvent être corrélées avec celles dans les plaines méridionales. Une partie inférieure argileuse et une partie supérieure sableuse sont décrites, la seconde consistant en des cycles régressifs de plate-forme continentale et d'avant-plage à progradation vers l'est, observés sous le contact avec la Formation de Blood Reserve.

[1] Contribution to the Eastern Cordillera NATMAP Project

INTRODUCTION

The southern Rocky Mountain Foothills of Alberta contain the westernmost exposures of the marine Bearpaw Formation strata. The shoreface of the Bearpaw Sea reached as far west as the footwall of the Lewis Thrust (Jerzykiewicz et al., 1996), but thickest Bearpaw strata of the Foothills occurs near the eastern boundary of the deformed belt within the Triangle Zone (Hume, 1931; Hage, 1943, 1945; Williams, 1949; Douglas, 1950, 1951). There, the Bearpaw shale and contiguous strata are intensively deformed, sedimentary structures are often obliterated, and fossils are rare. Both the lower and upper boundaries of the Bearpaw Formation in the Foothills are either faulted or covered. The lower boundary of the Bearpaw Formation in the deformed belt has not been positively identified and dated.

The purpose of this study is to report newly found ammonoids in the Crowsnest River section at Lundbreck. This discovery changes previous interpretations of the timing and character of the Bearpaw transgression into the Foothills. Correlation between the Lundbreck section and the reference section of the Bearpaw Formation on St. Mary River near Lethbridge, which is important for mapping the deformed belt, is also discussed.

BACKGROUND INFORMATION

The Bearpaw shale is part of a second-order transgressive-regressive marine cycle of Campanian age in the Western Interior Basin, and in the Canadian Great Plains (Caldwell, 1968; Gill and Cobban, 1973; Kauffmann, 1977; Kauffman and Caldwell, 1993). The Bearpaw cycle spans several third- and fourth-order sea level cycles, and several ammonite zones (Kauffman et al., 1993).

In the South Saskatchewan River valley of Saskatchewan, the Bearpaw Formation spans approximately 6 Ma, between the pre-*Exiteloceras jenneyi* Zone (approx. 75 Ma) or *Didymoceras nebrascense* Zone (approx. 76 Ma), and the *Baculites grandis* Zone (approx. 70 Ma; Caldwell, 1968; Caldwell et al., 1993). The transgression flooded the Alberta Plains during the time of the *Baculites compressus* Zone (approx. 73.4 Ma; Russell, 1970; Nascimbene, 1965; Folinsbee et al., 1966; Obradovich, 1993), as shown by the common occurrence of the index fossil *Baculites compressus*, almost at the bottom of the Bearpaw Formation in the Manyberries section of the Cypress Hills area, southwestern Alberta (Russell and Landes, 1940).

Until now, no ammonoids have been reported from the Foothills exposures of the Bearpaw Formation (cf. Riccardi, 1983). The biostratigraphy of the formation is based on foraminifers (Given and Wall, 1971; Rosene, 1972; Wall and Rosene, 1977; Caldwell et al., 1978, 1993). According to Rosene (1972), and Wall and Rosene (1977, p. 852), the Bearpaw transgression into the southern Foothills took place later, during the time interval of the *Baculites cuneatus* Zone, one zone later than in the southern plains. This would imply a marked diachroneity of the Bearpaw transgression between the plains and the Foothills of Alberta.

LITHOSTRATIGRAPHY AND SEDIMENTOLOGY OF THE LUNDBRECK SECTION

The Lundbreck section, which yielded the ammonoids described in this report, is located on the north bank of the Crowsnest River in LSD 15-26-7-2-W5 (Fig. 1). The section consists of several fault-repeated intervals of shale interbedded with siltstone and sandstone. The section has been divided into a lower shaly portion and an upper portion consisting of four coarsening-upward cycles (Jerzykiewicz, in press).

The lower portion of the section consists of shale interbedded with thin hummocky cross-stratified siltstone, and bentonite beds. The coarsening-upward cycles of the upper portion of the Lundbreck exposure consist of lower shaly facies and upper facies composed of thin beds of silty mudstone, sideritic siltstone, and fine grained sandstone, rhythmically alternating with mudstone. The lower boundaries of the siltstone and sandstone beds are sharp and characterized by sole markings. Groove and flute marks are the most common. The upper boundaries of the siltstone and sandstone beds with the shale are either gradational or abrupt. The latter are often covered with ripple marks and trace fossils. Internally, the siltstone and sandstone beds show delicate parallel lamination or small-scale hummocky crossbedding.

The type of stratification in the sandstone and siltstone beds and the nature of their contacts with the mudstone in the lower parts of the cycles indicate a predominantly quiet water, offshore environment of deposition. Silt and fine grained sand were transported by bottom currents into a quiet water environment of mud deposition, below and/or near the storm wave base. Few of the sandstone beds with sharp upper boundaries covered with current structures were eroded by bottom currents at the storm wave base. Siltstone beds that grade into mudstone were deposited below the level of current and wave activity. This conclusion is supported by the presence of planktonic foraminifera in the mudstone. Wall and Rosene (1977) recognized an offshore assemblage of foraminifera including *Heterohelix globosa,* a planktonic form that indicates normal-salinity shelf conditions of sedimentation.

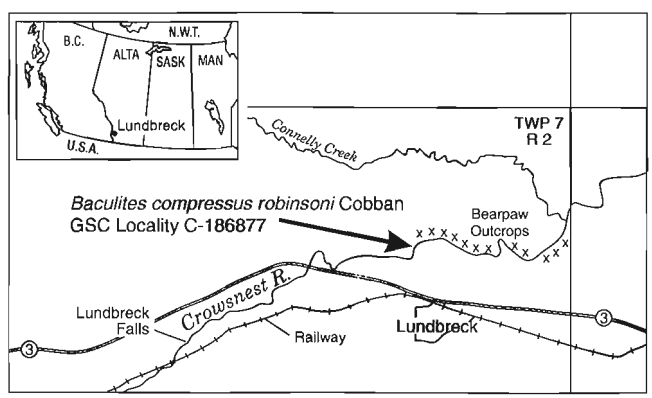

Figure 1. *Location map. The large arrow indicates GSC locality C-186877. The crosses indicate the Bearpaw Formation outcrops on the banks of Crowsnest River.*

Sea regression is marked by a change from the offshore, shale-dominated parts of the cycles into shoreface strata of the upper, sandy parts of the cycles. These cycles consist of alternating fine grained sandstone, showing lenticular and wavy stratification, and laminae of mudstone with some carbonaceous drapes. The upper sandy part of the fourth cycle is similar to the Blood Reserve sandstone of the plains; it shows a transition from the lower to the upper shoreface and it is capped by paleosols.

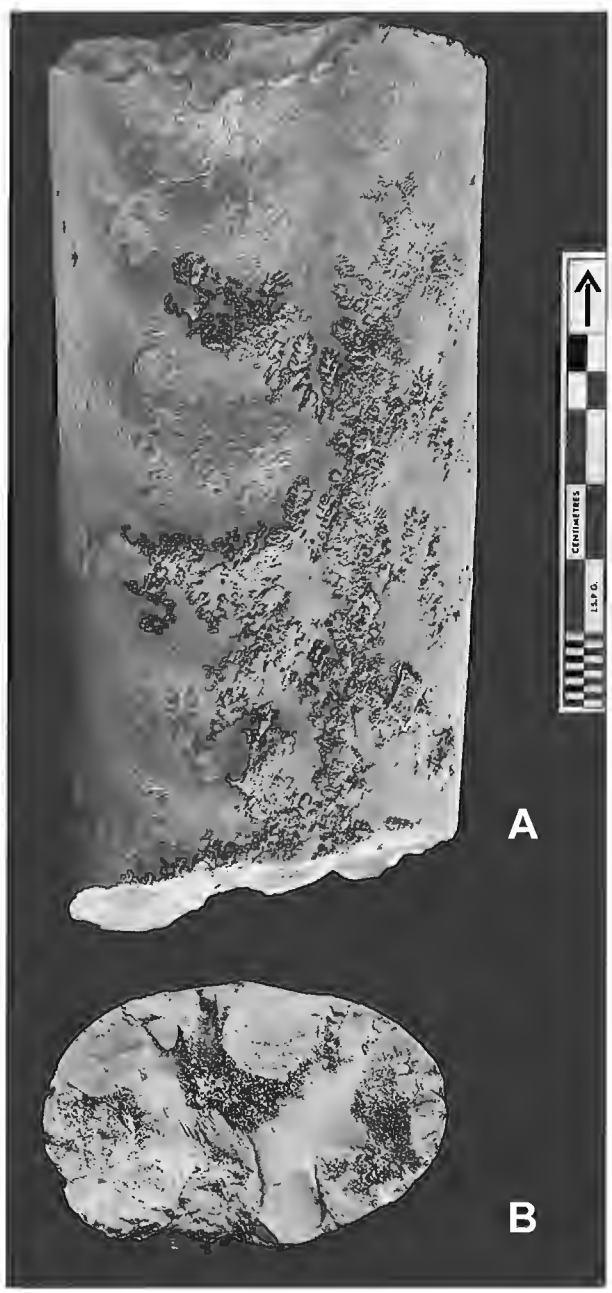

Figure 2. *Baculites compressus robinsoni Cobban; hypotype GSC 114593 (X 1), GSC locality C-186877 in the Bearpaw Formation from the Lundbreck section on Crowsnest River in LSD 15-26-7-2W5. Lateral* ***(A)*** *and cross-sectional* ***(B)*** *views. The hypotype is stored in the GSC type collection in Ottawa.*

The Lundbreck section is lithologically analogous to the Bearpaw section in the plains described by Link and Childerhose (1931, fig. 4), and Russell (1932) on the St. Mary River near Lethbridge. Both sections are of similar thickness (about 220 m), and consist of a lower, shaly portion overlain by an interval of coarsening-upward cycles below the shoreface sandstone of the Blood Reserve Formation.

FOSSIL DESCRIPTION

Occurrence. Two specimens of *Baculites compressus robinsoni* Cobban, including hypotype GSC 114593, were recovered in the lower shaly interval of the Bearpaw Formation at the Lundbreck section, a few metres above the lower boundary of the formation. The locality is indicated by an arrow on Figure 1. The exact height of the specimen above the base of the Bearpaw Formation is unknown because the lower part of the section is faulted and covered. Nevertheless, the ammonoids are estimated to occur less than 10 m above the base of the formation.

Description. The hypotype is an uncrushed, robust phragmocone 124 mm long with end diameters of 53.5 and 60.0 mm and a width to height ratio of 0.66 (Fig. 2). The growth angle of the shell is 3 degrees. The venter and dorsum are smooth, and crescentic flank ribs are present as shown in Figure 2.

The second specimen (not shown) consists of the last part of an uncrushed phragmocone and the older part of a crushed body chamber. The specimen is 131.5 mm long, its chambered part has a height of 58.7 mm, a width of 34.5 mm (width:height ratio 0.59), and a growth angle of 3 degrees. The only ornament consists of 4 weak flank ribs.

Comments. *Baculites compressus robinsoni* Cobban was described originally as *Baculites compressus* var. *ornatus* by Robinson (1945, p. 51, Pl. 1, fig. 1-4) from the lower part of the Bearpaw Formation in southern Saskatchewan. Since the name *ornatus* was preoccupied by *Baculites ornatus* d'Orbigny (1847), Cobban (1962, p. 128) renamed the Saskatchewan specimens as *B. compressus robinsoni*. He considered the species to be a northern subspecies of *B. compressus* Say (1820), which is common in the Pierre Shale in South Dakota and Colorado. *Baculites compressus robinsoni* differs from *B. compressus* (*sensu stricto*) chiefly in attaining lateral ornament (ribs) at a smaller size and, in many specimens, in having a more robust cross-section.

CONCLUSIONS

1. The occurrence of *Baculites compressus robinsoni* in the Lundbreck section indicates that the Bearpaw transgression flooded the area now occupied by the southern Rocky Mountain Foothills in or prior to the *B. compressus* Zone at approximately 73.4 Ma. The suggestion that the Bearpaw Formation of the southwestern Foothills of Alberta is restricted to the *Baculites cuneatus* Zone and the lower part of the *Baculites reesidei* Zone (Rosene, 1972) cannot be substantiated.

2. The suggestion that the Bearpaw Formation of the Lundbreck section lacks distinctive sand members (Wall and Rosene, 1977, p. 852) is not true. Sections of the Bearpaw Formation in the southern Foothills (on the Crowsnest River at Lundbreck) and southern plains (on the St. Mary River near Lethbridge) show similar thicknesses and successions of interbedded shale and sandstone. The sections in both areas contain shale representing the *B. compressus* Zone in the lower parts, and 3 to 4 coarsening-upward shale-sandstone cycles in the upper parts. The coarsening-upward cycles represent regressive, eastward prograding shelf-shoreface cycles related to the regression of the Bearpaw Sea.

3. Although the stratigraphic record of the Bearpaw transgression in the southern Rocky Mountain Foothills is obscure because of faulting and the general absence of fossils, it becomes clear that the transgression of the Bearpaw Sea flooded the southern Foothills and the southern plains synchronously at approximately 73.4 Ma and extended as far west as the footwall of the Lewis Thrust.

ACKNOWLEDGMENTS

W.A. Cobban of the United States Geological Survey is gratefully acknowledged for identifying and describing *Baculites compressus robinsoni* in this report.

REFERENCES

Caldwell, W.G.E.
1968: The Late Cretaceous Bearpaw Formation in the South Saskatchewan River valley; Saskatchewan Research Council Geology Division, Report 8.

Caldwell, W.G.E., Diner, R., Eicher, D.L., Fowler, S.P., North, B.R., Stelck, C.R., and von Holdt, W.L.
1993: Foraminiferal biostratigraphy of Cretaceous marine cyclothems; in Evolution of the Western Interior Basin, (ed.) W.G.E. Caldwell and E.G. Kauffman; Geological Association of Canada, Special Paper 39, p. 477-520.

Caldwell, W.G.E., North, B.R., Stelck, C.R., and Wall, J.H.
1978: A foraminiferal zonal scheme for the Cretaceous system in the Interior Plains of Canada; Geological Association of Canada, Special Paper 18, p. 495-575.

Cobban, W.A.
1962: New baculites from the Bearpaw Shale and equivalent rocks of the Western Interior; Journal of Paleontology, v. 36, p. 126-135.

Douglas, R.J.W.
1950: Callum Creek, Langford Creek, and Gap map-areas, Alberta; Geological Survey of Canada, Memoir 255, 124 p.
1951: Pincher Creek, Alberta; Geological Survey of Canada, Paper 51-22.

Folinsbee, R.E., Baadsgaard, H., Cumming, G.L., Nascimbene, J., and Shafiqullah, M.
1966: Late Cretaceous radiometric dates from the Cypress Hills of Western Canada; in Guidebook for the Alberta Society of Petroleum Geologists' 15th Annual Field Conference, Part 1: Cypress Hills Plateau, p. 162-174.

Gill, J.R. and Cobban, W.A.
1973: Stratigraphy and geologic history of the Montana Group and equivalent rocks, Montana, Wyoming, and North and South Dakota; United States Geological Survey, Professional Paper 776, 37 p.

Given, M.M. and Wall, J.H.
1971: Microfauna from the Upper Cretaceous Bearpaw Formation of south-central Alberta; Bulletin of Canadian Petroleum Geology, v. 19, p. 504-546.

Hage, C.O.
1943: Cowley map-area, Alberta; Geological Survey of Canada, Paper 43-1, 22 p.
1945: Cowley, Alberta; Geological Survey of Canada, Map 816A.

Hume, G.S.
1931: Turner Valley sheet, Alberta; Geological Survey of Canada, Map 257A.

Jerzykiewicz, T.
in press: Stratigraphic framework of the Uppermost Cretaceous to Paleocene strata of the Alberta Basin; Geological Survey of Canada, Bulletin.

Jerzykiewicz, T., Sweet, A.R., and McNeil, D.H.
1996: Shoreface of the Bearpaw Sea in the footwall of the Lewis Thrust, southern Canadian Cordillera, Alberta; in Current Research 1996-A; Geological Survey of Canada, p. 155-163.

Kauffman, E.G.
1977: Geological and biological overview: western interior Cretaceous basin; Mountain Geologist, v. 14, p. 75-99.

Kauffman, E.G., and Caldwell, W.G.E.
1993: The Western Interior Basin in space and time; in Evolution of the Western Interior Basin, (ed.) W.G.E. Caldwell and E.G. Kauffman; Geological Association of Canada, Special Paper 39, p. 1-30.

Kauffman, E.G., Sageman, B.B., Kirkland, J.I., Elder, W.P., Harries, P.J., and Villamil, T.
1993: Molluscan Biostratigraphy of the Cretaceous Western Interior Basin, North America; in Evolution of the Western Interior Basin, (ed.) W.G.E. Caldwell and E.G. Kauffman; Geological Association of Canada, Special Paper 39, p. 397-434.

Link, T.A. and Childerhose, A.J.
1931: Bearpaw shale and contiguous formations in Lethbridge area, Alberta; American Association of Petroleum Geologists Bulletin, v. 15, p. 1227-1242.

Nascimbene, G.G.
1965: Bentonites and the geochronolgy of the Bearpaw Sea; Bulletin of Canadian Petroleum Geology, v. 13, p. 537.

Obradovich, J.D.
1993: A Cretaceous time-scale; in Evolution of the Western Interior Basin, (ed.) W.G.E. Caldwell and E.G. Kauffman; Geological Association of Canada, Special Paper 39, p. 379-396.

d'Orbigny, A.D.
1847: Paleontology, pls. 1-6 (no text); in Voyage au Pôle Sud et dans l'Océanie sur les corvettes l'Astrolabe et la Zelée pendant les années 1837-1840 sous le commandement de M. Dumont d'Urville, Capitaine du Vaisseau, (éd.) M. Dumont d'Urville; Paris, Gide and J. Baudry.

Riccardi, A.C.
1983: Scaphitids from the Upper Campanian–Lower Maastrichtian Bearpaw Formation of the Western Interior of Canada; Geological Survey of Canada, Bulletin 354, 103 p.

Robinson, H.R.
1945: New baculites from the Cretaceous Bearpaw formation of southwestern Saskatchewan; Royal Society of Canada Transactions, ser. 3, v. 39, sec. 4, p. 51-54.

Rosene, R.K.
1972: Micropaleontology of the Bearpaw Formation, southwestern Alberta Foothills; M.Sc. thesis, University of Alberta, Edmonton, Alberta, 132 p.

Russell, L.S.
1932: Stratigraphy and structure of the eastern portion of the Blood Reserve, Alberta; Geological Survey of Canada, Summary Report 1931, Part B, p. 26-38.
1970: Correlation of the Upper Cretaceous Montana Group between southern Alberta and Montana; Canadian Journal of Earth Sciences, v. 7, p. 1099-1108.

Russell, L.S. and Landes, R.W.
1940: Geology of the southern Alberta Plains; Geological Survey of Canada, Memoir 221, 223 p.

Say, T.
1820: Observations on some species of zoophytes, shells etc., principally fossil; American Journal of Sciences, 1st ser. v. 2, p. 34-45.

Wall, J.H. and Rosene, R.K.
1977: Upper Cretaceous stratigraphy and micropaleontology of the Crowsnest Pass-Waterton area, southern Alberta Foothills; in Cordilleran Geology of Southern Alberta and Adjacent Areas, (ed.) M.S. Shawa; Canadian Society of Petroleum Geology, p. 842-867.

Williams, E.P.
1949: Cardston, Alberta; Geological Survey of Canada, Paper 49-3.

Geological Survey of Canada Project 930006

Interior Plains and Arctic Canada

Plaines intérieures et région arctique du Canada

Definition of a mappable contact between the Willow Creek and Porcupine Hills formations, southern Porcupine Hills, Alberta: a conformable boundary

M.E. McMechan and G.S. Stockmal
GSC Calgary, Calgary

McMechan, M.E. and Stockmal, G.S., 1996: Definition of a mappable contact between the Willow Creek and Porcupine Hills formations, southern Porcupine Hills, Alberta: a conformable boundary; in Current Research 1996-E; Geological Survey of Canada, p. 103-110.

Abstract: Recent mapping of the Willow Creek – Porcupine Hills formational boundary in southern Alberta has prompted reassessment of the traditional definition of the contact. Field and well cutting observations suggest that the thickness and relative predominance of sandstones should be the primary criterion for defining the Willow Creek – Porcupine Hills boundary, as at least one earlier worker proposed. In addition, examination of new, high-quality seismic reflection data across the Porcupine Hills indicates that this contact, which here is considered to be a facies boundary, climbs stratigraphically from west to east. The contact in the southern Porcupine Hills appears to be conformable and diachronous, and not a regional unconformity as interpreted previously.

Résumé : La cartographie récente de la limite entre les formations de Willow Creek et de Porcupine Hills dans la partie sud de l'Alberta est à l'origine d'une réévaluation de la définition classique de ce contact. Les travaux sur le terrain et l'observation des déblais de forage révèlent que l'épaisseur et la dominance relative des grès devraient être les premiers critères de définition de la limite entre ces deux unités, comme il l'a été proposé au moins une fois dans le passé. De plus, l'analyse de nouvelles données de sismique réflexion de haute qualité recoupant les collines Porcupine indique que ce contact, qui est considéré comme étant une limite de faciès, est de plus en plus haut dans la stratigraphie à mesure que l'on progresse d'ouest en est. Le contact dans la partie sud des collines Porcupine semble concordant et diachrone, contrairement à l'interprétation qu'on en faisait avant, selon laquelle il s'agit d'une discordance régionale.

[1] Contribution to the Eastern Cordillera NATMAP Project

INTRODUCTION AND PURPOSE

Recent mapping in the southern Porcupine Hills area, southern Alberta, in support of the Eastern Cordillera NATMAP Project, has raised questions regarding the definition and placement of the contact between the Maastrichtian to Paleocene Willow Creek Formation and the Paleocene Porcupine Hills Formation (Fig. 1). Consistent application of a workable, mappable definition of this contact is important for structural interpretations, and has implications for the nature of the contact itself.

The Porcupine Hills Formation is the youngest preserved stratigraphic unit in the foreland basin succession of southern Alberta (Fig. 1). Thick, resistant sandstones in the lower part of the formation form the tree-covered "porcupines" of the western portion of the Porcupine Hills. The Porcupine Hills lie along the axis of the Alberta Syncline (Fig. 2), an east-facing monocline with a shallow west-dipping east limb that reflects the regional dip of the autochthonous foreland basin, and a steeper east-dipping west limb that is due to uplift caused by a structural triangle zone that marks the eastern limit of significant Cordilleran deformation. Outcrop exposures on the east side of the Porcupine Hills differ from those on the west; eastern slopes are less heavily treed, less steep overall, and harbour better hillside and stream exposures higher in the section than the western slopes of the Porcupine Hills. The criteria for mapping the formational contact between the Willow Creek Formation and the Porcupine Hills Formation should be applicable in both these areas.

PREVIOUS DESCRIPTIONS AND DEFINITIONS

The placement of the Willow Creek – Porcupine Hills contact is dependent upon the definitions of these formations. Therefore, we briefly discuss previous definitions, including descriptions of the formational contact.

Willow Creek Formation

The Willow Creek and Porcupine Hills formations were first described by Dawson (1883), who referred to them as two "series". Regarding Dawson's description of the Willow Creek Formation, Bell (1949, p. 11) noted:

> "Dawson originally defined the Willow Creek formation as 'reddish and purplish clays, with grey and yellow sandstones' (1883, p. 4). Later (1884, p. 67) he amplified this description by stating that the beds comprise 'pale purplish, reddish and greenish grey clays or sandy clays, with soft sandstones and occasional bands of ironstone. The bedding is uniform and regular, and the whole series has a soft character, which causes it in some places to weather with miniature bad-land forms. In some clayey layers, peculiar whitish-weathering, irregularly reniform, and generally small sized concretions abound'".

Bell added that these concretions consist of lime carbonate, and are "similar to cornstone or kunkur." Jerzykiewicz and Sweet (1986) noted that "kunkur", also known as "kankar", is synonymous with "caliche".

Tozer (1956, p. 21) described the Willow Creek Formation as comprising "soft, grey, medium-grained sandstones, and friable or clayey shales of grey, green, and pink colour. The shales in many outcrops carry an abundance of white weathering calcareous concretions. ... In the upper part of the ... formation massive and crossbedded, buff weathering sandstones occur and these express the transitional relationship with the overlying Porcupine Hills formation."

The Lexicon of Canadian Stratigraphy (Glass, 1990, p. 693) discussed Douglas's (1950) five-fold subdivision of the Willow Creek Formation. Douglas (1950) used this subdivision and traced its members to the north to argue for a regional unconformity at the Willow Creek – Porcupine Hills contact. Contact relationships are discussed below.

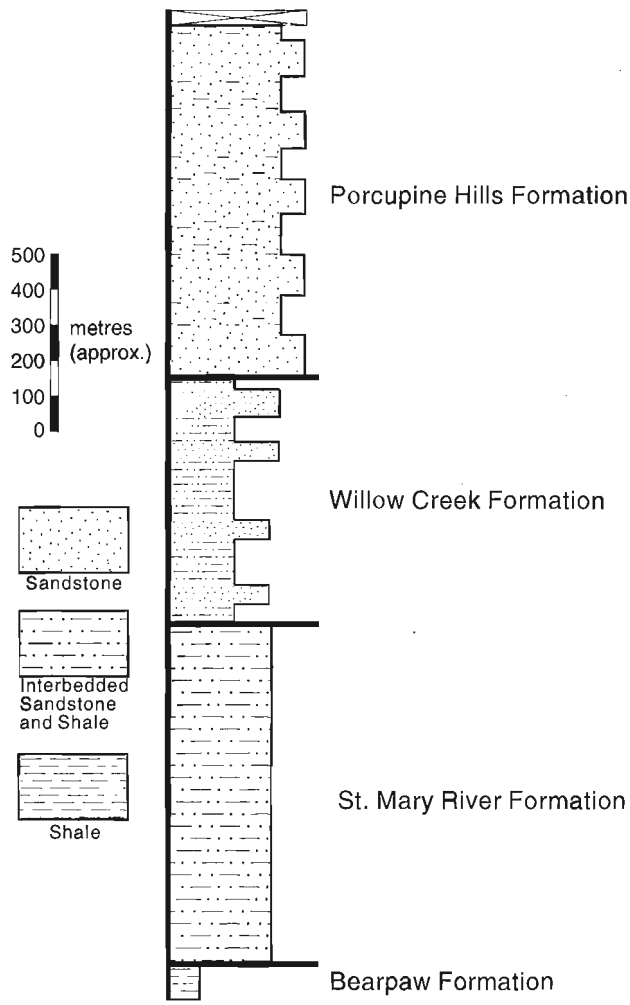

Figure 1. *Stratigraphic column showing the positions of the Willow Creek and Porcupine Hills formations in relationship to each other and to underlying units.*

Porcupine Hills Formation

The lexicon (Glass, 1990, p. 503) described the Porcupine Hills Formation, originally defined by Dawson (1883), as "composed of olive brown shales interbedded with fine to coarse grained brownish grey, cross-bedded limy sandstone and calcareous siltstone, in fairly well indurated beds from 6 to 15 m (20 to 49 ft) thick."

Williams and Dyer (1930, p. 62) described the Porcupine Hills Formation as consisting "mainly of fine-grained, cross-bedded, light grey, ledge-making sandstone with interbedded shaly clays. The ledge-making sandstones are the most markedly crossbedded sediments found in southern Alberta, the true bedding being determined with difficulty."

Willow Creek – Porcupine Hills contact

Williams and Dyer (1930, p. 59) stated that "the line between the Willow Creek and the Porcupine Hills is vague owing to the transitional relations, but is drawn at the point where hard beds of grey sandstone begin to comprise the major part of the rock." Bell (1949, p. 13) described the Porcupine Hills Formation to be "differentiated from the underlying Willow Creek formation by the dominance of thick sandstone beds, which are generally more strongly crossbedded and harder than those of the Willow Creek." Bell (1949) noted that conglomerate can occur locally at or near the base of the Porcupine Hills Formation, but added that mapping a boundary between these formations in some localities can be difficult (due to the gradational nature of the contact).

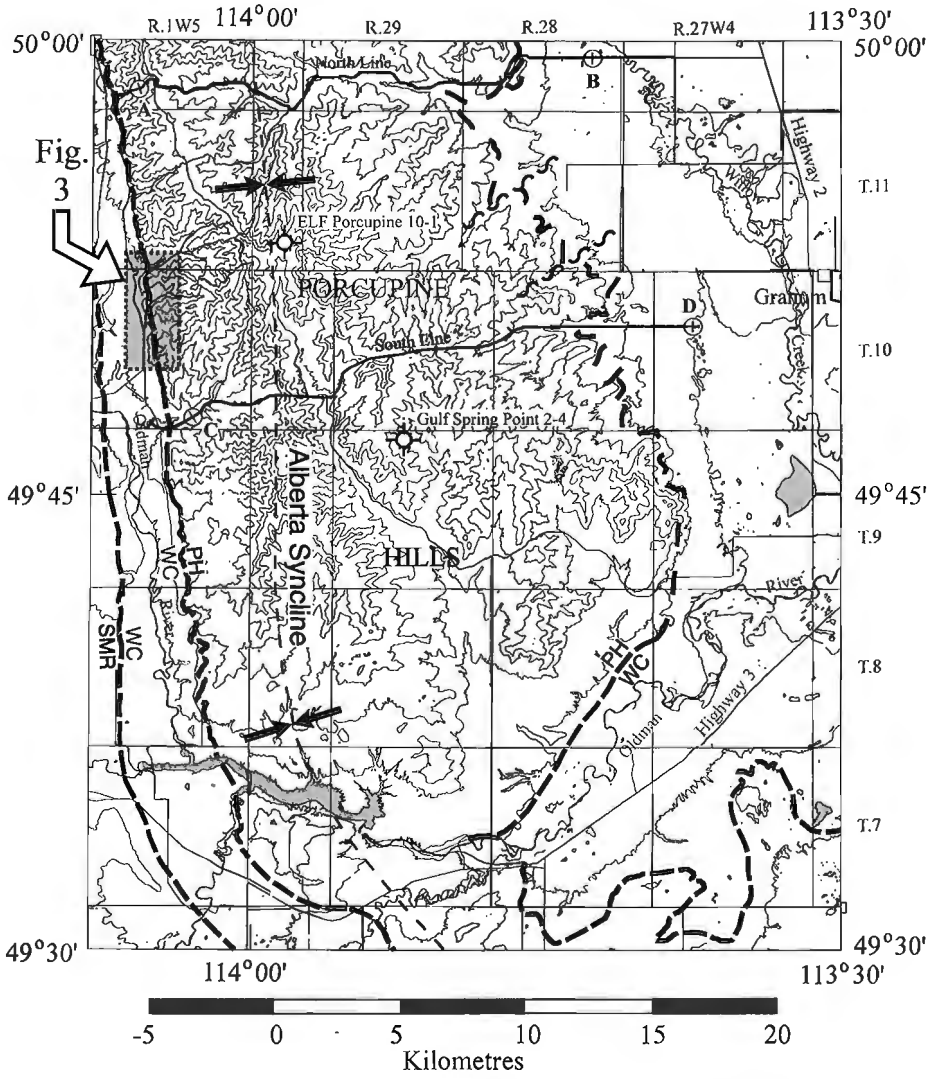

Figure 2.

Location map showing: the topography of the Porcupine Hills; the axial surface trace of the Alberta syncline; the location of the detailed map shown in Figure 3; the locations of wells utilized in Figure 4; the positions of seismic lines portrayed in Figure 5; the mapped positions of the Willow Creek (WC) – Porcupine Hills (PH) and St. Mary River (SMR) – Willow Creek formational contacts (heavy dashed lines); and the projected positions of the Willow Creek – Porcupine Hills contact on the seismic lines (points A, B, C, and D, see text). Map compiled from Stockmal (1996; north of lat. 49°45', west of long. 114°00'), Jerzykiewicz and Norris (pers. comm., 1996; south of lat. 49°45', west of long. 114°00'), Lebel (1996; south of lat. 49°45', east of long. 114°00'), and McMechan (unpub. data, 1996; north of lat. 49°45', east of long. 114°00').

As noted above, Douglas (1950) divided the Willow Creek Formation into five zones, or members. The uppermost member includes sandstones which are thicker, harder, and coarser than those below, perhaps suggesting gradation into the Porcupine Hills Formation above. However, Douglas (1950) interpreted the Willow Creek – Porcupine Hills formational contact to be an erosional unconformity. Douglas mapped the base of the Porcupine Hills Formation as cutting down-section through the Willow Creek Formation to the north, with progressive removal of the upper members of the formation. However, this interpretation is questionable on the basis of difficulties in correlating Douglas's (1950) basal beds of the Porcupine Hills Formation from one isolated stream exposure to the next, and clear evidence from structural dips and aerial photograph interpretation that the strike of obvious beds in the Porcupine Hills is oblique to Douglas's (1950) interpreted formational contact (Stockmal, 1996).

Bell (1949, p. 12), commenting on earlier descriptive notes by Douglas (1946), also argued against the apparent disconformity between these formations on the west limb of the Alberta syncline interpreted by Douglas on the basis of paleontological evidence and transitional relationships observed on the east limb. He added:

> "The Porcupine Hills formation is interpreted to be an alluvial deposit, and if so its base might be expected to transect the underlying Willow Creek formation with pronounced, local, erosional features. That the position of the contact ..., in some places at least, in the western as in the eastern limb of the syncline might depend on the viewpoint of the observer is evident from the rock section at the junction of Crowsnest and Oldman Rivers. The writer would place this contact on Oldman River about 600 feet east of its junction with the Crowsnest at the base of a thick, crossbedded sandstone ..., whereas C.O. Hage (1945) placed the contact more than half a mile to the west."

Tozer (1956) agreed with Bell's assessment of Douglas's unconformity, and proposed that this surface may represent the Cretaceous-Tertiary boundary.

Bossort (1957) suggested that the base of the Porcupine Hills Formation in the southern Porcupine Hills was an erosional unconformity of considerable magnitude which postdated Laramide deformation in the area. To support his conclusion that Laramide deformation was truncated at a "sub-Porcupine Hills unconformity", he used surface traverse data that revealed folding and faulting in the Willow Creek and older strata but not in the Porcupine Hills Formation, and subsurface seismic reflection data that showed Laramide faulting beneath the Willow Creek – Porcupine Hills contact. Modern seismic reflection data (e.g., Lawton et al., 1994; Bégin et al., 1996; Fig. 5) clearly show that the relative lack of deformation in the Porcupine Hills Formation, as compared to underlying strata, results from the existence of a zone of underthrusting (triangle zone) along the western side of the topographic Porcupine Hills. The upper roof thrust occurs within the Willow Creek Formation (Stockmal, 1996) and the Porcupine Hills Formation is gently folded above the upper detachment.

The mapped positions of the Willow Creek – Porcupine Hills contact along the Castle River and the Oldman River, where there are good to excellent exposures (Tozer, 1956), has changed significantly from author to author. Tozer (1956) noted a personal communication from Douglas that placed the Willow Creek – Porcupine Hills formational contact approximately 1300 ft. (~400 m) above the contact as mapped by Hage (1943). Tozer (1956, p. 28) also noted:

> "This sandstone may be correlated with a somewhat similar sandstone overlying typical Willow Creek sediments on Oldman River ... The base of the sandstone here is 440 feet above the contact suggested by Bell (1949, p. 12) and 1,090 ft. above that mapped by Hage (1943)."

Furthermore, Bell (1949, p. 12) questioned the use of colour as an aid to identifying the formational contact:

> "That the presence of maroon bands is not in itself a reliable criterion for the recognition of the Willow Creek formation is attested by the presence of two, thin, but well defined, maroon bands carrying small limestone concretions in the Porcupine Hills formation on Oldman River ..."

NEW OBSERVATIONS

Mapping and well logs

Detailed mapping along the western and eastern slopes of the Porcupine Hills in the Maycroft, east half (82G/16E; Stockmal, 1996), and Granum (82H/13; McMechan, unpub. map) map areas has included the examination of most outcrops in the upper Willow Creek – lower Porcupine Hills contact zone. On the west flank, a series of resistant sandstone intervals 5 to 20 m thick, separated by thick intervals of green grey, caliche nodule-bearing mudstones with thin sandstone interbeds form the base of the Porcupine Hills Formation (Fig. 3). On the east flank, near the south edge of Granum map area, the contact is mapped at the base of a resistant, 7 m thick sandstone above a red, white and grey weathering interbedded mudstone and sandstone interval displaying badlands topography. Local, thick (15 m) channels of crossbedded sandstone are exposed in the underlying Willow Creek Formation.

In the Gulf Spring Point 2-4-10-29W4 well (Fig. 2, 4), the contact suggested in the Lexicon of Canadian Stratigraphy (Glass, 1990, p. 502) projects to the east about 125 m above the contact suggested by surface mapping. Using this contact, the Willow Creek Formation would be 180 m thicker in the well than in the area of the mapped surface contact 15 km to the east. Thus it appears that the contact suggested in Glass (1990) is at a higher stratigraphic level than that suggested by surface mapping. Up to nine crossbedded, thicker (>5 m) sandstones are exposed in the 250 m of section above the

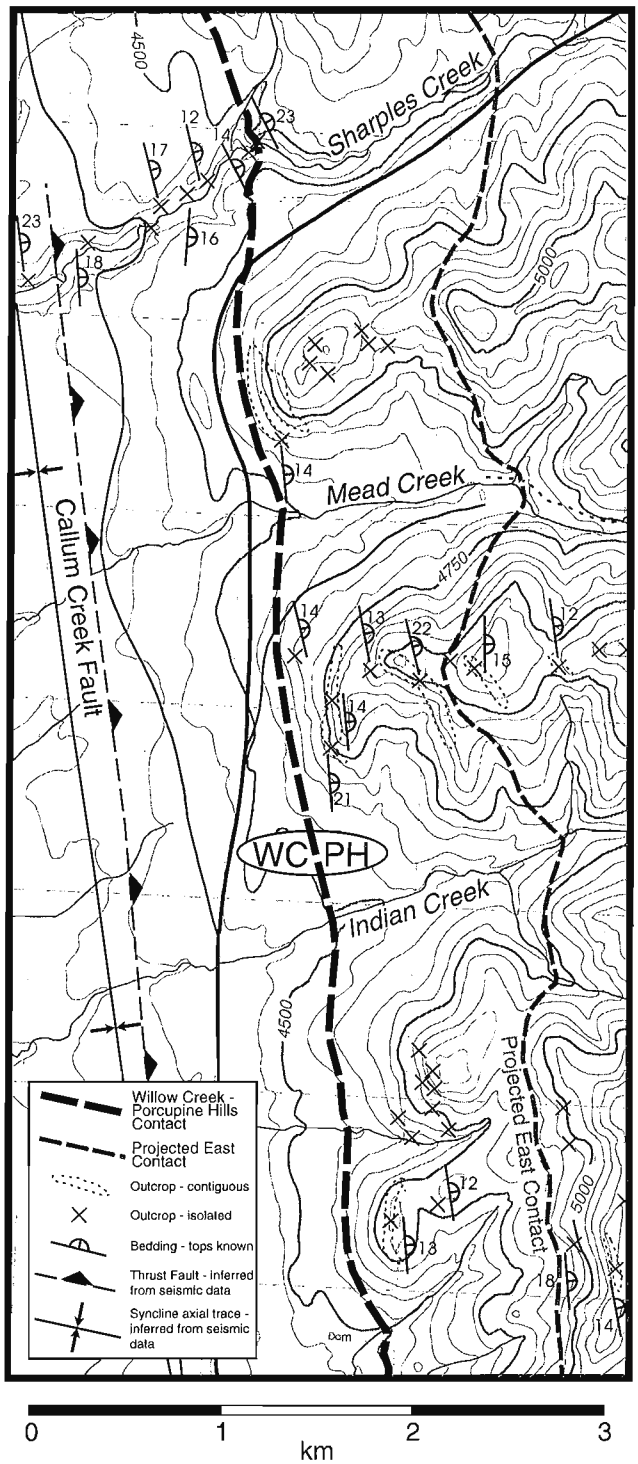

Figure 3. *Detailed map of the west flank of Porcupine Hills (modified after Stockmal, 1996). The mapped Willow Creek – Porcupine Hills formational contact is shown by a heavy, black, dashed line; the projected formational contact from the east flank of the Porcupine Hills is shown by a thinner, grey, dashed line. The projected contact lies well above classic physiographic "porcupines" underlain by thick and resistant sandstone intervals.*

mapped contact. There are no 15 m sandstones or distinctive mappable differences between these sandstone units; therefore, it would be extremely difficult to force a mappable contact within this zone. Since surface mapping requires a lower contact than that suggested in Glass (1990), we propose that the thick sandstone starting at 649 m (2130 ft.), rather than the sandstone zone starting at 518 m (1700 ft.) in the Gulf Spring Point well (Fig. 4), be used to mark the base of the formation.

Comparison of the gamma ray log signatures for the Porcupine Hills Formation in the Elf Porcupine 10-1-11-30W4 and Gulf Spring Point 2-4-10-29W4 wells shows that there is considerable variability in the amount of thick, clean sandstone found within the Porcupine Hills Formation. The Gulf Spring Point well contains a greater number of thicker sandstones than the Elf Porcupine well. In both wells, thicker sandstone is more abundant in the upper part of the logged Porcupine Hills section.

Well cuttings

Cuttings have been examined from the two petroleum exploration wells from which logs were recorded in the Porcupine Hills Formation. Examination of the cuttings corroborated Bell's (1949) observation that colour is a poor diagnostic indicator for interpreting the affinity of a particular section. Figure 4 shows the observed colours of mudstones in cuttings from portions of the Elf Porcupine 10-1-11-30W4 and Gulf Spring Point 2-4-10-29W4 wells. Red colours occur well above the formational contact reported in Glass (1990, p. 502) and above the contacts chosen by us.

Seismic reflection data

We examined new seismic reflection data gathered by BFR Geophysical Consultants Ltd, Calgary. Line drawings of selected portions of these data are shown (Fig. 5) with the kind permission of BFR. The quality of these data is excellent, allowing us to trace the mapped positions of contacts beneath the Porcupine Hills. No fault offsets were observed on the seismic data at the level of the Willow Creek – Porcupine Hills contact.

Mapped contacts on the west and east flanks of the Porcupine Hills, referenced onto the seismic data of Figure 5 and projected along and parallel to bundles of reflections, indicate that the mapped Willow Creek – Porcupine Hills formational contact is approximately 300 m higher stratigraphically in the east than in the west. This has resulted in a marked change in the position of the mapped contact (as compared to a constant stratigraphic level), particularly in the east where the structural dip is low. The approximate offset position of correlative strata to the east and west contacts is shown in Figure 5. The projected positions of the east and west contacts are also shown in Figure 2: points A and C are the projected positions of the east contact on the west ends of the seismic lines, whereas points B and D are the projected positions of the west contact on the east ends of the seismic lines.

DISCUSSION AND CONCLUSIONS

The history of mapping the Willow Creek – Porcupine Hills contact, as outlined above, reflects the basic ambiguity inherent in the definitions of the formations themselves. Red colouration of shales is not a reliable indicator to exclude strata from the Porcupine Hills Formation, as evidenced by the quote from Bell (1949), above, and by our own field and well cutting observations (Fig. 4).

Thin zones of red colouration were observed locally in the lower 200 m of the Porcupine Hills Formation along the east flank of the Porcupine Hills. In the subsurface, red mudstones occur in well cuttings up to 500 m above the estimated base of the Porcupine Hills Formation in the Elf Porcupine 10-1-11-30W4 well and 370 m above the estimated base in the Gulf Spring Point 2-4-10-29W4 well (Fig. 2, 4). Also, caliche nodules are commonly observed in mudstones or as intraclasts in sandstones of the Porcupine Hills to the highest exposed stratigraphic levels.

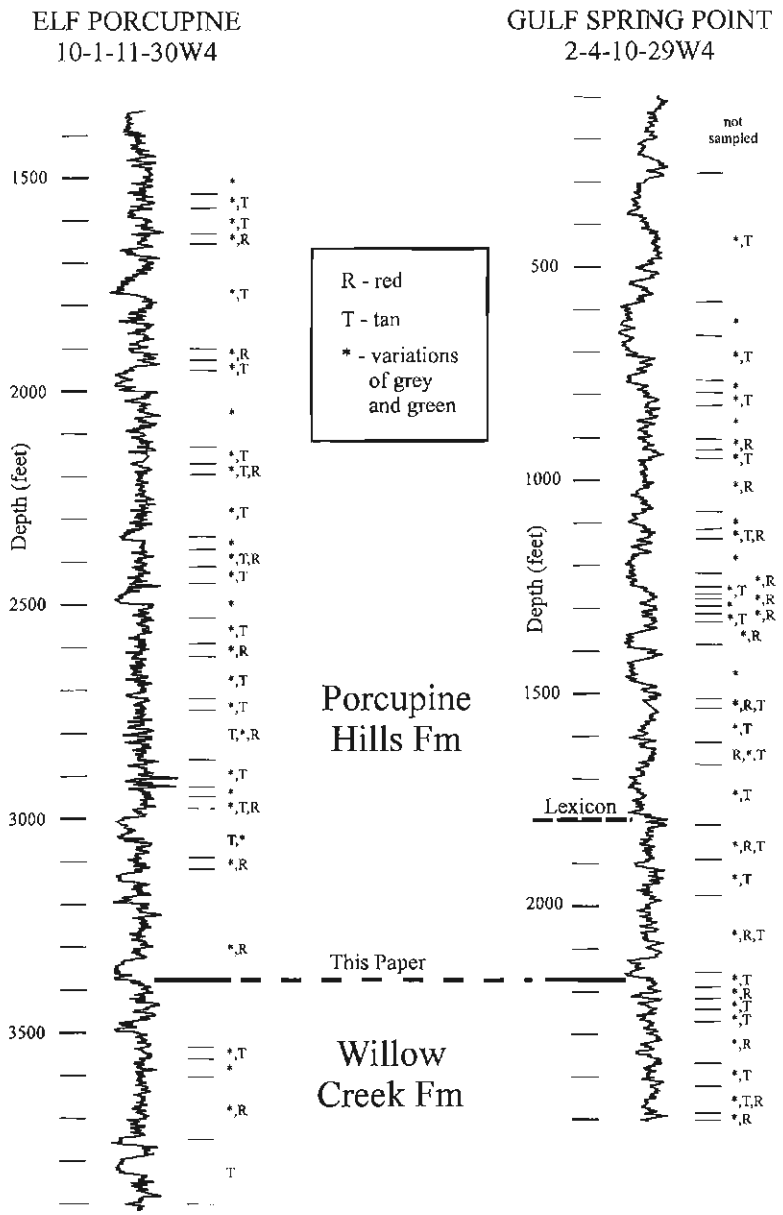

Figure 4. *Portions of gamma ray well logs from the Elf Porcupine 10-1-11-30W4 and Gulf Spring Point 2-4-10-29W4 wells. The logs indicate the colours of the mudstones observed in cuttings and locations of the Willow Creek – Porcupine Hills formational contact as chosen in this study and in the Lexicon of Canadian Stratigraphy (Glass, 1990, p. 502).*

Therefore, we follow the basic definition of Bell (1949), who emphasized the transitional though usually clear change from the soft, mudstone-dominated Willow Creek Formation below to the more resistant, thick bedded, sandstone-bearing Porcupine Hills Formation above. Red colouration and the presence of caliche nodules are not diagnostic indicators. Application of this definition results in mappable contacts on the west and east flanks of the Porcupine Hills, as in Figures 2 and 3 where the contacts generally follow clear topographic breaks.

Mapped contacts on the west and east flanks of the Porcupine Hills, referenced onto the seismic data of Figure 5, indicate that the Willow Creek – Porcupine Hills formational contact is approximately 300 m higher stratigraphically in the east than in the west. Because the formational contact is defined here as a facies boundary, the seismic data imply that the contact is diachronous, dropping stratigraphically to the west with the increase in abundance of thick sandstone channels. A facies boundary for the Willow Creek – Porcupine Hills contact is also implied in mapping by Lebel (1996) around the south end of the topographic Porcupine Hills (Brockett map area, 82H/12).

Our observations do not support the contention of Douglas (1950) and Bossort (1957), that the Willow Creek – Porcupine Hills contact is an erosional unconformity. Our interpretation suggests that the Willow Creek Formation may not be

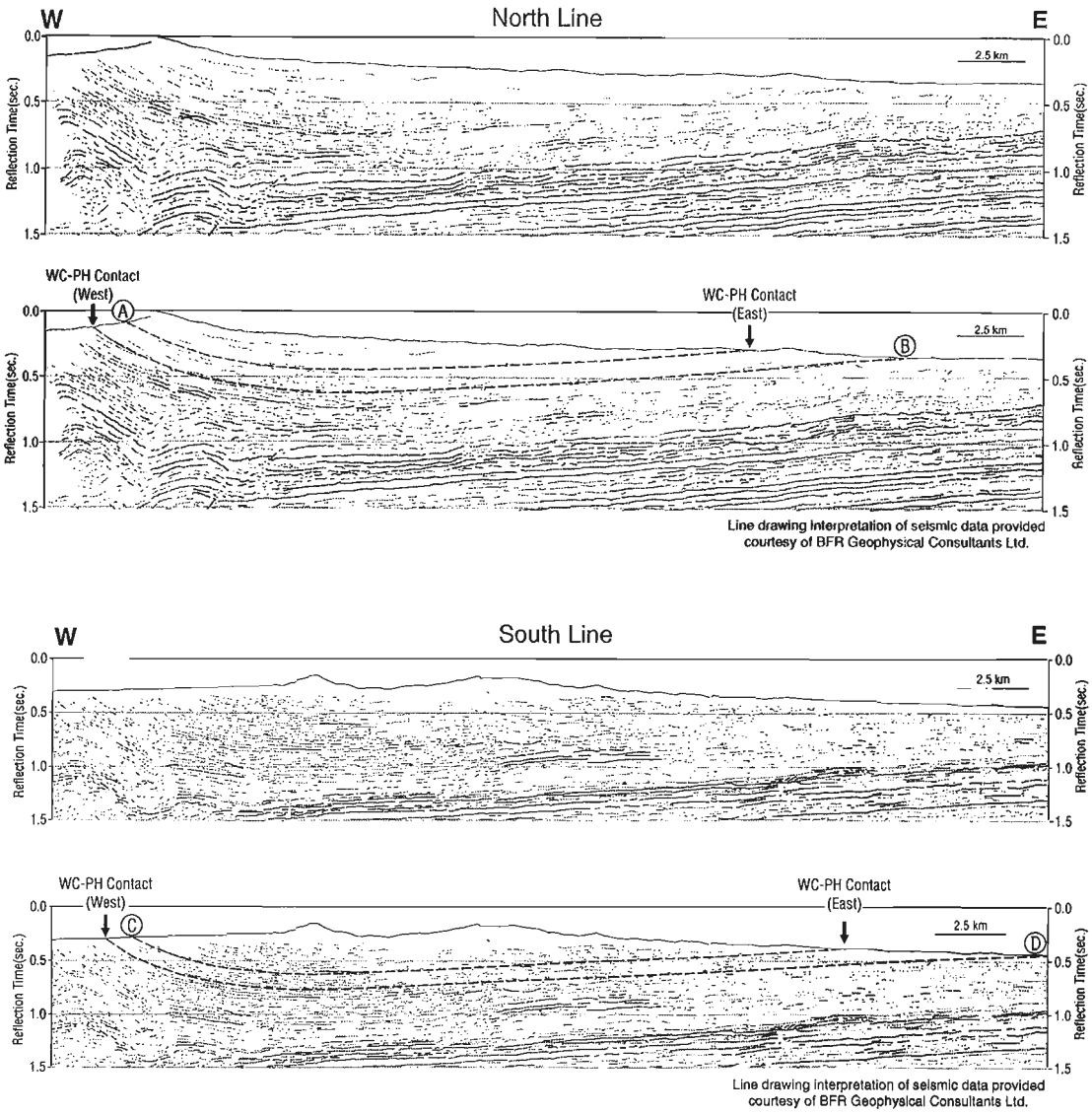

Figure 5. *Line drawings of seismic data from the area shown in Figure 2, courtesy of BFR Geophysical Consultants Ltd. Locations of mapped Willow Creek – Porcupine Hills contacts on the west and east flanks of the Porcupine Hills are shown on the interpreted sections and stratigraphic levels are projected beneath the hills. The mapped projections of A, B, C and D are located on Figure 2.*

removed by an unconformity to the north, but rather may thin to the north because of a facies change that resulted in progressively older strata being included in the Porcupine Hills Formation. Future field studies in support of the Eastern Cordillera NATMAP project, in Langford Creek (82J/1) and Stimson Creek (82J/8) map areas, will address the mappability of the Willow Creek – Porcupine Hills boundary in these areas.

Magnetostratigraphic and biostratigraphic studies by Lerbekmo et al. (1992) indicated a 2 to 4 Myr hiatus at the sub-Paskapoo disconformity in the Red Deer River Valley (Twp. 37-39, Rge. 25-27W4), 280 km north of the southern Porcupine Hills. They suggested that this middle Paleocene disconformity was probably regional in extent. The southern Porcupine Hills were much closer to the depocentre of the Paleocene foreland basin than the Red Deer River Valley area studied by Lerbekmo et al. (1992), and it is likely that a disconformity east of the basin depocentre would be replaced by more continuous sedimentation near the depocentre (e.g., Quinlan and Beaumont, 1984; Flemings and Jordan, 1990). Although a correlative of the sub-Paskapoo disconformity may indeed exist within the stratigraphic succession of the southern Porcupine Hills area, our observations require that it is not at the mappable Willow Creek – Porcupine Hills formational contact.

ACKNOWLEDGMENTS

We thank Daniel Lebel for numerous discussions both in and out of the field, and Phil Gregory of BFR Geophysical Consultants Ltd. for access to the seismic data. We thank Tomaz Jerzykiewicz and Daniel Lebel for helpful reviews of the manuscript.

REFERENCES

Bégin, N.J., Lawton, D.C., and Spratt, D.A.
1996: Seismic interpretation of the Rocky Mountain thrust front near the Crowsnest deflection, southern Alberta; Bulletin of Canadian Petroleum Geology, v. 44, p. 1-13.

Bell, W.A.
1949: Uppermost Cretaceous and Paleocene floras of western Alberta; Geological Survey of Canada, Bulletin 13, 93 p.

Bossort, D.O.
1957: Relationship of the Porcupine Hills to Early Laramide Movements; in Guidebook, Seventh Annual Field Conference, Waterton; Alberta Association of Petroleum Geologists, p. 46-51.

Dawson, G.M.
1883: Preliminary report on the geology of the Bow and Belly River region, North West Territory, with special reference to the coal deposits; Geological Survey of Canada, Report of Progress 1880-82, pt. B, p. 1-23.
1884: Report on the region in the vicinity of Bow and Belly rivers, North West Territory; Geological Survey of Canada, Report of Progress 1882-83-84, pt. C, p. 5-168.

Douglas, R.J.W.
1946: Preliminary Map, Callum Creek, Alberta; Geological Survey of Canada, Paper 46-10 (map scale 2 inches to 1 mile).
1950: Callum Creek, Langford Creek, and Gap Map-Area, Alberta; Geological Survey of Canada, Memoir 255, 124 p. (map scale 1 inch to 1 mile).

Flemings, P.B. and Jordan, T.E.
1990: Stratigraphic modeling of foreland basins: Interpreting thrust deformation and lithosphere rheology; Geology, v. 18, p. 430-434.

Glass, D.J. (ed.)
1990: Lexicon of Canadian Stratigraphy, Volume 4, Western Canada, Including Eastern British Columbia, Alberta, Saskatchewan, and Southern Manitoba; Canadian Society of Petroleum Geologists, Calgary, Alberta, 772 p.

Hage, C.O.
1943: Cowley Map-area, Alberta (Report and Map); Geological Survey of Canada, Paper 43-1 (map scale 2 inches to 1 mile).
1945: Cowley; Geological Survey of Canada, Map 816A, scale 1 inch to 1 mile.

Jerzykiewicz, T. and Sweet, A.R.
1986: Caliche and associated impoverished palynological assemblages: an innovative line of paleoclimatic research into the uppermost Cretaceous and Paleocene of southern Alberta; in Current Research, Part B; Geological Survey of Canada, Paper 86-1B, p. 653-663.

Lawton, D.C., Stockmal, G.S., and Spratt, D.A.
1994: Seismic definition of the triangle zone east of Maycroft, Alberta; in Current Research 1994-E; Geological Survey of Canada, p. 109-116.

Lebel, D.
1996: Brocket (82H/12), Alberta - Geology (preliminary); Geological Survey of Canada, Open File 3289, scale 1:50 000.

Lerbekmo, J.F., Demchuk, T.D., Evans, M.E., and Hoye, G.S.
1992: Magnetostratigraphy and biostratigraphy of the continental Paleocene of the Red Deer Valley, Alberta, Canada; Bulletin of Canadian Petroleum Geology, v. 40, p. 24-35.

Quinlan, G.M. and Beaumont, C.
1984: Appalachian thrusting, lithospheric flexure, and the Paleozoic stratigraphy of the Eastern Interior of North America; Canadian Journal of Earth Sciences, v. 21, p. 973-996.

Stockmal, G.S.
1996: Geology, Maycroft (East Half), Alberta (preliminary colour digital map); Geological Survey of Canada, Open File 3275, scale 1:50 000 (plus 1:25 000 inset).

Tozer, E.T.
1956: Uppermost Cretaceous and Paleocene non-marine molluscan faunas of western Alberta; Geological Survey of Canada, Memoir 280, 101 p.

Williams, M.Y. and Dyer, W.S.
1930: Geology of Southern Alberta and Southwestern Saskatchewan; Geological Survey of Canada, Memoir 163, 160 p.

Geological Survey of Canada Project 930006

Paleoenvironmental significance of biota of the Ostracode zone (Mannville Group) in south-central Alberta

I. Banerjee and I. Raychaudhuri[1]
GSC Calgary, Calgary

Banerjee, I. and Raychaudhuri, I., 1996: Paleoenvironmental significance of biota of the Ostracode zone (Mannville Group) in south-central Alberta; in Current Research 1996-E; Geological Survey of Canada, p. 111-122.

Abstract: The Ostracode zone (Late Aptian-Early Albian) is an informally designated lithostratigraphic unit that is a key stratigraphic interval within the Lower Cretaceous Mannville Group due to its regional extent, unique limestone-bearing lithology and inferred marine origin. The purpose of this subsurface study is two-fold: first, to present new data on trace fossils of this unit; and second, to review the paleoenvironmental significance of the entire fossil assemblage reported from this unit including macrofossils, microfossils and trace fossils.

Nineteen ichnogenera have been identified in this study. The softground ichnofossil assemblages are consistent with the *Cruziana* ichnofacies. Marginal marine environments are indicated by the small size of individual traces, overall low-abundance/moderate-diversity assemblages, and ichnofossil suites dominated by two to three genera with simple forms. Firmground and hardground examples of the *Glossifungites* and *Trypanites* ichnofacies, respectively, are also recognized.

A review of previous studies on the body fossils within the Ostracode zone (bivalves, ostracodes, foraminifera and dinoflagellates) corroborates a marginal marine interpretation. A very shallow, restricted inland seaway with fluctuating salinity, stagnant bottom conditions and repeated episodes of emergence, is indicated by the sedimentological and paleontological data.

Résumé : La zone à ostracodes (Aptien tardif-Albien précoce) est une unité lithostratigraphique informelle qui, pour plusieurs raisons, s'avère un intervalle stratigraphique clé dans le Groupe de Mannville du Crétacé inférieur; il s'agit en effet d'une lithologie calcarifère unique, qui s'observe dans toute la région et qu'on suppose d'origine marine. La présente étude de roches en subsurface vise un objectif à deux volets : présenter, d'une part, les nouvelles données recueillies sur les ichnofossiles de cette unité et analyser, d'autre part, la signification paléoenvironnementale de toute la cénozone dont l'existence a été établie dans cette unité, soit les macrofossiles, les microfossiles et les ichnofossiles.

Dix-neuf genres d'ichnofossiles ont été identifiés dans le cadre de cette étude. Les assemblages d'ichnofossiles de terrain mou correspondent à l'ichnofaciès à *Cruziana*. La petitesse des traces, la diversité modérée et la faible abondance globales des assemblages, mais aussi les suites d'ichnofossiles dans lesquelles dominent de deux à trois genres de forme simple sont l'indication de milieux marins marginaux. On a également relevé la présence d'ichnofossiles de terrain ferme et dur (ichnofaciès à *Glossifungites* et à *Trypanites*, respectivement).

[1] PanCanadian Petroleum Ltd., Pan Canadian Plaza, P.O. Box 2850, Calgary, Alberta T2P 2S5

Une analyse des études antérieures sur les fossiles à loges dans la zone à ostracodes (bivalves, ostracodes, foraminifères et dinoflagellés) corrobore l'interprétation d'un milieu marin marginal. Les données sédimentologiques et paléontologiques permettent d'en arriver à la conclusion d'un chenal maritime intérieur peu profond à circulation fermée, caractérisé par une salinité fluctuante, des conditions de fond stagnantes et des épisodes répétés d'émergence.

INTRODUCTION

Within the well studied, hydrocarbon-rich Mannville Group of Early Cretaceous age, the Ostracode zone, or Calcareous Member as it is known in outcrop, is a key stratigraphic unit used as a regional marker because of its unique limestone-rich lithology. A marginal marine assemblage of fossil flora and fauna (Finger, 1983; Banerjee and Davies, 1988; Banerjee and Kidwell, 1991) obtained from this unit, indicates that the Ostracode zone represents the leading edge of the Moosebar-Clearwater marine transgression (Caldwell, 1984) in south-central Alberta.

Although the molluscan macrofauna (Wanklyn, 1985), the microflora (Banerjee and Davies, 1988) and the microfauna (Banerjee, 1990) of this unit have been documented in some detail, the only published account of trace fossils is from an interpreted incised-valley fill of equivalent age (Geier and Pemberton, 1994). The present study documents the occurrence of trace fossils in the regional, limestone-bearing interval of the Ostracode zone in south-central Alberta, and reviews the present data and all other reported fossil occurrences in the unit with respect to their paleoenvironmental significance.

STUDY AREA AND STUDY METHODS

The study is based on cored intervals from 14 wells located between Townships 17 and 44 and Ranges 16 and 25W4 (Fig. 1). Detailed lithologs were recorded for each of the 14 cores, with particular focus on the type and occurrence of ichnofossils. Trace fossil identification was only possible at the genus level because of the small sizes and lack of well preserved forms. Furthermore, species differentiation commonly hinges on three-dimensional burrow morphology, which is particularly difficult to determine from 9 to 10 cm diameter drill cores. Ichnofacies designations were assigned

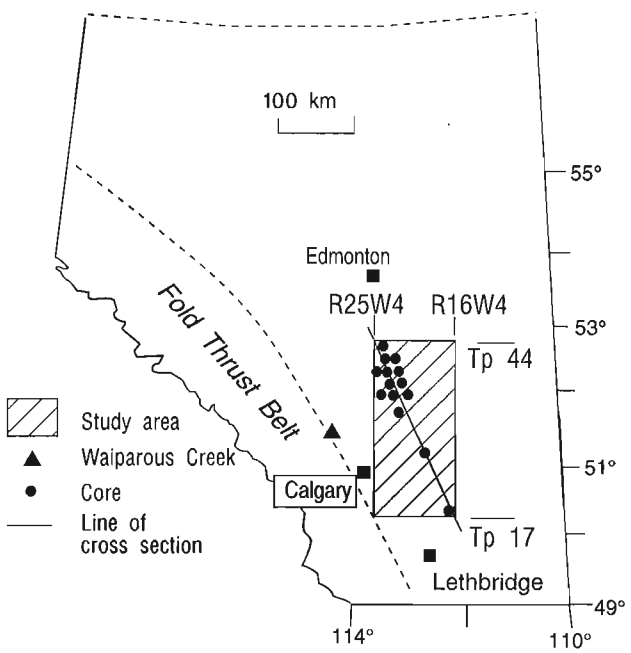

Figure 1. Map of the study area showing the locations of 14 cored wells, one outcrop section, and the line of stratigraphic cross-section illustrated in Figure 4. The outcrop section at Waiparous Creek is mentioned in Figure 10.

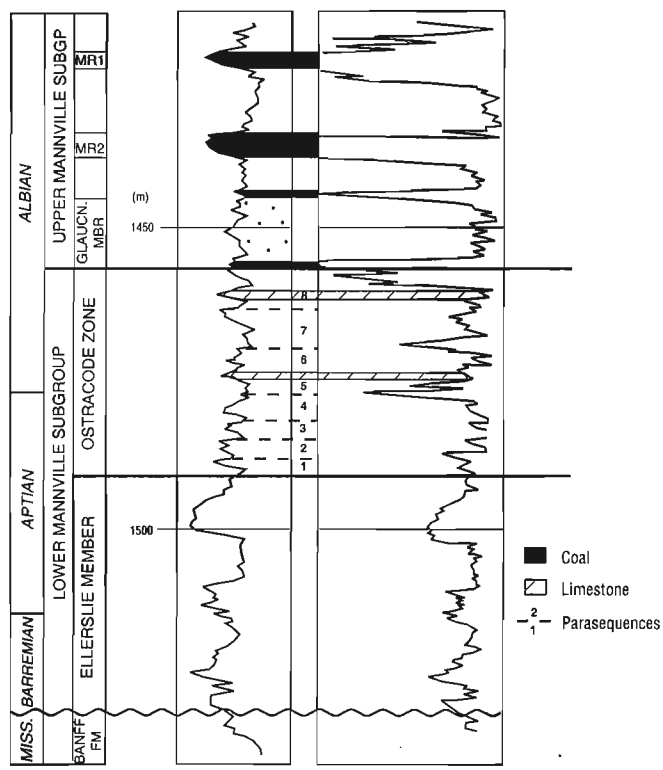

Figure 2. Type well log (Gamma-ray – Density) section of the study interval in the 14-32-44-25W4 well including labels of the surrounding stratigraphic nomenclature. The assigned ages shown in the figure are based on palynological data from Banerjee and Davies (1988).

based on the total assemblage and diversity of individual ichnofossil genera. Other aspects including average size of the forms, together with physical sedimentological data allowed general interpretation to be made. The degree of burrowing intensity within each core was visually estimated. In this way, vertical trends in burrowing intensity were noted and proved to be useful for correlation purposes.

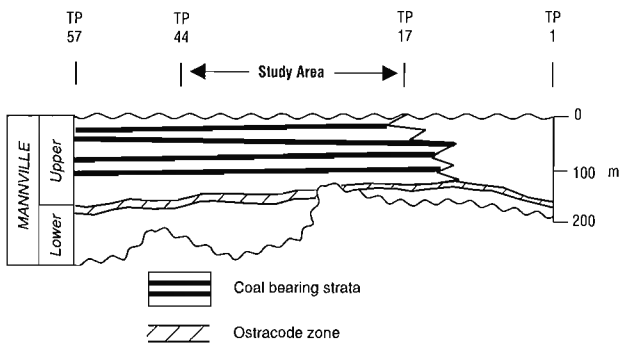

Figure 3. *Basic Mannville stratigraphy shown in a north-south cross-section across Alberta from Township 57 to the U.S.A. border. The coals are shown in black, the sandstone/shale lithologies are shown as blank areas. All limestone beds are confined to the Ostracode zone.*

The microfossil data are compiled from wells between Townships 1 and 54 and Ranges 8 and 26W4 and evaluated for their paleoenvironmental significance.

MANNVILLE STRATIGRAPHY

The Lower Cretaceous Mannville Group is a dominantly siliciclastic stratigraphic unit with the only limestones occurring within the Ostracode zone of the Lower Mannville subgroup (Banerjee, 1990) (Fig. 2). The Upper Mannville is coal bearing in the northern end of the study area, but the coals pinch out, and the Mannville Group thins as it is traced toward the south (Fig. 3).

The Ostracode zone (10-30 m thick) is a regionally continuous unit (Fig. 3, 4) comprising pyritic, organic-rich (Riediger and Banerjee, 1993) black shale interbedded with wave- to combined flow-rippled, burrowed, fine grained sandstone. The unique occurrence of one to four thin (<1.0 m) limestone beds characterizes this unit. The limestones are of two types: (i) coquinas or shell-hash limestones composed mostly of fragmented pelecypod shells, and (ii) dolomitized lime mudstones. The top of the Ostracode zone is easily identifiable at the base of the Glauconitic sandstone Member where present (Fig. 2), but the base is more difficult to locate because in many instances the interbedded sandstone/shale lithology of the Ostracode zone is similar to that of the

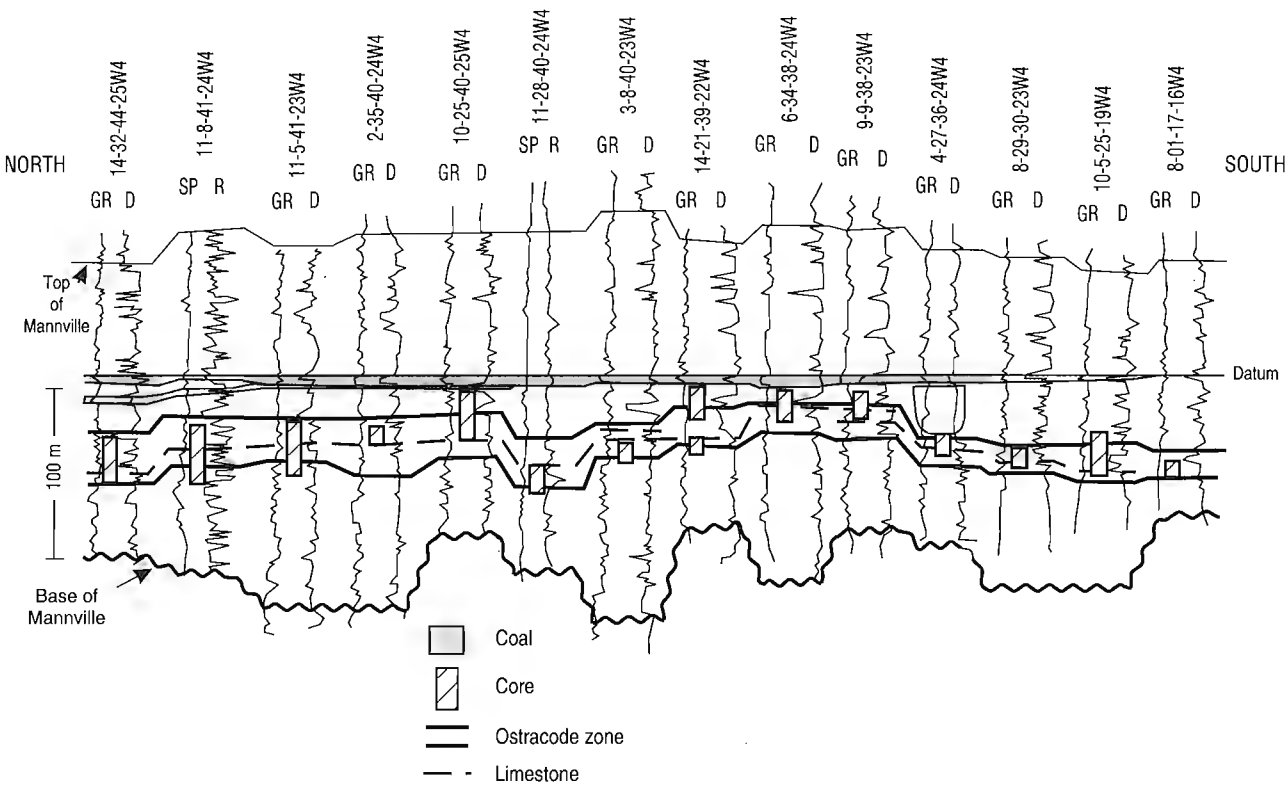

Figure 4. *Stratigraphic cross-section of the study area along the line shown in Figure 1. Types of logs: GR – Gamma Ray; D – Density; SP – Spontaneous Potential; R – Resistivity. Limits of the Ostracode zone and location of both cored intervals and limestone beds within the zone are shown.*

Ellerslie Member. In this study, the base has been chosen at the base of the first thick shale above the topmost thick (<2 m) sandstone of the Ellerslie Member (Fig. 2). The Ostracode zone itself is characterized by a succession of eight parasequences including 1 to 4 limestone beds (Fig. 2).

STRATIGRAPHY OF THE OSTRACODE ZONE

The stratigraphy of the Ostracode zone can be described in terms of eight, 2 to 6 m thick, coarsening-upward (CU) parasequences (Fig. 5). These parasequences typically start at the base with (i) a 1 to 3 m thick black shale unit containing 2 to 3 cm thick, normally graded beds of shell hash interpreted as distal tempestites, followed by (ii) an interval of interbedded, wave-ripple laminated (WRL) and combined flow-ripple laminated (CFRL), fine grained sandstones and black pyritic shales which gradationally pass upward into (iii) amalgamated units of micro-hummocky cross-stratified (HCS), fine grained sandstones. These siliciclastic parasequences are interpreted as offshore/distal lower shoreface deposits which coarsen upward into sandy wave- and storm-influenced lower shoreface deposits. The basal six parasequences comprise a retrogradational parasequence set, and the uppermost two parasequences comprise a progradational parasequence set. In this context, the base of the Ostracode zone represents an initial flooding surface, and a maximum flooding surface (MFS) separates the retrogradational parasequence set below from the progradational parasequence set above (Fig. 6).

A second, carbonate-dominated type of parasequence occurs in a few examples. This coarsening-upward parasequence type starts at the base with (i) black shale containing 1 to 2 cm lenses of combined flow-ripple laminated, fine grained sandstone, followed by (ii) burrowed micritic lime mudstone, and capped with (iii) an amalgamated shell bed.

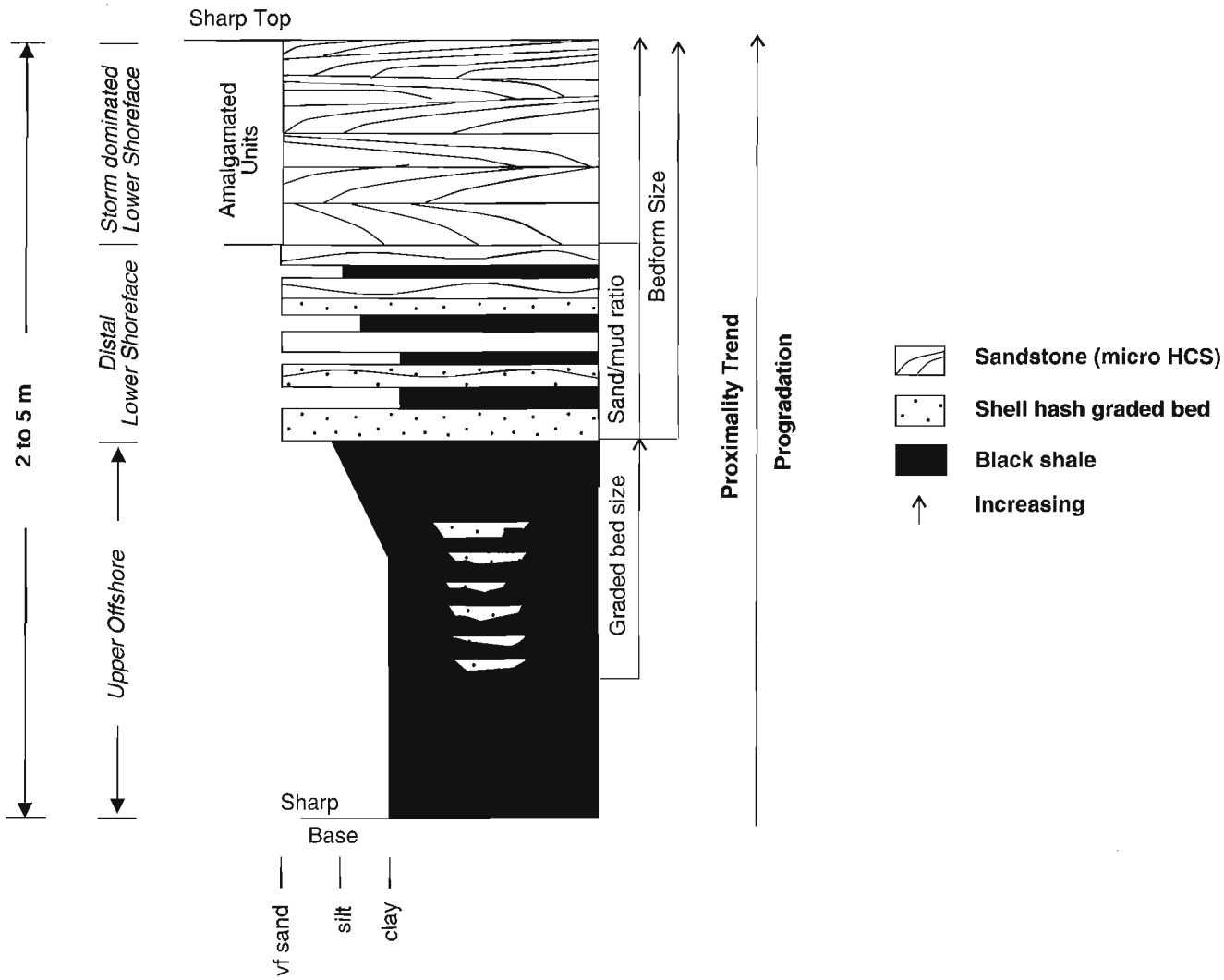

Figure 5. *A typical parasequence in the Ostracode zone and its environmental interpretation. A succession of eight such parasequences makes up the Ostracode zone (see Fig. 6). The thickness of normally graded beds, the sand/mud ratio, and the bedform sizes increase upward.*

This parasequence possibly represents a carbonate shoal, although its exact origin is obscure. The paucity of microbial mat-laminations, and the grey to medium brown colour (nonoxidized) of the lime mudstone indicate a subtidal origin.

ICHNOFOSSILS

The occurrence and relative abundance of different ichnogenera (Fig. 7) identified in the cored intervals of the 14 wells studied are summarized in Figures 8 and 9. The softground assemblages are generally dominated by horizontal traces of mostly deposit-feeding organisms, and can be assigned to the *Cruziana* ichnofacies (Pemberton et al., 1992). Note that a single ichnofacies corresponds to the different depositional environments previously discussed. The common occurrence and local dominance of *Chondrites* are interpreted as indicative of periodic anaerobic or dysaerobic bottom conditions (Bromley and Ekdale, 1984).

The total nature of the softground trace fossil assemblages indicates a stressed, impoverished marine ichnofossil suite. These assemblages are characterized by: (i) small individual trace fossil sizes, (ii) low overall abundances, (iii) low to moderate diversity of ichnogenera, and (iv) local abundance and dominance by a few behaviourally simple forms. The main stresses were likely fluctuating water salinity and reduced oxygenation at the sediment/water interface.

Substrate controlled ichnofacies

The trace fossil assemblages indicative of the *Cruziana* ichnofacies represent traces that were created by organisms that were reworking sediment that was still soft (i.e. softground). In other words, the reworking of biogenic sediment occurred penecontemporaneously with sediment deposition. In contrast to this, the Ostracode zone also contains examples of substrate dependent ichnofacies, namely the *Glossifungites* and *Trypanites* ichnofacies.

The *Glossifungites* ichnofacies occurs in stiff, but not completely lithified substrates (i.e. firmground). The *Trypanites* ichnofacies is found in hard, fully lithified substrates such as early cemented carbonate hardground. Both the *Glossifungites* and *Trypanites* ichnofacies are represented in cores examined in this study. Their significance, as discussed in the next section, is related to the relative sea-level history of the Ostracode zone.

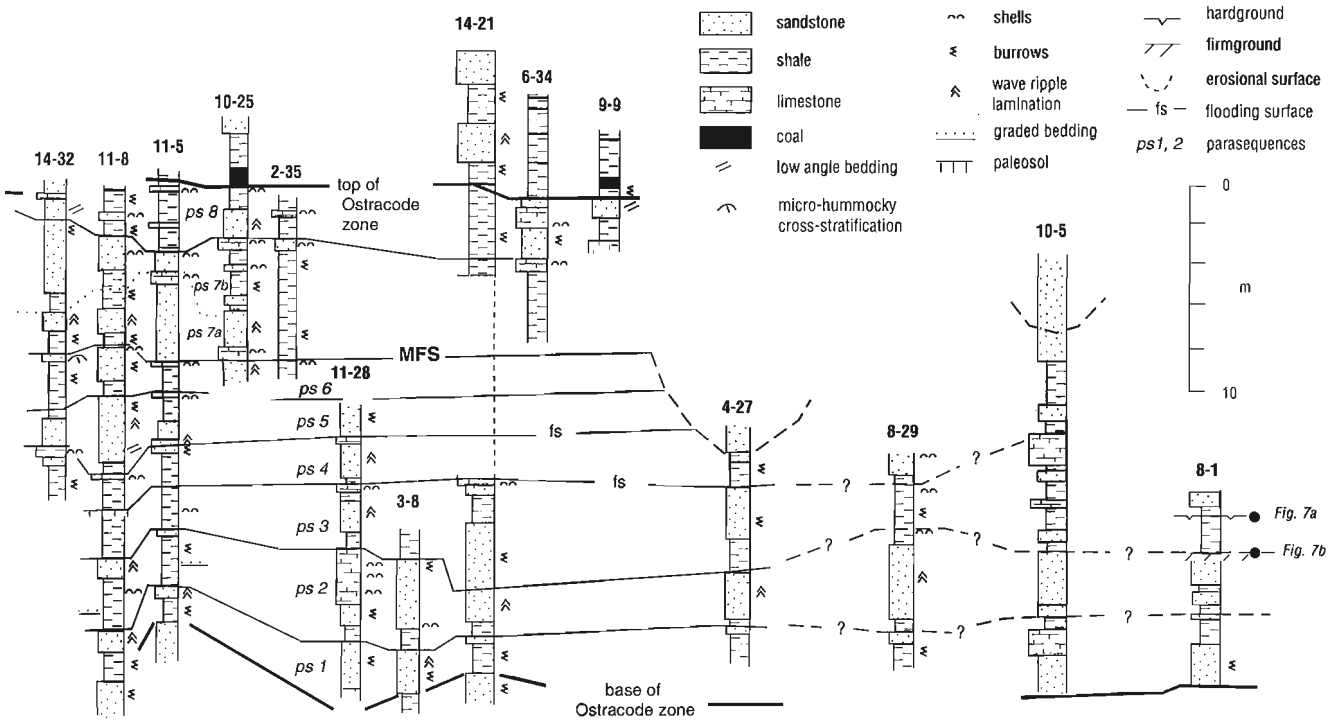

Figure 6. *The core lithologs of selected wells. The cored intervals have been subdivided into correlatable parasequences. The correlation lines for the last three wells have been marked with dashed lines and question marks to indicate uncertainty due to the great distances between core data. A retrogradational (thinning-upward) stacking pattern is apparent in the lower six parasequences and a progradational (thickening-upward) pattern can be recognized in the upper two. Accordingly, a maximum flooding surface (MFS) has been drawn separating the two parasequence sets. Locations of the wells are the same as in Figure 4. The locations of photographs of the hardground and the firmground seen in Figure 7 are demarcated in the 8-1-17-16W4 core litholog.*

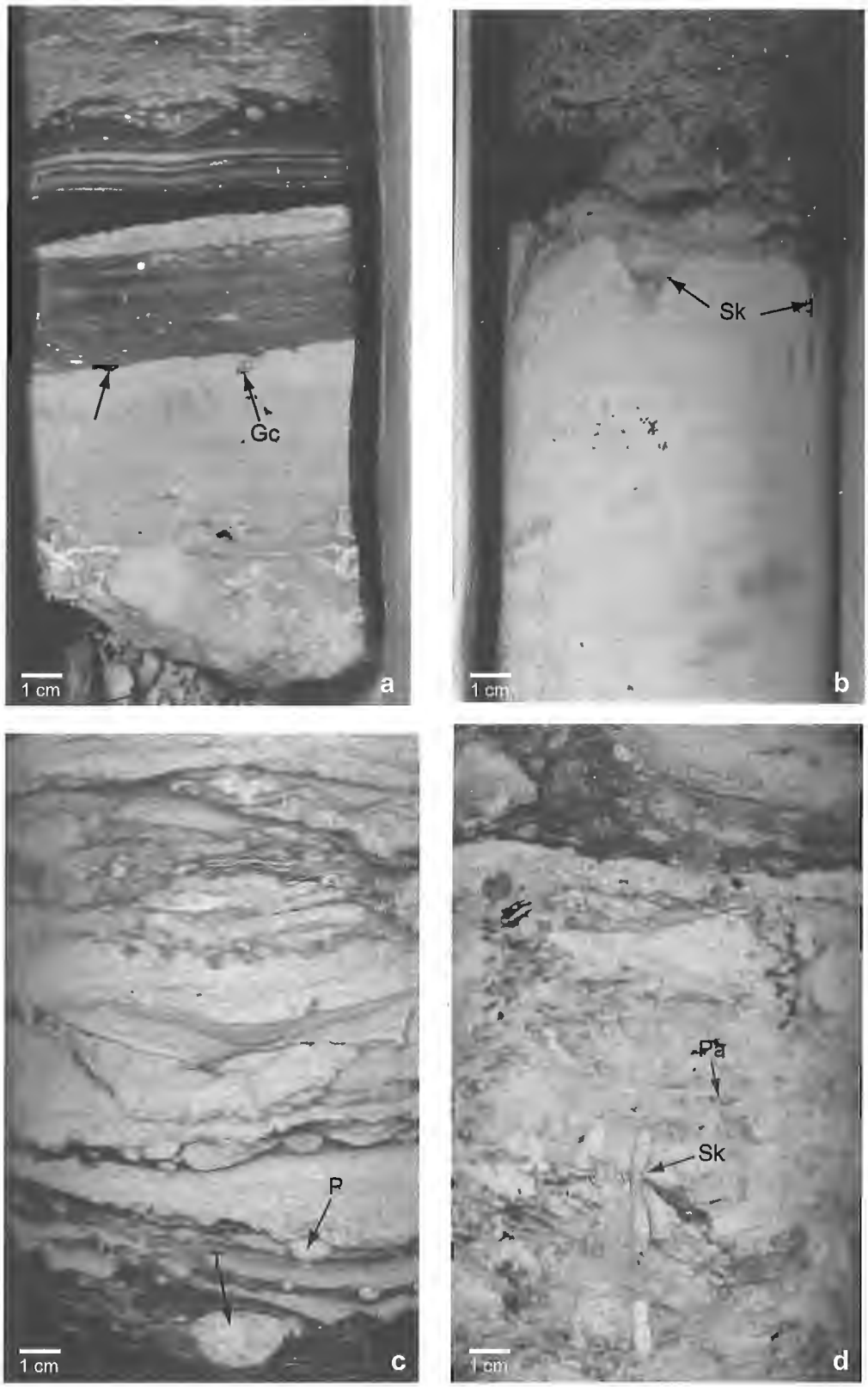

Figure 7. *Photographs of selected trace fossils.* ***a)*** Trypanites *ichnofacies demarcated by hardground* Gastrochaenolites *(Gc) boring into dolomitic lime mudstone. Note the sharp lithological contact (arrow) (8-1-17-16W4 at 3455 ft.) ISPG photo 4501-1;* ***b)*** Skolithos *(Sk) burrows demarcating an occurrence of the* Glossifungites *ichnofacies. Note the shaly medium grained sandstone piped into the vacated burrows in the underlying lime mudstone (8-1-17 16W4 at 3474.5 ft.) ISPG photo 4501-2;* ***c)*** Thalassinoides *(T) and* Planolites *(P) in a thinly interbedded sandstone and shale unit (11-8-41-24W4 at 5086.5 ft.) ISPG photo 4501-3;* ***d)*** *Mud-lined* Skolithos *(Sk) and* Palaeophycus *(Pa) (11-8-41-24W4 at 5086.5 ft.). ISPG photo 4501-4*

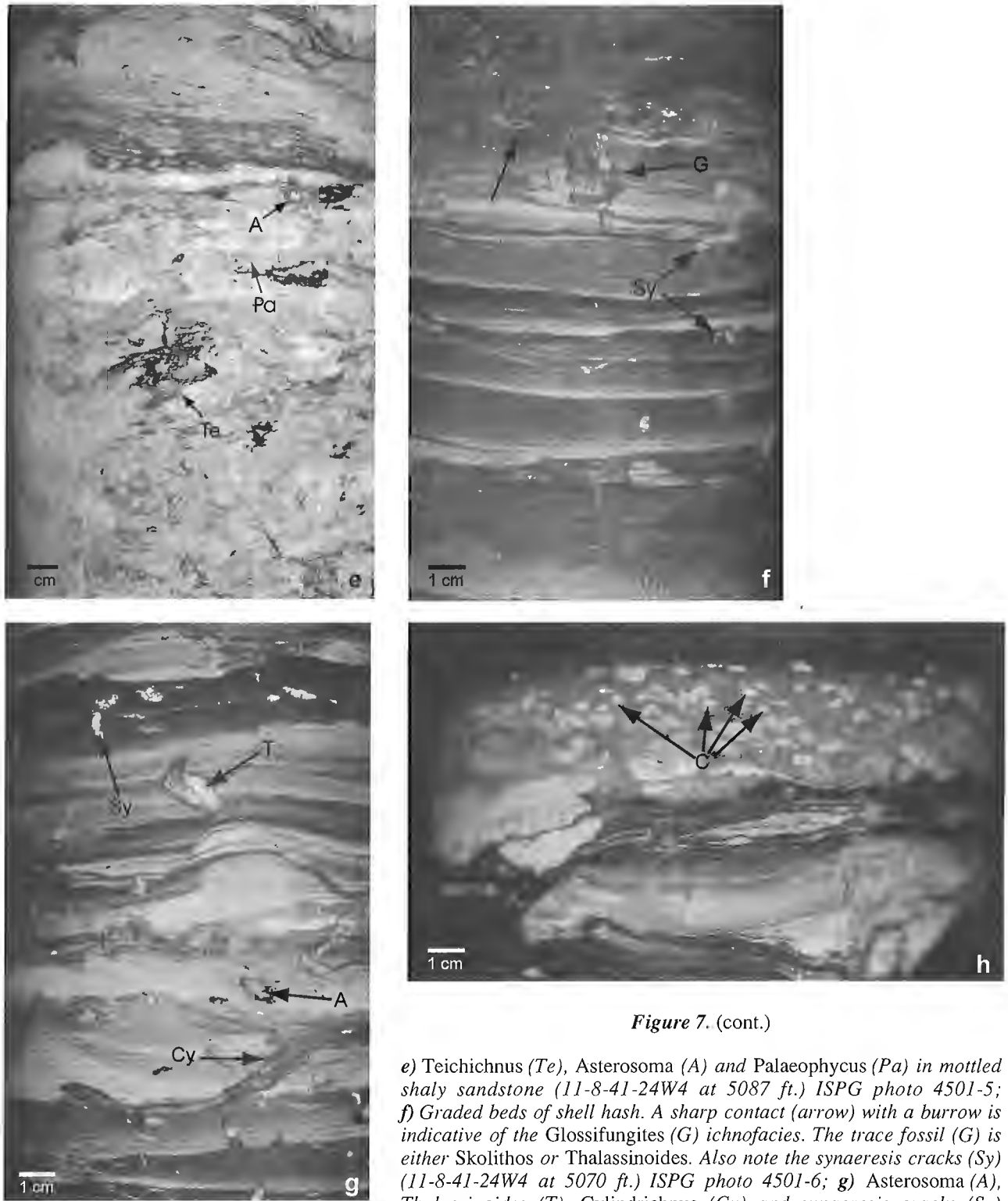

Figure 7. (cont.)

e) Teichichnus *(Te)*, Asterosoma *(A) and* Palaeophycus *(Pa) in mottled shaly sandstone (11-8-41-24W4 at 5087 ft.) ISPG photo 4501-5;* ***f)*** *Graded beds of shell hash. A sharp contact (arrow) with a burrow is indicative of the* Glossifungites *(G) ichnofacies. The trace fossil (G) is either* Skolithos *or* Thalassinoides. *Also note the synaeresis cracks (Sy) (11-8-41-24W4 at 5070 ft.) ISPG photo 4501-6;* ***g)*** Asterosoma *(A), Thalassinoides (T),* Cylindrichnus *(Cy) and synaeresis cracks (Sy) (11-8-41-24W4 at 5083.5 ft.) ISPG photo 4501-8;* ***h)*** *Robust* Chondrites *(C) (11-8-41-24W4 at 5059 ft.). ISPG photo 4501-7.*

Well Location	OZ cored interval	P	Pl	A	Th	C	T	S	Cy	H	O	E	Z	?L	?B	?P	Gl	Tr	G	Ar	Gc
8-01-17-16W4	3454'-3485'	x	x	x													x	x			x
10-05-25-19W4	4562.5'-4638'	x	x	x	x	x	x	x	x		x			x	x	x	x				
8-29-30-23W4	1508-1521 m		x	x	x	x															
4-27-36-24W4	1663.2-1674 m	x	x	x					x												
9-09-38-23W4	1487.5-1489.5 m	x	x																		
6-34-38-24W4	1542-1549 m	x	x	x																	
14-21-39-22W4	1390-1399.5 m	x	x	x		x				x	x	x									
3-08-40-23W4	5113'-5138.5'		x	x	x	x	x		x	x	x						x		x		
11-28-40-24W4	5215'-5304'	x	x	x	x	x	x	x	x	x											
2-35-40-24W4	1494-1504 m	x	x	x		x															
10-25-40-25W4	1571.5-1584 m	x	x	x		x		x	x			x								x	
11-05-41-23W4	4796'-4882'	x	x	x		x	x			x						x					
11-08-41-24W4	5002'-5092'	x	x	x	x	x	x	x	x	x	x			x	x		x				
14-32-44-25W4	1463-1481 m	x	x	x	x	x	x	x				x	x								

Figure 8. Table of occurrences of ichnogenera in the different wells studied. OZ – Ostracode zone; P – Palaeophycus; *Pl* – Planolites; *A* – Asterosoma; *Th* – Thalassinoides; *C* – Chondrites; *T* –Teichichnus; *S* – Skolithos; *Cy* – Cylindrichnus; *H* – Helminthopsis; *O* – Ophiomorpha; *E – Escape traces; Z* – Zoophycos; *?L* – Lockeia; *?B* – Bergaueria; *?P* – Polykladichnus; *Gl* – Glossifungites *ichnofacies; Tr* – Trypanites *ichnofacies; G* – Gyrolithes; *Ar* – Arenicolites; *Gc* – Gastrochaenolites.

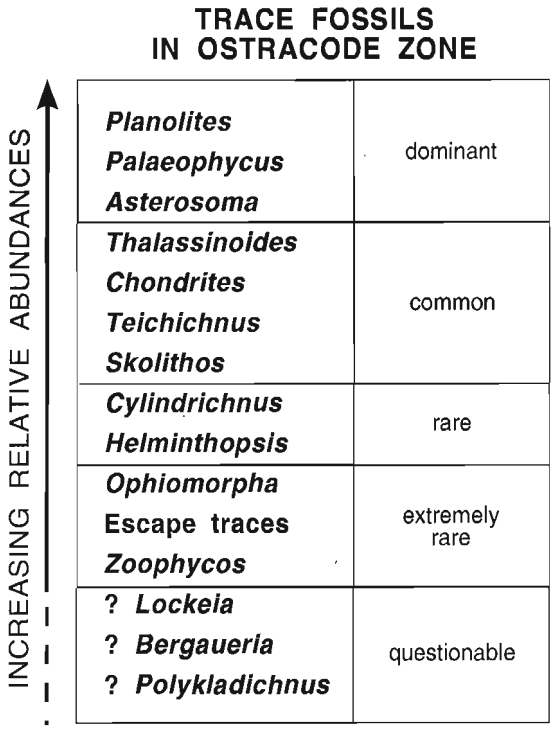

Figure 9. The trace fossil assemblage and the abundances of the different ichnogenera.

Parasequence boundaries and relative sea-level history

The tops of parasequences in the Ostracode zone commonly showed characteristic trace fossil expressions. In a few localities, a bored carbonate hardground (*Trypanites* ichnofacies) defines the boundary (Fig. 7a). In other localities, a firmground indicative of the *Glossifungites* ichnofacies is present at the boundary (Fig. 7b) with a concentration of vertical trace fossils like *Skolithos*. The implications of the *Glossifungites* ichnofacies are well documented by MacEachern et al. (1992) who inferred that the occurrence of *Glossifungites* at a particular surface implies that the surface was colonized and burrowed under marine or marginal marine conditions. Commonly, the firm substrates are exhumed by transgressive wave erosion and colonized by opportunistic organisms capable of exploiting the firm substrate niche by excavating burrow structures into the stiff, partially dewatered sediment. It is interpreted that as relative sea level rose during Ostracode zone time, transgressive wave erosion exhumed firm substrates that were subsequently colonized, vacated, and passively infilled by later sediment deposition. This process likely resulted in the occurrences of the *Glossifungites* ichnofacies observed at parasequence boundaries within the Ostracode zone. The overall transgression indicated by the six basal, retrogradationally stacked parasequences may have

occurred in pulses, with sufficient time and/or sediment available to allow progradational wedges of shoreface sediment to develop.

Paleoenvironmental interpretation

Evidence from trace fossil assemblages and sedimentological characteristics strongly support interpretation of Ostracode zone sediment deposition in a wave-dominated shallow embayment with restricted access to the open sea. Moreover, the embayment was subject to periodic influx of fresh water, and stagnant bottom water conditions.

EVIDENCE FROM BODY FOSSILS

Macrofauna

In a regional study of the paleoecology of the Ostracode zone, Wanklyn (1985) found a low-diversity molluscan assemblage dominated by corbulid and corbiculid bivalves. He classified the assemblages into 13 associations ranging from very brackish (i.e. most marine) to fresh water. Wanklyn (1985) recorded the assemblage shown in Figure 10 from the Waiparous Creek outcrop section (Township 28, Range 8W5; see Fig. 1 for location). According to his interpretation, this assemblage has the closest affinity to the marine realm among the ones studied.

Brackish:	*Corbula* sp. smooth form *Corbula engelmanni ?* (Meek) *Callistina ?* sp. *Corbicula ?* sp. *Modiolus* sp. *Pachychilioides* sp. aff. *P. chrysalis* (Meek) *Pachychilioides* sp. aff. *P. cleburui* (White) cf. *Cymbophora* sp.
Fresh:	cf. *Carinulortis* sp. ? (rare) *Lioplacoides ?* sp.

Figure 10. *The assemblage of bivalves found in the Waiparous Creek section (see Fig. 1 for location) by Wanklyn (1985). The assemblage has been identified as "very brackish".*

Microfauna

Microfossils representing both microflora and microfauna, have been studied to some extent in the Ostracode zone (Banerjee and Davies, 1988; Banerjee, 1990). Although a large database is lacking, the existing amount of data broadly supports a marginal marine interpretation (Banerjee and Kidwell, 1991). The references to published literature on the microfauna prior to 1983 can be found in Finger (1983).

Finger (1983) also reviewed the problems of paleoecological and taxonomical interpretation of the microfaunal data of the Ostracode zone previously published by Loranger (1951), Mellon and Wall (1963) and McLean and Wall (1981). The data presented in Figure 11 (right hand column) are based on analysis of microfossils by Finger (1983) from samples collected from cored intervals of five wells in central Alberta (Twp. 47-54, north of the current study area). This figure clearly demonstrates a mixed fauna of predominantly marginal marine origin.

In southern Alberta, Banerjee (1990) presented microfaunal data from five wells (Twp. 1-20) based on analysis by J.H. Wall (unpublished report no. 5, Geological Survey of Canada, 1983). In the 10-29-20-13W4 well at 3333 ft., a marine foraminiferal assemblage was obtained. Otherwise the data showed a mixed marine and freshwater assemblage (Fig. 11, left hand column).

One available dataset from central Alberta (Fig. 11, middle column) includes the study area (Twp. 21-44). The impoverished faunal assemblage observed suggests a brackish to freshwater environment (J.H. Wall, pers. comm., 1983). In conclusion, the existing regional data on microfaunal assemblages from the Ostracode zone support a marginal marine depositional interpretation.

Microflora

Both euryhaline and open marine dinoflagellates have been documented from regionally extensive core samples of the Ostracode zone (Banerjee and Davies, 1988). Of the 14 cores used in this study, the 11-08-41-24W4 location yielded 21 species of marine dinoflagellates (Fig. 12). In another core (10-25-40-25W4 at 1576-1577 m depth), two marine and two euryhaline forms were found (E.H. Davies, pers. comm., 1993). The dinoflagellate data clearly demonstrate a fully marine to marginal marine origin for the Ostracode zone.

Nature of the Ostracode zone sea

The Ostracode zone is a regionally extensive lithostratigraphic unit covering most of Alberta. Its origin has been the subject of continuous debate since Hunt (1950) first used the name and Loranger (1951) described the microfauna. The environmental interpretation ranged from a series of isolated freshwater lakes (Hayes, 1986) to marginal marine environments (Finger, 1983).

SUMMARY

The following brief summary of sedimentary facies and fossil and trace fossil evidence documented so far indicates that a marginal marine interpretation best fits the data.

1) Sedimentary facies

The overall low to moderately burrowed nature of the sediments, the presence of tempestites of shell hash within pyritic black shales, and the dominance of wave-generated combined flow-ripple laminated, wave-ripple laminated, and micro-hummocky cross-stratified structures in the sandstones, indicate that wave-dominated marginal marine environments were the norm in the Ostracode zone enclosed sea or embayment.

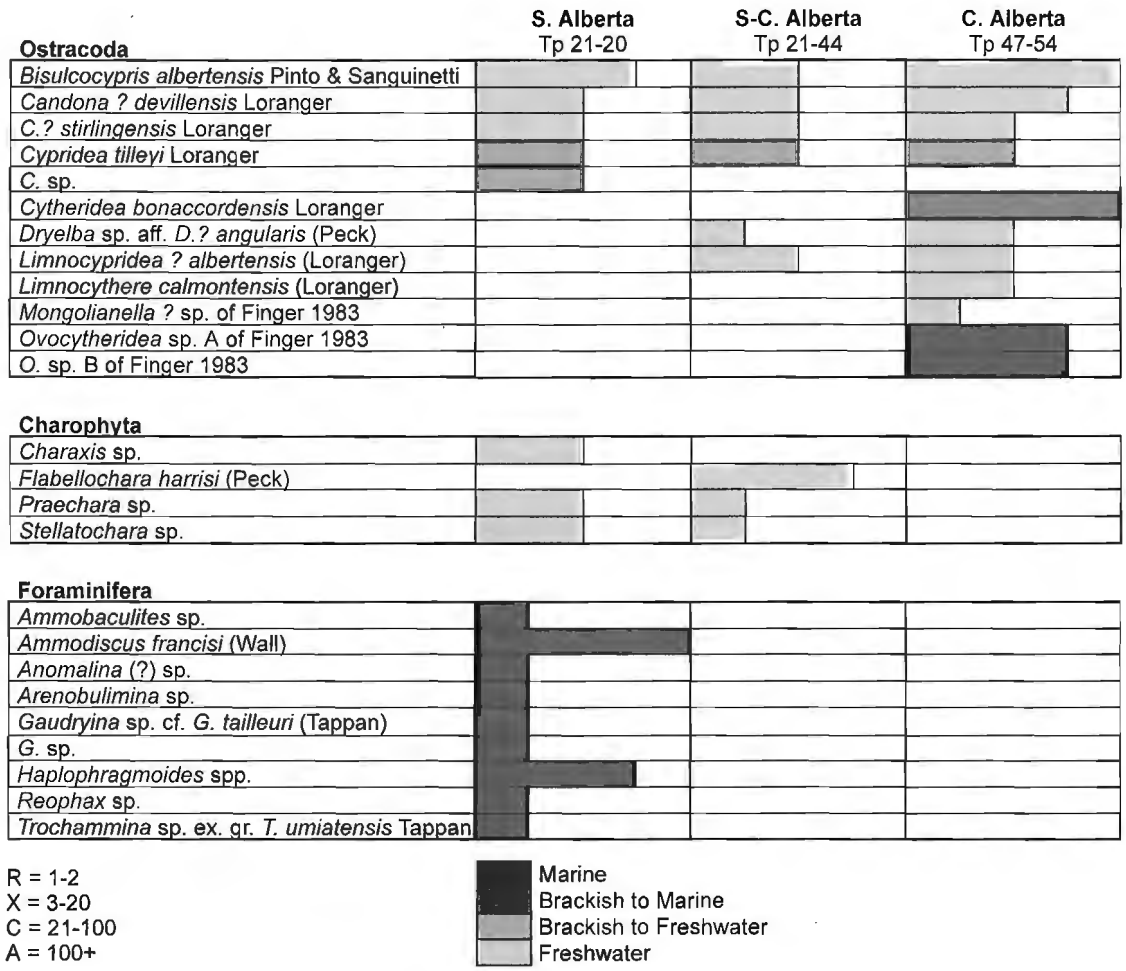

Figure 11. *Microfaunal abundances in southern, south-central and central Alberta. R – rare; X – normal; C – common; A – abundant. Numbers refer to microfaunal occurrences in individual samples.*

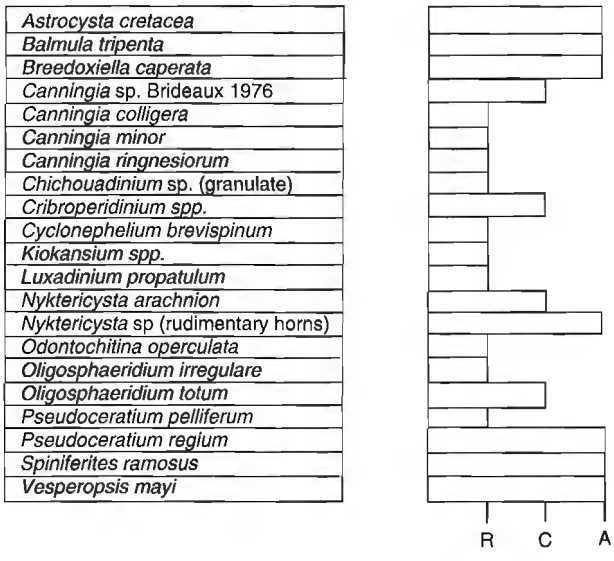

Figure 12. *Relative abundances of marine dinoflagellates found in the Ostracode zone (1-08-41-24W4). R – rare; C – common; A – abundant.*

Ubiquitous presence of synaeresis cracks in the sediments (see Fig. 7) supports the notion of deposition in an area influenced by the mixing of fresh and saline water (Burst, 1965).

The incipient paleosol horizons, rooted horizons and desiccation cracks in the lime mudstones collectively suggest repeated subaerial exposure of the sedimentary strata. Evidence of repeated emergence events may indicate a very shallow Ostracod sea that was particularly sensitive to even the slightest fluctuations in relative sea level (Fig. 13).

2) The body fossil evidence

Macro- and microfossil evidence presented above prove the presence of marine and brackish (i.e. impoverished marine) flora and fauna. The presence of freshwater fauna can be explained by periodic freshwater influx into an enclosed sea (Fig. 13).

3) The trace fossil evidence

Three ichnofacies (one softground and two substrate dependent) are present in the Ostracode zone within the study area. The softground trace fossil assemblages found are dominated by horizontal traces and can be assigned to the *Cruziana* ichnofacies. A marginal marine depositional environment characterized by local areas of reduced oxygen and lower than normal seawater salinity are reflected by the "stressed" nature of the softground ichnofossil suites. The substrate-controlled *Glossifungites* and *Trypanites* ichnofacies indicate colonization of firm and hard substrates under marine to marginal marine conditions, and enhance interpretation of the Ostracode zone's relative sea-level history.

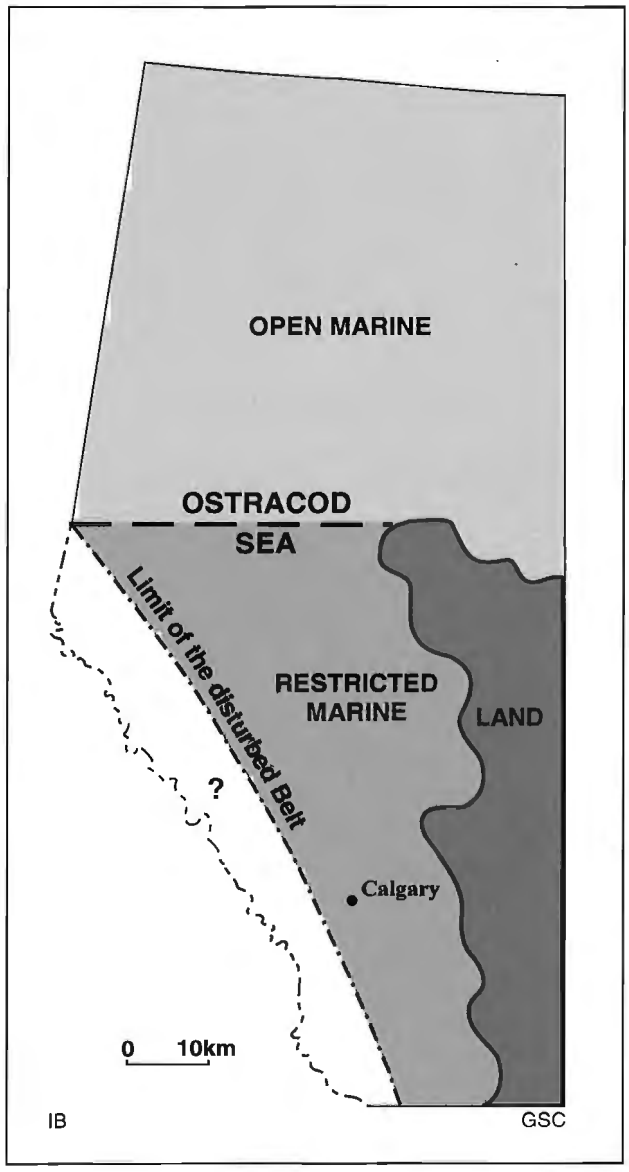

Figure 13. Paleogeography of the Ostracod sea showing the probable location of the shoreline and the limits of the restricted seaway (from Jackson, 1985).

CONCLUSIONS

A review of the sedimentological and body fossil evidence (both macro and micro) reported from previous studies, combined with trace fossil evidence from this study, indicate that sediments of the Ostracode zone were deposited in a wave-dominated, shallow enclosed sea with stagnant bottom conditions and periodic freshwater influx. The shallow nature of the sea rendered the sediments prone to subaerial exposure as a result of fluctuations in relative sea level.

ACKNOWLEDGMENTS

The microfaunal data tabulated in Figure 11 have been compiled and reviewed by J.H. Wall of the Geological Survey of Canada (Calgary). Much of the microfaunal data are based on a series of Wall's unpublished reports produced at GSC Calgary. The authors are deeply indebted to Wall for his help. Terry Poulton of GSC Calgary critically read the manuscript and made many helpful suggestions.

REFERENCES

Banerjee, I.
1990: Some aspects of Lower Mannville sedimentation in southeastern Alberta; Geological Survey of Canada, Paper 90-11, 44 p.

Banerjee, I. and Davies, E.H.
1988: An integrated lithostratigraphic and palynostratigraphic study of the Ostracode zone and adjacent strata in the Edmonton Embayment, central Alberta; in Sequences, stratigraphy, sedimentology: surface and subsurface, (ed.) D.P. James and D.A. Leckie; Canadian Society of Petroleum Geologists, Memoir 15, p. 261-274.

Banerjee, I. and Kidwell, S.M.
1991: Significance of molluscan shell beds in sequence stratigraphy: an example from the Lower Cretaceous Mannville Group of Canada; Sedimentology, v. 38, p. 913-934.

Bromley, R.G. and Ekdale, A.A.
1984: *Chondrites:* a trace fossil indicator of anoxia in sediments; Science, v. 224, p. 872-874.

Burst, J.F.
1965: Subaqueously formed shrinkage cracks in clay; Journal of Sedimentary Petrology, v. 35, p. 348-353.

Caldwell, W.G.
1984: Early Cretaceous transgressions and regressions in the southern interior plains; in The Mesozoic of Middle North America, (ed.) D.F. Stott and D.J. Glass; Canadian Society of Petroleum Geologists, Memoir 9, p. 173-203.

Finger, K.L.
1983: Observations on the Lower Cretaceous Ostracode zone of Alberta; Bulletin of Canadian Petroleum Geology, v. 31, p. 326-337.

Geier, M. and Pemberton, S.G.
1994: Ichnological and sedimentological aspects of the Ostracode zone, Bellshill-Lake Killam area, east-central Alberta; in Exploration Update 1994, (ed.) S.G. Pemberton, D.P. James, and D.M. Wightman; CSPG Mannville Core Conference, Canadian Society of Petroleum Geology, p. 315-330.

Hayes, B.J.R.
1986: Stratigraphy of the Basal Cretaceous Lower Mannville Formation, Southern Alberta and North-Central Montana; Bulletin of Canadian Petroleum Geology, v. 34, p. 30-48.

Hunt, C.W.
1950: Preliminary report on Whitemud oil field, Alberta, Canada; American Association of Petroleum Geologists Bulletin, v. 34, p. 1795-1801.

Jackson, P.C.
1985: Paleogeography of the Lower Cretaceous Mannville Group of Western Canada; in Elmworth - Case Study of a Deep Basin Gas Field, (ed.) J.A. Masters; American Association of Petroleum Geologists, Memoir 38, p. 49-77.

Loranger, D.M.
1951: Useful Blairmore microfossil zones in central and southern Alberta, Canada; American Association of Petroleum Geologists Bulletin, v. 35, p. 2348-2367.

MacEachern, J.A., Raychaudhuri, I., and Pemberton, S.G.
1992: Stratigraphic applications of the *Glossofungites* ichnofacies: delineating discontinuities in the rock record; in Application of Ichnology to Petroleum Exploration, a core workshop, (ed.) S.G. Pemberton; SEPM Core Workshop No. 17, Calgary, June 21, 1992, p. 169-198.

McLean, J.R. and Wall, J.H.
1981: The Early Cretaceous Moosebar Sea in Alberta; Bulletin of Canadian Petroleum Geology, v. 29, p. 334-377.

Mellon, G.B. and Wall, J.H.
1963: Correlation of the Blairmore Group and equivalent strata; Bulletin of Canadian Petroleum Geology, v. 11, p. 396-409.

Pemberton, S.G., MacEachern, J.A., and Frey, R.W.
1992: Trace fossil facies models: environmental and allostratigraphic significance; in Facies Models: response to sea level change, (ed.) R.G. Walker and N.P. James; Geological Association of Canada, p. 47-72.

Riediger, C.L. and Banerjee, I.
1993: Rock-Eval/TOC data from the Lower Cretaceous Ostracode zone (Mannville Group), Calcareous Member (Gladstone Formation) and Moosebar Formation, Alberta, Western Canada Sedimentary Basin; Geological Survey of Canada, Open File 2699, 16 p.

Wanklyn, R.P.
1985: Stratigraphy and depositional environments of the Ostracode Member of the McMurray Formation (Lower Cretaceous; Late Aptian-Early Albian) in west central Alberta; Master's thesis, University of Colorado, 289 p.

Geological Survey of Canada Project 930010

Canadian Shield

Bouclier canadien

The Duke of York and related Neoproterozoic inliers of southern Victoria Island, District of Franklin, Northwest Territories[1]

R.H. Rainbird[2], A.N. LeCheminant, and J.I. Lawyer[3]
Continental Geoscience Division, Ottawa

Rainbird, R.H., LeCheminant, A.N., and Lawyer, J.I., 1996: The Duke of York and related Neoproterozoic inliers of southern Victoria Island, District of Franklin, Northwest Territories; in Current Research 1996-E; Geological Survey of Canada, p. 125-134.

Abstract: Duke of York inlier contains a ~400 m-thick succession of sulphate evaporite, cherty dolostone, and siltstone-quartz arenite of the Neoproterozoic Shaler Supergroup. When linked with similar rocks to the north and south, these strata define a broad, gently northwest-dipping and northwest-concave arc. The arc parallels the inferred erosional edge of an intracratonic basin formed on the northwestern margin of Laurentia. The sedimentary rocks are intercalated with at least six gabbro sills, up to 125 m thick, intruded during a large magmatic outburst at 0.72 Ga (Franklin events) linked to break-up of a Neoproterozoic supercontinent. The intrusive suite also includes northwest-striking dykes and variably dipping, irregular gabbro sheets. A northeast-striking fault separates Victoria Island outcrops from down-dropped strata on the Richardson Islands. Proterozoic rocks are overlain by lower Paleozoic marine sandstones and carbonates, which can be correlated with the Old Fort Island and Cass Fiord formations, respectively.

Résumé : L'enclave de Duke of York contient une succession d'environ 400 mètres d'épaisseur d'évaporites sulfatées, de dolomie cherteuse et de siltstone-quartzarénite, faisant partie du Supergroupe de Shaler du Néoprotérozoïque. Lorsqu'on les corrèle à des roches semblables au nord et au sud, ces couches définissent un large arc faiblement incliné vers le nord-ouest et concave vers le nord-ouest. L'arc est parallèle au biseau d'érosion inféré d'un bassin intracratonique formé sur la marge nord-ouest de la Laurentie. Les roches sédimentaires sont intercalées avec au moins six filons-couches de gabbro mesurant jusqu'à 125 mètres d'épaisseur, qui ont fait intrusion il y a 0,72 milliards d'années pendant un important épisode magmatique (événements de Franklin); ce magmatisme était lié à la rupture d'un supercontinent néoprotérozoïque. La suite intrusive inclut en outre des dykes d'orientation nord-ouest et des nappes irrégulières de gabbro au pendage variable. Une faille d'orientation nord-est sépare les affleurements continentaux des successions affaissées sur les îles Richardson. Les roches protérozoïques sont sous-jacentes à des lithologies marines (grès et roches carbonatées) du Paléozoïque inférieur, que l'on peut corréler aux formations d'Old Fort Island et de Cass Fiord, respectivement.

[1] Industrial Partners Project 94-031, involving the Geological Survey of Canada and Ascot Resources Ltd., and Industrial Partners Project 95-012, involving the Geological Survey of Canada and WMC International Ltd.
[2] 1725 Grasmere Crescent, Ottawa, Ontario K1V 7V1
[3] WMC International Ltd., 22 Gurdwara Rd., Nepean, Ontario K2E 8A2

INTRODUCTION

Neoproterozoic rocks consisting of intercalated gabbro sills and Shaler Supergroup sedimentary rocks are exposed in topographic highs on the sub-Paleozoic surface in a discontinuous belt extending inland from Duke of York inlier to Surrey Lake (Fig. 1). The Proterozoic rocks were first mapped during a geological reconnaissance survey of Victoria Island in 1958 (Thorsteinsson and Tozer, 1962). Rugged coastal exposures in Duke of York inlier provide excellent sections through the sediment-sill complex for more than 50 km along the south shore of Victoria Island. Duke of York inlier and several smaller exposures to the west, north, and northeast were mapped from a helicopter-supported base camp during a three week period in July, 1995 (Rainbird et al., in press). The northernmost outcrops, near Surrey Lake, were examined in 1994 as part of a project to study Proterozoic successions and Archean basement rocks in northern Wellington inlier (Fig. 1; LeCheminant et al., 1996). Duke of York inlier was targeted for mapping because it is considered to hold potential for economic concentrations of Ni-Cu-PGEs, based on analogies to the Russian Noril'sk-Talnakh deposits and a previous reconnaissance survey that investigated the economic potential of gabbro sills from the Duke of York-Coppermine region (Jefferson et al., 1994).

REGIONAL GEOLOGY

Inliers of Shaler Supergroup rocks, intruded by gabbro sills of the Franklin suite, outcrop on Victoria Island, southern Banks Island, and on the northern mainland of the Amundsen Gulf region (Young, 1981; Rainbird et al., 1994b). The inliers are remnants of the formerly contiguous intracratonic Amundsen Basin, which is preserved on the northwest edge of cratonic North America (Laurentia). The Duke of York inlier (Dixon, 1979) is at the eastern end of an east to east-northeast arcuate trend, along strike with Shaler Supergroup strata in the Coppermine area (Fig. 1 and 2; Young and Jefferson, 1975; Dixon, 1979; Campbell, 1983). The Shaler Supergroup comprises an up to 5 km thick sequence of platformal marine carbonate, evaporite, and subordinate siliciclastic rocks overlain and underlain by fluvial and fluvio-deltaic siliciclastic rocks. It includes, in ascending stratigraphic order: Rae Group, Reynolds Point Group, Minto Inlet Formation, Wynniatt Formation, Kilian Formation, and Kuujjua Formation (Rainbird et al., 1994b) . Strata above the Minto Inlet Formation are preserved only in the Minto inlier on northern Victoria Island (Fig. 1), where the Shaler Supergroup is overlain an up to 1 km thick sequence of flood basalts, the Natkusiak Formation. The lower age limit of the Shaler Supergroup is constrained by a 1077 ± 4 Ma (U-Pb) detrital zircon obtained from fluvial braidplain quartz arenites of the Nelson Head Formation of the Rae Group (see below, Rainbird et al., 1994c).

Numerous gabbro sills and diabase dykes, coeval with the Natkusiak Formation flood basalts, intrude the Shaler Supergroup throughout Amundsen Basin. These sills are part of the Franklin igneous events and have U-Pb ages of 718-723 Ma (Heaman et al., 1992), which establishes a minimum age for the Shaler Supergroup. Gabbro sills are well exposed on the Richardson Islands in Duke of York inlier (Fig. 2), in the Duke of York Archipelago, and on islands in southern Coronation Gulf and adjacent mainland regions (Fig. 1). Up to fifteen 50-100 m thick sills are present within the Rae Group on the mainland (Robertson and Baragar, 1972). The geology of Duke of York inlier is also discussed in GSC reports by Dixon (1979), Campbell (1983,1985), and Rainbird et al. (1994b).

PROTEROZOIC GEOLOGY OF THE DUKE OF YORK INLIER

Sedimentary rocks of the Shaler Supergroup

Neoproterozoic sedimentary rocks in Duke of York inlier are assigned to the upper three formations of the redefined Rae Group of the Shaler Supergroup: the Mikkelsen Islands, Nelson Head, and Aok formations (Fig. 2; Rainbird et al., 1994b). Mikkelsen Islands Formation shelf carbonates are exposed in a belt extending from western Surrey Lake through eastern Duke of York inlier across the Duke of York Archipelago southwestward for about 300 km (see Baragar and Donaldson, 1973). In the inlier, the carbonates are confined primarily to the Richardson Islands, where they are variably preserved as thin (<30 m thick) layers sandwiched between several Franklin gabbro sills. Contact metamorphic effects are significant, as indicated by local recrystallization and metasomatism, including serpentinization of siliceous nodules in carbonate. Total thickness of the Mikkelsen Islands Formation is 100-120 m. The principal rock type is flat to slightly wavy bedded, grey, dolomitic microbialaminite. Thin carbonaceous siltstone interlaminations and dark chert nodules are common in the shoreline section at the easternmost edge of the map area (Fig. 2). These features are typical of the upper part of the formation in other areas (Rainbird et al., 1994b). Laterally linked domal stromatolites were observed on southern Edinburgh Island (Fig. 2); they are <1 m wide with synoptic relief of about 20 cm. The stromatolites pass upward into about 3 m of greyish white, thin parallel-bedded gypsum. Evaporites are not known elsewhere from the Mikkelsen Islands Formation and this occurrence represents their stratigraphically lowest occurrence in the Shaler Supergroup.

The Nelson Head Formation is exposed mainly to the west and northeast of Johansen Bay. Lowermost strata are silty, dark grey argillites, which overlie laminated carbonates of the Mikkelsen Islands Formation with abrupt conformity in an approximately 15 m thick section preserved between the stratigraphically highest sills in the eastern Richardson Islands (Fig. 2). The same section is repeated by a fault on adjacent Victoria Island. Gossans resulting from oxidation of finely disseminated pyrite in metamorphosed beds are common within this section. Basal Nelson Head Formation strata generally are thin, parallel-laminated carbonaceous mudstones, which coarsen upward to wavy bedded siltstone and fine sandstone. They are exposed throughout the eastern coastal region as a <10 m thick veneer on the upper chilled contact of the uppermost sill. The remainder of the Nelson Head Formation is composed of fine- to coarse-grained, well

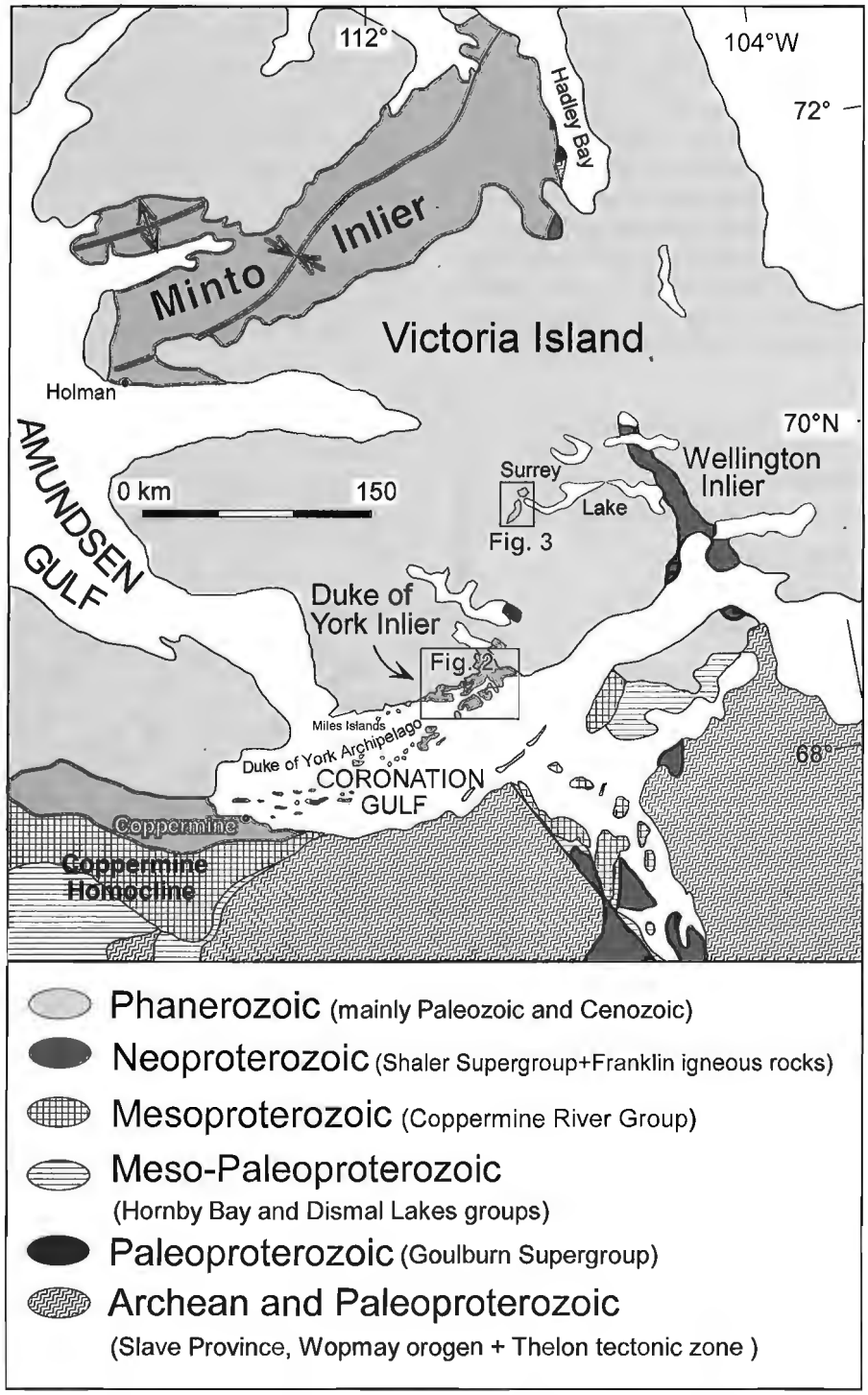

Figure 1. *Geological map of the north-central margin of Laurentia and adjacent regions, highlighting the distribution of Proterozoic inliers on Victoria Island and showing the location of detailed figures in this report.*

indurated quartz arenite. Subdued topography and poor continuity between rubbly exposures combined with the subhorizontal attitude of the strata provide insufficient data to construct a complete section for the Nelson Head Formation. Partial sections, combined with observations based on regional distribution and dip of strata (3-5°NW), indicate it to be about 200 m thick in northwestern Duke of York inlier. There, the Nelson Head Formation comprises one complete coarsening upward cycle beginning with the section described above and continuing above the uppermost sill into white- to buff-weathering, fine grained ripple crosslaminated to thin planar crossbedded quartz arenite/subarkose. This is overlain by a relatively thick section (~100 m) of pink to red, medium to very coarse grained quartz arenite containing large- to very large-scale tabular-planar to broad tabular-trough crossbeds and planar parallel beds. At the top of the section, at the western end of Johansen Bay, it comprises very clean, massive, tabular-bedded white quartz arenite. In Minto inlier, where it is at least twice as thick, the Nelson Head Formation comprises several such coarsening upward cycles produced by overlapping, prograding lobes of a river-dominated fan-delta (Young and Long, 1977; Rainbird et al., 1992; Conly, 1993). The massive white quartz arenites at the top of the Duke of York inlier section are interpreted to represent a marine-reworked delta top facies.

Paleocurrent data from crossbeds in the middle to upper part of the section indicate strong unimodal transport to the west-northwest (Fig. 2), supporting the braided fluvial transport interpretation. Our data are consistent with those

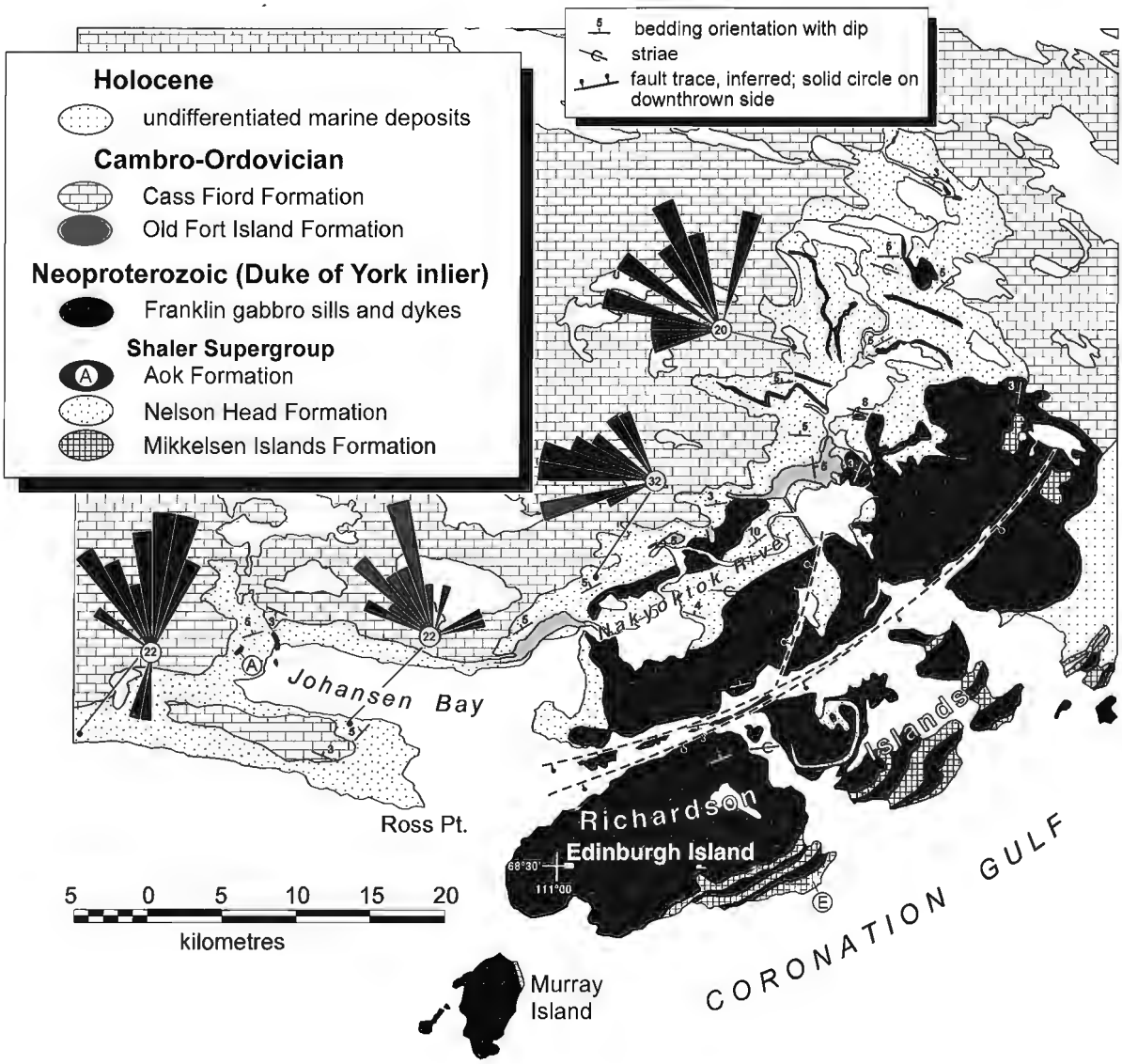

Figure 2. *Geological map of Duke of York inlier, simplified from Rainbird et al. (in press). Circled letter E shows location of evaporites; circled letter A shows location of Aok Formation outcrop. Paleocurrent roses are derived from crossbed dip azimuths (number of measurements in circle at center of rose). Petals are in 10° intervals and are equal-area plots.*

obtained from the middle part of the Nelson Head Formation elsewhere in Amundsen Basin and with data from a previous study of similar strata in this area (Campbell, 1983). We note, however, that the easternmost paleocurrent rose from Campbell (1983, Figure 6.3, p. 47) was derived from outcrops that we mapped as Cambrian Old Fort Island Formation (Rainbird et al., in press).

The Aok Formation occurs as a small (<50 m long) isolated outcrop at the west end of Johansen Bay (Campbell, 1985; Rainbird et al., 1994b; Rainbird et al., in press). Its contact with the underlying Nelson Head Formation is gradational over about 3 m from pure white quartz arenite into grey-green-weathering stromatolitic dolostone. Intervening strata are wavy to lenticular-bedded, brown sandy dolostone and red ferruginous siltstone. The preserved Aok Formation section is only about 10 m thick and is composed entirely of large, branching, digitate stromatolites of the form described by Jefferson and Young (1989).

Intrusive rocks of the Franklin igneous events

In Duke of York inlier, Franklin sills are well exposed on the Richardson Islands and adjacent coastal areas southeast of the Nakyoktok River (Fig. 2), where they are intercalated with carbonate rocks. In overlying quartz arenites of the Nelson Head Formation, the thick sills give way to variably dipping, arcuate, zig-zag and tabular gabbro sheets. As well, northwest-striking dykes intrude quartz arenites in the Nakyoktok River valley and northeast-striking dykes cut the lower sill complex. Isolated inliers, containing gabbro sills occur both west and northeast of the main outcrop area of the inlier. The sills, exposed through a thin cover of Paleozoic carbonates and glacial deposits, form an arcuate pattern of outcrops extending discontinuously to Surrey Lake (Fig. 1; Thorsteinsson and Tozer, 1962; Christie 1964; Christie et al., 1972).

GABBRO SILLS

Thick gabbro sills dominate the topography and geology of southern and eastern Duke of York inlier, where they comprise a series of at least six discrete, stacked, mainly tabular bodies. In contrast to sediment-dominated successions in Minto inlier and near Coppermine, in Duke of York inlier, thick sills are separated by relatively thin sedimentary layers (<30 m), mostly of Mikkelsen Islands Formation. The lower sills are well exposed in cliffs along the southeastern shores of the Richardson Islands and on the Victoria Island coast, at the eastern end of the inlier (Fig. 2). Northwest of the coastal cliffs on the Richardson Islands, remarkable flat-topped outcrops expose the upper chilled margin of the 25 m thick coastal sill, free of inter-sill carbonate rocks. The surface is flat, smooth and featureless, except for a few 10-30 cm patches characterized by oriented arrays of small vesicles. The smooth, aphanitic surface preserves abundant glacial striae and crag-and-tail structure indicating westerly transport. The overlying sill is also about 20-30 m thick. Sheeting in olivine gabbro near the base defines 0.5-1 m steps and black, amphibole-bearing seams accentuate the joint pattern. Middle and upper parts of the sill are medium grained poikilitic gabbro with 0.5-1 cm clinopyroxene oikocrysts. About 20 m of Mikkelsen Islands Formation carbonate separates this sill from the overlying thick poikilitic sill (sill 5) that forms many of the high cliff sections in the Richardson Islands.

Sill 5 is about 80 m thick and, except for a narrow zone at the base, it is poikilitic throughout. Above the fine grained base, the sill is a medium- to coarse-grained olivine gabbro; the coarse poikilitic texture that is characteristic of the sill occurs above the 40 m level. Pegmatitic patches occur irregularly in the upper third of the sill and, about 10 m below the sill top are associated with a discontinuous zone of gossans that contain minor chalcopyrite and up to 10% disseminated pyrite. Typically, on the eastern Richardson Islands, the upper chilled margin is not exposed and sill-top rocks are fine grained gabbros that crystallized about 1-3 m below the projected contact. However, upper parts of sill 5 are also exposed along the mainland coast of the channel northwest of the Richardson Islands. There, the sill is characterized by coarse, poikilitic texture and smooth fluted outcrops with low relief. The chilled top of the sill is locally well exposed; beneath it, thin sulphide-bearing seams weather out to produce small gossans. At one point, halfway along the channel between the Richardson Islands and coastal cliffs to the north, the poikilitic sill is cut by a gabbro sheet striking 020-030° and dipping 30-40°SE (Rainbird et al., in press). The gabbro sheet cuts uphill to the north and may be a feeder to the overlying columnar-jointed sill (sill 6). Locally, a sedimentary section containing the conformable contact between Mikkelsen Islands Formation carbonate and Nelson Head Formation siltstone separates sill 5 from sill 6. The carbonate sequence is up to 15 m thick and is overlain by flaggy, rusty-weathering, carbonaceous siltstone and fine grey sandstone.

Sill 6 is a brown-weathering gabbro, up to 125 m thick, with well defined columnar jointing near its base. In many areas, the aphanitic base is well exposed in rubbly cliff sections, and grades up into fine grained olivine gabbro. In general, the sill is olivine-bearing near its base and coarsens upwards to a medium- to coarse-grained gabbro with 'pocked' ophitic texture. In detail, the basal 20-30 m of the sill consists of columnar jointed, horizontally sheeted gabbro with up to 10% olivine. Above 40 m, the gabbro is more altered and contains coarser grained patches. Above 55 m, patches of coarse amphibole-bearing granophyre occur within medium- to coarse-grained gabbro.

The high plateau north of the Richardson Islands and southeast of the Nakyoktok River contains extensive exposures of sill 6, eroded into a complex topography (Rainbird et al., in press). Aphanitic upper contact rocks of sill 6 are exposed locally throughout the highest parts of the plateau; some are in contact with a thin veneer of basal Nelson Head Formation rocks. Several intrusive sheets have been mapped in the plateau area indicating that sill 6 is composite, in part conformable with Shaler Supergroup strata, and in part cross-cutting. One large north-striking intrusion forms a thick sheet that dips at 45-70° to the east. To the west, it overlies Nelson Head Formation sandstone and, to the east, it truncates an

older isolated 'piggyback' unit consisting of a 35 m thick granophyre-rich sill and underlying argillite (Rainbird et al., in press). The chilled basal contact of the 35 m sill caps 8-10 m of rusty-weathering, siltstone and black argillite of the basal Nelson Head Formation. On the east side of the plateau, a columnar-jointed sheet, likely a feeder to sill 6, truncates the poikilitic sill along a shallow north-dipping, west-striking contact (Rainbird et al., in press). All the intrusions have well defined chilled margins, suggesting that magmas feeding the columnar sills in the plateau region were emplaced under variable stress regimes over a time interval sufficient to allow for cooling between magma pulses.

GABBRO SHEETS AND DYKES IN THE NELSON HEAD FORMATION

Irregular gabbro sheets intrude the Nelson Head Formation and are well exposed at several localities in the valley of the Nakyoktok River. Generally these intrusions are tabular or broad arcuate sheets but some have shallow dips and very irregular shapes, such as the distinctive zig-zag-shaped intrusion exposed west of the river (Fig. 2). Dips of the contacts vary from 25-70°, with thicknesses estimated to be between 30-60 m. Cores of the intrusions are coarse grained gabbro with pegmatitic patches. Fine grained gabbros occur near chilled contacts and sheeted cooling fractures have developed parallel to contacts with the host sandstones.

A well exposed, 60 m wide dyke striking 150°/75-80° cuts sandstones of the Nelson Head Formation northwest of the plateau. The topographic top of the dyke is approximately at the same level as the base of the columnar sill(s) to the southeast, suggesting it could be a feeder to the plateau sills. Although sill 6 appears continuous across the projected strike of the dyke, field relationships are obscured by a east-northeast-striking fault (Fig. 2).

NORTHEAST-STRIKING DYKES

Several, near vertical, northeast-striking diabase dykes cut gabbro sills on the Richardson Islands and in coastal regions south of the gabbro plateau (Rainbird et al., in press). On the southeast coast of one island, a thick sill is cut by a 20 m wide, northeast-striking dyke. It has an unusual, 1 m wide coarse grained to pegmatitic zone in the center and is cut by irregular felsic dykes up to 10 cm wide. On the southeast side of the plateau area, a 035-055°-striking, vertical diabase dyke cuts coarse grained poikilitic gabbro (sill 5). The 5 m wide dyke is exposed along the shore and continues northeast as a recessive unit in the overlying columnar sill. On the plateau, an offset segment of the same (?) 5 m wide dyke cuts sill 6 at 215°/80° and continues as a linear to the northeast.

RELATED NEOPROTEROZOIC INLIERS OF SOUTHERN VICTORIA ISLAND

Coastal sills west of Duke of York inlier

Coastal outcrops of medium grained gabbro occur west of Duke of York inlier, along strike with sills exposed in the Miles Islands (Fig. 1). The gabbros contain irregular 10-100 cm patches of very coarse grained to pegmatitic granophyre, and are cut by an irregular array of pyrite-quartz veins up to 10 cm wide. The coastal sill has smooth fluted outlines in contrast to a parallel, east-striking gabbro ridge to the north which has poorly developed columnar jointing. There are no intervening Proterozoic sedimentary rocks; the coastal gabbro ridges are covered to the north by sandy Paleozoic dolostone of the Cass Fiord Formation.

Gabbro sills northeast of the main inlier

Isolated hills of medium- to coarse-grained gabbro surrounded by Paleozoic carbonates or glacial cover occur 10-15 km northeast of the main outcrop area of Duke of York inlier (Fig. 1). The isolated gabbro ridges correlate with two or three sills in the inlier, in particular, the line of hills defining the southeast limit of outcrop is correlated with the distinctive poikilitic sill (sill 5), and contains similar, pyritic gossan zones. The overlying thick sill to the northwest has a well exposed, flat, upper chilled surface that dips west at 3-5°, similar to sills in Duke of York inlier. Between the two sills is a >10 m section of Mikkelsen Islands Formation carbonates.

Western Surrey Lake area

An approximately 12 km long north- to northeast-striking spine of subhorizontal (<5°NW dip) gabbro sills is exposed about 50 km northeast of Duke of York inlier, at the western end of Surrey Lake (Fig. 1 and 3). The northern sill has a maximum exposed thickness of 65 m. Contacts with enclosing sedimentary rocks are not exposed except along the base of one hill, where gabbro overlies up to 10 m of greenish grey, calc-silicate preserving fine, planar microbial lamination and intercalated, 1-2 m wide, low-relief domal stromatolites. Bedding, wave-ripple marks, stylolitic seams, and black chert nodules are present within the poorly exposed unit, which extends for about 1 km along the basal chilled margin of the sill. We correlate this carbonate with the uppermost Mikkelsen Islands Formation of the Shaler Supergroup.

The northernmost gabbro outcrops are characterized by well developed sheeting dipping northwest at <5°. The sheeting is accentuated by prominent subhorizontal ribbing, which imparts a well defined stepped appearance to the hillside. The basal chilled margin coarsens to a medium grained gabbro above the 8-10 m level; coarse grained pegmatitic patches

appear above the 50 m level. Mineralogically, the gabbros contain strongly zoned plagioclase laths enclosed by large clinopyroxene oikocrysts, partly rimmed by hornblende.

Brown-weathering gabbros exposed in linear ridges south of the northern sill (Fig. 3) generally are coarse grained and have a prominent spotted texture due to uniformly distributed 1-2 cm clinopyroxene oikocrysts. The top surface of one outcrop consists of deeply weathered, coarse grained, red-brown gabbro with large feathery clinopyroxene crystals. Near the base of the ridge, the gabbro contains aligned plagioclase laths and is very red. Small areas contain up to 5% pyrite and minor chalcopyrite, but the zone is not extensive and sulphide distribution is heterogeneous.

The outcrop pattern of gabbro sills is accurately reflected in high resolution aeromagnetic maps (Ascot Resources Ltd. unpub. data, 1993). The exposed gabbros occur within a 6 km wide fault-bounded horst. Boundary faults, striking at 015°-020°(eastern fault shown on Fig. 3), define an uplifted

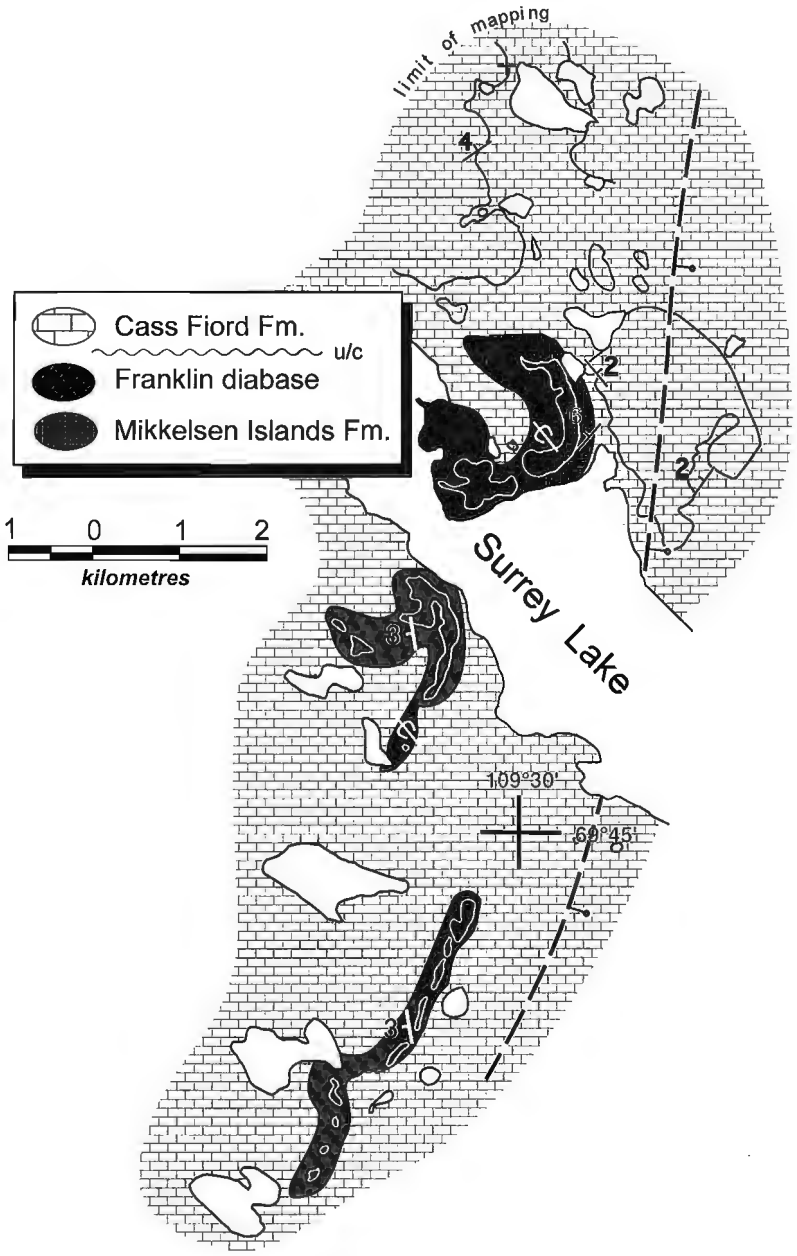

Figure 3. *Geological map of western Surrey Lake inlier. Solid lines define areas of outcrop. Dashed line is a fault inferred from geophysical data (see text); solid circle on down-dropped side*

central block responsible for the topographic high containing the exposed ridges of gabbro sills and inter-sill carbonates. The aeromagnetic maps indicate that the uplift narrows to the north-northeast and gently west-dipping gabbro sills within the horst are faulted out north of the exposed outcrops. The exposed sills and the underlying sill distribution interpreted from aeromagnetic maps closely mimic the shape and sequence of eroded sills exposed in coastal areas of Duke of York inlier.

STRUCTURE OF THE DUKE OF YORK INLIER

Neoproterozoic strata of Duke of York inlier, the Coronation Gulf and the Coppermine area define a broad east- to northeast arc, which parallels the inferred erosional edge of a huge intracratonic basin, formed on the northwestern margin of Laurentia during the Mesoproterozoic (Rainbird et al., 1996). The strata dip gently to the northwest (3-5°) as a result of folding, which is considered to have occurred at the same time as broad regional folding in strata of the Shaler Supergroup elsewhere in Amundsen Basin. The folding occurred during the approximately 200-250 million year interval between intrusion of the Franklin igneous suite and deposition of flat-lying Paleozoic sedimentary strata, which erosionally overlie the Proterozoic sequence (cf. Thorsteinsson and Tozer, 1962). In Duke of York inlier, the gently folded Proterozoic strata are cut by a prominent northeast-striking fault localized within the channel between Victoria Island and the Richardson Islands (Fig. 2). Strata on the southeast side of the fault are down-dropped at least 100 m; dip direction of the fault is unknown. A north- to northeast-striking set of faults, lineaments, and gabbro dykes also were mapped in this area (Rainbird et al., in press) and appear to have had some control on the location and style of gabbro intrusion. Some of the faults, therefore, are coeval with intrusion of the Franklin gabbros, similar to relationships observed in northern Minto inlier (Rainbird et al., 1994a). The temporal relationship between the two sets of faults is unresolved.

PALEOZOIC ROCKS

Published descriptions of the Paleozoic stratigraphic sequence of Victoria Island are limited to the work of Washburn (1947) and Thorsteinsson and Tozer (1962), who subdivided it into 3 units. The upper two units are confined to the extreme northwestern part of the island and only the lowermost unit (map unit 10 of Thorsteinsson and Tozer, 1962) is exposed over the rest of the island. Thorsteinsson and Tozer divided map unit 10 into a lower clastic member of possible Cambrian age and an upper carbonate member of possible Ordovician or Silurian age. Outcrops of the clastic member are restricted to the southern coastal region and a few isolated pockets around Minto inlier, whereas the upper unit has wide regional distribution. On the mainland and adjacent parts of Victoria Island, the clastic and carbonate units are mapped as an unnamed middle Cambrian sandstone member of the Saline River Formation and Cass Fiord Formation equivalent, respectively (Okulitch, 1992). We chose to adopt Cass Fiord for the widespread upper dolostone surrounding Duke of York inlier; however, we interpret the basal quartz arenite as Old Fort Island Formation because it better fits the definition of a basal Cambrian quartz arenite unit that infills topographic depressions (Okulitch, 1992). The age of the quartz arenite will be difficult to confirm owing to a lack of diagnostic body fossils. Descriptions below are from sections exposed along a prominent cliff-edge rim that defines the northwestern boundary of Duke of York inlier.

The Old Fort Island Formation is mainly composed of poorly indurated, white to buff, fine- to medium-grained quartz arenite. Thin- to moderate-scale tabular-planar crossbedding is the most recognizable sedimentary structure; trough crossbedding and planar-bedding are less common. Basal sections show consistent southeast paleocurrent transport but upper sections show polymodal distribution, indicating marine currents and decreasing influence from topographic channeling. The uppermost Old Fort Island is a sugary weathering, limonitic and calcareous quartz arenite interbedded with parallel to ripple crosslaminated sandy dolostone. Unidentified burrows of at least two different types occur commonly on bedding plane exposures. The thickness of the Old Fort Island Formation is extremely variable because it infills topography on the sub-Paleozoic unconformity. This also has been observed in Minto inlier, where paleo-relief of several hundred metres is preserved over karsted carbonates of the Wynniatt Formation. Paleorelief in Duke of York inlier generally is less pronounced, but may be up to 150 m as indicated by a small outlier on the western side of the map area, just west of the Nakyoktok River.

The Cass Fiord Formation gradationally overlies the Old Fort Island Formation. At its base, it is composed of thick laminated to thin wavy bedded sandy dolostone. Sandy interbeds give way to more massive and blocky weathering yellow dolostone, 5 m above the base. The blocky beds are separated by interbeds of strongly bioturbated dolosiltite (horizontal and vertical burrows). Above this, the Cass Fiord is characterized by thin, wavy bedded dolosiltite and dolarenite with minor interbeds of sandy dolarenite. Bedding in the Paleozoic rocks generally is horizontal; very open east-west folds were observed on the peninsula on the south side of Johansen Bay and a few kilometres northwest of the area outlined in Figure 2.

The basal Cass Fiord Formation surrounds the western Surrey Lake inlier (Fig. 3), where the basal pebbly quartzose dolostone exhibits normal grading, gutter casts, and small-scale, low-angle crossbedding, indicating high-energy shallow marine shelf deposition. As in Duke of York inlier and northern Wellington inlier, the sandy dolostone passes up into pure massive to wavy bedded dolostone.

ECONOMIC GEOLOGY

Jefferson et al. (1994) suggest that the Noril'sk model for Ni-Cu-PGE deposits is applicable to parts of Amundsen Basin and they assign a moderate to high mineral resource potential to Duke of York inlier, emphasizing the unusual thickness and

abundance of Franklin gabbro sills and their favourable chemistry. However, they caution that the mineral potential is somewhat reduced because only lower S-poor units of the Shaler Supergroup (Rae Group only) are preserved in Duke of York inlier and there are no known major faults. Field work in 1995 did not result in discovery of economic concentrations of Ni-Cu-PGE sulphides. However, a significant northeast-striking fault zone was recognized in the channel between Victoria Island and the Richardson Islands and sulphate evaporites were discovered along the southern shore of Edinburgh Island (Fig. 2). Discontinuous pyritic gossan zones characterize the upper part of the thick poikilitic sill (sill 5).

The Nelson Head Formation offers potential for sediment-hosted stratiform copper deposits (Rainbird et al., 1992). It has been explored extensively in northern Minto inlier and the Coppermine area, but not in Duke of York inlier. Preliminary reconnaissance during the present study did not locate any mineralization of this type.

CONCLUSIONS

Strata of the Rae Group, exposed in Duke of York inlier, are an along-strike extension of identical strata exposed in the Coppermine area. The Mikkelsen Islands Formation was deposited under quiet, moderate-depth marine conditions just prior to a regression that was accompanied by a voluminous clastic influx represented by sandstones of the Nelson Head Formation. Paleocurrents from crossbedding in the Nelson Head support the interpretation that this unit represents a huge braided fluvial system that transported craton-derived detritus northwesterly into Amundsen Basin (Rainbird et al., 1994c). Stromatolites of the regionally distinctive Aok Formation reflect a brief return to quieter marine depositional conditions. Rae Group strata in Duke of York inlier, Coppermine area, Duke of York Archipelago, and in several small inliers to the north, define a broad arc that is concave to the northwest. The arc parallels the nearby post-depositional edge of Amundsen Basin, which controlled sedimentary deposition on the northwest Laurentia margin for most of Mesoproterozoic-Neoproterozoic time.

Faulting as well as sedimentary and intrusive contact relationships suggest that uplift and deformation of Duke of York inlier likely occurred close to the time of intrusion of the Franklin igneous suite. These relationships have been documented in other Neoproterozoic inliers of the Amundsen Gulf and are consistent with the model that Franklin igneous events were caused by a mantle plume centred north (present co-ordinates) of Victoria Island (Heaman et al., 1992; Rainbird, 1993). The anomalous thickness, large volume, discordant relationships, and irregular morphology of the gabbro intrusions of Duke of York inlier suggest proximity to an intrusive center.

Erosional incision of the Proterozoic strata of the inlier is indicated by pronounced thickness variations in unconformably overlying Paleozoic quartz arenite of the Old Fort Island Formation. Widespread marine transgression followed by deposition of shallow water carbonates over most of Victoria Island and the adjacent islands and mainland. Duke of York inlier owes its present level of exposure to Pleistocene (Wisconsinan) glaciation that removed the Paleozoic cover to reveal a window of Neoproterozoic strata beneath.

ACKNOWLEDGMENTS

Fieldwork in the Surrey Lake area was carried out with logistical support from Ascot Resources Ltd. We thank Charlie Bolt of Coppermine for the use of his cabin on the Nakyoktok River and Danny Knopf of Great Slave Helicopter for excellent piloting. Dave Sharpe and Doug Hodgson kindly lent us air photos for some of the fieldwork. The manuscript was reviewed by Charlie Jefferson and Steve Lucas and we thank Tim de Freitas for helpful advice on lower Paleozoic stratigraphy and nomenclature.

REFERENCES

Baragar, W.R.A. and Donaldson, J.A.
1973: Coppermine and Dismal Lakes map areas; Geological Survey of Canada, Paper 71-39, 20 p.

Campbell, F.H.A.
1983: Stratigraphy of the Rae Group, Coronation Gulf area, District of Mackenzie; in Current Research, Part A; Geological Survey of Canada, Paper 83-1A, p. 43-52.
1985: Stratigraphy of the upper part of the Rae Group, Johansen Bay area, northern Coronation Gulf, District of Franklin; in Current Research, Part A; Geological Survey of Canada, Paper 85-1A, p. 693-696.

Christie, R.L.
1964: Diabase-gabbro sills and related rocks of Banks and Victoria Islands, Arctic Archipelago; Geological Survey of Canada, Bulletin 105, 13 p.

Christie, R.L., Cook, D.G., Nassichuk, W.W., Trettin, H.P., and Yorath, C.J.
1972: The Canadian Arctic Islands and Mackenzie region; 24th International Geological Congress, Montreal, Guide to Excursion A66, p. 146.

Conly, A.G.
1993: Sedimentology and stratigraphy of the upper clastic member, Glenelg Formation: Victoria Island, N.W.T.; B.Sc. thesis, Carleton University, Ottawa, Ontario, 59 p.

Dixon, J.
1979: Comments on the Proterozoic stratigraphy of Victoria Island and the Coppermine area, Northwest Territories; in Current Research, Part B; Geological Survey of Canada, Paper 79-1B, p. 263-267.

Heaman, L.M., LeCheminant, A.N., and Rainbird, R.H.
1992: Nature and timing of Franklin igneous events, Canada: implications for a late Proterozoic mantle plume and the break-up of Laurentia; Earth and Planetary Science Letters, v. 109, p. 117-131.

Jefferson, C. W. and Young, G. M.
1989: Late Proterozoic orange-weathering stromatolite biostrome, Mackenzie Mountains and western Arctic Canada; in Reefs, Canada and adjacent areas, (ed.) H.H.J. Geldsetzer, N.P. James, and G.E. Tebbutt; Canadian Society of Petroleum Geologists, Memoir 13, p. 72-80.

Jefferson, C.W., Hulbert, L.J., Rainbird, R.H., Hall, G.E.M., Grégoire, D.C., and Grinenko, L.
1994: Mineral Resource Assessment of the 723 Ma Franklin Igneous Events of Arctic Canada: Comparison with the Permo-Triassic Noril'sk-Talnakh Ni-Cu-PGE deposits of Russia, Geological Survey of Canada, Open File 2789, 48 p.

LeCheminant, A.N., Rainbird, R.H., and Villeneuve, M.E.
1996: Precambrian geology of northern Wellington inlier, Victoria Island, Northwest Territories, in Current Research 1996-C; Geological Survey of Canada, p. 1-10.

Okulitch, A.V.
1992: Geological Atlas, Horton River, Franklin-Mackenzie; Geological Survey of Canada, Map NR-9/10/11/12-G, scale 1:1 000 000.

Rainbird, R.H.
1993: The sedimentary record of mantle plume uplift preceding eruption of the Neoproterozoic Natkusiak flood basalt; Journal of Geology, v. 101, p. 305-318.

Rainbird, R.H., Darch, W., Jefferson, C.W., Lustwerk, R., Rees, M., Telmer, K., and Jones, T.
1992: Preliminary stratigraphy and sedimentology of the Glenelg Formation, lower Shaler Group and correlatives in the Amundsen Basin, Northwest Territories: relevance to sediment-hosted copper; in Current Research, Part C; Geological Survey of Canada, Paper 92-1C, p. 111-119.

Rainbird, R.H., Hodgson, D.A., and Jefferson, C.W.
1994a: Bedrock and surficial geology, Glenelg Bay, District of Franklin, Northwest Territories, NTS 78B/6, Geological Survey of Canada, Open File 2921, scale 1:50 000.

Rainbird, R.H., Jefferson, C.W., Hildebrand, R.S., and Worth, J.K.
1994b: The Shaler Supergroup and revision of Neoproterozoic stratigraphy in the Amundsen Basin, Northwest Territories; in Current Research 1994-C; Geological Survey of Canada, p. 61-70.

Rainbird, R.H., Jefferson, C.W., and Young, G.M.
1996: The early Neoproterozoic Succession B of northwest Laurentia: correlations and paleogeographic significance; Geological Society of America Bulletin, v. 108, p. 454-470.

Rainbird, R.H., LeCheminant, A.N., and Lawyer, J.I.
in press: Bedrock Geology of the Duke of York inlier, southern Victoria Island, District of Franklin, Geological Survey of Canada, Open File 3304, scale 1:50,000.

Rainbird, R.H., McNicoll, V.J., and Heaman, L.M.
1994c: Detrital zircon studies of Neoproterozoic quartz arenites from northwestern Canada: additional support for an extensive river system originating from Grenville orogen; in United States Geological Survey Circular No. 1107, Program with Abstracts, Eighth International Conference on Geochronology, Cosmochronology and Isotope Geology, p. 258.

Robertson, W.A. and Baragar, W.R.A.
1972: The petrology and paleomagnetism of the Coronation sills; Canadian Journal of Earth Sciences, v. 9, p. 123-140.

Thorsteinsson, R. and Tozer, E.T.
1962: Banks, Victoria and Stefansson Islands, Arctic Archipelago; Geological Survey of Canada, Memoir 330, 85 p.

Washburn, A.L.
1947: Reconnaissance geology of portions of Victoria Island and adjacent regions, Arctic Canada; Geological Society of America, Memoir 22, 142 p.

Young, G.M.
1981: The Amundsen Embayment, Northwest Territories; relevance to the upper Proterozoic evolution of North America; in Proterozoic Basins of Canada, (ed.) F.H.A. Campbell; Geological Survey of Canada, Paper 81-10, p. 203-211.

Young, G.M. and Jefferson, C.W.
1975: Late Precambrian shallow water deposits, Banks and Victoria Islands, Arctic Archipelago; Canadian Journal of Earth Sciences, v. 12, p. 1734-1748.

Young, G.M. and Long, D.G.F.
1977: A tide-influenced delta complex in the upper Proterozoic Shaler Group, Victoria Island, Canada; Canadian Journal of Earth Sciences, v. 14, p. 2246-2261.

Geological Survey of Canada Project 890011

Thermal regimes and diamond stability in the Archean Slave Province, northwestern Canadian Shield, District of Mackenzie, Northwest Territories

P.H. Thompson, A.S Judge[1], B.W. Charbonneau[2], J.M. Carson[2], and M.D. Thomas

Continental Geoscience Division, Ottawa

Thompson, P.H., Judge, A.S., Charbonneau, B.W., Carson, J.M., and Thomas, M.D., Thermal regimes and diamond stability in the Archean Slave Province, northwestern Canadian Shield, District of Mackenzie, Northwest Territories; in Current Research 1996-E; Geological Survey of Canada, p. 135-146.

Abstract: The combination of apparent heat production values derived from airborne radiometric surveys with outcrop and laboratory measurements, for the area bounded by 62°-66°N and 110°-116°W, indicates an arcuate zone (>30 000 km^2) with average heat production in excess of 2.5 μW/m^3 and anomalies tens of kilometres across that exceed 5.0 μW/m^3.

One-dimensional numerical models indicate that a lateral increase in average heat production in the upper crust from 1.7 μW/m^3 (surface heat flow = 40 mW/m^2) to 3.0 μW/m^3 (surface heat flow = 50 mW/m^2) corresponds to a reduction in lithospheric thickness from 215 to 180 km and in the thickness of the potentially diamondiferous zone in the lowermost lithosphere from 85 to 30 km.

According to a limited data set, kimberlite pipes close to or within heat production anomalies (Cross Lake, Yamba Lake) are significantly less diamondiferous than those near Lac de Gras. While many other factors may be involved, the significance of crustal heat production with respect to diamond potential merits careful consideration.

Résumé : Dans la région située entre, d'une part, 62° et 66° de latitude nord et, d'autre part, 110° et 116° de longitude ouest, les valeurs de la production de chaleur apparente obtenues par levé radiométrique aéroporté ont été combinées aux mesures faites sur des affleurements et en laboratoire; ce travail a permis de délimiter une zone arquée (> 30 000 km^2) où la production de chaleur moyenne dépasse 2,5 μW/m^3 et d'identifier des anomalies de plus de 5,0 μW/m^3 couvrant des dizaines de kilomètres.

Les modèles numériques unidimensionnels indiquent une augmentation latérale de la production de chaleur moyenne dans la croûte supérieure variant entre 1,7 μW/m^3 (flux thermique superficiel = 40 mW/m^2) et 3,0 μW/m^3 (flux thermique superficiel = 50 mW/m^2); cela correspond à une réduction de l'épaisseur de la lithosphère de 215 à 180 kilomètres et de la zone potentiellement diamantifère dans la lithosphère basale de 85 à 30 kilomètres.

Selon un ensemble de données limité, les cheminées kimberlitiques à proximité ou à l'intérieur des anomalies de production de chaleur (lac Cross, lac Yamba) sont significativement moins diamantifères que celles situées près du lac de Gras. Même s'il faudrait peut-être tenir compte d'autres facteurs, la signification de la production de chaleur dans la croûte par rapport au potentiel diamantifère mérite attention.

[1] Terrain Sciences Division, Ottawa
[2] Mineral Resources Division, Ottawa

INTRODUCTION

The concentration of diamondiferous kimberlites in Archean cratons is attributed to the presence of relatively thick, cool lithospheric mantle at the time of kimberlite emplacement. Where temperatures are low enough and mantle composition is appropriate, diamond is stable in the deeper portions of such a lithosphere (Gurney, 1989). Crustal radiogenic heat production and thermal conductivity can have a significant effect on geothermal gradients in the lower crust and lithospheric mantle (Pollack and Chapman, 1977). Using simple one-dimensional thermal models, measurements of present crustal radiogenic heat production and the radioactive decay rates for U, Th, and K, Thompson et al. (1995) calculated that lithosphere beneath much of the Slave Province, 2500 Ma ago, may have been too thin to contain diamonds. They speculated further that, wherever highly radioactive rock units are present in sufficient volume today, the lithosphere may be thinner than is typical of the Slave Province. In this paper, we use airborne and ground gamma-ray spectrometric data and gravity models to explore the possibility that lithospheric thickness, temperature and the potential for diamondiferous kimberlite across the province may be related, in part, to regional variations in crustal heat production.

A combination of surface geology and gravity data provides constraints for downward extrapolation of the geology and hence the distribution of heat sources in the crust. Two profiles were examined (Fig. 1): (1) a 350 km profile extending from Yellowknife to Lac de Gras; and (2) a less well-constrained profile farther to the northwest. Lithospheric thermal profiles are calculated using the model heat source distributions.

GEOLOGICAL SETTING

The Slave Province is distinguished from classic Archean granite-greenstone terranes of the Superior Province and Kaapvaal craton of southern Africa by the high proportion of metasedimentary rocks in the supracrustal sequence and the abundance of highly evolved granites. In the south-central part of the Slave Province (Fig. 1), thin belts of metavolcanic rocks separate extensive metasedimentary domains from angular granitoid complexes that comprise metagranitoid, quartzofeldspathic gneiss, and migmatite. The complexes are, at least in part, older than the predominant supracrustal sequence (ca 2.7 Ga). Massive, homogeneous plutons intrude both granitoid complexes and supracrustal domains. The younger granitoids (ca 2.6 Ga) are associated with Neoarchean orogenesis involving horizontal shortening and moderate overthickening of the crust and low pressure regional metamorphism. Relatively stable for the last 2500 Ma, the south-central Slave Province was intruded by two alkalic igneous complexes (Blatchford Lake, Big Spruce) and several swarms of diabase dykes in the interval 2100 to 1200 Ma. A thin sedimentary cover sequence was present in Cretaceous and early Tertiary time when kimberlites were intruded (Nassichuk and McIntyre, 1995).

CRUSTAL RADIOGENIC HEAT PRODUCTION

Knowledge of the distribution and magnitude of radiogenic heat sources within the crust remains limited. Values of radiogenic heat production measured on outcrop and on representative rocks in the laboratory and calculated from airborne gamma-ray spectrometric data map regional variations on the present surface.

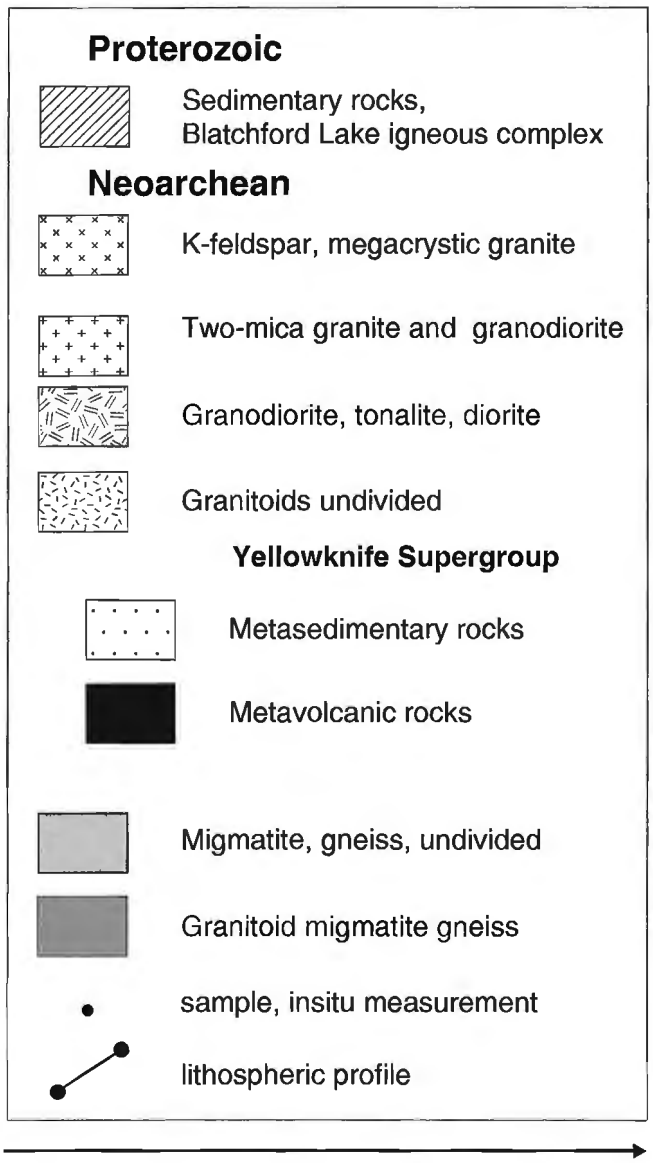

Figure 1. *Schematic geological map of the south-central Slave Province, Canadian Shield (modified after Hoffman and Hall, 1993; Thompson and Kerswill, 1994; Stubley, pers. comm., 1996) with location of Yellowknife-Lac de Gras and northwestern profiles. Straight line boundaries indicate change in scale of mapping. Outcrop measurement sites (data) are simplified where site density is high.*

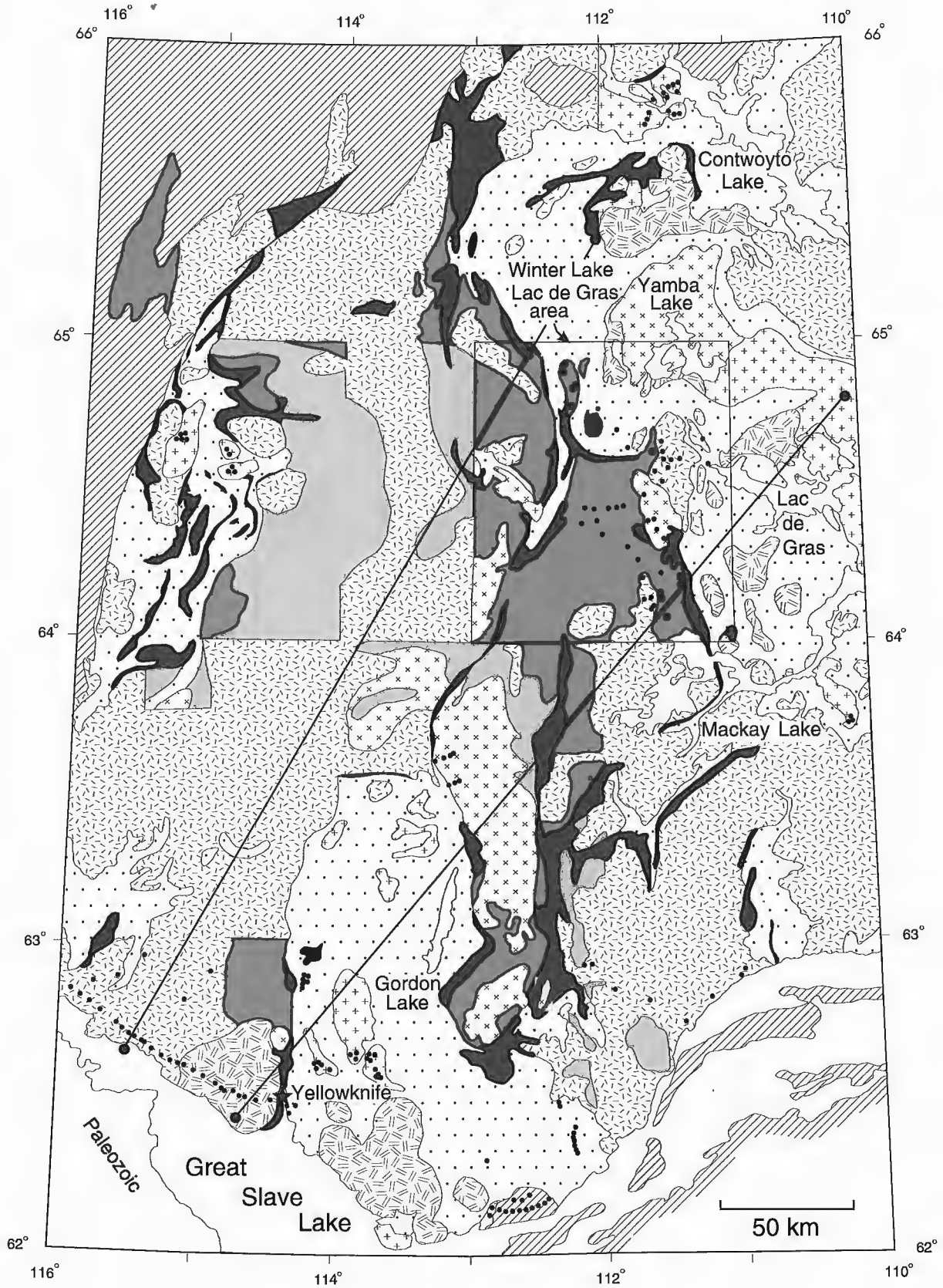
116°
114°
112°
110°
66°
65°
64°
63°
62°
Contwoyto Lake
Winter Lake
Lac de Gras area
Yamba Lake
Lac de Gras
Mackay Lake
Gordon Lake
Yellowknife
Paleozoic
Great Slave Lake
50 km

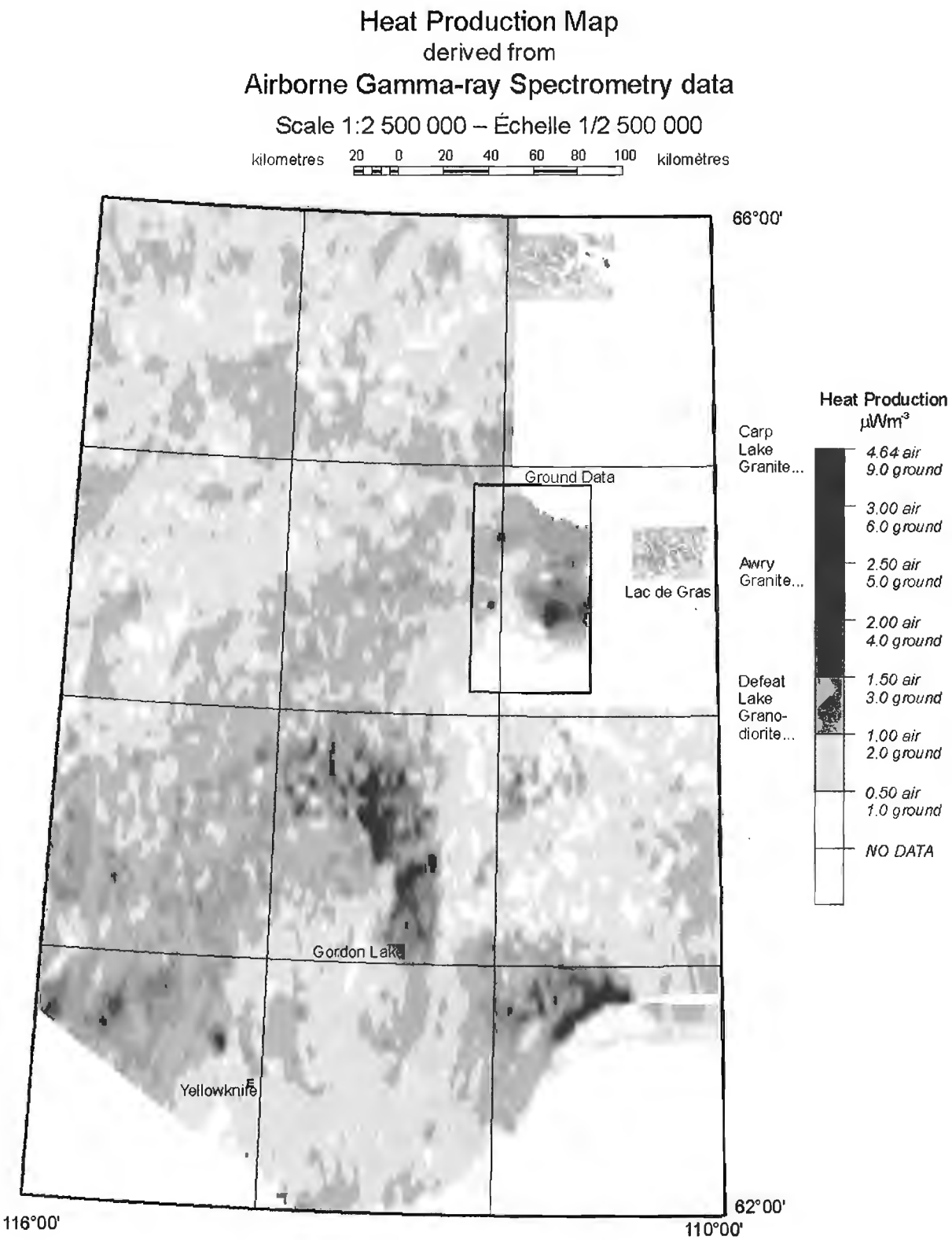

Figure 2. *Airborne gamma ray spectrometry coverage for the south-central Slave Province (Darnley et al., 1986). Heat production patterns within the "GROUND DATA" area were computed from laboratory analyses of bedrock samples. Note on the legend that ground (bedrock) heat production values are approximately twice the corresponding airborne value.*

Heat production – airborne data

Airborne gamma-ray spectrometric results (Fig. 2) for the south-central Slave Province (Darnley et al., 1986) are compiled from surveys with flight line spacings of 1.5-2.5 km south of 63°N and 5 km over the rest of the map area. Two small detailed surveys (spacing <1 km) are inset in Figure 2 north of Lac de Gras and west of Contwoyto Lake (Legault and Charbonneau, 1993). Conversion of total counts for U, Th, and K, as measured in airborne surveys, to "apparent" heat production values follows the method developed by Richardson and Killeen (1980).

Heat production values in Figure 2 range from <0.5 to >4.0 $\mu W/m^3$. These airborne values are less than the actual bedrock values, being reduced by the effects of glacial overburden, surface wetness, lakes, and vegetation cover; the airborne values are commonly one half of corresponding values measured on the ground on surface outcrops (Charbonneau et al., 1976; Richardson and Killeen, 1980), although considerable uncertainty is introduced by variable surface cover conditions. Laboratory and in situ outcrop measurements are available for most geological units (Fig. 1). These are in good agreement with, and thus serve to calibrate, regional variations of "apparent" heat production derived from airborne data (Fig. 2). The overall pattern of heat production shows that values are higher in the southern part of the study area (south of 64°N) than the north. The metasedimentary domain east of Yellowknife exhibits relatively low values. North of 64°N, areas with high heat production values are small.

Heat production – rock units

Heat production related to radioactive decay has been averaged for a variety of rock units in the south-central Slave Province (Fig. 1, Table 1) using nearly 900 determinations of K, U, and Th from a combination of outcrop and laboratory gamma-ray spectrometry. Outcrop measurements were made during follow-up of airborne surveys (Richardson and Charbonneau, 1973; Darnley et al., 1977; Ford, pers. comm., 1989; Legault and Charbonneau, 1993; Charbonneau and Legault, 1994). Laboratory gamma-ray measurements have been made on rock units near Yellowknife (Moore, 1972; Lewis and Wang, 1992; Thompson et al.,1995) and in the Winter Lake-Lac de Gras area (Thompson et al., 1995). The latter study estimated an average heat production of 1.7 $\mu W/m^3$ for the upper crust in the Winter Lake-Lac de Gras map area (11 000 km^2), substantially higher than the range of 0.8 to 1.0 $\mu W/m^3$ cited by Drury (1989) for the Superior Province.

Table 1. Radiogenic heat production

Rock Type	K %	U ppm	Th ppm	Average Heat Production ($\mu W/m^3$)	
				outcrop (sites)	laboratory (samples)
Blatchford Lake complex (SE of YK)	3.9	3.3	19.5	2.6 (132)	
K-feldspar megacrystic granite:					
Carp Lake granite	4.6	21.4	45.2	9.1 (75)	
Pink granite (West of Lac de Gras)	5.2	22.0	41.0		9.1 (5)
2-mica granite/granodiorite (6 plutons)	3.6	10.5	9.1	3.7 (466)	
Granodiorite/tonalite/diorite					
Defeat plutonic suite (YK)	2.5	1.7	14.0	1.7 (11)	
Granodiorite (Yamba Lake)	1.2	2.6	1.2		0.5 (1)
Granitoid undivided:					
White Granite (W, L. de Gras)	4.6	10.3	47.4		6.4 (8)
Quartz glob "granite" (SW of L. de Gras)	2.0	0.8	4.7		0.7 (6)
Awry plutonic suite (W of YK), East Arm	4.8	9.2	31.7	5.0 (26)	
Metasedimentary rocks - (PGC Lab)	2.6	2.8	8.6		1.4 (29)
- (MRD Lab)	1.8	1.8	8.9		1.3 (13)
Metavolcanic rocks - (PGC Lab)	0.7	0.9	2.0		0.5 (3)
- (MRD Lab)	2.2	1.6	6.9		1.1 (2)
Metagranitoid-migmatite-gneiss					
Hornblende metagranite	3.6	2.7	2.3		2.3 (6)
Metagranitoid	1.9	1.8	10.6		1.4 (15)
Granitoid migmatite					
paleosome	1.0	0.5	2.5		0.4 (3)
leucosome/dyke	4.4	17.9	59.3		9.2 (3)
Quartzofeldspathic gneiss	2.0	1.9	19.2		2.0 (6)
Weighted average					1.5 (33)

In general, as shown in Table 1, low regional heat production (<1-2 $\mu W/m^3$) is associated with extensive domains of metasedimentary rocks, mafic volcanic rocks, and metaplutonic complexes dominated by tonalite, migmatite, and gneiss. In several cases, however, small granitic dykes cutting the metaplutonic rocks and leucosomes in granitoid and metasedimentary migmatite yield moderate to high heat production. The suite of granodiorite-tonalite-diorite plutons (2.62-2.61 Ga: Henderson et al., 1987; van Breemen et al., 1992) is the least radioactive of the younger intrusive granitoids. Two-mica granites (2.59-2.58 Ga, van Breemen et al., 1992) yielded heat production values of 3.7 $\mu W/m^3$, in the middle of the measured range. The unit designated "Granitoids undivided" adjacent to the East Arm of Great Slave Lake and west of Yellowknife (Awry suite, 2.63-2.55 Ga; Stagg Lake suite, 2.58 Ga; Henderson et al., 1987) has relatively high average heat production values (5.0 $\mu W/m^3$), similar to those for the pluton located west of Lac de Gras (White Granite in Table 1).

The most prominent airborne radiometric anomaly occurs over pink, megacrystic K-feldspar granite (2630 km^2, Carp Lake area) north of Gordon Lake (Fig. 1, 2). Outcrop values of uranium exceed 25 ppm across tens of kilometres (Darnley et al., 1977), resulting in heat production averaging 9.1 $\mu W/m^3$. Comparable heat production is generated by a similar though smaller pluton (280 km^2) of pink granite in the Winter Lake-Lac de Gras area (Fig. 1, inset to Fig. 2, Table 1).

CRUSTAL HEAT SOURCE DISTRIBUTION

Although it is widely accepted that radiogenic heat production decreases with depth in the crust, the actual distribution of heat sources is not well known. Gravity and rock density data can provide a perspective on crustal compositional variation with depth. For example, thicknesses of 2 to 7 km have been estimated for metavolcanic and metasedimentary rocks near Yellowknife (Gibb and Thomas, 1980; McGrath et al., 1983). Farther east, Bleeker and Beaumont-Smith (1995) extend sedimentary rocks to depths greater than 8 km using structural projections. In this paper, gravity modelling is applied to the profile with better geological control (Yellowknife to Lac de Gras, Fig. 1).

We present two crustal models. One, based on the approach of Thompson et al. (1995), assumes that surface rock units other than the younger granitoids extend to depths of 10 km, that the bases of the plutons occur at a depth of 5 km, and that the units are block-shaped. The resulting high proportion of heat production in the upper 10 km of the crust is consistent with the heat flow province concept (Jessop, 1990). In a second crustal model, the geometry of upper crustal units in the uppermost 10 km is modelled from gravity anomalies by assigning densities to rock units. In both cases, middle crust (10 km thick) and lower crust (15 km thick) are taken to be compositionally homogeneous. The total crustal thickness of 35 km is in line with available seismic data (e.g. Barr, 1971).

GRAVITY INTERPRETATION

Gravity anomalies

The Bouguer gravity field illustrated in Figure 3 is defined by gravity stations spaced generally about 10 km apart. North-south trends dominate but northeasterly trends are significant, particularly in the southeast quadrant. The 10 km station spacing outlines anomalies associated with geological units of roughly equivalent or greater width. Nevertheless, there is a high degree of concordance between linear aspects of the gravity pattern, manifested as gravity highs, and the narrow northerly or northeasterly trending volcanic belts. Relatively low density granites, as expected, are usually associated with areas characterized by low to moderate Bouguer gravity anomalies. No correlation was observed between areas of Granitoids undivided or metasedimentary rocks and Bouguer gravity anomalies.

Rock densities

Mean densities of rock units are based on measurements made on hand or core samples obtained mainly in the Yellowknife (Gibb and Thomas, 1980; Kretz et al., 1982) and Lac de Gras (this study) areas. Gibb and Thomas (1980) calculated a mean density of 2.90 g/cm^3 for mafic volcanic rocks of the Yellowknife greenstone belt, using proportions of basaltic, andesitic, dacitic and sheared rocks as determined by Baragar (1966), and estimated that a likely upper limit was 2.96 g/cm^3. Mean densities of 2.64 g/cm^3 and 2.67 g/cm^3 were determined for large flanking bodies of granodiorite to the west and southeast of the Yellowknife belt (Fig. 1), respectively, and a mean density of 2.74 g/cm^3 was determined for metasedimentary rocks. Kretz et al. (1982) also obtained a mean density of 2.74 g/cm^3 for metasedimentary rocks in the same general area, and a mean density of 2.64 g/cm^3 for the Prestige pluton, one of 14 small muscovite-biotite granites mapped locally in the belt. Near Lac de Gras, metasedimentary and volcanic units were determined to have mean densities of 2.74 g/cm^3 and 2.96 g/cm^3, respectively, similar to values for the Yellowknife greenstone belt. A mean density of 2.69 g/cm^3 was calculated for undivided areas of migmatite and gneiss.

Gravity modelling

Quantitative modelling of gravity anomalies using a 2.5D program (Broome, 1989) has been carried out along the Yellowknife-Lac de Gras profile (Fig. 1, 3). Geological bodies are approximated by prisms having polygonal cross-sections and a strike length determined from the observed length of the body at surface coupled with the length of an assumed associated gravity anomaly. Optimum results are obtained when the profile is oriented at right angles to the geological strike and trend of gravity contours. Uncertainty ascribed to the model section is highest between the points 135 and 190 km from the southwest end, where the profile is essentially parallel to the gravity contours (e.g. shoe-shaped volcanic belt).

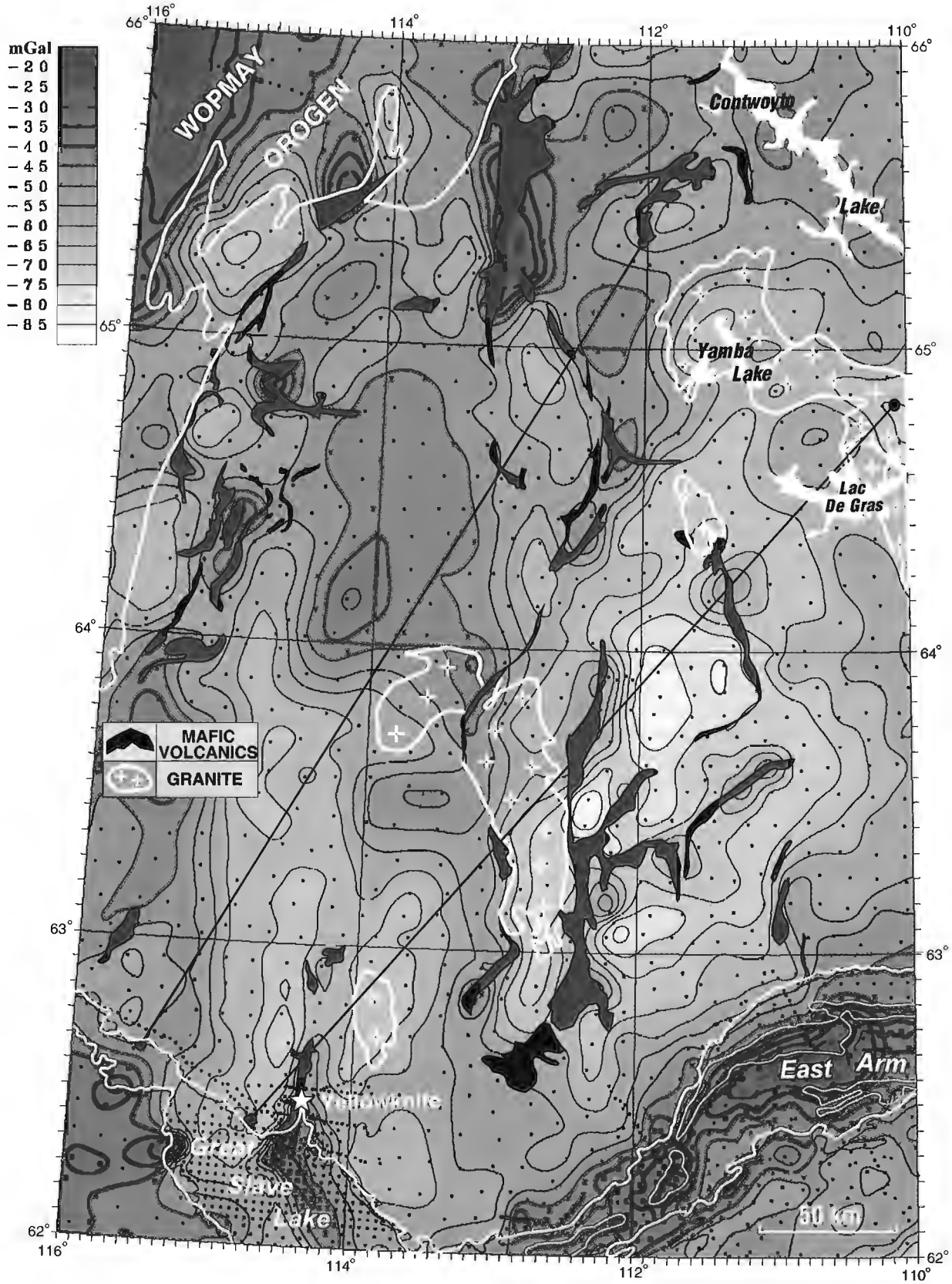

Figure 3. *Gravity map derived from Geological Survey of Canada gravity data base with 10 km station spacing. Geology from Figure 1.*

Modelling of gravity anomalies is more straightforward where the gravity field is relatively uniform over a reasonably large area, thereby providing a reference level for comparison with "anomalies". Such areas are usually underlain by a geological unit having fairly uniform density characteristics, which in turn provides an associated reference or standard density. In the study area, identification of a background field and associated density is equivocal, because of the generally rapidly fluctuating nature of the gravity field. A region of granitoid-migmatite-gneiss immediately north of the southwest end of the profile, estimated to have a mean density of 2.69 g/cm^3 and associated with a relatively extensive north-trending gravity low, was chosen as standard crust. The corresponding background gravity level is estimated to be -65 mGal. There is some support for this choice in that the calculated mean value of Bouguer gravity anomaly along the profile is -64 mGal.

The model gravity profile is linked to the observed profile at the southwest end of the profile (Fig. 4). Here the observed profile has a value of -68 mGal rather than the estimated -65 mGal background value, but is compatible with the assumed background if the granodiorite body overlying the granitoid-migmatite-gneiss unit is 1.25 km thick (density = 2.64 g/cm^3). A reasonable match of observed and model profiles is achieved for a model in which most surface geological units are considerably thinner (1-5 km) than the assumed thicknesses used in the Thompson et al. (1995) thermal models. Furthermore, their shapes differ significantly from those of the vertically bounded blocks assumed for the thermal models. Although the gravity model is constrained by some density data and surface geological contacts, gravity modelling is inherently ambiguous and the uncertainty in identifying a background field and related density contributes to the ambiguity. Nevertheless, with respect to depth extent of rock units, the model presents a plausible crustal section.

In view of the results of gravity model 1, the validity of the geometry of the upper crust assumed in the thermal model is examined by varying densities in the vertical blocks to obtain a best fit with respect to the observed anomaly profile (model 2, Fig. 5). Although an overall match between observed and calculated gravity is evident, there are several discrepancies relating to anomaly shape, amplitude, and gradient. The most noticeable is over the eastern part of the southwestern metasedimentary unit. In addition, some calculated densities become unreasonable. The calculated densities are indicated to fall within or outside the range of measured densities defined by the mean density plus or minus one standard deviation. One of the obvious results is the unreasonably low densities (2.72-2.75 g/cm^3) obtained for the volcanic units, which are generally considered to be dominated by mafic volcanic rocks, and should yield significantly higher densities. On the other hand, the proportion of felsic rocks in the less well-mapped belts may be higher than is presently assumed. In view of these differences, this model appears to maximize the thicknesses of surface geological units.

With respect to average upper crustal heat production, the variations in upper crustal heterogeneity represented by the two gravity models (Fig. 4, 5) are similar. The lower volume (compared to model 2) of supracrustal and plutonic rocks in model 1 is accompanied by a higher volume of granitoid migmatite gneiss. Therefore, the average crustal heat production for model 1 is only 10 per cent less than that for model 2.

LITHOSPHERIC THERMAL PROFILES

The thermal models illustrated here were developed using the method and assumptions of Thompson et al. (1995). It is assumed that at 1300°C peridotite is close enough to its solidus that it flows on a scale that is characteristic of the

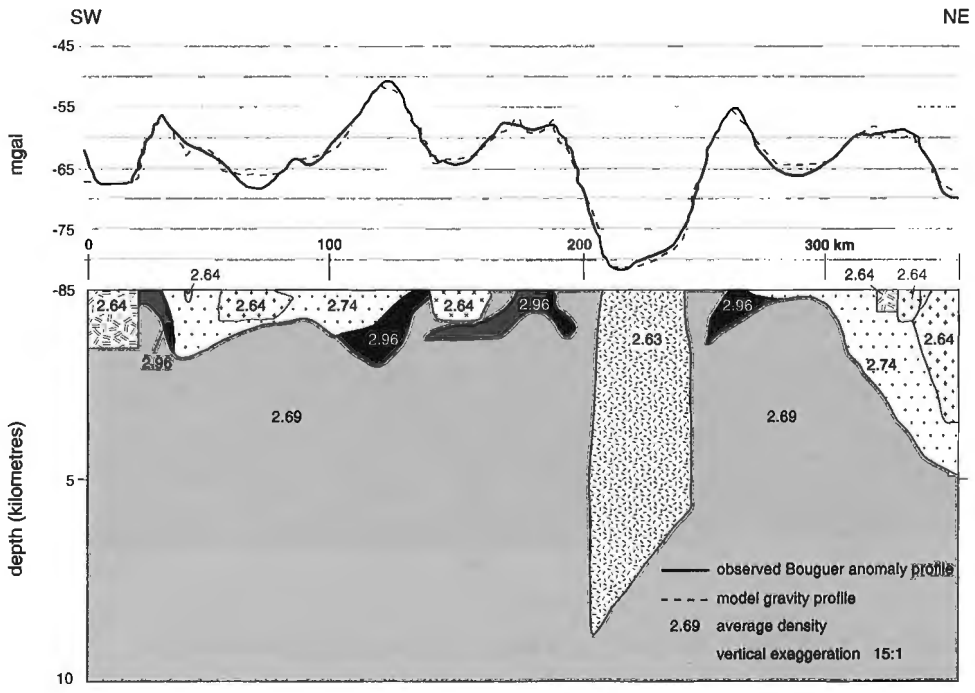

Figure 4.

Gravity model 1, Yellowknife-Lac de Gras profile. Density in g/cm^3.

asthenosphere, which thereby implies that this isotherm defines the base of the model lithosphere. The limitations on this assumption are recognized and discussed in Thompson et al. (1995, in press). Modelling was completed for two separate profiles, one crossing the relatively well-mapped geology between Yellowknife and Lac de Gras and a second, subparallel one located 50-80 km to the northwest that intersects the broad zone of relatively high heat production shown in Figure 2. In both cases, middle crust (10 km thick) and lower crust (15 km thick) are taken to be homogeneous with respect to heat production. The profiles demonstrate how variations in crustal heat production could affect lithospheric thickness and hence the potential for diamond stability beneath the Slave Province.

The method of calculation differs slightly from that used in Thompson et al. (1995) to take advantage of the increased information on the spatial variability of heat production along the profiles. Each determination of lithospheric thickness (i.e. depth to 1300°C isotherm) is made from the centre point of a 100 km wide section of the profile over which the heat production is averaged horizontally within each crustal layer. Adjacent determinations are made by stepping at 10 km intervals along the entire profile and repeating the procedure.

Yellowknife-Lac de Gras profile

Lithospheric thicknesses at the ends of the profile (Fig. 6) were taken from Thompson et al. (1995). For upper crust at Yellowknife, these authors used the heat production (2.3 $\mu W/m^3$) measured at the site of the single published heat flow measurement for upper crust in the Slave Province, even though the value is high for the surrounding region (Fig. 2). The weighted average heat production for the model upper crust along the 350 km profile (Fig. 1, 6) is calculated from laboratory and in situ measurements. The value of 2.0 $\mu W/m^3$ is somewhat higher than that for upper crust in the Winter Lake-Lac de Gras area (1.7 $\mu W/m^3$, Thompson et al., 1995), because of the presence of a larger pluton of very radioactive megacrystic pink granite, together with more two-mica granite/granodiorite and "Granitoids undivided" along the profile. Use of an upper crustal heat production of 2.0 $\mu W/m^3$ results in a model lithosphere that is approximately 180-200 km thick, with the lowermost 30 to 80 km lying within the stability field of diamond as determined by Kennedy and Kennedy (1976).

The relatively small volume of very radioactive Pink Granite intersected by the profile has a disproportionate effect on the average upper crustal heat production, but the unit is too small to have a major impact on the underlying thermal profile in the lithosphere. Only large wavelength 2-D variations, approaching lithospheric dimensions, in crustal heat production can produce significant variations in lithospheric thickness.

Northwestern profile

Figure 7 shows a profile across the extensive area of moderately radioactive rocks ("Granitoids undivided", Fig. 1, 2; 0.7-6.0 $\mu W/m^3$, Table 1) northwest of the Yellowknife-Lac de Gras profile. Heat production is lower than that for the hottest granite (Pink Granite north of Gordon Lake, Fig. 1, 2; Table 1), but moderate values extend across a wider area (airborne values, ca. 1.5 $\mu W/m^3$, Fig. 2; outcrop equivalent, 3.0 $\mu W/m^3$). Using an average heat production for Granitoids undivided of 5.0 $\mu W/m^3$ (outcrop measurements, Table 1), the average heat production for the crust in the southwestern two thirds of the profile is 27 per cent higher than that calculated by Thompson et al. (1995) for the heat flow measurement site near Yellowknife . If regional heat flow is also

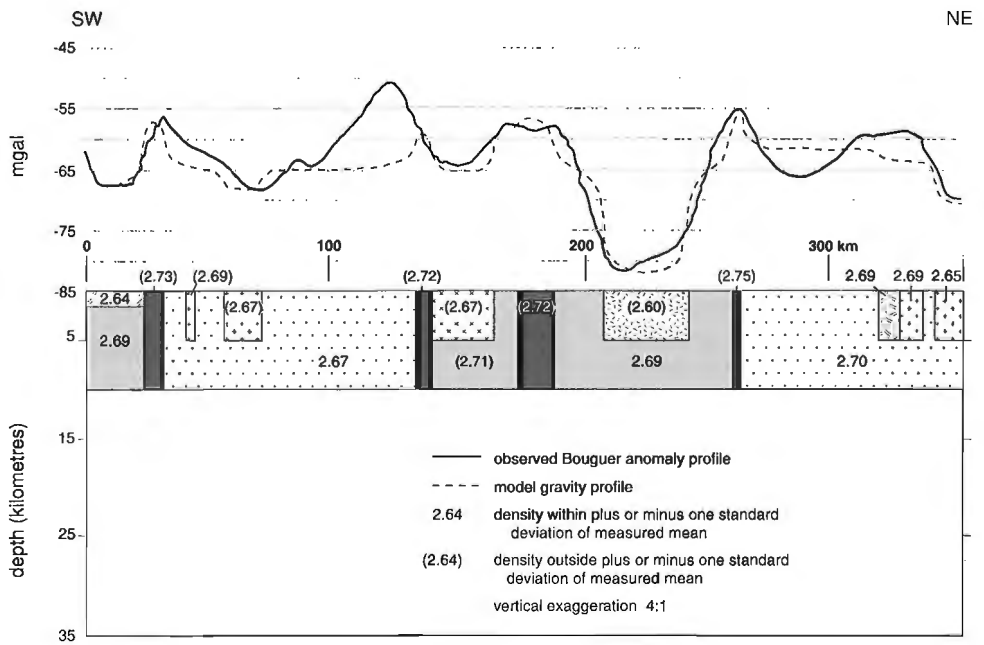

Figure 5.

Gravity model 2, Yellowknife-Lac de Gras profile. Density in g/cm³.

proportionally higher than at Yellowknife, the model lithosphere would be too thin to intersect the diamond stability field (Fig. 7).

Measurements compiled in Table 1 probably overestimate radiogenic heat production because ground measurements in the Granitoids undivided unit were taken in areas of anomalously high radioactivity (airborne data, Fig. 2). If a more representative heat production in the granitoid unit is assumed, for example, 3.0 $\mu W/m^3$ (estimated from Fig. 2), the average whole crustal value is close to that calculated for the Yellowknife locality by Thompson et al. (1995). In this case, assuming similar heat flow, the modelled lithosphere beneath the northwestern profile could contain a zone 30 km thick that is in the diamond stability field, similar to that calculated for the Yellowknife heat flow site. These conditions of heat flow and radiogenic heat production may restrict conditions for diamond formation beneath the southwest half of the profile at present and thus also in the past.

The absence of heat flow data along the length of the profiles or, indeed over the Slave Province, coupled with uncertainty about the vertical dimension of the rock units, are severe limitations on the practical application of these models to specific locations. It is interesting to note, however, that the model calculations indicate mantle heat flow (Thompson et al., 1995) close to that derived by Guillou-Frontier [*sic*, Frottier] et al. (1994) from surface heat flow measurements in the Superior Province.

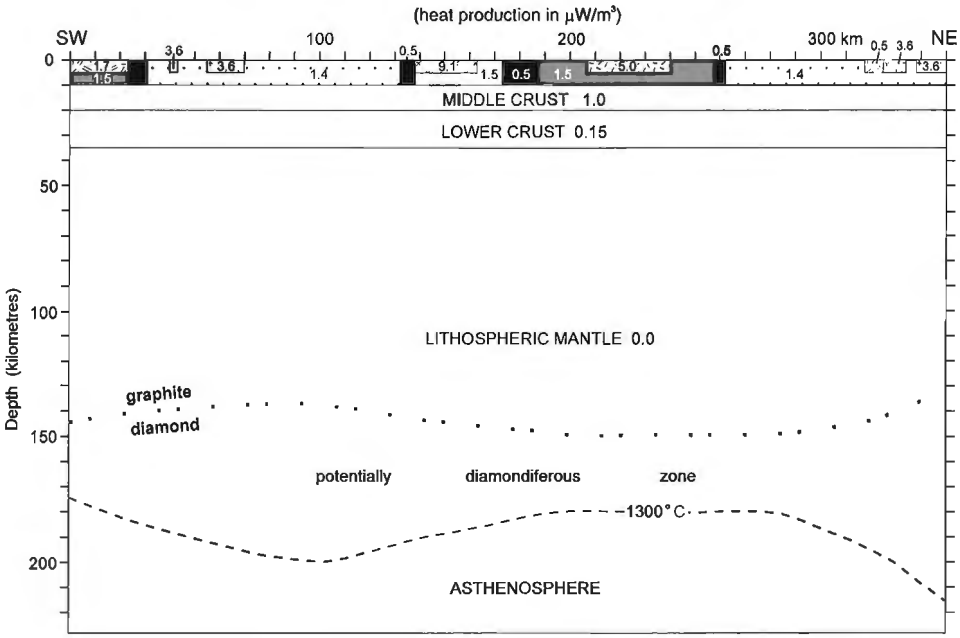

Figure 6.

Schematic profile of lithosphere between Yellowknife and Lac de Gras. Distribution of rock units (radiogenic heat sources, Table 1) within upper crust is extrapolated downward from surface geology (Figure 1). Thickness of middle and lower crust is assumed. See text for discussion of the calculation of lithospheric thickness (depth to 1300°C isotherm). Diamond stability after Kennedy and Kennedy (1976). Heat productions in middle and lower crust and mantle are from Thompson et al.(1995). Average heat production for the central portion of the profile is 3 $\mu W/m^3$.

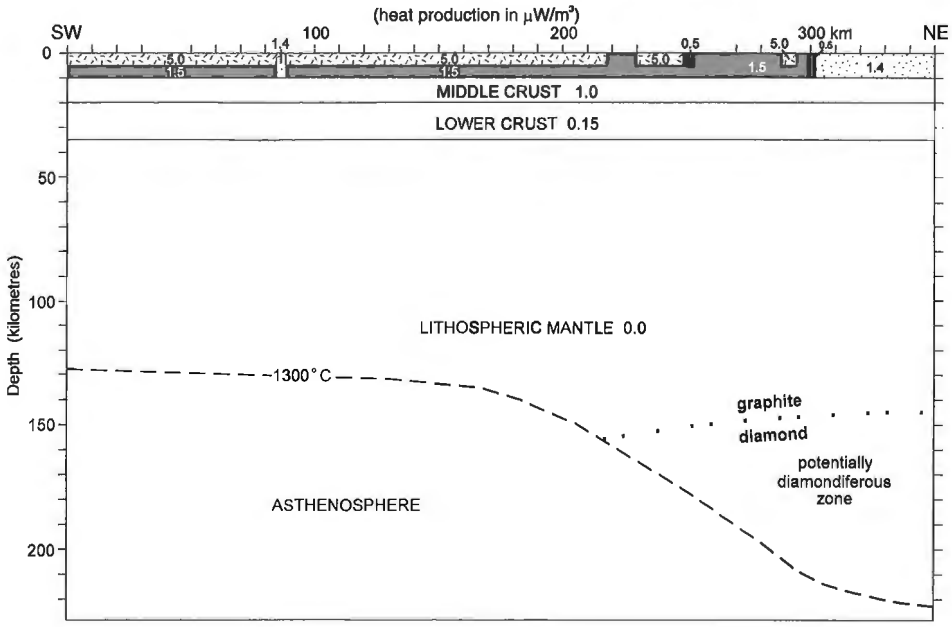

Figure 7.

Schematic profile of lithosphere between Great Slave Lake and a point northwest of Yamba Lake. Heat production at northeast end of profile is assumed to be similar to that calculated for the Lac de Gras area (Thompson et al., 1995). Distribution and magnitude of heat sources as in Figure 6.

DISCUSSION AND CONCLUSIONS

The strong influence of crustal radiogenic heat production and thermal conductivity means that these factors may have important effects on geothermal gradients in the lower crust and lithospheric mantle (Pollack and Chapman, 1977). Relatively low geothermal gradients and thick lithosphere are required for diamond stability. Back-calculation of radioactive decay processes indicates that crustal radiogenic heat production was twice as high 2500 Ma ago than it is today. Thompson et al. (1995) showed that a doubling of crustal heat production caused their modelled lithosphere to thin to a point where it no longer intersected the diamond stability field. They suggested that the geothermal gradients prior to 1800 Ma were too high for diamond to be stable in the Slave Province lithosphere. Spatial variations at the appropriate length scale in the concentration of heat producing elements, in the crust today may produce a similar effect on geothermal gradients, lithosphere thickness, and diamond stability.

Padgham and Fyson (1992) pointed out that the high proportion of highly evolved, potassium-rich granites distinguishes the Slave Province from classic Archean granite-greenstone terranes like the Superior Province. Radiogenic heat production for several of these granites (Table 1) is among the highest in the Canadian Shield and much higher than for the Superior Province as a whole (Darnley et al., 1977). However, while these granites have a disproportionate effect on average crustal heat production and hence on model lithospheric thickness, individual plutons are probably too small to have a direct influence on the depth to the 1300°C isotherm. The variations in lithospheric thickness revealed by the modelling (Fig. 6, 7) reflect broader, more diffuse changes in average crustal heat production. These are not high enough to eliminate the diamond stability field along the Yellowknife-Lac de Gras profile. However, the prominent heat production anomaly associated with pink megacrystic granite north of Gordon Lake is part of a much broader anomalous zone characterized by lower but still relatively high "apparent" heat production (Fig. 2). If there is a significant thickness (5 km) to this zone, the underlying mantle will be warmer and the diamond potential may be affected (Fig. 7).

Plutons of megacrystic pink granite several tens of kilometres across occur near the kimberlites at Cross Lake (north of Gordon Lake, Fig. 1) and at Yamba Lake. In view of the preliminary results based on heat production data from rock units along the schematic Yellowknife-Lac de Gras profile (Fig. 6), unless the granites are more than 5 km thick at these localities or the units are wider than the present surface expression, the relatively low diamond assays recorded (Pell, 1995, Table C) may be the result of factors other than proximity to radioactive megacrystic granite of limited lateral extent. Figure 7 on the other hand shows a transect of a large area of higher radiogenic heat production where the effect may be significant. Although poorly constrained thermally, preliminary models suggest a warmer mantle, a thinner lithosphere and a thinner or perhaps absent region of diamond stability.

FUTURE STUDIES

Several promising avenues of inquiry have been opened up as a consequence of this work on the interdependency of crustal heat production, lithospheric temperatures, and diamondiferous kimberlites.

1. More comprehensive knowledge of the distribution and economic potential of diamond-bearing kimberlites in the Slave Province and their relation to areas of high crustal heat production will provide a test of the idea that the long wavelength crustal heat production anomalies influence lithospheric thickness.
2. A test of models indicating thin lithosphere (100-150 km) beneath radiogenic upper crust would be to determine if any mantle xenoliths in kimberlites near or within the anomalous zone are derived from thick lithosphere (>200 km).
3. Collection of detailed gravity data along critical corridors to improve resolution of gravity anomalies and further constrain models of the upper crust.
4. Analysis of regional magnetic anomalies to investigate possible variations in depth to the Curie isotherm and the relation to areas of high surface heat production.
5. Measurements of terrestrial heat flow in exploratory boreholes linked to measurements of radiogenic heat production would provide a firmer basis for modelling of lithospheric thermal structure past and present. Ideally, boreholes would be located in areas of contrasting radiogenic heat production in order to develop a relationship between heat flow and heat production for the Slave Province and, to compare that relation with other Shield areas and areas worldwide with diamondiferous kimberlites.

ACKNOWLEDGMENTS

We thank Ray Hetu, Deborah Lemkow, Azad Rafeek and Katherine Venance for preparing the diagrams. Warner Miles compiled the gravity map. Keith Richardson and Steve Lucas provided constructive critical reviews.

REFERENCES

Baragar, W.R.A.
1966: Geochemistry of the Yellowknife volcanic rocks; Canadian Journal of Earth Sciences, v. 3, p. 9-30.

Barr, K.G.
1971: Crustal refraction experiment: Yellowknife, 1966; Journal of Geophysical Research, v. 76, p. 1929-1947.

Bleeker, W. and Beaumont-Smith, C.
1995: Thematic structural studies in the Slave Province: preliminary results and implications for the Yellowknife domain, Northwest Territories; in Current Research 1995-C; Geological Survey of Canada, p. 87-96.

Broome, J.
1989: MAGRAV2: An interactive magnetics and gravity modelling program for microcomputers (Version 1.5); Geological Survey of Canada, Open File 1334.

Charbonneau, B.W. and Legault, M.I.
1994: Interpretation of airborne geophysical data for the Thor Lake area, Northwest Territories; in Studies of Rare-metal Deposits in the Northwest Territories, (ed.) W.D. Sinclair and D.G. Richardson; Geological Survey of Canada, Bulletin 475, p. 17-31.

Charbonneau, B.W., Killeen, P.G., Carson, J.M., Cameron, G.W., and Richardson, K.A.
1976: Significance of radioelement concentration measurements made by airborne gamma ray spectrometry over the Canadian Shield; in Exploration for Uranium Ore Deposits; International Atomic Energy Agency, Vienna, p. 35-53.

Darnley, A.G., Charbonneau, B.W., and Richardson, K.A.
1977: Distribution of uranium in rocks as a guide to the recognition of uraniferous regions; in Recognition and Evaluation of Uraniferous Areas; International Atomic Energy Agency, Vienna 1977, p. 55-86.

Darnley, A.G., Richardson, K.A., Grasty, R.L., Carson, J.M., Holman, P.B., and Charbonneau, B.W.
1986: Radioactivity map of Canada; Geological Survey of Canada Map 1600A (1:5 000 000).

Drury, M.J.
1989: The heat flow-heat generation relationship: implications for the nature of continental crust; Tectonophysics, v. 164, p. 93-106.

Gibb, R.A. and Thomas, M.D.
1980: Correlation of gravity anomalies with Yellowknife Supergroup rocks, North Arm, Great Slave Lake; Canadian Journal of Earth Sciences, v. 17, p. 1506-1516.

Guillou-Frontier [*sic*, Frottier], L., Mareschal, J.-C., Jaupart, C., and Gariépy, C.
1994: Heat flow, gravity, and structure of the lithosphere; Trans-Hudson Orogen Transect Lithoprobe Report #38, p. 58-59.

Gurney, J.J.
1989: Diamonds; In Kimberlites and related rocks, v. 2., (ed.) J. Ross; Geological Association of Australia, Special Publication 14, p. 935-965.

Henderson, J.B., van Breemen, O., and Loveridge, W.D.
1987: Some U-Pb zircon ages from Archean basement, supracrustal and intrusive rocks, Yellowknife-Hearne Lake area, District of Mackenzie; in Radiogenic age and isotopic studies: Report 1; Geological Survey of Canada, Paper 87-2, p. 111-122.

Hoffman, P.F. and Hall, L.
1993: Geology Slave craton and environs, District of Mackenzie, Northwest Territories; Geological Survey of Canada, Open File 2559, scale 1:1 000 000.

Jessop, A.M.
1990: Thermal geophysics; Developments in solid earth geophysics 17, Elsevier Science Publishers, Amsterdam, 306 p.

Kennedy, C.S. and Kennedy, G.C.
1976: The equilibrium boundary between graphite and diamond; Journal of Geophysical Research, v.81, p.2467-2470.

Kretz, R., Garrett, D., and Garrett, R.G.
1982: Na-K-Li geochemistry of the Prestige pluton in the Slave Province of the Canadian Shield; Canadian Journal of Earth Sciences, v. 19, p. 540-554.

Legault, M.I. and Charbonneau, B.W.
1993: Geophysical, geochemical and petrological study of Contwoyto Batholith, Lupin gold mine area, Northwest Territories; in Current Research, Part E; Geological Survey of Canada, Paper 93-1E, p. 207-218.

Lewis, T.J. and Wang, K.
1992: Influence of terrain on bedrock temperatures; Paleogeography, Paleoclimatology, Paleoecology (Global and Planetary Change Section), v. 98, p. 87-100.

McGrath, P.H., Henderson, J.B., and Lindia, F.M.
1983: Interpretation of a gravity profile over a contact zone between an Archean granodiorite and the Yellowknife Supergroup using an interactive computer program with partial automatic optimization; in Current Research, Part B; Geological Survey of Canada, Paper 83-1B, p. 189-194.

Moore, H.D.
1972: The relationship between the geology and the K, U, Th concentrations in the Yellowknife, N.W.T. region; B.Sc. Thesis, Carleton University, Ottawa, Ontario.

Nassichuk, W.W. and McIntyre, D.J.
1995: Cretaceous and Tertiary fossils discovered in kimberlites at Lac de Gras in the Slave Province, Northwest Territories; in Current Research 1995-B; Geological Survey of Canada, p. 109-114.

Padgham, W.A. and Fyson, W.K.
1992: The Slave province: a distinct Archean craton; Canadian Journal of Earth Sciences, v. 29, p. 2072-2086.

Pell, J.
1995: Northwest Territories kimberlites; Indian and Northern Affairs Canada, NWT Geology Division, EGS 1995-2.

Pollack, H.N. and Chapman, D.S.
1977: On the regional variation of heat flow, geotherms and thickness of the lithosphere; Tectonophysics, v.38, p. 279-296.

Richardson, K.A. and Charbonneau, B.W.
1973: Gamma-ray spectrometry investigations, 1973; in Report of Activities, Part A; Geological Survey of Canada, Paper 74-1, Part A, p. 371-372.

Richardson, K.A. and Killeen, P.G.
1980: Regional radiogenic heat production mapping by airborne gamma ray spectrometry; in Current Research, Part B; Geological Survey of Canada, Paper 80-1B, p. 227-232.

Thompson, P.H. and Kerswill, J.A.
1994: Preliminary geology of the Winter Lake-Lac de Gras area, District of Mackenzie, Northwest Territories; Geological Survey of Canada, Open File 2740 (revised), 1:250 000 scale.

Thompson, P.H., Judge, A.S., and Lewis, T.J.
1995: Thermal parameters in rock units of the Winter Lake-Lac de Gras area, Central Slave province, Northwest Territories – implications for diamond genesis; in Current Research 1995-E; Geological Survey of Canada, p. 125-131.

in press: Thermal evolution of the lithosphere in the central Slave Province: implications for diamond genesis; in Searching for Diamonds in Canada, (ed.) A.N. LeCheminant, D.G. Richardson, R.N.W. DiLabio, and K.A. Richardson; Geological Survey of Canada, Open File 3228, p. 151-160.

van Breemen, O., Davis, W.D., and King, J.E.
1992: Temporal distribution of granitoid plutonic rocks in the Archean Slave Province, northwest Canadian Shield; Canadian Journal of Earth Sciences, v. 29, p. 2186-2199.

Geological Survey of Canada Projects 870008, 880029

Geological and geophysical signatures of a large polymetallic exploration target at Lou Lake, southern Great Bear magmatic zone, Northwest Territories[1]

Sunil S. Gandhi, Nirankar Prasad, and Brian W. Charbonneau
Mineral Resources Division, Ottawa

Gandhi, S.S., Prasad, N., and Charbonneau, B.W., 1996: Geological and geophysical signatures of a large polymetallic exploration target at Lou Lake, southern Great Bear magmatic zone, Northwest Territories; in Current Research 1996-E; Geological Survey of Canada, p. 147-158.

Abstract: Recent metallogenic studies and a multiparameter airborne geophysical survey have revealed a potentially large polymetallic exploration target in southern Great Bear magmatic zone. Its geological setting comprises an early Proterozoic metasedimentary platform sequence, intruded by granitic plutons and overlain unconformably by a gently dipping rhyolitic volcanic assemblage, which was emplaced during the Great Bear magmatic activity ca. 1865 Ma. The metasedimentary and volcanic rocks form a northwest-trending belt, and host numerous Bi-Cu-Co-Au-As-bearing arsenopyrite-pyrite-magnetite veins and disseminations, localized mainly at the unconformity. This hydrothermal mineralization is characterized by strong potassium enrichment over a 3 x 4 km area, coincident with high magnetic and low eTh/K ratio anomalies, detected by the airborne survey. Follow-up exploration by industry has revealed a coincident gravity anomaly that enhances potential for a large deposit of the type related to the giant Olympic Dam deposit in South Australia.

Résumé : Des études métallogéniques récentes et un levé géophysique aéroporté à plusieurs paramètres ont mis en évidence une cible d'exploration polymétallique potentiellement étendue dans la partie sud de la zone magmatique du Grand lac de l'Ours. Le contexte géologique de la cible comprend une séquence métasédimentaire de plate-forme du Protérozoïque précoce, injectée de plutons granitiques et recouverte en discordance par un assemblage volcanique rhyolitique à pendage faible; la mise en place de cet assemblage est associée à l'épisode magmatique du Grand lac de l'Ours, il y a environ 1 865 millions d'années. Les roches métasédimentaires et volcaniques forment une bande d'orientation nord-ouest et sont l'encaissant de nombreuses concentrations d'arsénopyrite-pyrite-magnétite à minéralisation en Bi-Cu-Co-Au-As, sous la forme de filons et de disséminations. Les concentrations s'observent principalement au niveau de la discordance entre la séquence de plate-forme et l'assemblage volcanique. Cette minéralisation de type hydrothermal se caractérise par un important enrichissement en potassium sur une superficie de 3 kilomètres sur 4 kilomètres, qui correspond aux anomalies (crête magnétique et faibles rapports eTh/K) détectées par le levé aéroporté. Un suivi par l'industrie a permis d'identifier une anomalie gravimétrique coïncidente, ce qui accentue le potentiel de découvrir un gros gisement du type de l'immense gisement d'Olympic Dam, en Australie méridionale.

[1] Contribution to a Canada-Northwest Territories Minerals Initiative Project (1991-1996), an initiative under the Canada-Northwest Territories Economic Development Cooperation Agreement

INTRODUCTION

Metallogenic studies carried out under the Canada-Northwest Territories Minerals Initiative Program (1991-96) in the southern part of Great Bear magmatic zone (Fig. 1) have provided new insights into the resource potential for the whole of the magmatic zone (Gandhi, 1994). These studies followed the 1974 discovery of the Sue-Dianne Cu-U-Au deposit by a regional gamma spectrometric survey (5 km line-spacing) by the Geological Survey of Canada (Charbonneau, 1988), and have revealed that mineralization is comparable with that of the giant Olympic Dam polymetallic deposit in South Australia (Reeve et al., 1990; Gandhi, 1994). A more detailed (500 m line-spacing) airborne multiparameter geophysical survey over a selected part of the magmatic zone, covering 1500 square kilometres (Fig. 1), was released recently by the Geological Survey of Canada (Hetu et al., 1994; Charbonneau et al., 1994). This survey provides a spectrometric, magnetic, and VLF-EM database to aid further assessment of the mineral potential of the area, and has generated exploration incentive throughout the magmatic zone. This paper describes a major exploration target revealed by the metallogenic studies and the geophysical survey (Fig. 2, 3), namely the Lou Lake Bi-Cu-Co-Au-As-bearing zone (Gandhi, 1994).

GEOLOGICAL SETTING

The Great Bear magmatic zone is a continental, 1870-1840 Ma old, volcano-plutonic zone on the west margin of the Wopmay Orogen, which culminated ca. 1900 Ma (Fig. 1 inset; Hildebrand et al., 1987; Gandhi and Mortensen, 1992; Gandhi, 1994). Older rocks in the Great Bear magmatic zone include remnants of an early Proterozoic metamorphosed platform-shelf sequence that has been intruded by foliated to massive granitic plutons. These supracrustal and plutonic rocks are regarded as equivalents of the Coronation Supergroup and the Hepburn intrusive suite, respectively, which form the core of the Wopmay orogen to the east. The eastern boundary of the Great Bear magmatic zone with this core zone is marked by the Wopmay fault zone, which forms a prominent north-trending topographic linear.

Volcanic assemblages of the Great Bear magmatic zone have an aggregate thickness of approximately 10 km in the north and 5 km in the south. Those in the north range from basalt to rhyolite, but dacite, rhyodacite, and rhyolite predominate over andesite and basalt. In the south, the volcanic rocks are in the dacite-rhyodacite-rhyolite range. Overall, the volcanic rocks of the magmatic zone display calc-alkaline trend, but in many places alkali metasomatism has been intense (Hildebrand et al., 1987; Gandhi, 1994). The older volcanic and associated volcaniclastic rocks (ca. 1865 Ma) include the Labine and Dumas groups in the north and the Faber Group in the south (Fig. 1). These volcanic and associated volcaniclastic rocks are gently folded, but lack the penetrative foliation seen in the metasedimentary rocks. They have been intruded by abundant subvolcanic porphyritic dacite and quartz monzonite plutons, which predate the younger Sloan

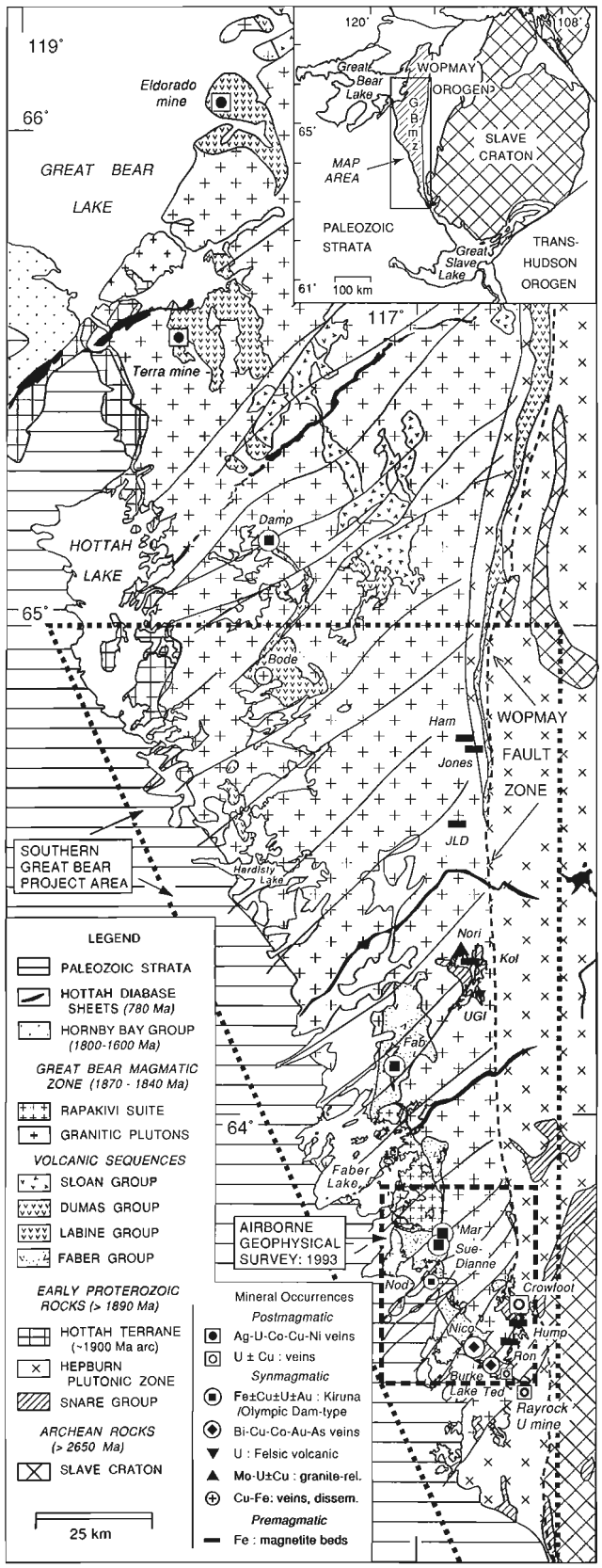

Figure 1. *General geology and main mineral occurrences of the Great Bear magmatic zone (GBmz), northwest Canadian Shield.*

Group in the north. Large granitic batholiths were emplaced during later stages of volcanic activity, including the rapakivi granite suite at Faber Lake (Fig. 1), which is characterized by high radioelement (K, eU, and eTh) concentrations.

The present study area (Fig. 2) is underlain by rocks of the four major groups of the Great Bear magmatic zone: i) metasedimentary rocks, ii) older intrusions, iii) the Great Bear volcanic rocks, and iv) younger intrusions. These are overlain by flat-lying Paleozoic strata to the southwest. The geological evolution of the area outlined below is based on work by McGlynn (1968) south of latitude 63°30′, Gandhi and Lentz (1990) around Lou Lake, Gandhi (1992) around Hump Lake, and on unpublished data from fieldwork done by the first two authors of this paper in the Bea Lake and Cole Lake areas in 1992, and around Betty Ray Lake during 1995.

Metasedimentary rocks are regarded as equivalents of the early Proterozoic Snare Group/Coronation Supergroup east of the Wopmay fault zone (Lord, 1942; McGlynn, 1968; Gandhi, 1994). The basement on which they were deposited is not exposed. They form a northwesterly trending ridge, as much as 100 m high between the Rayrock mine and Lou Lake, and a discontinuous zone in the Hump Lake-Cole Lake area, and also occur as numerous xenoliths in intrusions. The Lou Lake-Rayrock mine belt comprises a 1.5 km thick sequence (units 1 to 4) dipping 55° to 70° to the northeast, facing right-side up. Deformation and metamorphism are progressively more intensive in the metasedimentary rocks to the northeast, reaching amphibolite grade near the Wopmay fault zone in the Cole Lake-Hump Lake area.

The basal siltstone (unit 1) is approximately 1 km thick, and is fine grained, quartzofeldspathic, bedded on a centimetre scale, and commonly light grey, dark grey, and buff white. It includes a few argillaceous beds, and some weakly to strongly magnetic beds as much as 5 cm thick. The overlying unit of carbonate-rich beds (unit 2) is approximately 100 m thick and serves as a local marker unit. It includes carbonate, calcareous argillite and calc-silicate beds, and also some thin magnetite beds and elongate lenses. Much of it is thinly bedded, but thicker carbonate beds and lenses, erratically distributed and metamorphosed to marble, occur throughout the unit. The quartz arenite (unit 3) is 300 to 550 m thick, medium grained, and massive to well bedded on a decimetre scale. Graded bedding, crossbedding, and ripple marks, observed at several places, show that the beds are right side up. The unit includes pale pink to buff quartzofeldspathic and grey argillaceous siltstone beds, which are as much as 10 m thick in some places. It grades upward into a siltstone assemblage (unit 4) which exceeds 300 m in thickness. The siltstones are mainly grey biotite-rich, interbedded with buff white to pale pink, mafic-poor quartzofeldspathic beds. Magnetite is common in grey siltstones as finely disseminated grains and locally forms beds as much as a few centimetres thick. The unit includes beds of quartz arenite, argillite, and calcareous rocks. Northeast of the Lou Lake-Rayrock mine belt, most of the metasedimentary rocks are tentatively assigned to the four units, except for the biotite-rich quartzofeldspathic paragneiss (unit 5) at Hump Lake (Gandhi, 1992, 1994), and highly contorted biotite-hornblende quartzofeldspathic banded gneiss (subunit 1a), which has some remnants of amphibolitic rocks and resembles some of the Archean gneisses to the east.

The metasedimentary rocks were folded about northwest axes and have been intruded by syntectonic granodiorite gneiss of the Betty Ray Lake region (unit 6). Foliation in this hornblende-biotite-bearing pluton trends northwesterly. The pluton grades into a monzonitic marginal phase (unit 7). Both phases apparently grade into more massive varieties south and north of Betty Ray Lake, and these are difficult to distinguish in the field from compositionally similar, younger, Great Bear intrusions. Small leucogranitic bodies in metasedimentary rocks, with associated tourmaline-rich veins, may be phases of the older granites.

Following the uplift and erosion of these rocks, felsic volcanic activity formed the Lou Lake assemblage, which is approximately 1.5 km thick and dips gently to moderately to the northeast. Gandhi and Lentz (1990) recognized ten units in the assemblage (units 8 to 16) and some undivided rhyolitic rocks (unit 17). The basal unit is a lithologically variable agglomerate-lithic tuff, commonly fragmental but locally well bedded. It was deposited on uneven surface of folded metasedimentary rocks. The tuff is overlain by a massive to flow banded subporphyritic rhyolite (unit 9), which in turn is followed by a well bedded tuff-volcaniclastic siltstone (unit 10) with agglomerate lenses and thin rhyolite flows. The next units in the sequence are flow laminated, lithophysae-bearing subporphyritic rhyolite (unit 11), and grey, well banded to massive subporphyritic rhyolite (unit 12). These are succeeded in the north by a feldspar-hornblende porphyritic dacite (unit 13). A massive to ignimbritic rhyodacite (unit 14) occurs to the west, and is in part intrusive. A volcaniclastic conglomerate (unit 15) apparently grades to the north into tuff, siltstone, and rhyolite (unit 15a). The overlying coarse, quartz-feldspar porphyritic, massive rhyodacite, with a grey aphanitic matrix (unit 16) is also in part intrusive.

Rocks intrusive into the volcanic assemblage include diorites (unit 18) of more than one age, subvolcanic dacite (unit 19), quartz-feldspar porphyry dykes (unit 20), and quartz-monzonite-monzodiorite (unit 21) that is close in age to the volcanic rocks (Fig. 4; Gandhi and Mortensen, 1992). Granite-granodiorite forms a batholith to the northeast (unit 22), and a variety of granitic rocks (unit 23), ranging from hornblende-biotite-rich to leucocratic, underlie a large area to the southwest. Medium grained leucogranite bodies (unit 24) are probably phases of these granite plutons, although some or most of them may be coeval with the volcanism.

The magmatic activity was followed by brittle faulting, which formed a set of northeast-trending faults. Some of these faults host giant quartz veins (unit 25). A number of small diabase dykes of unknown age cut the volcano-plutonic zone. Paleozoic cover strata (unit 27) are less than 100 m thick in the study area.

Figure 2. *Geology and mineral occurrences of the Lou Lake-Rayrock mine area, southern Great Bear magmatic zone.*

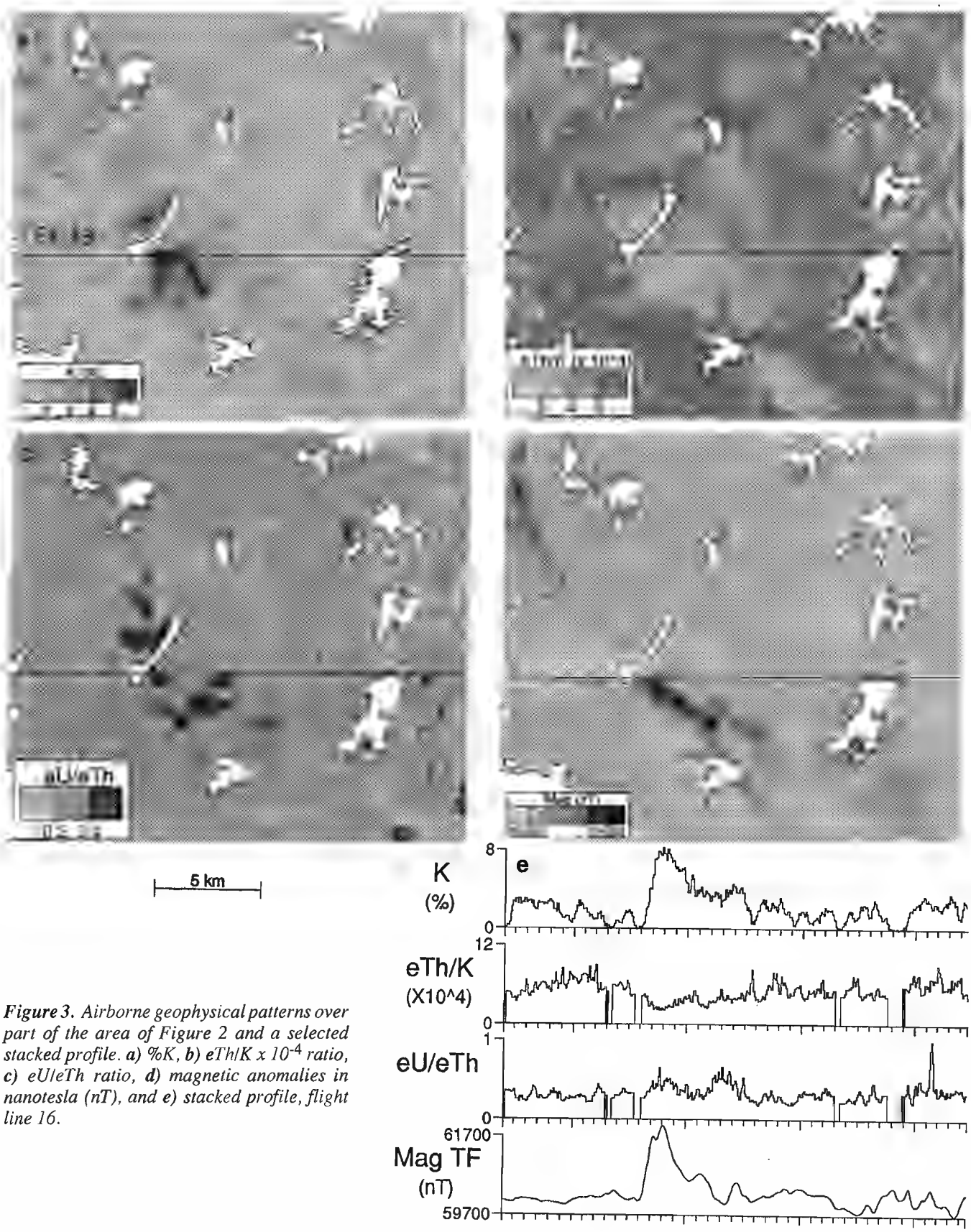

Figure 3. *Airborne geophysical patterns over part of the area of Figure 2 and a selected stacked profile.* ***a)*** *%K,* ***b)*** *eTh/K x 10^{-4} ratio,* ***c)*** *eU/eTh ratio,* ***d)*** *magnetic anomalies in nanotesla (nT), and* ***e)*** *stacked profile, flight line 16.*

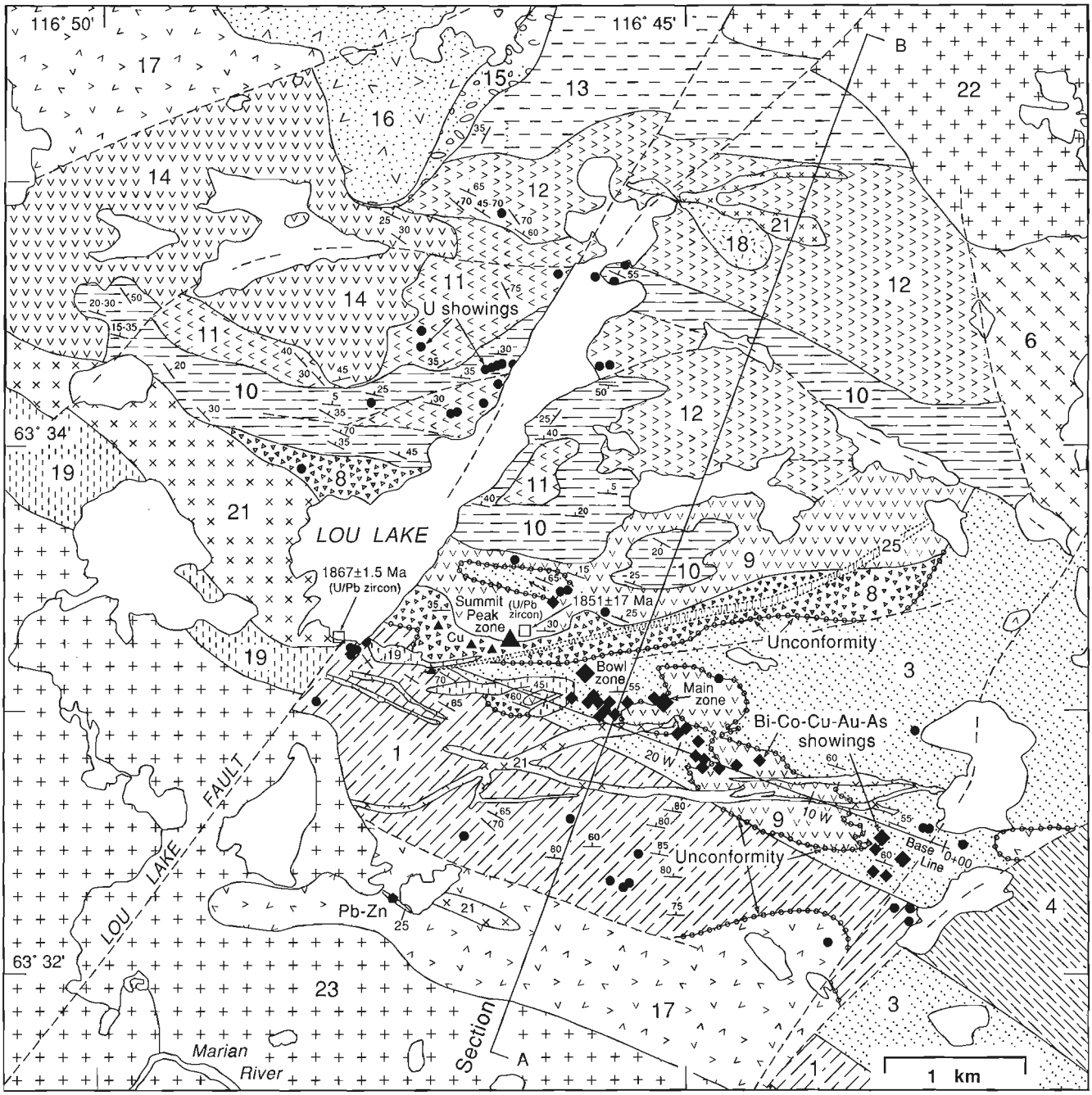

Figure 4. *Geology and mineral occurrences of the Lou Lake area. See legend Figure 2.*

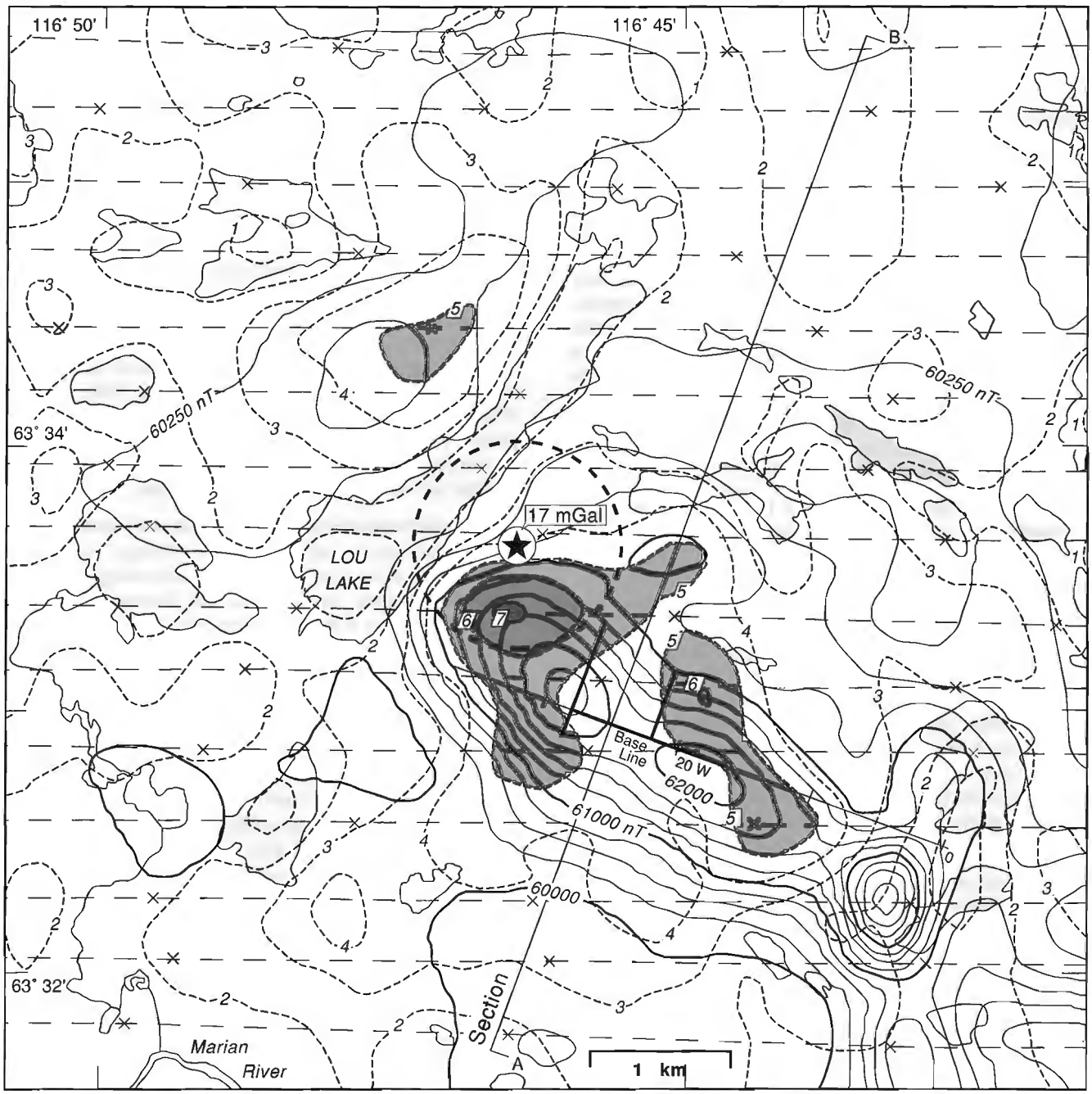

Figure 5. *Magnetic and potassium contours (solid and dashed lines) of the Lou Lake area from airborne survey (Hetu et al., 1994); contour intervals at 250 nanotesla and per cent potassium respectively; note east-west flight lines with fiducial points marked by 'X's; ground profiles over selected grid lines (thick lines) in Figure 6; gravity anomaly (heavy dashed circle) with peak value (Star).*

MINERAL OCCURRENCES

The main mineral occurrences of the region can be conveniently grouped with respect to the Great Bear magmatic activity into three broad groups, viz. premagmatic, synmagmatic, and postmagmatic (Fig. 1, 2). Most of the occurrences in the present study area (Fig. 2) have been described earlier by Gandhi and Lentz (1990) and Gandhi (1992, 1994), and hence they are only briefly mentioned below.

The main premagmatic metallic concentrations are in the metasedimentary sequence, mainly as stratiform magnetite beds and lenses in siltstone, argillite, and calcareous rocks. In addition, many siltstone sections are weakly to moderately magnetic because of the presence of disseminated magnetite. The best examples of stratiform magnetite are the Hump Lake north and Ron showings (Fig. 2), where some of the beds are 20 m thick and have a strike length of more than 200 m (Gandhi, 1992, 1994). The mapping done in 1995 near the Ron deposit revealed the presence of additional thick magnetite beds and lenses to the northwest, which have been intruded by massive quartz monzonite (unit 21).

The synmagmatic occurrences include i) mono- and polymetallic veins and breccia fillings of Kiruna-Olympic Dam type, ii) Bi-Cu-Co-Au-As-bearing hydrothermal arsenopyrite-pyrite-magnetite veins and disseminations, iii) felsic volcanic-associated uranium occurrences, and iv) pyrite-chalcopyrite veins and disseminations in shear zones (Fig. 1). Within the study area the most important are the Bi-Co-Cu-Au-As occurrences (Fig. 2, 4), and these are described further below. Kiruna-type magnetite-apatite-actinolite veins are found at the Tan showing, which have some uranium concentrations, and near Burke Lake, discovered in 1995. The uranium occurrences near Lou Lake are hosted by felsic volcanic rocks, and may be regarded either as volcanogenic or as an outer halo of the hydrothermal system that formed the Bi-Cu-Co-Au-As occurrences.

A number of Bi-Cu-Co-Au-As occurrences are known in the metasedimentary and volcanic rocks near Lou Lake close to the unconformity, and in the metasedimentary rocks near Burke Lake (Fig. 1, 2). Most of these are small, but a few larger zones of significant metal concentrations have been located near Lou Lake. The "Main zone" was discovered in 1965 (Fig. 4) and was explored by trenching and drilling during 1968-1969 by Precambrian Mining Services Limited-New Athona Mines Limited (Gandhi and Lentz, 1990). Metal concentrations encountered in this 300 m long, east-trending, steep zone are in the range of half a per cent each of Bi, Cu, and Co, and one ppm Au over widths of 5 to 20 m. Some samples contain as much as 6 ppm Au. Additional mineral occurrences were discovered during surface exploration carried out by Noranda Exploration Company Limited in 1978-1981. Since 1994, Fortune Minerals Limited has conducted more detailed sampling, prospecting, and trenching, and has recently initiated diamond drilling. Surface sampling revealed that a previously known zone 150 m south of the Main zone contains as much as 1.7% Co, 0.7% Bi, and 6 g/t Au over 4 m width, and has a strike length of 150 m. Prospecting by the company led to the discovery of two Bi-Co-Cu-Au-bearing zones, one 100 m north of the main zone, and the other called the 'Bowl zone' 300 m to the west-northwest Initial drilling on the latter has indicated undelimited mineralization over a strike length of 200 m, a width of 100 m, and a depth of 150 m down a moderate dip to the north, and intersected sections comparable in grades with those of the Main zone. In addition, chip samples from the copper-rich 'Summit Peak zone' to the northwest (Fig. 4), have returned assays averaging as high as 0.7% Cu over 44 m and some of them contain as much as 0.5% tungsten and 1 ppm Au (Fortune Minerals news releases, October 1995, April and May 1996).

The main minerals in these occurrences are arsenopyrite, pyrite, magnetite, chalcopyrite, and bismuthinite. Minor amounts of cobaltite, cobaltian arsenopyrite, bornite, chalcocite, pyrrhotite, emplectite, loellingite, wittichenite, tennantite, molybdenite, scheelite, wolframite, native bismuth, and native gold are also present (Gandhi and Lentz, 1990; Mulligan, 1995). Their proportions vary widely. Bismuthinite, native bismuth, native gold, and scheelite occur mainly as inclusions in arsenopyrite. Hematite, biotite, chlorite, and potassium feldspar are the principal alteration minerals.

The postmagmatic occurrences in the study area are pitchblende±chalcopyrite veins and fracture fillings hosted by the giant quartz veins along the northeast-trending, and rarely northwest-trending, brittle faults and fractures. The most important of these is at the old Rayrock mine (Gandhi, 1994), and in addition there are the Crowfoot and Ted showings. A few others contain only pyrite, and rarely Pb-Zn sulphides.

AIRBORNE GEOPHYSICAL SURVEY

An airborne geophysical survey was conducted during 1993 in the Mazenod Lake area (Fig. 1; lat. 63°30′-63°53′N; long. 116°27′-117°10′W). The survey results, published in 1994, comprised twelve coloured geophysical maps (K, eU, eTh, eU/eTh, eU/K, eTh/K, total count, ternary radiometric, magnetic total field, magnetic gradient, VLF-EM total field, and quadrature), a set of stacked profiles, and a geological map showing mineral occurrences (Hetu et al., 1994).

Selection of the survey area was based on the presence of a variety of known mineral occurrences and the potential for more economically attractive deposits in varied geological settings. The area has low to moderate relief and extensive bedrock exposures, which make it especially suitable for this type of multiparameter survey. The survey was funded by the Geological Survey of Canada, and was complementary to the regional metallogeny project supported by the Canada-Northwest Territories Minerals Initiative Program (1991-1996).

This geophysical data set provides valuable tools for geological mapping, metallogenic studies, mineral exploration, and resource assessment. It must be emphasized that, in addition to the contoured maps, the stacked geophysical profiles contain the fine detail of the anomalies along individual flight lines, and these should be examined during interpretation or selection of targets for field investigations.

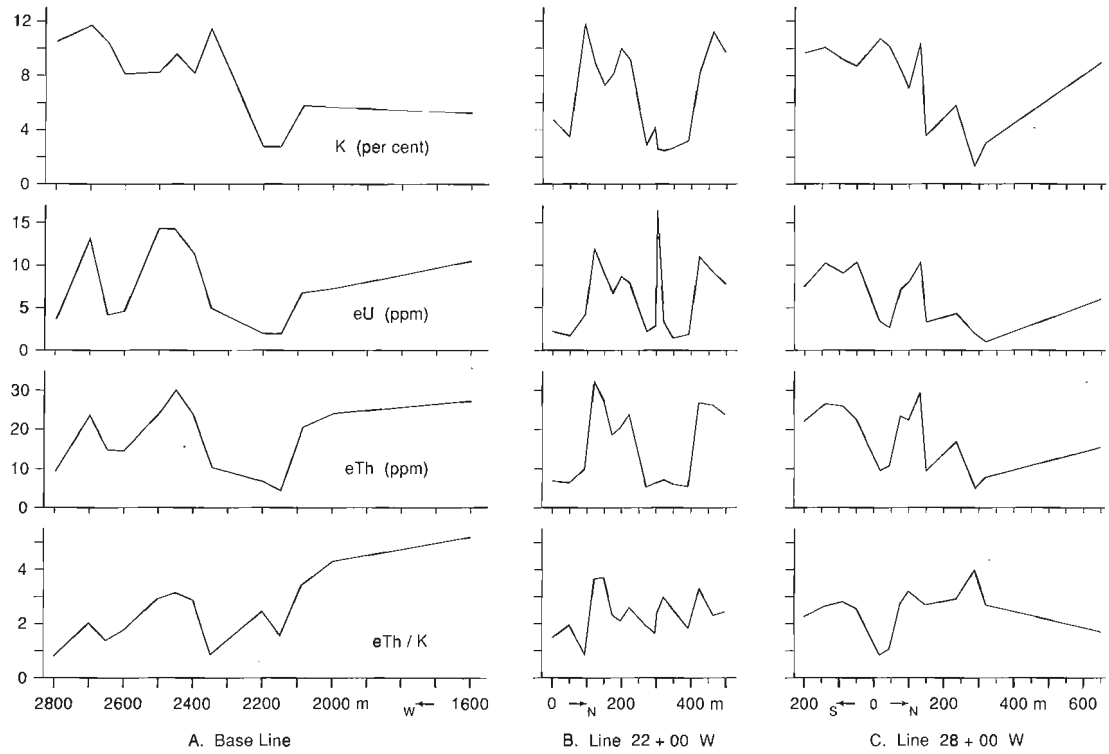

Figure 6. *Plots of K, eU, eTh and eTh/K along selected lines of the Lou Lake grid (Fig. 5); readings from Exploranium GRS-256 spectrometer.*

In general, geophysical patterns reflect the lithological units, faults, and various types of mineral occurrences. The geophysical signatures characterize different intrusions, e.g. the rapakivi granite in the northwestern corner of the surveyed area (Fig. 1), which is distinctive for its high radioelement content. A large segment of a granite-granodiorite batholith between the volcanic belt and the Wopmay fault zone shows variations in radiometric and magnetic patterns from core to margins suggesting zoned crystallization differentiation. An array of VLF-EM anomalies coincides with a set of northeast-trending right lateral brittle faults, which merge with, or terminate at the Wopmay fault zone to the northeast (Fig. 1).

Mineral occurrences in the area are characterized by a combination of high K, eU, eU/eTh ratio, and magnetic anomalies. For example, the Sue-Dianne deposit, which is a breccia-hosted Olympic Dam-type occurrence, has high eU, eU/eTh ratio and a high magnetic anomaly (Charbonneau, 1988). The group of veins and disseminated polymetallic (Bi-Cu-Co-Au-As) occurrences at Lou Lake and Burke Lake (Fig. 2) have high K, as well as anomalous eU, eU/eTh ratio, and magnetic field (discussed further below). The Ron stratiform Fe oxide occurrence is marked by a high magnetic anomaly alone. The Crowfoot uranium showing has high eU and eTh. The survey has also revealed several additional magnetic and radiometric anomalies not associated with known mineral occurrences, and thus enhances the exploration potential of the area (Charbonneau et al., 1994).

The present study covers the southeastern part of the airborne survey region, where several coincident geophysical anomalies (Fig. 3, 5) define exploration targets. The most important is a strong potassium anomaly which extends over a 3 x 4 km area, where numerous Bi-Co-Cu-Au-As occurrences are known (Fig. 4). Potassium concentrations peak at 7% K on the contoured maps approximately 1 km east of the south end of Lou Lake (Fig. 3a, 5). The maximum airborne profile value is, however, 8% K (Fig. 3e). This small difference arises because of the averaging inherent in the contouring technique.

The airborne survey results have been confirmed by ground spectrometer measurements along selected grid lines in the mineralized zone (Fig. 6). Although the grid lines surveyed were not in the area of maximum airborne response, values as high as 12% K were measured in rocks which would normally have background values less than 4% K. The high ground spectrometer values relate mainly to the abundance of K-feldspar in the alteration zone associated with the Bi-Co-Cu-Au-As mineralization. Samples of altered basal rhyolite near mineralization have K_2O contents of 12.5 and 12.7% (Gandhi and Lentz, 1990), and 13.67% (Mulligan, 1995).

The strong potassium anomaly is characterized by a very low eTh/K ratio (Fig. 3b, 6). This ratio is significant because it is commonly an excellent indicator of K alteration (Shives et al., 1995). Unaltered lithologies will show variation in

thorium and potassium proportional to the normal crustal abundance eTh/K ratio of about 5 x 10^{-4} (Galbraith and Saunders, 1983). During the process of potassium alteration, however, thorium does not accompany potassium at hydrothermal alteration temperatures, resulting in a low eTh/K ratio. Hence a very low eTh/K ratio, as seen at Lou Lake, enables distinction of K anomalies that have exploration significance from those related solely to lithological variations.

Uranium enrichment, apparent on the eU/eTh ratio map (Fig. 3c), is generally peripheral to the potassium anomaly. It reflects, at least in part, the presence of numerous small pitchblende veins (Fig. 2, 5).

The potassium anomaly is coincident with a strong magnetic anomaly, which has a peak intensity of 3000 nanoteslas (Fig. 3d, e, 5). The Bi-Cu-Co-Au-As mineralization occurs within the strongest part of the coincident magnetic and K anomalies. The general trend of the magnetic anomaly parallels the trend of the metasedimentary belt. As noted earlier, the metasedimantary rocks contain synsedimentary magnetite and magnetite-bearing veins that were introduced later. It is interesting to note the abrupt termination of this strong anomaly, and of exposures of the metasedimentary belt against the northeast-trending fault along Lou Lake. However, a notable K anomaly is detected across the fault northwest of the lake (Fig. 5).

Follow-up exploration by Fortune Minerals Limited in 1995 (Fortune Minerals news release, February 15, 1996), has revealed a strong 17 milligal gravity anomaly coincident with the potassium and magnetic anomalies (Fig. 5). Their work also showed a resistivity low in the region of Main, Bowl, and Summit Peak zones (R. Goad, pers. comm., 1996).

In addition to the main Lou Lake anomaly, interesting anomalies occur to the southeast near Burke Lake and to the northwest near Bea Lake (Fig. 2, 3). The Burke Lake anomaly is marked by a moderate increase in potassium, and a pronounced low eTh/K ratio and moderate magnetic response. Near Bea Lake there is a well defined, strong magnetic anomaly, and a coincident K anomaly with a corresponding low eTh/K ratio.

DEPOSIT MODEL AND EXPLORATION IMPLICATIONS

The polymetallic mineral occurrences at Lou Lake are numerous, and collectively define a 3 x 4 km area which is characterized by strong potassic alteration and a high magnetic anomaly. Gandhi and Lentz (1990) interpreted the mineralization as hydrothermal, related to a deep seated granitic pluton. They suggested that the mineralizing solutions moved upwards through the metasedimentary rocks (which include argillaceous beds enriched in metals), scavenged the metals, and redeposited them at the unconformity. The discovery of the large potassium enrichment zone by the airborne radiometric survey further emphasizes the hydrothermal character, and also points to the large size of the mineralizing system. This is illustrated in a combined geological/geophysical cross-section A-B (Fig. 7), which outlines a large potassium and iron enrichment zone associated with the polymetallic mineralization. It may be noted here that the maximum airborne contoured K value of 7% is located a kilometre west of the section.

The above interpretation has several geological and exploration implications. The unconformity between the metasedimentary and volcanic rocks provided a change in physico-chemical environment where metal deposition as seen in the known occurrences was favoured. Fractures and breccia zones, created in part at least by the hydrothermal activity, and possibly the permeable clastic rocks immediately above the unconformity, acted as channelways for the mineralizing solutions. There is some suggestion of lateral zoning, with copper-rich, bismuth-poor occurrences in the northwest compared with bismuth-cobalt-rich occurrences elsewhere in the system. More detailed studies and exploration data are, however, needed to establish this. It is conceivable that strong alkali metasomatism dispersed uranium towards the outer margin of the system as reflected by the airborne radiometric anomaly and a number of small uranium occurrences. It is also probable that there is vertical zoning of the mineralization, and hence the metal association may change with depth. A less intense potassium anomaly on the northwest side of Lou Lake may be an indication of deeper seated mineralization, possibly an extension of the known mineralization which has been down-faulted by a northeast-trending fault along the lake.

The element association, dominated by arsenic and bismuth, is somewhat different than that found at the giant Olympic Dam deposit in South Australia, which contains copper, gold, uranium, and rare-earth elements (Reeve et al., 1990; Gandhi and Bell, 1996). However the abundance of iron as oxide is a common feature. In this regard it is important to note that hematite dominates over magnetite at Olympic Dam, where associated magnetic and gravity anomalies have amplitudes of 1200 nT and 14 mGal respectively (Reeve et al., 1990; Gandhi and Halliday, 1993). The stronger magnetic anomaly of 3000 nT at Lou Lake reflects the relative abundance of magnetite. The main question that arises is how much of it is caused by stratiform magnetite in the host metasedimentary sequence and how much by magnetite introduced during hydrothermal mineralization. Observations to date show that the stratiform magnetite is restricted to thin layers in argillite and siltstone, and no major beds of the size seen at the Ron and Hump Lake deposits are found at Lou Lake. It can be argued that thick magnetite-rich beds exist at depth, presumably tightly folded, to account for the magnetic anomaly. On the other hand there are numerous veins of magnetite, and it is a common mineral in the hydrothermal assemblage here. Some of it occurs as breccia-fillings, and chalcopyrite is closely associated with it, thus showing a close resemblance to the Olympic Dam-type mineralization. It is conceivable that much of the iron in it may have been ultimately derived from the metasedimentary rocks, but this possibility does not detract from the strong capacity of the hydrothermal solutions for dissolution and transportation of iron. A further encouragement in terms of the exploration target is provided by the gravity anomaly of 17 mGal, reported recently by Fortune Minerals Limited, which is coincident with the magnetic and potassium anomalies.

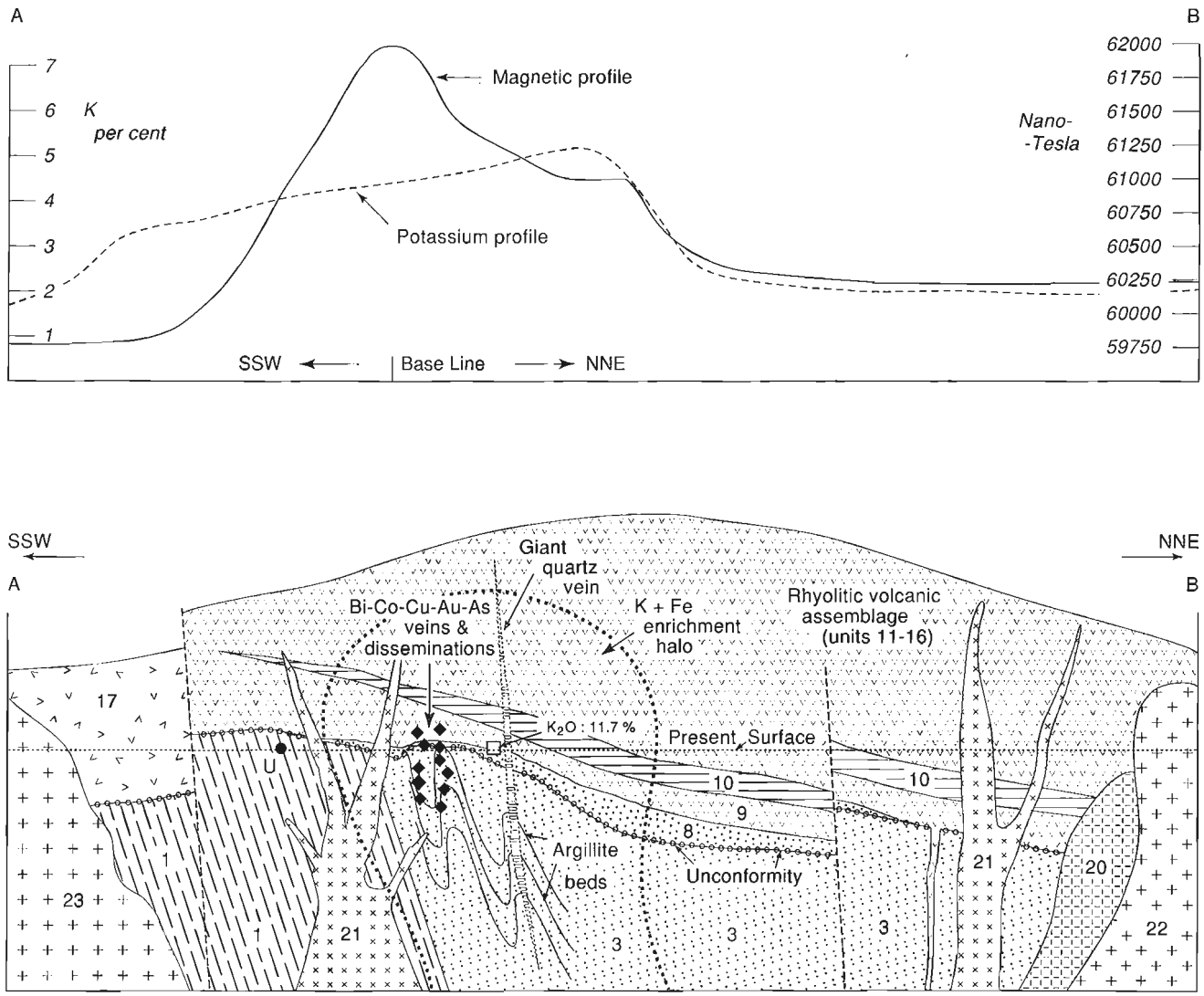

Figure 7. *Geological cross section and corresponding magnetic and potassium profiles along line A-B (Fig. 4, 5); note postulated enrichment halo of K and Fe associated with hydrothermal Bi-Co-Cu-Au-As mineralization, extending above the present surface into the volcanic pile now eroded.*

It is apparent that the metallogenic studies and the airborne survey results have revealed a promising large exploration target. The interpretations presented here at this early stage of exploration are tentative, and will undoubtedly be refined or modified as additional data become available.

ACKNOWLEDGMENTS

The authors thank Robin Goad of Fortune Minerals Limited for the close co-operation and help they received during the fieldwork in 1995, for access to exploration information, and a review of this paper. Derek Mulligan volunteered strenuous fieldwork for a month, and the authors appreciate his assistance as well as discussions on his own field observations made for Fortune Minerals Limited. Dave Webb and Catherine Richards, consulting for GMD Resources Limited, accompanied the group on a few of the traverses, and contributed interesting observations and discussions. The 1993 airborne survey and compilation were conducted by P.B. Holman and R.J. Hetu, respectively, of the Geological Survey of Canada. The manuscript benefited from critical reviews by R.I. Thorpe and R.B.K. Shives of the Geological Survey of Canada.

REFERENCES

Charbonneau, B.W.
1988: Gamma spectrometric and magnetic anomalies associated with Cu-U mineralization, Faber Lake volcanic belt, District of Mackenzie, N.W.T.; in Current Research, Part C; Geological Survey of Canada, Paper 88-1C, p. 255-258.

Charbonneau, B.W., Gandhi, S.S., Hetu, R.J., Holman, P.B., and Prasad, N.
1994: Multiparameter airborne geophysical survey of the Mazenod Lake area and its metallogenic implications (NTS 85N/10 and parts of 85N/11, 14 and 15); in Exploration Overview 1994, Northwest Territories, N.W.T. Geological Mapping Division, Indian and Northern Affairs Canada, p. 26-27.

Galbraith, J.H. and Saunders, D.F.
1983: Rock classification by characteristics of aerial gamma-ray measurements; Journal of Geochemical Exploration, v. 18, p. 49-73.

Gandhi, S.S.
1992: Magnetite deposits in metasiltstones of the Snare Group at Hump Lake, Northwest Territories; in Current Research, Part C; Geological Survey of Canada, Paper 92-1C, p. 225-235.
1994: Geology and genetic aspects of mineral occurrences in the southern Great Bear magmatic zone, Northwest Territories; in Studies of Rare-Metal Deposits in the Northwest Territories, (ed.) W.D. Sinclair and D.G. Richardson; Geological Survey of Canada, Bulletin 475, p. 63-96.

Gandhi, S.S. and Bell, R.T.
1996: Kiruna/Olympic Dam-type iron, copper, uranium, gold, silver; in Geology of Canadian Mineral Deposit Types, (ed.) O.R. Eckstrand, W.D. Sinclair, and R.I. Thorpe; Geological Survey of Canada, Geology of Canada, no. 8, p. 513-522 (also Geological Society of America, The Geology of North America, v. P-1)

Gandhi, S.S. and Halliday, D.
1993: Gravity survey of the Sue-Dianne deposit, Northwest Territories; in Current Research, Part E; Geological Survey of Canada, Paper 93-1E, p. 231-238.

Gandhi, S.S. and Lentz, D.R.
1990: Bi-Co-Cu-Au-As and U occurrences in the Snare Group metasediments and felsic volcanics of the southern Great Bear magmatic zone, Lou Lake, Northwest Territories; in Current Research, Part C; Geological Survey of Canada, Paper 90-1C, p. 239-253.

Gandhi, S.S. and Mortensen, J.K.
1992: 1.87-1.86 Ga old felsic volcano-plutonic activity in southern Great Bear magmatic zone, N.W.T.; in Program with Abstracts, Joint Annual Meeting, Geological Association of Canada-Mineralogical Association of Canada, v. 17, p. A37.

Hetu, R.J., Holman, P.B., Charbonneau, B.W., Prasad, N., and Gandhi, S.S.
1994: Multiparameter airborne geophysical survey of the Mazenod Lake area, Northwest Territories, 1993 (NTS 85N/10 and parts of 85N/11, 14, 15); Geological Survey of Canada, Open File 2806.

Hildebrand, R.S., Hoffman, P.F., and Bowring, S.A.
1987: Tectono-magmatic evolution of the 1.9-Ga Great Bear magmatic zone, Wopmay orogen, northwestern Canada; Journal of Volcanology and Geothermal Research, v. 32, p. 99-118.

Lord, C.S.
1942: Snare River and Ingray Lake map-areas, Northwest Territories; Geological Survey of Canada, Memoir 235, 35 p.

McGlynn, J.C.
1968: Tumi Lake, District of Mackenzie; Geological Survey of Canada, Map 1230A, scale 1:63 360.

Mulligan, D.L.
1995: Proterozoic iron oxide and As-Co-Bi-Cu vein mineralization at the NICO property, N.W.T.; B.Sc. thesis, University of Western Ontario, London, Ontario, 77 p.

Reeve, J.S., Cross, K.C., Smith, R.N., and Oreskes, N.
1990: Olympic Dam copper-uranium-gold-silver deposit; in Geology of the Mineral Deposits of Australia and Papua New Guinea, (ed.) F.E. Hughes; The Australasian Institute of Mining and Metallurgy, Melbourne, p. 1009-1035.

Shives, R.B.K., Ford, K.L., and Charbonneau, B.W.
1995: Applications of gamma ray spectrometry, magnetic/VLF-EM surveys "Workshop Manual"; Geological Survey of Canada, Open File 3061, 82 p.

Geological Survey of Canada Projects 750010, 880029

Electrical characteristics of rock samples from the La Ronge Domain of the Trans-Hudson Orogen, northern Saskatchewan

T.J. Katsube, A.G. Jones[1], N. Scromeda, and P. Schwann[2]
Mineral Resources Division, Ottawa

Katsube, T.J., Jones, A.G., Scromeda, N., and Schwann, P., 1996: Electrical characteristics of rock samples from the La Ronge Domain of the Trans-Hudson Orogen, northern Saskatchewan; in Current Research 1996-E; Geological Survey of Canada, p. 159-169.

Abstract: Electrical resistivities of rock samples (gneiss, greywacke and argillite), obtained from the western part of the La Ronge Domain, were studied to determine the source of elevated electrical conductivities observed deep in the subsurface of the region.

Analyses show that the resistivities of these rocks cover a wide range of values (0.3-2x10^4 Ω·m). While the larger values are typical for these types of rocks, the smaller ones are likely due to layers (thicknesses of about 1-5 mm) of sulphide concentrations. These layers are also a source of significant electrical resistivity anisotropy. These rocks are folded, with sulphide layers accumulated near the hinge of the fold forming a source of high electrical conductivity along its axis. Generally, the resistivities are 3-8 Ω·m in the direction of the fold axis, and 2000-20 000 Ω·m for samples from the host gneissic rock, which gives a bulk anisotropy of 200:1 to 7000:1 for the metasedimentary unit.

Résumé : La résistivité électrique d'échantillons de roches (gneiss, grauwacke et argilite) provenant de la partie ouest du Domaine de La Ronge a été mesurée pour déterminer la source des valeurs élevées de conductivité électrique observées dans les lithologies profondes de la région.

Les analyses indiquent que les valeurs de résistivité de ces lithologies couvrent un large intervalle (de 0,3 x 10^4 Ω·m à 2,0 x 10^4 Ω·m). Les valeurs les plus élevées sont caractéristiques des types de roches susmentionnées; quant aux valeurs faibles, elles sont probablement attribuables à des couches sulfurées (épaisseurs variant entre environ 1 et 5 millimètres). Ces couches sont en outre la source d'une anisotropie significative de la résistivité électrique. Les roches sont plissées et les couches sulfurées sont concentrées près de la charnière du pli, formant une source de conductivité électrique élevée le long de son axe. Généralement, les valeurs de résistivité atteignent 3-8 Ω·m dans la direction de l'axe du pli et 2 000-20 000 Ω·m dans les échantillons provenant de la roche gneissique hôte, ce qui donne une anisotropie apparente de 200:1 à 7 000:1 dans le cas de l'unité métasédimentaire.

[1] Continental Geoscience Division, Ottawa
[2] Saskatchewan Northern Affairs, Box 5000, La Ronge, Saskatchewan S0J 1L0

INTRODUCTION

Brief history of the discovery and early investigations of the NACP anomaly

The North American Central Plains (NACP) anomaly in electrical conductivity was discovered on the edge of an array of magnetometers by Gough and his colleagues in 1967 (Reitzel et al., 1970), and then located in the Black Hills region by a second array study in 1969 (Camfield et al., 1970; Porath et al., 1970, 1971; Gough and Camfield, 1972; Camfield and Gough, 1975). A subsequent magnetometer array in the Dakotas and Saskatchewan in 1972 traced the anomaly through those states and province (Alabi et al., 1975), and two later profiles of magnetometers tracked it through northern Saskatchewan and northern Manitoba (Handa and Camfield, 1984; Gupta et al., 1985; respectively). This curvi-linear feature, which affects natural electromagnetic fields from 10 s periodicity to periods of greater than one cycle per day, is estimated to be of at least 2000 km in length, and possibly connects to conductivity anomalies in Scandinavia (Jones, 1993). As such, it is the largest coherent crustal anomaly of enhanced electrical conductivity yet discovered.

In a bold and intuitive paper, Camfield and Gough (1977) suggested that the NACP was a geophysical expression of a Proterozoic plate boundary buried beneath the Phanerozoic cover of the mid-North American continent. Geological and geochronological investigations, using samples from basement-reaching boreholes (Peterman, 1981; Klasner and King, 1986), and interpretations of potential field maps (Green et al., 1979, 1985; Dutch, 1983; Klasner and King, 1986; Thomas et al., 1987) confirmed this subsurface extrapolation of structures exposed in northern Saskatchewan and Manitoba identified in the mid-1970s as an orogenic zone, termed the Trans-Hudson Orogen (THO) by Hoffman (1981), with a proposed Proterozoic plate boundary in southern Wyoming by Hills et al. (1975).

PanCanadian Oil Co. Ltd. was interested in basement control of sedimentary structures, and contracted a magnetotelluric (MT) survey over the NACP anomaly just north of the U.S./Canadian border in southern Saskatchewan in 1984. Due to the large spatial separation of Alabi et al.'s (1975) magnetometer sites (typically 75 km or greater), the actual position of the anomaly was mislocated, and a second survey farther east was undertaken in 1985 (Jones and Savage, 1986). This showed definitively that the NACP anomaly was located some 75 km east of the position identified by the array study. This view was contended by Maidens and Paulson (1988), but the comment on their paper and interpretation by Jones (1988), who pointed out their errors and stated that the NACP anomaly does indeed lie as detailed by Jones and Savage (1986), went unchallenged. Modeling of the PanCanadian MT data illustrated that the anomalies in electrical conductivity causing the anomaly were in the crust, and were arcuate in form with the centre of the arch being at about 103.25°W in southern Saskatchewan (Jones and Craven, 1990). A second major enhancement was also identified and named the TOBE anomaly because of the along-strike spatial association of aeromagnetic maps with the postulated subsurface extrapolation of the Thompson Belt (Jones and Craven, 1990; Rankin and Pascal, 1990). Two further MT profiles across the anomaly in central Saskatchewan illustrated that it is not a continuous feature, as implied by the magnetometer array work, and that it is displaced some 75 km to the west at around a latitude of 52°N (Jones and Craven, 1990).

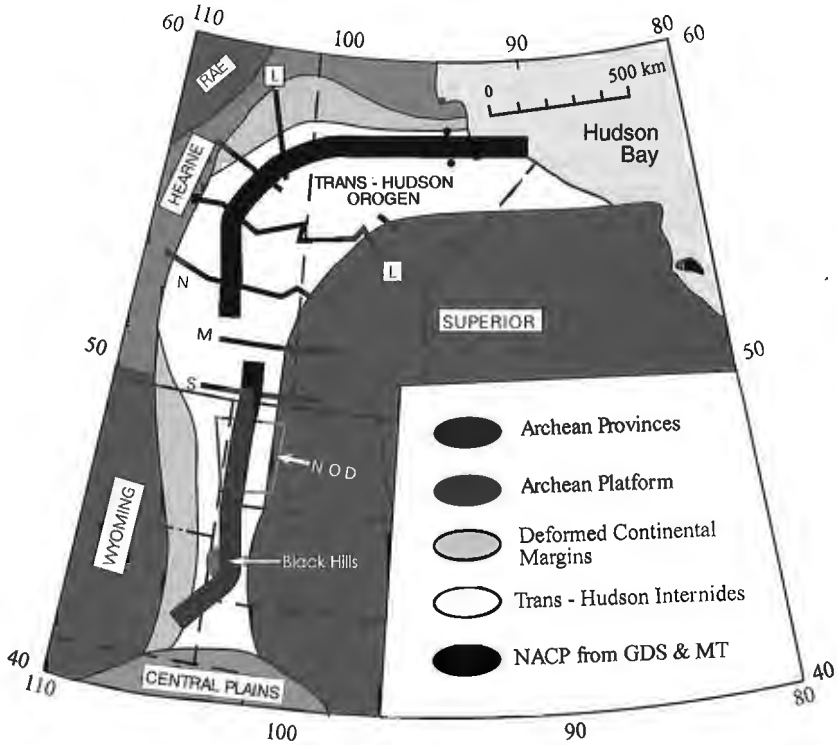

Figure 1.

Cartoon map of basement elements showing the Trans-Hudson Orogen (THO) and the trace of the North American Central Plains (NACP). S, M, N: South, Mid and North Saskatchewan MT profiles of Jones and Craven (1990); NOD: North Dakota MT studies by the University of Washington and the Geological Survey of Canada (unpubl.); L: Lithoprobe MT profiles.

Seismic reflection profiling in northern North Dakota imaged an arcuate non-reflecting deep crustal body with reflecting packages that lay on top of it. These reflecting packages correlated spatially with the locations of the zones of enhanced conductivity imaged by Jones and Craven (1990) just to the north (Nelson et al., 1993).

Figure 1 illustrates the trace of the NACP anomaly from all the above studies together with the generalized basement map of central North America. Note that the NACP lies virtually wholly within the Trans-Hudson Orogen, and is, for the most part, on its western or northern boundary.

Lithoprobe MT studies

Under the auspices of Lithoprobe (Clowes et al., 1993), magnetotelluric experiments have been undertaken on two campaigns. One in 1992 of 110 sites, and the other in 1994 of 30 sites. The 1992 experiment was along a single profile from one bounding craton (Superior to the east) to the other (Rae/Hearne to the west). The lines in Saskatchewan and the lithotectonic elements are shown in Figure 2. The MT data from the western part of the 1992 transect have been analyzed and modelled, and show that the NACP anomaly is associated with the western part of the La Ronge Domain, and that it dips beneath the Rottenstone Domain and the Wathaman Batholith, and ends at the Needle Falls Shear Zone (Jones et al., 1993). The model is illustrated in Figure 3, with the major seismic interfaces, determined from the reflection section, in bold lines.

Cause of enhanced conductivity

The actual cause of the enhanced conductivity in the NACP anomaly has been the subject of speculation since its discovery. Camfield and Gough (Camfield et al., 1970; Gough and Camfield, 1972; Camfield and Gough, 1977), considering the spatial correlation of the southern end of the NACP with graphitic schistose rocks in a belt mapped by Lidiak (1971), suggested that the enhanced conductivity is due to graphite sheets in highly metamorphosed and folded basement rocks. Green et al. (1985) suggested that it is due to partial serpentinization of oceanic mafic and ultramafic rocks at the ridge

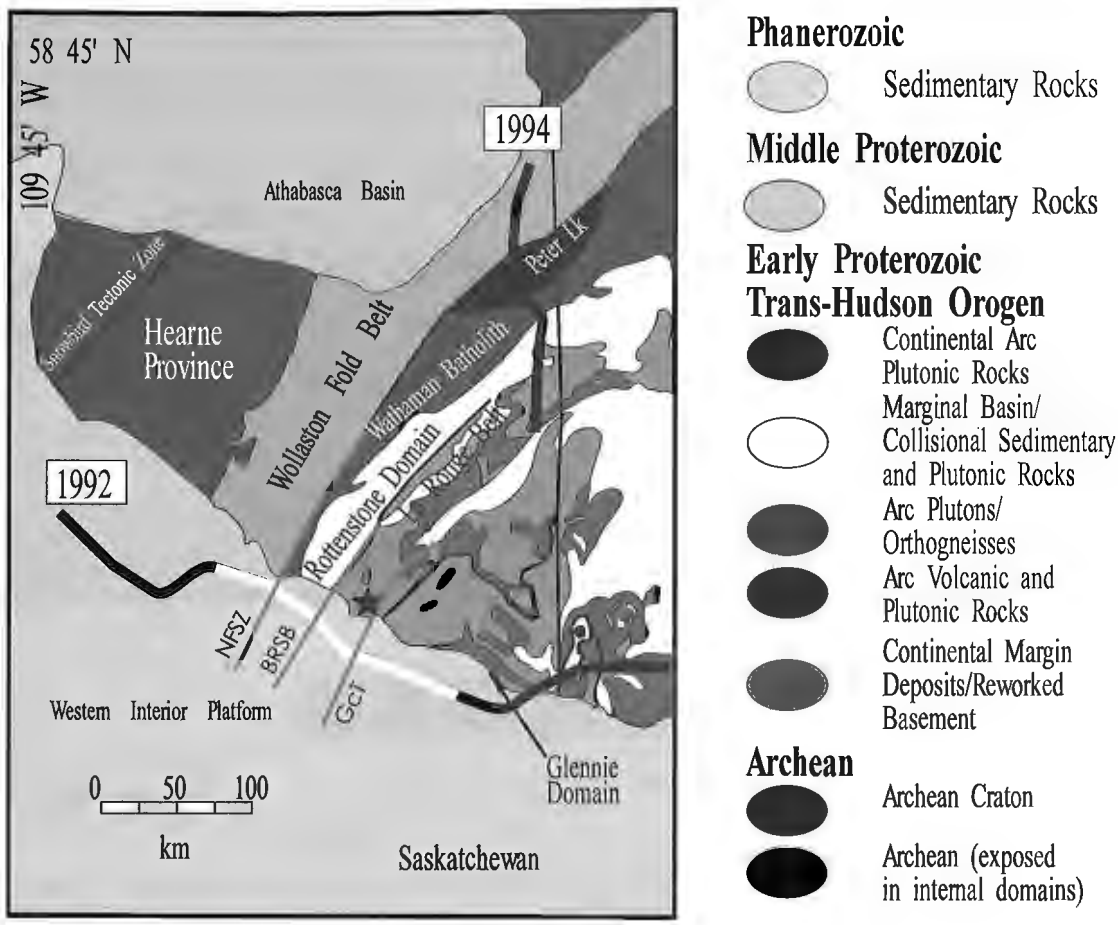

Figure 2. *Lithotectonic elements of the Trans-Hudson Orogran in Saskatchewan. The 1992 and 1994 MT profiles shown as solid lines, with that part of the 1992 profile modelled in Figure 3 in white. NFSZ: Needle Falls Shear Zone; BRSB: Birch Rapids Straight Belt; GcT: Guncoat Thrust. The star indicates the location of the rock samples in Figure 4.*

crest of ancient former oceanic crust, and Handa and Camfield (1984) proposed that it is due to trapped saline water in fractured rocks.

The conclusive spatial correlation of the NACP anomaly with the western La Ronge Domain by the 1992 Lithoprobe MT studies (Jones et al., 1993) gave an opportunity to identify the actual cause of enhanced conductivity. The anomaly is bounded by two high strain packages; the Guncoat Thrust and the Birch Rapids Straight Belt (Fig. 2). Within these packages are the only significant occurrences of graphite in the region (J.F. Lewry, pers. comm., 1993), but the data show that these bounding zones are not conductive compared to the units in between. The rocks within the western La Ronge Domain are mainly granodioritic-granitic gneisses interleaved with minor, discontinuous pelitic to psammitic sedimentary and plutonic rocks (Lewry and Slimmon, 1985), and associated mineralization, with economic deposits of gold, nickel, and copper in disjointed vein and disseminated sulphides, in the metasedimentary sequences. Conductors mapped by airborne electromagnetic surveys (compiled by Standing, 1973) are long, linear features that correlate spatially with surface exposures of the biotitic metasedimentary rocks. These observations led Jones et al. (1993) to associate the NACP anomaly with sulphides in the western La Ronge Belt.

Rock property studies

In order to determine conclusively the source of elevated electrical conductivities observed deep in the subsurface of the region, electrical resistivities of rock samples (gneiss, greywacke, and argillite) obtained from unit Lsn (L=La Ronge; sn=sedimentary), a biotitic metasedimentary unit in the western part of the La Ronge Domain of the Trans-Hudson Orogen, were measured. The electrical resistivity measurements were conducted in all three directions of the samples to ascertain the extent of electrical anisotropy in the rocks, and whether it might be related to the source of these subsurface anomalies. Hand-sample sized specimens were collected from seven locations deemed representative of the unit in the Nemeiben Zone of the western La Ronge Domain (Fig. 4).

METHOD OF INVESTIGATION

Samples and sample preparation

Seven rock samples (gneiss, greywacke, and argillite), each consisting of several sub-samples, and each weighing about 1-10 kg, were collected from the biotitic metasedimentary unit (unit Lsn) in the Nemeiben Zone of the western La Ronge Belt of the Trans-Hudson Orogen, northern Saskatchewan (Fig. 4). Information on their rock type is provided in Tables 1a and 1b. Many contained traces of up to 5 per cent

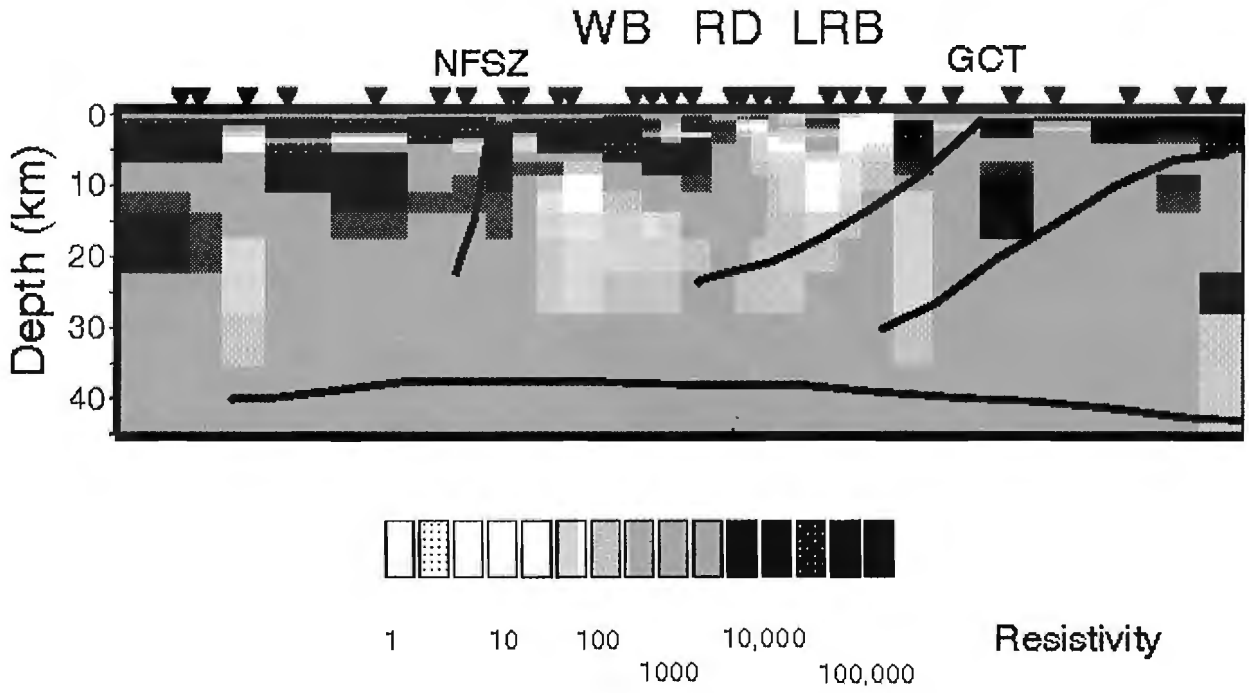

Figure 3. *Resistivity model from the Lithoprobe MT sites just on the Phanerozoic cover from the Glennie Domain to the Rae/Hearne craton (Fig. 2). Vertical exaggeration 1:1. White denotes resistivities <50 Ω·m, whereas black denotes resistivities >1000 Ω·m. The solid lines are from the seismic reflection section showing (a) the presumed projection of the Needle Falls Shear Zone (NFSZ), (b) the Guncoat Thrust (GCT), and (c) the top surface of the Archean microblock of unknown affinity, named the Sask craton. WB=Wathaman Batholith; RD=Rottenstone Domain; LRB=La Ronge Belt.*

Table 1a. Sample locations.

Sample	Location Description
LP94-001	On the Nemeiben Lake road
LP94-002	as LP94-001
LP94-003	as LP94-001
LP94-004	On the north side of English Bay
LP94-005	West side of Contact Lake
LP94-006	East side of MacKay Lake
LP94-007	On the Stanley Mission road close to Sulphide Lake

Table 1b. Sample information (rock type and strike/dip).

Sample	Rock Type	Strike/Dip
LP94-001	Quartz-feldspar-biotite gneiss	160/75SW
LP94-002	Quartz-feldspar-biotite gneiss	168/78SW
LP94-003	Quartz-feldspar-biotite gneiss	168/vert
LP94-004	Quartz-feldspar-muscovite gneiss with muscovite porphyroblasts	20/65SE
LP94-005	Biotite porphyroblastic greywaycke	-
LP94-006	Greywaycke	76/82S
LP94-007	Carbonaceous sulphidic argillite	72/70S

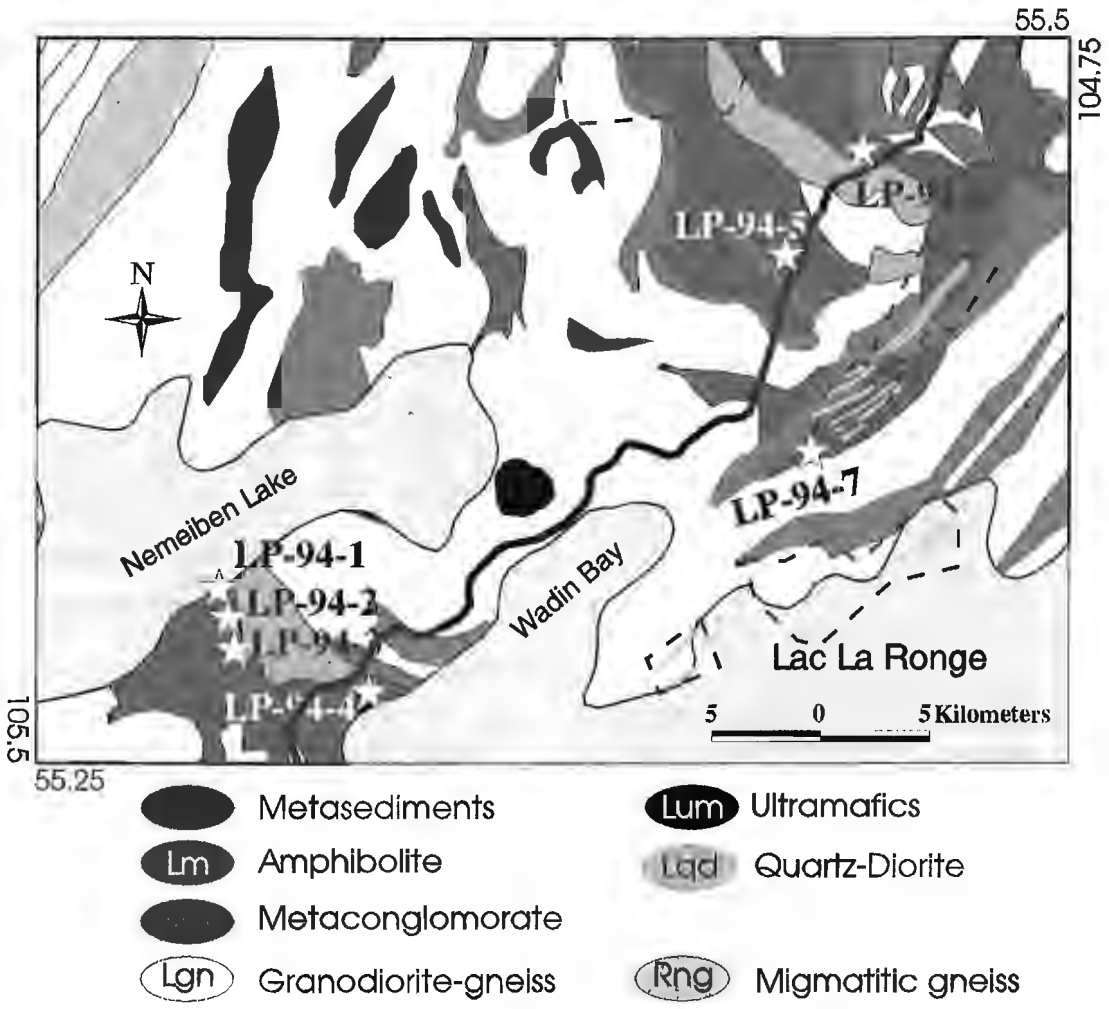

Figure 4. Rock sampling locations. Lsn: Biotitic metasedimentary unit in the La Ronge Domain; Lm: La Ronge amphibolite, hornblende gneiss and schist; Lum: La Ronge ultramafic rocks; Lqd: La Ronge quartz diorite-granodiorite-quartz monzonite-granite; Lgn: Granodiorite-granite complex; Rng: Birch Rapids Strait Belt – Migmatitic gneiss of the Rottenstone Domain. The dashed boxes show the regions where airborne EM observations were flown, and the solid lines indicate the locations of conductors mapped (Standing, 1973).

(estimate) sulphides. These 7 samples are represented by numbers LP94-001 to LP94-007. One to three sub-samples were selected as representative of each sample. In the case of sample LP94-007, the three sub-samples are coded with the letters A, B and C following the seven digit sample numbers. A second series of one to three sub-samples, represented by the letters a, b and c following the 7-8 digit sample or sub-sample numbers, were cut out from each sample or sub-sample. This amounts to a total of 15 sub-samples. One to two specimens were cut out of each sub-sample, one for bulk density (δ) and electrical resistivity (ρ_r) and one for effective porosity (ϕ_E) determinations. Those prepared for bulk density and electrical resistivity measurements were cut into rectangular shapes so that the latter could be measured in all three directions, identified by α, β and γ. Those prepared for effective porosity measurements were either rectangular or irregular in shape. The δ and ρ_r measurements were performed on all 15 sub-samples, and ϕ_E on only 12 of these sub-samples containing no visible sulphides. The geometric characteristics of the specimens used for ρ_r and δ measurements are listed in Tables 2a and 2b. The dimensions are in the range of 1.3-2.2 cm for the rectangular shaped specimens.

Bulk density and effective porosity measurements

The caliper method (API, 1960) has been used to determine the bulk density, δ, of the samples, by measuring the dimensions and weight of the rectangular specimens. This measurement constitutes part of the porosity determining procedure. Effective porosity, ϕ_E, in principle represents the pore volume of all interconnected pores. In this study, it is determined from the difference in weight between the oven-dried and water-saturated rock specimen.

Table 2a. Dimensions of specimens cut out from the samples for electrical measurements.

Sample	a_1 (cm)	a_2 (cm)	ℓ (cm)	W (g)	K_G (10^{-2}m)	δ (g/mL)
LP94-001α	1.741	2.219	1.405	14.5982	2.75	2.69
LP94-001β	1.405	2.219	1.741	14.5982	1.79	2.69
LP94-001γ	1.405	1.741	2.219	14.5982	1.10	2.69
LP94-002aα	1.493	1.744	1.386	9.7645	1.88	2.71
LP94-002aβ	1.386	1.744	1.493	9.7645	1.62	2.71
LP94-002aγ	1.386	1.493	1.744	9.7645	1.19	2.71
LP94-002bα	1.487	1.571	1.617	10.2456	1.45	2.71
LP94-002bβ	1.571	1.617	1.487	10.2456	1.71	2.71
LP94-002bγ	1.487	1.617	1.571	10.2456	1.53	2.71
LP94-003α	2.205	2.242	2.210	29.7555	2.24	2.72
LP94-003β	2.210	2.242	2.205	29.7555	2.25	2.72
LP94-003γ	2.205	2.210	2.242	29.7555	2.17	2.72
LP94-004aα	1.489	2.067	1.167	9.8381	2.64	2.74
LP94-004aβ	1.167	2.067	1.489	9.8381	1.62	2.74
LP94-004aγ	1.167	1.489	2.067	9.8381	0.84	2.74
LP94-004bα	1.589	1.657	1.705	12.2792	1.54	2.74
LP94-004bβ	1.657	1.705	1.589	12.2792	1.78	2.74
LP94-004bγ	1.589	1.705	1.657	12.2792	1.64	2.74
LP94-005α	1.319	2.211	1.753	13.9446	1.66	2.73
LP94-005β	1.753	2.211	1.319	13.9446	2.94	2.73
LP94-005γ	1.319	1.753	2.211	13.9446	1.05	2.73
LP94-006α	1.612	2.251	1.522	15.6995	2.38	2.84
LP94-006β	1.522	2.251	1.612	15.6995	2.13	2.84
LP94-006γ	1.522	1.612	2.251	15.6995	1.09	2.84
LP94-007Aaα	1.644	2.233	1.583	16.0573	2.32	2.76
LP94-007Aaβ	1.583	2.233	1.644	16.0573	2.15	2.76
LP94-007Aaγ	1.583	1.644	2.233	16.0573	1.17	2.76
LP94-007Abα	1.516	2.150	1.808	16.2846	1.80	2.76
LP94-007Abβ	1.808	2.150	1.516	16.2846	2.56	2.76
LP94-007Abγ	1.516	1.808	2.150	16.2846	1.28	2.76
LP94-007Acα	1.619	2.087	1.572	16.6943	2.15	3.14
LP94-007Acβ	1.572	2.087	1.619	16.6943	2.03	3.14
LP94-007Acγ	1.572	1.619	2.087	16.6943	1.22	3.14

a_1, a_2: Length of the two sides of the rectangular specimen.
ℓ: Thickness of specimen.
W: Weight of specimen under room dry conditions.
K_G: Geometric factor.
δ: Bulk density

Table 2b. Dimensions of specimens cut out from the samples for electrical measurements.

Sample	a_1 (cm)	a_2 (cm)	ℓ (cm)	W (g)	K_G (10^{-2}m)	δ (g/mL)
LP94-007Baα	1.785	2.159	1.619	17.0605	2.38	2.73
LP94-007Baβ	1.619	2.159	1.785	17.0605	1.96	2.73
LP94-007Baγ	1.619	1.785	2.159	17.0605	1.34	2.73
LP94-007Bbα	1.824	2.379	1.926	25.1178	2.25	3.01
LP94-007Bbβ	1.926	2.379	1.824	25.1178	2.51	3.01
LP94-007Bbγ	1.824	1.926	2.379	25.1178	1.48	3.01
LP94-007Caα	1.878	2.079	2.267	24.1118	1.72	2.72
LP94-007Caβ	2.079	2.267	1.878	24.1118	2.51	2.72
LP94-007Caγ	1.878	2.267	2.079	24.1118	2.05	2.72
LP94-007Cbα	1.925	2.213	1.591	20.4091	2.68	3.01
LP94-007Cbβ	1.591	2.213	1.925	20.4091	1.83	3.01
LP94-007Cbγ	1.591	1.925	2.213	20.4091	1.38	3.01

a_1, a_2: Length of the two sides of the rectangular specimen.
ℓ: Thickness of specimen.
W: Weight of specimen under room dry conditions.
K_G: Geometric factor.
δ: Bulk density

Table 3. Results of the effective porosity measurements.

Sample	δ (g/mL)	W_W (g)	W_D (g)	S_{ir} (%)	ϕ_E (%)
LP94-001	2.69	7.0147	6.9737	22.4	1.58
LP94-002	2.71	10.0792	9.9948	19.7	2.29
LP94-003	2.72	9.2004	9.1618	17.6	1.15
LP94-004a	2.74	6.5180	6.4977	24.1	0.86
LP94-004b	2.74	7.5839	7.5644	25.1	0.71
LP94-005	2.73	5.6994	5.6557	11.2	2.11
LP94-006	2.84	10.3938	10.3662	27.9	0.76
LP94-007Aa	2.76	6.3161	6.1386	21.7	7.98
LP94-007Ab	2.76	10.2831	10.1036	32.6	4.90
LP94-007Ac	3.14	7.4826	7.4094	51.5	3.10
LP94-007B	3.01	4.7395	4.6970	38.4	2.72
LP94-007C	3.01	7.9944	7.9390	40.1	2.10

W_w = wet weight
δ = bulk density (Equation 2)
S_{ir} = irreducible water saturation
ϕ_E = effective porosity
W_D = dry weight

The API Recommended Practice for Core-Analysis Procedures (API, 1960) has generally been followed in these measurements. The procedures routinely used in our measurements are described in the literature (Katsube and Scromeda, 1991; Katsube et al., 1992a; Scromeda and Katsube, 1994).

Bulk electrical resistivity measurements

The bulk electrical resistivity, ρ_r, is determined from the complex electrical resistivity (ρ^*) measurements made by methods described in recent publications (e.g. Katsube, et al., 1991; Katsube and Salisbury, 1991; Katsube and Scromeda, 1994). ρ^* is measured over a frequency range of 1-10^6 Hz, with ρ_r representing a bulk electrical resistivity at frequencies of about 10^2-10^3 Hz. It is a function of the pore structure and pore fluid resistivity, and is understood to exclude any other effects, such as pore surface, dielectric or any other polarizations (Katsube, 1975; Katsube and Walsh, 1987), including electrode polarization.

Table 4a. Results of electrical resistivity measurements.

Sample	Mes. #1	ρ_r, (10^3 Ωm) Mes. #2	Mean
LP94-001α	5.48	9.64	7.56
LP94-001β	2.03	3.57	2.80
LP94-001γ	1.85	2.97	2.41
LP94-002aα	14.37	14.27	14.32*
LP94-002aβ	11.49	12.29	11.89*
LP94-002aγ	9.51	8.45	8.98*
LP94-002bα	12.41	9.47	10.94*
LP94-002bβ	14.15	12.28	13.22*
LP94-002bγ	12.82	11.72	12.27*
LP94-003α	20.48	21.26	20.87*
LP94-003β	16.40	19.51	17.96
LP94-003γ	14.27	18.22	16.25
LP94-004aα	10.50	10.86	10.68
LP94-004aβ	5.88	6.91	6.40
LP94-004aγ	5.62	6.02	5.82
LP94-004bα	9.41	8.78	9.10
LP94-004bβ	12.71	12.56	12.64*
LP94-004bγ	10.31	10.68	10.50
LP94-005α	13.67	12.83	13.25
LP94-005β	15.06	14.55	14.81
LP94-005γ	8.27	8.59	8.43*
LP94-006α	3.56	3.95	3.76
LP94-006β	4.59	5.21	4.90
LP94-006γ	7.28	9.16	8.22*
LP94-007Aaα	0.020	0.017	0.019
LP94-007Aaβ	0.29	0.28	0.29
LP94-007Aaγ	0.033	0.032	0.033
LP94-007Abα	0.023	0.022	0.023
LP94-007Abβ	0.39	0.25	0.32
LP94-007Abγ	0.050	0.053	0.052
LP94-007Acα	0.0011	0.0009	0.0010
LP94-007Acβ	0.0006	0.0004	0.0005
LP94-007Acγ	0.0003	0.0002	0.0003

ρ_r= Bulk Electrical Resistivity.
Mes. (#1)= Measurement after 24 hours of saturation.
Mes. (#2)= Measurement after 48 hours of saturation.
*= Values determined from slightly distorted complex resistivity plots (Katsube et al., 1992).

EXPERIMENTAL RESULTS

The results of the bulk density (δ) determinations are listed in Tables 2a and 2b. They are in the range of 2.69-3.14 g/mL. The smaller values resemble those of a granitic gneiss (Daly et al., 1966), and the larger ones resemble those of a more basic rock. The results of the effective porosity (ϕ_E) measurements are listed in Table 3, displaying values in the range of 0.76-8.0%. The smaller values are typical of crystalline rocks (Katsube and Mareschal, 1993; Katsube and Scromeda, 1995) and the larger ones resemble those of a relatively competent sedimentary rock (Daly et al., 1966). In general, these porosities are relatively high for a crystalline rock.

The results of the electrical resistivity (ρ_r) measurements are listed in Tables 4a and 4b. Determinations have been made at 24 and 48 hours after water saturation, to ensure that they represent ρ_r values stable with time. Some examples of the complex resistivity plots used to determine the low values of ρ_r are shown in Figure 5. Details of this determination procedure are described elsewhere (e.g. Katsube and Scromeda, 1994). The ρ_r values are in the range of 0.3-2x10^4 Ω·m for these samples, the lower values in the range of rocks containing relatively large amounts of sulphides (Keller, 1982), and the higher values being typical of crystalline rocks (Katsube and Hume, 1987, 1989; Katsube and Mareschal, 1993). Some

Table 4b. Results of electrical resistivity measurements.

Sample	Mes. #1	ρ_r, (10^3 Ωm) Mes. #2	Mean
LP94-007Baα	0.40	0.25	0.33
LP94-007Baβ	1.35	0.60	0.98
LP94-007Baγ	5.74	1.94	3.84
LP94-007Bbα	0.049	0.046	0.048
LP94-007Bbβ	0.14	0.12	0.13
LP94-007Bbγ	0.0079	0.0077	0.0078
LP94-007Caα	0.089	0.076	0.083
LP94-007Caβ	0.89	0.68	0.79
LP94-007Caγ	0.53	0.46	0.50
LP94-007Cbα	0.015	0.014	0.015
LP94-007Cbβ	0.057	0.051	0.054
LP94-007Cbγ	0.0029	0.0032	0.0031

ρ_r= Bulk Electrical Resistivity.
Mes. (#1)= Measurement after 24 hours of saturation.
Mes. (#2)= Measurement after 48 hours of saturation.

complex resistivity plots showed slightly distorted arcs (Fig. 4a and 5a in Katsube et al., 1992b), implying that the ρ_r values obtained using these plots (denoted by an * in Table 4a) are likely to be slightly smaller than the true values.

DISCUSSION

The bulk densities observed (δ = 2.69-3.14 g/mL, Tables 2a and 2b) are not an unexpected range of values for these types of rocks. While the smaller effective porosity (ϕ_E=0.76-8.0%) values are typical of these types of crystalline rocks (Katsube and Mareschal, 1993; Katsube and Scromeda, 1995), the larger ones are not. Particularly, those displaying values above 3.0% (e.g. ϕ_E=4.9-8.0% for samples LP94-007Ab, LP94-007Aa) are unexpected for these rocks. This is probably a result of weathering, particularly of some of the sulphides, that has taken place because of these samples having been at or near the surface.

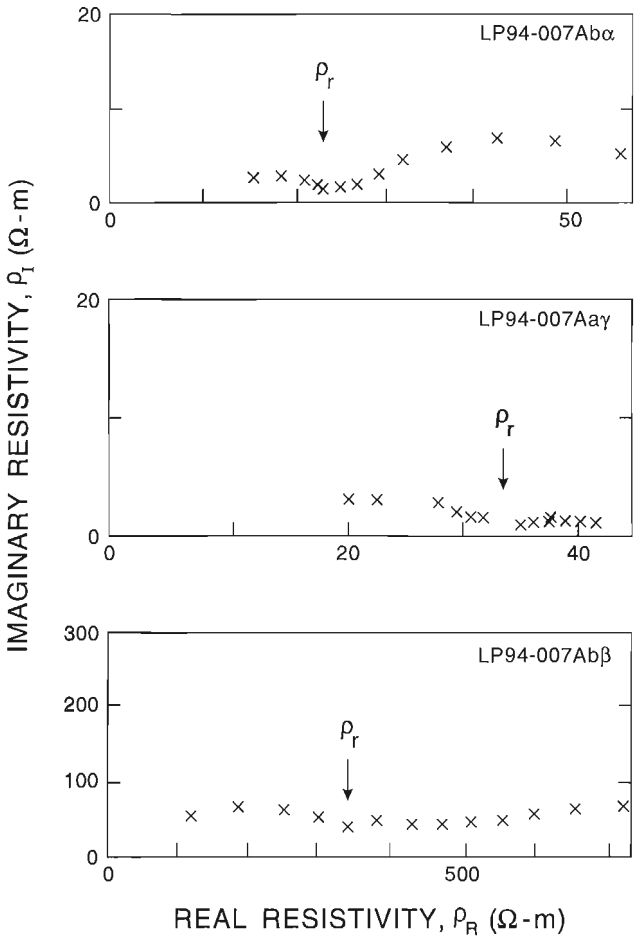

Figure 5. *Typical examples of complex resistivity plots used to determine low bulk electrical resistivity (ρ_r) values. These are examples for samples/specimens PL94-007Abα, PL94-007Aaγ, and PL94-007Abβ. Because of the low resistivities, strong electrode polarization effects (right-most arcs) are seen, but outside the range of influence on ρ_r. The relationship between ρ_I and ρ_R is described in the literature (e.g. Katsube and Walsh, 1987; Katsube et al., 1991, 1992b).*

The bulk electrical resistivities (ρ_r) of these rocks cover a wide range of values (ρ_r=0.3-2x10^4 Ω·m). While the larger values are typical for these types of rocks (Katsube and Mareschal, 1993; Katsube and Hume, 1987, 1989), the smaller values reflect effects of strong electrically conductive paths existing in some or some parts of these rocks. These are due to the visible layers, thicknesses of about 1-5 mm, which contain varied degrees of sulphide concentrations. These layers are a cause of significant electrical resistivity anisotropy, up to about 10:1 to 18:1, as seen in Tables 4a and 4b for samples/specimens LP94-007Ab, LP94-007Ba, LP94-007Bb, and LP94-007Cb.

The low ρ_r values (0.3-1.0 Ω·m) and large anisotropies of these rocks have significant implications on their bulk electrical characteristics. The slice of rock displayed in Figure 6 describes the distribution of layers of sulphide concentrations in sub-samples LP94-007B and LP94-007C. They both are parallel slices cut from sample LP94-007, and represent a cross-section of a folded rock with layers containing sulphides tending to concentrate towards the hinge of the fold. While the sulphide concentrations are not continuous along the folded bedding, they are continuous along the axis of the folding. Three discontinuous layers of sulphide concentrations are seen in this cross-section (Fig. 6), a highly concentrated thick layer (upper left), a highly concentrated thin layer (upper right), and a thick layer (lower section) with a low concentration of sulphides. A second series of three sub-samples (LP94-007Cb, LP94-007Bb, LP94-007Ba) representing these three layers, with very different sulphide concentration characteristics, were cut out of these two slices of rock.

The two second series of sub-samples (LP94-007Cb, LP94-007Bb), representing the highly concentrated layers, indicate resistivities of 3-8 Ω.m in the direction of the axis, and 15-130 Ω·m in the other two directions. If the resistivity values of the sections of the rock barren of sulphides (2000-20 000 Ω·m, Table 4a) are taken into consideration, the electrical model shown in Figure 7 can be constructed. This model represents the rock with folded layers containing highly concentrated sulphides accumulated near the head of the fold. These layers are discontinuous along the folded bedding, but continuous along the axis of the fold. When all the observed resistivity values are taken into consideration, this model suggests resistivities of 3-8 Ω·m in the direction of the axis, and 2000-20 000 Ω·m in the other two directions, an anisotropy of 200:1 to 7000:1. This model suggests an electrical anisotropy that has hitherto not been reported for laboratory studies of rock samples.

CONCLUSIONS

From regional-scale GDS array studies a crustal anomaly in electrical conductivity has been mapped from southern Wyoming through the Dakotas, Saskatchewan and Manitoba

to Hudson Bay. Tectonic and electrical similarities suggest that there may even be a counterpart of this anomaly in Scandinavia (Jones, 1993). As such, this anomaly, termed the North American Central Plains (NACP) anomaly, is arguably the largest yet discovered on Earth. Camfield and Gough's (1977) suggestion that the NACP is a geophysical marker for a Proterozoic continental collision zone has been shown to be correct, and the NACP can be definitively identified with the Paleoproterozoic Trans-Hudson Orogen.

Magnetotelluric studies over the NACP anomaly from the mid-1980s onwards have shown that the anomaly is not a contiguous or continuous feature, but indeed in section comprises discrete bodies of enhanced conductivity, and is broken along its length.

Lithoprobe studies in 1992 and 1994 have definitively correlated the anomaly at those latitudes with units in the western La Ronge Belt, and the only conductive rocks in that belt belong to the metasedimentary unit Lsn. Within that metasedimentary unit, conductors mapped by airborne EM observations are curvi-linear following, in the main, the structural trend of the region (Standing, 1973). Rock samples from that unit show that the only conductive sequences are sulphides concentrated along the hinges of folds. Accordingly, conclusively identified for this part of the NACP anomaly is the conduction mechanism: electronic conduction in concentrated sulphides in the hinges of folds aligned predominantly along the least compressive stress direction.

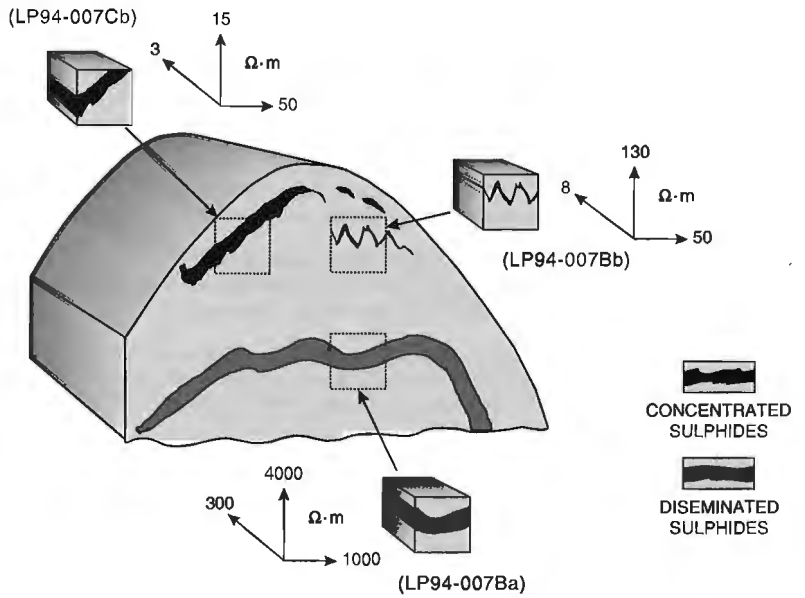

Figure 6.

Schematic representation of a cross-section of sample LP94-007, exemplified by sub-samples LP94-007B and LP94-007C, showing folded layers of sulphide concentrations, and locations from which the second series of sub-samples (LP94-007Cb, LP94-007Bb, LP94-007Ba) were taken. The 3-direction resistivity values of these sub-samples are also displayed.

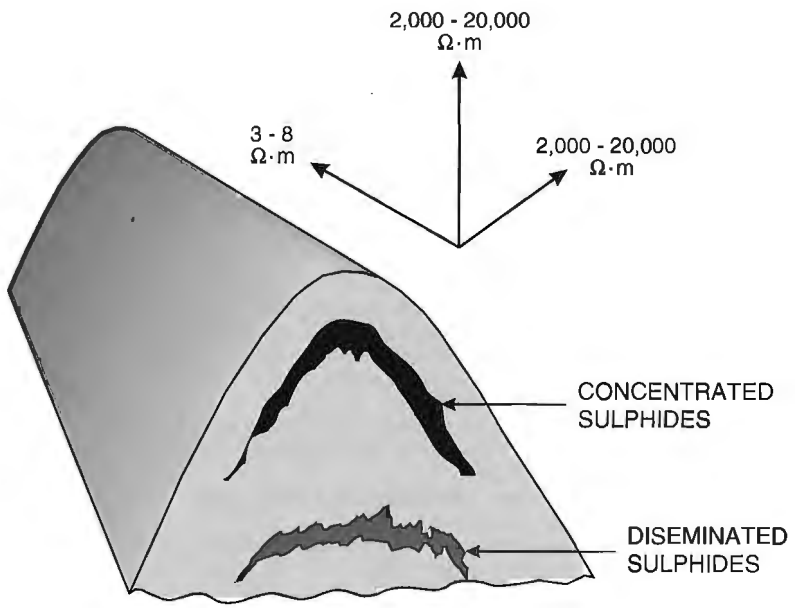

Figure 7.

Electrical model of these rocks, showing folded layers containing highly concentrated sulphides accumulated near the hinge of the fold. This suggests resistivities of 3-8 Ω·m in the direction of the axis, and 2000-20 000 Ω·m in the other two directions, for an anisotropy of 200:1 to 7000:1.

Whether this cause is also operating for the whole length of the anomaly is an open question. The along-strike continuity of the orogen would argue for this being the case. However, the southern terminus of the NACP anomaly, from the Black Hills to southeastern Wyoming (Fig. 1), is likely caused by a different mechanism. Camfield and Gough (1977) noted the spatial correlation of the NACP anomaly at that location with the Hartville Arch, which connects the Black Hills to the Laramie uplift. Within the Hartville Arch are mapped exposures of graphite (Osterwald et al., 1959) and major shear zones and fault systems that continue to the Sierra Madre. Modelling of the GDS responses at the Black Hills shows that the NACP anomaly at that location is both very shallow and highly conductive ($\rho < 1\Omega{\cdot}m$) (Jones and Craven, 1990). Such very low resistivities are necessary to explain that the anomalous horizontal east-west magnetic field is larger than the normal horizontal east-west magnetic field. This part of the conductor also follows the edge of the Wyoming province, rather than within the Trans-Hudson Orogen internides as in the rest of the NACP anomaly. It is possible that the foredeep hypothesis of Boerner et al. (in press) has caused this section of the anomaly. Accordingly, the apparent continuity of the NACP anomaly north and south of the Black Hills could be an artifact of the coarse spatial resolution of the GDS array studies. Rather, there could be two anomalies caused by different conducting mechanisms, one due to sulphides for most of the Trans-Hudson Orogen and one due to graphite at its southern terminus.

ACKNOWLEDGMENTS

The authors are thankful for the critical reviews of this paper by Don White and David Boerner (Geological Survey of Canada).

REFERENCES

API (American Petroleum Institute)
1960: Recommended practices for core-analysis procedure: API Recommended Practice 40 (RP 40) First Edition, American Petroleum Institute, Washington, D.C., p. 55.

Alabi, A.O., Camfield, P.A., and Gough, D.I.
1975: The North American Central Plains anomaly; Royal Astronomical Society Geophysical Journal, v. 43, p. 815-834.

Boerner, D.E., Kurtz, R.D., and Craven, J.A.
in press: Electrical conductivity and Paleoproterozoic foredeeps; Journal of Geophysical Research.

Camfield, P.A. and Gough, D.I.
1975: Anomalies in daily variation magnetic fields and structure under north-western United States and south-western Canada; Geophysical Journal of the Royal Astronomical Society, v. 41, p. 193-218.
1977: A possible Proterozoic plate boundary in North America; Canadian Journal of Earth Sciences, v. 14, p. 1229-1238.

Camfield, P.A., Gough, D.I., and Porath, H.
1970: Magnetometer array studies in the northwestern United States and southwestern Canada; Geophysical Journal of the Royal Astronomical Society, v. 22, p. 201-222.

Clowes, R.M., Cook, F.A., Green, A.G., Keen, C.E., Ludden, J.N., Percival, J.A., Quinlan, G.M., and West, G.F.
1993: Lithoprobe: new perspectives on crustal evolution; Canadian Journal of Earth Sciences, v. 29, p. 1813-1864.

Daly, R.A., Manger, E.G., and Clark, S.P., Jr.
1966: Density of rocks: Section 4; in Handbook of Physical Constants; Geological Society of America, Memoir 97, p. 19-26.

Drury, M.J. and Niblett, E.R.
1980: Buried ocean crust and continental crust geomagnetic induction anomalies: a possible association; Canadian Journal of Earth Sciences, v. 17, p. 961-967.

Dutch, S.I.
1983: Proterozoic structural provinces in the north-central United States; Geology, v. 11, 478-481.

Gough, D.I. and Camfield, P.A.
1972: Convergent geophysical evidence of a metamorphic belt through the Black Hills of South Dakota; Journal of Geophysical Research, v. 77, p. 3168-3170.

Green, A.G., Cumming, G.L., and Cedarwell, D.
1979: Extension of the Superior-Churchill boundary zone into southern Canada; Canadian Journal of Earth Sciences, v. 16, p. 1691-1701.

Green, A.G., Hajnal, Z., and Weber, W.
1985: An evolutionary model of the western Churchill Province and western margin of the Superior Province in Canada and the north-central United States; Tectonophysics, v. 116, p. 281-322.

Gupta, J.C., Kurtz, R.D., Camfield, P.A., and Niblett, E.R.
1985: A geomagnetic induction anomaly from IMS data near Hudson Bay, and its relation to crustal electrical conductivity in central North America; Royal Astronomical Society Geophysical Journal, v. 81, p. 33-46.

Handa, S. and Camfield, P.A.
1984: Crustal electrical conductivity in north-central Saskatchewan: The North American Central Plains anomaly and its relation to a Proterozoic plate margin; Canadian Journal of Earth Sciences, v. 21, p. 533-543.

Hills, F.A., Houston, R.S., and Subbarayudu, G.V.
1975: Possible Proterozoic plate boundary in southern Wyoming; Geological Society of America, Abstracts, v. 7, p. 614.

Hoffman, P.
1981: Autopsy of Athapuscow aulacogen: a failed arm affected by three collisions; in Proterozoic Basins of Canada, (ed.) F.H.A. Campbell; Geological Survey of Canada, Paper 81-10, p. 97-102.

Jones, A.G.
1988: Discussion of A magnetotelluric investigation under the Williston Basin of south-eastern Saskatchewan by J.M. Maidens and K.V. Paulson; Canadian Journal of Earth Sciences, v. 25, p. 1132-1139.
1993: Electromagnetic images of modern and ancient subduction zones; in Plate Tectonic Signatures in the Continental Lithosphere; (ed.) A.G. Green, A. Kroner, H.-J. Gotze and N. Pavlenkova; Tectonophysics, v. 219, p. 29-45.

Jones, A.G. and Craven, J.A.
1990: The North American Central Plains conductivity anomaly and its correlation with gravity, magnetics, seismic and heat flow data in the Province of Saskatchewan; Physics of the Earth and Planetary Interiors, v. 60, p. 169-194.

Jones, A.G. and Savage, P.J.
1986: North American Central Plains conductivity anomaly goes east; Geophysical Research Letters, v. 13, p. 685-688.

Jones, A.G., Craven, J.A., McNeice, G.A., Ferguson, I.J., Boyce, T., Farquarson, C. and Ellis, R.G.
1993: The North American Central Plains conductivity anomaly within the Trans-Hudson orogen in northern Saskatchewan; Geology, v. 21, p. 1027-1030.

Katsube, T.J.
1975: The electrical polarization mechanism model for moist rocks; Report of Activities, Part C; Geological Survey of Canada, Paper 75-1C, p. 353-360.

Katsube, T.J. and Hume, J.P.
1987: Electrical properties of granitic rocks in Lac du Bonnet batholith; in Geotechnical Studies at Whiteshell Research Area (RA-3); CANMET Report MRL 87-52, p. 205-220.

Katsube, T.J. and Mareschal, M.
1993: Petrophysical model of deep electrical conductors; Graphite lining as a source and its disconnection due to uplift; Journal of Geophysical Research, v. 98, B5, p. 8019-8030.

Katsube, T.J. and Salisbury, M.
1991: Petrophysical characteristics of surface core samples from the Sudbury structure; in Current Research, Part E; Geological Survey of Canada, Paper 91-1E, p. 265-271.

Katsube, T.J. and Scromeda, N.
1991: Effective porosity measuring procedure for low porosity rocks; in Current Research, Part E; Geological Survey of Canada, Paper 91-1E, p. 291-297.
1994: Physical properties of Canadian kimberlites; Somerset Island and Saskatchewan; in Current Research 1994-B; Geological Survey of Canada, p. 35-42.
1995: Accuracy of Low Porosity Measurements in Granite; in Current Research 1995-C; Geological Survey of Canada, p. 265-270.

Katsube, T.J. and Walsh, J.B.
1987: Effective aperture for fluid flow in microcracks; International Journal of Rock Mechanics and Mining Sciences and Geomechanics Abstracts, v. 24, p. 175-183.

Katsube, T.J., Best, M.E., and Mudford, B.S.
1991: Petrophysical characteristics of shales from the Scotian shelf; Geophysics, v. 56, p. 1681-1689.

Katsube, T.J., Scromeda, N., and Williamson, M.
1992: Effective porosity of tight shales from the Venture Gas Field, offshore Nova Scotia; in Current Research, Part D; Geological Survey of Canada, Paper 92-1D, p. 111-119.

Katsube, T.J., Scromeda, N., Mareschal, M., and Bailey, R.C.
1992b: Electrical resistivity and porosity of crystalline rock samples from the Kapuskasing Structural Zone; in Current Research, Part E; Geological Survey of Canada, Paper 92-1E, p. 225-236.

Klasner, J.S. and King, E.R.
1986: Precambrian basement geology of North and South Dakota; Canadian Journal of Earth Sciences v. 23, p. 1083-1102.

Keller, G.V.
1982: Electrical properties of rocks and minerals; in Handbook of Physical Properties of Rocks, Vol. I, (ed.) R.S. Carmichael; CRC Press, Inc., Florida, p. 217-293.

Law, L.K. and Riddihough, R.P.
1971: A geographical relation between geomagnetic variation anomalies and tectonics; Canandian Journal of Earth Sciences, v. 8, p. 1094-1106.

Lewry, J.F. and Slimmon, W.L.
1985: Compilation bedrock geology, Lac La Ronge NTS area 73P/73I; Saskatchewan Energy and Mines, Report 225 (1:250 000 scale map with marginal notes)

Lidiak, E.G.
1971: Buried Precambrian rocks of South Dakota; Geological Society of America Bulletin, v. 82, p. 1411-1420.

Maidens, J.M. and Paulson, K.V.
1988: A magnetotelluric investigation under the Williston Basin of southeastern Saskatchewan; Canadian Journal of Earth Sciences, v. 25, p. 60-67.

Nelson, K.D., Baird, D.J., Walters, J.J., Hauck, M., Brown, L.D., Oliver, J.E., Ahern, J.L., Hajnal, Z., Jones, A.G., and Sloss, L.L.
1993: Trans-Hudson orogen and Williston basin in Montana and North Dakota: New COCORP deep profiling results; Geology, v. 21, p. 447-450.

Osterwald, F.W., Osterwald, D.B., Long, J.S., and Wilson, W.H.
1959: Mineral resources of Wyoming; Geological Survey of Wyoming, Bulletin 50, p. 86-87.

Peterman, Z.E.
1981: Dating of Archean basement in northeastern Wyoming and southern Montana; Geological Society of America Bulletin, v. 92, p. 139-146.

Porath, H., Gough, D.I., and Camfield, P.A.
1971: Conductive structures in the northwestern United States and southwest Canada; Geophysical Journal of the Royal Astronomical Society, v. 23, p. 387-398.

Porath, H., Oldenburg, D.W., and Gough, D.I.
1970: Separation of magnetic variation fields and conductive structures in the western United States; Geophysical Journal of the Royal Astronomical Society, v. 19, p. 237-260.

Rankin, D. and Pascal, F.
1990: A gap in the North American Central Plains conductivity anomaly; Physics of the Earth and Planetary Interiors, v. 60, p. 132-137.

Rankin, D. and Reddy, I.K.
1973: Crustal conductivity anomaly under the Black Hills: a magnetotelluric study; Earth and Planetary Science Letters, v. 20, p. 275-279.

Reitzel, J.S., Gough, D.I., Porath, D.I., and Anderson III, C.W.
1970: Geomagnetic deep sounding and upper mantle structure in the western United States; Geophysical Journal of the Royal Astronomical Society, v. 19, p. 213-235.

Scromeda, N. and Katsube, T.J.
1994: Effect of temperature on drying procedures used in porosity measurements of tight rocks; in Current Research 1994-E; Geological Survey of Canada, p. 283-289.

Standing, K.F.
1973: Lac La Ronge conductivity anomaly locations 1:250 000 map; Saskatchewan Energy and Mines, Regina, map 73P.

Thom, A., Arndt, N.T., Chauvel, C., and Stauffer, M.
1990: Flin-Flon and Western La Ronge belts, Saskatchewan: Products of Proterozoic subduction-related volcanism; in The Early Proterozoic Trans-Hudson Orogen of North America, (ed.) J.F. Lewry and M.R. Stauffer; Geological Association of Canada, Special Paper 37, p. 163-176.

Thomas, M.D., Sharpton, V.L., and Grieve, R.A.F.
1987: Gravity patterns and Precambrian structure in the North American Central Plains; Geology, v. 15, p. 489-492.

Geological Survey of Canada Project 870057

Petrophysical characteristics of diatreme-facies kimberlites from Kirkland Lake, Ontario

T.J. Katsube, M.B. McClenaghan, and N. Scromeda
Mineral Resources Division, Ottawa

Katsube, T.J., McClenaghan, M.B., and Scromeda, N., 1996: Petrophysical characteristics of diatreme-facies kimberlites from Kirkland Lake, Ontario; in Current Research 1996-E; Geological Survey of Canada, p. 171-178.

Abstract: Electrical resistivity (ρ_r), effective porosity (ϕ_E) and bulk density (δ_B) have been measured on nine diatreme-facies kimberlite samples and six limestone samples from the Kirkland Lake area. One purpose of this study is to provide data required for interpretation of surface and airborne geophysical survey data. Another purpose is to determine if physical characteristics can distinguish between limestone xenoliths contained in these kimberlites and the source rock of the xenoliths.

Results indicate that the values for δ_B (2.3-2.5 g/mL), ϕ_E (13-25%) and ρ_r (30-470 Ω·m) for these kimberlites are generally within the reported range for Canadian kimberlites, and are similar to those of the crater facies kimberlites. This implies relatively low δ_B and ρ_r, and relatively high ϕ_E values. The values of δ_B (2.2-2.8 g/mL), ϕ_E (4-22%) and ρ_r (30-1.2 x 10^4 Ω·m) for the limestones are generally within the reported range. The only limestone xenolith measured displays the largest ϕ_E and smallest ρ_r values among the limestones.

Résumé : Des mesures de résistivité électrique (ρ_r), de porosité efficace (ϕ_E) et de masse volumique apparente (δ_B) ont été prises sur neuf échantillons de kimberlite à faciès de diatrème et sur six échantillons de calcaire provenant de la région de Kirkland Lake (Ontario). L'un des objectifs de la présente étude est de recueillir des données nécessaires à l'interprétation de levés géophysiques terrestres et aéroportés. De plus, elle vise à déterminer si les caractéristiques physiques peuvent servir à distinguer les xénolites de calcaire contenus dans ces kimberlites et la roche mère des xénolites.

Les résultats indiquent que les valeurs de δ_B (2,3-2,5 g/mL), de ϕ_E (13-25 %) et ρ_r (30-470 Ω·m) des échantillons de kimberlite sont généralement comprises dans l'intervalle indiqué pour les kimberlites canadiennes et sont semblables à celles des kimberlites à faciès de cratère. Cela suppose, d'une part, des valeurs relativement faibles de δ_B et de ρ_r et, d'autre part, des valeurs relativement élevées de ϕ_E. Les valeurs de δ_B (2,2-2,8 g/mL), de ϕ_E (4-22 %) et de ρ_r (30-1,2 x 10^4 Ω·m) des calcaires sont généralement situées dans l'intervalle indiqué. Le seul xénolite de calcaire sur lequel des mesures ont été effectuées affiche les valeurs les plus élevées de ϕ_E et les valeurs les plus faibles de ρ_r parmi les calcaires.

INTRODUCTION

Objectives of the study

Bulk electrical resistivity, ρ_r, effective porosity, ϕ_E, and bulk density, δ_B, measurements were made on nine diatreme-facies kimberlite and six limestone samples from the Kirkland Lake area in Ontario. One purpose of this study is to provide data to enable the physical property characterization of Canadian diatreme-facies kimberlites, to assist in the interpretation of surface and airborne geophysical survey data. Although a reasonable amount of petrophysical data exists, including bulk electrical resistivity (ρ_r) data, on Canadian hypabyssal and crater-facies kimberlites in the literature (e.g. Katsube et al., 1992a; Katsube and Scromeda, 1994; Scromeda et al., 1994; Richardson et al., 1995), there is a lack of such data for Canadian diatreme facies kimberlites.

The Kirkland Lake kimberlites, generally, contain considerable numbers of limestone xenoliths. A second purpose of this study is to determine if the physical properties of the xenolith and original Ordovician and Silurian limestones are different. Bulk electrical resistivity (ρ_r) was measured in three orthogonal directions, for these limestone samples, in order to determine if any electrical anisotropy related to the limestone bedding existed.

Geology of the Kirkland Lake kimberlite field

The Kirkland Lake kimberlite field is in the western part of the Abitibi Greenstone Belt (Fig. 1), in the Superior Province of the Canadian Shield, approximately 10 km north and east of Kirkland Lake and 100 km southeast of Timmins (McClenaghan, 1993, 1996). Kimberlites intruded into Archean metavolcanic and metasedimentary rocks during the Late Jurassic (160 to 155 Ma) (Brummer et al., 1992), and are blue-grey to grey-brown diatreme facies heterolithic tuffisitic kimberlite breccia. The groundmass consists of serpentine, phlogopite, chlorite, and calcite and varies from light to medium greenish-grey. Wallrock fragments of greenish-grey to white Paleozoic carbonate fragments are common, ranging in size from 1 cm to 1 m. The carbonate xenoliths indicate that Paleozoic rocks were present at this site during magma intrusion. Today, the nearest Paleozoic carbonate rocks are 40 km south of Kirkland Lake. Most of the known kimberlite pipes have distinct circular magnetic signatures (Ontario Geological Survey, 1979; Brummer et al., 1992; Geological Survey of Canada, 1993; Keating, 1995).

Kimberlite, being relatively soft, has been differentially eroded by preglacial and glacial erosion such that kimberlite pipes usually subcrop 20 to 50 m below the surrounding bedrock surface. Many deeply eroded kimberlites in the Lac de Gras kimberlite field in the Northwest Territories are detectable because they are now very deep lake basins. The Kirkland Lake kimberlites, in contrast, have been completely covered with thick sequences of glacial sediment and therefore have no surface expression. As a result, indicator mineral tracing combined with airborne geophysical surveys are used to explore for kimberlite in this area.

The kimberlite samples used in this study were obtained from four pipes: B30, C14, A4, and Diamond Lake (DL), as indicated in Table 1 and Figure 1. The B30 pipe appears to be the most weathered of the four pipes examined, with the

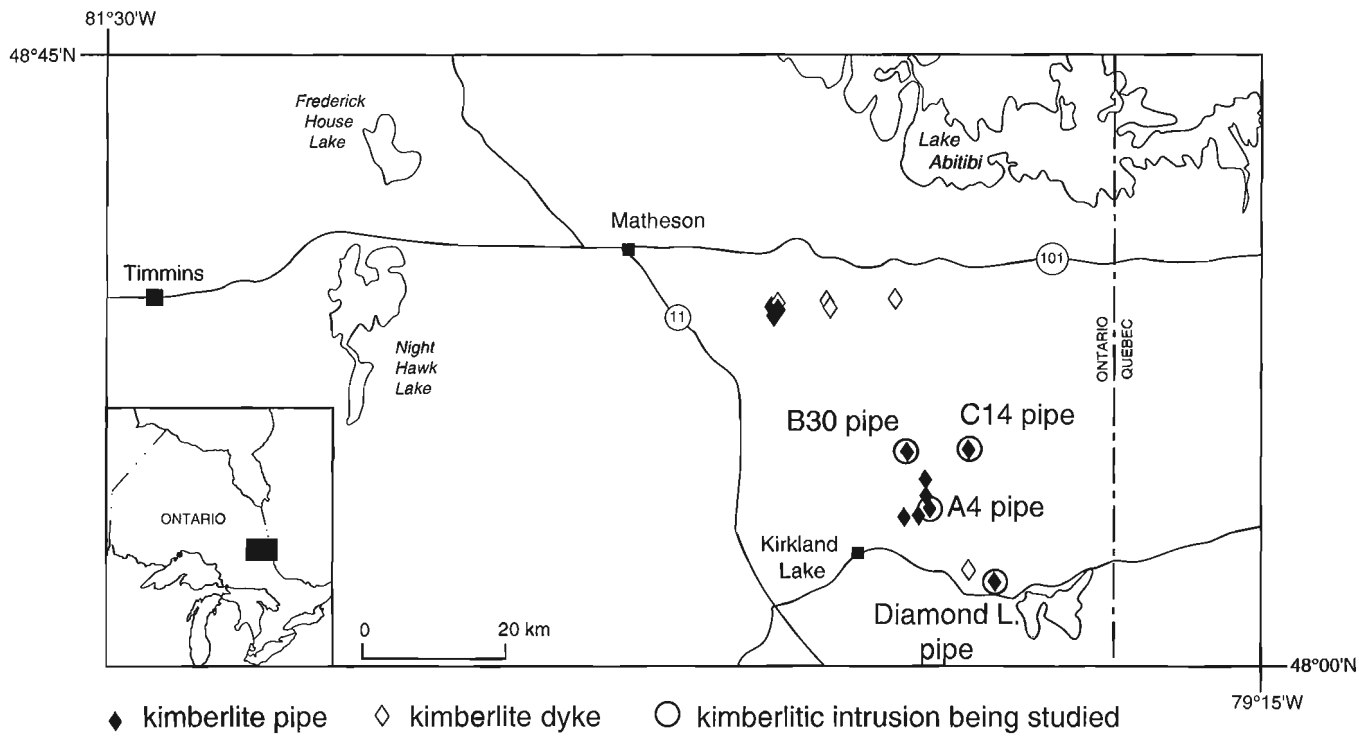

Figure 1. *Kimberlite pipe location map.*

matrix being weathered to a blue-grey clay. The core crumbles when cut open. The Diamond Lake and A4 pipes appear to be the least weathered, with the core being solid and hard.

METHOD OF INVESTIGATION

Method of sample collection

The uppermost 10 m of the A4, C14, and B30 kimberlite pipes were cored by the Geological Survey of Canada using a rotasonic overburden drill to obtain 9 cm diameter core. Samples for this study were collected at selected intervals in the drill core. The 4 cm diamond-drill core samples of kimberlite (Drillholes FL91-14 and FL92-23, Table 1) from the Diamond Lake pipe were collected by Sudbury Contact Mines Ltd. Six samples of Paleozoic limestone were collected from the nearest outcrops, approximately 40 km south of Kirkland Lake, for comparison to Paleozoic xenoliths in the kimberlite.

Samples and sample preparation

The nine kimberlite samples (KLM-1 to KLM-3 and KLH-1 to KLH-6) were drill cores, of 4 to 9 cm in diameter and 5 to 20 cm in length. The six (2 Ordovician and 4 Silurian) limestone samples (KLD-1 to KLD-6) were hand samples, of about 4x4x4 to 6x6x6 cm in dimensions. At least two specimens were cut from each of these core and hand samples, a rectangular one for bulk electrical resistivity (ρ_r) and bulk density (δ_B) measurements, and an irregularly shaped specimen for effective porosity (ϕ_E) measurements. Kimberlite sample KLM-1 was split into two sub-samples, one representing a limestone xenolith (KLM-1A) and the other (KLM-1B) representing the rest of the kimberlite section of the sample. These were then cut into the two or more specimens. Sample information, including field identification numbers and rock type are listed in Table 1. The geometric characteristics of the specimens used for electrical and bulk density measurements are listed in Table 2. The specimen dimensions are in the range of (1.1-2.3) x (1.3-2.3) cm for the cross-section, and 0.7-2.3 cm for thickness. The geometric factor (K_G), listed in Table 2, is a parameter derived from the specimen dimensions, and is used in the bulk electrical resistivity (ρ_r) determination (Katsube and Salisbury, 1991).

Bulk density and effective porosity measurements

The caliper method (API, 1960) has been used to determine the bulk density, δ_B, of the samples, by measuring the dimensions and weight of the rectangular specimens. This measurement constitutes part of the porosity determining procedure. Effective porosity, ϕ_E, in principle represents the pore volume of all interconnected pores. In this study, it is determined from the difference in weight between the oven-dried and water-saturated rock specimen. The API Recommended practice for core-analysis procedures (API, 1960) has generally been followed in these measurements. The procedures routinely used in our measurements are described in the literature (Katsube and Scromeda, 1991; Katsube et al., 1992b; Scromeda and Katsube, 1994).

Bulk electrical resistivity measurements

The bulk electrical resistivity, ρ_r, is determined from the complex electrical resistivity, ρ^*, measurements made by methods described in recent publications (e.g. Katsube and Scromeda, 1994; Katsube et al., 1991; Katsube and Salisbury, 1991).

Table 1. Kimberlite and limestone sample information.

Sample Number	Sample I.D.	Pipe	Drill Hole	Depth (m) DFS	Depth (m) DTKS	Rock Type
KLM-1A		B30	B30-10	45.0	41.0	LS Xenolith
KLM-1B		B30				KB
KLM-2		C14	C14-05	38.9	34.0	KB
KLM-3		A4	A4-01	61.0	51.0	KB
KLH-1		DL	DDH FL91-14	73	53.3	KB
KLH-2		DL	DDH FL91-14	191	53.3	KB
KLH-3		DL	DDH FL91-14	332	53.3	KB
KLH-4		DL	DDH FL92-23	108	53.3	KB
KLH-5		DL	DDH FL92-23	124	53.3	KB
KLH-6		DL	DDH FL92-23	135	53.3	KB
KLD-1	DKA-94-28B			0		LS
KLD-2	DKA-94-32E			0		LS
KLD-3	DKA-94-34D			0		LS
KLD-4	DKA-94-36H			0		LS
KLD-5	DKA-94-39B			0		LS
KLD-6	DKA-94-43			0		LS

DL = Diamond Lake Pipe (Fig. 1).
LS = Limestone.
DFS = Depth of sample from earth surface.
DTKS = Depth to kimberlite subcrop surface from earth surface.

Complex electrical resistivity (ρ^*) is measured over a frequency range of 1 to 10^6 Hz, with ρ_r representing a bulk electrical resistivity at frequencies of about 10^2 to 10^3 Hz. It is a function of the pore structure and pore fluid resistivity, and is understood to exclude any other effects, such as pore surface, dielectric or any other polarizations (Katsube, 1975; Katsube and Walsh, 1987).

EXPERIMENTAL RESULTS

The results of the bulk density (δ_B) determinations are listed in Tables 2 and 3. The δ_B values for the kimberlites are in the range of 2.3 to 2.5 g/mL. These values are on the lower end of those previously reported (2.2 to 3.2 g/mL) for Canadian kimberlites (Scromeda et al., 1994; Katsube and Scromeda, 1994), and resemble those of crater facies kimberlites. The δ_B values for the limestones are in the range of 2.4 to 2.8 g/mL, or 2.2 to 2.8 g/mL if the xenolith sample (KLM-1A) is included. This range of values is slightly wider than that (2.58 to 2.66 g/mL) normally accepted for limestones (Daly et al., 1966).

The results of the effective porosity (ϕ_E) measurements are listed in Table 3. The ϕ_E values for these diatreme facies kimberlites are in the range of 13 to 25%, well within the range (1.8 to 27%) of those previously reported (Katsube and Scromeda, 1994; Scromeda et al., 1994) for Canadian hypabyssal and crater facies kimberlites. The ϕ_E values for the limestone are in the range of 3.8 to 16%, or 3.8 to 22% if the limestone xenolith (KLM-1A) is included. These values are also within the range (0.4 to 26%) of those generally accepted for limestones (Daly et al., 1966).

The bulk electrical resistivity (ρ_r) values are listed in Table 4. Measurements have been made at 24 and 48 hours after saturation, to ensure that they represent ρ_r values stable with time. Typical examples of the complex resistivity measurements used to determine ρ_r are shown in Figures 2 and 3. Some complex resistivity plots (e.g. sample KLD-6aß)

Table 2. Dimensions of specimens cut out from the Kimberlite samples for electrical measurements.

Sample	a_1 (cm)	a_2 (cm)	ℓ (cm)	W (g)	V (cm^3)	K_G (10^{-2}m)	δ_B (g/mL)
KLM-1Aa	1.509	1.841	0.694	4.2968	1.93	4.00	2.23
KLM-1Ba	1.816	2.088	1.495	13.4467	5.67	2.54	2.37
KLM-2	1.929	1.961	1.175	11.0611	4.44	3.22	2.49
KLM-3	1.615	2.125	0.885	7.6054	3.04	3.88	2.50
KLH-1a	1.324	1.571	1.067	5.3503	2.2	1.95	2.41
KLH-2a	1.178	1.569	1.037	4.7705	1.9	1.78	2.49
KLH-3a	1.212	1.340	1.176	4.5692	1.9	1.38	2.39
KLH-4a	1.247	1.877	0.906	5.2966	2.1	2.58	2.50
KLH-5a	1.320	1.370	1.084	4.4989	2.0	1.67	2.29
KLH-6a	1.382	1.707	1.071	6.4292	2.5	2.20	2.54
KLD-1aα	1.411	1.541	1.083	6.5270	2.4	2.01	2.77
KLD-1aβ	1.083	1.541	1.411	6.5270	2.4	1.18	2.77
KLD-1aγ	1.083	1.411	1.541	6.5270	2.4	0.992	2.77
KLD-2aα	1.342	1.382	1.182	6.1276	2.2	1.57	2.80
KLD-2aβ	1.182	1.382	1.342	6.1276	2.2	1.22	2.80
KLD-2aγ	1.182	1.342	1.382	6.1276	2.2	1.15	2.80
KLD-3aα	2.347	2.283	1.855	26.3337	9.9	2.89	2.65
KLD-3aβ	1.855	2.347	2.283	26.3337	9.9	1.91	2.65
KLD-3aγ	1.855	2.283	2.347	26.3337	9.9	1.80	2.65
KLD-4aα	1.813	2.060	1.586	14.5254	5.9	2.35	2.45
KLD-4aβ	1.586	2.060	1.813	14.5254	5.9	1.80	2.45
KLD-4aγ	1.586	1.813	2.060	14.5254	5.9	1.40	2.45
KLD-5aα	1.715	2.340	1.474	15.4291	5.9	2.72	2.61
KLD-5aβ	1.474	2.340	1.715	15.4291	5.9	2.01	2.61
KLD-5aγ	1.474	1.715	2.340	15.4291	5.9	1.08	2.61
KLD-6aα	1.212	2.278	1.501	20.5206	7.6	3.36	2.71
KLD-6aβ	1.501	2.212	2.278	20.5206	7.6	1.46	2.71
KLD-6aγ	1.501	2.278	2.212	20.5206	7.6	1.55	2.71

a_1, a_2 : Length of the two sides of the rectangular specimen.
ℓ : Thickness of specimen.
W : Weight of specimen under room dry conditions.
V : Volume of specimen.
K_G : Geometric factor.
δ_B : Bulk density

showed slightly distorted arcs (Fig. 3b), similar to Figures 4a and 5a in Katsube et al. (1992b), implying that the ρ_r values obtained using these plots (denoted by an * in Table 4) are likely to be slightly smaller than the true values.

The ρ_r values for these diatreme kimberlites are in the range of 30 to 470 Ω·m, values in the lower end of those (10 to 6.2 x 10^4 Ω·m) previously reported for Canadian hypabyssal and crater facies kimberlites (Katsube and Scromeda, 1994; Scromeda et al., 1994). The ρ_r values for these limestones (xenolith included) are in the range of 34 to 1.2 x 10^4 Ω·m, a range of values commonly accepted (50 to 10^5 Ω·m, Keller, 1966) for these type of rocks. The limestone ρ_r values for the three directions (α, ß, γ) are also listed in Table 4. Some of the limestone samples (KLD-6 and KLD-3) show relatively strong electrical resistivity anisotropies (λ_ρ), which are in the range of 1.8:1 to 3.6:1. The electrical resistivity anisotropy (λ_ρ) is the ratio of the maximum ρ_r value, of the three orthogonal directions, over the minimum ρ_r value.

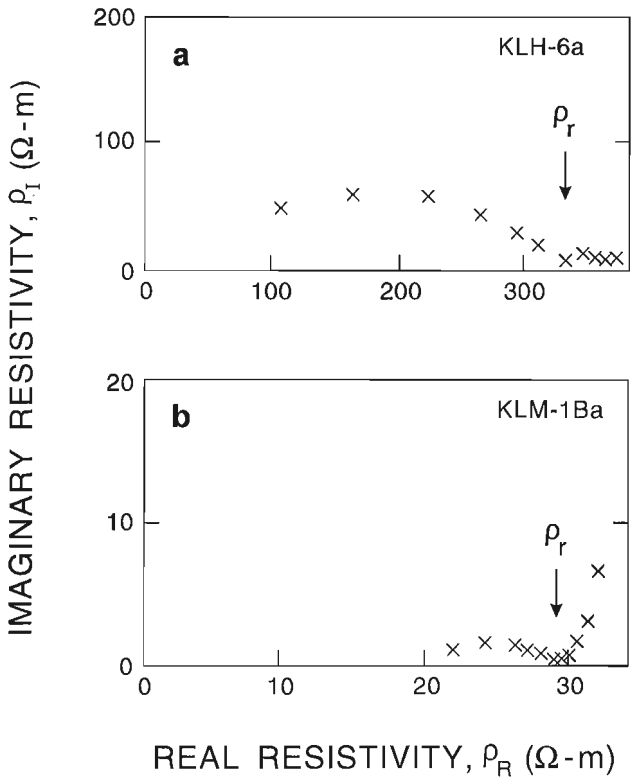

Figure 2. *Typical examples of complex resistivity (ρ^*) plots used to determine bulk electrical resistivity (ρ_r), **a)** for the imaginary resistivity (ρ_I) as function of real resistivity (ρ_R), of sample KLH-6a, displaying a normal to slightly suppressed arc, a pattern usually seen in rocks with intermediate resistivity, and **b)** for sample KLM-1Ba displaying a strongly suppressed arc with strong electrode polarization effects showing on its right hand side, a pattern usually seen in rocks with low resistivity.*

Table 3. Results of the effective porosity measurements.

Sample	δ_B (g/mL)	W_w (g)	W_D (g)	S_{ir} (%)	ϕ_E (%)
KLM-1Ab	2.23	2.1140	1.9271	7.1	21.63
KLM-1Bb	2.37	10.4189	9.4312	18.4	24.82
KLM-2	2.49	6.2125	5.8923	16.0	13.53
KLM-3	2.50	9.5317	8.9638	21.6	15.84
	2.41	4.9777	4.5816	5.5	20.84
KLH-1b	2.49	5.1852	4.8272	12.7	18.47
KLH-2b	2.39	5.7910	5.3244	4.2	20.94
KLH-3b	2.50	5.1995	4.7236	8.6	25.19
KLH-4b	2.29	5.2925	4.8772	7.2	19.50
KLH-5b	2.54	4.5208	4.1897	13.4	20.07
KLH-6b	2.77	4.7782	4.7110	14.3	3.95
KLD-1b	2.80	5.4292	5.3439	6.7	4.47
KLD-2b	2.65	13.1967	13.0110	6.6	3.78
KLD-3b	2.45	9.1203	8.5653	5.7	15.88
KLD-4b	2.61	9.5838	9.1618	2.3	12.02
KLD-5b	2.71	10.8024	10.6244	3.3	4.54
KLD-6b					

W_w = wet weight; W_D = dry weight; S_{ir} = irreducible water saturation; δ_B = bulk density; ϕ_E = effective porosity

DISCUSSIONS AND CONCLUSIONS

The results for all four parameters – bulk density (δ_B), effective porosity (ϕ_E), bulk electrical resistivity (ρ_r), and electrical resistivity anisotropy (λ_ρ) – are compiled in Table 5 for 16 kimberlite and limestone samples or sub-samples. The values of δ_B (2.3 to 2.5 g/mL), ϕ_E (13 to 25%) and ρ_r (30 to 470 Ω·m) for the kimberlites are generally within the reported range of values, 2.2 to 3.2 g/mL, 2 to 27% and 10 to 6 x 10^4 Ω·m, respectively, for Canadian kimberlites (Katsube and Scromeda, 1994; Scromeda et al., 1994). These kimberlites display petrophysical characteristics similar to those of the crater facies kimberlites, showing relatively low δ_B and ρ_r values, and relatively high ϕ_E values. The values of δ_B (2.2 to 2.8 g/mL), ϕ_E (4 to 22%), and ρ_r (30 to 1.2 x 10^4 Ω·m) for these limestones are generally within the reported range of values, 2.58 to 2.66 g/mL, 0.4 to 26%, and 50 to 5 x 10^5 Ω·m, respectively, given for limestones (Daly, et al., 1966). Two of these limestone samples show relatively strong electrical resistivity anisotropy (λ_ρ), of 1.8:1 and 3.6:1.

Effective porosity (ϕ_E) as a function of bulk electrical resistivity (ρ_r) is shown in Figure 4, for both the kimberlites and limestones. A relationship between the two parameters appears to exist for both rock types, with the variation of ϕ_E with ρ_r being larger for the limestones. The directional variation of ρ_r (represented by the horizontal bar in Fig. 4), or λ_ρ, tends to be larger for the limestones that show smaller values

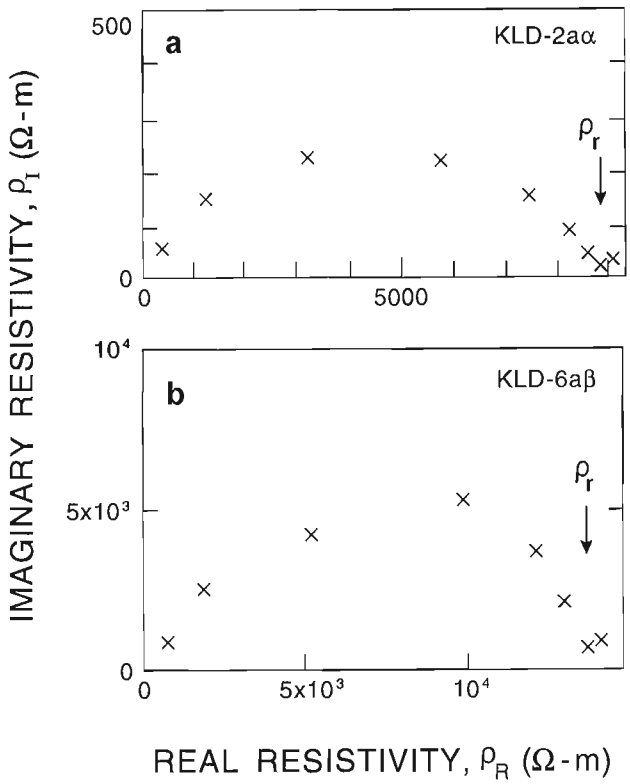

*Figure 3. Typical examples of complex resistivity (ρ^*) plots used to determine bulk resistivity (ρ_r), **a)** for the imaginary resistivity (ρ_I) as function of real resistivity (ρ_R), of sample KLD-2aα displaying a normal arc, a pattern usually seen in high resistivity rocks, and **b)** for sample KLD-6aβ displaying a slightly distorted arc, a pattern usually seen in very high resistivity rocks.*

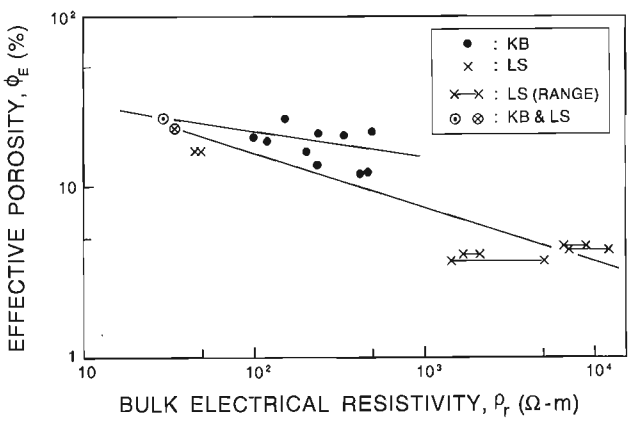

Figure 4. Effective porosity (ϕ_E) as a function of bulk electrical resistivity (ρ_r) for both the kimberlites (KB), represented by "•" in the figure, and limestones (LS), represented by "x". The limestone xenolith and the kimberlite host (sample KLM-1) are represented by "⊗" and "⊙", respectively, in the figure.

of ϕ_E, or larger values of ρ_r. The ϕ_E values for the kimberlites are generally larger than those for the limestones. The limestone xenolith displays the largest ϕ_E and smallest ρ_r values among the limestones. However, as the kimberlite sample that contained the xenolith also shows the largest ϕ_E and smallest ρ_r values among the kimberlites, it is not clear whether the large ϕ_E and small ρ_r values of the xenolith are due to the alteration process that it experienced or due to the ϕ_E and ρ_r characteristics of the kimberlite host. A systematic limestone xenolith study that is currently underway should provide more information.

Table 4. Results of electrical resistivity measurements.

Sample	ρ_r, (10^3 Ω·m) Mes. #1	Mes. #2	Mean**
KLM-1Aa	0.032	0.036	0.034
KLM-1Ba	0.028	0.029	0.029
KLM-2	0.21	0.22	0.22
KLM-3	0.20	0.19	0.20
KLH-1a	0.21	0.25	0.23
KLH-2a	0.11	0.12	0.12
KLH-3a	0.41	0.52	0.47
KLH-4a	0.15	0.15	0.15
KLH-5a	0.093	0.10	0.097
KLH-6a	0.33	0.33	0.33
KLD-1aα	1.87	2.31	2.09
KLD-1aβ	1.50	2.03	1.77
KLD-1aγ	1.50	1.80	1.65
KLD-2aα	8.73	9.24	8.99
KLD-2aβ	5.97	6.55	6.26
KLD-2aγ	5.70	7.17	6.44
KLD-3aα	1.38	1.41	1.40
KLD-3aβ	1.41	1.48	1.45
KLD-3aγ	4.79	5.37	5.08
KLD-4aα	0.042	0.048	0.045
KLD-4aβ	0.048	0.050	0.049
KLD-4aγ	0.043	0.047	0.045
KLD-5aα	0.42	0.49	0.46
KLD-5aβ	0.39	0.44	0.42
KLD-5aγ	0.43	0.46	0.45
KLD-6aα	5.70	7.96	6.83
KLD-6aβ	10.95	13.77	12.36*
KLD-6aγ	6.54	8.52	7.53

ρ_r = Bulk Electrical Resistivity.
Meas. (#1) = Measurement after 24 hours of saturation.
Meas. (#2) = Measurement after 48 hours of saturation.
*: Value determined from a slightly distorted complex resistivity arc (Katsube et al., 1992b), implying that this ρ_r value is likely to be slightly smaller than the true value.
**: Since the ρ_r values decrease immediately after saturation, it is necessary to make at least two measurements, reasonable timed apart, to ensure a stable value has been reached. Equal, or a larger value for the second ρ_r measurement, most likely, implies that stability has been reached.

Table 5. Summary of petrophysical properties.

Sample	Rock Type	δ_B (g/mL)	ϕ_E (%)	ρ_r (10^3 Ω·m)	λ_ρ
KLM-1A	LS Xenolith	2.23	21.63	0.034	
KLM-1B	Kimberlite	2.37	24.82	0.029	
KLM-2	Kimberlite	2.49	13.53	0.22	
KLM-3	Kimberlite	2.50	15.84	0.20	
KLH-1	Kimberlite	2.41	20.84	0.23	
KLH-2	Kimberlite	2.49	18.47	0.12	
KLH-3	Kimberlite	2.39	20.94	0.47	
KLH-4	Kimberlite	2.50	25.19	0.15	
KLH-5	Kimberlite	2.29	19.50	0.097	
KLH-6	Kimberlite	2.54	20.07	0.33	
KLD-1	Limestone	2.77	3.95	1.7-2.1	1.24
KLD-2	Limestone	2.80	4.47	6.3-9.0	1.43
KLD-3	Limestone	2.65	3.78	1.4-5.1	3.64
KLD-4	Limestone	2.45	15.88	0.045-0.049	1.09
KLD-5	Limestone	2.61	12.02	0.42-0.46	1.10
KLD-6	Limestone	2.71	4.54	6.8-12.4	1.82

LS = Limestone
δ_B = Bulk Density
ϕ_E = Effective Porosity
ρ_r = Bulk Electrical Resistivity
λ_ρ = Electrical Resistivity Anisotropy

ACKNOWLEDGMENTS

The authors are grateful to Sudbury Contact Mines Ltd. and Regal Goldfields Ltd. for providing the kimberlite samples and allowing access to their property. D.K. Armstrong (Ontario Geological Survey) provided the limestone samples from the Englehart area. The authors acknowledge support for this study from the Canada-Ontario Subsidiary Agreement on Northern Development (1991-95), a part of the Canada-Ontario Economic and Regional Development Agreement. The authors are thankful for the critical review of this paper by K.A. Richardson (Geological Survey of Canada).

REFERENCES

API (American Petroleum Institute)
1960: Recommended practices for core-analysis procedure; API Recommended Practice 40 (RP 40) First Edition, American Petroleum Institute, Washington, D.C., p. 55.

Brummer, J.J., MacFadyen, D.A., and Pegg, C.C.
1992: Discovery of kimberlites in the Kirkland Lake area, Northeastern Ontario, Part II: Kimberlite discoveries, sampling, diamond content, ages and emplacement; Exploration and Mining Geology, v. 1, p. 351-370.

Daly, R.A., Manger, E.G., and Clark, S.P. Jr.
1966: Density of rocks: Section 4; in Handbook of Physical Constants; Geological Society of America, Memoir 97, p. 19-26.

Geological Survey of Canada
1993: Magnetic anomaly map (Residual Total Field), Blake River Syncline, Ontario, parts of NTS 42A/1, 42A/8, 32D/4, 32D/5; Geological Survey of Canada, Maps C20369G and C203770G, scale 1:50 000.

Katsube, T.J.
1975: The electrical polarization mechanism model for moist rocks; in Report of Activities, Part C; Geological Survey of Canada, Paper 75-1C, p. 353-360.

Katsube, T.J. and Salisbury, M.
1991: Petrophysical characteristics of surface core samples from the Sudbury structure; in Current Research, Part E; Geological Survey of Canada, Paper 91-1E, p. 265-271.

Katsube, T.J. and Scromeda, N.
1991: Effective porosity measuring procedure for low porosity rocks; in Current Research, Part E; Geological Survey of Canada, Paper 91-1E, p. 291-297.
1994: Physical properties of Canadian kimberlites; Somerset Island and Saskatchewan; in Current Research, 1994-B; Geological Survey of Canada, p. 35-42.

Katsube, T.J. and Walsh, J.B.
1987: Effective aperture for fluid flow in microcracks; International Journal of Rock Mechanics and Mining Sciences and Geomechanics Abstracts, v. 24, p. 175-183.

Katsube, T.J., Best, M.E., and Mudford, B.S.
1991: Petrophysical characteristics of shales from the Scotian shelf; Geophysics, v. 56, p. 1681-1689.

Katsube, T.J., Scromeda, N., Bernius, G., and Kjarsgaard, B.A.
1992a: Laboratory physical property measurements of kimberlites; in Current Research, Part E; Geological Survey of Canada, Paper 92-1E, p. 357-364.

Katsube, T.J., Scromeda, N., Mareschal, M., and Bailey, R.C.
1992b: Electrical resistivity and porosity of crystalline rock samples from the Kapuskasing Structural Zone, Ontario; in Current Research, Part E; Geological Survey of Canada, Paper 92-1E, p. 225-236.

Keating, P.
1995: A simple technique to identify magnetic anomalies due to kimberlite pipes; Exploration and Mining Geology, v. 4, p. 121-126.

Keller, G.V.
1966: Electrical properties of rocks and minerals; in Handbook of Physical Constants, (ed.) S.P. Clark, Jr.; Geological Society of America, Memoir 97, p. 553-577.

McClenaghan, M.B.
1993: Location of known kimberlite bedrock, float and indicator minerals in drift in the Kirkland Lake area; Geological Survey of Canada, Open File 2636, scale 1:100 000.
1996: Kimberlite glacial dispersal studies near Kirkland Lake; in NODA Summary Report 1995-1996, Natural Resources Canada and Ministry of Northern Development and Mines, p. 50-55.

Ontario Geological Survey
1979: Airborne electromagnetic and total intensity magnetic survey, Kirkland Lake area, Bisley Township, District of Cochrane; Ontario Geological Survey, Maps P.2252, P.2253, P.2258, and P.2259, scale 1:20 000.

Patnode, H.W. and Wyllie, M.R.J.
1950: The presence of conductive solids in reservoir rocks as a factor in electric log interpretation; Transactions of the American Institute of Mining, Metallurgical and Petroleum Engineers, v. 189, p. 47-52.

Richardson, K.A., Katsube, T.J., Mwenifumbo, T.J., Killeen, P.G., Hunter, J.A.M., Gendzwill, D.J., and Matieshin, S.D.
1995: Geophysical studies of kimberlites in Saskatchewan; in Investigations Completed by the Saskatchewan Geological Survey and the Geological Survey of Canada under the Geoscience Program of the Canada-Saskatchewan Partnership Agreement on Mineral Development (1990-1995), (ed.) D.G. Richardson, Geological Survey of Canada, Open File 3119 (Saskatchewan Geological Survey Open File Report 95-3), p. 197-205.

Scromeda, N. and Katsube, T.J.
1994: Effect of temperature on drying procedures used in porosity measurements of tight rocks; in Current Research 1994-E, Geological Survey of Canada, p. 283-289.

Scromeda, N., Katsube, T.J., Bernius, G., and Kjarsgaard, B.A.
1994: Physical properties of Canadian kimberlites from Fort a la Corne, Saskatchewan; in Current Research 1994-E, Geological Survey of Canada, p. 171-175.

Geological Survey of Canada Project 870057

Eastern Canada and National and General Programs

Est du Canada et programmes nationaux et généraux

Groundwater prospects in the Oak Ridges Moraine area, southern Ontario: application of regional geological models[1]

D.R. Sharpe, L.D. Dyke, M.J. Hinton, S.E. Pullan, H.A.J. Russell[2], T.A. Brennand[3], P.J. Barnett[4], and A. Pugin[5]

Terrain Sciences Division, Ottawa

Sharpe, D.R., Dyke, L.D., Hinton, M.J., Pullan, S.E., Russell, H.A.J., Brennand, T.A., Barnett, P.J., and Pugin, A., 1996: Groundwater prospects in the Oak Ridges Moraine area, southern Ontario: application of regional geological models; in Current Research 1996-E; Geological Survey of Canada, p. 181-190.

Abstract: A geological model is presented for the glacial deposits of the Oak Ridges Moraine area of southern Ontario. The model contains four units as well as incised channels dissecting the strata. Channels eroded through the Newmarket Till, a regional aquitard, provide hydraulic connection between the aquifers of the overlying Oak Ridges Moraine and those of the underlying lower drift. Buried channels filled with silt, sand, and gravel, and preferentially oriented north-northeast-south-southwest, are indicated by drill core and seismic reflection profiles. The model, with two successful case studies, has significant implications for groundwater resource development in the Greater Toronto Area. Groundwater flow to the lower drift may occur through channels so that groundwater resources in the lower drift may be more productive than previously suggested. Gravel sequences within channels may be targets for high yield wells. Further investigations are required to examine buried channel locations, distribution, and sediment fill.

Résumé : Un modèle géologique montrant comment s'organisent les dépôts glaciaires de la région de la moraine d'Oak Ridges (partie sud de l'Ontario) est présenté dans le présent article. Le modèle tient compte de quatre unités de même que des chenaux découpant les couches. Les chenaux érodés traversant le till de Newmarket, un aquitard régional (couche semi-perméable), servent de connexion hydraulique entre les aquifères de la moraine d'Oak Ridges et ceux des sédiments glaciaires inférieurs. Les chenaux enfouis sont remplis de silt, de sable et de gravier et leur orientation préférentielle est NNE-SSW. Les carottes de forage et les profils de sismique réflexion corroborent l'existence de ces chenaux. Le modèle, selon lequel deux aquifères ont été identifiés, a des répercussions importantes sur la mise en valeur des eaux souterraines régionales dans le Toronto métropolitain. Il se peut que l'écoulement des eaux souterraines vers les sédiments glaciaires inférieurs emprunte les chenaux; ainsi, les ressources en eaux souterraines dans les sédiments glaciaires inférieurs pourraient être plus abondantes que prévu. Les séquences de gravier dans les chenaux pourraient être des cibles pour des puits à débit élevé. Des travaux supplémentaires sont nécessaires pour étudier l'emplacement des chenaux enfouis, la répartition des unités et la nature des sédiments de remplissage.

[1] Oak Ridges Moraine NATMAP Project

[2] University of Ottawa, Ottawa, Ontario
[3] Simon Fraser University, Burnaby, British Columbia
[4] Ontario Geological Survey, Sudbury, Ontario
[5] University of Geneva, Geneva, Switzerland

INTRODUCTION

The Oak Ridges Moraine (Fig. 1) and underlying sediments form an aquifer complex which supplies large amounts of potable water within the Greater Toronto Area. In 1993, the Geological Survey of Canada (GSC) began a three year regional hydrogeological study of the Oak Ridges Moraine to understand the extent of, and the geological controls on, the groundwater resource. The complex geology of the Oak Ridges Moraine area requires use of innovative subsurface investigations, including geophysical surveys and database syntheses. The study has relied heavily on co-operation from provincial government ministries, planning and engineering departments of all the Greater Toronto Area regional municipalities, consulting firms, and universities.

This paper presents a geological model for the Oak Ridges Moraine area. The stratigraphic model presented is used to define the major hydrostratigraphic elements and their influence on regional hydrogeology (Fig. 2). A case history involving the development of a high-yield municipal well is also presented, along with strategies for conducting future searches for similar high-yield water supplies.

WATER RESOURCE ISSUES IN THE GREATER TORONTO AND OAK RIDGES MORAINE AREAS

Adequate water supplies are essential and are an important consideration in planning from the residential to the national scale. On a regional scale, the Greater Toronto Area has to date had sufficient water supplies to enable large population growth without suffering major water shortages, although short-term water supply problems have been experienced in smaller communities.

In the Regional Municipality of York, for example, water is supplied from three major sources: Lake Ontario (76% of total supply in 1991) in the south, groundwater (21%) in the central and northwestern region, and Lake Simcoe (3%) in the northeastern region (Regional Municipality of York, 1993). Even with water conservation measures, long-term projections indicate that water demand will continue to grow. Groundwater has proven to be a reliable and economical resource, but the size of the resource is not well known. Stream baseflow into Lake Simcoe is not adequate to meet water supply needs for the region. Various options for supplying water by pipeline from Lake Ontario or from Georgian

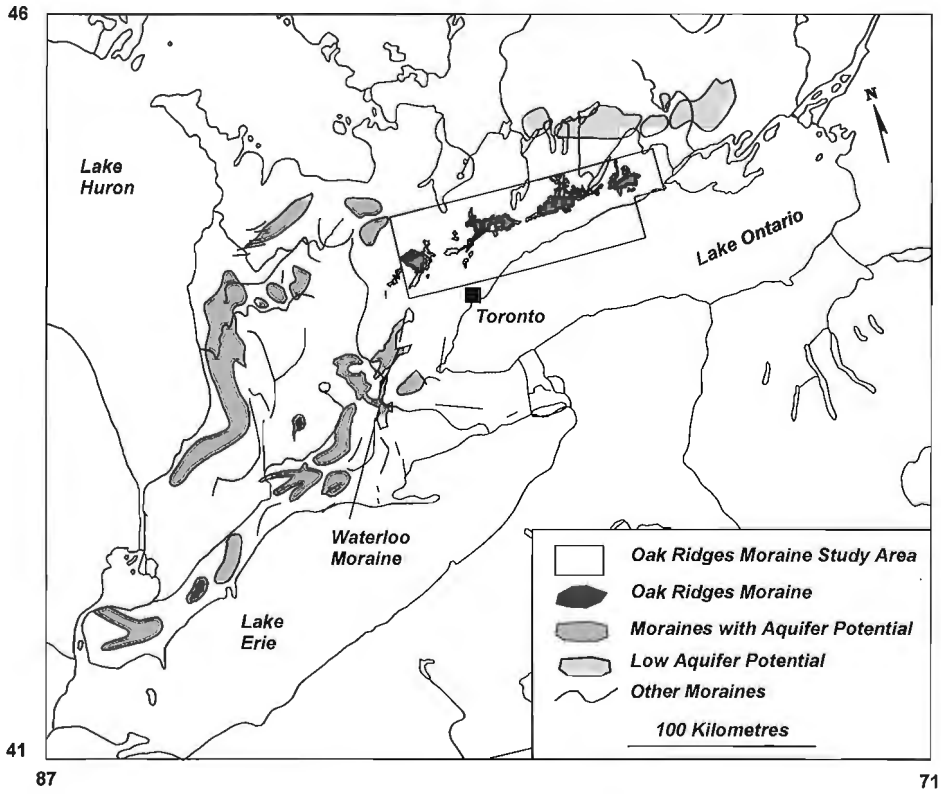

Figure 1. *Moraines of southern Ontario. (Digital file modified from Fulton, 1995).*

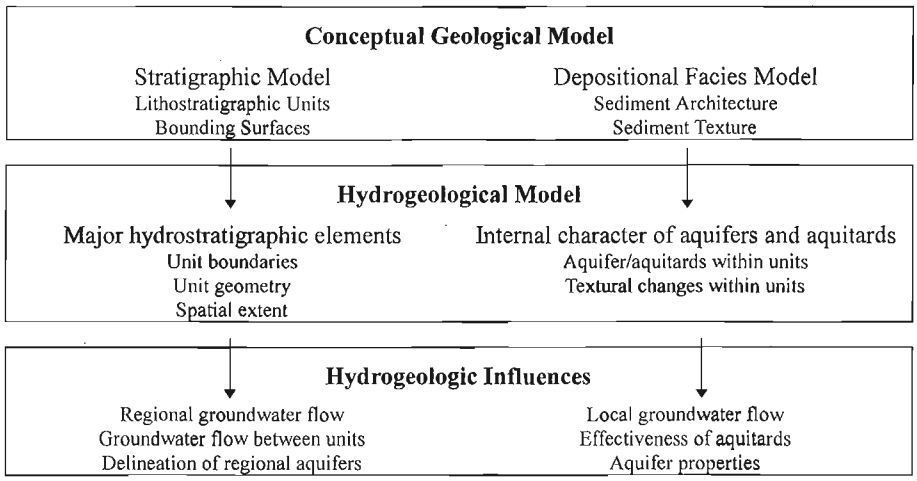

Figure 2. *Components of the geological and resulting hydrogeological model.*

Table 1. Investigative techniques used by the Oak Ridges Moraine project for aquifer delineation.

	Investigative Techniques		Application
Surface	Remote Sensing & GIS	Thematic mapper	Soil moisture, land cover,
		Spot	Image enhancement
		ERS-1	Soil moisture
		RADARSAT	Soil moisture
		Thermography	Spring locations
		Digital Elevation Model	Landscape / basin modelling / datum
	Mapping	Field sites	Detailed sediment characterization
		Stream gauging	Discharge
		Stream chemistry	Hydrogeology
Subsurface	Drilling	Sediment description	Geology
		Piezometer installations	Hydrogeology
	Geophysics	Reflection seismic	Stratigraphy / architecture
		Ground penetrating radar	Water table, structures
		EM-34, 47	Stratigraphy
		Gravity	Depth to bedrock
		Borehole	Physical properties
	Archival Boreholes	MOEE water wells	Geology, water levels
		Geotechnical	Geology, water levels
		Interim Waste Authority	Geology, hydrogeology

Bay are presently being considered. However, pipeline infrastructure is expensive and is estimated to cost approximately $550 million (Regional Municipality of York, 1993) without considering the high operational and maintenance costs of water transport.

Groundwater is a renewable resource that should be thoroughly evaluated. As groundwater is available closer to the water demand location and at a higher elevation than lake water, it can cost significantly less to supply than surface water. Even if groundwater resources prove to be insufficient to supply all future water needs, they could be used to supplement surface water supplies. Such a system is presently operating in Durham Region where Skinner's Spring has supplied 1.5 million litres per day to Bowmanville at low cost since 1914. In many small communities with more modest water demands, pipelines will be uneconomical and continued reliance on groundwater supplies is expected.

Similar considerations regarding the sources of future water supply have been discussed in several areas of the country where complex geology controls the water resource (e.g. Waterloo Moraine, Fig. 1). Better understanding of the geological controls on groundwater flow and the development of improved methods of groundwater investigation in the Oak Ridges Moraine may also be beneficial in addressing water supply issues in other areas.

INVESTIGATIONS BY THE GEOLOGICAL SURVEY OF CANADA

The principal objective of the Oak Ridges Moraine Hydrogeology project has been aquifer delineation. Work has focused on surface and subsurface investigations to map geological and hydrogeological features, with the aim of developing a regional geological model. The working geological model comprises two components: a) stratigraphic, and b) depositional facies, both of which are important to hydrogeological studies although only the stratigraphic component of the model will be discussed (Fig. 2). The development of the model relies on past geological mapping and on the interpretation of new high quality data collected by detailed geological mapping, geophysical surveys, and stratigraphic drilling. In parallel with this working model, a large quantity of archival surface and subsurface data has been collected (Table 1) to form a geological and hydrogeological database (T.A. Brennand, D.R. Sharpe, H.A.J. Russell, and C. Logan, 1994: poster H9 presented at 1994 Ontario Mines and Mineral Symposium, Toronto, Ontario; Russell et al., 1996; Brennand, in press a). Data integration, viewing, and analysis is being completed in a Geographic Information System (GIS) environment to advance geological and hydrogeological understanding.

Surface mapping is being completed by means of detailed field observations, remote sensing techniques, and hydrological surveys (Table 1). Geological mapping is the cornerstone for Oak Ridges Moraine model development, data integration, and field verification of remotely sensed data. Remotely sensed data are being combined with a digital elevation model (Kenny et al., 1996) to permit landform and land cover analysis, and materials mapping.

Subsurface investigations comprise archival borehole data, surface and downhole geophysical surveys, and analysis of new drilling (Table 1). The project has drilled four new stratigraphic boreholes and used existing Ontario Geological Survey (OGS) boreholes in the area. Geophysical surveys (including seismic reflection profiling, ground penetrating radar, and a regional gravity survey; e.g. Pullan et al., 1994) provide lateral extensions of point data, enhancing the stratigraphic and structural understanding of the study area. Analysis incorporates an upgraded (locations improved by ~15%) Ontario Ministry of Environment and Energy (MOEE) waterwell database (Hunter, 1996), with other archival data to provide regional information on sediment distribution and therefore aquifer/aquitard distribution.

GEOLOGICAL MODEL

The geological model (Fig. 3) of the Oak Ridges Moraine has been constructed (Sharpe et al., 1994a, b) using detailed mapping (e.g. Barnett, 1992, 1993, 1994, 1995; Barnett and Henderson, 1995), published data (e.g. Sibul et al., 1977), recent borehole data (Barnett, 1993), logging of sediment exposures, and shallow seismic reflection profiles (Pullan et al., 1994; see Fig. 6). These high-quality data are most abundant in the moraine corridor between Uxbridge in the east and Nobleton in the west, and thus the model best applies to this area, the Uxbridge wedge. Nevertheless, it appears that some of the key strata comprising the model extend to the east

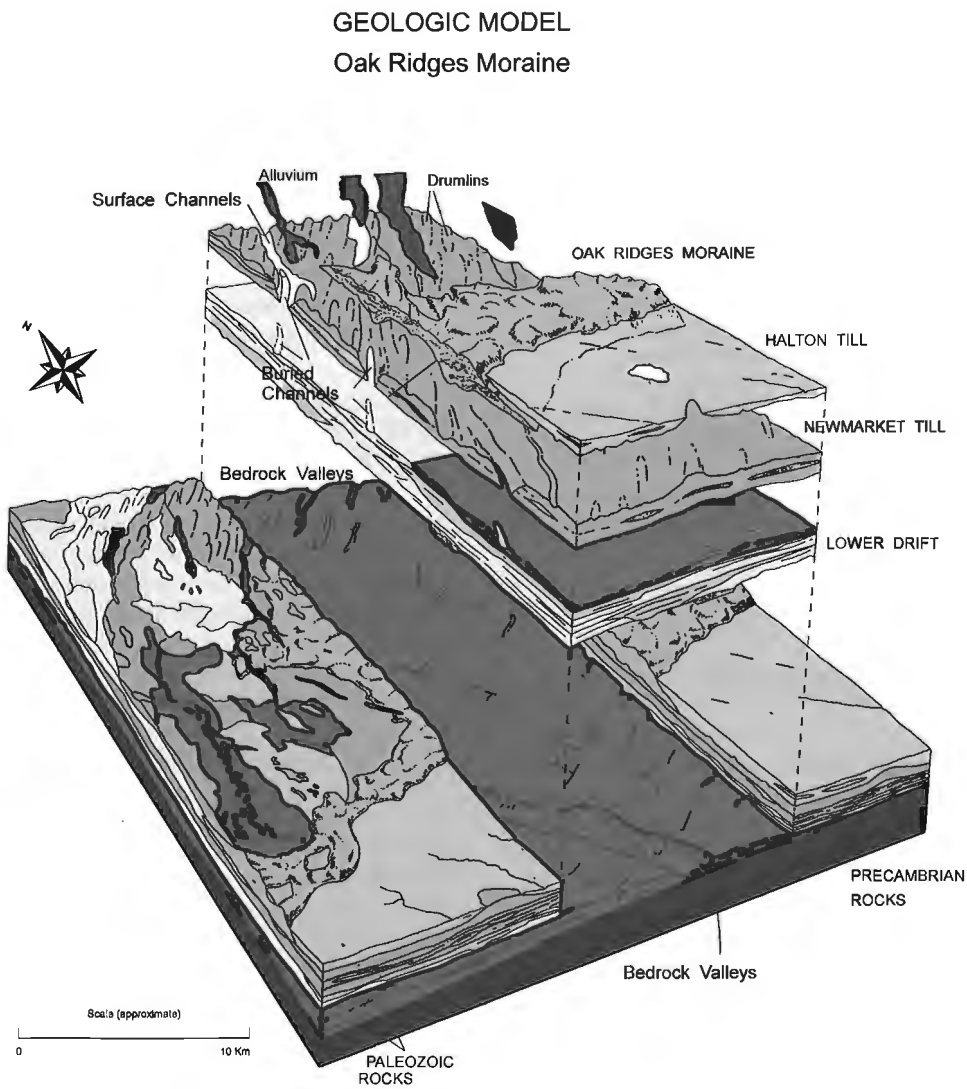

Figure 3. *Geological model of major strata in Oak Ridges Moraine area. (Kettleby not shown) (Drawing by J. Glew; computer rendering by D. Finley, March 1994).*

or west of the Uxbridge wedge (e.g. mapping and recent borehole data from the Interim Waste Authority (IWA), 1994a, b.

From the youngest units downwards, four major units and two erosional surfaces are identified (Fig. 3):

1. Halton/Kettleby drifts
2. Oak Ridges Moraine
3. Channellized erosional surface on the Newmarket Till
4. Newmarket Till
5. Lower drift
6. Erosional bedrock surface

1. Halton/Kettleby drifts

Halton and Kettleby drifts form the highest stratigraphic units, and occur as surface tills and lake sediments south (Halton) and north (Kettleby) of Oak Ridges Moraine (Fig. 4). These different drifts are dominantly clayey silt to silt till with interbedded sand and silt. The Halton Till is thickest in the Humber River area (20-30 m) and thins towards the north and east. Along the southern flank of the Oak Ridges Moraine the Halton overlaps the moraine where it characterized by a zone of hummocky terrain (e.g. Barnett and Henderson, 1995).

2. Oak Ridges Moraine

The Oak Ridges Moraine forms an extensive surface deposit 160 km long and 2 to 11 km wide. Its surface form can be divided into four sediment bodies or wedges, each widening westward. The Oak Ridges Moraine may be more extensive in the subsurface, particularly beneath the Halton drift. Rhythmically interbedded fine sands and silts are the dominant sediments, but coarse sands and gravels are prominent locally. Core logging indicates that areas of the moraine are composed of two to four fining upward packages. Regional landform relations and textural trends indicate paleoflow from the northeast. The lower contact of the moraine is an irregular channelled Newmarket Till surface (Fig. 5). Where this underlying till sheet has been completely eroded, Oak Ridges Moraine sediments may reach thicknesses of 150 m, and rest either on the lower drift or bedrock.

3. Channellized erosional surface on the Newmarket Till

A network of channels mapped north of the Oak Ridges Moraine, and oriented north-northeast to south-southwest (Fig. 5), is cut on the Newmarket Till (Barnett, 1990; Brennand and Shaw, 1994). The surface expression of the channels disappears beneath the moraine. Mapping (e.g. Barnett, 1992), seismic reflection profiling (Fig. 6; Pugin et al., in press), and drilling (e.g. Barnett, 1993) have shown

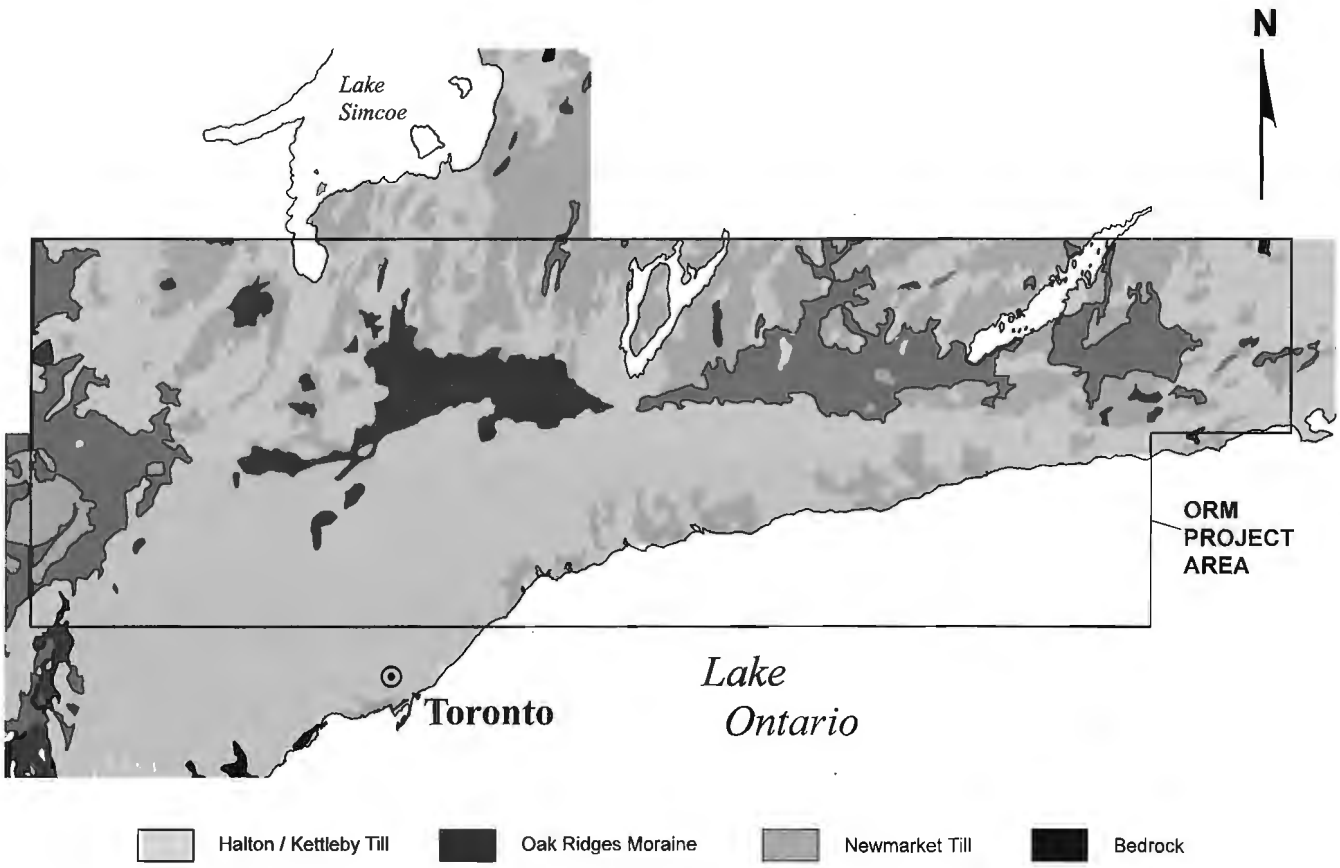

Figure 4. Surficial Geology of the Oak Ridges Moraine area (from Barnett et al., 1994).

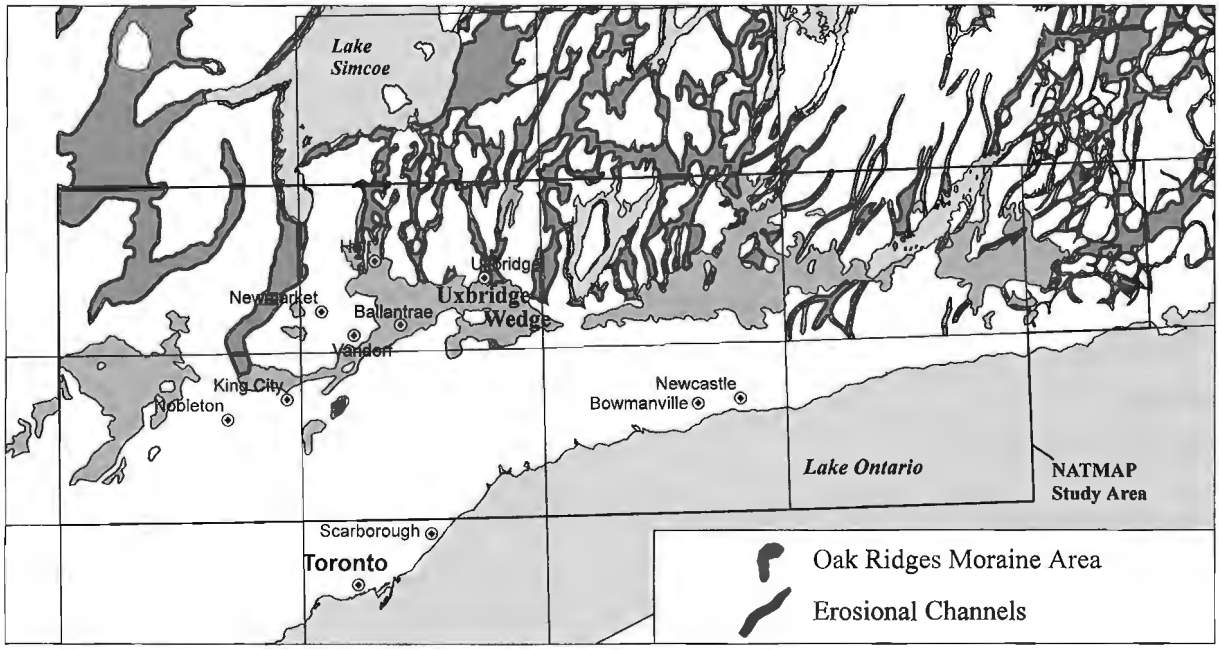

Figure 5. *Channels eroded in the Newmarket Till (preliminary map). Data from Barnett, 1990; Shaw and Gorrell, 1991; Gorrell and Sharpe, 1994; Brennand and Shaw, 1994.*

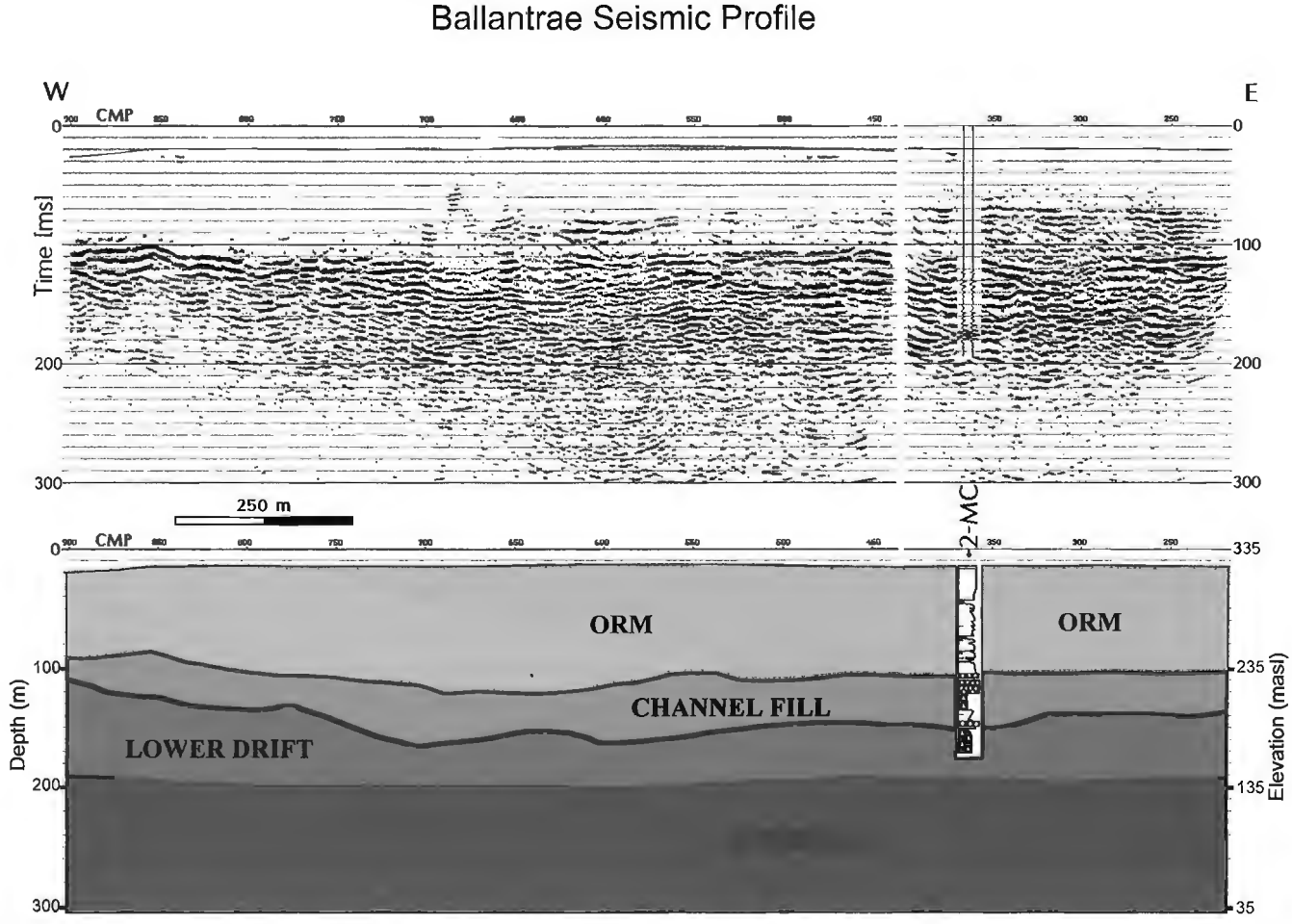

Figure 6. *Seismic reflection profile from Ballantrae area, showing the geometry of broad subsurface channels and channel fill confirmed by core logging (ORM = Oak Ridges Moraine).*

that channels continue beneath the Oak Ridges Moraine. The channels may be confined within, or have eroded through, the Newmarket Till into the lower drift. The channel geometry at surface indicates features 1-4 km wide and tens of meters deep; subsurface geometry reveals features 1-2 km wide and tens of meters deep. The channels contain mainly sandy sediments related to the Oak Ridges Moraine complex; however, at least some channels contain thick (10-15 m) gravels.

4. Newmarket Till

Newmarket Till occurs at the surface north of Oak Ridges Moraine (Gwyn and DiLabio, 1973), and has both streamlined (drumlins) and erosional (channels) elements. It is less extensively exposed south of the moraine but has been mapped in the subsurface at Musselman Lake (see Barnett et al., 1991; Sharpe, in press), Sutton, and Newcastle, and at the surface near Kleinburg (Russell, in press) and Port Hope (Brennand, in press b). This sediment is a dense, stony, silty sand till, observed to be 5-30 m thick in surface outcrop. Newmarket Till is characterized by high seismic velocities in downhole seismic logs obtained over widespread areas, and the contrast in velocities between it and overlying sediments make it a prominent reflection on seismic profiles (Pullan et al., 1994; Boyce et al., 1995). The base of the unit typically occurs between 200 and 220 m a.s.l. within the Uxbridge wedge (see also Hunter, 1996).

5. Lower drift

Lower drift units defined as Don and Scarborough formations and Sunnybrook Till at Scarborough Bluffs (Karrow, 1967), may extend north of the Oak Ridges Moraine (Eyles et al., 1985). These units are exposed north of the Lake Ontario shoreline along some river banks and at Woodbridge (White, 1975). The sandy Don Formation has been identified as a prominent seismic unit in the Nobleton area (A. Pugin, unpub. report to Geological Survey of Canada, 1996) and confirmed by drillcore data (Sado et al., 1983). Overlying Scarborough Formation sands have been confirmed as far north as the GSC borehole in Vandorf. These sands have regional extent as a unit tens of metres thick and are well displayed on seismic profiles (Pugin et al., in press). The Sunnybrook diamicton, a fine grained unit, may occur in a GSC borehole east of Newmarket and thus appears to form a regional aquitard within the lower drift sequence. Where the Newmarket Till is completely eroded, lower drift sediments may also have been eroded.

6. Bedrock surface

Attempts to define the bedrock topography in the Oak Ridges Moraine area have been made using unedited water well records (e.g. Eyles et al., 1985). However, beneath the moraine and in the Laurentian channel, is a buried valley extending from Georgian Bay to Lake Ontario; the precise definition of the bedrock surface is poorly constrained as few water wells intersect bedrock. Investigations west of Bolton indicate that several tributary channels may descend toward the Laurentian Channel (Hunter, 1996). Regional gravity surveys are providing a means of better delineating buried bedrock valleys including the Laurentian Channel (e.g. Belisle, 1995).

HYDROGEOLOGICAL SIGNIFICANCE OF THE GEOLOGICAL MODEL AND PROSPECTS FOR WATER SUPPLY

The geological model indicates that at least four geological units or subsurface structures are potential aquifer targets and at least two units that are aquitards. The Halton and Kettleby drifts are mainly surficial aquitards that reduce local groundwater recharge and that may serve to reduce the exposure of underlying aquifers to contamination (hydraulic conductivities from 10^{-8} to 10^{-4} cm/s; Interim Waste Authority, 1994a). Where the Newmarket Till is present, it is a regional aquitard that overlies the lower drift and may limit groundwater recharge from the ground surface or groundwater flow from the Oak Ridges Moraine sediments. Newmarket Till is an aquitard that may reduce groundwater recharge and contaminant migration. Core samples have low hydraulic conductivities (10^{-9} to 10^{-8} cm/s), but those calculated from piezometer or pump tests have a wider range (10^{-9} to 10^{-4} cm/s). It has been reported that larger-scale fractures could serve as pathways for groundwater flow through the till (Interim Waste Authority, 1994b).

The four main aquifer targets are:

1. extensive Oak Ridges Moraine sediments exposed at the surface;
2. channel structures cut into or through the Newmarket Till and filled by Oak Ridges Moraine sediments;
3. extensive sands within the lower drift sequence; and
4. lower drift sands filling valleys on the bedrock surface.

The Oak Ridges Moraine sediments form near surface aquifers across most of the moraine. These aquifers supply sufficient water for individual residential water demand, so wells have simply been drilled where water is required. Coarse sand and gravel beds within the moraine sediments offer good prospects for larger capacity wells. The location of these beds depends primarily on the type and distribution of depositional facies (e.g. gravel). Therefore, facies changes within the moraine are more important than the generalized stratigraphy as a guide for productive aquifers.

The high topographic position and predominantly sandy texture of the Oak Ridges Moraine implies that it plays a significant role in regional groundwater flow and groundwater resources in terms of its high recharge potential and subsequent flow to other down gradient aquifers. Thus, the long term integrity of groundwater supplies in the region depends, in part, on the recharge of groundwater within the Oak Ridges Moraine and on protecting these groundwaters from contamination.

Mapping, geophysical surveys, and drilling carried out for the Oak Ridges Moraine project have identified channel structures below the moraine that are eroded into or through

the regionally extensive Newmarket Till. Infilled channels may extend to elevations comparable to those of the lower drift sediments, so that productive 'lower' aquifers in some areas may be composed of moraine sediments. The high density of channels in the Newmarket Till north of the moraine suggests that these channels could significantly influence groundwater flow on a regional scale (Fig. 5). These channels are hydrogeologically significant for two reasons: 1) they can form significant hydraulic connections between the Oak Ridge Moraine sediments and the lower drift, and 2) gravel deposits within the channels may form high yield aquifers.

Since these channels are filled with silt, sand, and gravel, they are probably more permeable ($\approx 10^{-7}$ to $>10^{-3}$ cm/s) than the Newmarket Till and are potential pathways for groundwater flow (and potential contaminants) to the lower drift. Estimates of groundwater recharge to the lower drift (30 and 250 mm per year) are based on calculations which assume that groundwater flows through a continuous aquitard (Regional Municipality of York, 1993; Smart, 1994). Channels cut to lower drift likely provide greater recharge to portions of the lower drift than previously estimated.

Some channels contain gravel sequences which are potential targets for municipal water supplies. The extent and prevalence of these gravel deposits within channel structures will require further mapping. Since these channel aquifers are hydraulically connected to the Oak Ridge Moraine sediments, groundwater flow to the gravel could be high and aquifers may capture recharge from a broad surface area. The channels have little or no surface expression where they are covered by the moraine, so it is difficult to effectively predict the locations of channels without geophysical mapping.

The lower drift is composed of several geological and hydrostratigraphic units. South of the Oak Ridges Moraine, at least two confined aquifer units have been identified within the lower drift by logging sections (Sibul et al., 1977), but their regional extent and interconnectedness are not well known. Where the Oak Ridges Moraine is not present, sands within the lower drift are the primary aquifers. If vertical flow through the channels is significant, recharge through the moraine could also supply much of the regional groundwater flow to lower drift aquifers. Since lower drift may be supplying a significant portion of the groundwater supply in York Region and in parts of Peel Region, it is important to evaluate whether the geological model is appropriate in these areas. The lower drift is also a good groundwater supply target for small communities on the north side of the moraine in York and Durham regions, where continued reliance on groundwater is anticipated. Groundwater within the lower drift may be less susceptible to contamination than groundwater from the surficial units.

Finally, it is suggested that there could be productive aquifers in buried bedrock valleys. Recent GSC and Interim Waste Authority drillholes in bedrock valleys identified a thin gravel zone near the bedrock surface. Several municipal wells in the vicinity of the Laurentian Channel obtain their water from productive zones in the lowermost aquifers (Regional Municipality of York, 1993); some of these wells may be located within the fill of bedrock valleys. At present, the stratigraphy within the Laurentian Channel is poorly known, and therefore it is difficult to assess the potential for recharge to these aquifers.

CASE STUDIES IN WATER SUPPLY LOCATION

In the course of the field investigations carried out as part of this project, two potential high-yield water supplies have been identified; one of which is now under development as a municipal water well.

The Regional Municipality of York has recently completed aquifer testing and supply well installation for the community of Ballantrae (Fig. 5). Although the location of the well was partly determined by the availability of municipal lands and earlier exploratory drilling, GSC (Fig. 6) and OGS work in the area provided geological support for the decision to proceed with supply well installation. The municipal well is close to a GSC borehole interpreted to have intersected a channel cut through the Newmarket Till. One hundred meters of Oak Ridges Moraine sediments were logged in the borehole above a prominent 15 m thick (north-northeast-south-southwest) sand and gravel horizon (240 m a.s.l.). The association of the gravel with a channel supported the prospects for finding an aquifer in the same channel. A producing gravel horizon was found at the same depth in the Regional Municipality of York borehole located one-half kilometre to the north. Pumping tests demonstrate direct hydraulic connection between the gravels at the two locations and indicate that this well will meet the municipal water requirements.

The second example, near Nobleton, is untested as yet in terms of water production, but drill core combined with seismic reflection profiles suggest that it could also be a high yield water supply. Geological Survey of Canada, supported by both Peel and York regions, completed the continuously cored Nobleton borehole to bedrock at ~192 m depth. This borehole intersects a 12 m sand, and coarse gravel unit at a depth of 50 m (210 m a.s.l.). A shallow seismic reflection profile which runs by the borehole clearly shows this gravel sequence as a complex reflection package that can be traced westward for a distance of approximately 500 m. Detailed logging of the core is required to determine whether this gravel unit is part of the Oak Ridges Moraine sediments, or is another example of gravel within an erosional channel beneath the moraine. In either case, this gravel intersection and its significant lateral extent imply the possibility of groundwater reserves on a production well scale.

PROSPECTS FOR GROUNDWATER SUPPLIES IN THE OAK RIDGES MORAINE AREA

Historically, municipal production wells have been drilled close to consumption areas or located according to previous drilling experience with little geophysical profiling. Although a concept of the distribution of water-bearing zones does emerge as wells are added to a system, this approach will ultimately fail to define groundwater potential because of the complexity of the geology and the lack of a geological basis for extending searches for additional water. The geological model developed during this study provides a local and regional strategy for locating new groundwater supplies as well as subsequent aquifer protection strategies. The two case studies demonstrate the application of this model to successful groundwater searches.

The geological model includes four potential stratigraphic targets for groundwater searches 1) channels in drift; 2) Oak Ridges Moraine sediments; 3) lower drift; and 4) bedrock channels. The prime stratigraphic drilling targets identified in the model are buried channels which may host gravel deposits and are at moderate depths. While channels are relatively narrow targets, the model provides some guidance by defining the dominant channel orientations and size, and mapping out the surface occurrences north of the moraine. Exploration strategies should focus on east-west surveys that are most likely to intersect buried channels. The recognition that the base of the Newmarket Till commonly occurs around 200 m a.s.l. (in the Uxbridge wedge) provides a stratigraphic marker to help identify whether drilling has encountered the lower drift or a buried channel. However, at the present time, the model is not sufficiently detailed, or requires supplemental depositional facies information to be fully effective as a prospecting tool for high-yield water supplies in the Oak Ridges Moraine sediments, lower drift units, or bedrock channels.

Groundwater flow through channels may be high enough to permit sustainable groundwater extraction from the lower drift in the vicinity of channels. Regional groundwater flow in the lower drift could also provide a sustainable groundwater supply to many areas both north and south of the moraine.

The geological model of the Oak Ridges Moraine area presented in this paper should be updated and revised as more information becomes available. Municipal water supplies should be assessed in terms of the current working geological model to better understand the geological controls on the groundwater resources being tapped. Exploration for new water supplies should include subsurface investigations such as geophysical surveys and stratigraphic drilling as reconnaissance tools. As well as aiding particular water searches, such surveys constitute invaluable investments because of the geological and hydrogeological information made available for refining the understanding and promoting wise resource management within the Oak Ridges Moraine area.

CONCLUSIONS

A regional geological model and its possible hydrogeological significance have been presented for the central portion of the Oak Ridges Moraine. The model emphasizes the importance of channel structures eroded into or through the Newmarket Till, a regional aquitard. New mapping, seismic reflection profiles, and drilling support this stratigraphic model.

Gravel sequences within channels have been identified as potentially productive aquifers. Application of the model suggests that groundwater flow through channels to aquifers within the lower drift may be higher than implied by current estimates. Consequently, channels could influence how groundwater resources are assessed and managed on a regional scale. Further research is needed to delineate buried channels and the infilled sediments. Hydrogeological work is also required to assess vertical groundwater flow through these channels to the lower drift. The development of depositional facies models will improve our understanding of the internal structure of the geological units and assist in the development of improved strategies to locate productive aquifers.

A valid geological model is a critical tool in hydrogeological assessments and exploration. The regional model influences perceptions of the prospects for groundwater resources in the Oak Ridges Moraine area and provides a stratigraphic context in which geological and hydrogeological data can be examined. More work remains to be done in refining and validating the model in the central portion of the Oak Ridges Moraine, and in verifying and adapting the model for other areas. However, the tools and methods required for this work have been tested and proven, and can now be put to effective use in searching for and evaluating the potential of groundwater resources in the Oak Ridges Moraine area.

ACKNOWLEDGMENTS

The authors would like to thank Charles Logan, Paul Stacey, and Wendy Lewis for logistical support. Drafting of Figure 3 was completed by John Glew, James Ross assisted with Figure 5. Funding for this project is provided by the National Geoscience Mapping Program (NATMAP) and the Hydrogeology Committees of the Geological Survey of Canada. The Ontario Geological Survey funded work by Peter J. Barnett. Mapping support has also been received from Ontario Ministry of Environment and Energy (S. Singer) and Ministry of Natural Resources (Fred Johnson). H.A.J. Russell is partially supported by an NSERC Operating Grant to Dr. W. Arnott (University of Ottawa).

REFERENCES

Barnett, P.J.
1990: Tunnel valleys: evidence of catastrophic release of subglacial meltwater, central-southern Ontario Canada (abstract); in Abstracts with Programs, Northeastern Section, Geological Society of America, Syracuse, New York, p. 3.
1992: Geological investigations within the Oak Ridges Moraine area, Whitchurch-Stouffville and Uxbridge Township Municipalities, Ontario; in Summary of Fieldwork and Other Activities 1992; Ontario Geological Survey, Miscellaneous Paper 160, p. 144-145.
1993: Geological investigations in the Oak Ridges Moraine area, parts of Scugog, Manvers and Newcastle Township Municipalities and Oshawa Municipality, Ontario; in Summary of Fieldwork and Other Activities 1993; Ontario Geological Survey, Miscellaneous Paper 162, p. 158-159.
1994: Project 92-19, Geology of the Oak Ridges Moraine area, parts of Peterborough and Victoria counties and part of Durham Regional Municipalities, Ontario; in Summary of Fieldwork and Other Activities 1994; Ontario Geological Survey, Miscellaneous Paper 163, p. 155-156.
1995: Project 92-19, Geology of the Oak Ridges Moraine area, parts of Peterborough and Victoria counties and Durham and York Regional Municipalities, Ontario; in Summary of Fieldwork and Other Activities 1995; Ontario Geological Survey, Miscellaneous Paper 164, p. 155-160.

Barnett, P.J. and Henderson, L.A.
1995: Quarternary geology of the Port Perry area; Ontario Geological Survey, Map 2635, scale 1:20 000.

Barnett, P.J., Cowan, W.R., and Henry, A.P.
1991: Quaternary geology of Ontario, southern sheet; Ontario Geological Survey, Map 2556.

Belisle, J.
1995: The effectiveness of the gravity method for mapping bedrock topography beneath the Oak Ridges Moraine, Ontario; BSc. thesis, Queen's University, Kingston, Ontario, 32 p.

Boyce, J.I., Eyles, N., and Pugin, A.
1995: Seismic reflection, borehole, and outcrop geometry of Late Wisconsin tills at a proposed landfill near Toronto, Ontario; Canadian Journal of Earth Sciences, v. 32, p. 1331-1349.

Brennand, T.A.
in press a: Urban geology note: Oshawa, Ontario; in Urban Geology of Canadian Cities, Geological Association of Canada, Special Paper 42.
in press b: Glacial Geology of the Port Hope (30 M/16) 1:50 000 NTS map sheet; Geological Survey of Canada, Open File 3298.

Brennand, T. and Shaw, J.
1994: Tunnel channels and associated landforms: their implication for ice sheet hydrology; Canadian Journal of Earth Sciences, v. 31, p. 505-522.

Eyles, N., Clark, B.M., Kaye, B.G., Howard, K.W.F., and Eyles, C.H.
1985: The application of basin analysis techniques to glaciated terrains; an example from the Lake Ontario Basin, Canada; Geoscience Canada, v. 12, p. 22-32.

Fulton, R.J. (comp.)
1995: Surficial materials of Canada; Geological Survey of Canada, Map 1880A, scale 1:3 000 000.

Gorrell, G.A. and Sharpe, D.R.
1994: Stop 20, Oak Ridges Moraine; in A field guide to the glacial and postglacial landscape of southeastern Ontario and part of Quebec, (ed.) R. Gilbert; Geological Survey of Canada, Bulletin 453, p. 69-70.

Gwyn, Q.H.J. and DiLabio, N.N.W.
1973: Quaternary geology of the Newmarket area, southern Ontario; Ontario Division of Mines, Preliminary Map P836, scale 1:50 000.

Hunter, G.
1996: Technical Report, Hydrogeological Evaluation of the Oak Ridges Moraine Area; part of Background Report No. 3 for The Oak Ridges Moraine Planning Study, Volume 1, (prepared for Oak Ridges Moraine Technical Working Committee), Ontario Ministry of Natural Resources.

Interim Waste Authority (IWA)
1994a: Detailed assessment of the proposed site C-34b: Appendix C Geology/Hydrogeology; prepared for the IWA by Golder Associates. (available at Ontario Ministry of Development and Mines Library, Queen's Park, Toronto).
1994b: Detailed assessment of the proposed site EE11: Appendix C Geology/Hydrogeology; prepared for the IWA by M.M. Dillon Ltd. (available at Ontario Ministry of Development and Mines Library, Queen's Park, Toronto).

Karrow, P.F.
1967: Pleistocene geology of the Scarborough area; Ontario Department of Mines, Geological Report 46, 108 p.

Kenny, F.M., Russell, H.A.J., Hinton, M.J., and Brennand, T.A.
1996: Digital elevation models in environmental geoscience: Oak Ridges Moraine, southern Ontario; in Current Research 1996-E; Geological Survey of Canada.

Pugin, A., Pullan, S.E., and Sharpe, D.R.
in press: Observation of tunnel channels in glacial sediments with shallow land-based seismic reflection; Annals of Glaciology.

Pullan, S.E., Pugin, A., Dyke, L.D., Hunter, J.A., Pilon, J.A., Todd, B.J., Allen, V.S., and Barnett, P.J.
1994: Shallow geophysics in a hydrogeological investigation of the Oak Ridges Moraine, Ontario; in Proceedings, Symposium on the application of geophysics to engineering and environmental problems, (ed.) R.S. Bell and C.M. Lepper; March 27-31, Boston, Massachusetts, v. 1, p. 143-161.

Regional Municipality of York
1993: Long term water supply: Stage 1, Volume 2 – Appendices; Prepared for the Regional Municipality of York by Gore and Storrie Ltd. and MacViro Consultants Inc.

Russell, H.A.J.
in press: Glacial Geology of the Bolton (30 M/13) 1:50 000 NTS map sheet; Geological Survey of Canada, Open File 3299.

Russell, H.A.J., Logan, C., Brennand, T.A., Hinton, M., and Sharpe, D.R.
1996: Regional geoscience database for the Oak Ridges Moraine project southern Ontario; in Current Research 1996-E; Geological Survey of Canada.

Sado, E., White, O.L., and Sharpe, D.R.
1983: The glacial geology, stratigraphy and geomorphology of the North Toronto area: A field excursion; in Correlation of Quaternary Chronologies, (ed.) W. Mahaney; Geobooks, Norwich, England, p. 505-517.

Shaw, J. and Gorrell, G.A.
1991: Subglacially formed dunes with bimodal and graded gravel in the Trenton drumlin field, Ontario; Géographic physique et Quaternaire, v. 45, p. 21-34.

Sharpe, D.R.
in press: Glacial Geology of the Markham (30M/14) 1:50 000 NTS map sheet; Geological Survey of Canada, Open File 3300.

Sharpe, D.R., Dyke, L.D., and Pullan, S.E.
1994a: Hydrogeology of the Oak Ridges Moraine; Geological Survey of Canada, Open file 2869.

Sharpe, D.R., Barnett, P.J., Dyke, L.D., Howard, K.W.F., Hunter, G.T., Gerber, R.E., Paterson, J., and Pullan, S.E.
1994b: Quaternary geology and hydrogeology of the Oak Ridges Moraine area; Geological Association of Canada-Mineralogical Association of Canada, Joint Annual Meeting, Waterloo, 1994, Field Trip A7: Guidebook, 32 p.

Sibul, U., Wang, K.T., and Vallery, D.
1977: Ground-Water Resources of the Duffin Creek-Rouge River Drainage Basins; Ministry of the Environment, Water Resources Report 8, 109 p.

Smart, P.J.
1994: A water balance numerical groundwater flow model analysis of the Oak Ridges Aquifer Complex, south-central Ontario; MSc. dissertation, University of Toronto, Scarborough, Ontario, 155 p.

White, O.L.
1975: Quaternary Geology of the Bolton area, southern Ontario; Ontario Division of Mines, Geological Report 117, 119 p.

Geological Survey of Canada Project 930042

Regional geoscience database for the Oak Ridges Moraine project (southern Ontario)[1]

H.A.J. Russell[2], C. Logan, T.A. Brennand[3], M.J. Hinton, and D.R. Sharpe

Terrain Sciences Division, Ottawa

Russell, H.A.J., Logan, C., Brennand, T.A., Hinton, M.J., and Sharpe, 1996: Regional geoscience database for the Oak Ridges Moraine project (southern Ontario); in Current Research 1996-E; Geological Survey of Canada, p. 191-200.

Abstract: To assist in completing surface and subsurface mapping in the Oak Ridges Moraine area a geoscience database is being developed. The database consists of three data storage elements: a) relational database, b) GIS layers, and c) flat files. The relational database is the repository for new and archival point data obtained by mapping and borehole studies. The GIS layers include a library of remotely sensed imagery, a regional Digital Elevation Model, and thematic layers. The flat file format has been used for subsurface geophysical data, particularly reflection seismic and ground penetrating radar profiles. Most of the database is on desktop PC platforms with UNIX systems being incorporated for specific tasks. A simple example is provided to illustrate the potential for database querying and spatial interpolation in a GIS.

Résumé : Une base de données géoscientifiques est élaborée dans le but d'aider à la finalisation de la cartographie des dépôts en surface et en subsurface dans la région de la moraine d'Oak Ridges. Elle se compose de trois éléments : a) une base de données relationnelles, b) des couches de données intégrées à un système d'information géographique (SIG) et c) des fichiers plats. La base de données relationnelles sert à stocker toutes les données ponctuelles, tant les nouvelles que les anciennes, obtenues dans le cadre des travaux de cartographie et de forage. Le SIG comprend une imagethèque de télédétection, un modèle altimétrique numérique à l'échelle régionale et des couches thématiques. Le format «fichier plat» est utilisé pour consigner les données géophysiques souterraines, en particulier les profils de sismique réflexion et de géoradar. La base de données est en grande partie sur des ordinateurs personnels et le système d'exploitation UNIX permet d'effectuer des tâches spécifiques. Un exemple simple est présenté pour illustrer le potentiel qu'offre la base de données pour la consultation et l'interpolation spatiale dans un SIG.

[1] Oak Ridges Moraine NATMAP Project

[2] Department of Geology, University of Ottawa, Ontario K1N 6N5

[3] Department of Geography, Simon Fraser University, Burnaby, British Columbia V5A 1S6

INTRODUCTION

The Oak Ridges Moraine NATMAP Project was initiated in the spring of 1993 as a collaborative multi-agency multidisciplinary project with the Ontario Geological Survey (OGS). The project is a response to the need for a better understanding of the regional geology and groundwater resources in an area of intense urban growth. The absence of a regional geological understanding was highlighted at the time by the Interim Waste Authority (IWA) search for waste disposal sites in the Greater Toronto Area and by the Oak Ridges Moraine Technical Working Committee of the Ontario Ministry of Natural Resources (MNR).

The Oak Ridges Moraine area provides interesting challenges for geological mapping. In most regions of the country mapping is completed primarily for mineral resource assessment. In contrast, issues in the Oak Ridges Moraine are related to urbanization: water resources – extraction, protection; land use – agriculture, real estate development, golf courses, waste disposal; and planning and development – urban expansion, aggregate extraction, shoreline erosion. The thick Quaternary sediments are being mapped both at the surface and in the subsurface to define the sedimentary architecture and stratigraphic succession. Understanding the three dimensional geological architecture will provide the basis for delineating the extent of aquifers in the area. To achieve these objectives the project initiated a comprehensive database development (T.A. Brennand, D.R. Sharpe, H.A.J. Russell, and C. Logan, 1994: poster H9 presented at 1994 Ontario Mines and Mineral Symposium, Toronto, Ontario).

This paper provides an overview of the project objectives in establishing the database. The computer platforms and software used are briefly discussed. The database structure is defined and data sets are reviewed. To demonstrate the application of the database, a regional drift thickness map has been generated from a database query in a GIS.

DATABASE OBJECTIVES

The GSC has been a leader in the collection, transfer, and dissemination of digital geoscience information in Canada since the mid-1970s (Belanger, 1975; Belanger and Harrison, 1980). Digital databases are now a standard component of geological projects at the GSC (Broome et al., 1993; Woodsworth and Ricketts, 1994; Harris et al., 1995; Belanger, in press). In the Greater Toronto Area there are a number of Urban geology databases (e.g., Oshawa; Brennand, in press) which were compiled by the GSC UGAIS (Urban Geology Automated Information System) project (Belanger, 1975). With increasing improvements in PC/desktop technology and the evolving nature of software, particularly GIS, databases have evolved from single component relational databases (e.g., Belanger, 1975) to multicomponent GIS projects (Bonham-Carter, 1989; Broome et al., 1993). The Oak Ridges Moraine database is a synthesis of relational database and GIS as the project attempts to integrate large three-dimensional data sets (T.A. Brennand, D.R. Sharpe, H.A.J. Russell, and C. Logan, 1994: poster H9 presented at 1994 Ontario Mines and Mineral Symposium, Toronto, Ontario; Brennand, in press). To meet the geological objectives and to disseminate the collected information to the largest possible user group, the principal database objectives are:

1. Create an integrated GIS database for geological analysis on PC based platforms.
2. Create an integrated geographically keyed digital geoscience database for the Oak Ridges Moraine area.
3. Complete spatial data analysis and map production in a GIS.
4. Package digital data in a format which can be distributed to, and easily accessed, by investigators in a broad range of science, engineering, and planning disciplines.

THE STUDY AREA

The study area comprises eight 1:50 000 scale National Topographic System (NTS) map sheets north of Lake Ontario, representing approximately 63% of the Greater Toronto Area (GTA). The Quaternary geology comprises a glaciolacustrine-glaciofluvial sequence which is divided into stratigraphic units by a regional till sheet and unconformities (Sharpe et al., 1994; Sharpe et al., 1996). The sediment is up to 200 m thick in the west and generally thins towards the east. The western margin of the survey area coincides with the Niagara Escarpment. The east-trending Oak Ridges Moraine forms the major landform element of the study area and defines the drainage divide between Lake Ontario and Georgian Bay drainage basins (Fig. 1).

DATABASE PLATFORM

The database has been developed around two computer software/hardware combinations. The relational database is supported by Microsoft Access and shared on a Local Area Network (LAN) using Windows/Windows NT based PCs. The GIS database has been developed on PC based MapInfo software and in unison on UNIX based ArcInfo and PCI systems. Microsoft Access was chosen as the relational database management system (RDBMS) because it: permits multiple user connectivity on a LAN, has a flexible and easily designed user interface, provides for enforceable relational integrity, contains built-in Visual BASIC language, supports Open Database Connectivity (ODBC) format and the ability to share data with other Windows based applications that support Dynamic Data Exchange (DDE). The UNIX based systems are being employed to deal with study-wide data sets which have large file sizes (up to 350 megs) and/or where processing is computationally intensive (e.g., Landsat TM and RADARSAT imagery, DEM). Following processing and reclassification many of these map and image layers can be handled in MapInfo and other PC based programs.

A main objective of the database is to use this GIS database on a PC platform. MapInfo was selected because of its multi-platform capabilities (Windows, Apple, UNIX), ease of use, functionality, and low cost. As a vector based program MapInfo does not meet all the projects requirements. As a result, the GSC has collaborated with Northwood Geoscience Ltd. in the development of Vertical Mapper, a software package that enables point-to-area data transformations. Specifically, Vertical Mapper allows point data interpolation, contouring, DEM generation, DEM perspective viewing, and some modelling.

THE ORM DATABASE STRUCTURE

The project has collected a geographically keyed data set and developed a database comprised of three data storage formats (Fig. 2): a) a relational database, b) a spatial GIS data set, and c) a flat file data format.

Relational database

The relational database management system contains point data which possess multiple attributes. To date the database contains seven principal tables linked by index fields (key fields) (Fig. 2). The common field linking all tables is "site number". This field is the primary key field in the header table and is part of multiple-field primary keys or "foreign keys" in the other tables (see Microsoft Corporation, 1994). Data retrieval is achieved through the Microsoft Access query forum, or Microsoft Access BASIC.

GIS data layer

This component represents spatial data of either a vector or raster model. The data are stored as a library of layers in ArcInfo and MapInfo, and can be queried or compared with other data sets within a GIS. There are no direct-map-to-database relations as in some ArcInfo-Oracle database combinations (Broome et al., 1993).

Flat file data

This data set contains geophysical data, seismic, ground-penetrating radar profiles (GPR) and borehole geophysics data. The bulk of the data reside in proprietary file formats and are managed within DOS, Windows, or appropriate data processing packages.

DATA CAPTURE

Data capture involves both the transfer of reported data (e.g. geological, geotechnical, etc.), drilling information (e.g. type of drilling, company), and location information (e.g. geographic co-ordinates, etc.) to the database. Data has been transferred to the database by digital transfer (Ministry of Energy and Environment (MOEE) waterwell data, location data) and by manual entry (all geotechnical site investigation descriptions). Manual keyboard entry of hardcopy data files is the most time-consuming task of the database assembly and a potential source of error. To maximize data entry efficiency, data entry forms with links between database tables were created. The enforcement of data type restrictions and obligatory fields minimizes data entry errors. Subsequent data verification is an important task in the database development.

Data within the database must be georeferenced. This has proven to be a problem for a number of the data sets. It is not uncommon for reports to lack geographic coordinates, to have site maps with no geographic coordinates, or to have incorrect geographic coordinates on site maps and in the tabulated data. When necessary, geographic coordinates are obtained from site location maps by georeferencing identifiable points and digitizing or scanning site plans. Where the datum is not stated explicitly the availability of both North American Datum (NAD) 27 and 83 has increased the source of error in defining geographic coordinates. While the project has adopted the NAD 83 datum for output, it is critical that the datum of the original source is known to enable co-ordinate transformations. Where site location data can not be determined the data are not entered in the database.

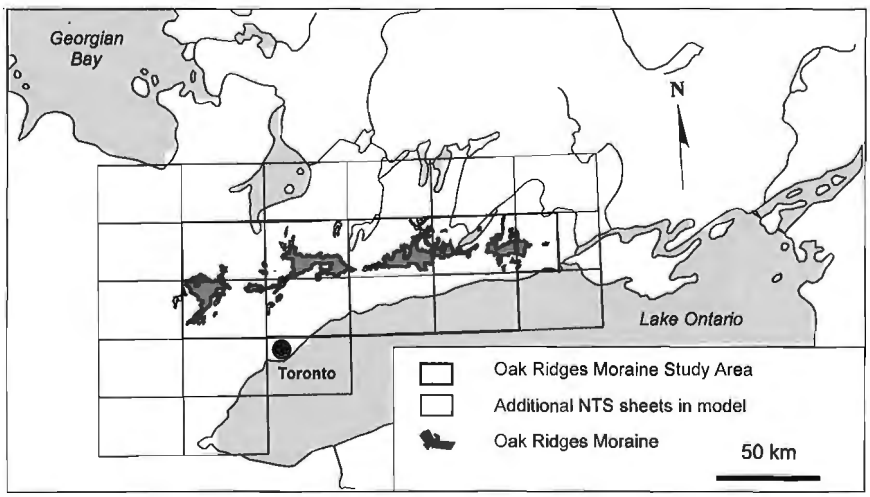

Figure 1.

Location diagram of the study area in southern Ontario.

Descriptions of geological materials in the archival data have been completed by a large number of people over a long period of time (>30 years). To ensure meaningful comparisons and to facilitate entry of sediment descriptions, two coding schemes have been developed. Sediment descriptions in reports have been entered using an adjective noun sequence (e.g. sandy silty diamicton), where the first descriptor is subordinate to each successive descriptor. The second coding system has two components, a material code and a preliminary unit attribute. The material coding system has ten generic, nonstratigraphic groupings (e.g. gravel, sand). The preliminary unit attribute coding has eleven genetic units (e.g. glaciofluvial, glaciolacustrine). The application of the second coding system has ensured a standard sediment description regardless of data sets and an easily managed number of units which are common to the archival borehole and Oak Ridges Moraine field mapping.

DATA SOURCES

Archival and new data are being compiled in the database (Table 1, 2, 3). Data collected as part of the current program have been obtained by surveys completed by the GSC, OGS, Canadian Centre for Remote Sensing, and Provincial Remote Sensing Office. Archival data have been obtained from a range of government agencies (MOEE, Metro Toronto Conservation Authority, Ministry of Transport, Metro Toronto, and Municipalities of York, Peel, and Durham), Universities (Guelph), and the private sector (Consumers Gas, Canadian National Railway). Archival data can include hardcopy reports, digital file formats, and sediment cores.

Point data

Field data have been collected in support of the geological mapping program. These data include sedimentological and geochemical information from shallow (1 m) probe holes and road side excavations and deeper (1 to 25 m) river and lake shore sections (Table 1). Hydrogeological field data have also been collected along streams where baseflow discharge has been measured to determine the spatial distribution of groundwater discharge (Hinton, in press).

The geochemistry survey comprises 412 A and C horizon sample pairs providing a baseline data set for the Greater Toronto Area. This survey provides the first regional geochemical sample set for the area and allows comparison of anthropogenic and geological signatures.

Field data from previous OGS mapping programs (e.g. Karrow, 1967; White, 1973; Gwyn and White, 1973; Sharpe, 1980a, b) have been provided to the project in hardcopy

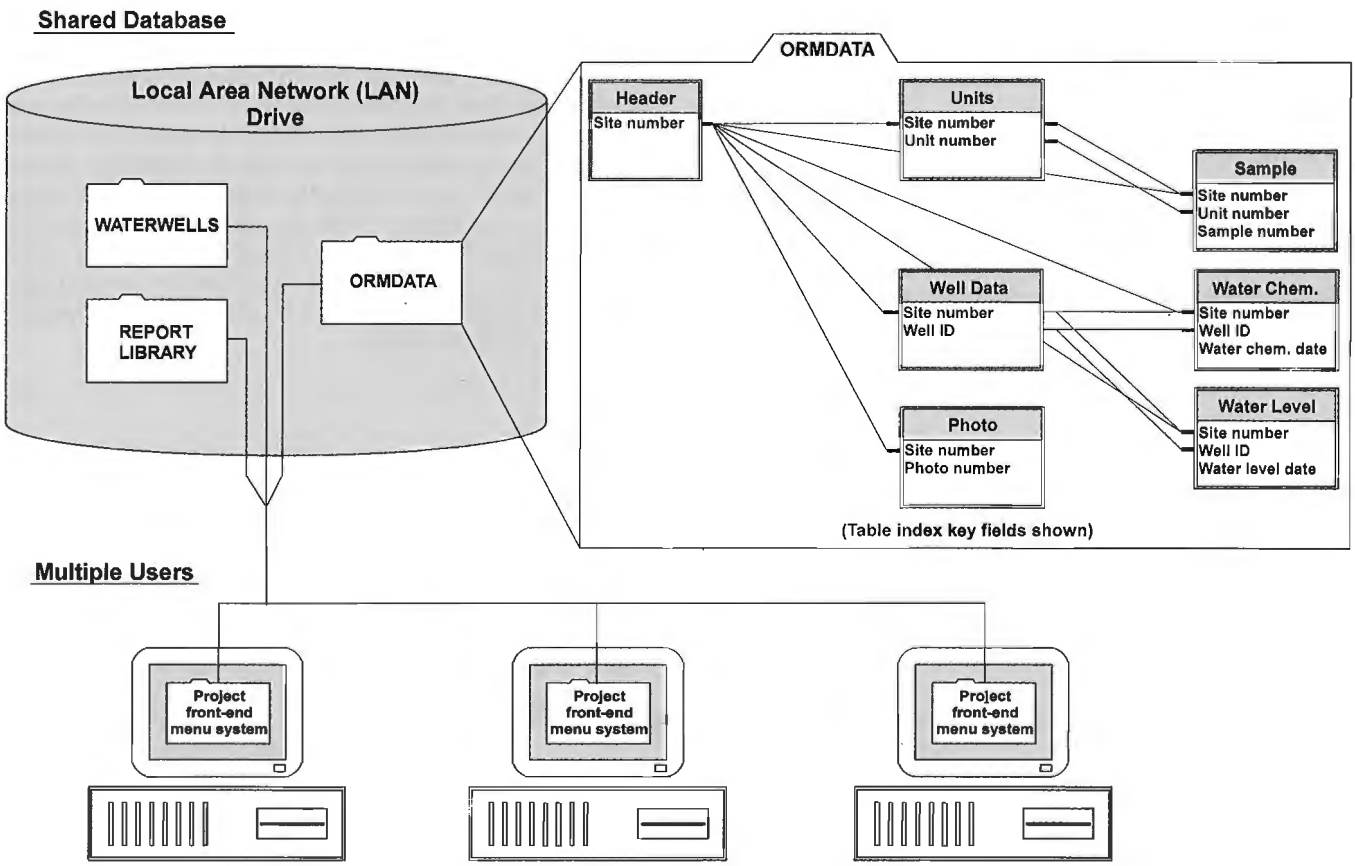

Figure 2. *Relational Database Structure.*

format. Data for seven map sheets (Bolton, Alliston, Markham, Brampton, Guelph, Trenton, and Toronto) collected by these surveys have been integrated into the database. The location of bedrock outcrops mapped by the OGS have been captured from the 1:50 000 scale bedrock geology maps (Telford, 1976a, b, c; Carson, 1980a, b, c) and bedrock topography maps (Holden et al., 1993a, b, c). Sedimentological data collected along the north shore of Lake Ontario has been provided by researchers from the University of Guelph and OGS (Brookfield et al., 1982; H. Gwyn, unpub. field notes 1976).

The borehole dataset can be separated into three categories on the basis of geological data quality: boreholes with continuous core recovery, borehole data from geotechnical reports, and MOEE waterwell database (Table 1). Boreholes with continuous core recovery provide the highest quality data and allow detailed sedimentological logging, which is crucial for the reliable interpretation of sedimentary processes and depositional environments. Continuously cored boreholes have been drilled by the GSC, OGS, and IWA. Borehole data from geotechnical reports have not been continuously sampled and have been described primarily for engineering purposes. While providing valuable information on sediment properties the descriptions have limited use for interpreting sedimentary processes. The waterwell data reported in the MOEE database have limited applications due to the absence of sediment sampling. The sediment descriptions rely on washings brought to the surface during the drilling process and do not describe solid sediment core. Individual boreholes from this data set have low reliability; however, as an ancillary data set and as a group, they are a useful subsurface mapping tool.

The GSC and OGS have drilled 10 boreholes with near continuous core recovery (>80%) These boreholes are providing detailed sedimentological data; hydrogeological data are being collected through the monitoring and sampling of nested piezometers (Table 1). The OGS has also contributed other drilling results, notably from the Woodbridge area (Kelly, 1994).

The IWA completed an extensive site specific drilling program within the three regional municipalities of the Greater Toronto Area (Durham, York, Peel) as part of a regional landfill search. This drilling program drilled nested sets of wells for hydrogeological monitoring, with depths ranging from 10 to 160 m. The project has entered data from published IWA reports (Interim Waste Authority 1993, 1994a, b, c, d, e). Following the termination of the IWA investigation in 1995 the GSC became the depository of approximately 6 km of IWA drill core from 140 boreholes. Relogging of some of this material is providing detailed sedimentological and stratigraphic information. The IWA has also provided access to the digital geological and hydrogeological data files retained by the respective consulting companies. This data set is of high quality and provides an unsurpassed examination of the geological conditions on a site basis (cf. Boyce et al., 1995). Data from similar site investigations have been obtained from the Port Hope area (unpub. report prepared for Low Level Radioactive Waste Management Office, by Gartner Lee Ltd., 1992) (Table 1).

Geotechnical boreholes are commonly drilled for site investigations of roads, bridges, railway crossings, gas pipelines, utility substations, hydro towers, lighting networks, and buildings prior to construction. This data set provides regional information on geotechnical parameters and water levels (Table 1). Boreholes of this data set are 5 to 30 m depth and include information on sediment texture, standard penetration testing ("N" values), grain size analysis, water levels, Atterberg limits, and shear strength.

The MOEE have provided the largest single data set to the project. For the Greater Toronto Area and peripheral areas there are approximately 57 000 boreholes (current to 1985). This data set is compiled by the MOEE through legislation requiring drillers to submit information on wells drilled. The data set provides a unique opportunity to expand sediment mapping regionally from sites of high quality data. This data set is particularly important for defining the bedrock surface as it is the only regional data set to reach bedrock. Each record contains information documenting location, sediment descriptions, well construction, and hydrogeological characteristics (Table 1).

GIS layers

Information in this category includes both archival data (e.g. original Landsat TM) and thematic data layers (e.g. interpreted TM, geology). As the project progresses, the number of thematic layers will increase as data is interpreted and interpolated from point to spatial data sets (e.g. field points via airphoto interpretation to surface geology maps) (Fig. 3). A hydrologically sound 1:50 000 scale DEM with a 30 m grid resolution is being developed with the assistance of the Ontario Provincial Remote Sensing Office (Kenny et al., 1996; Skinner and Moore, in press) (Fig. 1). This DEM will provide an elevation datum for project data, permit landform analysis, and aid watershed mapping. To supplement sparse bedrock elevation data beneath the moraine, a regional gravity survey has been completed along the road system with station intervals of 500 m (east-west) and 3-4 km line spacing (north-south) (~3000 stations).

Landsat TM coverage of the study area supplemented by partial SPOT, ERS-1, and RADARSAT data coverage has been obtained (Table 2). These data are proving to be invaluable for terrain analysis, wetland, and landcover mapping. A thermal image flown along the south side of the Oak Ridges Moraine by PRSO has been incorporated into the database. These data highlight open water on a cold (-20°C) March night in 1994 and are providing insights concerning spring locations and related geological correlations.

Flat file layers

Extensive geophysical surveys have been conducted to define the 3-D sediment architecture and hydrostratigraphy (Table 3) (Pullan et al., 1994). For regional analysis the reflection seismic data has proven key to understanding the stratigraphic succession (Sharpe et al., 1996). The ground penetrating radar data has provided information on sediment

Table 1. Listing of data sources, nature of data, and summary information, (modified from Brennand, in press).

		NATMAP Field Sites	OGS Field Sites	NATMAP/ OGS BH	IWA	Laidlaw	LLRWMO	STFS	MTO	Misc. Geotechnical	Oshawa UGAIS	U. Guelph	MOEE
Geographic Location													
Site Description													
Soil Description													
Sediment Description:	Depth Interval												
	texture												
	Colour												
	Structure												
	Contacts												
	Paleoflows												
	Clast Lithology												
Sample Type:	Geotechnical												
	Geochemical												
	Heavy Mineral												
	Organic												
Bedrock Description and Depth													
Hydrogeology:	Static Levels												
	Piezometric Level												
	Hydraulic Conductivity												
	Water Chemistry												
	Stream Gauging												
Data Format Aquired		Hardcopy	Hardcopy	Hardcopy	Hardcopy	Hardcopy	Hardcopy	Hardcopy	Hardcopy	Hardcopy	Digital	Hardcopy	Digital
Current Format		Digital	Digital	Digital	Digital	Digital	Digital	Digital	Digital	Digital	Digital	Digital	Digital
Numbr of Records, approximate counts		3000	4000	9	146	61	91	67	2000	100	3777	35	57,000
Location Problem Identified		No	Minor	No	No	No	No	No	Some	Some	Uncertain	No	Yes
Data Quality Questions		No	No	No	No	Uncertain	Uncertain	Uncertain	Uncertain	Uncertain	Uncertain	No	Yes

LEGEND: Data Entered

Table 2. Listing of GIS data layers and summary information.

Type	Format	Scale	Horizontal Resolution (m)	Source	Coverage
Anthropogenic	Vector	1:50 000 & 1:250 000	NA	Geomatics Canada	Complete
Hydrology	Vector	1:50 000 & 1:250 000	NA	Geomatics Canada	Complete
Topography	Vector	1:50 000 & 1:250 000	NA	Geomatics Canada	Complete
Soils	Vector	1:64 000	NA	Ag Canada	Partial
Surficial Geology	Vector	1:1 000 000	NA	OGS	Complete
Surficial Geology	Vector	1:50 000	NA	Project	Complete
Bedrock Geology	Vector	1:1 000 000	NA	OGS	Complete
Tunnel Channels	vector	1:50 000	NA	Project	Complete
Drainage Basins	Vector	1:50 000	NA	Project	Complete
TM bands 2,3,4	Raster	1:50 000 & 1:250 000	30	CCRS/PRSO	Complete
Spot	Raster	1:50 000	10	PRSO	Partial
ERS-1	Raster	1:50 000		PRSO	Partial
RadarSat	Raster	1:10 000	9 to 30	CCRS	Partial
Thermography	Hardcopy	1:50 000		PRSO	Partial
DEM	Raster	1:50 000	30	Project	Complete
DEM	Raster	1:250 000	?	MNR	Complete
Gravity	Raster	NA	NA	Project	Complete

Table 3. Listing of Flat File data and summary information.

Type	Agency	Format	Quantity	Purpose
Seismic	GSC/IWA	TIF and SIG2	45 km	Architecture & Stratigraphy
GPR	GSC	TIF and SSI	N/A	Architecture, Water Table
EM-34, 47	GSC	ASCII	N/A	Bedrock / Stratigraphy
Downhole	GSC/IWA	ASCII	10 holes	Physical Properties

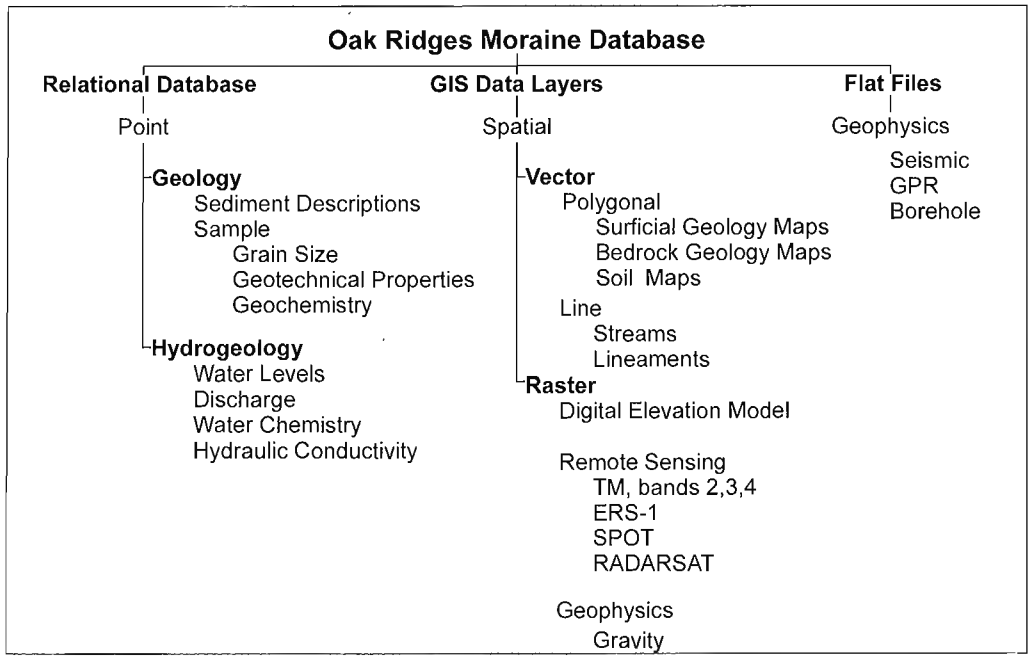

Figure 3. *Three components of the Oak Ridges Moraine database.*

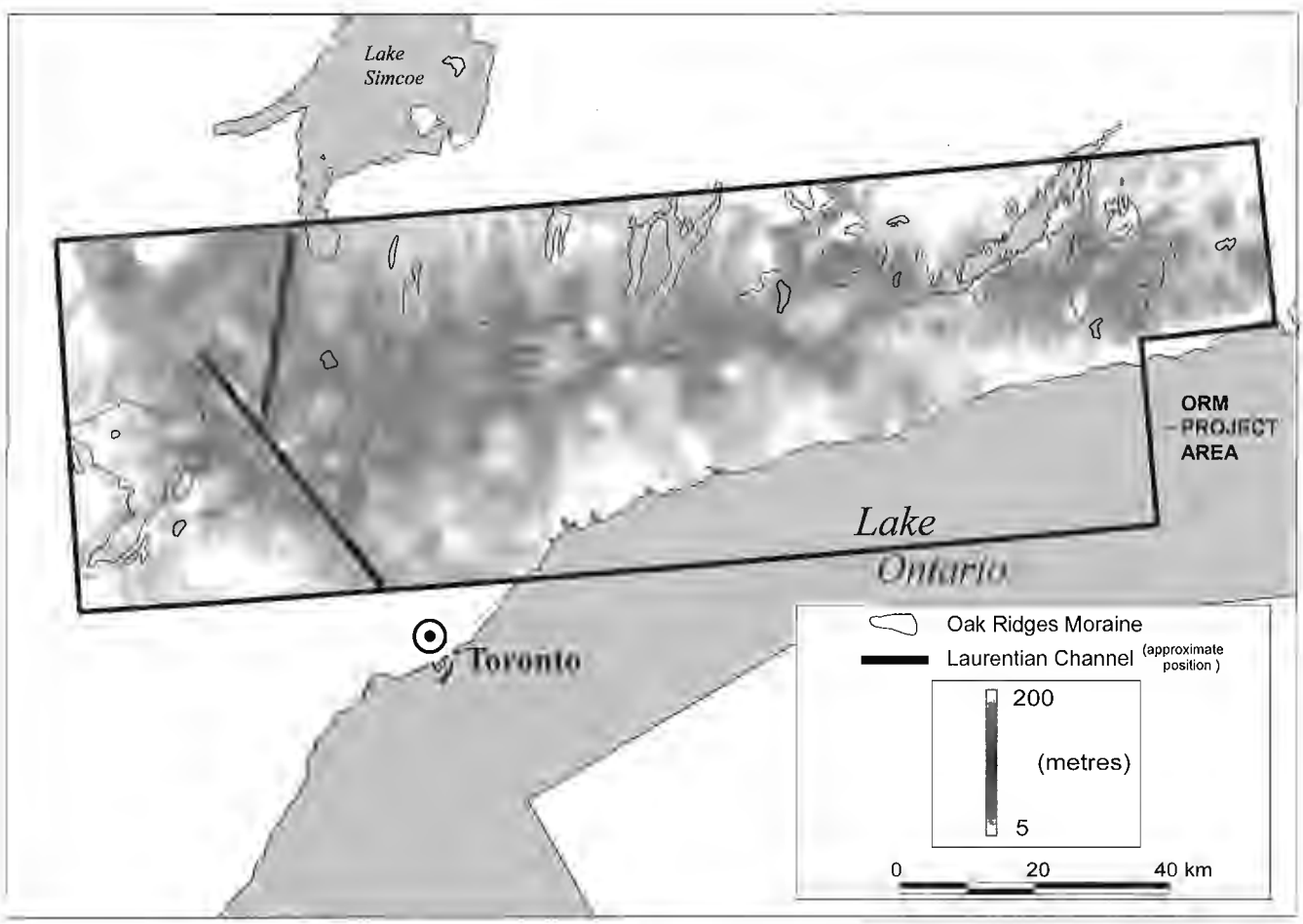

Figure 4. *Drift thickness map of the Oak Ridges Moraine (ORM) study area.*

architecture and depth to the water table. The borehole geophysics (borehole seismic, gamma, magnetic susceptibility, and conductivity) have provided valuable data for reflection seismic correlations and sediment property characterization.

All geophysical survey locations have been entered in the header table of the relational database and flagged appropriately. Selected vertical measurements have been taken from interpreted seismic profiles and entered as interpreted seismic logs. Reflection seismic profiles and ground penetrating radar are also captured as TIF images and can be used as a backdrop when plotting database borehole queries.

AN EXAMPLE OF A REGIONAL DATABASE MANAGEMENT SYSTEM QUERY AND GIS OPERATION

The Oak Ridges Moraine database is being used primarily to define the 3-D geometry of sedimentary deposits in the study area. This involves the formulation of selected queries of the relational database, and data interpolation and integration in a GIS. The following example demonstrates the combined use of an integrated database/GIS analysis. Production of a sediment thickness map of the study area requires delineation of two surfaces: the underlying bedrock surface and the landscape topography. Using the DEM as a reference, the surface elevations of all boreholes were standardized. The bedrock surface was defined using a database query to select the points to bedrock, and then interpolated within a GIS to produce a surface. The landscape surface is defined by the DEM (Skinner and Moore, in press). A common grid cell resolution was defined for the two surfaces, in this case the 30 m grid size of the DEM. The drift thickness map was then generated from the elevation difference between the two surfaces. The resulting map is a derivative surface of the previous two surfaces and highlights thick drift along the moraine and in the vicinity of the Laurentian Channel (Fig. 4). The strong correlation in the drift thickness and surface topography reflects the small number of original points to bedrock (~12 000) and resultant low resolution image of the bedrock surface.

FUTURE WORK

Work is ongoing with respect to data entry and verification. Data entry is approximately 90% complete: additional archival data are being added as it becomes available. During the course of preliminary data analysis (Hunter, 1996, pers. comm.) it has become apparent that the MOEE data set has between 20 and 30% location errors. The project is in the process of completing a systematic verification of locations for the MOEE data. A level of data verification for subsequent users is being incorporated by flagging duplicate locations, ambiguous sediment descriptions, and inconsistent data reporting.

It is anticipated that components of the database will be released in both digital (CD-ROM) and hardcopy formats as appropriate. The proprietary nature of some of the data will influence which data are released. Final formats have not been determined for CD-ROM releases but will probably include runtime viewing software for both the relational database and GIS data layers.

CONCLUSION

The choice of PC/Windows platform and software has proven to be a functional option for the scope of this project. The database has been able to provide complex data processing and querying abilities in a variety of formats along with network sharing functionality. MapInfo with Vertical Mapper has proven to be a low-cost solution for most of the map production and analysis needs. Some of the more intensive image processing and analysis have needed to be done with ArcInfo and PCI, but for the display and integration of these images MapInfo has proven suitable.

The ability to obtain archival data from a broad range of agencies working in the Toronto area has allowed the project to focus on specific geographic areas and hydrogeological and geological problems. This has permitted the optimization of scarce funds and minimized duplication of research efforts.

Queries on the database and GIS operations completed to date have demonstrated the functionality of the database (D.R. Sharpe, M. Hinton, L.D. Dyke, S.E. Pullan, T.A. Brennard, H.A.J. Russell, C. Logan, and A. Morre, 1995: poster presented at 1995 Ontario Mines and Minerals Symposium, Toronto, Ontario). Data analysis is starting to progress from local high quality sources and conceptual model development to the regional testing of models. The database will be an invaluable component of GIS analysis as an attempt is made to map the subsurface geology with the same rigor commonly applied to regional surface mapping.

The range of geoscience data in the database makes it of interest to a broad spectrum of users in the Greater Toronto Area. Consultants and municipalities in the area have shown an interest in the database and its release to the public. Subsurface components are useful to hydrogeologist, geochemistry to environmental agencies, and surface geology mapping to planners and agriculture. The DEM and some of the remote sensing and thematic map products can be used in applications involving architecture, engineering, land management, recreational planning, fisheries management, hydrology, hydrogeology, geology, and agriculture.

ACKNOWLEDGMENTS

Funding for this project has been provided by the Geological Survey of Canada NATMAP and Hydrogeology committees. H.A.J. Russell is partially funded by an NSERC operating grant to W. Arnott, University of Ottawa. A critical review by R. Belanger led to significant improvements in the paper. The authors would like to thank all those involved in data entry during the course of this study, particularly: J. Bjornson, S. Dumas, C. Helmer, W. Lewis, L. Morotti, J. Ross, and T. Shaw. Supporting GIS operations have been completed by P. Chin, R. Laframboise, A. Moore, and P. Stacey.

REFERENCES

Belanger, J.R.
1975: UGAIS data record instruction manual; Geological Survey of Canada, Open File 292, 11 p.
in press: Urban geology of Canada's national capital area; in Urban Geology of Canadian Cities; Geological Association of Canada, Special Paper 42.

Belanger, J.R. and Harrison, J.E.
1980: Regional geoscience information Ottawa-Hull;. Geological Survey of Canada, Paper 77-11, 18 p.

Bonham-Carter, G.F.
1989: Integrating geological datasets with a raster-based geographic information system; in Digital Geological and Geographic Information Systems; (ed.) J.N. Van Driel and J.C. Davis; America Geophysical Union, Short Course in Geology, v. 10, p. 1-14.

Boyce, J.I., Eyles, N., and Pugin, A.
1995: Seismic reflection, borehole and outcrop geometry of Late Wisconsin tills at a proposed landfill near Toronto, Ontario; Canadian Journal of Earth Sciences, v. 32, p. 1331-1349.

Brennand, T.A.
in press: Urban geology note: Oshawa, Ontario, in Urban Geology of Canadian Cities; Geological Association of Canada, Special Paper 42.

Brookfield, M.E., Gywn, Q.H.J., and Martinin, I.P.
1982: Quaternary sequences along the north shore of Lake Ontario: Oshawa-Port Hope; Canadian Journal. of Earth Sciences, v. 19, p. 1836-1850.

Broome, J., Brodaric, B., Viljoen, D., and Baril, D.
1993: The NATMAP digital geoscience data-management system; Computers and Geosciences; v. 19, p. 1501-1516.

Carson, D.M.
1980a: Paleozoic geology of the Rice Lake-Port Hope area, southern Ontario; Ontario Geological Survey, Preliminary Map P. 2338, Geological Series, scale 1:50 000.
1980b: Paleozoic geology of the Bannock-Campbellford area, southern Ontario; Ontario Geological Survey, Preliminary Map P. 2374, Geological Series, scale 1:50 000.
1980c: Paleozoic geology of the Trenton-Consecan area, southern Ontario; Ontario Geological Survey, Preliminary Map P. 23375, Geological Series, scale 1:50 000.

Gywn, Q.H.J. and White, S.
1973: Quaternary geology of the Alliston area, southern Ontario; Ontario Division Mines, Preliminary Map P.835, Geological Series, scale 1:50 000.

Harris, J.R., Broome, J., and Heather, K.B.
1995: Swayze Greenstone Belt GIS project; in NODA Summary Report-1993-1994, Natural Resources and Ministry of Northern Development and Mines, Paper 57, p. 115-121.

Hinton, M.J.
in press: Measuring stream discharge to infer the spatial distribution of groundwater discharge; Canadian Water Resources Journal.

Holden, K.M., Thomas, J., and Karrow, P.F.
1993a: Bedrock topography of the Alliston area, southern Ontario; Ontario Geological Survey, Preliminary Map P.3213, scale 1:50 000.

Holden, K.M., Mitchell, D., and Karrow, P.F.
1993b: Bedrock topography, Oshawa area; Ontario Geological Survey, Preliminary Map P.3192, scale 1:50 000.

Holden, K.M., Mitchell, D., and Karrow, P.F.
1993c: Bedrock topography, Port Hope area; Ontario Geological Survey, Preliminary Map P.3193, scale 1:50 000.

Hunter, G.
1996: Technical Report, Hydrogeological Evaluation of the Oak Ridges Moraine Area; part of Background Report No. 3 for The Oak Ridges Moraine Planning Study, Volume 1, (prepared for Oak Ridges Moraine Technical Working Committee), Ontario Ministry of Natural Resources.

Interim Waste Authority (IWA)
1993: IWA landfill site search Peel Region, step 6 hydrogeological report site B-21c; prepared by Golder Associates Ltd. (Available at Ontario Ministry of Northern Development and Mines library, Queen's Park, Toronto).
1994a: Geology/hydrogeology technical appendix 5; in Detailed assessment of the proposed site KK2; prepared by M.M. Dillon for Durham Region landfill site search, EA Document V. (Available at Ontario Ministry of Northern Development and Mines library, Queen's Park, Toronto).
1994b: Detailed assessment of the proposed site EE11; prepared by M.M. Dillon for Durham Region landfill site search. (Available at Ontario Ministry of Northern Development and Mines library, Queen's Park, Toronto).
1994c: Appendix C-Geology/Hydrogeology; in Interim Waste Authority Peel Region landfill site search, detailed assessment of the proposed site C-34B; prepared by Golder Associates Ltd. (Available at Ontario Ministry of Northern Development and Mines library, Queen's Park, Toronto).
1994d: Technical Appendices (Part 2 of 5); in Detailed assessment of the proposed site V4A; prepared by Fenco MacLaren Inc. for the Metropolitan Toronto and York Region landfill site search. (Available at Ontario Ministry of Northern Development and Mines library, Queen's Park, Toronto).
1994e: IWA landfill site search Metro/York Region, step 6 hydrogeological report site M6; prepared by Fenco MacLaren Inc. (Available at Ontario Ministry of Northern Development and Mines library, Queen's Park, Toronto).

Karrow, P.F.
1967: Pleistocene geology of the Scarborough area; Ontario Department of Mines, Geological Report 46, 108 p.

Kelly, R.I.
1994: Results of a Quaternary geology hollow stem auguring program; Ontario Geological Survey, Open File Report 5887, 52 p.

Kenny, F.M., Russell, H.A.J., Hinton, M.J., and Brennand, T.A.
1996: Digital Elevation Models in environmental geoscience, Oak Ridges Moraine, southern Ontario; in Current Research 1996-E, Geological Survey of Canada.

Microsoft Corporation
1994: MS Access Relational Database Management System for Windows, version 2.0, Users Guide; Microsoft Press.

Pullan, S.E., Pugin, A., Dyke, L.D., Hunter, J.A., Pilon, J.A., Todd, B.J., Allen, V.S., and Barnett, P.J.
1994: Shallow geophysics in a hydrogeological investigation of the Oak Ridges Moraine, Ontario; in Proceedings: Symposium on the Application of Geophysics to Engineering and Environmental Problems, (ed.) R.S. Bell and C.M. Lepper; March 27-31, Boston, Massachusetts, v. 1, p. 143-161.

Sharpe, D.R.
1980a: Quaternary geology of Toronto and surrounding area; Ontario Geological Survey, Map P.2204, scale 1:100 000.
1980b: Quaternary geology of the Brampton area; in Summary of Fieldwork and Other Activities 1980; Ontario Geological Survey, Miscellaneous Paper 149, p. 104-105.

Sharpe, D.R., Barnett, P.J., Dyke, L.D., Howard, K.W.F., Hunter, G.T., Gerber, R.E., Paterson, J., and Pullan, S.E.
1994: Quaternary geology and hydrogeology of the Oak Ridges Moraine area; Geological Association of Canada-Mineralogical Association of Canada, Joint Annual Meeting, Waterloo, 1994 Field Trip A7: Guidebook, 32 p.

Sharpe, D.R., Hinton, M., Dyke, L.D., Pullan, S.E., Russell, H.A.J., Brennand, T.A., and Barnett, P.J.
1996: Groundwater prospects in the Oak Ridges Moraine area, southern Ontario: application of regional geological models; in Current Research, 1996-E, Geological Survey of Canada.

Skinner, H. and Moore, A.
in press: A Digital Elevation Model of the Oak Ridges Moraine, southern Ontario; Geological Survey of Canada and Ministry of Natural Resources, Government of Ontario; Geological Survey of Canada, Open File 3297, scale 1:250 000.

Telford, P.
1976a: Paleozoic geology of Orangeville; Ontario Division of Mines, Ministry of Natural Resources. Map 2339, scale 1:50 000.
1976b: Paleozoic geology of Bolton; Ontario Division of Mines, Ministry of Natural Resources, Map 2338, scale 1:50 000.
1976c: Paleozoic geology of Brampton; Ontario Division of Mines, Ministry of Natural Resources, Map 2337, scale 1:50 000.

White, O.L.
1973: Bolton, Quaternary geology; Ontario Division of Mines, Map 2275, Geological Series, scale 1:50 000.

Woodsworth, G.J. and Ricketts, B.D.
1994: A digital database for groundwater data, Fraser Valley, British Columbia; in Current Research 1994-A; Geological Survey of Canada, p. 207-210.

Geological Survey of Canada Project 930042

Digital Elevation Models in environmental geoscience, Oak Ridges Moraine, southern Ontario[1]

F.M. Kenny[2], H.A.J. Russell[3], M.J. Hinton, and T.A. Brennand[4]
Terrain Sciences Division, Ottawa

Kenny, F.M., Russell, H.A.J., Hinton, M.J., and Brennand, T.A., 1996: Digital Elevation Models in environmental geoscience, Oak Ridges Moraine, southern Ontario; in Current Research 1996-E; Geological Survey of Canada, p. 201-208.

Abstract: Knowledge of topography is often a basic requirement for studies undertaken in the natural sciences, specifically, geomorphology, hydrology, and geology. Digital Elevation Models (DEM) can be developed using Geographical Information Systems and digitally structured topographic maps to provide contiguous information of a landscape. Once terrain information is captured as a DEM, the potential for multidisciplinary geoscience applications increases dramatically.

A 1:10 000 scale DEM was constructed and used to develop integrated image analysis techniques for geological and landform mapping within a 15 by 20 km test site of the Oak Ridges Moraine. The techniques developed in the test area are being applied on a 1:50 000 scale DEM that includes the entire Greater Toronto Area. Examples of DEM applications are provided from both the test site and regional models. The DEM is also being used by geologists on desktop PC systems as an aid in geological mapping.

Résumé : La connaissance de la topograhie est souvent une exigence de base pour les études entreprises dans les divers domaines des sciences naturelles, en particulier en géomorphologie, en hydrologie et en géologie. Des modèles altimétriques numériques (MAN) peuvent être conçus en faisant appel aux systèmes d'information géographiques et aux cartes topographiques numérisées pour obtenir les informations sur tous les secteurs contigus d'un paysage. Lorsque des informations sur un terrain sont intégrées sous la forme d'un MAN, les possibilités d'application multidisciplinaire en sciences de la Terre s'accroissent à un rythme fulgurant.

Un MAN à l'échelle de 1:10 000 a été produit et utilisé pour élaborer des techniques d'analyse d'images intégrées; le but consistait à établir des cartes (géologie et formes du relief) d'un site d'essai de 15 kilomètres sur 20 kilomètres de la moraine d'Oak Ridges. Les techniques mises au point dans la zone d'essai sont actuellement appliquées dans l'élaboration d'un MAN à une échelle de 1:50 000 qui englobe l'ensemble de la région du Toronto métropolitain. Des exemples d'applications de MAN sont donnés tant dans le cas du site d'essai que dans celui de modèles régionaux. Les géologues se servent également des MAN sur des ordinateurs portatifs en tant qu'outil de cartographie géologique.

[1] Oak Ridges Moraine NATMAP Project
[2] Provincial Remote Sensing Office, Ministry of Natural Resources, North York, Ontario M2N 3A1
[3] Department of Geology, University of Ottawa, Ottawa, Ontario K1N 6N5
[4] Department of Geography, Simon Fraser University, Burnaby, British Columbia V5A 1S6

INTRODUCTION

An essential component of the GSC NATMAP (NATional MApping Program) and Hydrogeology projects is digital data integration within a Geographic Information System (GIS). To achieve this objective the Oak Ridges Moraine project has developed a multicomponent database (Russell et al., 1996). A key element of this data set is the digital topographic bases and associated anthropogenic layers. The Oak Ridges Moraine (ORM) project is completing surface and subsurface geological mapping in the Greater Toronto Area. Traditionally, this type of mapping has been compiled through airphoto interpretation and field verification. Remote sensing and GIS technologies provide an additional approach and opportunities for streamlining and automating some aspects of the mapping process. Surfical geology mapping is comprised of two components, landform analysis and sediment texture mapping. Remote sensing and GIS techniques can be used to perform both these tasks. Digital Elevation Models (DEM) are suitable for landform analysis, while remote sensing imagery can provide information on both sediment textures and landform elements (Kenny et al., 1994; Kenny and Barnett, in press). With carefully selected image analysis techniques, multispectral imagery can be enhanced to identify specific elements of geological interest.

The Oak Ridges Moraine project, through collaboration with the Ontario Provincial Remote Sensing Office (PRSO) within the Ontario Ministry of Natural Resources (MNR), are integrating both remote sensing imagery (Landsat TM, SPOT, ERS-1, RADARSAT) and DEM for surface mapping and hydrogeology investigations. This paper outlines several examples of the use of DEM to environmental geosciences.

STUDY AREA

The Oak Ridges Moraine area project is mapping the surface and subsurface geology within nine 1:50 000 NTS map sheets north of Lake Ontario (Fig. 1). The study area is centred on the Oak Ridges Moraine, a 150 km long east-trending landform. This moraine is one of several prominent glaciofluvial-glaciolacustrine moraines in southern Ontario (cf. Barnett et al., 1991; Fulton, 1995). The study area is predominantly composed of glacial sediments which reach a thickness of up to 200 m. The stratigraphy is complex with sediments having been deposited during a succession of glacial events and with major erosional events incising older deposits (Sharpe et al., 1994, 1996). The surface sediments and landforms of the area record a complex series of events related to the erosional and the depositional history of the area. In some areas surface landforms may be controlled or influenced by subsurface features.

METHODOLOGY

Background

With the introduction of digital topographic maps covering broad areas of Canada, such as the Ontario Base Maps and the National Topographic Series, and the wide availability of GIS, the ability to create and use DEM for numerous geoscience applications has increased dramatically. As GIS and DEM move onto geoscientists' desktops, they are providing new opportunities for viewing and analyzing data. Satellite and airborne digital stereo imaging technology is advancing rapidly, as are the automated DEM extraction algorithms that use these data, but until these technologies become fully operational and cost effective, the best source of DEM will be from structured topographic maps.

There has been a constant refinement in the methods used to generate DEM from topographic maps and the tools used to analyze them. Some earlier DEM programs used only contour and point elevation data to interpolate a terrain surface which usually resulted in significant differences between the generated surface and the actual terrain surface. Many improvements to these early models have been developed and can be grouped broadly into two categories: drainage enforcement techniques and improved interpolation methods.

A major improvement in developing DEM is the incorporation of the digitally mapped drainage network into the model generation process, ensuring that streams and rivers represent local minima in the DEM. This process was improved by using drainage enforcement procedures on the drainage network to create 'hydrologically sound' DEM (Hutchison, 1989, 1993). The process of drainage enforcement

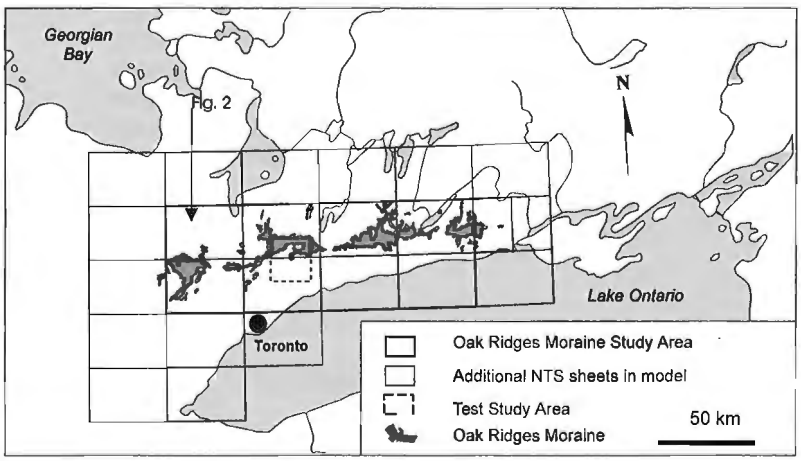

Figure 1.

Location map of the study area and area covered by the respective DEM models.

ensures the continuous downslope flow direction for all connected drainage networks to the extent of altering original point and contour elevation data to conform to drainage conditions. Recognizing that closed drainage networks are relatively rare in a natural terrain, the drainage enforcement process attempts to automatically remove, subject to user-specified tolerances, closed drainage from the DEM. With properly selected tolerances, true closed drainage conditions such as occur in areas of kettle lakes and karstic terrain can exist in the final DEM. The use of drainage networks as enforcement in the DEM generation process often requires a significant effort in restructuring and ensuring the accuracy of the drainage network.

The second largest area of improvement in DEM generation has been in the interpolation algorithms used to generate the models. Early DEM did not sufficiently represent ridge and valley lines as distinct breaks in the terrain. In elevation contour data, the location of valleys and ridge lines can be identified as points of local maximum curvature in the contours. By connecting such points between contours lines, both valley and ridge lines can be delineated automatically and used in generating DEM (Hutchison, 1989, 1993) to produce a much more realistic and informative terrain surface. These new developments in generating DEM are being used more frequently as software packages such as Arc/Info TOPOGRID and ANUDEM become available.

Once elevation data is in a digital raster format, such as a DEM, it can be treated as an image product, where image enhancement and image integration techniques can be applied (Harris et al., 1994). Common viewing enhancements for DEM include hillshading, perspective hillshading, and perspective mesh net or wireframe. Alternatively, other data sets or images can be draped on the DEM to provide a visual representation of the relationship between a secondary attribute (ie. geology, Landsat TM imagery) and topography. The DEM can also be integrated with other image products to produce stereo-imagery for analysis using either traditional stereo or digital techniques (Toutin and Rivard, 1995).

At a cursory level, interpretation of DEM surfaces relies on similar techniques as applied in airphoto interpretation, such as, assessment of surface roughness, linearity, form, spatial associations, and elevation relationships. More sophisticated analysis can be applied using mathematical morphological operators to enhance or minimize specific features (Bonham-Carter, 1994). As well the information derived using such methods can be used with other geo-referenced data sets in knowledge-based models (Srinivasan and Richards, 1993).

Model development

DEM have been developed at both the 1:10 000 and 1:50 000 scales by using the vector contour and point elevation data. The 1:10 000 model has been built using twelve, 5 m contour interval Ontario Base Maps (OBM). The 1:50 000 model presently consists of eleven NTS map sheets, with an original 10 m contour interval (Skinner and Moore, 1996). The model is presently being enlarged to 23 sheets (Fig. 1). Both models have been developed using similar interpolation techniques: contour-to-point, point-to-Triangulated Irregular Network (TIN), TIN-to-lattice, and lattice-to-Grid. The elevation data was then interpolated and grided at horizontal resolutions of 10 and 30 m for the 1:10 000 and 1:50 000 DEM respectively. A 30 m grid scale was used as this matches the resolution of TM imagery being used within the study. At the 1:50 000 scale, the major streams and lakes were incorporated. Drainage enforcement and some of the newer interpolation techniques have not yet been used on the present DEM, which make them inadequate for hydrological modelling. To use the NTS drainage network in the 1:50 000 scale DEM generation process, it must first be restructured to ensure that it is contiguous. Vector segments must be properly positioned and orientated in a downslope direction, and double line rivers replaced by single line segments. The process of restructuring the drainage network has, to a large degree, been automated by the use of recently developed macros (Paquette, 1996). The final DEM will be constructed using full drainage enforcement techniques available in ArcInfo TOPOGRID and as a result will be hydrologically sound. To assist in this task and to provide an added level of quality control, a Landsat Thematic Mapper (TM) image, georeferenced at 1:50 000 scale, and Ontario Base Map drainage are being used as backdrops. Where discrepancies between the NTS and other networks are encountered they will be investigated and corrected. This process is necessary as field mapping has identified discrepancies between the published NTS mapsheets, NTS digital files, and present stream courses.

There has not been an assessment of the accuracies of the models generated to date. For qualitative terrain mapping, accuracy is not a major issue, but for quantitative applications, including hydrological modelling an accuracy assessment of the model will be essential. Surface verification of the final model will be achieved by the integration of geodetic benchmark information available across the study area. An attempt will be made to follow United States Geological Survey (USGS) protocol, where for 7.5 minute DEM, 28 test points are selected and compared with the geodetic benchmarks (United States Geological Survey, 1990).

An additional source of terrain information, fifteen 1:25 000 scale digital lake bathymetric field sheets have been ordered from the Canadian Hydrographic Survey for portions of Lake Ontario, Lake Simcoe, Lake Scugog, and Rice Lake. These bathymetric data will be used to generate an offshore DEM which will be incorporated with the onshore DEM to provide an integrated model.

GEOSCIENCE APPLICATIONS

DEM have been applied to terrain mapping since the early 1970s (Collins, 1975). The lack of widespread use has resulted from problems associated with the generation and viewing of models which required extensive computing power and operator expertise. Desktop GIS systems now enable geologists to create and view DEM on PC systems (PCI Terrain Analysis, Spans Explorer, MapInfo/Vertical Mapper) and assorted shareware software (Microdem). The project has four principal applications for the DEM within the

surface-subsurface mapping and hydrogeology program: a) regional datum, b) terrain mapping, c) DEM and satellite image integration, and d) watershed and drainage analysis.

a) Regional datum

For the Oak Ridges Moraine project an extensive database derived from many sources has been developed (Russell et al., 1996). The elevation control on this data has been assigned from a variety of sources and in places is erroneous. As the project is interested in analyzing subsurface data with respect to depth from surface or elevation above sea level, it is necessary to have a unique project elevation datum. The DEM will provide an important role as a means of assigning new elevation control to all the data being used by the project. In addition, the projects largest subsurface data set, the Ministry of Environment and Energy waterwells, has approximately 20 to 25% location errors (G. Hunter, pers. comm., 1994). A systematic process of identifying these errors has been developed using the Ontario Base Map lot and concession fabric and elevation control (Hunter, 1996). The project anticipates comparing the DEM and waterwell elevations as a method of location error checking during a second round of verification.

b) Terrain mapping

The DEM can serve a number of functions in terrain mapping, and this role can be optimized by image enhancement and visualization techniques. Here we present three enhancements of the DEM data; hillshaded, perspective shaded relief, and filtered perspective shaded relief as a basic illustration of the power and versatility of working with elevation data in a DEM format.

From the regional 1:50 000 scale DEM a hillshaded representation is presented for the Alliston (31D/4) mapsheet (Fig. 2). This image has been generated by sampling the regional 30 m grid cell Oak Ridges Moraine DEM at a reduced resolution of 100 m spacing. This example highlights the flexibility available to geologists for regional terrain analysis. While lacking the resolution of 1:50 000 airphotos traditionally

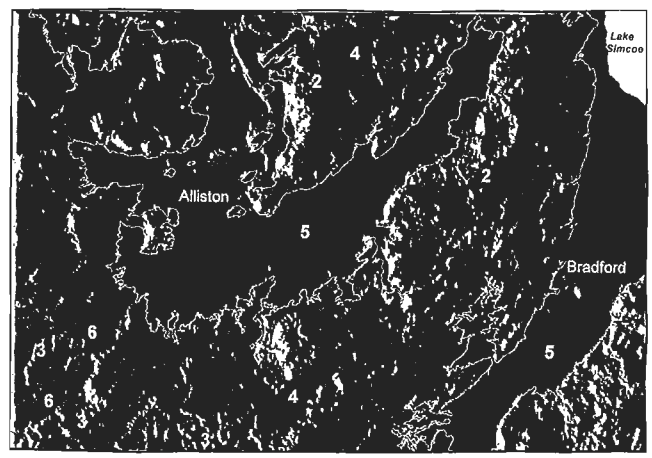

Figure 2.

A shaded relief DEM of the Alliston NTS map sheet showing a general visual classification.

Table 1. Classification table for Figure 2, indicating DEM characteristics and supplemental data layers used to assign surface classifications.

Label	Topographic character	Supplemental information from drainage & anthropogenic layers	Interpretation
6	incised, smooth	drainage layer, air photos	paleofluvial system
5	smooth, tight elevation range, below 230m	contour overlay	Lake Algonquin bottom sediments
4	smooth, elevation,		lacustrine silts
3	roughness, incoherent, elevation	mapped sand and gravel pits	ORM sands
2	elevation, roughness	mapped sand and gravel pits	sand & gravel
1	streamlined, roughness, elevation		till surface

used for regional synthesis, it provides distinct advantages of economy of time, ability to integrate or overlay other data sets, ease of topographic analyses, and optimizing advantages offered by other viewing combinations (rotation, shaded relief, vertical exaggeration, scale changes). In this example a visual analysis permits the identification of several terrain categories (Table 1). Identification of some elements has been aided by drainage and anthropogenic layers from the digital topographic bases.

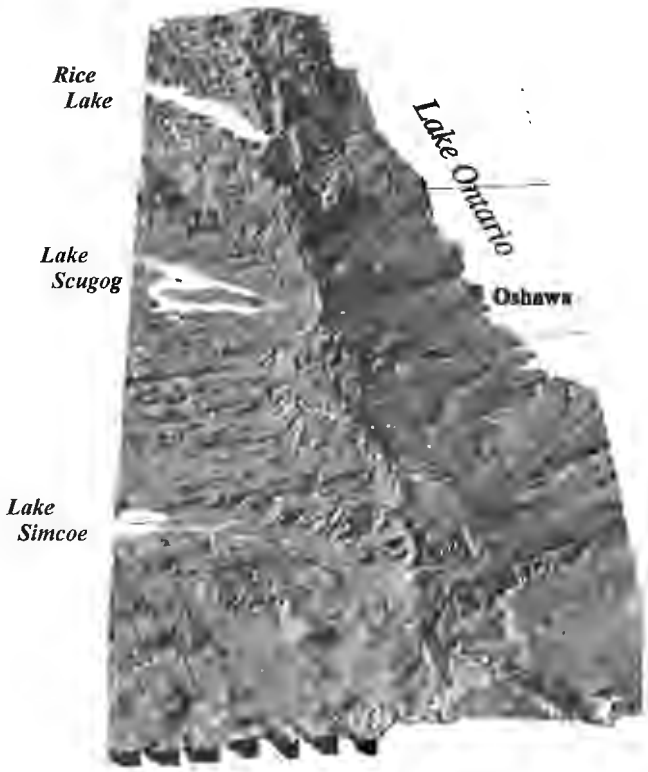

Figure 3. *A shaded relief perspective view (west to east of Whole ORM) of the 1:50 000 scale Oak Ridges Moraine DEM.*

Perspective viewing of DEM can be an effective tool for conceptual understanding of landscape relationships. A shaded relief enhancement of the moraine, (observer 25°, altitude 30°, and distance 284 km, and a sun azimuth 25°, declination of 35°, and a vertical exaggeration 12 times (Fig. 3), highlights the strong linear form of the moraine, variations in moraine width, the variable nature of the moraine crest and variations in the elevation of the moraine crest along its length.

For surficial geology mapping, a shaded relief representation of the test area was found to be an effective interpretative aid. Illumination from the northeast, at an elevation of 26°, and a vertical exaggeration of three effectively displays several of the major terrain elements (Fig. 4). To further enhance terrain characteristics, a smoothing filter (3 x 3 neighbourhood low pass) gave the terrain surface a smoother, more realistic appearance. In this view, several of the major terrain elements and terrain features can be clearly delineated, including the Halton till plain, the streamlined features on the Halton till plain, an area of hummocky moraine, an area of kames, and a glaciofluvial outwash area (Fig. 4). Other views highlighted different terrain features for mapping; an illumination set from the southeast enhances the terrain transition between the hummocky terrain and glaciofluvial outwash deposits.

c) DEM and satellite image integration

For the test site, Landsat TM imagery was merged with a SPOT Panchromatic image. An image integration methodology was selected that best preserved the spectral characteristics of the Landsat imagery (6 spectral bands @ 28 m spatial resolution), while at the same time taking advantage of the high spatial resolution of the SPOT image (single and @ 10 m spatial resolution) (Chavez et al., 1991). A stereo pair

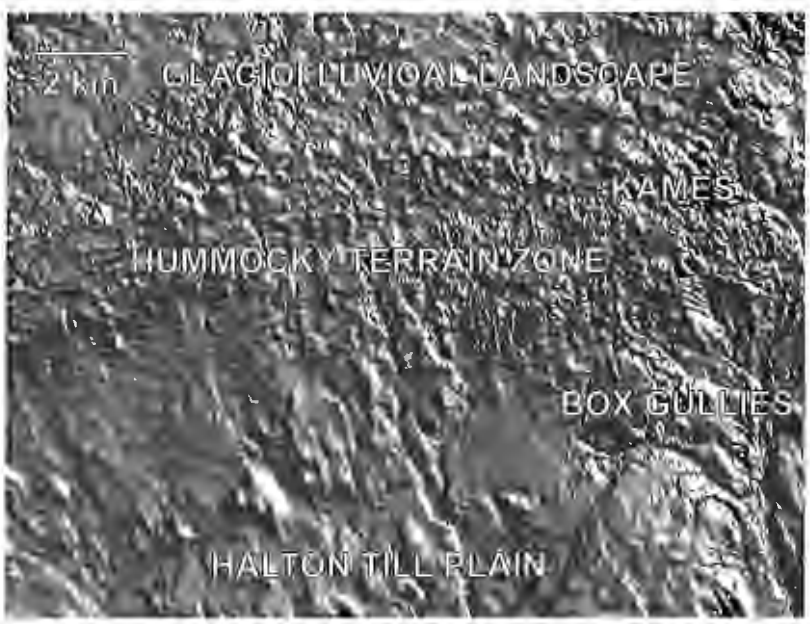

Figure 4.

Shaded relief enhancement of the test site 1:10 000 DEM with physiographic regions indicated.

was generated from the merged satellite imagery using the test site DEM (Fig. 5). This stereo-pair was generated by calculating a parallax for each pixel in the original image as a function of elevation, derived from the DEM, and a user supplied stereoscopic factor. For the processing of this image a stereoscopic factor of 15 was applied to produce the stereo effect. While such a stereoscopic factor produces a vertical exaggeration, it is not more than usually found in stereo aerial photography. Although these images are the result of several enhancements, merging techniques, and contain imagery from two different sensors and a DEM they are prepared for very traditional image/photo interpretation. A user with experience in interpreting multi-spectral imagery and stereo aerial photography can apply these skills directly on the merged imagery.

The stereo-pair shows a portion of the hummocky terrain zone at the northern margin of the Halton till plain. This hummocky terrain is a common element of moraine topography and can be delineated easily in such stereo-pairs. This hummocky terrain zone marks the most northerly advance of the Lake Ontario ice following formation of the Oak Ridges Moraine during the Late Wisconsinan.

d) Watershed and drainage analysis

A component of the hydrogeology field program is delineating the spatial distribution of groundwater discharge within watersheds by measuring stream baseflow at a number of stream locations (Hinton, in press). The net increase in stream discharge along stream segments is a measure of the groundwater discharge within each segment. The net discharge can be normalized to the length of the stream segments or to the contributing area of each stream segment (Fig. 6).

The final DEM will be used to facilitate both data presentation and analysis. The determination of stream length and drainage area requires the stream to be segmented and the subcatchment boundaries to be delineated for each flow gauging location. A hydrologically sound DEM generated using full drainage enforcement procedures will be used with existing subroutines to automate subcatchment delineation (Jenson and Dominique, 1988) and generate drainage networks based solely on terrain (Jenson and Dominique, 1988; Jensen, 1993). The DEM will also be useful for interpreting the survey results to help determine how geological and topographic factors may influence groundwater discharge. Using the DEM within a GIS, groundwater discharge along stream segments can be analyzed with respect to elevation, topographic slope, and surficial geology.

A common element of glacial landscapes are kettle lakes or hummocky moraine (Prest, 1983). In the Oak Ridges Moraine numerous kettle lakes and depressions are associated with parts of the moraine. Groundwater level measurements indicate that these landforms are frequently associated with groundwater recharge conditions. The DEM will be useful for automatically delineating kettle lakes and depressions which will aid the interpretation of regional groundwater flow

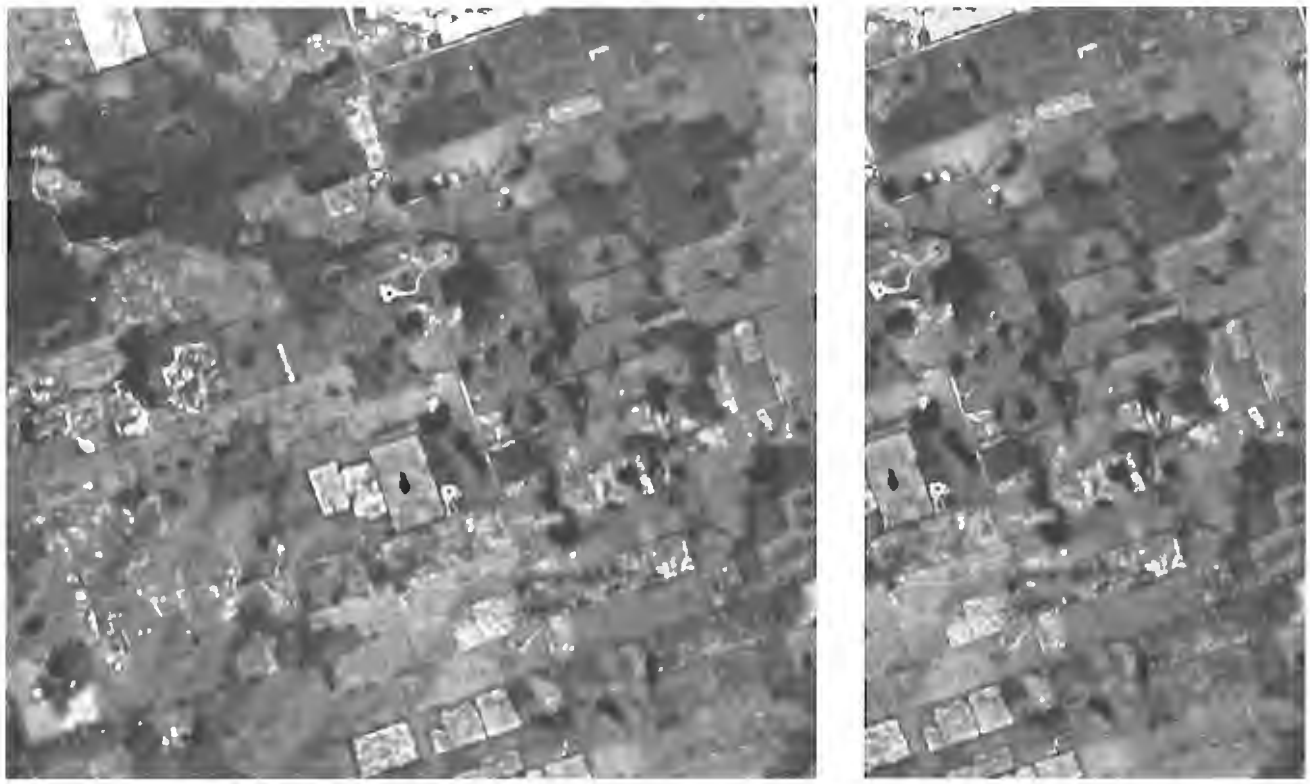

Figure 5. *Stereo-Pair showing hummocky terrain on the south central flank of the Oak Ridges Moraine. Imagery generated from merged Landsat TM, a SPOT Panchromatic image and a DEM.*

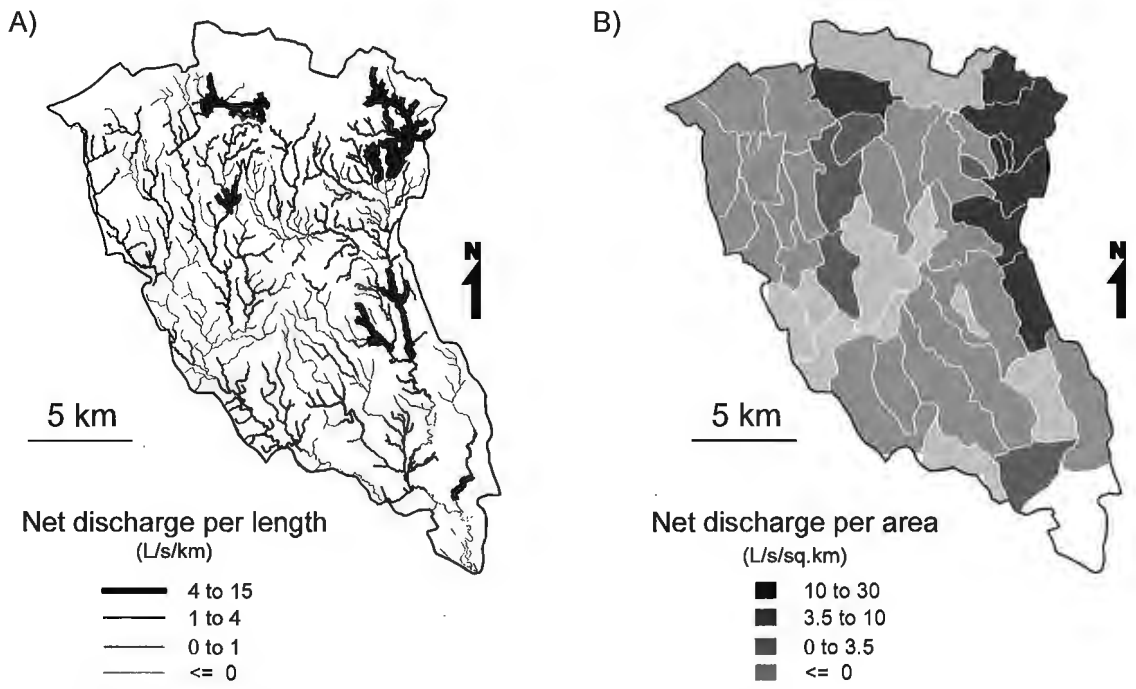

Figure 6. *Net baseflow discharge in the Duffins Creek watershed expressed with respect to* ***A)*** *stream length, and* ***B)*** *catchment area.*

conditions. Since drainage enforcement techniques may fill depressions, kettle lakes emphasize the importance of careful selection and application of DEM generation procedures.

CONCLUSIONS

Improvements in DEM generation procedures, PC hardware, and GIS and image analysis software are making the models more accurate and more accessible for multiple uses in environmental geoscience projects. Hydrologically sound DEM are being developed and tested for the Oak Ridges Moraine area of southern Ontario. These DEM will be particularly useful for several tasks including: 1) verifying georeferenced data, 2) automating various mapping procedures, 3) landform analysis, 4) integration with other imaging techniques, 5) topographic analysis of spatial data, and 6) data display and presentation.

Topographic maps are used as base maps for data presentation and analysis in geoscience projects. With the increased use and availability of GIS, digital databases, and digital maps in the geosciences, the digital representations of a topographic surface are becoming as important a tool as the topographic map.

ACKNOWLEDGMENTS

The authors would like to thank Harry Skinner for his efforts in developing the 1:50 000 DEM, Andy Moore for data visualization, and Jules Paquette for work on structuring of the drainage. We would also like to thank Andy Moore for his useful comments on a draft of this paper. Paul Stacey and Charles Logan helped on figure preparation. Funding for this work has been through the Geological Survey of Canada NATMAP and hydrogeology committees and PRSO of the Ontario Ministry of Natural Resources. H.A.J. Russell is partially supported by an NSERC Operating Grant to Dr. W. Arnott (University of Ottawa).

REFERENCES

Barnett, P.J., Cowan, W.R., and Henry, A.P.
1991: Quaternary geology of Ontario, southern sheet; Ontario Geological Survey, Map 2556.

Bonham-Carter, G.F.
1994: Geographic Information Systems for Geoscientists: Modelling with GIS; Pergamon, New York, 598 p.

Collins, S.H.
1975: Terrain parameter directly from a digital terrain model; The Canadian Surveyor, v. 29, no. 5, p. 507-518.

Chavez, P.S., Sides, S.C., and Anderson, J.A.
1991: Comparison of three different methods to merge multiresolution and multispectral data: Landsat TM and SPOT Panchromatic; Photogrammetric Engineering and Remote Sensing, v. 57, no. 3, p. 295-303.

Fulton, R.J.
1995: Surficial materials of Canada; Geological Survey of Canada, Map 1880A, scale 1:3 000 000.

Harris, J.R, Bowie, C., Rencz, A.N., and Graham, D.
1994: Computer enhancement techniques for the integration of remotely sensed imagery, geophysical, and thematic data for the geosciences; Canadian Journal of Remote Sensing, v. 20, no. 3, p. 210-221.

Hinton, M.J.
in press: Measuring stream discharge to infer the spatial distribution of groundwater discharge; Canadian Water Resources Journal.

Hunter, G.
1996: Technical Report, Hydrogeological Evaluation of the Oak Ridges Moraine Area; part of Background Report No. 3 For The Oak Ridges Moraine Planning Study, Volume 1, (prepared for Oak Ridges Moraine technical Working Committee), Ontario Ministry of Natural Resources.

Hutchison, M.F.
1989: A new procedure for griding elevation and stream line data with automatic removal of spurious pits; Journal of Hydrology, v. 106, p. 211-232.
1993: Development of a continent-wide DEM with applications to terrain and climate analysis; in Environmental Modelling with GIS, (ed.) M.F. Goodchild, B.O. Parks, and L.T. Steyaert; Oxford University Press, New York, p. 392-399.

Jensen, S.K.
1993: Applications of hydrologic information automatically extracted from digital elevation models; in Terrain Analysis and Distributed Modelling in Hydrology; (ed.) K.J. Beven and I.D. Moore; John Wiley and Sons Ltd., Chichester, p. 35-48.

Jensen, S.K. and Dominque, J.O.
1988: Extracting topographic structure from digital elevation data for Geographic Information System analysis; Photogrammetric Engineering and Remote Sensing, v. 54, no. 11, p. 1593-1600.

Kenny, F.M. and Barnett, P.J.
in press: Relating satellite radar signatures to glacial surficial materials; Canadian Water Resources Journal.

Kenny, F.M., Singhroy, V.H., and Barnett, P.J.
1994: Integration of SPOT panchromatic, ERS-1, and digital elevation data for terrain and surficial mapping; Proceedings of Tenth Thematic Conference on Geological Remote Sensing, San Antonio, Texas, 9-12 May 1994, p. 503-516

Paquette, J.
1996: Digital Elevation Models for hydrological applications in Oak Ridges Moraine, southern Ontario: the necessity for structured drainage networks; in Current Research 1996-E, Geological Survey of Canada.

Prest, V.K.
1983: Canada's hertiage of glacial features; Geological Survey of Canada, Miscellaneous Report 28, 119 p.

Russell, H.A.J., Logan, C., Brennand, T.A., Hinton, M., and Sharpe, D.R.
1996: Regional geoscience database for the Oak Ridges Moraine project (southern Ontario); in Current Research 1996; Geological Survey of Canada.

Sharpe, D.R., Barnett, P.J., Dyke, L.D., Howard, K.W.F., Hunter, G.T., Gerber, R.E., Paterson, J., and Pullan, S.E.
1994: Quaternary geology and hydrogeology of the Oak Ridges Moraine area; Geological Association of Canada-Mineralogical Association of Canada, Joint Annual Meeting, Waterloo, 1994, Field Trip A7: Guidebook, 32 p.

Sharpe, D.R., Dyke, L.D., Hinton, M.J., Pullan, S.E., Russell, H.A.J., Brennand, T.A., Barnett, P.J., and Pugin, A.
1996: Groundwater prospects in the Oak Ridges Moraine area southern Ontario: application of regional geological models in Current Research 1996-E, Geological Survey of Canada.

Skinner, H. and Moore, A.
1996: A Digital Elevation Model of the Oak Ridges Moraine, southern Ontario; Geological Survey of Canada and Ministry of Natural Resources, Government of Ontario; Geological Survey of Canada, Open File 3297, scale 1:200 000.

Srinivason, A. and Richards, J.A.
1993: Analysis of GIS spatial data using knowledge-based methods; International Journal of Geographic Information Systems, v. 7, no. 6, p. 479-500.

Toutin, T. and Rivard, B.
1995: A new tool for depth perception of multi-source data; Photogrammetric Engineering and Remote Sensing, v. 61, no. 10, p. 1209-1212

United States Geological Survey
1990: US GeoData, Digital Elevation Models; Data Users Guide 5, United States Department of the Interior, United States Geological Survey, 51 p.

Geological Survey of Canada Project 930042

Digital Elevation Models for hydrological applications in Oak Ridges Moraine, southern Ontario: the necessity for structured drainage networks[1]

J. Paquette
Terrain Sciences Division, Ottawa

Paquette, J., 1996: Digital Elevation Models for hydrological applications in Oak Ridges Moraine, southern Ontario: the necessity for structured drainage networks; in Current Research 1996-E; Geological Survey of Canada, p. 209-213.

Abstract: A Digital Elevation Model (DEM) is being developed for landform and hydrologic analysis of the Oak Ridges Moraine study area. The model, at a grid scale of 30 m, is derived from 1:50 000 scale vector data containing accurate contour lines, elevation points, and well structured drainage data for breakline enforcement. In order to use drainage vector information as breaklines, the data must respect certain conditions, such as connectivity of line segments and correct vector orientation.

The preprocessing of drainage data can involve considerable time and cost, therefore a minimum user interaction macro-process was developed using a Geographic Information System (GIS). The macro defines watershed outlets, then compares the distance of line segment nodes in order to reorient the segments as necessary. The corrected drainage database is then used as input for a hydrologically sound DEM.

Résumé : Un modèle altimétrique numérique (MAN) est en cours d'élaboration pour analyser le relief et l'hydrologie de la région de la moraine d'Oak Ridges. Le modèle (quadrillage aux mailles de de 30 mètres de côté) est élaboré à partir de données vectorielles à l'échelle de 1:50 000, lesquelles comprennent des courbes de niveau précises, des points d'altitude et des données structurées sur le réseau hydrographique pour l'établissement de bris de continuité. Pour utiliser les informations vectorielles sur le bassin hydrographique en tant que bris de continuité, les données doivent respecter certaines conditions, comme la connectivité des segments de lignes et l'orientation correcte des vecteurs.

Comme le traitement des données hydrographiques nécessite beaucoup de temps et d'argent, une instruction automatisée minimisant l'interaction de l'utilisateur (macro) a été intégrée à un système d'information géographique. La macro définit les exutoires du bassin hydrographique et compare ensuite la distance jusqu'aux noeuds des segments linéaires (afin de réorienter les segments au besoin). La base de données hydrographiques corrigée est ensuite incorporée à un MAN; à partir de ce moment, l'aspect hydrologie est considéré.

[1] Oak Ridges Moraine NATMAP Project

INTRODUCTION

The wide availability of spatial data integration software combined with increasing access to digital topographic data has resulted in Digital Elevation Models (DEM) becoming a standard data layer in geographic analysis. Geographic Information Systems (GIS) compile and integrate topographic data to build these models for use in numerous applications, such as erosion modelling, classification of landforms, and modelling of climatic phenomena (Hutchinson, 1989).

The Geological Survey of Canada NATMAP and Hydrogeology projects are developing a Digital Elevation Model of the Oak Ridges Moraine study area for landform and hydrological analysis. The algorithm used to create the model uses elevation data (contour lines and elevation points) and incorporates a drainage enforcement constraint which requires accurate drainage segments. To be useful in the interpolation, this drainage must respect certain conditions, such as connection of all line segments to create a continuous flow, eliminating "induced" closed drainage systems, and the correction of each arc segment direction so the actual terrain drainage flow is respected.

The manual processing and verification of the extensive digital drainage data sets covering the Oak Ridges Moraine study area would involve considerable work. The basis of an semi-automated process (macro) for partial drainage database correction is presented here. The macro corrects specifically line segment orientation to produce a continuous flow direction in the drainage database.

METHODOLOGY

The Oak Ridges Moraine project uses extensive National Topographic Series (NTS) base data covering twenty-three 1:50 000 scale map sheets (Kenny et al., 1996). The DEM is being developed with elevation and drainage features from these data sets. An image resolution of 30 m is used for compatibility with LANDSAT TM data. A present DEM for the NATMAP study area has been developed for nine 1:50 000 scale NTS sheets (Skinner and Moore, in press).

The DEM is to be built using the TOPOGRID module in ARC/INFO (GIS software; ESRI, 1995). This module is based on the ANUDEM interpolation program (Hutchinson, 1991). The NETWORK module, which is designed for spatial network modelling, was not available for this study so the hydrology correction work was done in the ARCEDIT and GRID modules using line feature characteristics.

Background

A variety of general purpose interpolation algorithms are available to produce DEM from irregularly distributed data. Methods using only topographic data can build elevation surfaces with a wide range of detail. An acceptable representation of regional terrain shape results when macro-scale (global) interpolation methods are used or more localized surfaces when micro-scale (local) interpolation methods are employed. The global methods become computationally inefficient with large data sets and the local methods can produce spurious edge effects and large errors where input data is sparse. In any case, use of these general purpose methods on elevation data incorporate a number of spurious low elevation points (pits or sinks) which limit the usefulness of the output DEM in hydrological applications (Hutchinson, 1989).

This effect can be overcome by a drainage enforcement algorithm which attempts to remove all undesirable pits to increase the accuracy of the drainage properties in the interpolated DEM. This is done because pits, or closed drainage systems, are usually quite rare in nature (Hutchinson, 1993). Obviously, some landforms are exceptions, such as karstic or glacial landscapes, in which case the actual pit positions and elevations can be used as input to the interpolation. These particular features can also be maintained through careful use of the tolerances during the sink removal.

The drainage enforcement factor removes the anomalous sinks which were originally incorporated in the model by the interpolation algorithm. To do so, every spurious sink, which is not an input elevation data point, is connected by a vector (links) to the lowest surrounding saddle (ridge that connects higher elevation points). The correct drainage flow is established by modifying the elevations of the sink to be above the saddle. These sink and saddle links are then joined to existing data points or previously determined links and are used as a drainage factor in the DEM. The connection of all the links produces an estimated drainage network. The drainage becomes even more accurate than by the automated estimation procedure once actual drainage vector data is incorporated in the model. The result is hydrologically sound DEM.

The interpolation algorithm used by TOPOGRID is designed to take advantage of commonly available input data and known characteristics of elevation surfaces (TOPOGRID command reference, ESRI, 1995). The algorithm incorporates the elevation interpolation and the drainage enforcement. The input data for this module includes a structured digital topographic base data (Geomatics Canada, 1994).

Vector terminology

The input topographic data consists of geographically referenced linear and point features available in vector format. The definition of these features and their associated attributes must be described in order to understand the concepts.

ARC/INFO defines a line segment (arcs) as a series of linked points or vertices. Both end vertices of an arc are called nodes; the staring vertex being the 'from-node' and the ending vertex being the 'to-node'; nodes are points where arcs intersect. This node order determines the orientation of the arc.

Additional information can be extracted from an arc network by using it to define route systems, or route attribute subclasses (ESRI, 1994). A route is a logical collection of line segments defining specific linear features, such as bus or delivery routes. Every linear feature will be stored as a different route subclass. A route feature can also be used to define drainage basins within a drainage data set. Routes are described by measuring distances along a series of line segments. These measures can then be used to locate any position along the route.

DRAINAGE CORRECTION

The drainage database required as input to TOPOGRID must contain a properly oriented, single line stream network. This implies a number of steps in database preparation:

a) Missing line segments must be added to produce a continuous drainage system and closed drainage systems are removed.

b) Double line rivers and lakes (areal features) included in the stream network must be replaced by single line vectors (centerlines) since the algorithm used for drainage enforcement requires single line vectors.

c) Finally, line segments must be reoriented so every set of segments is oriented in a common flow direction.

To obtain an appropriate drainage database, for use in TOPOGRID, these three steps must be completed. The presented order is preferable to minimize errors but it is not essential. Missing data for the first two steps in the drainage correction of the NTS topographic data for the Oak Ridges Moraine study area precipitated the work on segment orientation correction (step c). This step can be done at the beginning of the drainage correction process since every line segment will have been properly oriented in the final output, including lines defining areal features. If the segment connection step (step a) was not previously completed, the macro will therefore be applied on a greater number of drainage basins (considering erroneous closed drainage basins).

The first step in drainage correction (step a) will be done by comparing the available drainage data (1:50 000 scale) to the Ontario Base Maps (OBM; 1:10 000 scale) and satellite imagery (LANDSAT TM, SPOT; Kenny et al., 1996). The elevation data (1:50 000 scale) will also be used for additional information. Missing segments will be identified and added to ensure complete drainage systems.

The area feature replacement by single line vectors (step b) is essential as TOPOGRID requires stream line data to be connected and free of areal features. An automated procedure which transposes the double line features to a raster and establishes cost-distance paths, is being developed to create these vectors.

A semi-automated procedure was developed for the correction of segment orientation (step c). This macro is based on the sample program presented in the TOPOGRID command reference (ESRI, 1995) and line segment definitions. The guiding principle is that, as in actual drainage networks, every line segment in the drainage database must be oriented towards a specific point representing the stream outlet. This simulates a continuous flow direction. To achieve this, the data is treated sequentially (Fig. 1). The example in Figure 2 shows different stages in the procedure with data from the Bolton area, NTS 30M/13 (Geomatics Canada, 1994). Anomalies in this sample drainage data set, such as missing segments and areal features, were removed to emphasize the flow correction process.

At the beginning of the process, a route system is created on the raw drainage database (Fig. 2a) so that every drainage basin, or separate group of arcs, is defined as a distinct route. This determines the total number of drainage basins and relates every arc to a single route (Fig. 1, stage 1). A stream outlet is then determined for every one of the created routes.

To determine stream outlets, the macro starts by selecting arcs that are oriented away from other arcs in the basin. Only arcs with a 'to-node' not connected to other arcs are selected. As an additional condition, an arc is removed from the selected set if all connecting arcs point towards its 'from-node'. This produces a selected set of arcs that are pointing outwards without having a local orientation trend. An arc reorientation (flipping) procedure then corrects the selected arcs (Fig. 1, stage 2). This stage is essential since it reduces the number of outward pointing arcs (Fig. 2b).

Once the automated procedure has selected the revised set of outward pointing arcs, user interaction is necessary to modify the selection until one single arc, which corresponds to the stream outlet, is selected for every route (Fig. 1, stage 3). The user can update the selected arcs, verify the basins that don't have an arc selected, or the basins that have more than one in order to obtain the stream outlets. The to-nodes of the final selected set of arcs become the outlet point for each of the individual drainage basins. A preliminary DEM, built without a corrected drainage network, could be used to determine general flow patterns and reduce user interaction.

A new route subclass is created using the outlets as starting points for distance measurements on each route. These measurements now become important since the from-nodes and to-nodes of every arc will have a distance attribute field which determines its position on the route. Since every arc in a drainage basin should be oriented towards the stream outlet, the to-node must be closer to the outlet than the from-node. Using the new measurements, arcs which have a greater

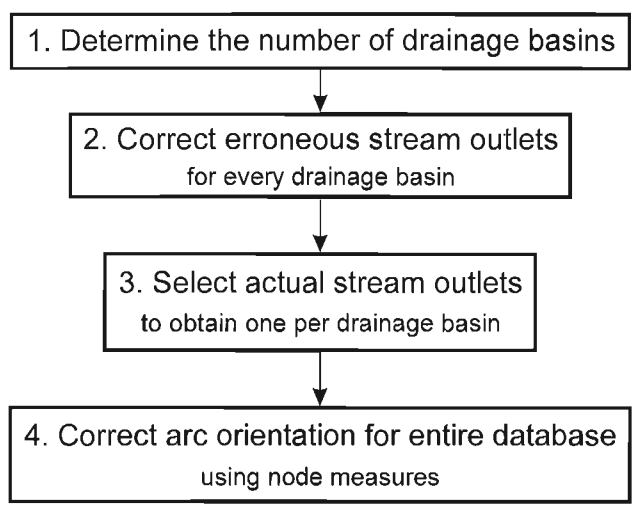

Figure 1. Flow chart showing the four stages in the line segment orientation correction process.

to-node distance than a from-node distance can be selected and reoriented (Fig. 1, stage 4). This produces an output database where every arc is pointing towards its associated stream outlet by means of continuous line segments (Fig. 2c).

CONCLUSION

Drainage enforcement factors applied in the generation of a DEM reduces the number of spurious pits incorporated in the surface by general purpose interpolation algorithms. The DEM is even more accurate when stream line data is used as the drainage factor. A number of processing steps are required to use the stream line data for breakline enforcement and elevation correction, such as addition of missing line segments, replacement of area features by a centerline and correction of line segment orientation.

A semi-automated procedure was developed for line segment orientation correction. This significantly reduces the amount of work necessary to correct these errors in a raw drainage database. The algorithm described for correction is basically an iterative selection process and can be used in any

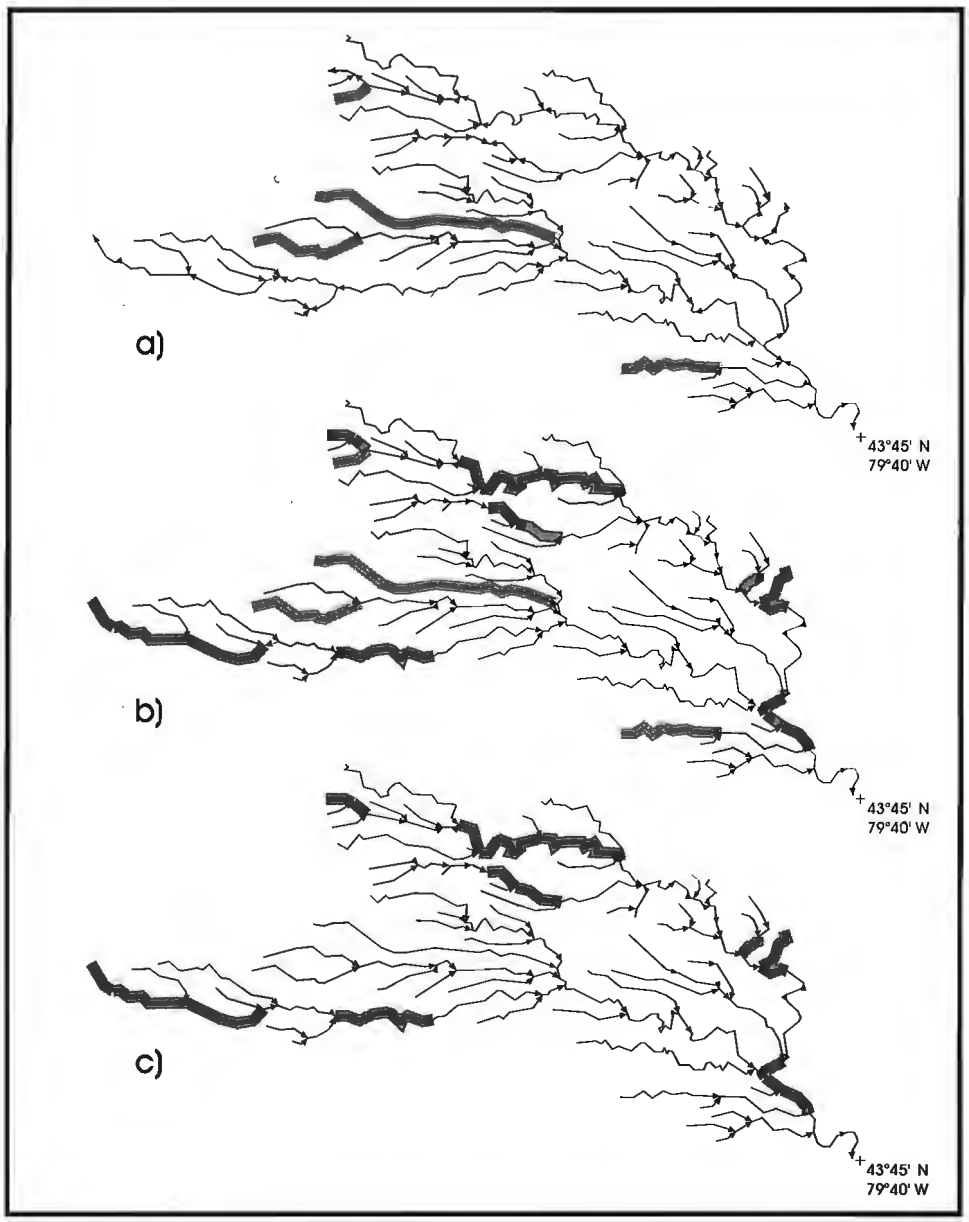

Figure 2. *Changes on the drainage database during the correction process;* ***a)*** *raw database;* ***b)*** *after stage 2, where erroneous stream outlets are corrected;* ***c)*** *the output database with continuous flow direction; pale highlights were corrected from a to b; dark highlights were corrected from b to c; (Geomatics Canada, 1994).*

GIS software with macro capabilities. The corrected data set is a first step towards the development of a hydrologically sound DEM for the Oak Ridges Moraine study area.

ACKNOWLEDGMENTS

The author would like to thank Hazen Russel for supporting this project and his helpful comments for this report and Andy Moore for his assistance. Funding for this project was provided by the Geological Survey of Canada NATMAP and Hydrogeology committees.

REFERENCES

Environmental Systems Research Institute (ESRI), inc.
1994: ARC/INFO Data Management: Concepts, data models, database design, and storage; Environmental Systems Research Institute (ESRI), inc., 393 p.
1995: ArcDoc; online help, version 7.0, Environmental Systems Research Institute (ESRI), inc.

Geomatics Canada
1994: Bolton, 30M/13; National Topographic Series (NTS) digital topographic map, Geomatics Canada.

Hutchinson, M.F.
1989: Procedure for griding elevation and stream line data with automatic removal of spurious pits; Journal of Hydrology, v. 106, p. 211-232.
1991: ANUDEM, Centre for Resource and Environmental Studies, Australian National University, Canberro, Australia, 8 p.
1993: Development of a continent-wide DEM with applications to terrain and climate analysis; in Environmental Modelling with GIS, (ed.) M.F. Goodchild, B.O. Parks, and L.T. Steyaert; Oxford University Press, p. 392-399.

Kenny, F.M., Russel, H.A.J., Hinton M.J., and Brennand, T.A.
1996: Digital Elevation Models in environmental geoscience, Oak Ridges Moraine, southern Ontario; in Current Research 1996-E, Geological Survey of Canada.

Skinner, H. and Moore, A.
1996: A Digital Elevation Model of the Oak Ridges Moraine, Southern Ontario; Geological Survey of Canada and Ministry of Natural Resources, Government of Ontario, Geological Survey of Canada, Open File 3297.

Geological Survey of Canada Project 930042

Le glissement de terrain d'avril 1996 à Saint-Boniface-de-Shawinigan, Québec : observations et données préliminaires

C. Bégin, S.G. Evans[1], M. Parent, D. Demers[2], G. Grondin[2], D.E. Lawrence[1], J.M. Aylsworth[1], Y. Michaud, G.R. Brooks[1], et R. Couture[3]

Centre géoscientifique de Québec, Sainte-Foy

Bégin, C., Evans, S.G., Parent, M., Demers, D., Grondin, G., Lawrence, D.E., Aylsworth, J.M., Michaud, Y., Brooks, G.R., et Couture, R., 1996 : Le glissement de terrain d'avril 1996 à Saint-Boniface-de-Shawinigan, Québec : observations et données préliminaires; dans Recherches en cours 1996-E, Commission géologique du Canada, p. 215-223.

Résumé : Dans l'après-midi du 21 avril 1996, la municipalité de Saint-Boniface-de-Shawinigan (Québec) a été touchée par un important glissement de terrain qui s'est produit dans les sédiments de la Mer de Champlain, le long de la rivière Machiche. Le glissement, de type rétrogressif multiple, a affecté un secteur de 31 hectares occupé surtout par des plantations de pins et a impliqué un volume de matériel d'environ 8 X 10^6 m^3, ce qui en fait probablement le plus considérable de ce siècle dans les basses terres du Saint-Laurent. Le faible degré de liquéfaction des argiles et l'exiguïté de la vallée expliqueraient la rétrogression limitée du glissement (moy. 125 m) et sa forme. Le glissement n'a entraîné ni pertes de vie ni dommages aux bâtiments résidentiels ou agricoles, mais a provoqué une hausse importante du niveau de la rivière en amont, puisque le matériel emporté a complètement remblayé le fond de la vallée. L'inondation qui en a résulté a mis en péril la sécurité de certaines infrastructures routières et hydroélectriques.

Abstract: During the afternoon of April 21, 1996, a massive landslide occurred in Champlain Sea sediments along the Machiche River, 5 km south of St-Boniface-de-Shawinigan, Quebec. The slide occurred in a wooded area following a period of intense rainfall. The landslide is thought to be a multiple retrogressive type with a volume estimated to be about 8 X 10^6 m^3. It is one of the largest landslides (31 ha) to have occurred in the St-Lawrence Lowlands in this century. The debris blocked the valley of the Machiche River and caused a lake to form upstream. This landslide has shown the vulnerability of hydroelectric facilities and roads to major landslides in Champlain Sea sediments.

[1] Division de la science des terrains
[2] Ministère des transports du Québec, Service géotechnique et géologie, 930, chemin Sainte-Foy (Québec) G1S 4X9
[3] Département de géologie et de génie géologique, Université Laval, Sainte-Foy (Québec) G1K 7P4

INTRODUCTION

Dans l'après-midi du 21 avril 1996, un important glissement de terrain de type rétrogressif multiple (fig. 1A, B), d'environ 1 km de largeur, s'est produit dans les sédiments de la Mer de Champlain sur la rive est de la rivière Machiche dans la municipalité de Saint-Boniface-de-Shawinigan, à 25 km au nord-ouest de Trois-Rivières, au Québec (fig. 2). La masse mobilisée est venue buter contre le flanc ouest de la vallée, bloquant complètement le cours de la rivière Machiche. À l'endroit du glissement, la vallée a été remblayée sur près de la moitié de sa dénivelée. Le déplacement de matériel n'a pas causé de pertes de vie ni de dommages aux bâtiments résidentiels ou agricoles mais a partiellement détruit des plantations de pins. Il a également exigé la fermeture temporaire d'un tronçon de la route 153 ainsi que du pont qui s'y trouve, en raison de la hausse rapide du niveau de la rivière en amont de la zone mobilisée. Au plus fort de l'inondation (26 au 28 avril), les eaux de la rivière avaient monté de plus de 10 m, submergeant les forêts sur les versants de la vallée ainsi que la base du remblai du pont de la route 153. Bien qu'ayant eu un impact mineur sur le plan humain et économique, le glissement de Saint-Boniface a brusquement rappelé aux habitants de la Mauricie que leurs terres, de par leurs caractéristiques géotechniques et géomorphologiques, présentent des risques élevés de mouvements de masse qu'il importe de documenter le plus précisément possible, afin de minimiser les conséquences des catastrophes futures.

Les objectifs de ce manuscrit sont (1) de présenter un premier compte rendu des données disponibles; et (2) de faire état des observations effectuées sur place les 28 et 29 avril, soit environ sept jours après le glissement. Suit une description du contexte géologique général, des propriétés géotechniques des argiles impliquées ainsi que des caractéristiques physiques du glissement. En outre, bien qu'une discussion soit présentée des causes possibles de la rupture en relation avec le contexte météorologique, il reste que les explications définitives nécessiteront des travaux additionnels.

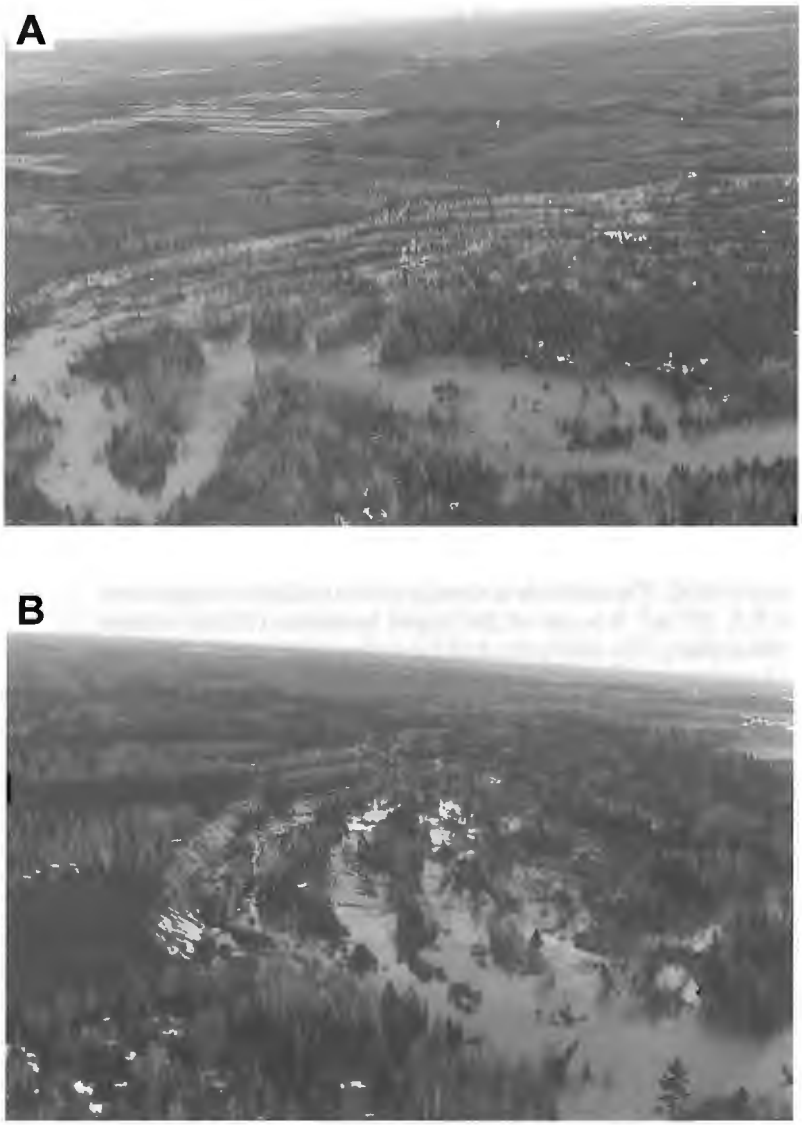

Figure 1.

*Vue générale vers l'est (**A**) et, plus rapprochée, vers le sud-est (**B**) du glissement de terrain de Saint-Boniface. On peut observer sur les photos la forme évasée de l'amphithéâtre qui s'étend sur 1,1 km ainsi que quelques-unes des sections de terrasse (gradins) qui ont glissé successivement et bloqué la vallée de la rivière Machiche. À noter, le caractère continu des gradins parallèles à l'escarpement. Les dépressions entre les crêtes ont été comblées par les eaux de la rivière qui ont monté d'environ 10 m. À noter aussi, la proximité de la ligne de transmission électrique à haut voltage. Les photos ont été prises le 28 avril, entre 15h00 et 16h00.*

CONTEXTE GÉOLOGIQUE DU SITE

Géologie du Quaternaire et cadre stratigraphique

Grâce aux travaux pionniers de Gadd et Karrow (1959) et de Gadd (1971), la géologie du Quaternaire de cette région de la Mauricie est l'une des mieux connues du Québec. De plus, elle a fait l'objet de mises à jour récentes par Occhietti (1980) et par Parent et Occhietti (1988), notamment en ce qui a trait aux faciès et à la chronologie des sédiments de la Mer de Champlain.

Le glissement d'avril 1996 est situé à un peu plus d'un kilomètre au nord de la Moraine de Saint-Narcisse, au sein du paléo-delta du Saint-Maurice dans la Mer de Champlain (fig. 3: unité Md). À l'endroit du glissement et dans ses environs, la séquence des sédiments quaternaires est conforme à celle démontrée par Parent et Occhietti (1988). Au sommet de la séquence (fig. 4), à une altitude d'environ 110 m, les sédiments deltaïques sont constitués de sables fins et moyens à litage oblique sur une épaisseur d'environ 5 m. Ceux-ci surmontent des sédiments prodeltaïques épais d'environ 1 m et constitués de turbidites sableuses fines. Cette séquence deltaïque, dont l'épaisseur d'ensemble varie régionalement de 6 à 10 m, date de la fin de l'épisode champlainien, soit entre 10 300 et 10 000 ans BP (Parent et Occhietti, 1988).

Les nombreux sondages réalisés dans la région immédiate du glissement (fig. 3) indiquent que les argiles marines atteignent plus de 40 m d'épaisseur sous les sédiments deltaïques. Le toit de la séquence argileuse se situe à une altitude d'environ 100 m. La partie supérieure de l'unité est un silt argileux finement laminé et comportant des interlits de sable très fin; son épaisseur n'a pu être mesurée précisément à l'endroit du glissement mais, d'après les données de forage, elle est d'environ 2 ou 3 m dans la région immédiate. Les silts laminés surmontent une unité de silt argileux massif et plutôt homogène, où le pourcentage d'argile varie de 30 à 40 %. La sédimentation argileuse marine aux environs de Saint-Boniface-de-Shawinigan a débuté après la mise en place de la Moraine de Saint-Narcisse, soit après 10 800 ans BP (Parent et Occhietti, 1988).

L'âge de l'exondation finale du delta n'est pas connu avec exactitude; toutefois, les datations ^{14}C disponibles pour la région indiquent un âge compris entre 10 000 et 9 500 ans BP pour le niveau de 110 m, celui sur lequel le glissement s'est produit. Les autres glissements apparaissant sur la figure 3 ont eu lieu durant l'intervalle compris entre 9500 ans BP et aujourd'hui. L'encaissement des cours d'eau dans les sédiments de la Mer de Champlain est évidemment le processus principal menant à la déstabilisation des versants formés dans les sédiments marins de la région.

Importance des glissements de terrain dans la région

La région de Shawinigan est notoire pour l'importance des glissements de terrain qui y ont eu lieu (Karrow, 1972; Chagnon et al., 1979). Plusieurs cicatrices de coulées boueuses, souvent

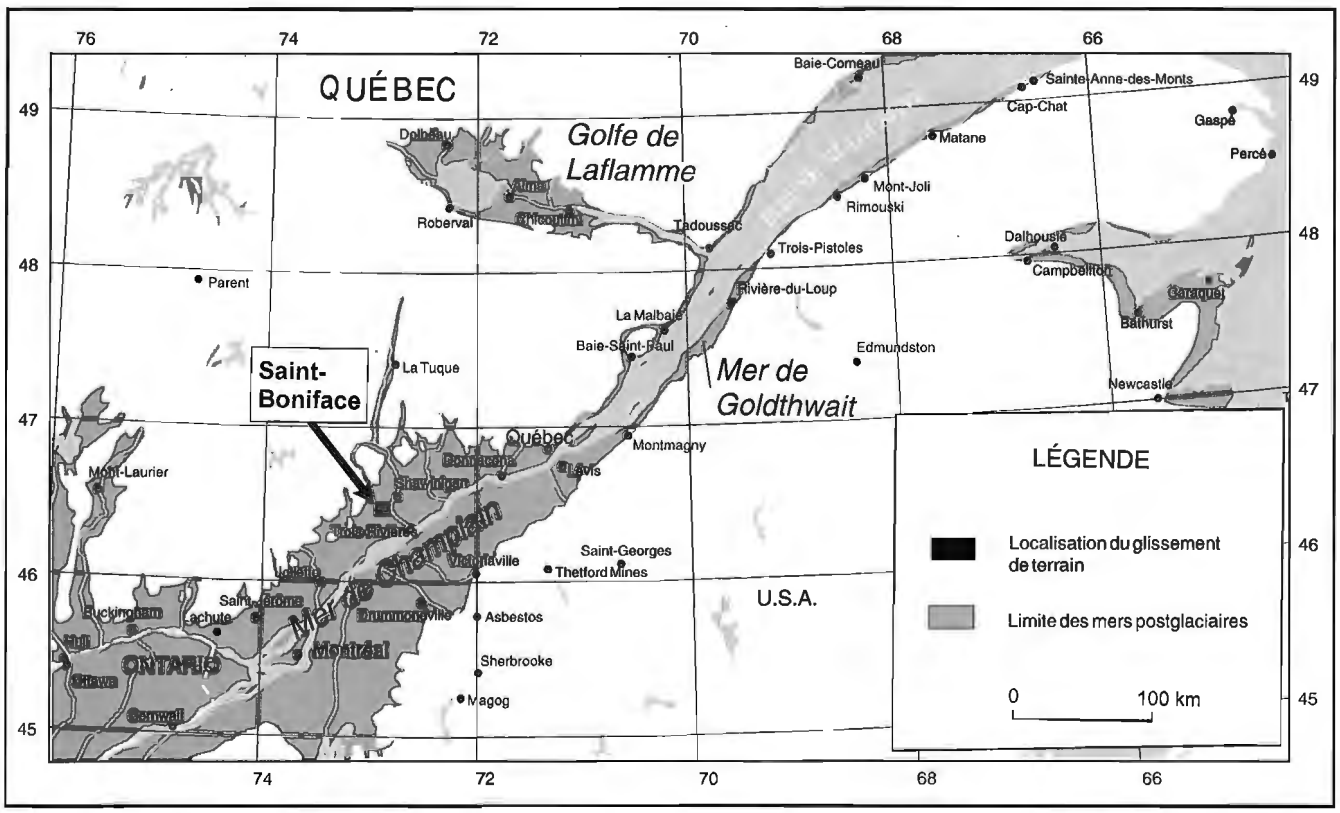

Figure 2. *Carte schématisée des limites des mers postglaciaires (Mer de Champlain, Mer de Goldthwait et Golfe de Laflamme) de l'Est du Canada (adaptée de Parent et Occhietti, 1988).*

de grande envergure, ont été identifiées le long de de la rivière Yamachiche et de la rivière du Loup, généralement au sud de la Moraine de Saint-Narcisse (Karrow, 1972). Comme le montre la figure 3, il existe également plusieurs glissements au nord de cette moraine, notamment ceux de Saint-Étienne-des-Grès et de Saint-Boniface, de même que celui de Shawinigan-Sud (La Bissonnière, *in* Desjardins, 1980). Les datations disponibles semblent indiquer plusieurs générations de glissements, souvent imbriqués les uns dans les autres, comme le tristement célèbre cas de Saint-Jean-Vianney (Tavenas et al., 1971). Les plus vieilles coulées dans le secteur de Saint-Boniface ont été datées à 8 510 ans BP; elles seraient donc légèrement postérieures au retrait de la Mer de Champlain. Par la suite, plusieurs autres coulées, dont les âges sont centrés sur 3 900 ans BP, 690 ans BP et 390 ans BP, sont survenues dans la région (Chagnon et al., 1979; Desjardins, 1980). Celles datées à 390 ans BP ont été associées au tremblement de terre du 5 février 1663 (Desjardins, 1980). Plus récemment, en mai 1883, un glissement de terrain de 18 ha s'est produit le long de la rivière Yamachiche, près de Charette (fig. 3). De plus, il existe juste à l'aval du glissement de 1996, mais sur le versant ouest de la rivière, deux autres glissements de type rétrogressif (fig. 3).

Propriétés géotechniques des argiles

Plusieurs sondages ont été réalisés dans la région par le ministère des Ressources naturelles du Québec et par le ministère des Transports du Québec (fig. 3). La figure 5, qui illustre les résultats de deux sondages au pénétromètre statique pratiqués à 0,5 et 2,8 km de part et d'autre du glissement, montre que la stratigraphie et les propriétés des sédiments sont remarquablement homogènes. Au sommet, un sable fin de compacité moyenne devient stratifié vers la base, jusqu'à une altitude d'environ 100 m. Sous ce niveau, les sols sont constitués d'un silt argileux homogène. Ces deux unités passent graduellement de l'une à l'autre par l'entremise d'une zone de transition stratifiée dont l'épaisseur est de quelques mètres seulement. Les sédiments argileux ont une épaisseur minimale de 40 m.

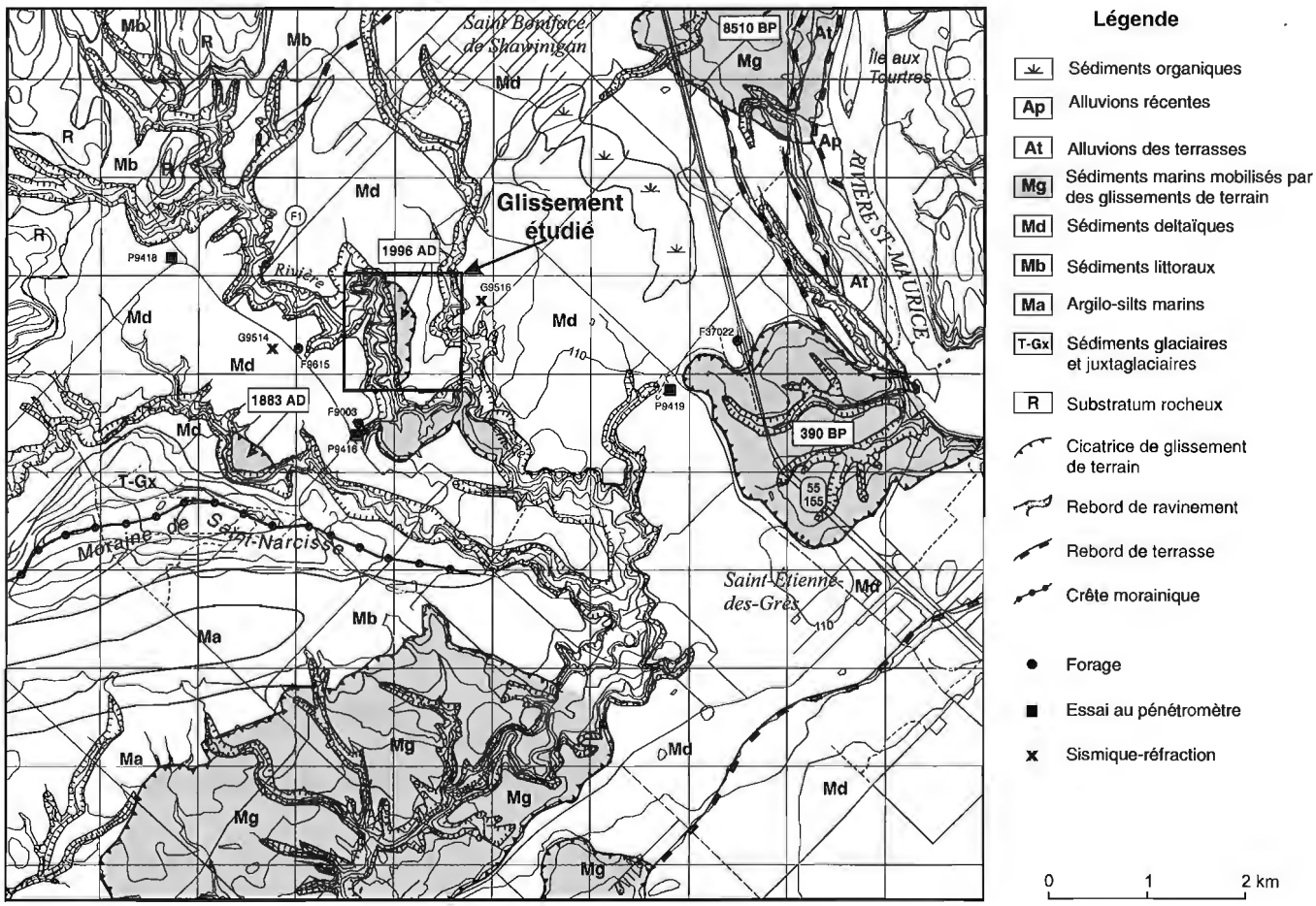

Figure 3. *Carte simplifiée de la géologie du Quaternaire, montrant la localisation du glissement d'avril 1996 et les autres glissements survenus dans la région ainsi que les sites de forages et autres essais géotechniques. Partie du feuillet SNRC 31 I/7 (Trois-Rivières).*

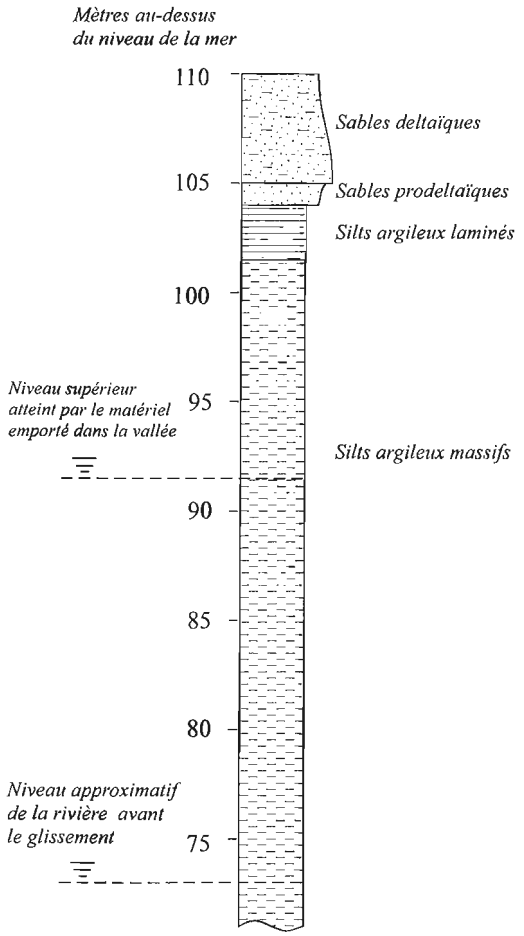

Figure 4. *Coupe stratigraphique schématique des sédiments de la Mer de Champlain à l'endroit du glissement.*

La figure 6 donne les principales propriétés géotechniques de la partie supérieure du dépôt argileux dans un forage (F1) pratiqué à moins de 1 km en amont du glissement. De façon générale, la granulométrie est relativement uniforme. La fraction argileuse (inférieure à 2 µm) est généralement comprise entre 30 et 40 % et le sable n'est présent que sous forme de traces, sauf lorsqu'il constitue de petits interlits. L'indice de plasticité du matériau est pratiquement constant à une valeur de 20. La teneur en eau, qui se situe entre 34 et 53 %, est toujours légèrement supérieure à la limite de liquidité. L'indice de liquidité varie entre 1,1 et 1,4, ce qui n'est pas élevé pour les argiles postglaciaires de l'Est du Canada. La résistance au cisaillement non drainé, mesurée au scissomètre de chantier, montre un profil qui suit deux segments. Du sommet jusqu'à 19 m de profondeur, la résistance diminue linéairement, passant de 95 kPa au sommet à 75 kPa plus en profondeur. Sous l'élévation 80,5 m environ, on observe un changement de pente et la résistance augmente par la suite avec la profondeur. À l'altitude de 60 m, soit environ 50 m de profondeur par rapport à l'endroit du glissement, la résistance atteint 160 kPa.

Mesurée à l'état remanié à l'aide du cône suédois, la résistance est relativement faible, oscillant entre des valeurs de 0,7 à 2,6 kPa, ce qui donne des valeurs de sensibilité comprises entre 15 et 92. De plus, des observations faites sur le terrain suite au glissement ont permis d'identifier des couches de sensibilité très variable. Si l'on utilise les relations de Leroueil et al. (1983) pour évaluer la pression de préconsolidation, le rapport de surconsolidation (OCR) atteint une valeur de 12 au sommet du dépôt et décroît par la suite jusqu'à une valeur de 1,7 à 18 m de profondeur.

Les conditions piézométriques ne sont pas bien connues dans le secteur du glissement. Les quelques renseignements disponibles pour le moment proviennent des trois (3) piézomètres en sommet de talus au forage F1 (fig. 3). Selon le seul relevé disponible, datant d'août 1984, les conditions d'eaux souterraines présentent un léger gradient vers le bas en sommet de talus, ce qui est conforme à ce que l'on observe généralement dans de telles conditions géométriques et stratigraphiques (Lafleur et Lefebvre, 1980). Cependant, il est fort probable que les conditions au pied du talus présentent un fort gradient vers le haut, en raison de la présence des nombreux affleurements rocheux que forment les contreforts laurentiens situés au nord-est et de l'immense crête de la Moraine de Saint-Narcisse située à 2 km au sud-ouest. Ces deux éléments topographiques constituent des zones de recharge majeure de la nappe d'eau souterraine. De nombreux cas similaires ont déjà été rapportés (La Rochelle et al., 1970; Lefebvre, 1986; Grondin et Demers, 1996), des coulées argileuses s'étant formées dans des conditions de gradients de pied ascendants très élevés.

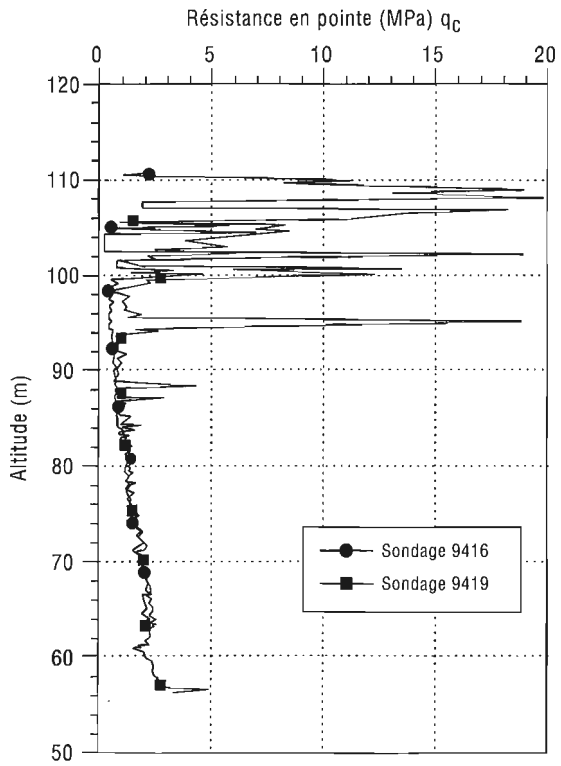

Figure 5. *Comparaison des résultats d'essais CPI à proximité du glissement (voir fig. 3 pour la localisation).*

LE GLISSEMENT DE SAINT-BONIFACE

Morphologie et mécanisme

Le glissement de terrain s'est produit dans un secteur très dynamique de la rivière Machiche, caractérisé surtout par de nombreux méandres et d'anciennes cicatrices de glissements. Avant la rupture du versant, plusieurs sections convexes de méandres étaient soumises à l'érosion fluviale et affectées par des glissements de type pelliculaire. La couronne de l'amphithéâtre du glissement de 1996 s'étend sur plus d'un kilomètre (1,1 km) sur la rive est de la rivière Machiche (fig. 1 et 3). En projection plane, elle se présente comme un arc de cercle très étiré, composé de trois lobes distincts. La hauteur du mur de l'amphithéâtre est d'environ 18 m et la distance de rétrogression moyenne est de 125 m (max.: 175 m). La cicatrice est d'une superficie d'environ 0,176 km^2 (16 ha) alors que l'ensemble de la zone touchée par le glissement avoisine 0,31 km^2 (31 ha). En tenant compte des différents niveaux de terrasse impliqués, de la profondeur estimée du glissement et de la taille de l'amphithéâtre, un volume de 7,75 X 10^6 m^3 de matériel emporté a été évalué. Un tel volume de matériel fait du glissement de Saint-Boniface probablement le plus important à s'être produit dans les basses terres du Saint-Laurent au cours du dernier siècle (Landry et Mercier, 1983).

La morphologie de la surface du glissement est typique des glissements rétrogressifs multiples. Elle est caractérisée par la présence d'au moins huit gradins (ou terrassettes), correspondant à autant de sections subparallèles de terrasse qui ont basculé dans l'axe du glissement. La largeur des gradins varie entre 5 et 15 m. L'orientation des arbres sur le revers des terrassettes indique le sens de la rotation (fig. 7). Les dépressions entre les gradins sont inondées ou occupées par des amas de matériel partiellement remanié. Des blocs d'argile de plusieurs dizaines de mètres de diamètre ont été observés dans la zone d'accumulation. La rétrogression multiple par glissement rotationnel est sans aucun doute le mécanisme dominant dans le cas du glissement de Saint-Boniface. Cependant, la présence sporadique de crêtes triangulaires, peut-être associées aux «prismes et coins» décrits par Carson (1979), porte à croire que l'étalement latéral a pu jouer un rôle.

L'essentiel du matériel emporté s'est accumulé au fond de la vallée en une masse relativement compacte d'une hauteur d'environ 17 m. L'importance des blocs de matériel non

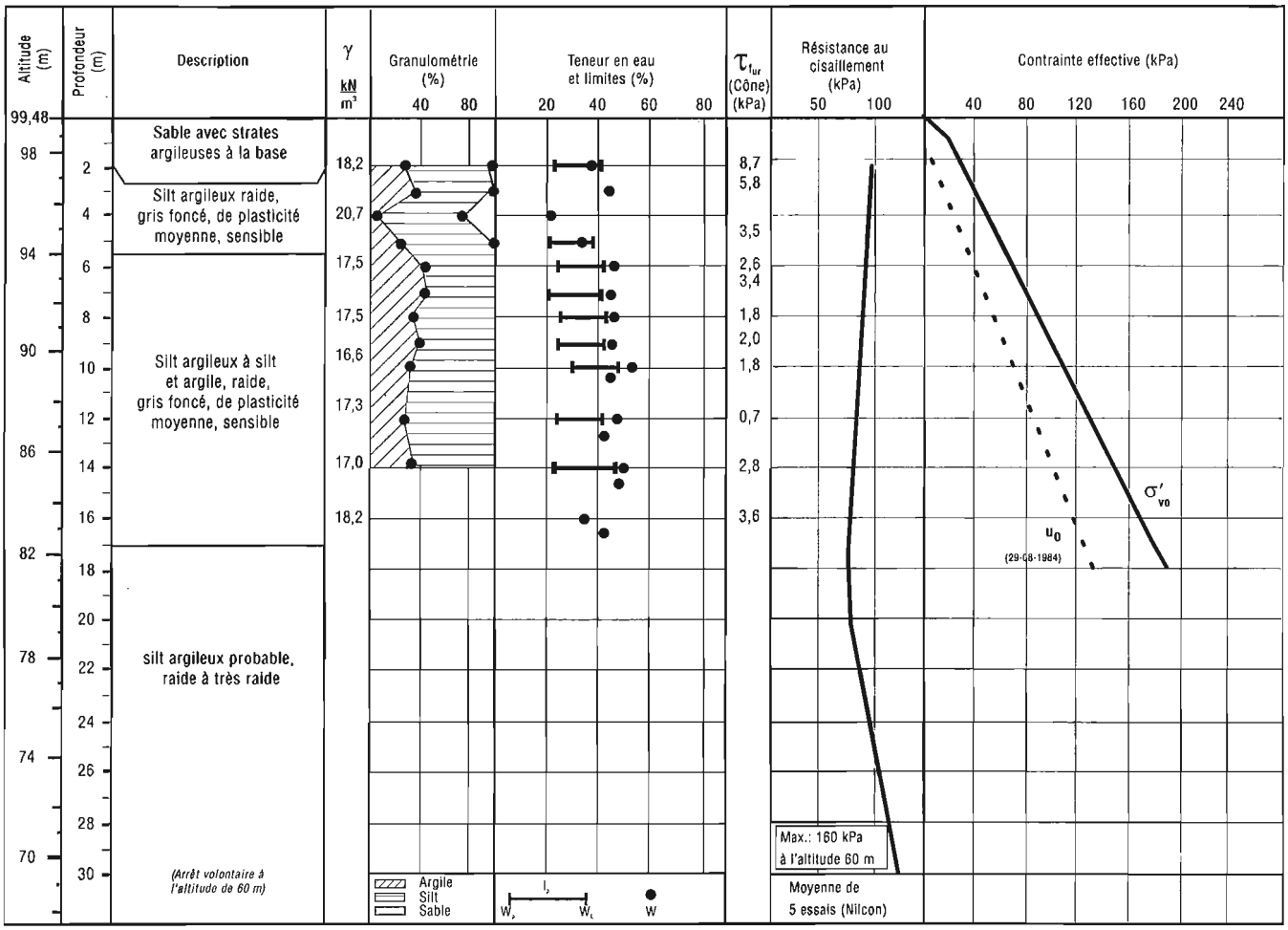

Figure 6. *Profil géotechnique à l'intersection de la route 153 et de la rivière Machiche.*

déformé dans la zone de glissement, ainsi que l'absence d'amas de matériel transporté en aval du glissement, indiquent un degré de liquéfaction peu élevé, contrairement à ce qui avait été observé au glissement de Lemieux en 1993 (Brooks et al., 1994; Evans and Brooks, 1994). Cette observation concorde avec les valeurs de sensibilité des argiles mesurées dans un forage adjacent (fig. 6). Cette caractéristique des argiles, alliée à l'exiguïté de la vallée, pourrait expliquer la rétrogression limitée du glissement et la forme qui en résulte, comme l'ont déjà suggéré Carson et Lajoie (1981).

Évolution du niveau de la rivière Machiche

Le matériel emporté a non seulement bloqué le cours de la rivière Machiche mais aussi complètement remblayé le fond de la vallée, entraînant la formation d'un lac de retenue sur plus de 3 km en amont (fig. 8). Le niveau des eaux a rapidement monté de plus de 10 m, jusqu'à l'altitude de 86 m, à un rythme de 30 cm/heure et serait demeuré stable jusqu'au 28 avril. Les eaux de la rivière auraient surmonté le barrage de débris dans la matinée du 28 avril. Un écoulement d'eau important, canalisé dans plusieurs chenaux, a été observé vers 11h30 (28 avril) dans le secteur aval du glissement.

DISCUSSION

Le glissement de terrain de Saint-Boniface se serait produit dimanche le 21 avril 1996 vers 15h00. Le moment relativement précis du glissement a été rapporté par M. É. Gélinas qui, ce même dimanche après-midi, a entendu et senti une quinzaine de détonations sourdes venant du sol. M. Gélinas a indiqué que les détonations se sont produites à un intervalle de 30 secondes à une minute et que l'ensemble de l'événement a duré de cinq à dix minutes. D'autre part, le niveau anormalement élevé de la rivière Machiche a été constaté par M. É. Gauthier mardi matin, le 23 avril. Le glissement de terrain aurait donc eu lieu quatre jours avant d'avoir été signalé aux autorités civiles.

La détermination du moment précis du glissement s'avère une donnée importante dans l'interprétation des causes de la rupture. Il devient alors possible de relier l'initiation du glissement à des événements ponctuels d'origine naturel le ou anthropique, comme cela est souvent le cas (Lebuis et al., 1982), ou encore, à un contexte paléoclimatique particulier (Bégin et Filion, 1988). Il est, bien connu par exemple, que des événements séismiques peuvent déclencher d'importantes ruptures dans les dépôts marins sensibles (Desjardins, 1980; Keefer, 1984; Filion et al., 1991; Lefebvre et al., 1992).

Figure 7. *Gradins dans la zone de glissement correspondant à des sections de terrasse qui ont glissé successivement (rétrogression). L'inclinaison des arbres permet d'établir le sens de la rotation.*

Figure 8. *Vue aérienne d'une partie de l'inondation créée par le glissement qui a complètement bloqué la vallée de la rivière Machiche. Le glissement est visible au centre de la photo (entre les deux flèches). La photo a été prise vers le sud-est, le 28 avril, vers 16h00.*

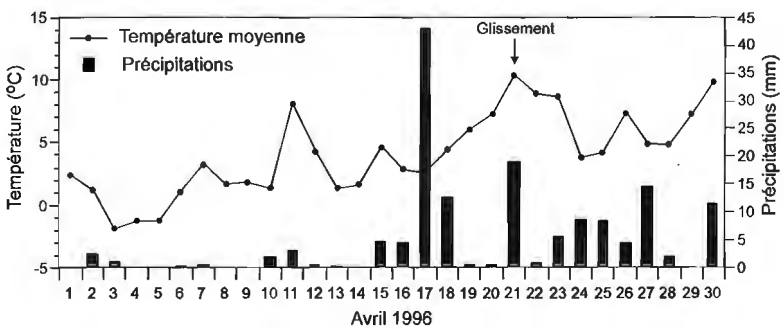

Figure 9.

Températures moyennes et précipitations d'avril 1996 enregistrées à la station de Trois-Rivières (données fournies par Environnement Canada).

Les vérifications effectuées auprès du Réseau sismographique canadien ont montré qu'aucune secousse sismique n'a été enregistrée dans la région au moment du glissement (M. Lamontagne, comm. pers.). Les enquêtes réalisées à la municipalité de Saint-Boniface confirment également qu'aucun travail important d'excavation ou de remblaiement n'aurait été effectué au cours de la période du glissement de terrain. En revanche, deux importants orages électriques accompagnés de très fortes pluies ont eu lieu les 17 et 21 avril (fig. 9). Il appert donc, comme cela a déjà été observé ailleurs (Eden et al., 1971), que le glissement se soit produit peu après un important orage.

Sur le plan météorologique, le mois d'avril 1996 aura été propice aux glissements de terrain. Dans la région, les municipalités de Lyster et de Saint-Tite ont également été touchées par des ruptures de versants (Le Nouvelliste, 27 avril 1996). Les précipitations d'avril 1996 ont atteint des valeurs records partout dans le sud du Québec (Le Soleil, 1er mai 1996). À la station de Trois-Rivières, les précipitations d'avril ont atteint 149 mm et ont été ponctuées de deux averses exceptionnelles les 17 et 21 avril (fig. 9). La période du 18 au 21 avril a également été marquée par un réchauffement accéléré des températures ayant causé la fonte rapide du couvert de neige et, à certains endroits, le dégel du sol. L'infiltration des eaux de fonte n'aurait cependant pas été un facteur déterminant dans le cas du glissement de Saint-Boniface puisque, le 28 avril, le sol était encore gelé à l'intérieur de la pinède surplombant l'amphithéâtre et le couvert de neige y a été estimé à plus de 20 %. À la même date, 6 cm de gel ont été mesurés sur le revers des gradins à l'intérieur de la zone de glissement. Comme l'ont démontré Kenney et Lau (1984), il est fort peu probable que l'orage précédant le glissement ait provoqué des augmentations significatives des pressions interstitielles dans le massif argileux. Toutefois, le ruissellement des eaux de fonte peut grandement contribuer à la crue printanière des rivières et ainsi augmenter l'activité érosive des cours d'eau. De plus, il est possible qu'un gradient hydraulique ascendant au pied des talus ait participé à la diminution de la stabilité du versant.

Les informations disponibles à ce jour semblent indiquer que le niveau exceptionnellement élevé de la rivière Machiche, lié aux fortes précipitations du mois d'avril et à la fonte rapide des neiges, pourrait être à l'origine du glissement de Saint-Boniface. Ce haut niveau d'eau aurait entraîné des conditions d'érosion fluviale critiques pour la stabilité des berges. Des décrochements mineurs se seraient alors produits et auraient lourdement hypothéqué l'équilibre du versant est de la rivière où les pentes étaient parmi les plus abruptes du secteur.

CONCLUSIONS

Le glissement de Saint-Boniface s,est produit vers 15h00 le 21 avril 1996 en réponse aux précipitations exceptionnelles du mois d'avril. La rétrogression multiple par rotation dans un contexte de liquéfaction limitée des argiles serait le mécanisme dominant en cause. Au moins huit rétrogressions successives ont entraîné le recul de la terrasse supérieure sur une distance maximum de 175 m et ont impliqué un volume de matériel avoisinant les 8×10^6 m^3. La faible liquéfaction des argiles ainsi que l'exiguïté de la vallée expliqueraient la rétrogression limitée du glissement et sa forme. La rupture du versant, ainsi que l'inondation qu'elle a causée en amont, n'ont entraîné ni pertes de vie ni dommages aux bâtiments résidentiels ou agricoles. Elles auraient pu cependant avoir des lourdes conséquences sur certaines infrastructures routières et hydro-électriques.

REMERCIEMENTS

Les auteurs remercient M. C. Gélinas (Saint-Boniface) pour les informations pertinentes concernant les événements qui se sont produits sur ses terres. Ils sont également reconnaissants envers R. Boivin, É. Boisvert et M. Boutin pour leur aide à la réalisation des figures. Enfin, ils remercient S. Paradis pour sa lecture critique du manuscrit.

RÉFÉRENCES

Bégin, C. and Filion, L.
1988: Age of landslides along the Grande Rivière de la Baleine estuary, eastern coast of Hudson Bay, Québec (Canada); Boreas, v. 17, p. 289-299.

Brooks, G.R., Aylsworth, J.M., Evans, S.G., and Lawence, D.E.
1994: The Lemieux landslide of June 20, 1993, South Nation valley, southeastern Ontario – a photographic record; Geological Survey of Canada, Miscellaneous report 56, 18 p.

Carson, M.A.
1979: Le glissement de Rigaud (Québec) du 3 mai 1978: Une interprétation du mode de rupture d'après la morphologie de la cicatrice; Géographie physique et Quaternaire, v. 33, p. 63-92.

Carson, M.A. and Lajoie, G.
1981: Some constraints on the severity of landslide penetration in sensitive deposits; Géographie physique et Quaternaire, v. 35, p. 301-316.

Chagnon, J.Y., Lebuis, J., Allard, J.D., et Robert, J.M.
1979: Argiles sensibles, pentes instables, mesures correctives et coulées des régions de Québec et de Shawinigan; Réunion annuelle conjointe AGC-AMC, Québec 1979. Livret-guide de l'excursion B-11, 40 p.

Desjardins, R.
1980: Tremblement de terre et glissements de terrain: corrélations entre des datations au ^{14}C et des données historiques à Shawinigan, Québec; Géographie physique et Quaternaire, v. 34, p. 359-362.

Eden, W.J., Fletcher, E.B., and Mitchell, R.J.
1971: South Nation River Landslide, 15 May 1971; Canadian Geotechnical Journal, v. 8, p. 446-451.

Evans, S.G. and Brooks, G.R.
1994: An earthflow in sensitive Champlain Sea sediments at Lemieux, Ontario, June 20 1993, and its impact on the South Nation River. Canadian Geotechnical Journal, v. 31, p. 384-394.

Filion, L., Quinty, F. and Bégin, C.
1991: A chronology of landslide activity in the valley of Rivière du Gouffre, Charlevoix, Québec; Canadian Journal of Earth Sciences, v. 28, p. 250-256.

Gadd, N.R.
1971: Pleistocene geology of the central St. Lawrence Lowland; Geological Survey of Canada, Memoir 359, 153 p.

Gadd, N.R. and Karrow, P.F.
1959: Surficial geology, Trois-Rivières, Quebec; Geological Survey of Canada, Map 54-1959.

Grondin, G. and Demers, D.
(sous presse): The 1989 Saint-Liguori flakeslide: characterization and remedial work; Proceedings of Seventh International Symposium on Landslides, Trondheim, Norway, June 1996.

Karrow, P.F.
1972: Earthflows in the Grondines and Trois-Rivières areas, Québec; Canadian Journal of Earth Sciences, v. 9, p. 561-573.

Keefer, D.K.
1984: Landslides caused by earthquakes; Geological Society of America Bulletin, v. 95, p. 406-421.
Kenney, T.C. and Lau, K.C.
1984: Temporal changes of groundwater pressure in a natural slope of nonfissured clay; Canadian Geotechnical Journal, v. 21, p. 138-146.
Lafleur, J. and Lefebvre, G.
1980: Groundwater regime associated with slope stability in Champlain clay deposit; Canadian Geotechnical Journal, v. 17, p. 44-53.
Landry, B. et Mercier, M.
1983: Notions de géologie, avec exemples du Québec; Modulo Éditeurs, 426 p.
La Rochelle, P., Chagnon, J.-Y., and Lefebvre, G.
1970: Regional geology in the marine clay deposits of eastern Canada; Canadian Geotechnical Journal, v. 7, p. 145-156.
Lebuis, J., Robert, J.-M., and Rissman, P.
1982: Regional mapping of landslide hazard in Québec; Symposium on Slopes on Soft Clays, Proceedings; Swedish Geotechnical Institute, report 17, p. 205-262.
Lefebvre, G.
1986: Slope instability and valley formation in Canadian soft clay deposits; Canadian Geotechnical Journal, v. 23, p. 261-270.
Lefebvre, G., Leboeuf, D., Hornych, P., and Tanguay, L.
1992: Slope failures associated with the 1988 Saguenay earthquake, Québec, Canada; Canadian Geotechnical Journal, v. 29, p. 117-130.
Leroueil, S., Tavenas, F., et Le Bihan, J.P.
1983: Caractéristiques des argiles de l'est du Canada; Revue canadienne de Géotechnique, v. 20, p. 681-705.
Occhietti, S.
1980: Le Quaternaire de la région de Trois-Rivières-Shawinigan, Québec. Contribution à la paléogéographie de la vallée moyenne du Saint-Laurent et corrélations stratigraphiques; Université du Québec à Trois-Rivières, Paléo-Québec, v. 10, 227 p.
Parent, M. and Occhietti, S.
1988: Late Wisconsinan deglaciation and Champlain Sea invasion in the St. Lawrence Valley, Québec; Géographie physique et Quaternaire, v. 42, p. 215-246.
Tavenas, F., Chagnon, J.-Y., and La Rochelle, P.
1971: The Saint-Jean-Vianney landslide: observations and eyewitnesses accounts; Canadian Geotechnical Journal, v. 8, p. 463-478.

Projets 960001 et 950030 de la Commission géologique du Canada

Résultats initiaux de la caractérisation géochimique des aquifères du piémont laurentien dans la municipalité régionale de comtés de Portneuf (Québec)

É. Bourque, M.R. LaFlèche[1], R. Lefebvre[1] et Y. Michaud
Centre géoscientifique de Québec, Sainte-Foy

Bourque, É., LaFlèche, M.R., Lefebvre, R., et Michaud, Y., 1996 : Résultats initiaux de la caractérisation géochimique des aquifères du piémont laurentien dans la municipalité régionale de comtés de Portneuf (Québec); dans Recherches en cours 1996-E; Commission géologique du Canada, p. 225-232.

Résumé : Une caractérisation hydrogéochimique des eaux souterraines est en cours dans la municipalité régionale de comtés (MRC) de Portneuf, dans le cadre d'un projet de cartographie hydrogéologique régionale. L'étude de la qualité de l'eau souterraine a débuté par l'analyse de paramètres inorganiques et microbiologiques de 37 échantillons d'eau souterraine. On constate des variations importantes de la composition et de la qualité des eaux souterraines, ainsi que des dépassements d'objectifs esthétiques fréquents. On observe une dégradation de la qualité des eaux souterraines. Une présence significative de nitrates a été mesurée dans 41 % des puits échantillonnés. De plus, l'aménagement et l'entretien des puits privés semblent déficients puisque 50 % des échantillons provenant de ces puits ne respectaient pas les normes microbiologiques.

Abstract: A hydrogeochemical groundwater study is underway in the Portneuf MRC (municipalité régionale de comtés) as part of a regional groundwater mapping project. This groundwater quality investigation has analyzed 37 groundwater samples for inorganic and bacteriologic parameters. We noticed significant variations in the groundwater composition and quality, with several samples exceeding aesthetical objectives. We observed a degradation of the groundwater quality. Significant concentrations of nitrates have been measured for 41% of the samples. Moreover, private well installations and maintenance seem to be deficient since 50% of the samples taken from those wells exceeded the microbiological norms.

[1] INRS-Géoressources, 2535, boul. Laurier, Sainte-Foy (Québec) G1V 4C7

INTRODUCTION

Les eaux souterraines représentent une ressource renouvelable de première importance, très exploitée partout dans le monde. Au Québec, environ 17 % de la population dépend des eaux souterraines pour son approvisionnement en eau. En milieu rural, cette proportion est de l'ordre de 90 %. Les eaux souterraines sont utilisées comme source d'approvisionnement en eau potable, mais également pour des fins agricoles et industrielles.

L'eau souterraine possède un avantage économique par rapport à l'eau de surface comme source d'approvisionnement en eau potable pour les petites municipalités. En effet les coûts de captage et de traitement sont normalement beaucoup moins élevés que pour les eaux de surface. Des facteurs importants sont aussi la régularité de la qualité de l'eau souterraine et le fait qu'elle soit habituellement exempte de solides en suspension et de micro-organismes pathogènes, en raison de la filtration à laquelle elle est sujette lors de sa circulation. Les eaux souterraines ont également généralement un caractère extensif et une accessibilité qui en font une ressource appropriée pour les villages et les fermes.

L'eau souterraine est une composante fondamentale du cycle de l'eau. Elle résulte de l'infiltration des précipitations et circule à travers un milieu perméable fait de matériaux granulaires ou fracturés. L'eau souterraine émerge dans les cours d'eau, permettant ainsi leur alimentation. Les caractéristiques chimiques et physico-chimiques de l'eau souterraine sont fonction de la composition de l'eau s'infiltrant dans l'aquifère, mais également des réactions avec les minéraux présents dans le sol et dans la formation aquifère. En effet, l'eau est impliquée dans de nombreux processus géochimiques (altération, dissolution, précipitation et sorption). Sa composition est donc modifiée progressivement tout au long de son parcours. Les modifications de composition chimique sont également fonction du temps de résidence de l'eau dans l'aquifère, qui peut varier de quelques mois à plusieurs années, en fonction des vitesses d'écoulement.

L'origine de l'eau souterraine et son cheminement à travers les formations géologiques peuvent en principe être déduits indirectement par l'étude de la signature géochimique des eaux, suite aux réactions chimiques qui se produisent dans les aquifères (par ex., gains d'ions dus à la dissolution, ou pertes occasionnées par précipitation de phases minérales). La composition chimique et isotopique de l'eau souterraine est donc susceptible de contribuer efficacement aux études portant sur la délimitation des aquifères, l'identification des zones de recharge et d'émergence et la nature des liens entre les aquifères.

La qualité de l'eau souterraine peut être compromise par des activités polluantes anthropiques d'origine : 1) domestique (aménagement de fosses septiques); 2) agricole (épandage d'engrais chimiques, de fumier, d'herbicides et de pesticides); 3) industrielle (fuites d'hydrocarbures, etc.) et 4) communautaires (aménagement de lieux d'enfouissement sanitaire, etc.). La géologie du sous-sol peut également affecter la qualité naturelle des eaux souterraines. En effet, certains éléments comme le fer, le soufre, le manganèse, le calcium et le magnésium (dureté), le fluor et l'arsenic sont parfois présents dans les eaux à des concentrations particulièrement élevées sans que des sources de contamination anthropique ne soient en cause.

La nécessité de mettre au point des approches préventives à la contamination et d'instaurer des mesures de protection de l'eau souterraine est de plus en plus reconnue par les scientifiques et les principaux intervenants en matière de gestion des eaux souterraines. Ces mesures sont d'autant plus justifiées que les travaux de recherche en eau, d'aménagement d'unités de captage et de restauration d'aquifères contaminés impliquent des coûts très imposants. Le ministère de l'Environnement et de la Faune du Québec (MEF) finalise présentement une nouvelle politique de gestion des eaux souterraines qui responsabilisera les MRC face à la protection des eaux souterraines.

La présente étude s'inscrit dans le cadre d'un projet pilote d'étude hydrogéologique des aquifères du piémont laurentien dans la MRC de Portneuf (fig. 1). Ce projet a pour but le développement d'une méthodologie utile pour caractériser les aquifères, évaluer leurs potentiels en terme de quantité et de qualité, évaluer leur vulnérabilité à la contamination, les classifier et, finalement, mettre sur pied des mesures adéquates de gestion et de protection de cette ressource. Les usagers visés sont les MRC. Il s'agit, en effet, de pourvoir ces unités administratives d'une méthodologie et d'outils qui leur permettront de respecter la politique des eaux souterraines qui sera implantée ainsi que les règlements qui en découleront.

Le volet «caractérisation hydrogéochimique» du projet-pilote permettra principalement de mesurer les concentrations «naturelles» des éléments chimiques contenus dans l'eau souterraine. Les paramètres inorganiques analysés sont les ions majeurs (cations et anions), les principaux nutriments (par ex. nitrates, phosphates) et les métaux à l'état de traces (tableau 1). Ces éléments ou composés sont d'abord dosés afin de vérifier le respect des normes de potabilité et d'objectifs

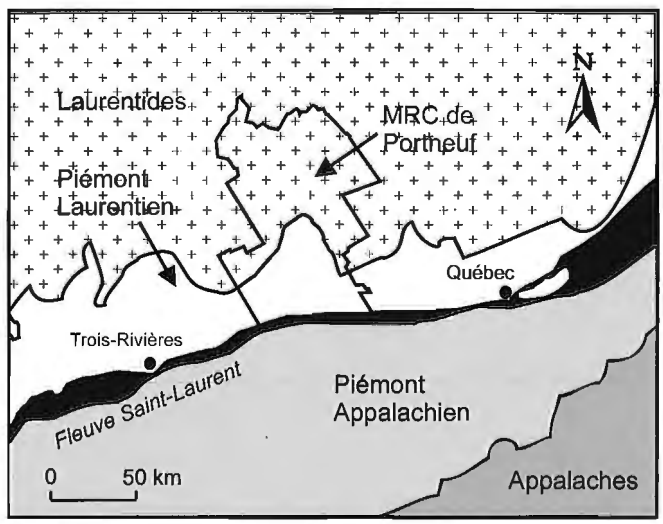

Figure 1. *Localisation du piémont Laurentien et de la MRC de Portneuf.*

Tableau 1. Paramètres analysés, méthodes d'analyse et préservation des échantillons.

paramètres	méthode d'analyse	préservatifs
Al, B, Ba, Ca, Cr, Cu, Fe, K, Mg, Mn, Na, Ni, Si, Sr, Zn	ICP-AES	HNO_3
Ag, As, B, Ba, Be, Bi, Cd, Co, Cr, Cu, Cs, La, Li, Mn, Mo, Ni, Pb, Rb, Sb, Se, Sn, Sr, Th, U, Va, Zn	ICP-MS	HNO_3
NH_3, $NO_3 + NO_2$, PO_4	colorimétrie	H_2SO_4
CN	colorimétrie	NaOH
F, SO_4	colorimétrie	-------
sulfures	colorimétrie	AcZn/NaOH
Cl	conductivité	-------
Hg	fluorimétrie	$K_2Cr_2O_7$*HNO_3
As	génération d'hydrures	HNO_3

esthétiques. Ils sont également nécessaires à l'identification des sources de contamination anthropique et à la modélisation géochimique des différentes formations aquifères.

CONTEXTE HYDROGÉOLOGIQUE DE LA MRC DE PORTNEUF

La MRC de Portneuf est située sur la rive nord du Saint-Laurent, à mis chemin entre les villes de Québec et de Trois-Rivières (fig. 1). Elle chevauche les unités physiographiques des basses-terres du Saint-Laurent et des Laurentides. Les eaux souterraines s'y écoulent dans trois types de formations géologiques différentes : 1) des sédiments non consolidés mis en place dans la mer de Champlain (principaux aquifères exploités par les municipalités); 2) des roches sédimentaires paléozoïques (calcaires et schistes argileux; plutôt utilisées lorsqu'aucune autre formation n'est présente); et 3) des roches cristallines du socle précambrien (gneiss granitiques et tonalitiques; surtout exploités par des puits de particuliers).

MÉTHODOLOGIE

Les paramètres dosés et les techniques analytiques utilisées sont présentés au tableau 1. De plus, des analyses microbiologiques ont été faites pour les coliformes totaux et fécaux, les streptocoques fécaux et les B.H.A.A. (bactéries hétérotrophes viables aérobies ou anaérobies facultatives). Toutes ces analyses ont été effectuées dans les laboratoires du MEF et de l'INRS-Géoressources. Certaines mesures ont été effectuées sur place afin de pouvoir déterminer quantitativement des paramètres qui évoluent après l'échantillonnage : le pH, l'alcalinité, l'oxygène dissous, la conductivité et la quantité de solides dissous totaux.

L'étude des métaux à l'état de traces et d'ultra-traces nécessite la prise de précautions particulières. Ainsi, le matériel d'échantillonnage (bouteilles et instruments utilisés pour les prélèvements : tubes à clapet, membranes filtrantes, seringues utilisées pour la filtration) a été décontaminé à l'aide d'eau nanopure acidifiée (10 à 15 % d'acide nitrique Aristar^{MD} 69 %) et rincé abondamment à l'eau nanopure (système Millipore^{MD}). Les échantillons pour l'analyse de métaux ont été acidifiés afin d'éviter la précipitation ou l'adsorption des métaux sur les parois des contenants et de minimiser la prolifération bactérienne ainsi que certaines réactions d'oxydation. Ces échantillons ont également été filtrés, afin de pouvoir mesurer les concentrations dissoutes (fraction <0,45µm) et non la contribution provenant de la dissolution partielle de particules en suspension. L'utilisation de divers préservatifs a également été nécessaire pour l'analyse de paramètres supplémentaires (tableau 1).

L'échantillonnage a été réalisé de septembre à novembre 1995. Trente-sept (37) échantillons d'eau souterraine ont été prélevés. Le choix des sites a été fait de façon à ce qu'ils soient représentatifs du territoire à l'étude ainsi que des principaux aquifères et des principales sources d'approvisionnement existantes (fig. 2). Parmi les puits échantillonnés, 24 sont aménagés dans des dépôts meubles et 13 dans le roc. De ces derniers, huit puits sont dans des formations de gneiss granitique, deux dans des schistes argileux (ou shales) et trois dans des calcaires. Il est à noter que dans l'ensemble, 31 puits sont aménagés dans des nappes libres et six se situent dans des aquifères confinés. L'échantillonnage impliquait des puits de particuliers, des unités de captage reliées à des aqueducs municipaux ou privés, des réservoirs et des bassins de rétention aménagés afin de capter une source ou résurgence. Des précautions ont été prises afin de minimiser la contamination lors de l'échantillonnage et ainsi un remplissage direct des bouteilles a été effectué lorsque l'occasion le permettait (par ex., accès à un robinet). Un tube à clapet en Téflon^{MD} (par ex., dans le cas de réservoirs ou de puits de surface) ou un contenant (par ex., dans le cas de bassins de rétention) préalablement décontaminés ont été utilisés à l'occasion. L'eau des robinets était purgée jusqu'à ce que la température devienne stable, afin de s'assurer qu'elle n'ait pas résidé dans la tuyauterie. Les échantillons d'eau, auxquels étaient ajoutés des préservatifs au besoin, ont été conservés à 4°C et dans l'obscurité jusqu'à leur analyse.

La qualité des dosages et du matériel d'échantillonnage a été évaluée par l'analyse de duplicatas et de blancs de lavage (environ 10 % des échantillons dans chaque cas). Des vérifications de l'équilibre chimique (électro-neutralité de la solution) ont également été faites pour chaque échantillon.

RÉSULTATS

La composition géochimique en ions majeurs de certains échantillons représentatifs des eaux souterraines est illustrée sous forme de diagrammes de Schoeller aux figures 3 et 4. De plus, la qualité de l'eau souterraine est représentée, géographiquement, à l'aide de diagrammes de Stiff à la figure 5.

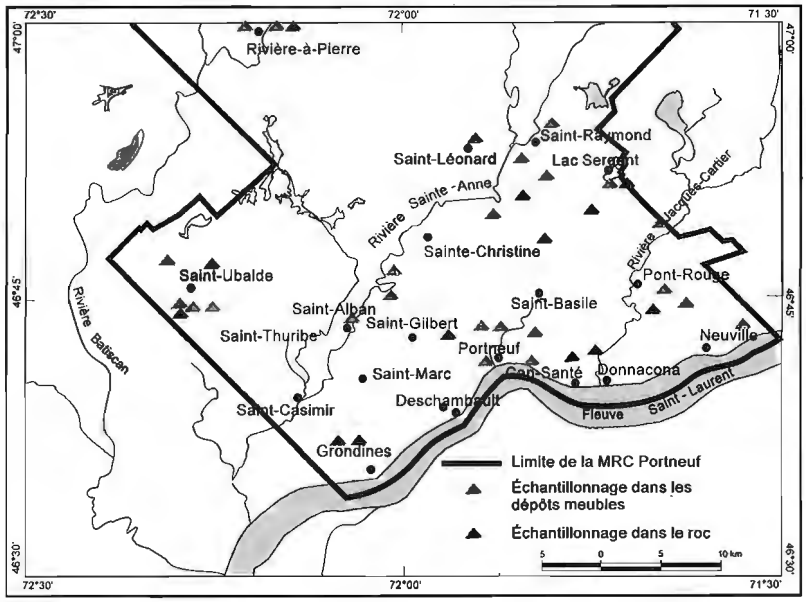

Figure 2.

Localisation des échantillons d'eau souterraine prélevés.

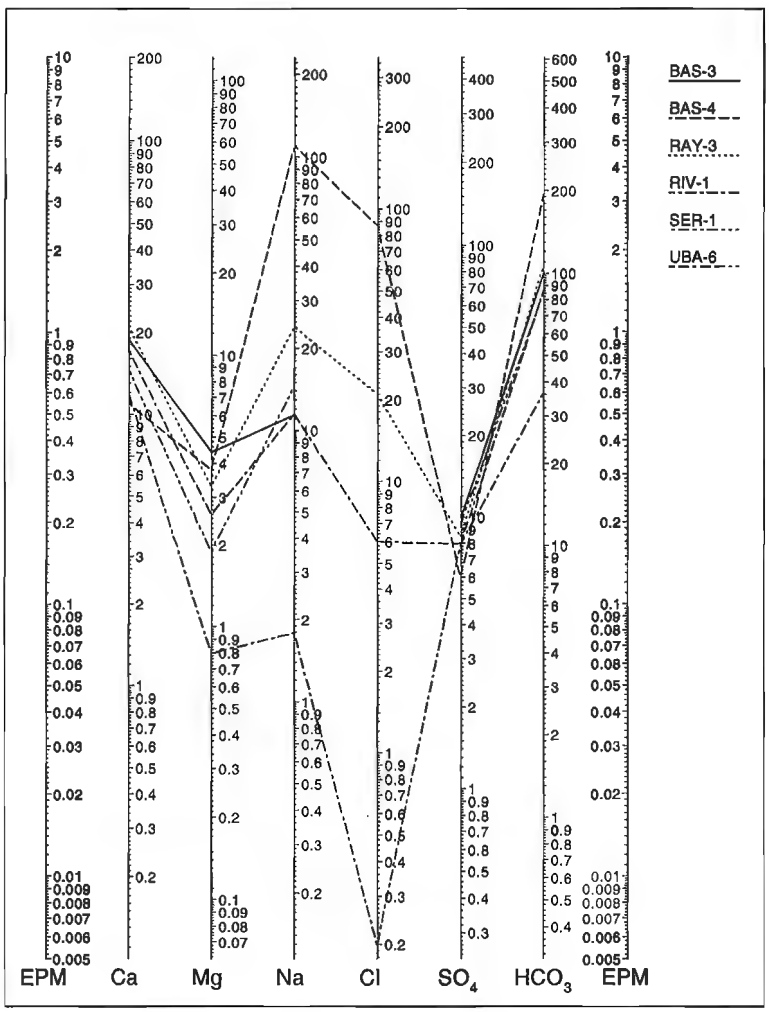

Figure 3.

Diagramme de Schoeller pour des échantillons d'eau souterraine prélevés dans des formations de gneiss granitique.

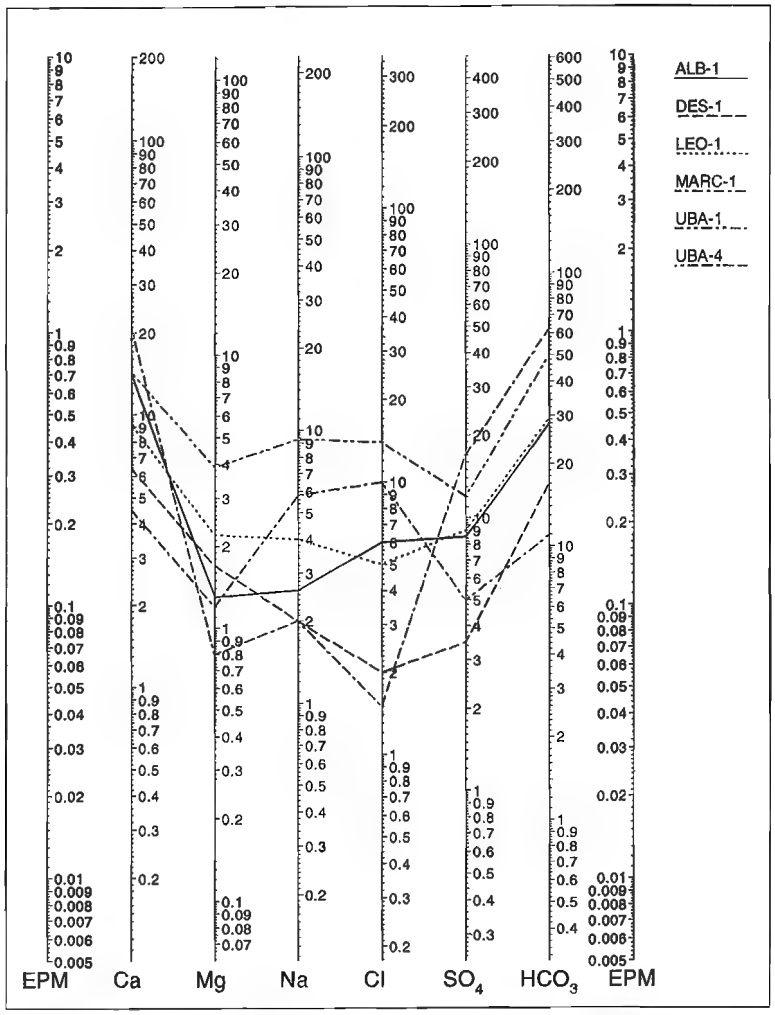

Figure 4.

Diagramme de Schoeller pour des échantillons d'eau souterrainne prélevés dans des formations de sable.

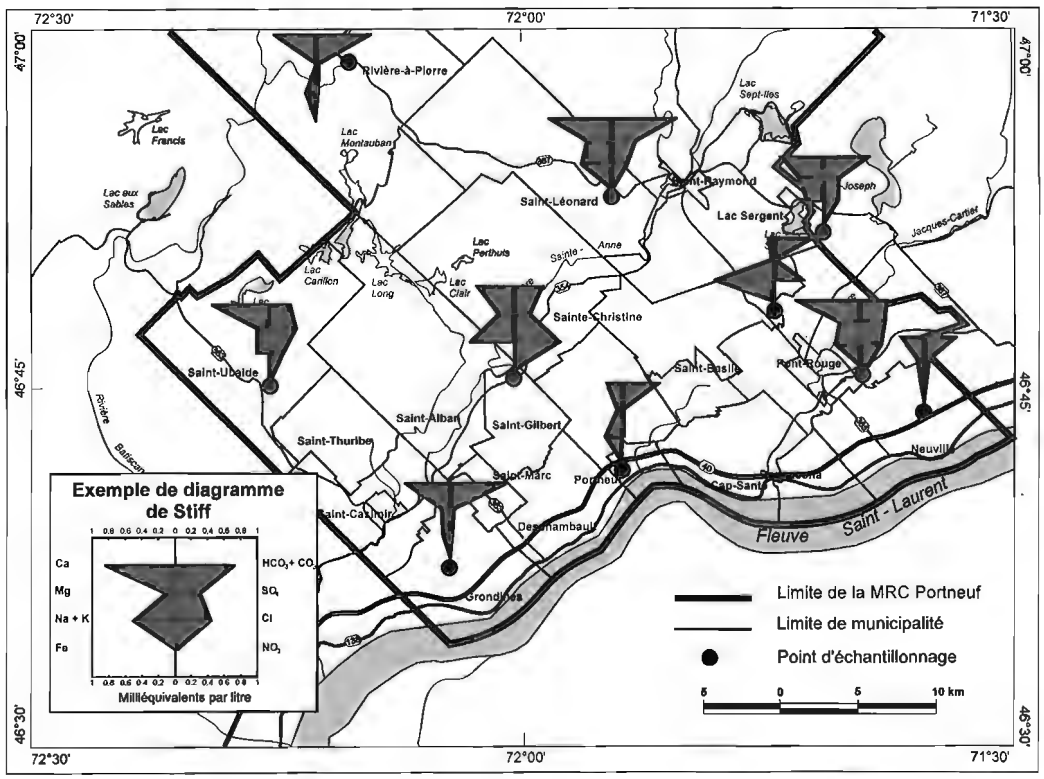

Figure 5.

Représentation de la qualité de l'eau souterraine par diagrammes de Stiff.

Les résultats d'analyses chimiques ont été comparés à des normes de potabilité (Gouvernement du Québec, 1993) et à des objectifs esthétiques (Santé et Bien-être social Canada, 1987). Aucun dépassement des normes de potabilité n'a été observé à l'exception des fluorures (2/37 échantillons) et du mercure (1/37 échantillons). Des dépassements d'objectifs esthétiques sont fréquents pour les paramètres comme le manganèse, les sulfures, la dureté, le pH et le fer. Pour l'ensemble des puits échantillonnés, au moins un de ces paramètres ne respecte pas les objectifs esthétiques pour 100 % des échantillons et au moins deux (2) de ces paramètres sont dépassés pour 18 % des échantillons (fig. 6 à 9). La figure 10 présente géographiquement les concentrations en solides dissous totaux (SDT) pour les échantillons prélevés dans les dépôts meubles.

Du point de vue microbiologique, environ 50 % (6/13) des échantillons prélevés dans des puits de particuliers ne respectaient pas les normes de potabilité microbiologiques (coliformes totaux, coliformes et autres organismes d'origine fécale). Pour ce qui est des aqueducs privés et municipaux ne subissant pas de chloration ultérieurement au point d'échantillonnage, on observe respectivement 2/9 (dont un résultat supérieur à 120 coliformes fécaux/100 ml) et 1/15 dépassements des normes microbiologiques. Des neuf (9) cas de dépassement, sept (7) sont reliés uniquement à des dépassements de la norme pour les coliformes totaux.

Finalement, une présence significative de nitrates (NO_3) a été notée pour 41% (15/37) des échantillons prélevés. La notion de *présence significative* correspond à une concentration arbitraire supérieure à 1 mg/L, la norme de potabilité étant de 10 mg/L.

DISCUSSION

Les diagrammes de Schoeller et de Stiff révèlent des patrons différents pour les échantillons prélevés dans les différentes formations aquifères (fig. 3 à 5), justifiant ainsi les travaux de cartographie hydrostratigraphique et hydrogéochimique du système d'aquifères.

La présence de fortes concentrations en fluorures de sources naturelles a été identifiée ponctuellement (2 dépassements). Cette observation concorde avec les résultats d'études antérieures qui démontrent que les fluorures sont présents à des concentrations élevées à certains endroits dans les

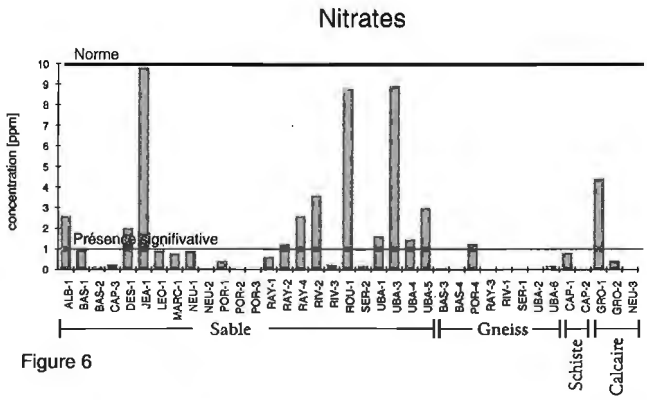

Figure 6

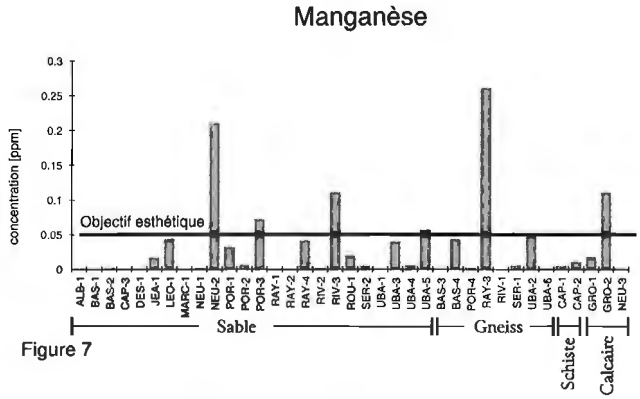

Figure 7

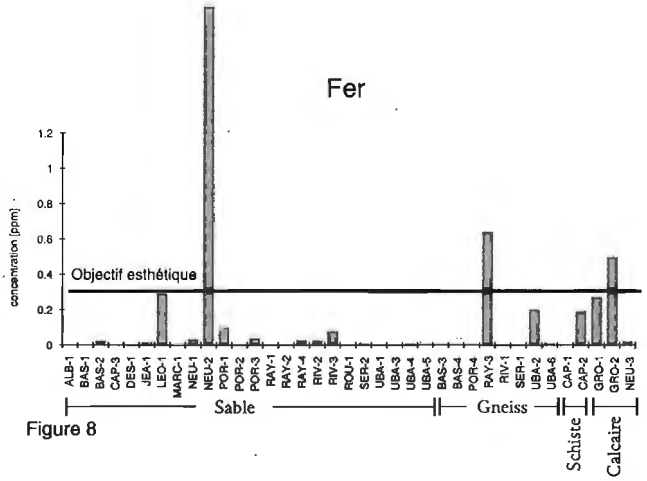

Figure 8

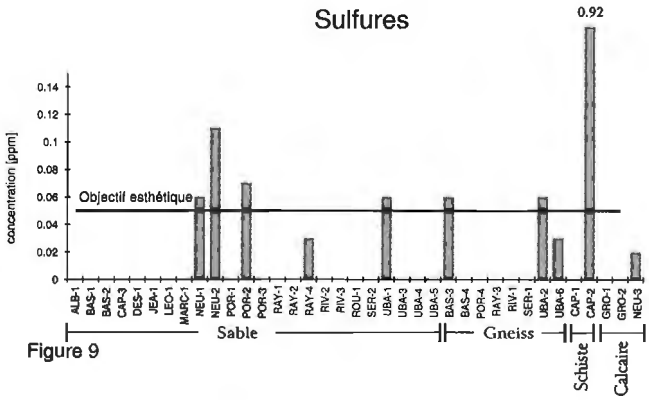

Figure 9

Figure 6 à 9. *Concentrations pour des échantillons d'eau souterraine prélevés dans différentes formations aquifères.*

secteurs de Deschambault (SNC-Lavalin, 1992), de Saint-Ubalde et de Montauban (Kirouac, 1987). On rapporte des concentrations en fluorures aussi élevées que 5,4 mg/L à Deschambault et 3,2 mg/L dans la région de Saint-Ubalde et Montauban, la norme de potabilité étant de 1,5 mg/L.

Les résultats des analyses microbiologiques démontrent que l'aménagement et l'entretien des puits privés sont parfois déficients et que des efforts d'information et de sensibilisation de la population seraient bénéfiques.

Les principaux contaminants inorganiques de nature anthropique identifiés sont les nitrates (NO_3). Ceux-ci sont particulièrement abondants dans certains secteurs agricoles. L'interprétation des résultats microbiologiques montre que les concentrations élevées en nitrates ne semblent pas reliées à des contaminations microbiologiques et vice versa. Les endroits où l'on retrouve des concentrations élevées sont des secteurs où la culture de la pomme de terre est importante (fig. 11). Cette observation semble indiquer que la présence de nitrates est principalement reliée à l'épandage d'engrais chimiques. L'échantillonnage ne ciblait pas les secteurs où la contamination par les nitrates est soupçonnée, et les puits échantillonnés étaient parfois très profonds et donc moins susceptibles d'être contaminés. Il en découle que ces résultats ne concordent pas entièrement avec une étude réalisée par le MEF (Paradis et al., 1991) dans laquelle des valeurs encore plus élevées en nitrates ont été mesurées dans la MRC de Portneuf, et ceci de façon plus généralisée. Cette fois l'échantillonnage ciblait des secteurs où la culture de la pomme de terre est intensive. Des nitrates ont été retrouvés dans 68 des 70 puits analysés. De plus, la valeur moyenne des nitrates dépasse la norme de 10 mg/L dans 29 des 70 puits et cette valeur moyenne dépasse même 20 mg/L dans huit (8) des puits. La valeur maximale rencontrée est de 33 mg/L. Les

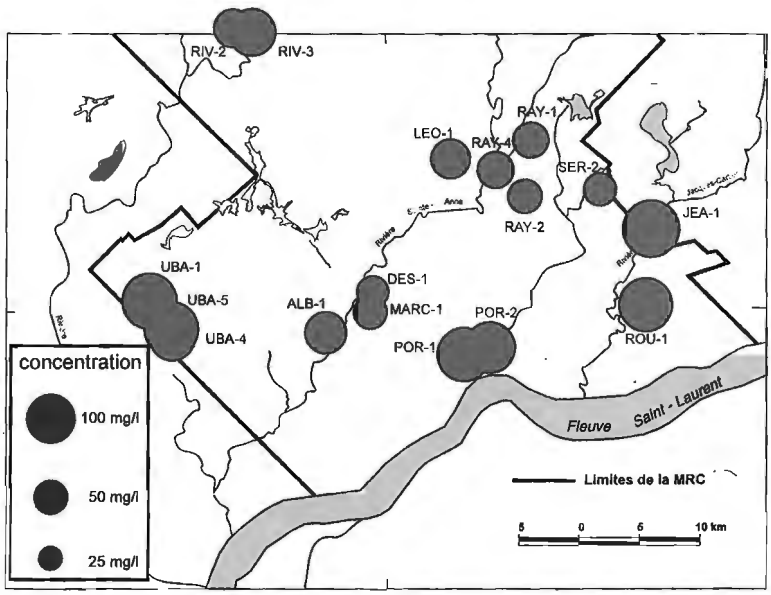

Figure 10.

Concentrations en SDT d'échantillons prélevés dans des aquifères de dépôts meubles (non confinés).

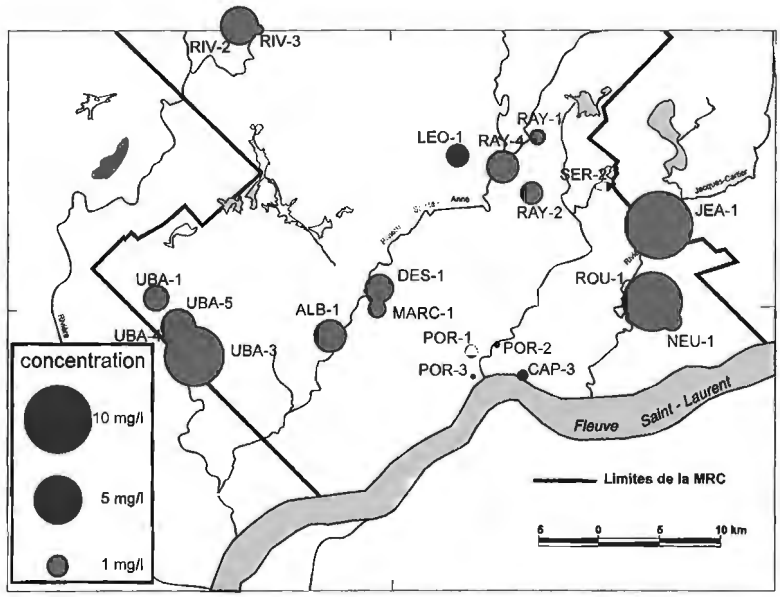

Figure 11.

Concentrations en nitrates d'échantillons prélevés dans des aquifères de dépôts meubles (non confinés).

aquifères utilisés en agriculture (dépôts meubles) sont particulièrement vulnérables aux effets de la contamination diffuse d'origine agricole. La protection des eaux souterraines impliquerait donc des modifications des pratiques agricoles. Des chercheurs de l'Université Laval (projet Écorecherche) se penchent sur l'influence des pratiques agricoles sur la qualité des eaux souterraines.

CONCLUSION

Les représentations faites à l'aide de diagrammes de Schoeller et de Stiff ont démontré que la qualité naturelle (fer, manganèse, dureté, etc.) des eaux souterraines est très variable pour les différentes formations aquifères exploitées dans la MRC de Portneuf. La contamination microbiologique très répandue dans les puits de particuliers montre que des efforts d'information et d'éducation du public concernant l'aménagement et l'entretien de leur unité de captage seraient bénéfiques. Une présence significative de nitrates a été relevée. Une surveillance à proximité de certaines unités de captage municipales, dans les secteurs où des activités agricoles sont pratiquées (épandage d'engrais chimiques) serait donc nécessaire. Cette surveillance pourrait être assurée par l'aménagement d'infrastructures comme des puits de surveillance. La détermination de périmètres de protection à l'intérieur desquels certaines activités seraient proscrites ou limitées est également recommandée.

À l'aide des données recueillies au cours de cette campagne d'échantillonnage et de celle prévue pour 1996, des cartes géochimiques de la qualité de l'eau faisant état des ions majeurs seront réalisées pour les principaux aquifères. L'étude de la qualité de l'eau sera complétée par des analyses isotopiques qui serviront d'outils de caractérisation additionnels.

Finalement, les résultats d'analyse pourraient être ultérieurement utiles, par exemple, pour l'identification des zones de recharge et d'émergence ainsi que pour la délimitation des aquifères et l'identification des liens entre ces derniers.

REMERCIEMENTS

Cette contribution fait partie d'un projet conjoint avec le MEF, financé par le comité d'hydrogéologie de la Commission géologique du Canada. Les auteurs aimeraient remercier R. Racine pour sa participation à la campagne d'échantillonnage, É. Desrochers qui a réalisé les figures, N. Tassé pour ses commentaires suite à la lecture du manuscrit et, finalement, la population et les municipalités de la MRC de Portneuf, pour leur collaboration et l'intérêt qu'elles ont manifesté pour cette étude.

RÉFÉRENCES

Santé et Bien-être social Canada
1987: Recommandations pour la qualité de l'eau potable au Canada, 20 p.
Gouvernement du Québec
1993: Règlement sur l'eau potable; éditeur officiel.
Kirouac, F.
1987: Géochimie des eaux souterraines-Région de Montauban; Ministère de l'Énergie et des Ressources, manuscrits bruts, MB 87-12, 70 p.
SNC-Lavalin
1992: Étude de l'état zéro de l'environnement, Projet d'implantation de l'aluminerie Lauralco; rapport soumis à Lauralco.
Paradis, D., Bernier, P. J., Levallois, P.
1991: Qualité de l'eau souterraine dans la MRC de Portneuf; rapport soumis aux Ministère de l'Environnement, Ministère de l'Agriculture des Pêcheries et de l'Alimentation et au Département de santé communautaire du Centre hospitalier de l'Université Laval, 32 p.

Projet 960001 de la Commission géologique du Canada

Detailed gravity studies in support of the EXTECH II Program, Bathurst mining camp, New Brunswick[1]

M.D. Thomas, D. Jobin[2], M. Daniels[2], C. Chamberlain[2], D.B. Hearty[2], G. Zhang[2], and J.F. Halpenny[2]

Continental Geoscience Division, Ottawa

Thomas, M.D., Jobin, D., Daniels, M., Chamberlain, C., Hearty, D.B., Zhang, G., and Halpenny, J.F., 1996: Detailed gravity studies in support of the EXTECH II Program, Bathurst mining camp, New Brunswick; in Current Research 1996-E; Geological Survey of Canada, p. 233-242.

Abstract: The multidisciplinary EXTECH II program in the Bathurst mining camp has included detailed gravity surveys over and/or around several massive sulphide occurrences. Targets include the Half Mile Lake, Canoe Landing Lake, and Key Anacon deposits, and the Willett property, where small bodies of sulphide have been located at surface and at depth. A total of 977 gravity observations were made. Most of these are positioned along local property grids, where they are spaced on the order of tens of metres apart. The remainder were surveyed around the properties at wider intervals, ranging from about 400 m to 3 km, with the objective of outlining the background gravity fields. The latter provide a broader context in which to examine local signatures that may be associated with sulphide deposits or spatially related structures. Results of the surveys are illustrated in this report and brief comment is made on their geological significance.

Résumé : Des levés gravimétriques détaillés au-dessus et autour de plusieurs indices de sulfures massifs ont été effectués dans le cadre du programme multidisciplinaire EXTECH II dans le camp minier de Bathurst. Les cibles des levés ont été les gisements de Halfmile Lake, de Canoe Landing Lake et de Key Anacon, ainsi que la propriété de Willett, où de petits amas de sulfures ont été localisés à la surface et en profondeur. Au total, 977 observations gravimétriques ont été faites. La plupart étaient positionnées le long des quadrillages des propriétés (échelle locale) et espacées de quelques dizaines de mètres. Le reste des observations provient des zones entourant les propriétés; les mesures ont été prises à des intervalles plus grands, variant entre environ 400 mètres et 3 000 mètres, afin de délimiter les champs gravimétriques de fond. Les observations plus espacées permettent de définir un contexte plus vaste et d'examiner les signatures locales qui peuvent être associées aux gisements de sulfures ou aux structures qui leur sont reliées spatialement. Le présent article fait état des résultats des levés et comprend un bref commentaire sur leur signification géologique.

[1] Contribution to the 1994-1999 Bathurst Mining Camp. Canada-New Brunswick Exploration Science and Technology (EXTECH II) Initiative.

[2] Geomatics Canada, Ottawa

INTRODUCTION

The EXTECH II program in the Bathurst mining camp (Fig. 1) is a co-operative multidisciplinary program involving participants from the federal government, the New Brunswick government, industry, and academia. It embraces a variety of geological, geochemical, and geophysical studies. Because the physical properties of massive sulphide deposits invariably differ significantly from those of their host rocks, they generally produce distinct geophysical responses (anomalies). Typically, the deposits have a density of around 4 g/cm^3, which compares with values that range characteristically from about 2.7 g/cm^3 to 2.8 g/cm^3 for host rocks. Hence, massive sulphide deposits generate associated positive gravity anomalies or 'highs', which are keenly sought in mineral exploration. Active interest by industry in the Half Mile Lake, Canoe Landing Lake, and Willett properties prompted the undertaking of detailed gravity surveys (station spacing 15 m to 30 m) on the properties. Small surveys in which station spacing ranged from about 400 m to 3 km, termed semi-regional surveys, were also conducted around these properties, and around the Key Anacon deposit, where a detailed property survey had already been completed by Rio Algom Exploration Inc.

GEOLOGICAL SETTING

A simplified geological map of the Bathurst mining camp is shown in Figure 1. According to McCutcheon (1992) there are some 100 Zn-Pb-Cu massive sulphide occurrences in the camp. These are hosted by the Middle Ordovician Tetagouche Group, a volcanic-sedimentary assemblage that was probably produced in an ensialic back-arc rifting environment (van Staal et al., 1992). Most of the hosting lithologies are fine grained sedimentary rocks, felsic tuffs, or metamorphic equivalents, and many sulphide developments are reported to occur at the contact between tuffaceous and sedimentary rocks (McCutcheon, 1992). Summaries of the geology of the region and of the base-metal deposits are provided by van Staal et al. (1992) and McCutcheon (1992), respectively.

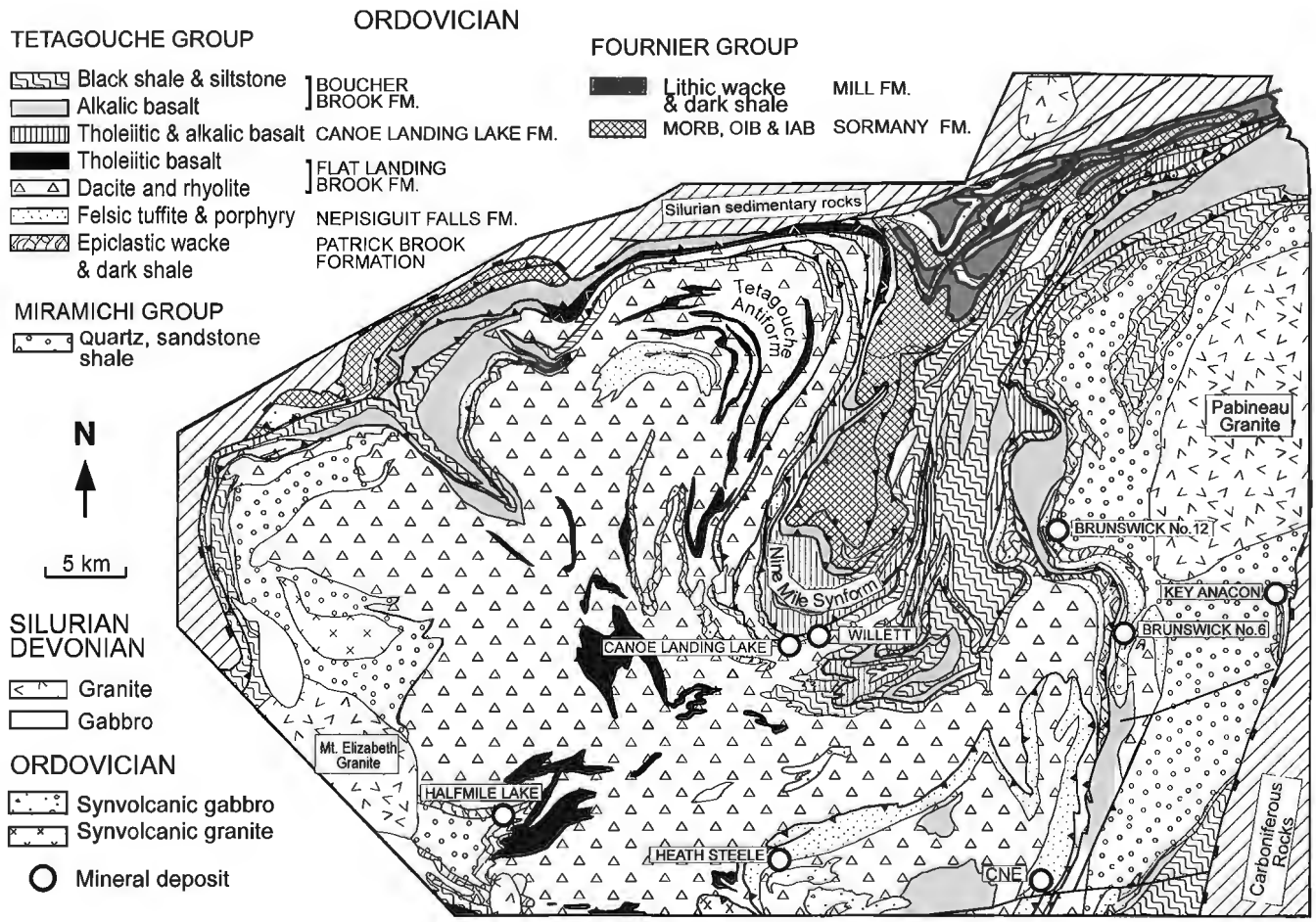

Figure 1. *Geological map of the Bathurst mining camp showing locations of mineral deposits examined in this study, and some other deposits. The map is modified from a digital image provided courtesy of Cees van Staal, Geological Survey of Canada.*

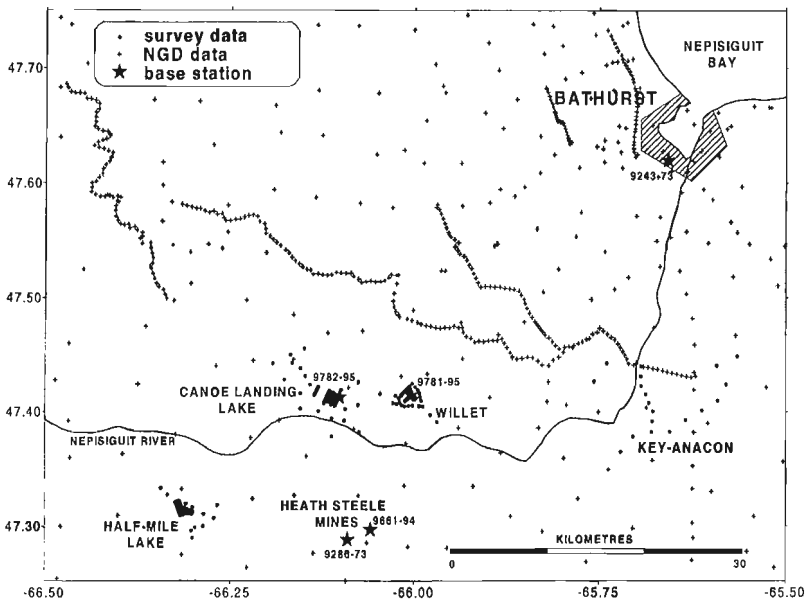

Figure 2.

Plot of gravity stations in the region of the Bathurst mining camp. Stations observed in the new surveys are indicated by dots. NGD, National Gravity Database. Values on axes are decimal degrees of latitude and longitude.

Table 1. Number of gravity readings by area.

Area	No. gravity readings	Repeats	Rejections
Willett detailed grid	341	12	-
Canoe Landing Lake detailed grid	249	1	19
Half Mile Lake detailed grid	307	-	-
Willett semi-regional	31	32	
Canoe Landing Lake semi-regional	19	-	-
Half Mile Lake semi-regional	11	-	-
Key Anacon semi-regional	19	-	-
TOTAL	977	45	19

GRAVITY SURVEYS

The locations of the Half Mile Lake, Canoe Landing Lake, Willett, and Key Anacon surveys are indicated on the geological map of Figure 1, and in Figure 2, which illustrates also gravity coverage in the area of the mining camp based on data in the National Gravity Database. Stations generally have an average spacing of about 6 km, although in several detailed road surveys spacing is much closer, ranging from 0.5 km to 1 km (Thomas et al., 1991). A total of 977 gravity observations was achieved by the new surveys. Details are provided in Table 1.

Survey specifications

Surveys on exploration properties were designed to detect small gravity anomalies that might be directly related to sulphide bodies. Stations were positioned at pickets along selected lines of property grids. On the Willett property most stations are spaced 50 ft. (≈ 15 m) apart. On two short lines near the principal exposed body of sulphide, the spacing is reduced to half this distance. At the Canoe Landing Lake and Half Mile Lake properties, stations are 25 m and 100 ft (≈ 30 m) apart, respectively.

Surveys around properties were conducted with the objective of obtaining a broader perspective of the local gravity field. For the purpose of this report these are termed semi-regional surveys. Stations were located along tracks and roads and were spaced from about 400 m to 3 km apart.

Gravity control

All gravity observations are referenced to the Canadian Gravity Base Network (CGBN). Local control stations were established at the Willett, Canoe Landing Lake, and Half Mile Lake properties through ties to CGBN stations in Bathurst and at Heath Steele Mines using a minimum of four acceptable ties. Adjusted gravity values were computed using a least squares technique, and were added to the National Gravity Database. However, the station sites were not documented for permanent status. Gravity meters were transported to the survey sites in a case mounted on air shocks to prevent or minimize instrumental tares that may arise from excessive vibration.

Gravity instrumentation

Two Scintrex CG-3 AUTOGRAV gravity meters (X054, X111) and two LaCoste and Romberg gravity meters (G291, G255) were used in the surveys. Three meters (G291, G255, X054) were used to establish local control stations at the Willett and Canoe Landing Lake properties. Scintrex meter X111 was used to establish local control at Half Mile Lake property. The Scintrex meter is a digital instrument and was used for most observations along the cut lines of property grids, operating with a sample rate of one second and gathering 60 samples. An error limit and a rejection limit of 0.02 mGal were specified in the software. These parameters, respectively, rejected a bad sample reading or stopped the sampling if the standard deviation of the one second samples dropped below that value within the 60 sample limit. The instrument proved to be robust, quick, and reliable, even on

unstable, spongy ground. A LaCoste and Romberg meter was used only on two short traverses, on the Willett property, for comparison purposes. It was more difficult to read on unstable ground and productivity was approximately 50% of that achieved using the Scintrex meter in a given time period.

A measure of the accuracy of the property surveys was obtained by repeating gravity readings at 12 stations. The average difference was 0.0265 mGal (standard deviation ± 0.0214 mGal), and the maximum difference was 0.071 mGal.

Vertical and horizontal positioning

Elevations for traverses along all three property grids were established under contract using conventional rod and automatic level surveying techniques. Closure errors are estimated to be less than 10 cm. In all cases the traverse elevations are tied to a local datum, which is itself tied to a geodetic benchmark. At Half Mile Lake these ties were completed under contract for Noranda Exploration Co. Ltd., and picket elevations and horizontal positions were supplied by the company. At Willett and Canoe Landing Lake properties, positional control points were established coincident with the local gravity control stations using a Global Positioning System (GPS) comprising two TurboRogue model SNR-8000 receivers (base and roving unit), which were operated in differential mode. The properties are located approximately 35 and 40 km, respectively, from the GPS base station. The roving unit was observed on site for 20 to 30 minutes. A difference in errors in the elevations of the Willett and Canoe Landing Lake control stations, estimated to be ±5 and ±10 cm, respectively, results from differences in observation times. Overall, elevations of detailed stations are estimated to be accurate to within ±10 cm.

The elevation of the GPS base unit, permanently installed on the roof of the New Brunswick Natural Resources and Energy Building in Bathurst during the course of the surveys, was determined by measurements made at provincial geodetic benchmark 25963. This is located in a sand pit 16 km south of Bathurst, and was selected to eliminate the multipath effects of overhead power lines and trees. The orthometric height of the base unit was determined to be 17.26 m. The geoid separation using the model 'gsd95' is -20.77 m, and the height determined from the Geodetic Survey active control station at Algonquin Radio Observatory, 963 km away, is 16.9 m. The value of 17.26 m derived by comparison with the local benchmark was adopted for the gravity surveys because it is tied to the local geoid.

For regional gravity stations, which lie within 25 to 60 km of the GPS base unit, GPS data were recorded at a 10 second rate for a minimum of 5 minutes, and the formal errors of the determined heights are normally less than 0.25 m, with a maximum error of 0.78 m.

Horizontal positions of the semi-regional stations were also determined from GPS observations. Their accuracy is evaluated to be within ±3 m, resulting in an error of less than 0.01 mGal in gravity anomalies. Horizontal positions for the detailed gravity stations on the Willett and Canoe Landing Lake properties were initially determined using local co-ordinate systems related to the property grids. Absolute positions were established using several GPS control points located on the grids.

Processing of data and error estimates

All gravity data were processed using the PCGRAV software package developed and maintained by the Geodetic Survey of Canada. Gravity readings are referenced to the International Gravity Standardization Net 1971 and theoretical values used in the computation of anomalies are obtained using the Geodetic Reference System 1967. A standard density of 2.67 g/cm^3 and a sea level datum were used for Bouguer anomaly calculations. A free air correction for the height of the tripod above ground level is incorporated into the Bouguer value. Error estimates based on accuracies specified for the measured parameters are computed by the PCGRAV software. Accordingly, the computed accuracies for Bouguer anomalies range from 0.11 to 0.27 mGal.

Apart from Figures 10 and 11, for the Half Mile Lake property, terrain corrections have not been applied to the data illustrated in figures in this report. However, estimates of slope out to a radius of 25 m around gravity stations were made for all stations for the purpose of computing the near-terrain effects. Corrections for these effects have been made for Half Mile Lake data.

GRAVITY MAPS AND PRELIMINARY GEOLOGICAL INTERPRETATIONS

Key Anacon Deposit

The Key Anacon property straddles Highway 360 and the Nepisiguit River (Fig. 3). South of the highway, east of the river, the Main zone Cu-Pb-Zn deposit includes four zones consisting of small near-surface sulphide bodies. Of these, the No. 2 zone is potentially the richest with proven reserves of about 1.1 million tonnes (Irrinki 1992). Across the highway, about 1.5 km to the north-northeast, massive sulphides occur in the Key Anacon East zone (Lentz, 1995), but apparently there are no published estimates of tonnage. A detailed gravity survey has been carried out over the property grid by Rio Algom Exploration Inc. This defined a broad gravity high oriented approximately east-northeast-west-southwest. To the north and northwest it is bounded by relatively steep gradients, which are probably influenced to a large extent by a flanking negative anomaly associated with the Pabineau granite (Thomas et al., 1991).

To establish a better link between the Rio Algom grid survey and the regional gravity field, 19 stations were measured on roads adjacent to and crossing the property. These provided improved coverage mainly to the east of the property, because access elsewhere is limited. Just two new stations were measured west of the Nepisiguit River. Even without the incorporation of Rio Algom data, the new data define the gravity high, which was not apparent in the earlier regional data sets.

A major control on the high appears to be mafic volcanic rocks of the Boucher Brook Formation. A small gravity high is defined over the No. 2 zone, partially superposed on a westward-decreasing regional gradient. Subtraction of the regional from the observed profile results in a residual gravity high of about 0.25 mGal. A theoretical anomaly computed for the No. 2 zone using a section published by Irrinki (1992) and densities determined on drill core has an amplitude and shape similar to those of the residual high.

Willett Property

On the Willett property a small lens of Cu-Zn-Pb massive sulphides about 10 m long is located at surface within argillitic rocks of the Patrick Brook Formation, which are associated locally with felsic volcanics. A drilling program conducted by Freewest Resources Canada detected discrete concentrations of massive sulphide at depth, to a maximum thickness of about 2.6 m. Given the apparent disconnected nature of the intersections, and possible structural scenarios resulting from faulting and folding, the potential for other occurrences was considered favourable. To investigate this possibility, gravity observations were conducted along a series of lines in the vicinity of the surface sulphide lens. Semi-regional observations were also made around the property. Modelling conducted prior to the surveys, on the basis of sulphide geometries as outlined by drilling, indicated that gravity signatures for such bodies would be very small, of the order of a few hundredths of a mGal. Nevertheless, given the geological setting, it was anticipated that if a larger body were present, its signature would be readily recognized.

A Bouguer gravity map derived from the combined results of the detailed and semi-regional surveys is shown in Figure 4. A more detailed map for the area of the grid lines, with a simplified geological overlay is presented in Figure 5. A small gravity high about 0.45 mGal amplitude extends

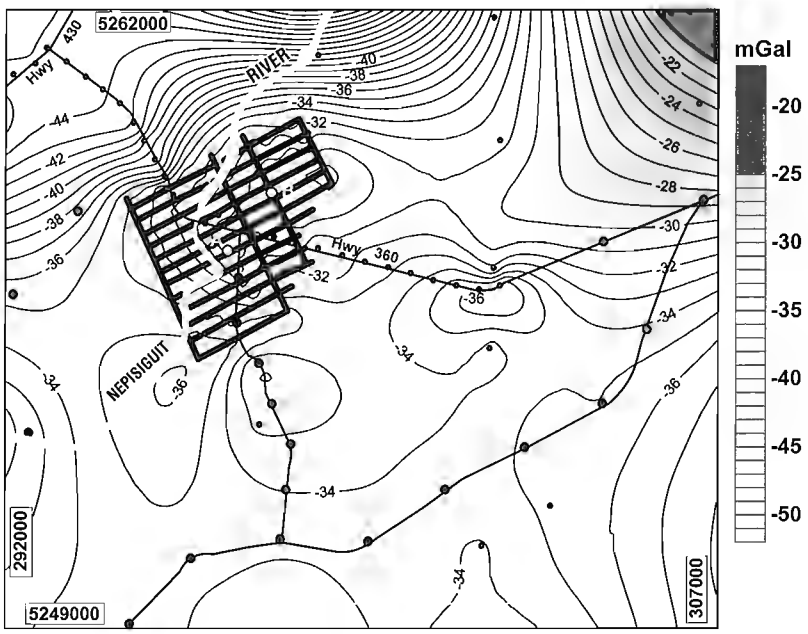

Figure 3.

Gravity map of area around Key Anacon property. The map incorporates data from the National Gravity Data Base (small dots), from Rio Algom Exploration Inc. (grid), and the new survey (large dots). Contour interval = 1 mGal. Limits of area indicated by UTM co-ordinates related to North American Datum (NAD) 1983. A, Main zone sulphide deposits; B, East zone.

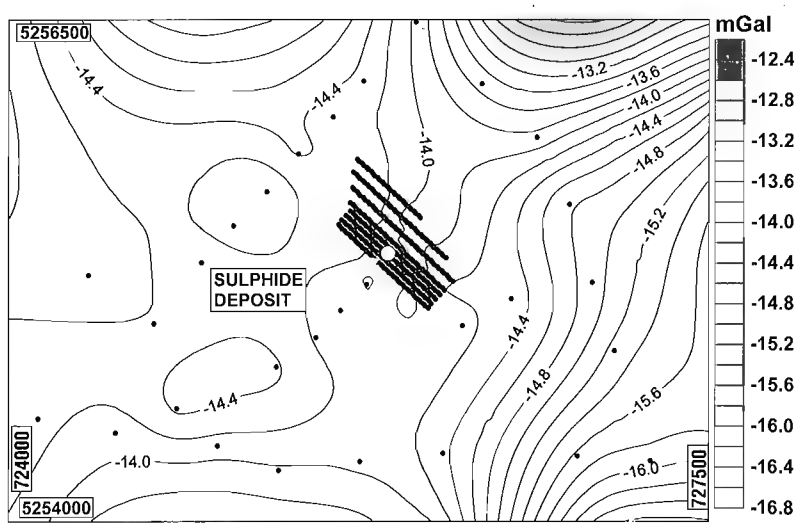

Figure 4.

Bouguer gravity anomaly map for Willett property based on grid line and semi-regional observations. Contour interval = 0.2 mGal. Boundaries of area defined by UTM co-ordinates related to NAD 1927.

northeastward across the grid lines, spatially coincident with small intrusions of gabbro lying within less dense siltstones and phyllites. The ore-bearing unit of argillite lies on the northwestern flank of the high. There are minor perturbations on this flank, but no persistent positive feature that might signal a sizable ore deposit. The sulphide showing at surface corresponds with a weak gravity high that is flanked by small lows of restricted extent. The lows are explained by the presence of mounds of earth scraped from above the sulphide deposit. Since gravity measurements were made on the mounds themselves, the negative values are attributable to terrain effects. This has been confirmed by computing terrain corrections for a single profile (line 200W).

Figure 6 shows a preliminary model derived from the Bouguer anomaly profile along line 200W. The ore-bearing argillite unit and an adjacent phyllite unit correlate with two small positive perturbations on the northwestern flank of the gravity high. If a background trend such as that portrayed by model curve 1 is adopted, the two perturbations (A and B) of the observed curve could be regarded as small highs signalling the presence of small sulphide deposits (curve 1 represents the gravity effect of the modelled geological section without consideration of the two sulphide bodies). A better match between observed and model curves is obtained when two small vertical sheet-like bodies of sulphide are added to the model. However, it is not possible to reproduce the low between highs A and B, strongly suggesting that this series of small undulations is related to very shallow source(s), such as variations in overburden thickness. Furthermore, the somewhat spiky nature of the observed profile and the small amplitudes of the perturbations **caution that they might also be related to measurement "noise" produced by such phenomenon as unstable ground and small errors in elevation**. Further studies are required before a more definitive assessment of the potential for buried sulphide deposits can be realized.

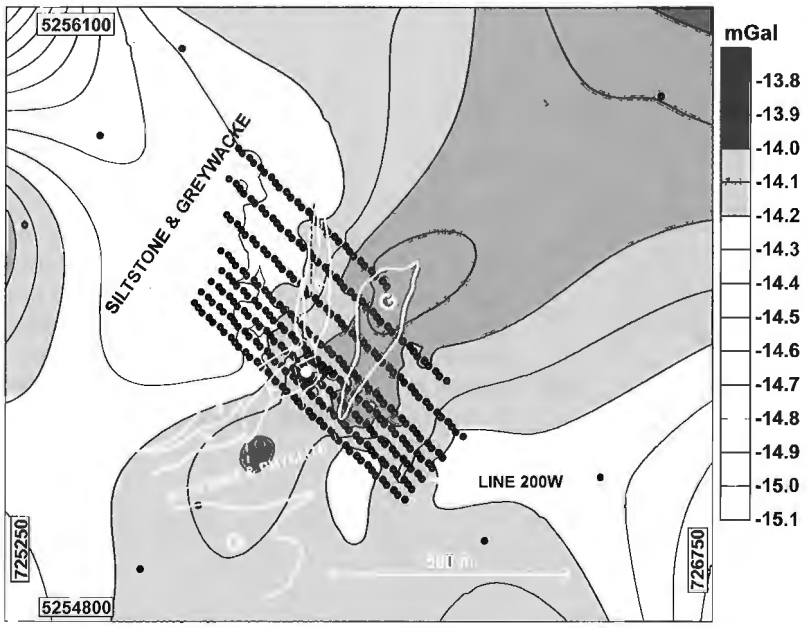

Figure 5.

Detail of Bouguer gravity anomaly map shown in Figure 4 for area immediate to grid lines. Contour interval = 0.1 mGal. Geology, based on a map supplied by Freewest Resources Inc., is superposed. A, argillite; G, gabbro; P, phyllite. White dot is location of sulphide body at surface. Boundaries of area defined by UTM co-ordinates related to NAD 1927.

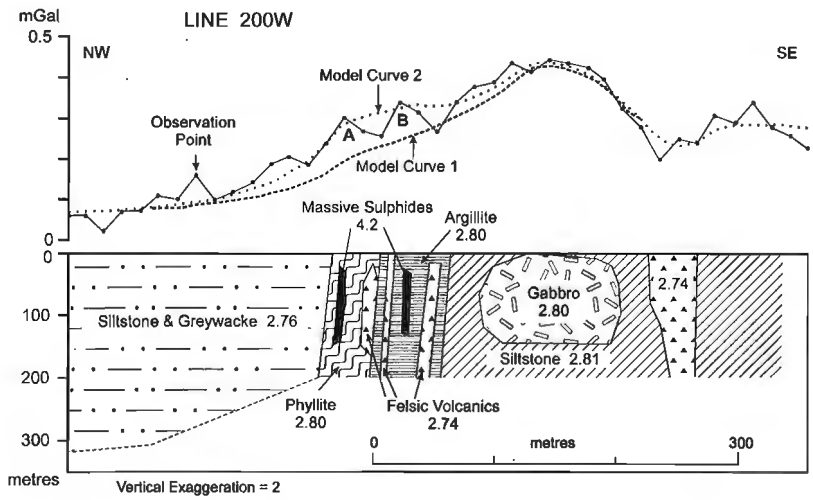

Figure 6.

Observed gravity profile along line 200W of the Willett property, and modelled geological section. A and B are gravity highs discussed in text. Densities of rock units are in the unit of g/cm^3.

Canoe Landing Lake Property

The pyrite-rich Canoe Landing Lake Cu-Zn-Pb deposit is hosted by slate of the Boucher Brook Formation (Fig. 7). Its geometry, defined by a series of drillholes, takes the form of a steeply dipping thin sheet (Walker and McDonald 1995). It correlates with a strong electromagnetic (VLF) anomaly outlined by surveys undertaken by Nebex Resources Ltd. in 1994 (Trapnell, 1994). It is speculated that several other VLF anomalies on the property are possibly or probably related to sulphide sources.

The presence of conductors having possible economic potential (Trapnell, 1994), ongoing exploration by Nebex Resources Ltd., and the recent geological and geochemical investigations by Walker and McDonald (1995) provided an incentive to investigate the property using the gravity method. Brooks (1982) and Brooks and Macintosh (1982) reported briefly on results of detailed gravity surveys carried out by Brunswick Mining and Smelting Corporation Ltd. in 1981 along the cut-line grid system existing at that time. The survey defined a fairly uniform gravity gradient having northward-increasing values. Inspection of the individual line gravity anomaly profiles reveals several small positive departures from the estimated background gradient. These generally have amplitudes of about 0.1 to 0.2 mGal, but occasionally attain 0.3 mGal.

Brooks and Macintosh (1982) stated that they interpret only a small anomaly over the Canoe Landing Lake deposit that locally attains 0.3 mGal amplitude. Our inspection of the gravity data suggests the maximum amplitude is smaller at about 0.2 mGal. Furthermore, the anomaly peaks between about 80 to 130 m north of the surface position of the sulphide horizon as currently portrayed on a geological map compiled by Nebex Resources Ltd. (Johnson, 1995). Whereas the spatial registration of various maps consulted in this study involved some approximation in obtaining a best fit, any spatial offsets caused by this process are estimated to be far less than the aforementioned displacements. This particular anomaly, therefore, probably has a source other than the sulphide deposit. Some likely sources are suggested by drilling elsewhere on the property to test gravity anomalies associated with weak electromagnetic anomalies. Sediments that include a zone of pyrite, flanked by less dense acid volcanics, is interpreted as the likely source of one anomaly (Brooks, 1982), and two other anomalies are attributed to stringered pyrite, up to 10% locally, in graphitic argillite (Brooks and Macintosh, 1982).

In the present gravity survey, 249 observations were made at 25 m intervals along 6 lines (Fig. 7) crossing the known deposit and the most prominent sections of the VLF conductors described by Trapnell (1994). Nineteen observations were made around the deposit. A Bouguer anomaly map based on all of these measurements shows the gravity field to increase steadily northeastward across the property (Fig. 8). The higher values in the northeast can be attributed to dense basaltic rocks in the Nine Mile synform (Fig. 1).

The gravity profile along line 650W is selected to illustrate results of the detailed line surveys (Fig. 9). Breaks in the profile represent sites where unstable ground conditions yielded unacceptable data. A small break occurs over the Canoe Landing Lake sulphide body, but adjacent parts of the profile are well defined and show no hint of a related gravity high. An anomaly of about 0.4 mGal had been expected for a uniform sheet 5 m thick having the 1220 m strike length and minimum 925 m depth extent as described by Walker and McDonald (1995). The lack of signature is interpreted to indicate that the ore body thins and/or becomes lower grade near surface on this line. Preliminary inspection of the other five gravity profiles indicates that gravity highs are not associated with any of the VLF anomalies.

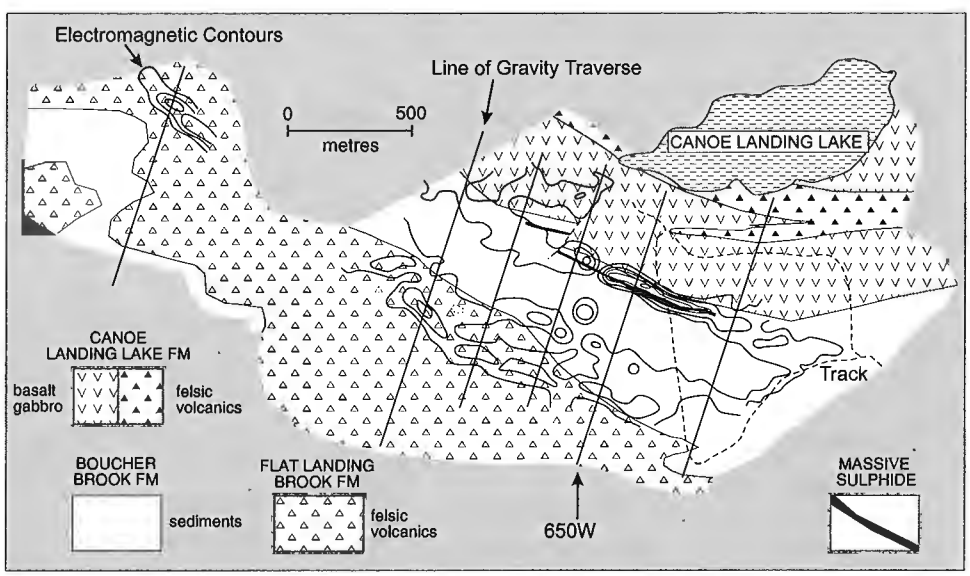

Figure 7. *Simplified geological map of Canoe Landing Lake property (after Johnson, 1995) with VLF electromagnetic contours (after Trapnell, 1994) superposed.*

Half Mile Lake deposit

The Half Mile Lake is one of the largest undeveloped sulphide deposits in the Bathurst mining camp (Adair, 1992). It comprises an estimated 26 million tonnes of iron and base-metal sulphides. The sulphides occur within a northward-dipping, structurally inverted sequence of felsic pyroclastics and fine grained sediments, underlain by andesitic volcanics and intruded by bodies of quartz feldspar porphyry.

A gravity survey completed by Noranda Exploration Company Ltd. over the section of the property known as Half Mile South, indicated a total range of Bouguer gravity anomalies of about 1 mGal. The general pattern of anomalies there showed low values over the andesitic volcanics, separated by a distinct belt of relatively steep gradients from a higher plateau of values over argillite, greywacke, and volcanic tuff to the north. The gradient lies close to, but does not necessarily coincide with the boundary between andesitic volcanics and the sediments-tuff package. The source of the gradient is somewhat puzzling since the available data suggest that there is little difference in densities of the volcanics (2.79 g/cm^3) and sediments (2.80 g/cm^3) – tuff (2.75 g/cm^3).

At Half Mile South the surface trace of the principal sulphide and associated stringer horizon, lying close to the northern boundary of the andesitic volcanics, coincides with a variable expression of the gravity field. At one point, where the horizon widens significantly, it does coincide with a

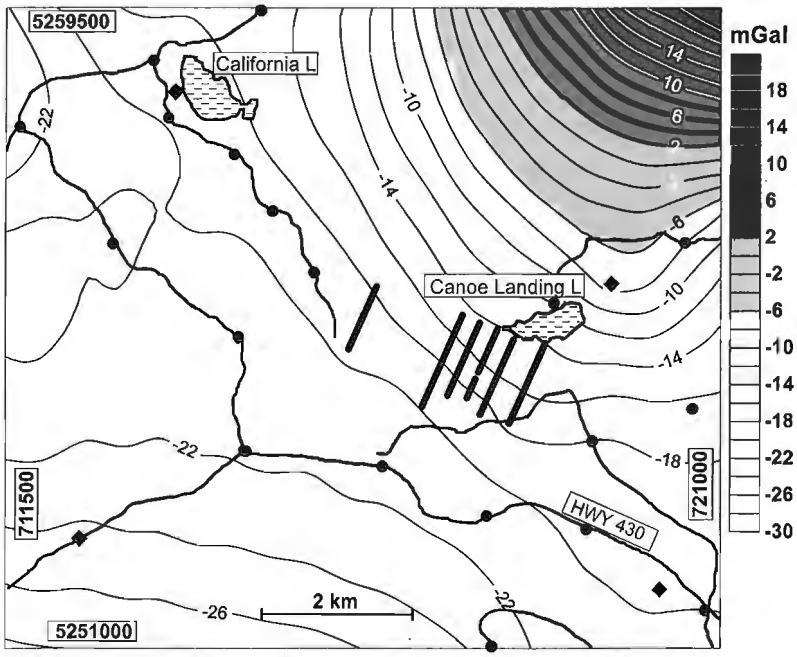

Figure 8.

Bouguer gravity anomaly map of area around Canoe Landing Lake deposit. Dots, new gravity stations; diamonds, gravity values from National Gravity Database. Boundaries of area defined by UTM co-ordinates related to NAD 1927.

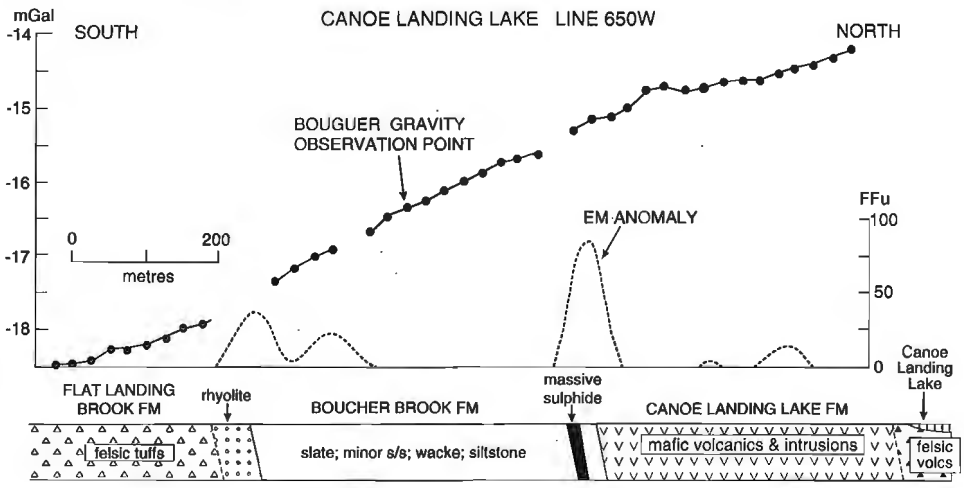

Figure 9. *Gravity profile, electromagnetic (EM) anomaly expressed as Fraser filter profile, and schematic near-surface geological section along line 650W on Canoe Landing Lake property. FFu, Fraser filter units.*

distinct gravity high. This occurs as a localized peak having an amplitude of about 0.15 mGal, superposed at the top of the belt of steeper gradients.

As part of the EXTECH II initiative, a detailed gravity survey was completed along grid lines to the northeast of the area covered by the Noranda survey, on a section of the property known as Half Mile Lake North. Observations were also made around the property to obtain information on the background field. Results of the two surveys are combined in Figure 10. A detailed gravity map of the immediate area of the grid lines with geology superposed is presented in Figure 11. The most prominent feature outlined by the survey is a northeast-trending positive anomaly, about 0.6 mGal amplitude, that coincides with bands of argillite-greywacke and felsic tuff. This is flanked to the north and south by areas of low gravity over quartz feldspar porphyry and andesite, respectively. There do not appear to be any discrete gravity highs that can be tied to sulphide deposits. However, it is noted that a sulphide-stringer horizon coincides with the southeastern flank of the main positive anomaly.

SUMMARY

Notwithstanding the fact that significant gravity anomalies indicative of large sulphide deposits have not been encountered in the series of described surveys, new data sets are now available. These can help answer questions about the potential for new discoveries or the size of reserves, even if they are not overly optimistic. Furthermore, the gravity anomalies can be modelled to reveal information on structure at depth, which is an important consideration in exploration. The gravity method is one that will reveal massive sulphides if the size

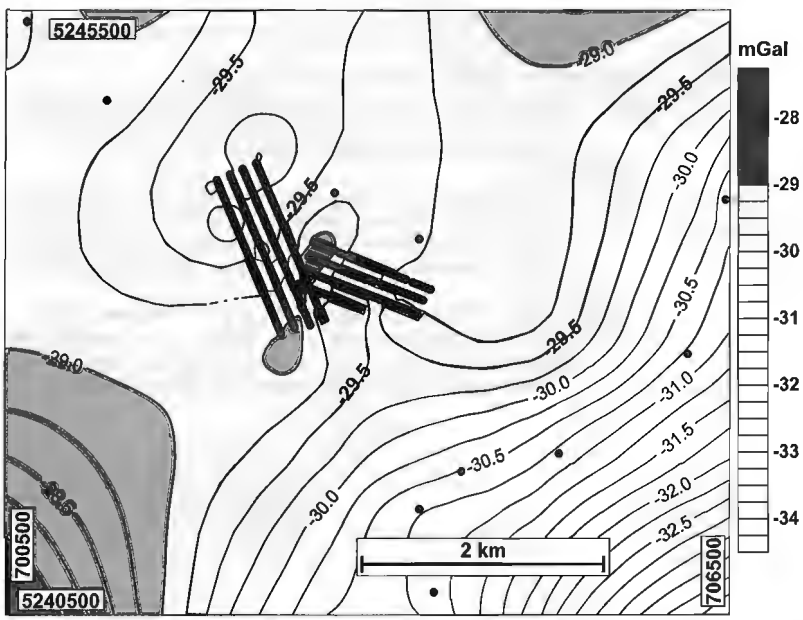

Figure 10.

Gravity map of portion of Half Mile Lake property based on detailed grid and semi-regional surveys. Contour interval = 0.25 mGal. Boundaries of area defined by UTM co-ordinates related to NAD 1927. (A recent revision to a gravity control station requires that 0.08 mGal be added to values on this map).

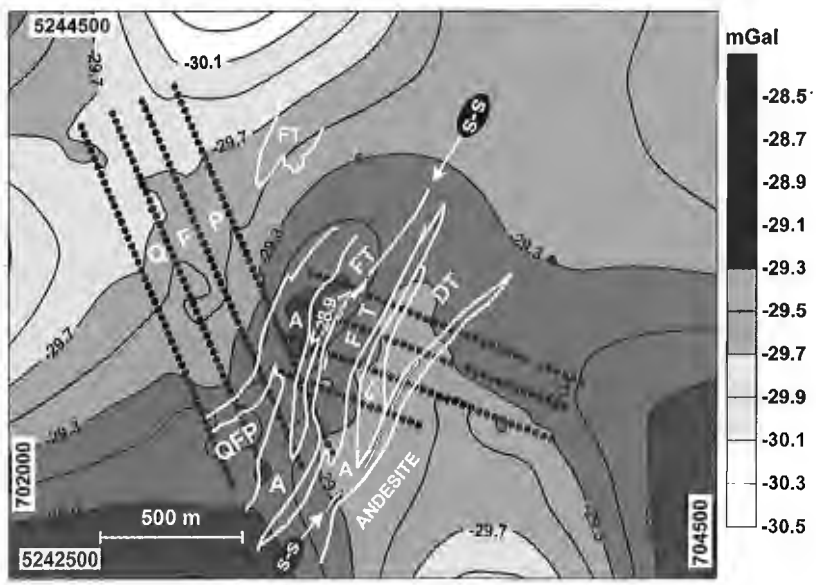

Figure 11.

Gravity map of area of Half Mile Lake property immediate to the detailed grid survey. Contour interval = 0.2 mGal. Geology is superposed in area of grid lines (after R. Adair, unpub. map, 1993). A, argillite-greywacke; DT, dacite tuff; FT, felsic tuff; QFP, quartz felspar porphyry; S-S, sulphide-stringer horizon. Boundaries of area defined by UTM co-ordinates related to NAD 1927. (A recent revision to a gravity control station requires that 0.08 mGal be added to values on this map).

and depth of burial of the deposit are of dimensions favourable to detection. It is a method that should be applied routinely in the screening of properties for mineral potential.

ACKNOWLEDGMENTS

The authors wish to thank the following people, and their organizations, for discussion, data and information, and permission to reproduce various material displayed here:

Graham Ascough, Noranda Exploration Co. Ltd., Bathurst.
Don Hoy, Freewest Resources Canada Inc., Bathurst.
Jim Kelly, Nebex Resources, Calgary.
Dave Lentz, New Brunswick Natural Resources & Energy, Bathurst.
Arnie McAllister, Rio Algom Exploration Inc., Fredericton.
Warner Miles, Geological Survey of Canada, Ottawa.
Cees van Staal, Geological Survey of Canada, Ottawa.
Jim Walker, New Brunswick Natural Resources & Energy, Bathurst.

The ready help of Steve McCutcheon, Regional Geologist, and his staff at the Bathurst office of the New Brunswick Natural Resources & Energy is also greatly appreciated. We thank colleagues, Wayne Goodfellow, EXTECH II co-ordinator, for continuing support and encouragement, and Mark Pilkington for constructive comments on the manuscript.

REFERENCES

Adair, R.N.
1992: Stratigraphy, structure, and geochemistry of the Halfmile Lake massive-sulphide deposit, New Brunswick; Exploration and Mining Geology, v. 1, p. 151-166.

Brooks, E.A.
1982: Brunswick Mining and Smelting Corporation Limited Mining Division. Report for assessment on B.M. & S. property project 211, Canoe Landing Lake extension. Claim Nos. 306623-625, 306657-684, 308822-825, 304979-980, 307196-215. N.T.S. No. 21 O/8 east (H, 2, 5); New Brunswick Department of Natural Resources and Energy, Bathurst Office, Assessment File 472811.

Brooks, E.A. and Macintosh, J.A.
1982: Brunswick Mining and Smelting Corporation Limited Mining Division. Assessment report on mining license 1231, B.M. & S. project 212 (Canoe Landing Lake property). N.T.S. 21 O/8 E (21 O/8 H(b)); New Brunswick Department of Natural Resources and Energy, Bathurst Office, Assessment File 472867.

Irrinki, R.R.
1992: Key Anacon sulfide deposit, Gloucester County, New Brunswick; Exploration and Mining Geology, v. 1, p. 121-129.

Johnson, W.
1995: Geological mapping and diamond drilling, Canoe Landing Lake property, Northumberland County, N.B., NTS 21/O8e; 66°06'30"W, 47°24'50"N. Mapping: June-July, 1994, Drilling: Dec. 5, 1994-March 27, 1995 for Nebex Resources Ltd.; New Brunswick Department of Natural Resources and Energy, Bathurst Office, Assessment File 474581.

Lentz, D.R.
1995: Stratigraphy and structure of the Key Anacon massive-sulphide deposits compared with the Brunswick deposits, Bathurst Mining Camp, New Brunswick; in Geoscience Research 1994, (comp., ed.) J.P. Langton; New Brunswick Department of Natural Resources and Energy, Minerals and Energy Division, Miscellaneous Report 15, p. 23-44.

McCutcheon, S.R.
1992: Base-metal deposits of the Bathurst-Newcastle District: characteristics and depositional models; Exploration and Mining Geology, v. 1, p. 105-119.

Thomas, M.D., Halliday, D.W., and O'Dowd, D.V.
1991: Detailed gravity surveys in the Appalachian Dunnage and Gander terranes, northern New Brunswick; in Current Research, Part D, Geological Survey of Canada, Paper 91-1D, p. 101-109.

Trapnell, M.L.
1994: Nebex Resources Ltd. Report on the 1994 VLF survey, Canoe Landing Lake Property, Claims 335560-335584, Northumberland County, New Brunswick, NTS 21 O/8; New Brunswick Department of Natural Resources and Energy, Bathurst Office, Assessment File 474479.

van Staal, C.R., Fyffe, L.R., Langton, J.P., and McCutcheon, S.R.
1992: The Ordovician Tetagouche Group, Bathurst camp, northern New Brunswick, Canada: history, tectonic setting, and distribution of massive-sulfide deposits; Exploration and Mining Geology, v. 1, p. 93-103.

Walker, J.A. and McDonald, S.M.
1995: Preliminary investigation of the Canoe Landing Lake massive-sulphide deposit, NTS 21 O/8 e; in Geoscience Research 1994, (comp., ed.) J.P. Langton; New Brunswick Department of Natural Resources and Energy, Minerals and Energy Division; Miscellaneous Report 15, p. 78-99.

Geological Survey of Canada Project 940001

Chemical and stable isotopic composition of ground and surface waters from the Restigouche Zn-Pb massive sulphide deposit, Bathurst mining camp, northern New Brunswick – EXTECH II[1]

Matthew I. Leybourne[2], Wayne D. Goodfellow, and Dan R. Boyle
Mineral Resources Division, Ottawa

Leybourne, M.I., Goodfellow, W.D., and Boyle, D.R., 1996: Chemical and stable isotopic composition of ground and surface waters from the Restigouche Zn-Pb massive sulphide deposit, Bathurst mining camp, northern New Brunswick – EXTECH II; in Current Research 1996-E; Geological Survey of Canada, p. 243-254.

Abstract: A deposit-scale study of the hydrology and hydrochemistry of surface and groundwaters has been initiated in the Bathurst Mining Camp as part of the EXTECH II program. The purpose of this study is to investigate the effectiveness of hydrogeochemical methods in the exploration for buried deposits within the Bathurst Mining Camp. Preliminary work has focussed on the Halfmile Lake and Restigouche Zn-Pb deposits. At the Restigouche deposit, samples of stream, spring, seep, and borehole waters have been collected and measured for a wide range of trace elements and stable isotopes. Surface waters are dominantly low total dissolved solids (TDS) Ca-HCO_3^- waters, with differences between streams reflecting underlying lithology. Ore-related elements (e.g. Pb, Zn, K) are well correlated with proximity to the Restigouche deposit. Groundwaters at Restigouche are highly variable in composition and range from shallow waters similar to stream waters, to deeper Na-Ca-Cl saline waters resembling brines from the Canadian Shield. Groundwaters at Restigouche are very different from those at the Halfmile Lake deposit, reflecting differences in hydrology and recharge history.

Résumé : Une étude hydrologique et hydrogéochimique des eaux souterraines et de surface à l'échelle du gisement a été entreprise dans le camp minier de Bathurst, dans le cadre du programme EXTECH II. L'étude a pour but de vérifier l'efficacité des méthodes hydrogéochimiques en exploration des gisements enfouis, en recueillant des données sur le camp minier de Bathurst. Les travaux préliminaires ont été concentrés autour des gisements de Zn-Pb de Halfmile Lake et de Restigouche. Au gisement de Restigouche, des échantillons d'eaux (de ruisseau, de source, d'infiltration et de forage) ont été analysés pour une grande variété d'éléments en traces et d'isotopes stables. Les eaux de surface sont généralement riches en Ca et en HCO_3^-, mais contiennent peu de matières totales dissoutes. Il existe cependant des écarts d'un ruisseau à l'autre, ce qui est le reflet des lithologies sous-jacentes. Les éléments qui forment des minerais, comme par exemple le plomb, le zinc et le potassium, sont plus abondants à proximité du gisement de Restigouche. Les eaux souterraines, quant à elles, sont très variables en composition aux environs du gisement de Restigouche; ainsi, la composition s'échelonne de celle des eaux de surface (s'apparentant aux eaux d'un ruisseau) à celle des eaux salines riches en Na-Ca-Cl observées à de plus grandes profondeurs (semblables aux saumures du Bouclier canadien). Les eaux souterraines aux environs du gisement de Restigouche sont très différentes de celles aux environs de celui de Halfmile Lake, témoignant ainsi d'écarts en ce qui a trait à l'hydrologie et à l'évolution des apports.

[1] Contribution to the 1994-1999 Bathurst Mining Camp. Canada-New Brunswick Exploration Science and Technology (EXTECH II) Initiative.
[2] Ottawa-Carleton Geoscience Centre, Department of Geology, University of Ottawa, Ottawa, Ontario K1N 6N5

INTRODUCTION

This report describes preliminary results of geochemical studies of ground and surface waters collected in the vicinity of the Restigouche Pb-Zn deposit during the summer of 1995 (Fig. 1). The purpose of this study, and a companion study at Halfmile Lake (Leybourne et al., 1995 and presentation at GSC Forum 1995), is to characterize groundwater-rock reactions occurring within volcanogenic massive sulphide deposits and their alteration envelopes, to document chemical signatures appropriate to such interacting groundwaters, and thereby to develop and improve hydrogeochemical exploration methods. Hydrogeochemical methods in exploration are receiving renewed attention, although application in Canada in the past has primarily been restricted to uranium exploration and few detailed studies around other types of deposits.

Groundwater geochemistry is potentially highly effective in exploring for buried sulphide deposits, particularly in a mature mining camp such as Bathurst where the geological controls on mineralization are relatively well understood. Transport of indicator elements in groundwaters is controlled by a variety of factors including pH, redox state, complexing reactions, adsorption-desorption reactions, and mineral solubility. In order to understand and characterize these processes, it is necessary to construct a water-rock reaction model. Study of the Restigouche deposit was initiated in part to discern mechanisms of rock-water reactions occurring among the Restigouche massive sulphide deposit, its altered host rocks, and the local groundwater regime. Interpretations of hydrogeochemical anomalies will be more rigorous if the processes controlling oxidation and dissolution of sulphide minerals, their subsequent dispersion, and concentration of constituent trace metals into stream waters and sediments, are well

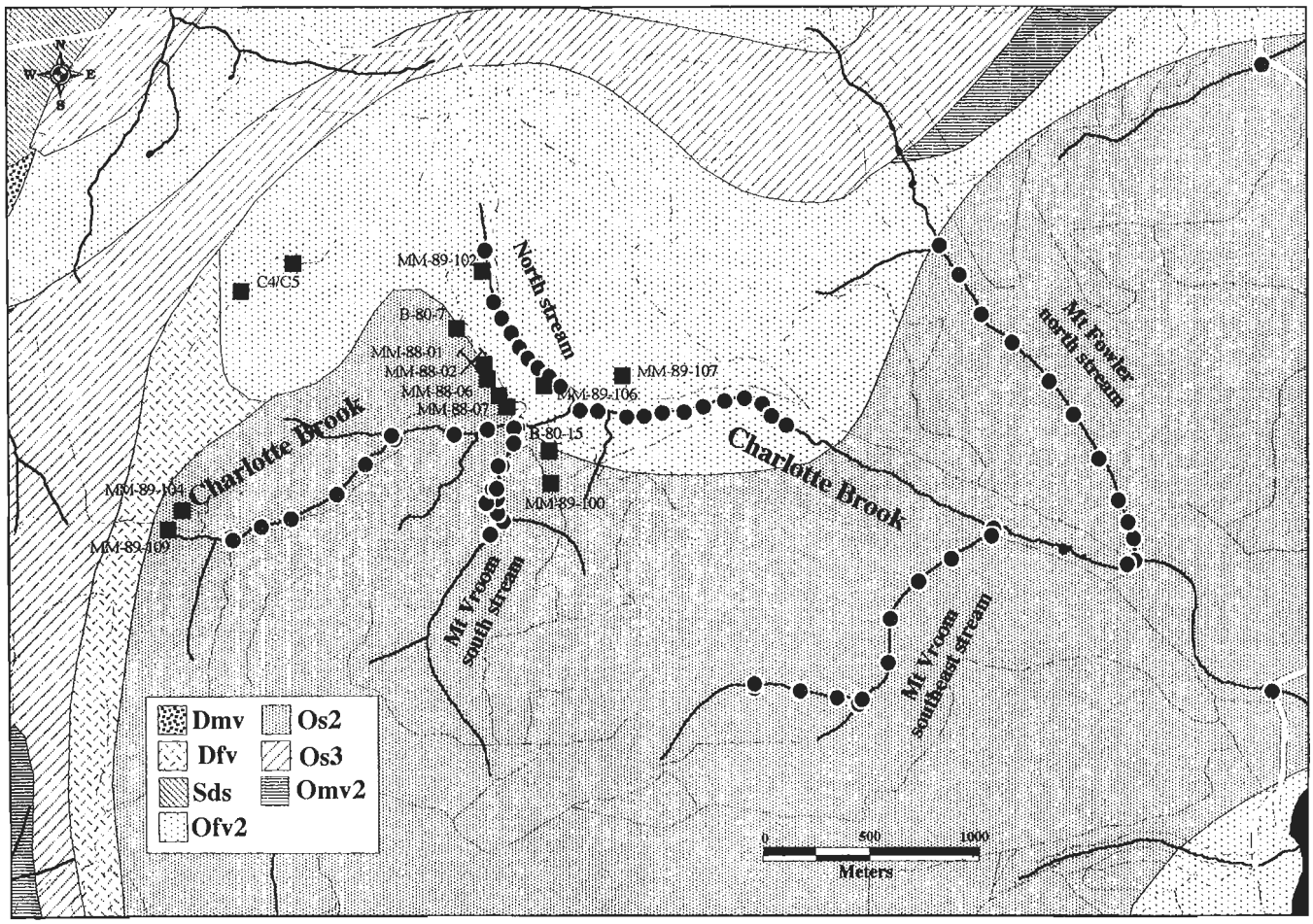

Figure 1. *Location of study area, showing location of surface samples and boreholes sampled during 1995 summer field season. Geology after Davies (1979). Dmv, amygdaloidal basalt, mafic tuff and breccia; Dfv, flow-banded and massive rhyolite, tuff and breccia; Sds, calcareous siltstone, sandstone and shale; Ofv2, quartz and quartz feldspar porphyry and related schists; Os2, phyllite, metagreywacke and graphitic schist; Os3, phyllite, graphitic slate, red and green manganiferous slate and chert, feldspathic lithic and quartzose greywacke; Omv2, metabasalt, pillow metabasalt. Dark lines are streams and light lines are roads.*

understood. This study is part of a larger multi-disciplinary program, EXTECH II, designed to improve exploration techniques for buried massive sulphide deposits in the Bathurst Mining Camp.

GENERAL GEOLOGY

The Restigouche deposit, part of the Tetagouche Group comprising a sequence of metasedimentary and metavolcanic rocks, is in fault contact to the north with Upper Ordovician-Lower Silurian mafic volcanic rocks, and to the northwest with Upper Silurian to Lower Devonian conglomerate, sandstone, and intercalated volcanic rocks. Three major sedimentary units cross the Restigouche property (south to north): 1) sandstones, argillites, and local pockets of graphitic argillite, 2) siltstones, graphitic and mafic tuff, and 3) ferruginous and graphitic argillites. There are two major felsic units, a southern felsic unit which hosts the Restigouche deposit and a northern unit which hosts the C4 and C5 mineralized zones (Barrie, 1982). The general stratigraphy for the Restigouche deposit follows the sequence: banded argillite to siltstone in sharp contact and intercalated with feldspar crystal and lapilli tuff, grading upwards to coarse pyroclastic lithic tuff, lithic lapilli and fragmental units intercalated with massive and disseminated sulphides (Barrie, 1982). The massive pyritic sulphides are in sharp contact with overlying massive rhyolite tuff grading upwards to lapilli and lithic tuffs and crystal tuff.

The Restigouche deposit is a volcanogenic Pb-Zn-Ag-(Cu-Au) massive sulphide deposit and differs from the Halfmile Lake deposit and most other deposits in the Bathurst Mining Camp in that it is hosted within felsic volcanic rocks. The Restigouche deposit is elongate and composed of a series of four vertically contiguous lenses and two satellite lenses in the hanging wall (Burns and Westoll, unpublished report to Marshall Minerals Corp., 1989). The massive sulphide lenses are up to 40 m thick. The major sulphide minerals are pyrite, marcasite, galena, sphalerite, and minor chalcopyrite; accessory minerals are enargite, tennantite and cassiterite. There is a stringer zone, indicating that the massive sulphides are not displaced from the feeder system. There is a northeast-trending mafic dyke swarm that cross-cuts the deposit and in places appears to infill fault zones. The diabase is variably altered to carbonate. Quartz and carbonate veins are common in both the footwall and hanging wall units. The ore zone outcrops on the south side of Charlotte Brook in a small gossan pit.

FIELD AND ANALYTICAL METHODS

Surface water samples were collected during the summer of 1995 from streams, springs, and seeps draining the Restigouche deposit. Borehole waters were collected using a flow-through bailer system and a high-pressure straddle-packer system. The straddle-packer system consists of two packers, spaced 1.5 m apart which are inflated with N_2 gas. The packed-off zone is sampled using N_2 gas through a sampling head located above the packers. Water flowing through the packed-off zone enters the sample head through a uni-directional 1 psi cracking valve. Several samples are taken at different time intervals dependant on the hydraulic conductivity of the zone being developed until the electrical conductivity of the recovered water reaches a steady state. Zones to be sampled are selected based on analysis of fracture patterns and fault densities in drill core. Parameters measured in the field were pH, Eh, conductivity, temperature, and dissolved oxygen (DO). All samples were hand-pump filtered in situ through 0.45 µm sterile filters in a 500 mL filter holder. All samples were refrigerated, and those for cation determination were acidified with ultrapure nitric acid at base camp prior to transport back to Ottawa for chemical and isotopic analyses. Major cations were analyzed by ICP-ES (Si, Ti, Fe, Mg, Ca, Na, K, B), trace elements by ICP-MS (Al, As, Ba, Cd, Co, Cr, Cu, Li, Mn, Mo, Ni, Pb, Rb, Sb, Sr, U, V, Zn), major anions by ion chromatography (NO_2, NO_3, F, PO_4, Br, SO_4, Cl) and alkalinity by titration at the Geological Survey of Canada. Representative analyses are presented in Table 1. Stable isotopes (^{18}O and D) were analyzed at the University of Ottawa. Reproducibility is better than ±15‰ for ^{18}O and ± 1.5‰ for D. Data are presented in standard δ notation:

$$\delta^{18}O = 10^3 \cdot \frac{(^{18}O/^{16}O)_{sample}}{(^{18}O/^{16}O)_{SMOW}} - 1$$

where SMOW is standard mean ocean water (Craig, 1961).

GEOCHEMISTRY OF SURFACE WATERS

The Restigouche area is characterized by steep hills (typical relief is in the order of 200-500 m) with generally poorly developed soils and very thin till cover (usually on the order of 1 m or less in thickness). Streams range from rock and pebble bottoms in steeper gradient areas to swampy wetlands. Surface waters are dominantly calcium-bicarbonate type waters (Fig. 2, 3) and typically have low concentrations of total dissolved solids (TDS; <85 mg/L; Table 1, Fig. 4a).

Although all surface waters are dominated by Ca and HCO_3^-, the streams surrounding the Restigouche deposit exhibit different chemical characteristics (Fig. 3, 4) reflecting variations in residence times, flow paths, and underlying lithologies. The North stream flowing adjacent to the main ore zone has low TDS (Fig. 4a) but is elevated in elements related to mineralization including Pb, Zn, and K (Fig. 4b, c, d). On a plot of K vs HCO_3^- for surface waters, two trends are evident; one trend shows increasing K with little increase in HCO_3^-, whereas the other trend shows more rapid increase in HCO_3^- compared to K (Fig. 3). The first trend is dominated by waters from the North stream (Fig. 4d). It is thus the stream most intimately associated with potassic (sericitic) alteration around the ore body, and is consistent with the predominance of illitic clays in fracture zones.

Total dissolved solids are highest for Charlotte Brook, especially upstream of the deposit. In this area there is a series of beaver dam lakes, resulting in greater surface evaporation

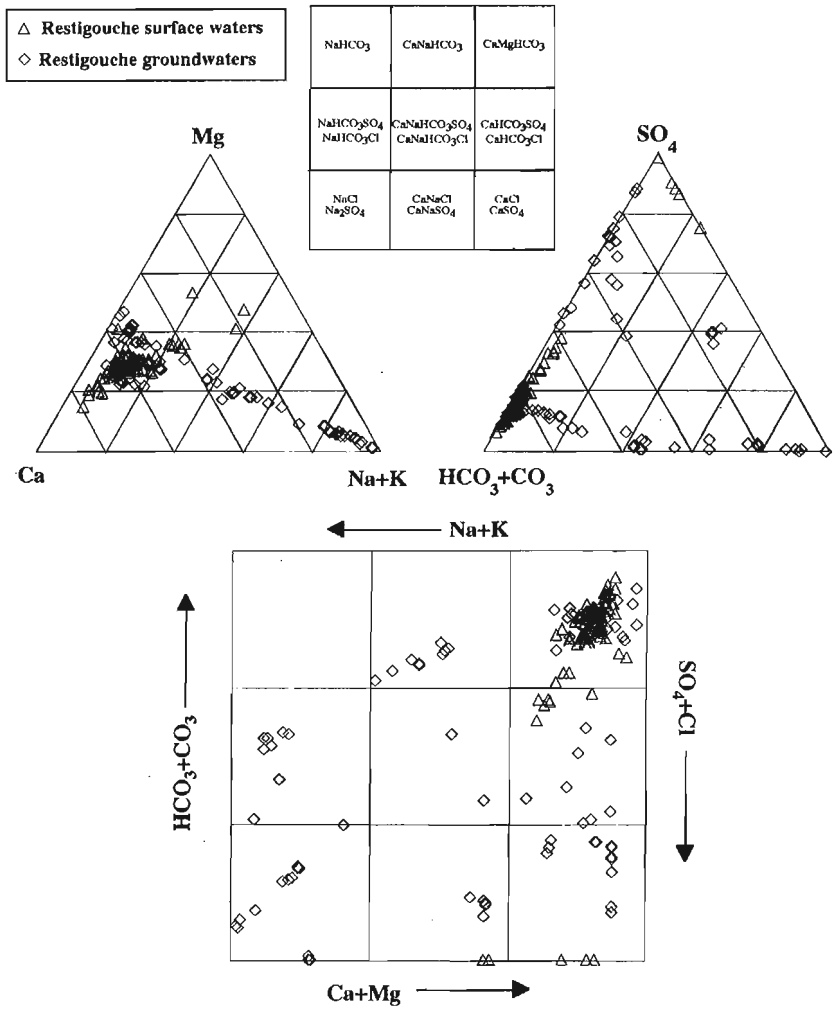

Figure 2.

Modified Piper plot of surface and borehole waters from the Restigouche deposit. Surface waters are tightly clustered and have Ca and HCO_3^- dominated compositions. Groundwaters show a strong trend towards the Na apex. Some groundwaters are dominated by Cl and some are SO_4^{2-}-rich.

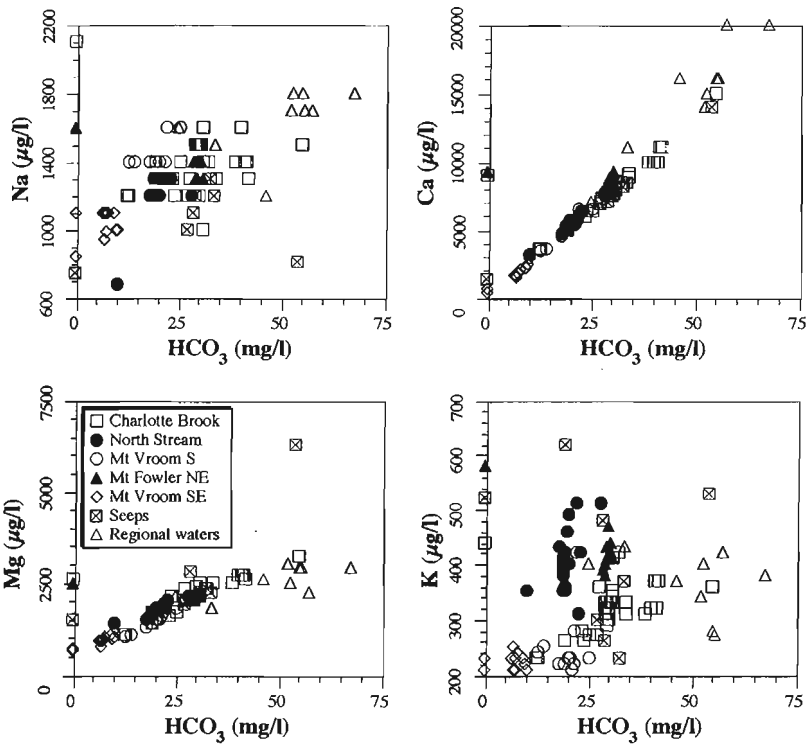

Figure 3.

Major cations plotted against HCO_3^- for surface waters. Mg and Ca are strongly correlated with HCO_3^-, whereas Na and K exhibit greater scatter between the different streams.

and thus an increase in TDS (Fig. 4a). Downstream of the deposit, the TDS values in Charlotte Brook are lower due to dilution from input by the lower TDS North and Mt. Vroom south streams.

The surface waters around the Restigouche deposit illustrate the potential for the use of hydrogeochemistry in mineral exploration. The geometry and location of the deposit are highly amenable to the production of hydromorphic anomalies. For example, Pb values are highest in the North stream, adjacent to the strike of the deposit, and in Charlotte Brook where the deposit comes to surface. Pb values decrease downstream, reflecting the low solubility of Pb (Fig. 4b). There is a single Pb anomaly on the Mt. Vroom southeast stream, which is coincident with Zn (Fig. 4c) and Al (Fig. 4e) anomalies. The Al values reflect the influence of pH on Al solubility

Table 1. Selected geochemical analyses of Restigouche surface and groundwaters

Sample #	MLW95-302	MLW95-430	MLW95-384	MLW95-398	MLW95-454	MLW95-465	MLW95-300	MLW95-581	MLW95-305	MLW95-606	MLW95-503	MLW95-370
Borehole	Surface	Surface	Surface	Surface	Surface	Surface	Surface	B-80-7	MM-88-01	MM-88-02	MM-89-106	EH-1
Depth (m)								173	20	511	243	75
Stream/type	Charlotte Bk	Charlotte Bk	North stream	Vroom south	Mt Fowler n	Mt Vroom SE	Seep	Packer	Baller	Packer	Packer	Baller
Do	10.3	9.72	10.63	10.77	9.47	10	7.92	na	4.8	na	na	na
pH	6.09	7.07	6.91	7	7.31	6.41	2.87	8.32	8.36	7.83	9.33	6.6
Eh		207	232	268	277	312	na	153	na	-113	197	308.5
Cond	32.8	64	43.7	44.3	80.1	45.7	467	305	202	40800	4870	70.7
Temp	8.1	11.5	8.4	6.2	12.9	11.3	13.3	na	8.1	na	na	na
pH (lab)	6.85	7.32	7.10	7.16	7.2	6.77	2.90	8.61	7.45	pending	7.74	7.03
Alkalinity	10.85	22.65	16.01	17.49	25.32	6.18	NA	123.85	46.90	pending	173.58	15.19
mg/L												
HCO_3 (calc)	13.24	27.63	19.53	21.34	30.89	7.54		151.10	0.00		211.77	0.00
SO_4	2.57	4.32	3.80	2.65	5.49	3.14	71.10	19.5	38.5	<0.05	0.21	13.9
Cl	0.27	0.3	0.26	0.35	0.42	0.28	0.68	13.6	0.43	13255	1485	0.31
NO_2	<50	<50	<50	<50	<50	<50	<50	<50	<50	nd	nd	<50
NO_3	<50	<50	<50	<50	<50	<50	196	<50	803	<50	<50	<50
F	<50	<50	<50	<50	59	<50	172	704	87	<50	<50	<50
PO_4	<50	<50	<50	<50	<50	<50	<50	<50	<50	<50	<50	<50
Br	<50	<50	<50	<50	<50	<50	<50	<50	<50	<50	<50	<50
µg/L												
Si	2600	3300	3200	3500	3500	2700	3900	3000	2800	3100	2200	4300
Ti	<1	1	<1	<1	<1	<1	1	1	<1	<1	3	<1
Al	8.1	3.1	3.7	2	5.6	7	890	7.5	36	14	110	2.6
Fe	<3	48	<3	<3	25	<3	4400	<3	230	1300	<3	<3
Mn	0.3	12	0.4	<0.2	0.4	1	82	17	370	81	280	6.2
Mg	1100	2300	1600	1500	2100	900	1500	7800	9500	320000	5000	2500
Ca	3600	7000	5000	5400	9100	1800	1300	22000	20000	780000	11000	7500
Na	1200	1200	1200	1300	1400	980	740	35000	3000	6200000	940000	2000
K	230	270	420	210	420	210	520	550	710	19000	1900	730
Ag	<0.2	<0.2	<0.2	<0.2	<0.2	<0.2	1.1	<0.2	<0.2	<0.2	<0.2	<0.2
As	<2	<2	<2	<2	<1	<1	2	1	4	7	13	4
B	<16	<16	<16	<16	<16	<16	<16	24	<16	6800	6900	<16
Ba	1.5	7	10	0.6	11	1.9	12	66	36	93000	550	16
Be	<1	<1	<1	<1	<1	<1	<1	<1	<1	<1	<1	<1
Bi	<0.2	<0.2	<0.2	<0.2	<0.2	<0.2	<0.2	<0.2	<0.2	<0.2	<0.2	<0.2
Cd	<0.5	<0.5	<0.5	<0.5	<0.5	<0.5	12	<0.5	3.2	<0.5	<0.5	<0.5
Co	<0.2	<0.2	<0.2	<0.2	<0.2	<0.2	1.5	<0.2	0.8	2.1	0.8	<0.2
Cr	<0.2	<0.2	<0.2	<0.2	0.3	<0.2	0.3	<0.2	<0.2	1.8	2.7	<0.2
Cs	<0.2	<0.2	<0.2	<0.2	<0.2	<0.2	<0.2	<0.2	<0.2	8.7	0.6	<0.2
Cu	<0.5	<0.5	1.6	<0.5	<0.5	<0.5	200	<0.5	3	12	2	1.6
Ga	<0.2	<0.2	<0.2	<0.2	<0.2	<0.2	<0.2	<0.2	<0.2	<0.2	<0.2	<0.2
Hg	<0.2	<0.2	<0.2	<0.2			<0.2		<0.2			<0.2
In	<0.2	<0.2	<0.2	<0.2	<0.2	<0.2	<0.2	<0.2	<0.2	<0.2	<0.2	<0.2
Li	1	<1	<1	<1	<1	<1	2	6	2	2600	1800	<1
Mo	<0.5	<0.5	<0.5	<0.5	<0.5	<0.5	<0.5	0.5	<0.5	0.5	19	<0.5
Ni	<1	<1	<1	<1	<1	<1	1	<1	3	21	6	<1
Pb	2.4	0.5	0.9	0.5	0.3	0.3	4000	<0.2	2.5	0.8	1.3	3.4
Rb	0.3	0.2	0.4	0.2	0.5	0.3	0.7	0.4	1.1	25	3.7	0.6
Sb	<0.2	<0.2	<0.2	<0.2	<0.2	<0.2	<0.2	1.4	<0.2	<0.2	0.3	4.3
Sc	<0.4	<0.4	<0.4	<0.4	<0.4	<0.4	<0.4	<0.4	<0.4	<0.4	<0.4	<0.4
Se	<2	<2	<2	<2	<2	<2	<2	<2	<2	<2	<2	<2
Sr	12	13	10	18	22	9.8	8.4	220	92	89000	610	29
Tl	<0.2	<0.2	<0.2	<0.2	<0.2	<0.2	0.3	<0.2	<0.2	<0.2	<0.2	<0.2
U	<0.2	<0.2	<0.2	<0.2	<0.2	<0.2	0.3	0.4	<0.2	<0.2	1.3	<0.2
V	<0.2	<0.2	<0.2	<0.2	<0.2	<0.2	<0.2	<0.2	<0.2	<0.2	<0.2	<0.2
Zn	4	<2	9	<2	<2	<2	3600	<2	1400	1700	14	97

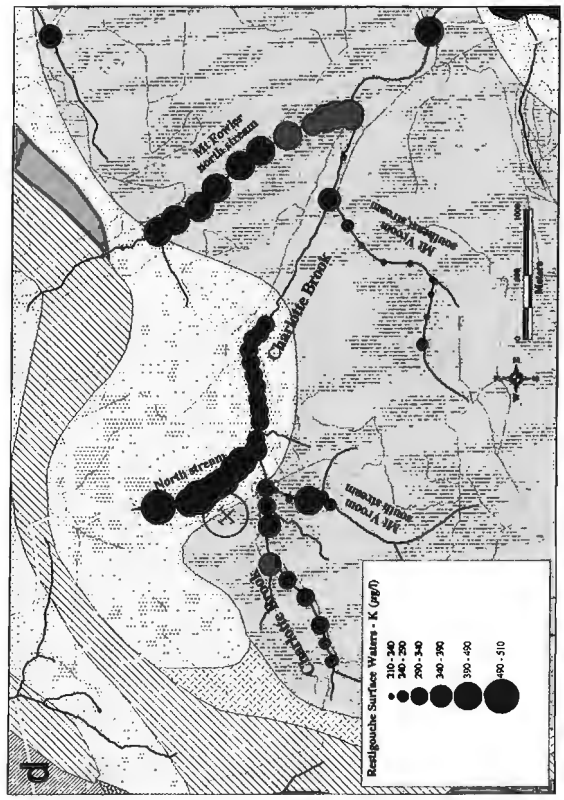
Mt. Fowler north stream
Mt. Vroom south stream
Mt. Vroom southeast stream
Charlotte Brook
North stream
Charlotte Brook
Restigouche Surface Waters - K (µg/l)
210 - 240
240 - 290
290 - 340
340 - 390
390 - 490
490 - 510
d

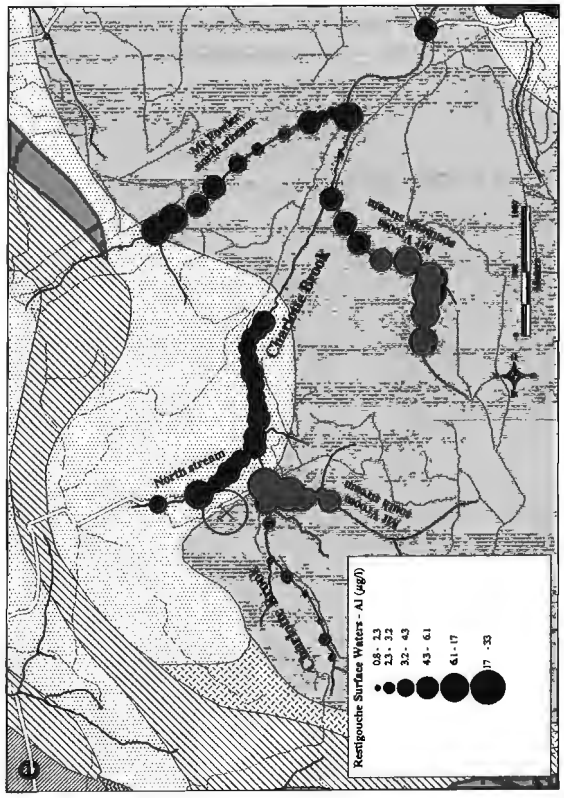
Mt. Fowler north stream
Mt. Vroom south stream
Mt. Vroom southeast stream
Charlotte Brook
North stream
Charlotte Brook
Restigouche Surface Waters - Al (µg/l)
0.8 - 2.3
2.3 - 3.2
3.2 - 4.3
4.3 - 6.1
6.1 - 17
17 - 33
c

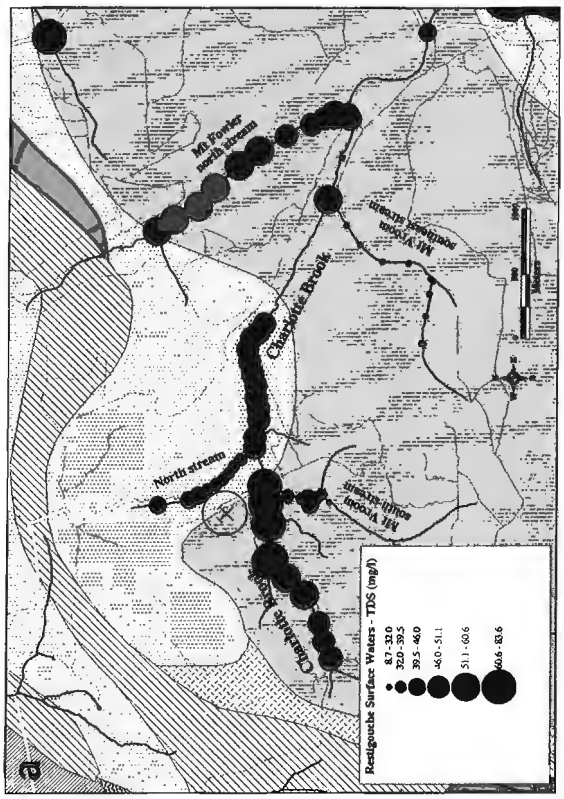
Mt. Fowler north stream
Mt. Vroom south stream
Mt. Vroom southeast stream
Charlotte Brook
North stream
Charlotte Brook
Restigouche Surface Waters - TDS (mg/l)
8.7 - 32.0
32.0 - 39.5
39.5 - 46.0
46.0 - 51.1
51.1 - 60.6
60.6 - 83.6
a

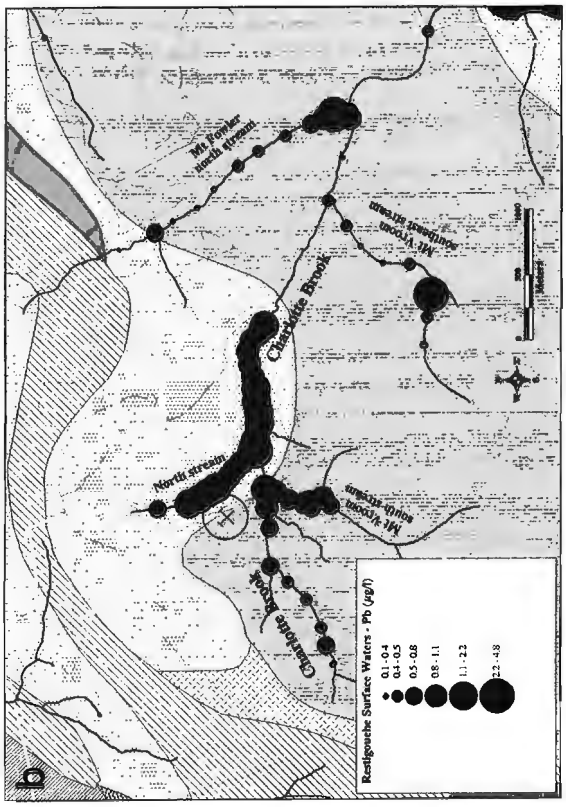
Mt. Fowler north stream
Mt. Vroom south stream
Mt. Vroom southeast stream
Charlotte Brook
North stream
Charlotte Brook
Restigouche Surface Waters - Pb (µg/l)
0.1 - 0.4
0.4 - 0.5
0.5 - 0.8
0.8 - 1.1
1.1 - 2.2
2.2 - 4.8
b

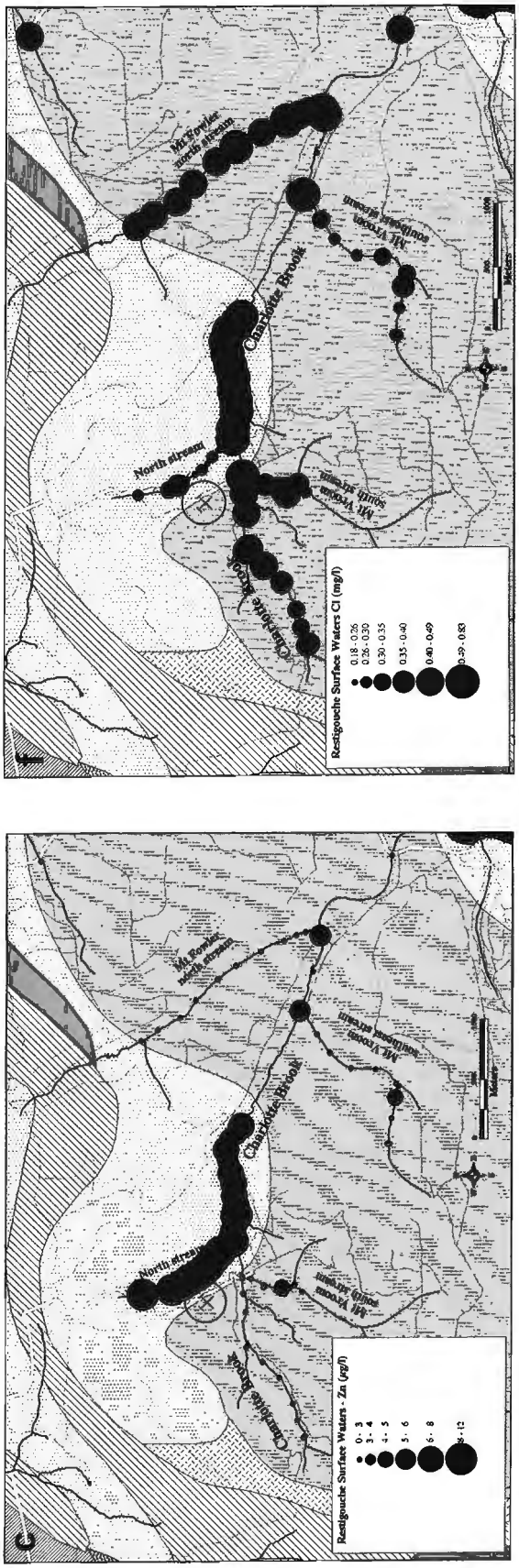

Figure 4. *Proportional circle plots of: **a)** TDS, **b)** Pb, **c)** Zn, **d)** K, **e)** Al, and **f)** Cl for Restigouche surface waters showing the spatial distribution of water chemistry. These diagrams clearly show the differences in chemistries for the different streams and the influence of the Restigouche ore body on surface water compositions.*

(Hooper and Shoemaker, 1985). Elevated Al values are also evident near the deposit, again reflecting more acidic waters. A seep in the gossan (not shown in Fig. 4e) has a pH of 2.9 and Al concentration of 890 µg/L. Zn concentrations are mostly below detection (<2 µg/L), but are clearly elevated in the immediate vicinity of the deposit and in Charlotte Brook downstream of the deposit. Zn is below detection in waters adjacent to the gossan. This is due to the very low Zn concentrations in the gossan; Zn is easily mobilized in acid weathering conditions, whereas Pb typically is immobilized as sulphate minerals, e.g. jarosite (Boyle, 1995).

One of the more interesting aspects of the hydrochemistry at Restigouche is occurrence of brackish to high salinity groundwaters at depth (>150 m; see below). These waters were recovered only in or near the deposit from the drillholes. However, Cl concentrations are somewhat elevated in the streams closest to, and downstream from, the ore body (Fig. 4f), suggesting that there may be some degree of hydrological connection between deeper saline groundwaters and the low TDS meteoric waters which feed the stream system.

GEOCHEMISTRY OF BOREHOLE WATERS

Selection of boreholes for sampling of groundwaters was based on several criteria. The main criterion was whether the drillhole was open to sufficient depth to warrant sampling. For the straddle packer system, two holes were selected that intersected mineralization and two holes that were east of the main zone of mineralization, but which penetrated footwall units. In general, cased NQ holes drilled in 1988 and 1989 by Marshall Minerals were open and accessible, whereas older holes were generally blocked at or near surface, with exception of two holes drilled in 1980 by Billiton Inc. The bailer method of groundwater sampling proved useful in that it is a much more rapid technique than the straddle-packer. However, although downhole increases in salinity are evident in bailer samples, the magnitude of the changes are variably masked by diffusion and advection in the borehole. The straddle-packer provides a more accurate representation of downhole chemical changes because it permits sampling at discrete depth intervals.

Groundwaters at Restigouche are variable in composition and range from shallow, low TDS Ca-HCO_3 groundwaters which are similar to surface waters in major ions (Fig. 2), to deeper brackish and saline waters. Most groundwaters are enriched in either Cl or $SO_4$2- over HCO_3- compared to surface waters (Fig. 2). Groundwaters also show a strong trend with increasing TDS and Cl concentration away from Ca-Mg dominated compositions to Na dominated compositions (Fig. 2). This relationship is evident from the strong correlation between Na and Cl concentrations (Fig. 5) which indicates either that Cl is increasing due to enhanced water-rock reaction, or that there are mixing relationships between dilute shallow groundwaters and deeper saline groundwaters. It is likely that both processes are occurring.

Calcium and Mg are highly correlated for all borehole waters (Fig. 5, 6), regardless of concentration, suggesting a common control over their concentrations. This is most likely

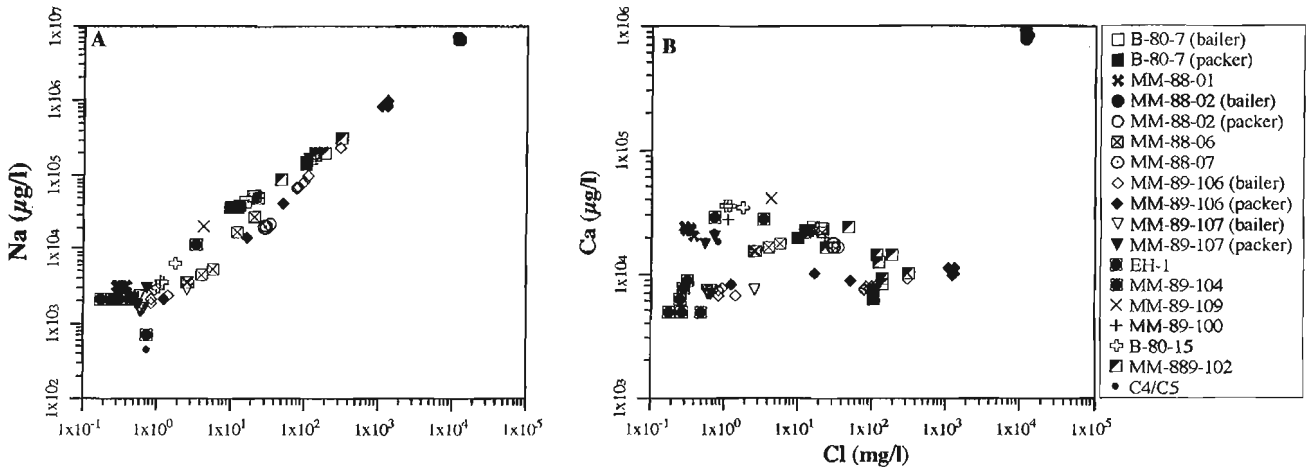

Figure 5. Plots of Na and Ca versus Cl for borehole waters from Restigouche. Na is strongly correlated with Cl, whereas Ca decreases with increased Cl, with the exception of the high salinity waters from borehole MM-88-02.

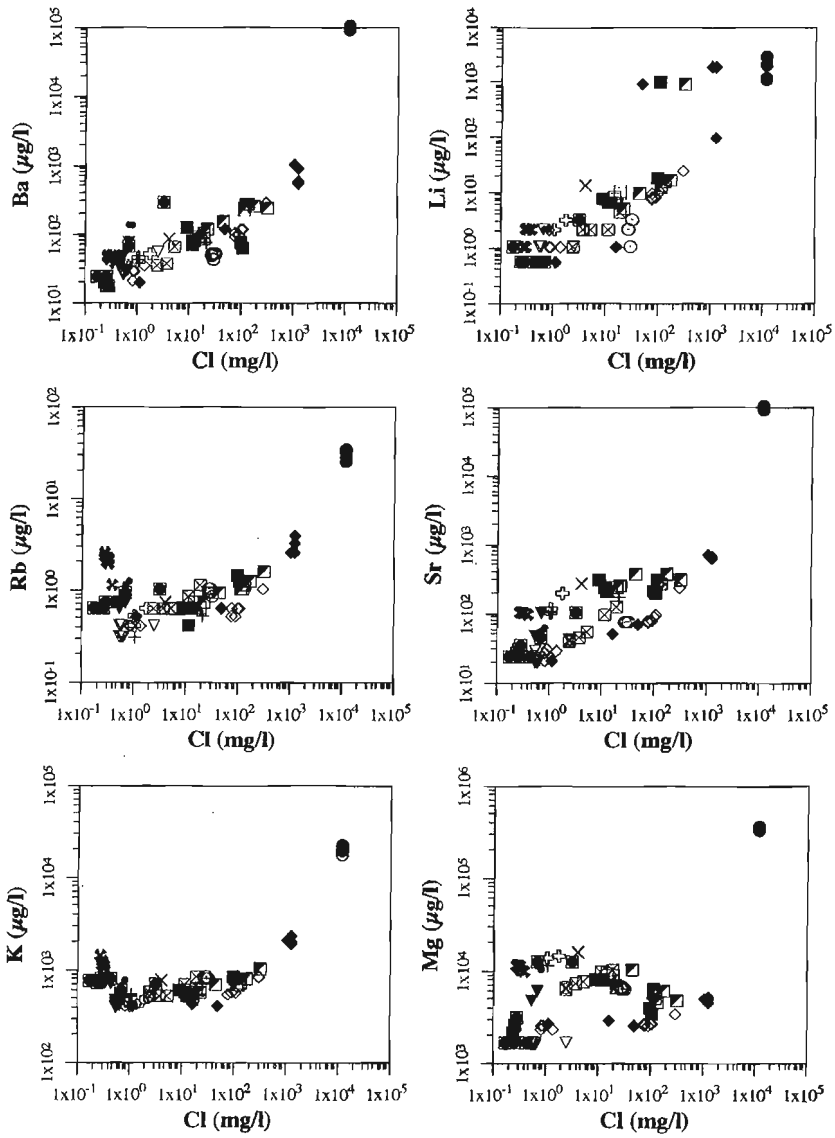

Figure 6.

Major and trace cations plotted against Cl. Most elements increase with increasing Cl, but some elements, such as K and Rb, show more complex behaviours, probably reflecting solubility control by fracture zone minerals. See Figure 5 for symbol legend.

due to carbonate minerals; Ca-Mg-Fe carbonates are common vein minerals in the Restigouche stratigraphy. Both Ca and Mg correlate positively with Cl, but groundwaters with Cl concentrations >10 mg/L decrease somewhat in Ca and Mg with further increases in Cl (Fig. 5, 6). This may indicate saturation of these waters with respect to carbonate minerals. Preliminary speciation and saturation modelling of Restigouche groundwaters supports this conclusion; all borehole waters except those from MM-88-01 and EH-1 are saturated or supersaturated with respect to calcite.

Trace elements show similar patterns as the major cations. In general, the trace metals increase with increasing chloride content. For example, Sr, Ba, and Li all increase with increasing Cl (Fig. 6). Potassium and Rb mimic each other and exhibit more complex behaviour (Fig. 6). Concentrations of K and Rb are higher in the lowest salinity groundwaters from boreholes penetrating hanging wall and footwall alteration zones, than in more saline waters, and probably originate from sericitic clays in the fractures by cation exchange reactions. Potassium and Rb contents are lowest for groundwaters with Cl concentrations 0.7-20 mg/L above which concentrations of both elements increase. Again, preliminary solubility modelling is consistent with K and Rb being controlled by saturation with respect to muscovite and illite.

The SO_4^{2-} concentrations are generally highest in the vicinity of the sulphides, indicating sulphide oxidation (e.g. Nordstrom et al., 1992). Boreholes MM-88-06 and MM-88-07 are close to the surface outcrop of the deposit and have elevated sulphate. Borehole MM-88-01 is further removed from the outcrop, but still intersects the main zone of mineralization and has the highest SO_4 values (38-87 mg/L; Fig. 7). The waters in this borehole are more oxidizing than those from 88-06 or 88-07 (Dissolved oxygen = 4-5 mg/L vs <3 mg/L). Fe contents are generally low, perhaps reflecting the precipitation of Fe-oxyhydroxides by oxidizing shallow groundwaters (Fig.7). The exceptions are MM-88-06 and MM-88-07, closest to where the deposit outcrops, which have elevated Fe; Fe concentration correlates with proximity to the massive sulphide deposit. MM-88-01, which has the highest SO_4 and highest Zn contents, has relatively low Fe compared to MM-88-06 and MM-88-07. Boreholes MM-89-106 and MM-89-107 are low in all the base metals and SO_4^{2-}, consistent with the location of these holes to the east of the main ore zone.

The water samples from the bottom of borehole MM-89-106, and to a lesser extent MM-89-107, show an increase in Cu and base metals as well as alkali and alkaline-earth elements indicating an association with hydrothermal alteration. The core logs for these holes noted that the units near the bottom of the holes were correlative with the stringer zone in the main ore body, but without major mineralization.

ORIGIN OF HIGH SALINITY GROUNDWATERS AT RESTIGOUCHE

The saline waters from borehole MM-88-02 have TDS values in excess of 20 000 mg/L, nearly two thirds the salinity of seawater. On the Piper plot (Fig. 2), these waters plot in the Na-(Ca)-Cl field. The MM-88-02 waters have Na/Cl molar ratios of 0.7-0.8 and (Cl-Na)/Mg molar ratios >6 indicating

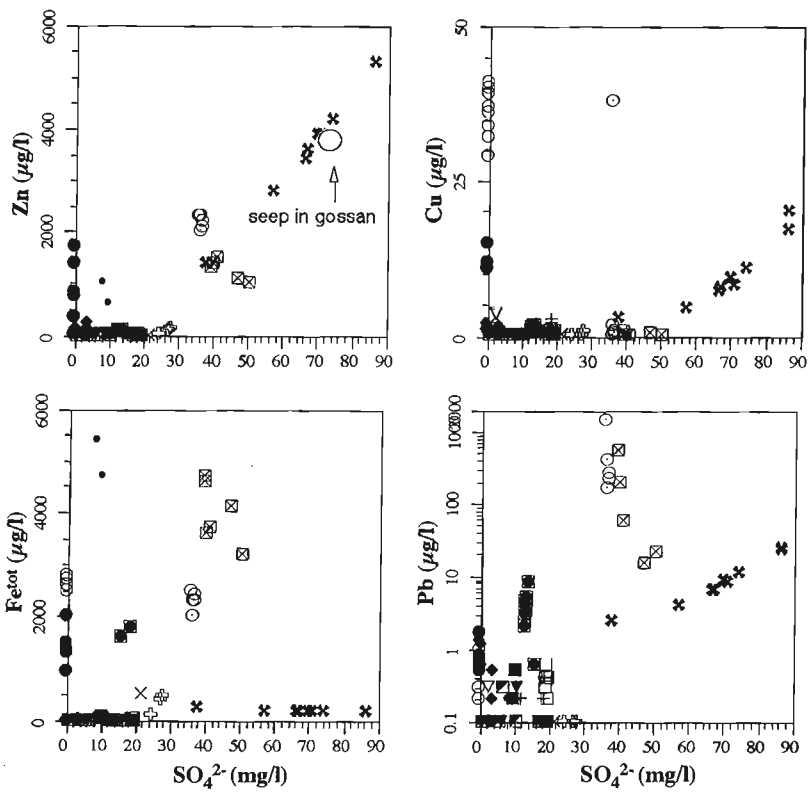

Figure 7.

Plots of Zn, Cu, Pb and Fe versus SO_4^{2-} for groundwaters from Restigouche. Sulphate and base metal concentrations are high for shallow groundwaters near the deposit, reflecting oxidation of sulphides. See Figure 5 for symbol legend.

that at least part of the chloride is balanced by Ca. This relationship is also defined as $Ca/(SO_4 + HCO_3) > 1$, indicating that there has been relative depletion in sulphate and bicarbonate. Although these high salinity waters from Restigouche have lower TDS than seawater with proportionately lower Cl and Na, they have considerably lower Mg and higher Ca, producing larger Ca/Mg ratios than seawater. Ba and Sr, along with Li and Cs, are elevated compared to seawater, whereas Rb and K are depleted compared to seawater. If the high salinity waters from Restigouche are modified seawater, water-rock reaction has depleted the alkali metals and enriched the alkali-earth metals. The relative enrichment in Ca, Sr, and Ba and depletion in Na, K, and Rb of the Restigouche saline groundwaters compared to seawater is suggestive of water-rock interaction involving silicate hydrolysis, probably dominated by feldspar dissolution.

The critical question is what is the source of the salinity, especially the high Cl content and the low concentrations of the other anions. There are several origins of high salinity including 1) long time periods of water-rock interaction, similar to waters from the Canadian Shield (e.g. Frape et al., 1984); 2) evaporation of fresh waters during pre-glacial times; 3) incursion of seawater in pre-glacial times; 4) deposition of marine aerosols; and 5) interaction of meteoric waters with fluid inclusions in the host rocks.

Deposition by seawater-derived aerosols is an unlikely mechanism due to the low sulphate concentrations of the saline waters at Restigouche and because the distance between Restigouche and Halfmile Lake deposits is not sufficient to explain the chemical differences between them.

Fluid inclusions from host rocks to the Brunswick #12 deposit are saline with daughter crystals present (Peter, pers. comm., 1993). However, if this is a source of Cl, it again raises the question of why such waters are not found at Halfmile Lake, and why such waters occur at shallow depths at Restigouche; groundwater salinities generally increase with depth in the Heath Steele mine but do not come close to the concentrations observed at Restigouche, even at depths up to 1 km. Nordstrom et al. (1989) concluded that the most likely origin for the deep saline waters at the Stripa mine, Sweden, was leakage from fluid inclusions. One of the lines of evidence for a fluid inclusion origin was the high Ca/Mg ratios of the inclusions and of the deep Stripa groundwaters, which had ratios up to 1000; the only type of waters with these ratios is geothermal water (Nordstrom et al., 1989). The saline waters at Restigouche all have low Ca/Mg ratios, suggesting that these waters are not related to fluid inclusion leakage.

One of the difficulties with evaporation is that this process typically results in a residual brine which is more concentrated in SO_4 and Br (e.g. Frape et al., 1984; Vengosh et al., 1995); in fact virtually all saline waters and brines from the Canadian Shield are enriched in SO_4 and Br (Frape et al., 1984). Waters from MM-88-02 have non-detectable SO_4. Br contents for the MM-88-02 waters were not detected by standard analytical methods and are being reanalyzed by a more sensitive technique.

Bottomley et al. (1994) invoked an allochthonous origin for the saline waters and brines from the Canadian Shield. They noted that much of the shield was covered by ocean during the Early Paleozoic, as shown by salt deposits of that age in the Alberta and Michigan Basins, and in the Hudson Bay region. If this mechanism were applicable to the MM-88-02 waters, significant modification must have taken place since seawater incursion occurred. The Ca, Sr, Ba, Li, and Cs concentrations are all higher than seawater, whereas, the Mg, Rb, and K concentrations are lower. The waters from MM-88-02 have lower Na/Cl ratios than seawater, reflecting either loss of Na if derived from halite dissolution or seawater or derivation from dissolution of silicates due to long periods of water-rock interaction. If the high saline waters are autochthonous, that is produced entirely by in situ enhanced water-rock reactions, the source of Cl becomes problematic (Bottomley et al., 1994). The oxygen and deuterium systematics are more consistent with an origin similar to shield-type brines than burial formation waters.

One of the most critical questions surrounding the saline waters is how they have been preserved over time in their present location. One answer may be that in the Bathurst Camp there are pockets of saline brines that because of their density and possible location in areas of low hydraulic gradient are effectively decoupled from the active groundwater flow systems (e.g. Bottomley et al., 1994).

STABLE ISOTOPE CHEMISTRY

Groundwaters at Restigouche show considerably greater variation in stable isotopic compositions compared to waters from Halfmile Lake (Leybourne et al., 1995), reflecting the greater variation in groundwater major and trace element compositions, greater water-rock interaction, and water evolution. Surface waters and low TDS shallow groundwaters are isotopically similar to those from Halfmile Lake, ranging from between -13.4 and -13.8 for $\delta^{18}O$ and -90 and -98 for δD (Fig. 8). Brackish groundwaters from the lower portions of MM-89-102 and MM-89-106 (990-2660 mg/L TDS) are isotopically heavier, whereas the saline waters from borehole MM-88-02 are the most isotopically enriched with compositions around -11‰ and -67 to -72‰ for $\delta^{18}O$ and δD, respectively. Waters from Heath Steele and Brunswick #12 mines fall between the saline and the brackish Restigouche groundwaters (Fig. 8). In general, isotopic composition is well correlated with Cl for the brackish to saline groundwaters.

Surface waters and shallow groundwaters are isotopically depleted compared with published compilations of groundwaters in Canada (Fritz et al., 1987), which indicates that groundwaters in the Bathurst regions should be between -10 and -11‰ on average. Excess deuterium is high, ranging from 10.5 to 17 (where excess deuterium is defined as 'd' = $\delta D - 8 \cdot \delta^{18}O$), which, combined with the depleted nature of the waters, suggests that recharge is dominated by winter precipitation, as was interpreted for Halfmile Lake meteoric waters (Leybourne et al., 1995).

The more isotopically enriched nature of the saline groundwaters and mine waters can be accounted for by several mechanisms. The more isotopically enriched compositions may reflect recharge during a warmer climatic regime, however the timing of such recharge is unconstrained. Alternatively, these waters may have been produced by mixing with a more saline end-member groundwater, such as a shield-type brine (Fritz and Frape, 1982; Frape et al., 1984; Bottomley et al., 1994). These saline waters may not be the true end-members; the act of drilling may have perturbed the local hydrology and resulted in mixing with low salinity meteoric waters. Although some form of mixing is the most likely option, simple two-component mixing is ruled out by the chemistry of the waters. For example, the Ca and Mg contents are inconsistent with simple mixing (Fig. 5, 6).

COMPARISON WITH WATERS FROM HALFMILE LAKE

The ground and surface waters at Restigouche differ from those at Halfmile Lake. Although broadly similar, surface waters at Restigouche are proportionally more Mg- and Ca-rich and Na-poor compared to those from Halfmile Lake. This is a reflection of the greater amount of carbonate within the Restigouche stratigraphy compared to Halfmile Lake, to the geochemistry of the host rocks, the fracture zone mineralogy and pre-glacial and modern weathering histories. Surface waters at Restigouche are uniformly proportionally enriched in HCO_3- at the expense of SO_4^{2-} and Cl compared to Halfmile Lake waters.

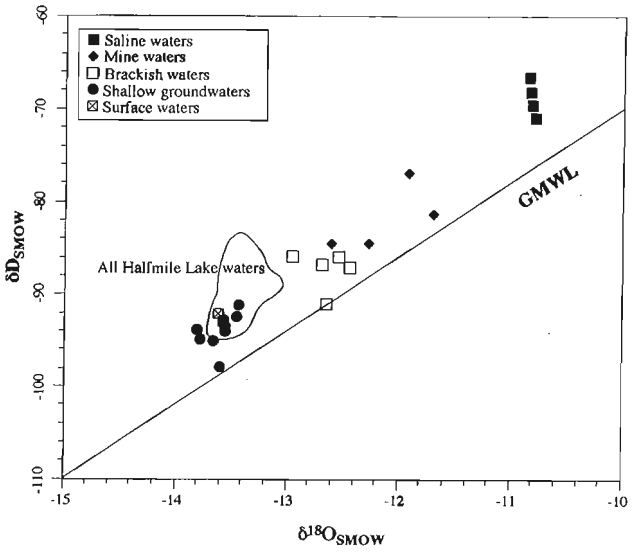

Figure 8. *$\delta^{18}O_{SMOW}$ vs δD_{SMOW} plot of surface and borehole waters from Restigouche. GMWL is the global meteoric water line. The field enclosing surface waters and groundwaters from Halfmile Lake is from Leybourne et al. (1995). Mine waters are from Heath Steele and Brunswick #12.*

Restigouche groundwaters trend towards very Na- and Cl-rich compositions (Fig. 2) and are more Ca- and Mg-rich than those from Halfmile Lake. Groundwaters closest to the Restigouche sulphide orebody are much more SO_4-rich than Halfmile Lake groundwaters (Leybourne et al., 1995). This reflects the lower degree of water-rock interaction at Halfmile Lake and the more shallow nature of the Restigouche ore body and therefore the greater degree of sulphide oxidation at Restigouche. The only borehole at Halfmile Lake with similar SO_4^{2-}/HCO_3- ratios is HT55-43 in the Upper AB zone (Leybourne et al., 1995). This hole penetrates the gossan and is therefore most analogous to the boreholes at Restigouche (i.e. associated with near-surface sulphides).

All of the borehole waters with the exception of those from MM-88-01 are low in Al (<5 ppb). One of the major controls on Al solubility is pH; Halfmile Lake groundwaters have generally lower pH than those from Restigouche.

The major differences in geochemical signatures in groundwaters between the two deposits is interpreted to reflect differences in host lithologies and fracture mineralogy as well as physical hydrology as a function of structure, geometry, and recharge characteristics. The Halfmile Lake ore-body and associated structures are steeply dipping, which combined with the deeply buried nature of the main part of the ore results in limited recharge to depth. Groundwaters collected at depth from boreholes at Halfmile Lake are most likely to reflect shallower groundwaters flowing downhole. In contrast, the orebody at Restigouche is shallow dipping and close to surface. As a result of the different geometry, recharge depth is much less than at Halfmile Lake, and pockets of old, more saline groundwater are preserved at Restigouche.

CONCLUSIONS

The chemical and stable isotopic compositions of the surface waters at the Restigouche deposit are broadly similar to those of low salinity shallow groundwaters. With increased depth, groundwater salinities typically increase reflecting increased residence time, increased interaction with the host rock, and possibly mixing with a deeper more saline groundwater. Surface waters show good correlations between potential ore pathfinder elements and proximity to the Restigouche massive sulphide deposit, especially for Pb, Zn, K, and Al. The presence of deep saline waters may be reflected in slightly higher Cl contents for surface waters near the deposit, suggesting some hydrological connection between deep groundwaters and surface waters.

Groundwaters at Restigouche are variable in major ions, total dissolved solids, and stable isotopes. Saline waters occur at depth and these waters are chemically and isotopically similar to shield brines with the exception of low sulphate concentrations.

The stable isotopes indicate that shallow groundwaters and surface waters are isotopically depleted compared to deeper brackish and saline waters, and are consistent with recharge dominated by winter precipitation. The more

enriched isotopic compositions of the saline waters may reflect recharge during warmer climatic regimes, but more likely reflects enhanced water-rock reactions.

Differences in compositions between surface waters at Restigouche and those at Halfmile Lake are a function of lithology and depth of the massive sulphides. The ore body at Restigouche is shallow producing larger chemical anomalies in ore-related elements. Groundwaters at Restigouche are very different to those at Halfmile Lake. This is most likely a reflection of differences in hydrology related to structures and to differences in host lithology.

The extent of hydromorphic dispersion of ore elements away from massive sulphide deposits is clearly quite limited (see Fig. 4). At Halfmile Lake, because the main ore zone is much deeper compared to Restigouche, the hydrogeochemical anomalies are smaller than at Restigouche. This has important implications for the design and implementation of hydrogeochemical surveys for more deeply buried deposits in mature base metal districts such as the Bathurst Camp and requires detailed sampling at small sample spacings.

ACKNOWLEDGMENTS

We would like to thank Steve McCutcheon, Mike Parkhill, and the rest of the staff at the New Brunswick Department of Natural Resources for access to assessments files and local knowledge. Peter Belanger is thanked for overseeing the geochemical analyses. Ian Jonasson is thanked for reviewing the manuscript.

REFERENCES

Barrie, C.Q.
1982: Summary Report, Restigouche Project, N.T.S. 21O7E and 10E; Billiton Canada Ltd.

Bottomley, D.J., Gregoire, D.C., and Raven, K.G.
1994: Saline groundwaters and brines in the Canadian Shield: geochemical and isotopic evidence for a residual evaporite brine component; Geochimica et Cosmochimica Acta, v. 58, p. 1483-1498.

Boyle, D.R.
1995: Geochemistry and genesis of the Murray Brook precious metal gossan deposit, Bathurst Mining Camp, New Brunswick; Exploration and Mining Geology, v. 4, p. 341-363.

Craig, H.
1961: Standard for reporting concentrations of deuterium and oxygen-18 in natural waters; Science, v. 133, p. 1833-1834.

Davies, J.L.
1979: Geological map of Northern New Brunswick; New Brunswick Department of Natural Resources and Energy, Mineral Resources Branch, Map NR-3.

Frape, S.K., Fritz, P., and McNutt, R.H.
1984: Water-rock interaction and chemistry of groundwaters from the Canadian Shield; Geochimica et Cosmochimica Acta, v. 48, p. 1617-1627.

Fritz, P. and Frape, S.K.
1982: Saline groundwaters in the Canadian Shield – a first overview; Chemical Geology, v. 36, p. 179-190.

Fritz, P., Drimmie, R.J., Frape, S.K., and O'Shea, K.
1987: The isotopic composition of precipitation and groundwater in Canada; in Isotopic Techniques in Water Resources Development, Symp. 299, March 1987, International Atomic Energy Agency, p. 539-550.

Hooper, R.P. and Shoemaker, C.A.
1985: Aluminum mobilization in an acidic headwater stream: temporal variation and mineral dissolution equilibria; Science, v. 229, p. 463-465.

Leybourne, M.I., Goodfellow, W.D., and Boyle, D.R.
1995: Chemical composition of ground and surface waters at the Halfmile Lake deposit, Bathurst Mining Camp, northern New Brunswick – EXTECH II; in Current Research 1994, (ed.) S.A.A. Merlini; New Brunswick Department of Natural Resources and Energy, Minerals and Energy Division, Miscellaneous Report 18, p. 113-126.

Nordstrom, D.K., Ball, J.W., Donahoe, R.J., and Whittemore, D.
1989: Groundwater chemistry and water-rock interactions at Stripa; Geochimica et Cosmochimica Acta, v. 53, p. 1727-1740.

Nordstrom, D.K., McNutt, R.H., Puigdomènech, I., Smellie, J.A.T., and Wolf, M.
1992: Ground water chemistry and geochemical modeling of water-rock interactions at the Osamu Utsumi mine and the Morro do Ferro analogue study sites, Poços de Caldas, Minas Gerais, Brazil; Journal of Geochemical Exploration, v. 45, p. 249-287.

Vengosh, A., Chivas, A.R., Starinsky, A., Kolodny, Y., Baozhen, Z., and Pengxi, Z.
1995: Chemical and boron isotope compositions of non-marine brines from the Qaidam Basin, Qinghai, China; Chemical Geology, v. 120, p. 135-154.

Geological Survey of Canada Project 940001

Spatially linked relational database management of petrology and geochemistry using Fieldlog v3.0: a worked example from the Bathurst mining camp, New Brunswick[1]

Neil Rogers and Boyan Brodaric
Continental Geoscience Division, Ottawa

Rogers, N. and Brodaric, B., 1996: Spatially linked relational database management of petrology and geochemistry using Fieldlog v3.0: a worked example from the Bathurst mining camp, New Brunswick; in Current Research 1996-E; Geological Survey of Canada, p. 255-260.

Abstract: Advances in personal computing power have enhanced the geological mapping process considerably. The recently developed Fieldlog v3.0 provides a geologist with the ability to store information in spatially linked relational databases and to organize data in a customized form without having to deal with the complexities of relational database design. Furthermore, it automatically links these data sets spatially to a digital base map, thus enabling the on-screen editing of data, whilst providing data analysis tools such as stereonets and chemical plots.

The reclassification of the Patrick Brook Formation from the Tetagouche Group to the Miramichi was implemented following a combined chemical, petrological, spatial, and structural re-analysis of sedimentary rock data from the Bathurst mining camp, northern New Brunswick. The methodology behind this reclassification is presented as an example of how Fieldlog v3.0 can be used to enhance geological models.

Résumé : Les progrès accomplis au niveau de la puissance des ordinateurs personnels ont permis d'améliorer considérablement le processus de cartographie géologique. Le nouveau logiciel Fieldlog v3.0 donne aux géologues la capacité de stocker des informations dans des bases de données relationnelles (liens spatiaux) et de personnaliser l'organisation des données, sans se perdre dans les complexités de la conception d'une telle base de données. De plus, le logiciel relie automatiquement et de façon spatiale les ensembles de données à un fond de carte numérique, permettant ainsi des corrections à l'écran, tout en fournissant des outils d'analyse de données (comme la possibilité de faire des stéréogrammes et des diagrammes chimiques).

La reclassification de la Formation de Patrick Brook, qui du Groupe de Tetagouche est passée à celui de Miramichi, a été effectuée après une nouvelle analyse chimique, pétrologique, spatiale et structurale des données sur les roches sédimentaires du camp minier de Bathurst (partie nord du Nouveau-Brunswick). La méthodologie derrière cette reclassification est présentée comme un exemple de la façon dont Fieldlog v3.0 peut être utilisé pour améliorer les modèles géologiques.

[1] Contribution to the Canada 1994-1999 Bathurst Mining Camp, Canada – Brunswick Exploration and Science Technology (EXTECH II) Initiative.

INTRODUCTION

The recent proliferation and ever increasing power of personal computers has provided an opportunity to develop new techniques for geological mapping. In the following paper we intend to outline one such procedure using the Fieldlog v3.0 spatially linked relational database that has assisted in the reclassification of a stratigraphic unit from the Bathurst mining camp, New Brunswick.

Digital compilation of geological data sets has a number of advantages over traditional techniques, most notably the ability to effectively manage far more information. For example, in a regional mapping program petrological information could be spread across hundreds of airphotos and several dozen field notebooks. Traditionally, compiling all the D_1 structures for a rose diagram, would have been a major project, whereas a computerized system could perform the task in a matter of seconds. The use of relational databases enables complex searches to be performed that combine information from different sources. Furthermore, it allows multiple entities to be linked to a single feature, such as various structures and samples from a single location. The advantage for geologists of having a relational database that is spatially linked cannot be overstated. Whereas simply cataloguing data into a more accessible form assists certain aspects of research (e.g. the production of stereonets), having this data linked into a mapping system allows for the visualization of this information. The ability to visualize and edit the relation between structure and rock type is an essential part of the cartographic process required to produce a geological map. The methods outlined in this paper illustrate how such techniques have accelerated geological interpretation, and how data from numerous sources can be incorporated together.

FIELDLOG V3.0

Fieldlog was originally developed by the Ontario Geological Survey in 1988 as a relational database system for use in their mapping programs. It was adopted by the Geological Survey of Canada in 1990, where it was redeveloped during 1991 and 1992. Fieldlog v3.0 was first developed in 1995 and has been under beta testing since that field season. Fieldlog v3.0 differs from the previous releases in that it operates solely as a module within AutoCAD r12 for both Windows and DOS, rather than a stand-alone DOS program that could be linked into DOS versions of AutoCAD. This enables it to maintain the advantages of a database system while incorporating the functionality of a graphical user interface and enabling data entry directly onto a base map. It has also been designed to make data entry easier and more reliable with the development of user-definable dictionaries that can handle long text strings (i.e. geologically relevant terms rather than contractions). When used in concert with the multitasking capabilities of the Windows95 operating system, it is possible to run a whole series of other programs in the background, such as a wordprocessor or spreadsheet, which can assist in the data handling without affecting the operation of Fieldlog. Other features of Fieldlog v3.0 that offer improved productivity for a geological study include the ability to run data analysis tools (e.g. stereonet production, geochemical plots), project locations into alternative co-ordinate systems, and export data to geographical information systems (GIS).

Most geological field surveys consist of collecting data at discrete locations throughout a designated region, from which the geological relationships (i.e. contacts) are inferred. At each location the geologist is liable to record a whole series of observations, such as rock type, colour, grain size, mineralogy, strike, and dip. Such observations exceed what can be displayed on a base map, without even considering the possibility for numerous structural readings, collection of multiple samples, and/or the presence of several lithologies at the same outcrop. Furthermore, it is difficult to effectively compile this data into a single table as it would require enough columns to account for every possible occurrence (i.e. the table would have to be large enough to accommodate the maximum number of rock types, along with their description, etc., that could possibly occur at an outcrop). This would create a table with an extremely large number of columns, many of which would be unused for any particular outcrop. The resulting sparse matrix is unwieldy and consequently difficult to visualize and search. For example, an outcrop could have many different rock types occurring at it, each of which may require a unique set of features to accurately record its description (i.e. the porosity is important feature of a sandstone, but not of crosscutting mafic dykes). Furthermore, numerous samples could be collected of each rock type, with many different methods of analysis (i.e. chemistry, thin section, etc.) applied to each sample. These problems are overcome in Fieldlog by handling the data in a relational database format, which consists of a collection of inter-related tables linked by common attributes, such as station number and sample number.

Each of the user defined tables in a Fieldlog database is registered as the particular type (e.g. station, rock, composition, process, sample, and analysis) that is most relevant for the field or laboratory observations it records. The tables themselves can be imported from other systems, such as spreadsheets, or created to suit the project within Fieldlog. Generally, the station table records the location at which the observations were recorded and samples collected (obtained from GPS (Geographical Positioning Satellite) or digitized from an airphoto, etc.) and refers it to a *station number*. Separate tables are then designed to deal with the other various forms of data, such as structure, lithology, samples, photographs, and other geological attributes. Each of these tables are linked together by the station number as well as potentially other numbers (e.g. sample number). This multitable approach enables multiple occurrences to be recorded in the appropriate table as often as required (i.e. each sample at a location would have its own record in the *samples* table). As search functions can be performed across multiple tables this enables complex data manipulation (e.g. retrieval of all the samples that have thin sections within a certain map sheet).

All database activities are performed by Fieldlog in a relatively transparent manner, with the user thus insulated from the technical aspects of using a relational database. While operating in AutoCAD, Fieldlog can act as an intermediary to a variety of underlying relational databases such as

dBASE (via AutoCAD's internal client-server environment) or Microsoft Access using ODBC (Open Database Concept) in Windows. Thus databases constructed with Fieldlog can also be directly manipulated by other systems outside the AutoCAD environment. These mechanisms permit the user to select from a wide variety of databases for any project, while maintaining Fieldlog's standard interface to the map and data.

In addition to automating database management, Fieldlog also provides spatial tools, such as projections from one co-ordinate system to another. The net result of these features is that the geologist can easily design a unique system for each mapping project using the most appropriate co-ordinate system, while maintaining full compatibility with any other projects. Furthermore, because Fieldlog accesses user defined dictionaries of geological terms, these may be shared between projects, thus also allowing for terminological standardization where desired.

Data sets may be accessed via user defined search routines, with the output presented in one several different forms (e.g. as a text file or a chemical plot). As Fieldlog v3.0 runs within a CAD environment all the various aspects of data can be displayed, edited, and saved directly on base maps, with the different features allocated to unique layers and/or symbols so that large quantities of data can be accessed rapidly or hidden from view, as required. This simplifies the drafting of geological boundaries to the extent that a geological map may be digitally drafted in the field.

STRATIGRAPHIC REVISION IN THE BATHURST MINING CAMP

The following sections present the methods used in order to reorganize the local stratigraphy of the Bathurst mining camp so that it is consistent both internally and with the rest of the Canadian Appalachians. This is illustrated by focusing on the techniques that resulted in the reclassification of the Patrick Brook Formation. The details of the regional geology and the resulting revised stratigraphy are beyond the scope of this paper.

Database Set-up

Petrographic and geochemical information from four field seasons have been compiled into a customized Fieldlog database, with all the locations linked to one of eight 1:50 000 digital base maps. This provides direct access to nearly 400 whole-rock chemical analyses, and well over a 1000 petrographic descriptions complete with stratigraphic classification. In addition, there are tables recording the samples, thin sections, and photographs, plus links to information not readily represented in tabular form which is contained in other formats (e.g. wordprocessor documents). Furthermore, several thousand structural readings from an earlier project (de Roo et al., 1993), recorded with an earlier version of Fieldlog, were incorporated into this study, illustrating the portability of digitized data sets.

Geological Setting

The Bathurst mining camp forms the northern extent of the Miramichi Highlands, a belt of pre-Silurian rocks extending across New Brunswick (Ruitenberg et al., 1977; van Staal and Fyffe, 1991). These pre-Silurian rocks have been divided into three groups – the clastic sedimentary Miramichi Group; the bimodal volcanic and sedimentary Tetagouche Group; and the ophiolitic Fournier Group (van Staal and Fyffe, 1991; van Staal et al., 1991; van Staal and Langton, 1990). The original contact between the Miramichi and Tetagouche groups is, where preserved, marked by a mélange at the top of the Miramichi Group (Miramichi Mélange, van Staal, 1994) that is unconformably overlain by the Tetagouche Group. This boundary is considered to be equivalent to parts of the Dunnage-Gander boundary as mapped in Newfoundland (van Staal and Williams, 1991).

The entire region has undergone intense alteration, with at least five phases of deformation and metamorphism to greenschist and locally blueschist facies. The strain distribution is extremely heterogeneous, with numerous mylonite zones interspersed with pockets of virtually no deformation. Consequently, the appearance of identical lithologies or stratigraphic units may vary radically from one location to the next. Combined with inaccessibility due to the afforestation and limited exposure, it renders the standard mapping techniques of traverses and following contacts largely invalid. The result is that geological units and their map distribution are, in many cases, defined by immobile element chemistry (Rogers, 1994).

The Patrick Brook Formation was originally defined as a sequence of interbedded black shales and impure sandstones, with resinous quartz clasts, which together form the basal clastic sedimentary unit within the Tetagouche Group (van Staal and Fyffe, 1991). These were thought to be contemporaneous with the early volcanism, and are locally the host rock to some of the volcanogenic massive sulphide deposits that occur within the Tetagouche Group.

Reclassification of the Patrick Brook Formation

Initial doubts over the classification of the Patrick Brook Formation became apparent after a regional study of the clastic sediment whole-rock chemistry. This study showed that the clastic sedimentary rocks of the Bathurst mining camp follow one of two distinct trends as defined on the basis of the Zr/Cr-V/Nb chemical plot. With the notable exception of the Patrick Brook Formation, the Tetagouche (Dunnage) Group rocks follow the high V/Nb trend, whereas the Miramichi (Gander) Group rocks follow the high Zr/Cr trend. The distinction between these trends is particularly apparent for the sandstones. Furthermore, recent fieldwork demonstrated that disrupted sedimentary horizons occur throughout the type locality for the Patrick Brook Formation, implying that the Miramichi Mélange sits at a slightly different stratigraphic position. Both of these factors seem to contradict with the evidence of an intradepositional relationship between Patrick Brook Formation clastic sediments and the initial stages of Tetagouche Group felsic volcanism.

The clastic sedimentary rock data set was re-analyzed by plotting the position of all the outcrops classified as Patrick Brook Formation, along with the rock type. This was important because the chemical characteristics of the shales differ from those of the sandstones. A specific symbol and colour combination were designated for each rock type from each formation, and plotted the location on an unique layer. A similar procedure was followed for the structural data and previous interpretations of the geological boundaries. This provided a geographical link into the project database, and a mechanism to edit or hide data as required, so that the relevant data under investigation was not "lost". The next phase of the investigation consisted of producing chemical plots for subsets of the sedimentary rocks, and incorporating these into important regions of the geological map (e.g. Fig. 1, 2, 3). Finally, the outcrop symbols were associated to specific attributes, such that the size of the symbol on the map corresponded directly to the abundance of certain elements.

A significant advantage that this approach is the direct presentation of chemical data on the map at its geographic location, which can be combined with a petrographic description. The chemical plots can be produced directly within Fieldlog v3.0 or by exporting the data as a text file for conversion by a spreadsheet into a format acceptable to proprietary geochemical plotting programs. There are advantages to both of these methods of displaying the chemical analyses: each system was used at different times during this study. Proprietary geochemical software is useful in that it allows for rapid generation of numerous chemical plots, including spidergrams which are not currently supported by Fieldlog v3.0. Furthermore, using the multitasking capabilities of Windows95, data sets can be updated and converted on a spreadsheet and presented on a chemical plot without needing to close Fieldlog or AutoCAD. However the presentation of chemical plots directly from Fieldlog onto the base map has one major advantage over separate geochemical programs, in that reallocation of samples to different groups on a chemical basis immediately results in the updating of the complete database. In contrast, if the chemistry is analyzed via another system, then this subset of the project data has to be constantly compared with the Fieldlog database to ensure that they are consistent. The on-screen editing capabilities of Fieldlog, enabling access to the database via both the sample's location or its chemistry, is illustrated in Figure 3.

In this particular study, it was shown that Patrick Brook-type sandstones do indeed follow the Miramichi Group chemical trend, whereas the interbedded shales are generally chemically indistinct from the other sediments in the region. However, this type of sediment occurs both contemporaneously with the base of the felsic volcanic pile and stratigraphically below the Miramichi Mélange (i.e. within the Miramichi Group). Consequently, the sediments classified as Patrick Brook Formation had to be split between one unit at the top of the Miramichi Group and another at the base of the Tetagouche Group. As the type locality for the Patrick Brook Formation occurs in the unit below the Miramichi Mélange, it follows that the Patrick Brook Formation is reclassified to the Miramichi Group. The remaining sediments that formed after the mélange (i.e. in the Tetagouche Group) were then allocated as the clastic sedimentary Rosehill Member of the contemporaneous Vallée Lourdes Formation. As these two units are effectively chemically and petologically

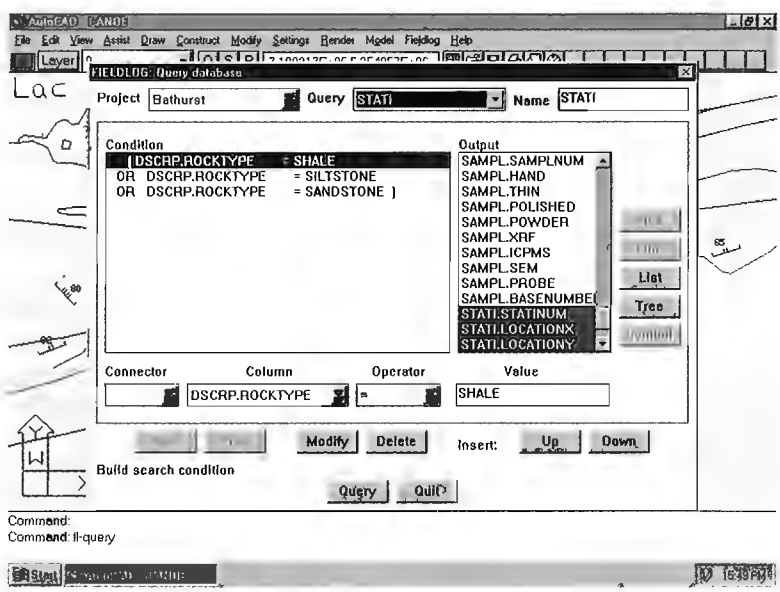

Figure 1. *A Fieldlog query (implemented by the FL-QUERY command) is created by specifying conditions which, when applied against the project database, return a thematic subset of the database. In this example, certain sedimentary rock types are being queried, while also returning data on the location and chemistry. This is a multiple table search, combining the rock description table with the station and chemistry tables. Including the station location in the query permits the rocks to be plotted on the map at their outcrop position.*

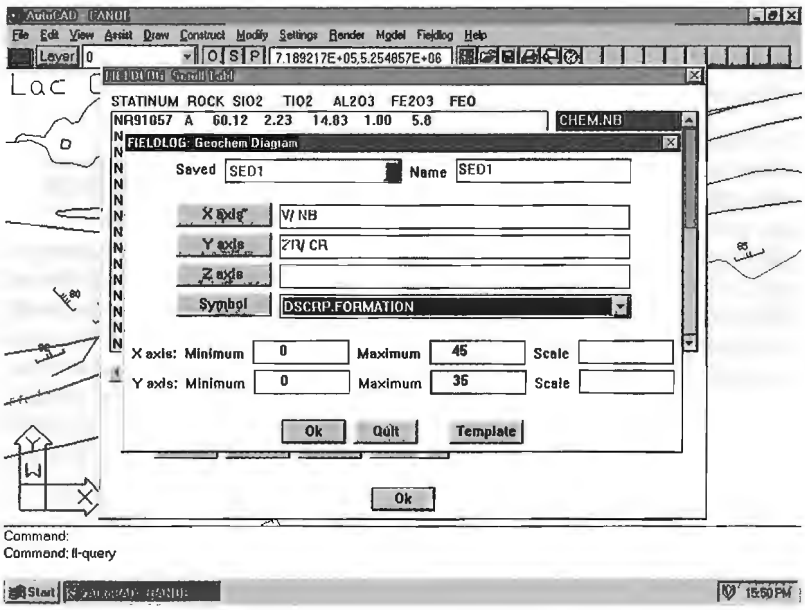

Figure 2. *The results of a query are initially presented in a table, from which the data can be output in a variety of formats: (i) AutoCAD map; (ii) database or text tables; (iii) ArcInfo, MapInfo, and SPANS GIS systems; and (iv) analytical diagrams such as a stereonet, a rose diagram or, as in this case, a geochemical plot. Fieldlog produces binary or ternary plots, for which the user can define formulae for the x, y, or z axis, scale the axis, symbolize the resultant points and place the diagram on the map. This example is a binary plot where V/Nb is plotted against Zr/Cr and the resultant points are symbolized according to their formation.*

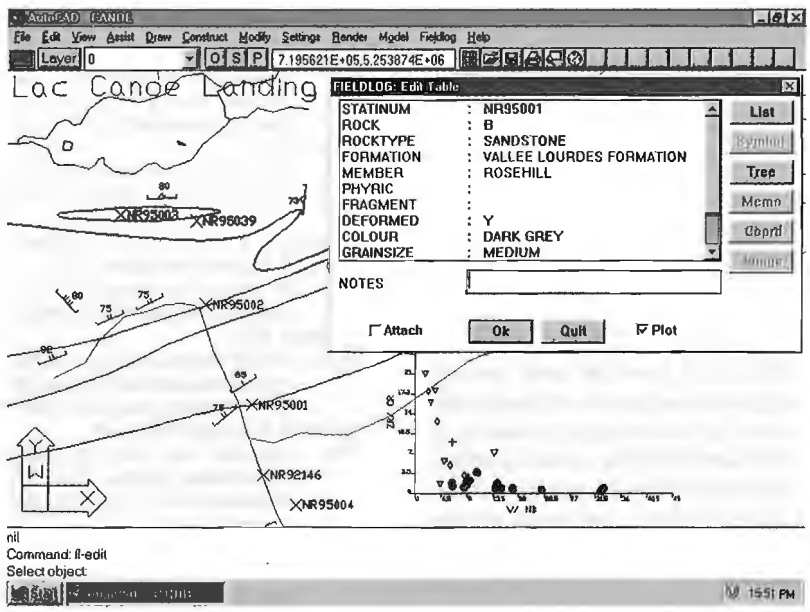

Figure 3. *Data entered with Fieldlog, or plotted from Fieldlog via a query, remains attached to the database. Thus both map and plot data can be "clicked-on" and the database item then displayed and if necessary edited. In this example, the top-most inverted triangle on the geochemical plot was selected, returning the description database item for one of the rocks occurring at locality NR95001. The same data table can also be retrieved by selecting the outcrop. Therefore, if required, the rock description can be altered either on a basis of its location in respect to other outcrops or by its chemical characteristics.*

identical, they would not have been discriminated from one another had they not been proven to occur at different stratigraphic positions by vitue of their relationship to adjacent rocks.

Without the benefit of a spatially linked relational database, this discrimination process would have been a very long and tedious operation, requiring the geologist to keep in mind not only the geographic locations of each of the Patrick Brook samples, but their petrographic type, and indeed, the geology of all the surrounding outcrops. Although it is envisaged that most reclassifications could be completed via global replacement of the formation and/or member status of a subset of the database obtained through a specific search function (i.e. all the black shales with greater than 4.5 wt.% MgO), this was not possible in this case. The classification of an outcrop as either Patrick Brook Formation (Miramichi Group) or Rosehill Member (Tetagouche Group) depends on information not necessarily directly related to that particular station number. For example, a sedimentary rock may not have any uniquely distinguishing features; however, if it is interbedded with felsic volcanic rocks, it must belong to the Rosehill Member of the Vallée Lourdes Formation (i.e. Tetagouche Group). Furthermore, updating the database would be difficult without on-screen editing following identification of the correct stratigraphic correlation of the station or sample.

SUMMARY AND CONCLUSIONS

Spatially linked relational databases are an extremely effective way to store and edit geological information. Fieldlog v3.0 offers the benefits of a relational system in a form that can be fully customized for each research project, without the geologist having to deal with details of database design and management. Furthermore, it enables field and laboratory data to be presented in numerous ways other than just points and lines on a map, such as chemical plots and stereonets.

The study outlined above used the power of the Fieldlog database system to split a petrographically and chemically indistinct subset of sediments between the Miramichi and Tetagouche groups in the Bathurst mining camp, northern New Brunswick. The similarities between the two units implies that they were both derived from the same source, only at separate times in the geological history of the region. It follows that there was a time lag between the initiation of the Tetagouche Group sedimentation and the switch from the granitic-sourced sediments that typify the Miramichi Group to the ophiolitic source that accounts for most of the Tetagouche Group sediments. This is thought to be related to the time it took to exhume the ophiolitic material responsible for the high V/Nb chemical in Tetagouche sediments.

Compiling data into a system such as Fieldlog presents potential benefits beyond the rapid classification or reclassification of samples into their relevant stratigraphic units and the preparation of geological maps. The availability and range of information contained within the database allows data to be incorporated easily into a geographical information system (GIS). Fieldlog v3.0 can export data to ArcInfo, SPANS, and MapInfo GIS systems, allowing more complex analyses to be performed through integration of field data with other data sets (e.g. aeromagnetics, gravity). Furthermore, the potential to record and export field data in digital format enhances its long-term usefulness.

ACKNOWLEDGMENTS

This paper would not have been possible without the assistance of Cees van Staal, John Winchester, and all the staff at the New Brunswick Department of Natural Resources who assisted in the geological investigations. The chemical analyses used in the study were produced by John Winchester at the Department of Earth Sciences, Keele University, England. Jacob de Roo is acknowledged for his structural data set, which was compiled for use in this project by Janice Bishop. This paper was critically reviewed by Graeme Bonham-Carter, Steve Lucas, and Cees van Staal.

Boyan Brodaric wishes to thank all the people who have assisted in the beta testing of Fieldlog v3.0 over the past year. Neil Rogers is a National Science and Engineering Research Council Visiting Fellow at the Geological Survey of Canada as part of the Extech II project.

The following companies are acknowledged for the use of their computer software products: AutoCAD is a registered trademark of Autodesk Inc; Windows95 and Microsoft Access are registered trademarks of the Microsoft Corporation; and dBASE is a registered trademark of Borland International Inc.

REFERENCES

de Roo, J.A., van Staal, C.R., and Brodaric, B.
1993: Application of FIELDLOG software to structural analysis in the Bathurst mining camp, New Brunswick; in Current Research, Part D; Geological Survey of Canada, Paper 93-1D, p. 83-92.

Rogers, N.
1994: The geology and geochemistry of the felsic volcanic rocks of the Acadians Range Complex, Tetagouche Group, New Brunswick; Ph.D. thesis, Keele University, United Kingdom, 420 p.

Ruitenberg, A.A., Fyffe, L.R., McCutcheon, S.R., St. Peter, C.J., Irrinki, R.R., and Venugopal, D.V.
1977: Evolution of pre-carboniferous tectonstratigraphic zones in the New Brunswick Appalachians; Geoscience Canada, v. 4, p. 171-181.

van Staal, C.R.
1994: The Brunswick subduction complex in the Canadian Appalachians: record of the Late Ordovician to Late Silurian collision between Laurentia and the Gander margin of Avalon; Tectonics, v. 13, p. 946-962.

van Staal, C.R. and Fyffe, L.R.
1991: Dunnage and Gander Zones, New Brunswick: Canadian Appalachian Region; New Brunswick Department of Natural Resources and Energy, Mineral Resources Branch, Geoscience Report 91-2, 39 p.

van Staal, C.R. and Langton, J.P.
1990: Geology of the Ordovician massive sulphide deposits and their host rocks in northern New Brunswick; in Mineral deposits of New Brunswick and Nova Scotia; (ed.) D.R. Boyle; Geological Survey of Canada, Open File 2157, p. 1-21.

van Staal, C.R. and Williams, H.
1991: Dunnage Zone-Gander Zone relationships in the Canadian Appalachians; Geological Society of America, Program with Abstracts, v. 23, p. 143.

van Staal, C.R., Winchester, J.A., and Bédard, J.H.
1991: Geochemical variations in Middle Ordovician volcanic rocks of the northern Miramichi Highlands and their tectonic significance; Canadian Journal of Earth Sciences, v. 28, p. 1031-1049.

Geological Survey of Canada Project 940001

Differential subsidence and tectonic control of sedimentation in the Stellarton Basin, Pictou Coalfield, Nova Scotia

John W.F. Waldron[1]
Continental Geoscience Division

Waldron, J.W.F. 1996: Differential subsidence and tectonic control of sedimentation in the Stellarton Basin, Pictou Coalfield, Nova Scotia; in Current Research 1996-E; Geological Survey of Canada, p. 261-268.

Abstract: The Stellarton Basin, containing the Pictou Coalfield, has been recently interpreted as a pull-apart basin formed on a dextral strike-slip system during Westphalian time. Core logs from part of the basin fill show, after correction for tilt and decompaction, a consistent southward increase in thickness, transverse to the basin axis. Thickness variations parallel to the basin axis are minor. Coal seams represent approximate paleo-horizontal datum planes; southward thickening therefore indicates synsedimentary tilting of the basin. The southern basin margin is interpreted as fault-bounded. Subsidence at the fault-bounded southern margin of the basin created accommodation space which trapped clastic sediment; peat accumulation occurred on the sediment-starved flexural basin margin in the north.

Résumé : Le bassin de Stellarton, dans lequel se trouve le champ houiller de Pictou, a récemment été interprété comme un bassin d'extension formé au niveau d'un décrochement dextre pendant le Westphalien. Des carottes de certains matériaux de remplissage du bassin indiquent, après application des corrections d'inclinaison et de décompaction, une augmentation continue de l'épaisseur des couches vers le sud, transversalement à l'axe du bassin. Les variations d'épaisseur parallèles à l'axe du bassin sont mineures. Les couches de charbon représentent des plans de référence qui étaient approximativement horizontaux dans le passé; l'épaississement vers le sud des couches indique donc une inclinaison synsédimentaire du bassin. La marge sud du bassin est interprétée comme étant délimitée par une faille. La subsidence au niveau de cette marge a créé un espace dans lequel ont été piégés des sédiments clastiques; la tourbe s'est accumulée sur la marge du bassin de flexure à faible remplissage sédimentaire dans le nord.

[1] Geology Department, Saint Mary's University, Halifax, Nova Scotia B3H 3C3

INTRODUCTION

The Stellarton Basin is a fault-bounded Westphalian basin located on a complex of faults in central mainland Nova Scotia (Fig. 1). The basin is located at the junction between the Cobequid Fault to the west, and the Hollow Fault to the east. The Stellarton Basin contains the entire Pictou Coalfield and has historically been the site of substantial coal mining; there has been recent exploration for coalbed methane. As a result of many years of exploration, the basin contains over 400 recorded boreholes. In this data set, approximately 35 coal seams and about 60 oil shale horizons may be correlated laterally between boreholes (e.g. Naylor et al., 1989).

The basin-fill rocks overlie intensely deformed rocks assigned to the Namurian Mabou (formerly Canso) Group. At the base of the succession within the basin, the Westphalian A Middle River Formation overlies the Mabou Group with profound angular unconformity. The Middle River Formation occupies a geographically restricted part of the southwest basin margin; the overlying Stellarton Formation onlaps onto Mabou Group at the basin margins. The Stellarton Formation consists mainly of Westphalian C lacustrine and fluvial sediments; the formation ranges up to Westphalian D age at the top. Palynological results suggest that the Westphalian B unit is missing at the disconformable base of the Stellarton Formation.

In this report the sedimentary record of subsidence within the basin is examined, using selected lithological logs from the database of borehole records, and a tectonic model for basin subsidence during deposition of the economically important coals of the Albion member of the Stellarton Formation is suggested.

REGIONAL GEOLOGICAL SETTING

The Stellarton basin is largely fault-bounded, except at its southwest margin where erosion has exposed the basal contacts of Stellarton and Middle River formations on highly deformed (vertical to overturned) older Carboniferous units. The northwest basin margin is marked by a complex of fault slices (the Alma fault zone) connecting with the Cobequid Fault to the west. To the north of the Cobequid fault lie Precambrian and Carboniferous granitoids, and Early Paleozoic and older Carboniferous rocks of the Cobequid Highlands. These are overlain to the east (north of the Stellarton basin) by late Carboniferous rocks of the Trenton Syncline (Fig. 1).

Towards the east end of the basin, a complex and poorly exposed area of faults separates the basin fill from slices of Windsor, Mabou, and other Cumberland group rocks (Fig. 1, 2). Some of these faults connect to the Hollow Fault, defining the

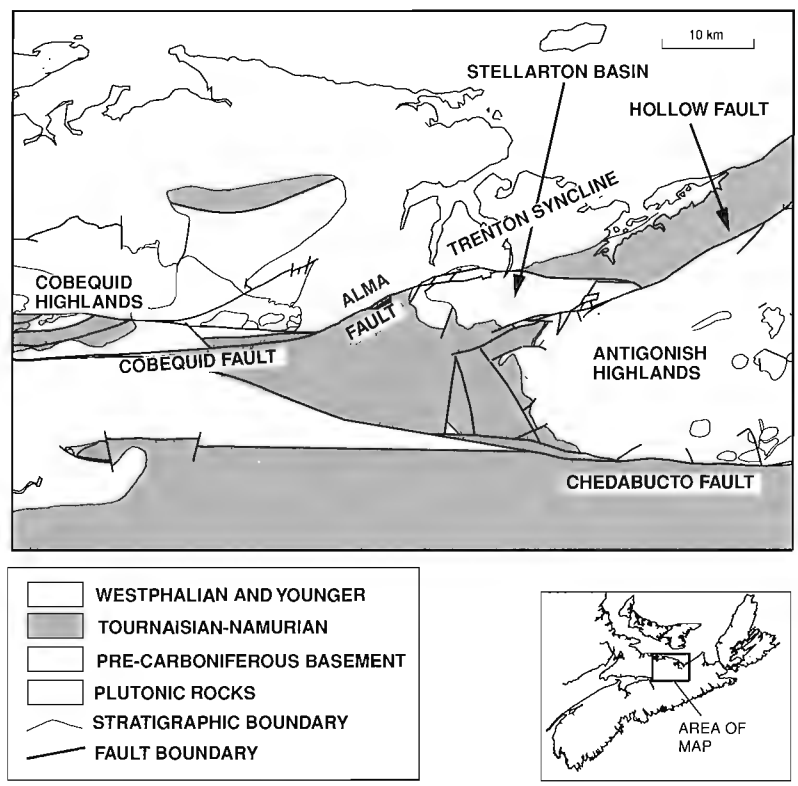

Figure 1. *Regional map of the Stellarton area showing the location of the Stellarton basin and surrounding units.*

northwest margin of the Antigonish Highlands. The highlands consist mainly of Precambrian and Silurian units, overlain to the southwest by limestones, minor evaporites, and clastic sediments of the Windsor Group (Giles, 1982).

The Stellarton Formation has been divided (Bell, 1940; Yeo and Gao, 1987) into six members (Fig. 2). At the base, the Skinner Brook Member consists largely of redbeds. It is overlain by the coal-bearing Westville Member; an interdigitation of Westville and Skinner Brook lithologies has been mapped towards the basin margins (e.g. Daigle, 1988). Redbeds at the south basin margin contemporary with the upper Westville and the lower part of the overlying Albion Member are assigned to the Plymouth Member; a thin interval of Plymouth Member redbeds extends into the central part of the basin. An second coal-rich interval occurs in the Albion Member; the thickest seam is the Foord, marking the top of the member. Albion Member coals show great lateral variability in both thickness and composition; in general the thickest coals are found close to the north margin of the basin, in an area where historic mining was hampered by intense faulting. Overlying the Albion Member is an oil-shale dominated lacustrine succession, the Coal Brook Member. The highest part of the formation is again coal-bearing, and is assigned to the Thorburn Member.

Stratigraphic analysis of the Stellarton Formation by Naylor et al. (1989) and others has shown that coarse clastic facies (mainly sandstones, local conglomerates) are concentrated at the south, east, and west basin margins. The present structural margins of the basin in these areas are therefore inferred to approximately follow the syndepositional basin margins. The thickest coal and oil shale successions are found in the centre of the basin and extend into the highly deformed northern marginal zone.

PREVIOUS STRUCTURAL WORK

Structural work in the Stellarton Basin dates back to the last century, when the geological setting of coal mines was investigated by Poole (1904). Subsequent extension of coal mines into the Albion Syncline led to further work by the Geological Survey of Canada, culminating in the study of Bell (1940),

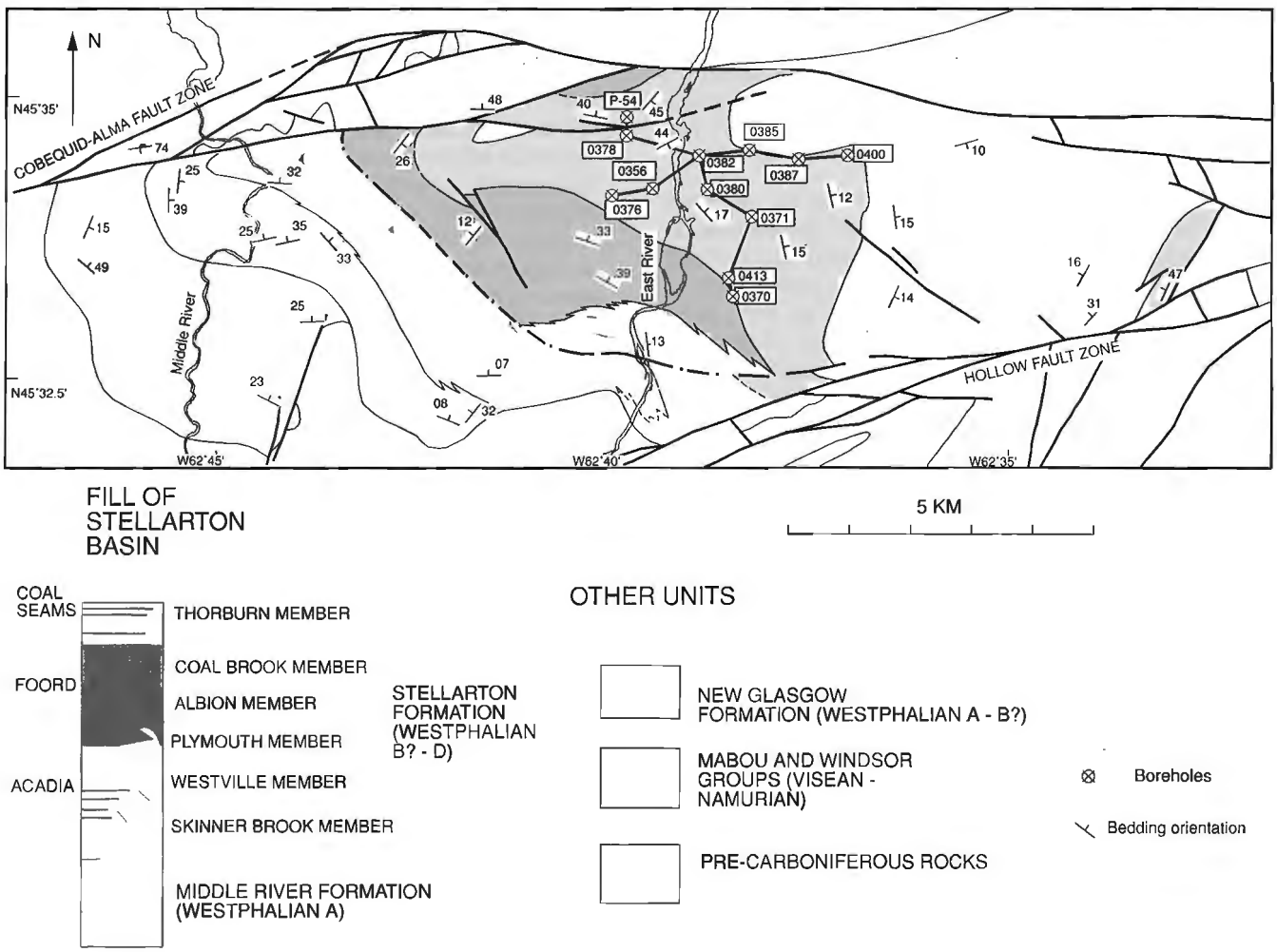

Figure 2. Geological map of the Stellarton basin showing the location of boreholes shown in Figures 3 to 5.

which identified many of the major faults in the area. During the 1940s and 1950s exploration and mining by the Acadia Coal Company led to the preparation of detailed contour plans of coal seams (T.B. Haites, unpub. data held at Nova Scotia Department of Natural Resources, 1953). Haites (1950) interpreted these results in a model involving substantial tectonic shortening. In this hypothesis, the coal seams of the Albion and Westville members were interpreted as equivalent. Subsequent paleobotanical studies (e.g. Hacquebard and Donaldson, 1969) have not confirmed this hypothesis. Yeo and Gao (1987) carried out structural studies in the basin and suggested a model for basin formation involving extension at a releasing bend (pull-apart) in a dextral fault system. Subsequent work by Gillis (1991) revealed an array of structures consistent with the dextral pull-apart model, a conclusion supported by Waldron et al. (1995) in an earlier report on this study.

BOREHOLE ANALYSIS

Data set

The Stellarton Basin is cut by about 400 recorded boreholes, lithological logs from which have been compiled into a computer database at GSC (Calgary) by Hughes (1993). Lithological logs in this database vary in quality; some early logs from the Acadia Coal Company record only the location of coal seams; more recent logs, particularly those dating from coal exploration in the 1980s, show detailed subdivision into units less than a metre thick.

Many coal seams in these boreholes can be correlated widely within the basin. Although coals vary greatly in thickness, showing interdigitation with clastic rocks near the basin margins, there is no indication that they are grossly diachronous. Because they were deposited close to the water table, these coals must represent approximate 'paleo-horizontal' datum planes within the stratigraphic pile. Thus it is possible to assess first-order differences in subsidence across the basin by examining thickness variations in sediment packages that are bounded by correlated coal seams.

Method of decompaction

Differential compaction has affected the present-day thicknesses of the various sedimentary units within the basin; for example a unit of originally constant thickness that grades laterally from sandstone into shale will show differential compaction such that the shale is now thinner. To assess differential subsidence we must therefore attempt to remove the effects of such differential compaction.

The method of decompaction adopted here is based on the relationship developed by Sclater and Christie (1980) for North Sea clastic sediments; this method has been widely used in studies of various sedimentary basins (e.g. Pitman and Andrews, 1985; King, 1994). The method uses an empirically calibrated exponential relationship between porosity and depth, given by

$$\text{Porosity at depth y: } \phi = \phi_0 e^{-cy}$$

The porosity at a given depth is dependent on two parameters that vary between types of sediment. The initial porosity ϕ_0 of the sediment is a measure of the total amount of compaction possible; the quantity c (known as the phi-depth coefficient) measures the rate at which this compaction will occur with increasing depth. The values of these parameters for typical sandstones and shales are well known (see Table 1), but values of the compaction parameters for peat and coal have been little investigated. In coal-bearing basins where the volume of coal is small compared with the clastic sediments, its compaction can sometimes be neglected. In the Stellarton Basin, coal makes up a significant proportion of the basin fill, especially in the relatively thin successions at the northern basin margin. Information on compaction during the peat-coal transformation is needed in order to determine how much of the apparent northward thinning of strata is due to compaction. Compaction parameters for peat were obtained from data presented by Salinas et al. (1989), using a best-fit to the exponential curve represented by the equation of Sclater and Christie (1980). The resulting values are shown in Table 1; the corresponding compaction ratio for coal is 7.7:1, which is in good accord with other estimates of coal compaction (e.g. Ryer and Langer, 1980).

Table 1. Parameters used for decompaction, based on data from Sclater and Christie (1980) for clastic sediments and Salinas et al. (1989) for coal.

Lithology	Initial porosity	Phi-depth coefficient (km^{-1})
Sandstone	0.49	0.27
Siltstone	0.56	0.39
Shale	0.63	0.51
Coal	0.87	2.00

Decompaction also requires information on the present-day state of compaction based on porosity measurements or on the maximum thickness of overburden accumulated during the subsequent geological history. Systematic data on the present-day porosity of the sediments are not available; however, available fission track data suggest that possibly 2 km of overburden may have been removed from the area (R.J. Ryan, pers. comm., 1994). Models were therefore run assuming 2 km of overburden above the present level of exposure; closely comparable results were obtained in trials using higher (3 km) and lower (1 km) overburden values.

Thicknesses values for selected cores were first corrected for tectonic tilt using dip angles from the core database. Solution of the porosity depth equation requires an iterative calculation (Allen and Allen, 1990), which was carried out using a Microsoft Excel spreadsheet.

Preliminary results

Figure 3 shows the general variation in thickness in the upper Albion Member along a roughly north-northwest-south-southeast traverse, perpendicular to the basin axis, through the central part of the basin. The columns in Figure 3 show present-day thicknesses, with thickness corrected only for tectonic tilt. There is a substantial stratigraphic thickening towards the south margin of the basin. All this thickening is accounted for by increase in clastic, especially coarse clastic, facies. However, coals and oil shales thin and interdigitate with clastics towards the south basin margin.

This southward thickening represents a combination of primary thickness changes and differential compaction. In order to represent the original thickness of strata, the effects of subsequent compaction must be removed. This is done using the decompaction algorithm described above and the results are shown in Figure 4. Clearly a southward thickening is still present, presumably reflecting increased subsidence towards the southern basin margin.

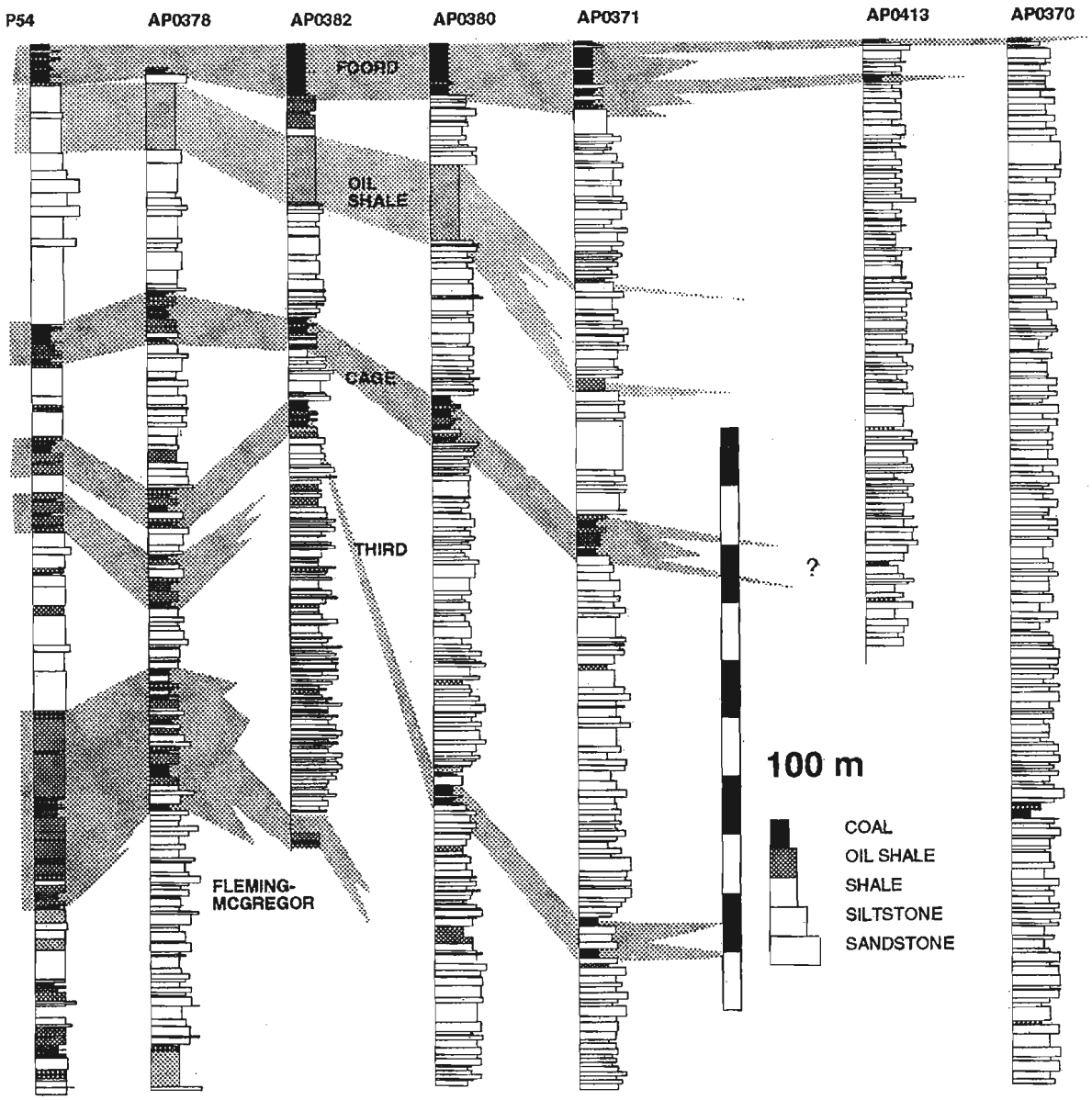

Figure 3. *Logs of cores on north-south profile through Albion member of Stellarton Formation, thicknesses corrected for dip. Borehole locations shown in Figure 2.*

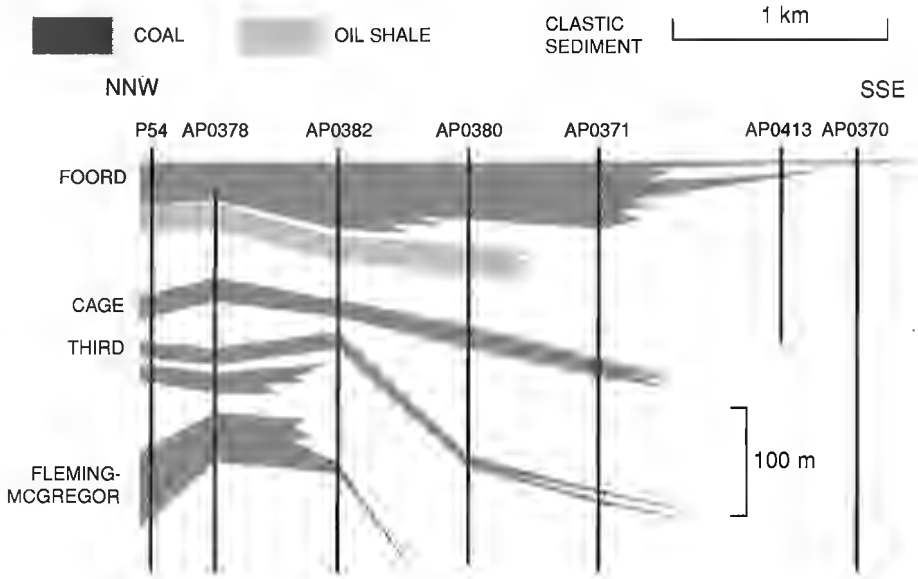

Figure 4. *Logs based on cores on profile through Albion Member of Stellarton Formation transverse to the basin axis. Thicknesses are shown as they existed at time of end of Foord seam deposition, corrected for present day tilt and decompacted. Vertical exaggeration x5. Borehole locations shown in Figure 2.*

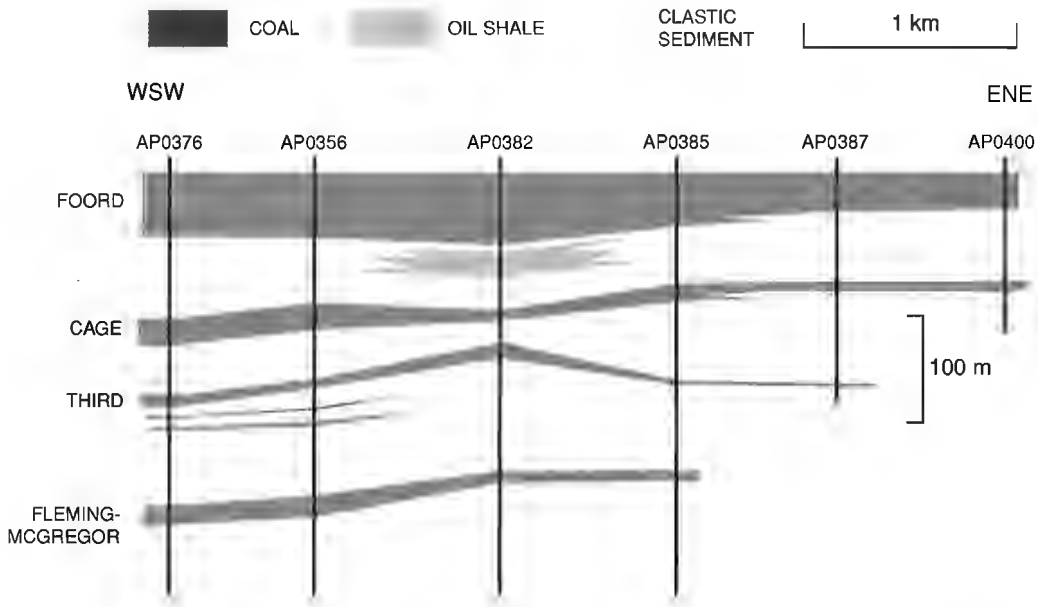

Figure 5. *Logs of cores on longitudinal profile of basin, through Albion Member of Stellarton Formation, thicknesses corrected for dip and decompacted as in Figure 4.*

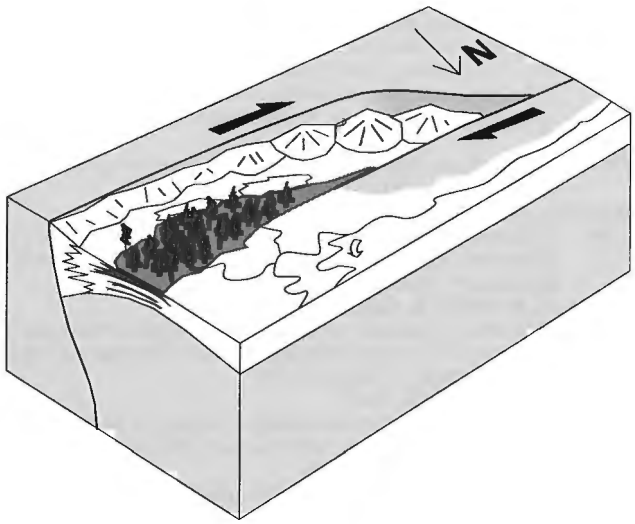

Figure 6. Simplified model for deposition of the Albion Member of the Stellarton Formation during pull-apart subsidence. Dark grey shading with tree ornament represents possible tectonic setting of peat-forming mires.

Results of a similar analysis along a traverse longitudinally along the basin (location shown in Fig. 2) are shown in Figure 5. Note that the thickness variations shown are much more subdued, indicating that the tilting axis was approximately parallel to the overall basin axis.

DISCUSSION

Localized facies changes and the geometry of the Stellarton Basin indicate that Westphalian subsidence was largely fault-controlled. In previous interpretations, the strong concentration of coal and fine grained facies at the north edge of the basin has been assumed to indicate greater subsidence in the north. However, the southward thickening of Stellarton basin-fill successions clearly indicates that the tectonic regime created more accommodation space near the south basin margin during deposition of the Albion Member. Most reasonably, the coincidence of greatest subsidence with coarsest clastic facies indicates that the southern margin of the basin was fault-controlled, and that coarse clastics were shed from a basin-bounding fault scarp at the south margin of the basin. Restriction of coarse clastics to a zone close to the south margin indicates derivation from a relatively small drainage basin.

Tilting in pull-apart basins is largely controlled by curvature of bounding fault surfaces, which commonly show negative flower structure (e.g. Harding, 1985) profiles in cross-section. Figure 6 shows a schematic model for deposition in a pull-apart basin, in which accommodation space for sediment accumulation is provided by an extensional dextral fault at the basin margin. Tilting of the basin fill results from movement along the listric upper part of the bounding fault surface. A gentle arch is created at the opposite, flexural basin margin. Pulses of tectonic movement at the basin margin result in increased accommodation space close to the bounding fault, and create a surface gradient that prevents sediment from escaping from the marginal region until this space is filled. This provides the ideal setting for peat accumulation (high water table relative to sediment surface, lack of clastic input) at the more slowly subsiding flexural basin margin. During deposition of the Albion Member coals, the faulted margin lay along the south of the basin; coal is interpreted to have accumulated preferentially along the northern, flexural margin. In the block diagram (Fig. 6), regional drainage is shown diverted northward away from the basin, consistent with the paleocurrent data of Yeo and Gao (1987). Subsequently, the north basin margin was cut by faults that generated the present, positive flower structure along the north basin margin, and deformed the Albion coals in the subsurface.

CONCLUSIONS

After decompaction and correction for tectonic tilt, thicknesses of coal-bearing successions can indicate first-order features of basin subsidence geometry. During deposition of the Albion Member of the Stellarton Formation, subsidence and sediment accumulation were most rapid at the southern basin margin, interpreted as fault-bounded. Peat formation was concentrated at the north basin margin where overall syndepositional subsidence was slowest. The geometry of the basin is consistent with a dextral pull-apart model, in which active faulting occurred at the southern basin margin and flexure of the basin floor took place in the north.

ACKNOWLEDGMENTS

I am grateful to Dave Hughes and Don MacNeil for facilitating access to the database of borehole information, without which this study would not be possible. I also acknowledge useful discussions with Kevin Gillis, Rob Naylor, John Calder, Fred Chandler, and Peter Giles, and helpful reviews by Brendan Murphy and Fred Chandler. I thank Fred Chandler and Peter Giles for their logistical assistance and support of the project.

REFERENCES

Allen, P.A. and Allen, J.R.L.
1990: Basin Analysis: Principles and Applications; Blackwell, Oxford, England, 451 p.

Bell, W.A.
1940: The Pictou Coalfield, Nova Scotia; Geological Survey of Canada, Memoir 225.

Daigle, L.
1988: Deposition of the lower three members of the Stellarton Formation; Nova Scotia Department of Natural Resources Report 88-3, p. 199-202.

Giles, P.S.
1982: Geological Map of the Eureka area, central Nova Scotia; Nova Scotia Department of Mines and Energy, Map 82-03, scale 1:50 000.

Gillis, K.S.
1991: Report on the structural setting and coal resources of the Stellarton Graben, Pictou County, Nova Scotia; Nova Scotia Department of Mines and Energy, Open File Report 91-014, 24 p.

Hacquebard, P.A. and Donaldson, J.R.
1969: Carboniferous coal deposition associated with flood-plain and limnic environments in Nova Scotia; Geological Society of America, Special Publication 114, p. 143-191.

Haites, T.B.
1950: Some geological aspects of the Pictou Coalfield with reference to their influence on mining operations; in Conference on the Origin and Constitution of Coal, (ed.) J.P. Messervey and H.D. Smith, Nova Scotia Department of Mines and Nova Scotia Research Foundation, Halifax. p. 39-93.

Harding, T.P.
1985: Seismic characteristics and identification of negative flower structures, positive flower structures, and positive structural inversion; American Association of Petroleum Geologists, Bulletin, v. 69, p. 582-600.

Hughes, J.D.
1993: GEOMODEL - An expert system for modeling layered geological sequences applied to the assessment of coalfields; in Mineral Deposit Modeling, (ed.) R.V. Kirkham, W.D. Sinclair, R.I. Thorpe and J.M. Duke; Geological Association of Canada, Special Paper, v. 40, p. 707-734.

King, L.M.
1994: Subsidence analysis of Eastern Avalonian sequences: implications for Iapetus closure; Journal of the Geological Society, v. 151, p. 647-657.

Naylor, R.D., Kalkreuth, W., Smith, W.D., and Yeo, G.M.
1989: Stratigraphy, sedimentology, and depositional environments of the coal-bearing Stellarton Formation, Nova Scotia; Geological Survey of Canada, Paper 89-8, p. 2-13.

Pitman, W.C. and Andrews, J.A.
1985: Subsidence and thermal history of small pull-apart basins; in Strike-Slip Deformation, Basin Formation and Sedimentation, (ed.) K.T. Biddle and N. Christie-Blick; Society of Economic Paleontologists and Mineralogists, Special Publication, v. 37, p. 45-49.

Poole, H.S.
1904: Report on the Pictou Coal Field; Geological Survey of Canada, Annual Report v. XIV, part M, p. 1-38.

Ryer, T.A. and Langer, A.W.
1980: Thickness change involved in the peat-to-coal transformation for a bituminous coal of Cretaceous age in central Utah; Journal of Sedimentary Petrology, v. 50, p. 987-992.

Salinas, E., Beaudoin, B., Cojan, I., and Mercier, D.
1989: Sedimentary dynamics in French coal-measures reconstituted by decompaction and litho-/bio-facies analysis; International Journal of Coal Geology, v. 16, p. 171-174.

Sclater, J.G. and Christie, P.A.F.
1980: Continental stretching: an explanation of the post Mid-Cretaceous subsidence of the central North Sea basin; Journal of Geophysical Research, v. 85, p. 3711-3739.

Waldron, J.W.F., Gillis, K.S., Naylor, R.D., and Chandler, F.W.
1995: Structural Investigations in the Stellarton pull-apart basin, Nova Scotia; in Current Research 1995-D; Geological Survey of Canada, p. 19-25.

Yeo, G. and Gao, R.-X.
1987: Stellarton graben: an upper Carboniferous pull-apart basin in northern Nova Scotia; in Sedimentary Basins and Basin-Forming Mechanisms, (ed.) C. Beaumont and A.J. Tankard; Canadian Society of Petroleum Geologists, Memoir 12, and Atlantic Geoscience Society, Special Publication 5, p. 299-309.

Geological Survey of Canada Project 760027

The Dorset showings: mesothermal vein-type gold occurrences associated with post-Ordovician deformation along the Baie Verte-Brompton Line, Baie Verte Peninsula, Newfoundland[1]

Michèle Bélanger, Benoît Dubé, and Michel Malo[2]
Quebec Geoscience Centre, Sainte-Foy

Bélanger, M., Dubé, B., and Malo, M., 1996: The Dorset showings: mesothermal vein-type gold occurrences associated with post-Ordovician deformation along the Baie Verte-Brompton Line, Baie Verte Peninsula, Newfoundland; in Current Research 1996-E; Geological Survey of Canada, p. 269-279.

Abstract: The Dorset gold showings are mesothermal vein-type gold occurrences located close to the Baie Verte-Brompton Line. Mineralization occurs in fault-fill veins hosted by Ordovician and Silurian volcanic and volcaniclastic rocks of the Dunnage zone. Auriferous quartz veins are located in the central part of high strain zones and are spatially associated with fine grained mafic dykes. Development of high strain zones is facilitated by strength anisotropy induced by the mafic dykes. Deformation-induced secondary permeability in high strain zones concentrates the fluid circulation which is responsible for the gold mineralization. Structural elements suggests that development of the high strain zones and the gold mineralization are related to a major compressive event. The timing of the mineralizing event is syn- to post-Silurian and could be related to the Silurian reactivation of the Baie Verte-Brompton Line. Late movements contributed to deform the gold-bearing quartz veins.

Résumé : Les indices de Dorset sont des exemples de minéralisation aurifère mésothermale. La minéralisation est contenue dans des veines de quartz en "remplissage de faille" spatialement associées à la ligne Baie Verte-Brompton (BBL). Elles sont encaissées dans les roches volcaniques et volcanoclastiques ordoviciennes et siluriennes de la zone de Dunnage. Les veines de quartz aurifères sont situées dans la partie centrale d'étroites zones de forte déformation et sont spatialement associées à des dykes de composition mafique. Le développement des zones de forte déformation est favorisé par la différence de compétence induite par la présence des dykes mafiques. La perméabilité secondaire qui en résulte a permis la circulation de fluides hydrothermaux responsable de la minéralisation aurifère dans les zones de forte déformation. Les éléments structuraux suggèrent que le développement des zones de forte déformation et la minéralisation aurifère sont reliés à un événement tectonique majeur en compression. L'événement minéralisateur est syn- à post-Silurien et pourrait être relié à la réactivation de la BBL au Silurien. Des mouvements tardifs ont contribué à la déformation des veines minéralisées.

[1] Contribution to Canada-Newfoundland Cooperation Agreement on Mineral Development 1990-1994. Project funded by the Geological Survey of Canada.
[2] Institut National de la Recherche Scientifique-Géoressources, Sainte-Foy, Quebec, Canada

INTRODUCTION

The Dorset gold showings, located 3 km southwest of the town of Baie Verte (Fig. 1), are mesothermal vein-type gold occurrences (Dubé, 1990; MacDougall and MacInnis, 1990; Dubé and Lauzière, 1992). They consist of a series of high grade fault-fill quartz veins hosted by Ordovician and Silurian volcanic and volcaniclastic rocks of the Dunnage zone. These mineralized veins are spatially associated with the Baie Verte-Brompton Line. The Dorset gold showings were discovered by Noranda Exploration in 1987. Previous work include regional studies by Kidd (1974, 1977), Bursnall (1975), Williams (1977), and Hibbard (1983), and detailed mapping by Noranda exploration geologists (MacDougall and MacInnis, 1990) and Dubé and Lauzière (1992).

The aim of this paper is to define the geological setting and characteristics of the structures hosting gold mineralization. We also address the possible structural relationship between the Baie Verte-Brompton Line and gold mineralization as previously proposed for the Baie Verte Peninsula area by, among others, Tuach et al. (1988), Dubé (1990), and Swinden (1990).

GEOLOGICAL SETTING

The principal structural feature of the Baie Verte Peninsula is the Baie Verte-Brompton Line, a major suture between the ancient North American continental margin, the Humber Zone, and Iapetus Ocean domain, the Dunnage Zone (Williams and St-Julien, 1982, Hibbard, 1983) (Fig. 1). The Dorset gold showings are hosted by the Ordovician Advocate Complex and the Silurian Flat Water Pond Group, both included in the Dunnage Zone. The Advocate Complex is defined as steeply dipping, northeasterly striking, and intensely dismembered and deformed mafic and ultramafic plutonic rocks, mafic volcanic and volcaniclastic rocks, as well as dark grey to black slates (Hibbard, 1983). On a broad scale, it can be viewed as three incomplete, dismembered ophiolite sheets, southwest-facing and imbricated with their presumed cover sequence (Hibbard, 1983). The Flat Water Pond Group, is a Silurian volcanic-sedimentary assemblage, that is interpreted as graben-fill deposited along the Baie Verte-Brompton Line during rapid exhumation of the bounding eastern Humber and western Dunnage zones (Cawood and Dunning, 1993).

Hibbard (1983) divided the Flat Water Pond Group into four mappable rock associations. From the bottom to the top, they are: (1) The Kidney Pond conglomerate and associated

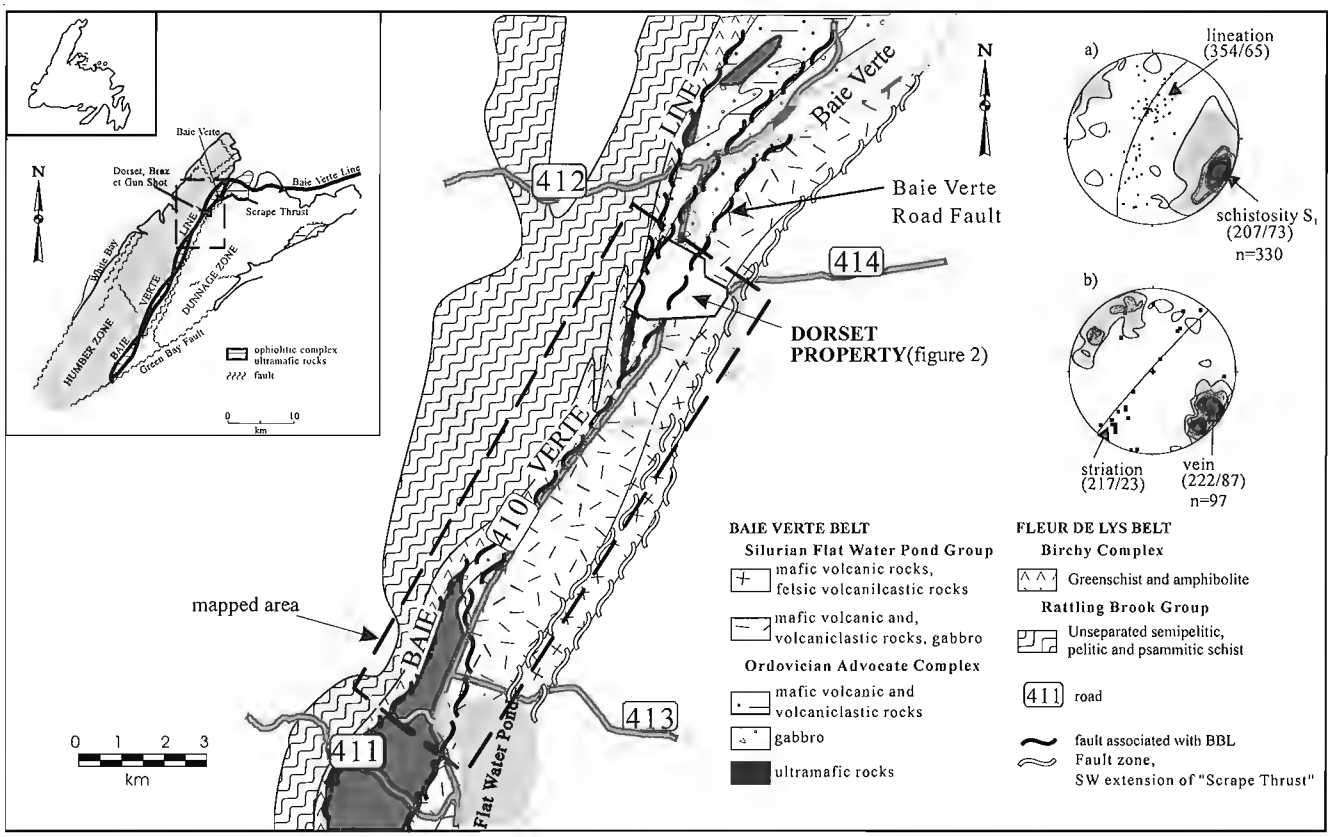

Figure 1. *Map of the Dorset gold showing and other mesothermal gold showings along the Baie Verte-Brompton Line (modified from Tuach et al., 1988). Geology of the Baie Verte area (modified from Hibbard, 1983). Compilation of the main structural elements on equal area projection (lower hemisphere);* ***a)*** *pole of S_1 foliation and stretching lineation;* ***b)*** *pole of vein and striation.*

rocks, (2) undivided mafic volcaniclastic rocks with subordinate conglomerate and minor pillow lava which form the major part of the group, (3) mixed mafic and felsic volcanic and volcaniclastic rocks, and finally (4) local co-magmatic mafic sills and pillow lavas (Kidd, 1974; Hibbard, 1983).

The study area is characterized by numerous northeast oriented fault zones subparallel to the Baie Verte-Brompton Line. Rocks are regionally affected by a weak to strong foliation (N207/74) which contains a moderately-plunging to down-dip stretching lineation (Fig. 1a). Along the Baie Verte Road Fault (Fig. 2), rocks are mylonitized and locally contain both moderately-plunging stretching lineation and subhorizontal striations (Fig. 1b). Striations and steps indicate late dextral and sinistral movements along the Baie Verte-Brompton Line (Bélanger, 1995).

A large part of the regional deformation is concentrated along the Baie Verte-Brompton Line and its subsidiary structures (e.g. Baie Verte Road Fault). The tectonic history of the Baie Verte-Brompton Line is complex and not well understood. It is commonly divided into two main events: ophiolite obduction on the Fleur de Lys Belt, ascribed to the Ordovician Taconian orogeny (Bursnall, 1975; Bursnall and de Wit, 1975; Williams et al., 1977; Hibbard, 1983), and subsequent movements, heterogeneously distributed along the Baie Verte-Brompton Line and attributed to the Devonian Acadian and the Carboniferous Alleghanian orogenies (Bursnall and de Wit, 1975; Williams et al., 1977; Hibbard, 1983). Recently, Cawood et al. (1994) demonstrated that the main tectonic event in the Dunnage Zone is related to a Silurian orogenic event (e.g. Dunning et al., 1990). Cawood et al. (1994) suggested that the Iapetus Ocean was closed by the Silurian and that orogenic activity was taking place within a continent-continent collision zone between the Laurentia and Gondwana plates. They attributed late movements on high strain zones to the Devonian Acadian orogeny.

Goodwin and Williams (1990) and Goodwin (pers. comm., 1994) described the Baie Verte-Brompton Line as a ductile-brittle deformation zone, active from the Ordovician to at least the Carboniferous. According to them, the Baie Verte-Brompton Line recorded five structural events: 1) early reverse motion at amphibolite metamorphic grade, 2) overprinting by dextral strike slip motion still at amphibolite

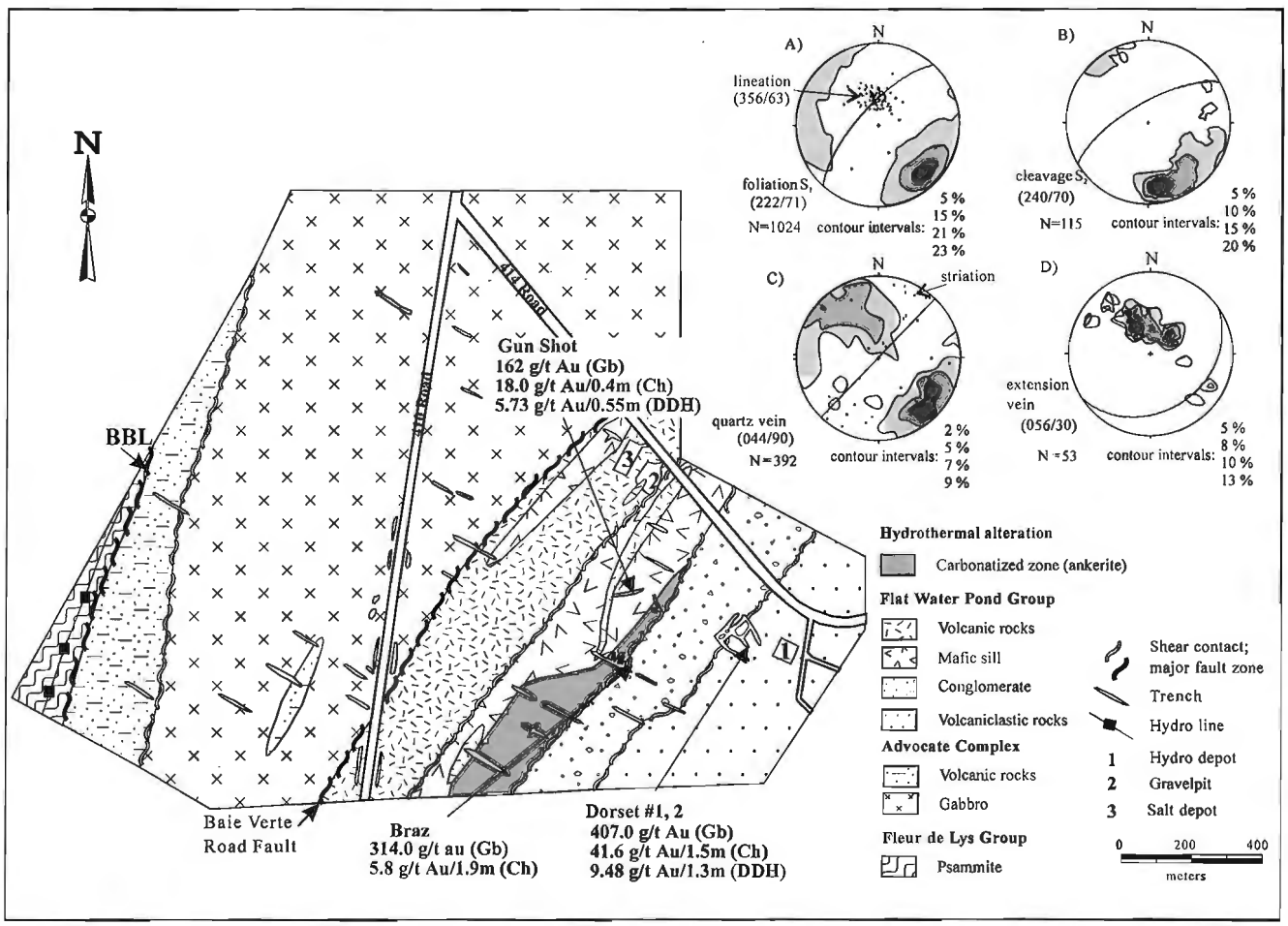

Figure 2. *Geological map of the Dorset property and localization of the main gold showings, Braz, Gun Shot, Dorset #1, and Dorset #2 (modified from unpub. company map, Noranda Exploration, 1989). Compilation of the main structural elements on equal area projection (lower hemisphere);* ***A)*** *pole of S_1 foliation and lineation;* ***B)*** *pole of S_2 cleavage;* ***C)*** *pole of quartz vein and striation;* ***D)*** *pole of extention vein.*

grade, 3) sinistral strike slip motion with associated retrogradation to greenschist facies, 4) a major reverse-dextral ductile event at greenschist facies with strain partitioning from reverse to dextral motions recorded within the Silurian Flat Water Pond Group, and 5) late extension overprinting everything (Goodwin, pers. comm., 1994).

In this study, secondary faults of the Baie Verte-Brompton Line are recognized and well mapped. On the Dorset property, the Advocate Complex and the Flat Water Pond Group are in structural contact along the Baie Verte Road Fault, a secondary structure (or a splay?) of the Baie Verte-Brompton Line.

GEOLOGY OF THE DORSET GOLD SHOWINGS

Gabbros and volcanic rocks of the Advocate Complex occupy most of the northwestern part of the Dorset property whereas the southeastern part is occupied by mafic sills and pillow lavas units and by the undivided mafic volcaniclastics and subordinate conglomerate of the Flat Water Pond Group (Fig. 2). All units are in tectonic contact with each other.

Despite variations in colour, grain size, and composition, gabbros of Advocate Complex were grouped into a single mappable unit. Generally, they are dark green to black and medium to coarse grained. Most of the gabbro is leucocratic, with 60-70% plagioclase and 30-40% mafic minerals, mainly amphibole and pyroxene that are partly altered to chlorite. Quartz, magnetite, pyrite, and/or leucoxene are accessory minerals. Gabbros are generally weakly strained, except near quartz veins. Numerous mafic dykes cut the gabbro: they are grey to greenish, fine grained, and their thickness varies from 10 to 25 cm. Deformation is generally more important in the dykes.

Volcaniclastic rocks form rectilinear strips, of 4 to 60 cm thick and 2 to 5 m long, that pinch out. Generally, volcaniclastic rocks are fine to medium grained and their composition varies from mafic to intermediate. Variations in granulometry, composition, and presence or absence of phenocrysts or amygdules permitted the differentiation of units. It was impossible to distinguish between pyroclastic and epiclastic volcanics because they are highly deformed and altered. Plagioclase, potassic feldspar, chlorite, and epidote are the major components, with minor carbonate, muscovite, pyroxene, and pyrite.

Polymictic conglomerate contains subrounded to subangular clasts in a fine grained, chloritic matrix. The clasts, dominantly composed of gabbro and mafic to intermediate lavas, are derived from the surrounding units. Generally, clasts are as much as 1 to 7 cm long, but plagioclase-phyric mafic lava fragments up to 2 m are locally present.

The contacts between conglomerate and mafic sills are characterized by strong iron carbonate alteration. These are characterized by a rusty weathering colour due to iron oxidation. This intense alteration zone is best developed in the mafic sills and forms a mappable unit 10 to 30 m wide and 800 m long (Fig. 2). Other smaller similar hydrothermal alteration zones were mapped elsewhere on the property.

Mafic sills of the Flat Water Pond Group are differentiated into three main units, based on grain size and compositional variations. A very coarse leucogabbro is characterized by presence of irregular lenses of plagioclase ranging from 2 to 20 cm; a fine- to medium-grained leucogabbro, and a fine grained melagabbro containing 2-4% leucoxene, indicating Fe-Ti enrichment. The thickness of each unit varies from metres to decimetres.

Pillow lavas occur in two localities within the Flat Water Pond Group. Mean pillow diameter is 40 cm. Phenocrysts and amygdules are common. Chlorite, epidote, and carbonate alterations affect the deformed pillows.

STRUCTURE

The study area is characterized by a number of decametre-scale high strain zones subparallel to the Baie Verte-Brompton Line. These high strain zones are heterogeneously distributed, but preferentially located at lithological contacts (Fig. 2). These high strain zones are dominated by a weak to moderate S_1 foliation, oriented northeast-southwest, and containing a steeply to moderately northwest-plunging stretching lineation (Fig. 2A). Foliation is penetrative and becomes mylonitic near the Baie Verte Road Fault. Locally a northeast-southwest oriented S_2 cleavage crenulates S_1 (Fig. 2B).

The Dorset showings include four main mineralized zones hosted by discrete high strain zones developed within the gabbro unit (Gun Shot showing) and in the undifferentiated volcaniclastic rocks with subordinate conglomerate (Braz, Dorset #1, and Dorset #2 showings) of the Flat Water Pond Group (Fig. 2).These discrete high strain zones are oriented northeast-southwest. They are metre-wide, up to 100 m long (Fig. 3A) and are characterized by an intense foliation (S_1) with a northwest-oriented steeply plunging stretching lineation (L_1) (Fig. 3B). The S_2 cleavage is also well developed (Fig 3C).

Kinematic of the mineralized high strain zone is difficult to determine due to absence of unambiguous kinematic indicators. Bélanger et al. (1992) suggested a reverse-oblique movement deduced from the down-dip stretching lineation and from the apparent sinistral movement suggested by displacement of a gabbro unit on opposite sides of the high strain zone (Fig. 4). However, the sinistral displacement of the gabbro is most probably induced by the projection of the horizontal component of movement along the down dip stretching lineation (L_1) and thus cannot be used to infer sinistral motion along the high strain zone.

The S_2 cleavage is particularly well developed at the Gun Shot showing where it is oriented at a slight angle to the main fabric. The intersection between S_1 and S_2 produces a pseudo CS-type fabric in plan view (Fig. 3C), but as the intersection between these two fabrics is coaxial with the stretching lineation, no kinematic significance can be attributed to these two noncontemporanous structures.

In thin section, two kinds of potential kinematic indicators were found: pressure shadows on pyrite and protected zones around clasts. Analysis of the pressure shadows around euhedral crystals can be use to evaluate the deformation history subsequent to the crystal growth (Ramsay and Huber, 1983). In this study, only euhedral pyrites were observed with face-controlled fibres. Where crystal faces are oriented parallel to the foliation, fibres have grown parallel with it, without rotation. In some cases, S_2 cleavage overprints fibres and produces an apparent rotation, but again no kinematic significance can be attributed to this rotation (Fig. 3D). Where crystal faces are not parallel to the foliation, strain history cannot be determined from the direction of face controlled fibres, but it can be determined from the geometry of the contact suture which separates different fibre groups (Ramsay and Huber, 1983). In most cases this contact line is straight, suggesting pure shear deformation. Protected zones on clasts are symmetric and no evidence of rotation was found.

As indicated by pressure shadows on pyrite cubes, the late increments of S_1-related deformation was of the pure shear type. Given the absence of evidence of non-coaxial deformation, the high strain zones are interpreted as zones probably dominated by flattening strain, as opposed to zones with

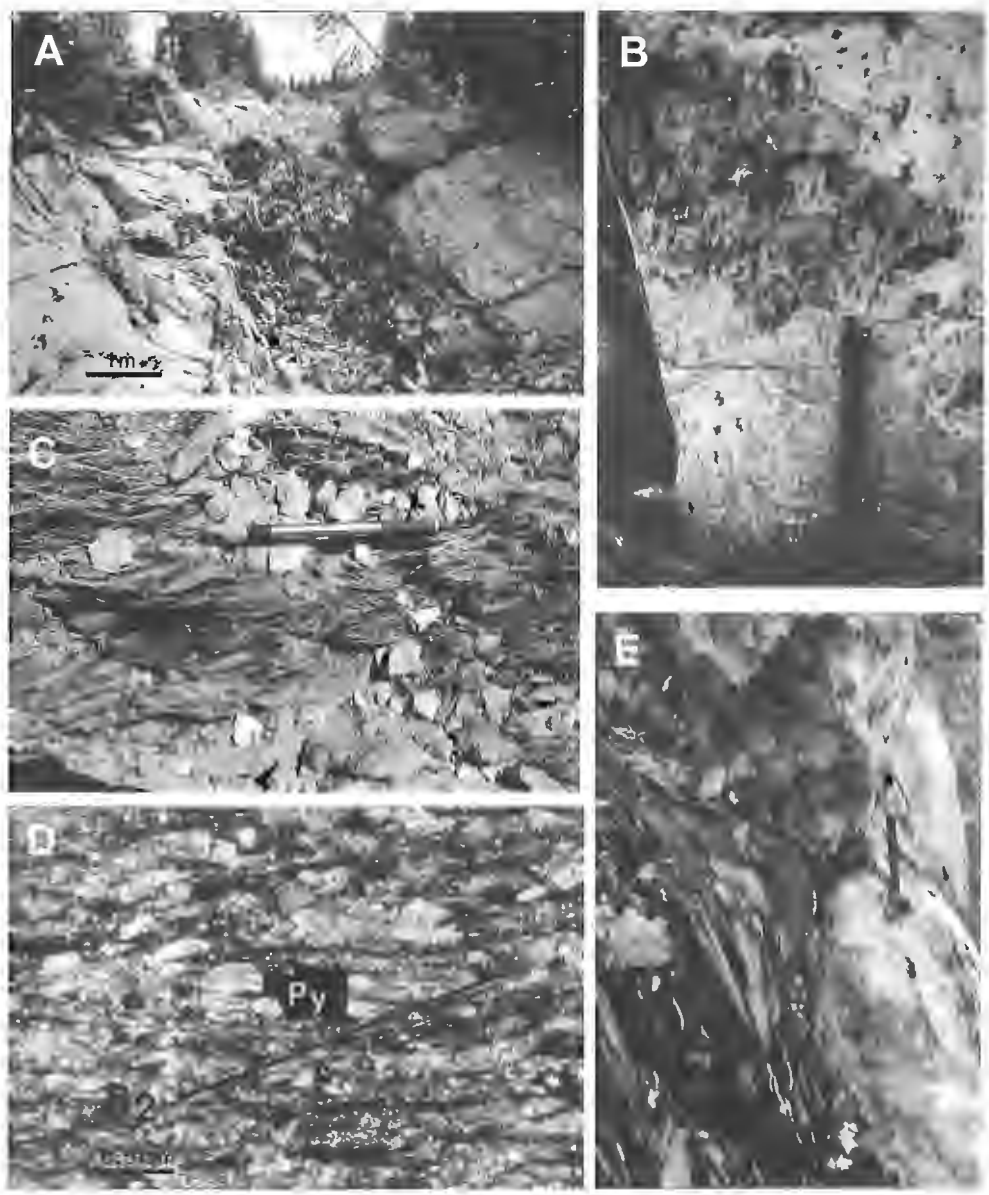

Figure 3. *A) Southwest-view of the Dorset #2 showing, high strain zone is about 2 m. wide.* ***B)*** *Longitudinal view showing down-dip stretching lineation in mafic dyke.* ***C)*** Plan view showing intersection between S_1 *and* S_2 *producing a pseudo-CS fabric.* ***D)*** *Face controlled fibres growth parallel with foliation* S_1 *on euhedral pyrite.* ***E)*** *Cross-section view showing subhorizontal quartz vein observed in boudin necks.*

significant movement. Thus, the high strain zones are recording subhorizontal northwest-southeast shortening and subvertical to oblique extension.

The gold-bearing veins (see descriptions below) are discontinuous and display chocolate tablet boudinage. On the most part of the study area, subvertical boudinage is better developed and subhorizontal extensional quartz veins are locally observed in boudin necks (Fig. 3E). Where it is possible to measure two set of boudins, they intersect at 90°. Geometry of boudins suggests a single deformation event to produce chocolate tablet boudinage (Ramsay and Huber, 1983), with a vertical extension as major component and a minor northeast-southwest extension. The chocolate tablet boudinage combine with the absence of rotation of the pressure shadow around pyrite cubes suggest a post-pyrite and most probably post-vein flattening related to a northwest-southeast compression, in a pure shear deformation regime.

MINERALIZATION

Gold mineralization occurs in northwest-southeast oriented and steeply dipping fault-fill quartz veins (e.g. Robert et al. 1994 for nomenclature) located in the central part of the high strain zones. Veins are subparallel to the S_1 foliation (Fig. 4).

The veins are 10 to 70 cm wide and their lateral extent is variable due to the effects of superimposed deformation. On the Braz and Gun Shot showings (Fig. 2), the veins appeared only in 2 to 4 m sections, whereas on the Dorset #2 showing the veins can be trace for a distance of 60 m along the high strain zone.

Veins are laminated (Fig. 5A) and contain about 90% quartz, 5-10% sulphides, 1-2% carbonate, and less than 1-2% foliated rock fragments. On Dorset #2 showing, a poorly mineralized vein with only traces of sulphides is present to the southeast of the auriferous one and parallel to it. It is characterized by nonoriented euhedral quartz forming a 1 cm thick layer on the northeast wall of the vein. Locally, subhorizontal extensional veinlets, subperpendicular to stretching lineation, are present within the iron carbonate alteration zone. Subvertical idiomorphic quartz and iron carbonate fill these veinlets.

In thin section, the gold-bearing veins contain 90% quartz (Qz1), which is xenomorphic, strongly deformed, and shows undulatory extinction and intense recrystallization. Neoblasts are fine grained but relics of original grains are 1 to 2.5 mm long. Locally, the quartz is idiomorphic with an oblique orientation to vein walls (Fig. 6). It probably represents filling of the last vein cavities.

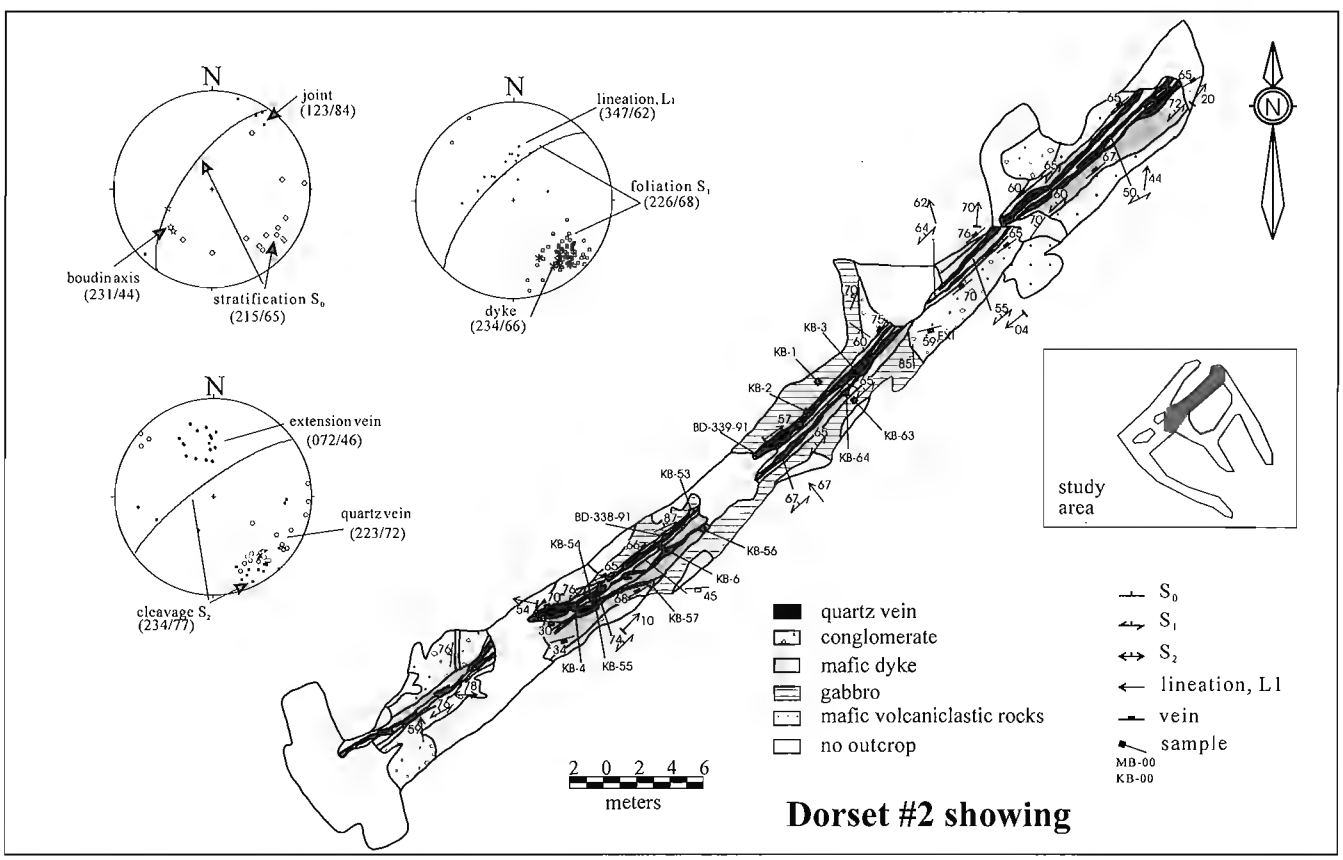

Figure 4. *Detailed geological map of Dorset #2 showing and compilation of the main structural elements on equal area projection (lower hemisphere).*

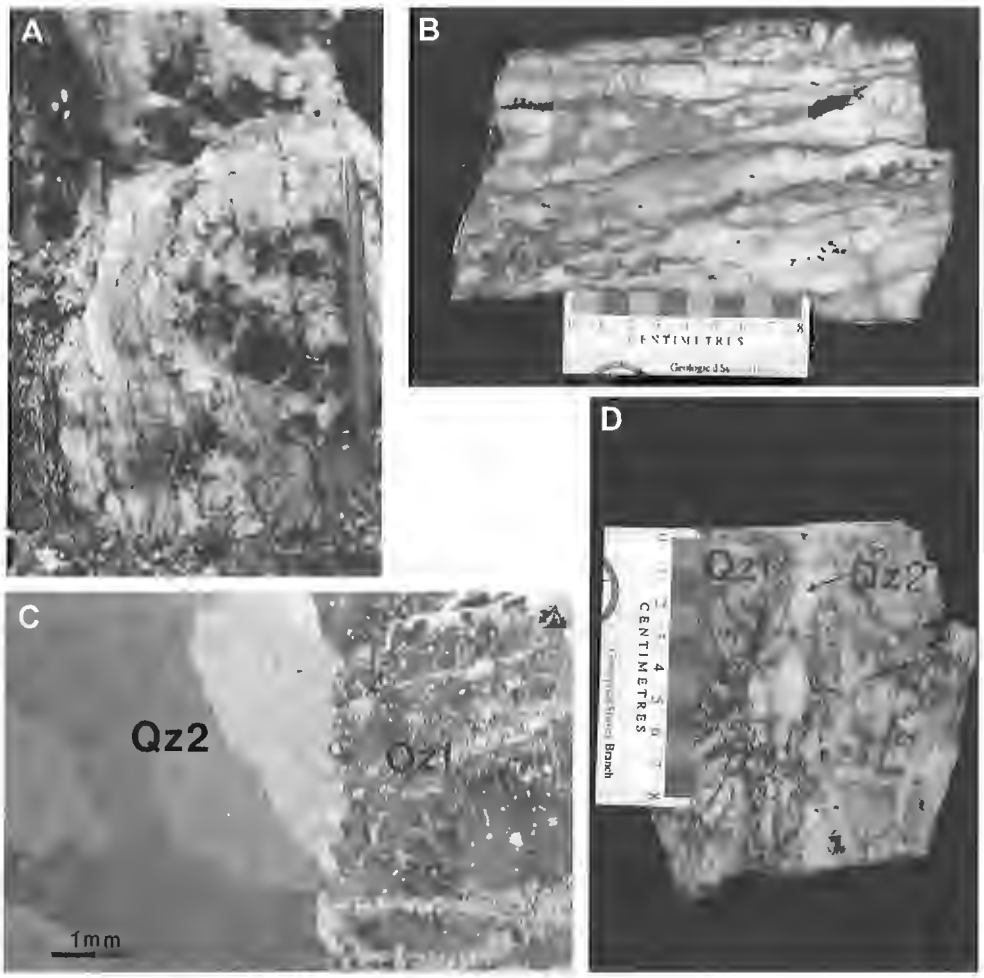

Figure 5. *A) Cross-section showing the fault-fill vein from Dorset #2.* ***B)*** *Laminated vein with sulphides (pyrite and sphalerite) in 1-2 cm thick stripe.* ***C)*** *Subeuhedral milky quartz (Qz2) crosscuts the strongly deformed xenomorphic quartz (Qz1).* ***D)*** *Two set of milky quartz (Qz2) veinlets crosscut xenomorphic quartz (Qz1) in the mineralized quartz vein of Braz showing.*

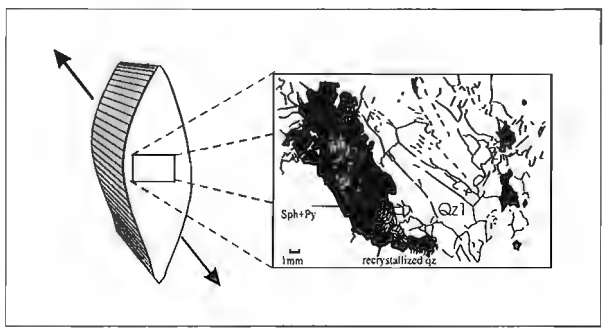

Figure 6. *Sketch of idiomorphic quartz (Qz1) in thin section from mineralized quartz vein of Dorset #2 showing.*

As described above, the veins are boudinaged, the boudin axes are moderately plunging to the southwest and sometimes steeply to the northeast. Idiomorphic quartz is present in subhorizontal necks indicating vertical extension (Fig. 3E). Subhorizontal extensional veinlets with idiomorphic quartz crystals perpendicular to veinlet walls are also present at the Braz and Gun Shot showings. In thin section those subhorizontal extensional veinlets are composed of milky quartz (Qz2) which crosscuts xenomorphic quartz (Qzl) (Fig. 5C). On Braz showing, late milky quartz-type unmineralized veinlets parallel to the principal vein are also observed. These two systems of veinlets are most probably contemporaneous (Fig. 5D).

The principal sulphides are pyrite, sphalerite, arsenopyrite, chalcopyrite, and galena with minor covellite and gold (Table 1). They form layers 1-2 cm thick in xenomorphic quartz (Fig. 5B). Pyrite and arsenopyrite are medium grained (1 mm) and, generally idiomorphic to hypidiomorphic. Locally, cataclastic texture is developed within pyrite suggesting syn- to postdepositional deformation. Subangular pyrite fragments are surrounded by recrystallized quartz. Sphalerite, galena, and chalcopyrite are fine grained, xenomorphic, and rounded to subangular. They are also surrounded by recrystallized quartz. Gold occurs as inclusions or in microfractures in pyrite, galena, and the Qz1; (xenomorphic quartz Fig. 7A, B). Assays of mineralized quartz veins (Table 2) shows a positive correlation between base metal (Cu, Zn, Pb) and As and gold.

Table 1. Occurrence of sulphides in thin sections from mineralized quartz vein. Dorset* is the poorly mineralized vein from Dorset #2 showing.

Sample	%sulphide	Py	Apy	Sp	Gn	Ccp	Cv	Gold
MB-22 (Braz)	1-2%	40%	-----	10%	-----	50%	-----	-----
KB-5 (Dorset*)	1%	60%	-----	40%	-----	-----	-----	-----
MB-64b (Gun)	<1%	100%	-----	-----	-----	-----	-----	-----
MB-116 (Dor.ext)	20%	82%	1-2%	5-7%	-----	10%	1%	tr
BD-340 (Dorset)	20-25%	42%	<1%	47%	3%	3-4%	<1%	tr
MB-121 (Dorset)	20-25%	55%	5%	15%	5%	13%	5%	tr
KB-6 (Dorset)	5%	20%	7%	5%	25%	35%	2%	tr

Py: pyrite; Apy: arsenopyrite; Sp: sphalerite; Gn: galena; Ccp: chalcopyrite; Cv: covellite; Dorext: Dorset extension

Except for the broad iron carbonate alteration zone present in the gabbro (Fig. 2), the alteration in the gold-bearing high strain zones is weakly developed and confined to the deformation zones. Toward the central part of high strain zone, chlorite, carbonate, and white mica become more important than epidote and actinote. The lack of rusty weathering on most intensely altered rocks suggests the presence of calcite and dolomite rather than iron carbonate. At the Braz showing, which is closest to the iron carbonate alteration zone, iron carbonates are present within the high strain zone.

CONTROLS ON HIGH STRAIN ZONE DEVELOPMENT

The auriferous fault-fill quartz veins are spatially associated with fine grained mafic dykes that crosscut all other lithologies (Fig. 4, 8). The veins occur adjacent to, or locally within these dykes. These mafic dykes most probably played a key role in the development and localization of the high strain zones.

The influence of strength anisotropy on the development of high strain zones was discussed by Ramsay and Huber (1987), Dubé et al. (1989), and more recently by Robert et al. (1994). Figure 9 is a simplified representation of the influence of strength anisotropy for the two dimensional case of a single oblique layer in an otherwise isotropic host rock. Where the layer is much more competent than its host, most of the strain will be taken up by the host rock, and it is expected that the layer will be submitted to an extension (or shortening) parallel to its length (Fig. 9a). In this case, high strain zones will develop in the host rocks along their contact with the competent layer. In the intermediate cases where there is less contrast between the layer and its host, the interface becomes the locus of deformation and the strain will be better developed in the weaker unit (Fig. 9b). In the case where the layer is much weaker than its host, strain will be localized within the layer. As a result, the weak layer will effectively become a shear zone (Fig. 9c).

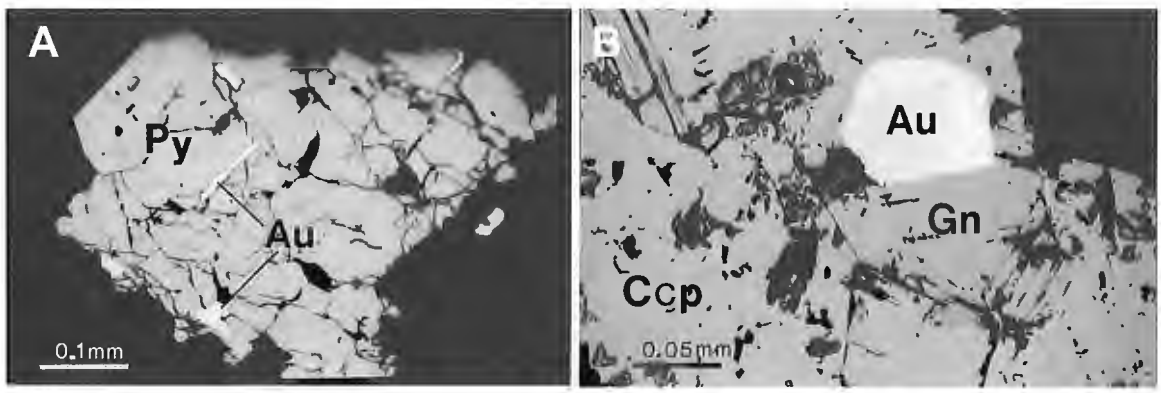

Figure 7: A) Gold (Au) in micro-fractures of cataclastic pyrite (Py). B) Gold (Au) in galena (Gn) associated with chalcopyrite (Ccp).

Table 2. Chemical analysis of the mineralized quartz veins. Dorset* is the poorly mineralized vein from Dorset #2 showing. Analysis done at X-ray Assay Laboratories Limited, Don Mills, Ontario.

	Au (ppm)	Ag (ppm)	Cu (ppm)	Zn (ppm)	Pb (ppm)	Au/Ag
Braz (MB-22)	0.064	0.05	11	5.0	18	1.3
Dorset* (KB-5)	0.462	0.05	14	67.0	149	9.2
Gun Shot (MB-62b)	5.55	0.05	359	9.4	640	111.0
Dorset ext. (MB-116)	50.90	0.80	1360	303.0	1170	63.6
Dorset (BD-340)	261.00	28.90	2300	41700.0	764	9.0
Dorset (MB-121)	489.00	35.60	143	11400.0	3900	13.7

Dorset ext: Dorset extension

Figure 8. *Plan view showing spatial relationship between mineralized quartz vein and the mafic dyke on Dorset #2 showing.*

At the Dorset showing, host rocks are not isotropic and their composition is variable. Differences in grain size and composition between the dyke (fine grained) and its host (medium- to coarse-grained conglomerate, gabbro, and volcaniclastic rocks) induce a competency contrast. At the Dorset #2 showing, there are variations in host rock from a conglomeratic unit in the southwest to gabbro and volcaniclastic to the northeast (Fig. 4). In the southwest segment, the high strain zone is confined to the dyke whereas it extended to host rocks in the northeast segment of the showing. Thus, in the southwest segment, the dyke appears less competent than conglomeratic units, and accommodated the major part of the strain.

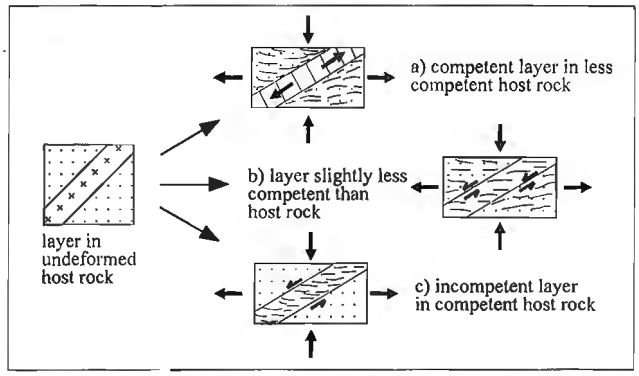

Figure 9. *Simplified representation illustrating the influence of strength anisotropy in shear zone development (modified from Robert et al., 1994).*

However, where the host rocks are volcaniclastics or gabbro, differences in grain size and composition are weaker and the strain was accommodated by both the dyke and its host rocks.

Dorset showings are far from isotropic ideal cases as described by Robert et al. (1994), but it seems that the dykes have induced a strength anisotropy such that most of the strain was accommodated within or adjacent to them. Development of high strain zones may have enhanced secondary permeability and facilitated the circulation of hydrothermal fluids. The localization of the veins in the central part of the high strain zones, laminations in quartz veins, and variation of deformation in quartz ribbons suggest that they were emplaced when the high strain zones were still active.

The early history of the high strain zones is unclear. But, the presence of steep to oblique stretching lineation suggest that deformation may have been noncoaxial. Such an interpretation is compatible with the major reverse-dextral ductile event at greenschist facies recorded within the Flat Water Pond Group along the Baie Verte-Brompton Line (L.B. Goodwin, pers. comm., 1994). By analogy with other situations (e.g. Robert et al., 1994), we suggest that the gold-bearing veins at Dorset were formed during shear zone deformation although the exact timing remains unknown.

DISCUSSION AND CONCLUSION

Conglomerates of the Flat Water Pond Group, which are confined to the Baie Verte-Brompton Line, contain granodiorite clasts and deformed and metamorphosed siliclastic rock debris interpreted to be derived from the Burlington Granodiorite (432 ± 3 Ma; Cawood and Dunning, 1993) and the Fleur de Lys Supergroup, respectively. The Flat Water Pond Group and the Burlington Granodiorite are unconformably overlain by the Mic Mac Lake Group which is correlated with the Cape St. John and Springdale groups (both dated at around 430-425 Ma). This implies a Silurian age for at least parts of the Flat Water Pond Group (Cawood and Dunning, 1993).

The time of peak metamorphism and associated regional deformation along the Baie Verte-Brompton Line, between Corner Brook and Baie Verte, is restricted to a narrow time span of ~435-425 Ma (Cawood et al., 1994). Cawood et al. (1994) recognized a phase of Early to Middle Silurian deformation, metamorphism, and plutonism clearly temporally separated from either the Ordovician Taconian orogeny or the Devonian Acadian orogeny.

Structural elements recorded in the Flat Water Pond Group indicates that it was affected by a major compressive event. Deposition and deformation of the Flat Water Pond Group have been interpreted as a continuous succession of events through Silurian tectonic activities (P.A. Cawood, pers. comm., 1994).

Even if the age of gold mineralization and high strain zones at the Dorset showings are unknown, their position in the Silurian Flat Water Pond Group indicates that they are younger than it. The main planar fabric (S_1) and the L_1 down dip stretching lineation present in high strain zones recorded a northwest-trending compression. Similarities between structures observed in the gold-bearing high strain zones and elsewhere in the Flat Water Pond Group suggest a possible contemporaneous deformation event which has occurred during the Silurian orogeny or a younger event.

Mineralized veins are overprinted by a flattening deformational event dominated by a vertical extension and a minor northeast-southwest extension as indicated by chocolate tablet boudinage. Goodwin (pers. comm., 1994) identified late strike-slip movement due to strain partitioning along the Baie Verte-Brompton Line, which could have contributed to the northeast-southwest extension of the veins and could be responsible for the actual distribution of quartz veins.

The Dorset showings are an example of mesothermal vein-type gold mineralization associated with a major fault in Baie Verte Peninsula. Mineralization is interpreted to be genetically associated to discrete high strain zones. Competency contrast induced by mafic dykes contributed to localize the strain and favour the development of the high strain zones. Deformation-induced secondary permeability in high strain zones focused the fluid circulation which was responsible for the gold mineralization.

Similarities in structural elements strongly suggest a structural link between the mineralized high strain zones and the Baie Verte-Brompton Line. Second order structures such as the Baie Verte Road Fault, as well as some lithological contacts, were loci for fluid circulation and produced a strong iron carbonate hydrothermal alteration without significant gold mineralization as typically found in the Archean. Discrete shear zones, hosting mineralization, could represent third order structures related to the Baie Verte-Brompton Line and developed during compression. The timing of the mineralizing event is syn- to post-Silurian and could be related to the Silurian reactivation of the Baie Verte Brompton Line. However, the lack of direct dating of the hydrothermal system and of specific increments of deformation along the Baie Verte-Brompton Line preclude direct genetic links.

Late movements on the Baie Verte-Brompton Line and its subsidiary structures, probably related to the Devonian Acadian orogeny or a younger Carboniferous event, may be responsible for the boudinage which overprints the gold-bearing quartz veins.

ACKNOWLEDGMENTS

The authors express their sincere thanks to C. MacDougall, Ian Perry, A. Huard, and D. MacInnis of Noranda Exploration for their great scientific collaboration, access to unpublished information and material, and logistic support. Thanks are especially due to K. Lauzière and to François Robert, H.K. Poulsen, and Jayanta Guha for stimulating comments in the field and to L. Goodwin and P. Cawood for their collaboration. H. Bouchard and K. Bureau provided excellent field assistance. The manuscript has benefited from the constructive criticism of François Robert and Paul Sacks.

REFERENCES

Bélanger, M.
1995: Contrôle structural et contexte métallogénique de l'indice aurifère Dorset, péninsule de Baie Verte, Terre-Neuve; MSc. thesis, Université du Québec INRS, Géoressources, Ste-Foy, Québec, 81 p.

Bélanger, M., Dubé, B., and Lauzière, K.
1992: A preliminary report of the structural control of the mesothermal Dorset gold showing, Baie Verte Peninsula, Newfoundland; in Newfoundland Department of Mines and Energy, Report of Activities 1992, p. 3-4.

Bursnall, J.T.
1975: Stratigraphy, structure and metamorphism west Baie Verte, Burlington Peninsula, Newfoundland; PhD. thesis, Cambridge University, England, 337 p.

Bursnall, J.T. and de Wit, M.J.
1975: Timing and development of the orthotectonic zone in the Appalachian orogen of northwest Newfoundland; Canadian Journal of Earth Sciences, v. 12, p. 1712-1722.

Cawood, P.A. and Dunning, G.R.
1993: Silurian age for movement on the Baie Verte Line: implications for accretionary tectonics in the Northern Appalachians; Geological Society of America, Abstracts with Programs, v. 25, no. 6, p. A422.

Cawood, P.A., Dunning, G.R., Lux, D., and van Gool, J.A.M.
1994: Timing of peak metamorphism and deformation along the Appalachian margin of Laurentia in Newfoundland: Silurian, not Ordovician; Geology, v. 22, p. 399-402.

Dubé, B.
1990: A preliminary report on contrasting structural styles of gold-only deposits in western Newfoundland; Current Research, Part B; Geological Survey of Canada, Paper 90-1B, p. 77-90.

Dubé, B. and Lauzière, K.
1992: The Dorset gold showing: structural control of a mesothermal gold deposit in the Baie Verte Peninsula, Newfoundland; in Gold mineralization in Western Newfoundland. (ed.) B. Dubé, K. Lauzière, S. Swinden, and M. Wilson; Geological Association of Canada, Joint Annual Meeting, Wolfville '92, Field Trip A-4: Guidebook, p. 53-58.

Dubé. B., Poulsen, K.H., and Guha, J.
1989: The effects of layer anisotropy on auriferous shear zones: the Norbeau mine, Quebec. Economic Geology, v. 84, p. 871-878.

Dunning, G.R., O'Brien, S.J., Colman-Sadd, S.P., Blackwood, R.F., Dickson, W.L., O'Neill, P.P., and Krogh, T.E.
1990: Silurian Orogeny in the Newfoundland Appalachians; Journal of Geology, v. 98, p. 895-913.

Goodwin, L.B. and Williams, P.F.
1990: Strike-slip motion along the Baie Verte Line, Newfoundland (abstract); in Abstracts-Geological Association of Canada, Newfoundland section, 1990 Annual Spring Meeting, Atlantic Geology, v. 26 no. 2, p. 170.

Hibbard, J.
1983: Geology of the Baie Verte Peninsula, Newfoundland; Newfoundland Department of Mines and Energy, Mineral Division, Memoir 2, 279 p.

Kidd, W.S.F.
1974: The evolution of the Baie Verte lineament, Burlington Peninsula, Newfoundland; Unpublished PhD. thesis, Cambridge University, England, 294 p.
1977: The Baie Verte Lineament: ophiolite complex floor and mafic volcanic fill of a small Ordovician marginal basin; in Island Arcs, Deep Sea Trenches and Back Arc Basins, (ed.) M. Talwani and W.C. Pitman; Maurice Ewing Series, v. 1, p. 407-418.

MacDougall, C. and MacInnis, D.
1990: The Dorset showing: a structurally controlled lode gold occurrence adjacent to the Baie Verte Line; in Metallogenic Framework of Base and Precious Metal Deposits, Central and Western Newfoundland, (ed.) H.S. Swinden, D.T.W. Evans, and B.F. Kean; 8th International Association on the Genesis of Ore Deposits Symposium, Field Trip Guidebook, Geological Survey of Canada, Open File 2156, p. 162-164.

Ramsay, J.G. and Huber, M.I.
1983: The Techniques of Modern Structural Geology, Volume 1: Strain analysis; Academic Press, London, England, 307 p.
1987: The Techniques of Modern Structural Geology, Volume 2: Folds and Fractures; Academic Press, London, England, 700 p.

Robert, F., Poulsen, K.H., and Dubé, B.
1994: Structural analysis of lode gold deposits in deformed terranes; Geological Survey of Canada, Open File 2850, 140 p.

Swinden, H.S.
1990: Regional geology and Metallogeny of the Central Newfoundland; in Metallogenic Framework of the Base and Precious Metal Deposits, Central and Western Newfoundland, (ed.) H.S. Swinden, D.T.W. Evans, and B.F. Kean; 8th International Association on the Genesis of Ore Deposits Symposium, Geological Survey of Canada, Open File 2156, p. 1-31.

Tuach, J., Dean, P.L., Swinden, H.S., O'Driscoll, C.F., Kean, B.F., and Evans, D.T.W.
1988: Gold mineralization in Newfoundland: a 1988 review; in Current Research, (ed.) R.S. Hyde, D.G. Walsh and R.F. Blackwood; Newfoundland Department of Mines, Report 88-1, p. 279-306.

Williams, H.
1977: Ophiolitic mélange and its significance in the Fleur de Lys Supergroup, northern Appalachians; Canadian Journal of Earth Sciences, v. 14, p. 987-1003.

Williams, H. and St-Julien, P.
1982: The Baie Verte-Brompton Line: Early Paleozoic continent-ocean interface in the Canadian Appalachians; in Major Structural Zones and Faults of the Northern Appalachians, (ed.) P. St-Julien and J. Béland; Geological Association of Canada, Special Paper 24, p. 177-207.

Williams, H., Hibbard, J., and Bursnall, J.T.
1977: Geologic setting of asbestos-bearing ultramafic rocks along the Baie Verte Lineament, Newfoundland; Geological Survey of Canada, Paper 77-1A, p. 351-360.

Geological Survey of Canada Project 920004

Reprint Explorer, a paleontological reprint database for Microsoft Windows

D.C.A. Stanley and J.W. Haggart
GSC Pacific, Vancouver

Stanley, D.C.A. and Haggart, J.W., 1996: Reprint Explorer, *a paleontological reprint database for Microsoft Windows; in Current Research 1996-E; Geological Survey of Canada, p. 281-284.*

Abstract: A new dBASE for Microsoft Windows program allows a research scientist to efficiently catalogue a paleontological reprint collection. In addition to being able to capture bibliographic information describing each reprint in the collection, taxonomic details regarding taxa covered in each reprint can be recorded. The resulting database can then be queried to easily locate specific papers or those dealing with specific taxa.

Résumé : Un nouveau programme dBASE pour Windows de Microsoft permet aux scientifiques de cataloguer efficacement une collection d'articles traitant de paléontologie. En plus de donner la possibilité de consigner l'information bibliographique sur chaque article d'une collection, le programme permet d'intégrer les détails concernant les taxons couverts dans chaque article. La base de données obtenue peut alors être consultée pour localiser facilement un article en particulier ou pour identifier ceux qui traitent de taxons spécifiques.

INTRODUCTION

The literature in a particular paleontological field is generally voluminous, and includes many older publications which are always relevant to the modern literature. Indeed, many paleontological species are based on taxonomic descriptions and specimens figured in literature commonly dating back to the early 19th century or before. In contrast to many other disciplines within the geological sciences where older contributions become outdated as the science progresses, the paleontologist must continue to study the older literature and incorporate it in any modern taxonomic work. The classic treatises are compared with more recent papers to arrive at satisfactory systematic and biostratigraphic conclusions. Thus, maintaining the necessary database linking the old and new literature becomes an ever-increasing challenge.

Traditionally, paleontologists have relied on card files to maintain their taxonomic databases. Such files, while able to store much information, typically become bulky in short order. In addition, the capacity to integrate the various data contained in many different references is limited in such systems. The personal computer, in contrast, can provide more thoroughly integrated and much smaller database files, readily accessible at the keyboard and easily integrated into other work.

We designed a PC-based database program, using the dBASE 5.0 for Microsoft Windows development environment, that would address several specific paleontological needs. Foremost is our long-term goal to catalogue our literature on Cretaceous mollusc paleontology so that its systematic, biostratigraphic, and biogeographic content is readily accessible to the researcher. We wanted a system that allows searching for all references discussing a particular taxon, as well as providing stratigraphic and geographic data about taxa distributions at both regional and global scales.

Although this system is designed for paleontological needs, it could easily be modified for use with several other types of earth science literature, allowing users to track mineral occurrences, stratigraphic names, and geographical names, for example.

Table 1. Structures of database tables used by *Reprint Explorer*.

JOURNAL.DBF			
Field Name	*Data Type*	*Length*	*Description*
ID	Numeric	5	Number providing link between the two databases
AUTHOR	Character	85	The name(s) of the paper's author(s)
TITLE	Character	201	The paper's title
YEAR	Character	10	The year of publication
VOL	Character	3	The volume number the paper appears in
NUM_PART	Character	4	The number or part of the publication the paper appears in
PAGES	Character	9	The page number(s) the paper appears on
PLATES	Character	20	The number of plates in the paper
JRN_BK	Character	123	The journal or book in which the paper appears
ABSTRACT	Logical	1	Checked if the paper is an abstract
EDS	Character	43	The editors of the publication in which the paper appears
PUB	Character	50	The publishers of the paper
READ	Logical	1	Checked if the paper has been read (unique to our needs)
NOTES	Character	250	An area to record personal comments about the paper
REPRINT	Logical	1	Checked if a reprint was received from the author
VERIFIED	Logical	1	Checked if the data-entry has been verified for accuracy
LIB_LOC	Character	30	Location of paper in reprint library organised by region or age
TAXONOMY.DBF			
Field Name	*Data Type*	*Length*	*Description*
ID	Numeric	5	Number providing a link between the two databases
GENUS	Character	25	The generic name of the taxon
SUB_GENUS	Character	25	The sub-generic name of the taxon
SPECIES	Character	25	The trivial name of the taxon
SUB_SPECIE	Character	25	The sub-trivial name of the taxon
OPEN_NOM	Character	20	Any open nomenclatural terms used in naming the taxon
TAXON_AUT	Character	50	The taxon author(s)
PAGE_NUM	Character	9	The page number(s) on which the taxon is mentioned
DIAGNOSIS	Logical	1	Checked if a diagnosis is given
EMENDED	Logical	1	Checked if a diagnosis is emended
FIGURED	Logical	1	Checked if the taxon is figured
DESCRIP	Logical	1	Checked if a description of the taxon is given
LISTING	Logical	1	Checked if the taxon only appears in a list in the paper
ERECTED	Logical	1	Checked if the taxon is erected in the paper
STR_HORIZN	Character	20	The stratigraphic horizon in which the taxon was found
GEOG_AREA	Character	30	The geographic area in which the taxon was found

The illustrations in this paper show *Reprint Explorer* running under the Windows 95 operating system; however, the program also runs under Windows 3.X. Due to incompatibilities between dBASE 5.0 and Visual dBASE 5.5, the program only runs under dBASE 5.0. While a simpler DOS-based version of this program was written in 1990 using dBASE III+, this has been superseded by the more flexible Windows version. No Macintosh versions are planned.

USING THE SYSTEM

While the bibliographic and taxonomic data accessed by the program are stored in two separate dBASE-format database files (the structures of which are given in Table 1), all these data are displayed on a single user-interface screen (Fig. 1). The program can access the data stored in these files based on bibliographic or taxonomic criteria. To define either of these two types of queries, the user presses the "Set Filter..." button in the "Action" area of the screen. The program will render inactive all fields except those with which a query may be defined. Additionally, the label on the "Set Filter..." button will change to read "Filter Data". By default, upon pressing the "Set Filter..." button, the fields used in defining a query on *specific taxa* are left active, all others being disabled. Selecting either the "Taxonomic" or "Bibliographic" radio buttons in the "Type of Filter" area of the screen will set-up the program to allow the respective types of queries to be defined.

Bibliographic queries

The database can be queried using the Author, Title, Year, and Journal/Book fields (Fig. 1). When the program executes a query, criteria are considered to be satisfied if database records *contain* the text given in the query definition. Thus, an Author-based query on the name "Jeletzky" will return all papers where Jeletzky was an author, either individually, or as a junior or senior co-author. Likewise, a Title-based query on the word "shale" will return all papers whose title contains the word "shale". It can be useful to limit a query by date of publication, for example eliminating all historical literature published prior to a certain date. This can be done by entering a date in the Year field, and selecting either the <, > or = radio button to cause the program to only return papers whose date of publication is, respectively, less than, greater then, or equal to the specified year.

To execute the query, the user presses the "Filter Data" button in the "Action" area of the screen. This will cause all the fields that were previously disabled to become active again, and the label on the "Filter Data" button will revert to reading "Set Filter...". Pressing the "Next" and "Previous" buttons will navigate the user through the records that satisfied the query criteria. To define a new query, pressing the "Set Filter..." button clears the previous query results, and allows the user to type in new criteria.

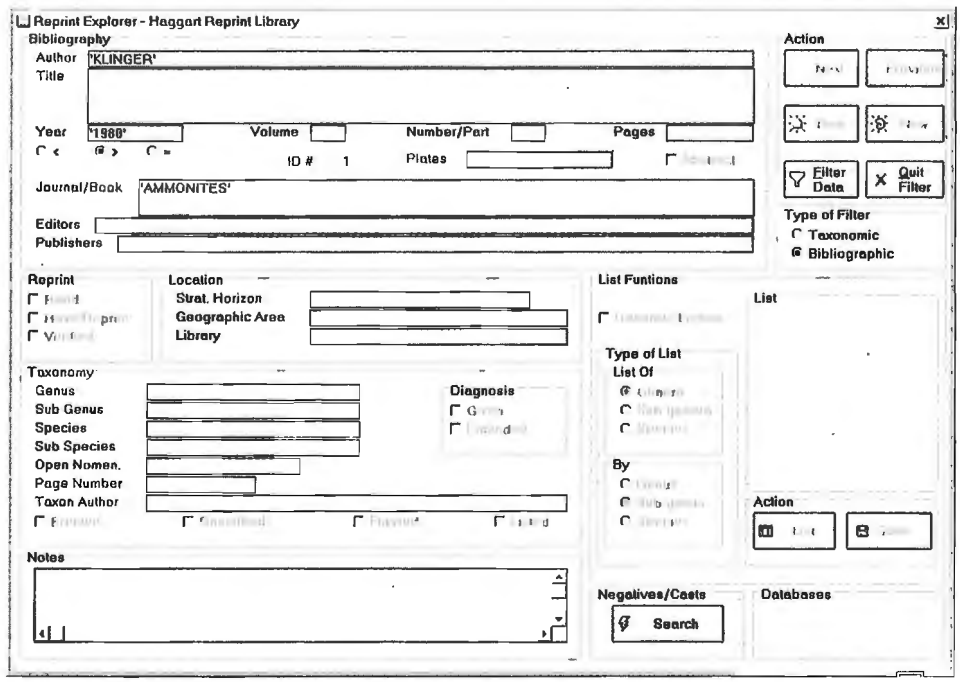

Figure 1. *Example of using* Reprint Explorer *to locate papers using bibliographic criteria. In the illustration, the user has defined a query to identify papers by Klinger published after 1980 containing the word "ammonites" in their title.*

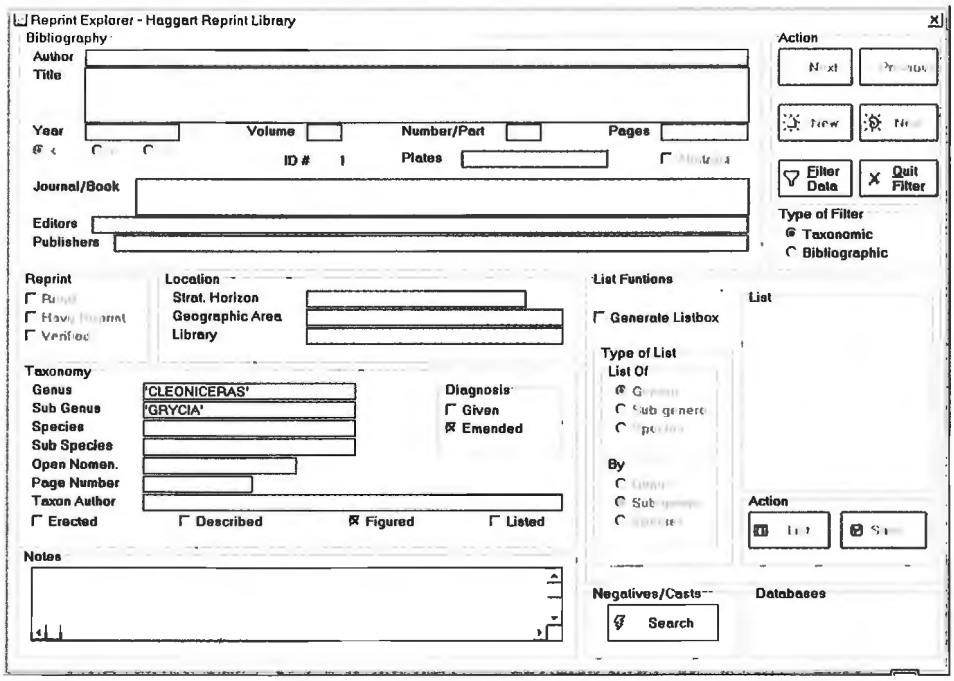

Figure 2. *Example of using* Reprint Explorer *to locate papers using taxonomic criteria. The user has defined a query that will find all the papers in the database that illustrate and provide an emended diagnosis of Cleoniceras (Grycia).*

Taxonomic queries

Although Bibliographic queries are useful in determining which publications are in a reprint collection, many commercially available reprint-tracking software packages allow one to do this. The principle purpose of this program, however, is to allow a research paleontologist (or biologist, for that matter) to easily identify which papers in their collection deal with specific taxa, and in what fashion. Does the paper contain a diagnosis of the taxon in question? Is an illustration provided, or is the taxon just mentioned in the text? This program allows users to easily identify papers in their collection based on such criteria.

Taxonomic queries can be made by specifying a genus, sub-genus, species, sub-species, and open-nomenclature term (cf., aff., sp. nov., etc.). Additionally, by clicking the appropriate check-box when defining a search, users can limit the results to papers where the specified taxa are erected, described, figured, just listed, or diagnosed (original vs. emended diagnoses can be specified). The process of defining a taxonomic query is similar to that used in defining a bibliographic query. The user first presses the "Set Filter..." button in the "Action" area of the screen. This will cause all the fields other than those which can be used in defining the query to be disabled. By default, the program sets up the screen for a taxonomic query (Fig. 2). The user then defines the query by entering the name of a taxon. If desired, a list of, for example, species associated with a specific genus can be generated. This process is explained in more detail under "Generating lists of taxa" below. Pressing the "Filter Data" button executes the defined query, and the user navigates through the resulting records by pressing the "Next" and "Previous" buttons.

Generating lists of taxa

In the initial stages of researching a genus (or sub-genus) with which a researcher is unfamiliar, it can be helpful to be able to generate a list of species (or sub-species) associated with that genus. To do so, the user checks the "Generate Listbox" check-box in the "List Functions" area of the screen when defining a taxonomic query. By default, the screen is then set-up to allow the user to specify a genus for which a list of species should be generated. However, by clicking on the various radio buttons in the "List of" and "By" sections of the screen, the user can tailor the type of list generated to their particular needs.

Once the type of list desired has been specified, pressing the "List" button will cause the list to be generated and displayed in a list-box. If the user double-clicks on an item in the list-box, that item will then be placed in the appropriate query-definition field. Pressing the "Filter Data" button causes the program to display all the publications in the database dealing with this taxon.

ACKNOWLEDGMENTS

We thank Glenn Woodsworth for critically reviewing the manuscript. dBASE is a registered trademark of Borland International Inc.. Windows is a registered trade mark of Microsoft Corporation.

Geological Survey of Canada Project 870070

AUTHOR INDEX

NOTE TO CONTRIBUTORS

Submissions to the Discussion section of Current Research are welcome from both the staff of the Geological Survey of Canada and from the public. Discussions are limited to 6 double-spaced typewritten pages (about 1500 words) and are subject to review by the Chief Scientific Editor. Discussions are restricted to the scientific content of Geological Survey reports. General discussions concerning sector or government policy will not be accepted. All manuscripts must be computer word-processed on an IBM compatible system and must be submitted with a diskette using WordPerfect. Illustrations will be accepted only if, in the opinion of the editor, they are considered essential. In any case no redrafting will be undertaken and reproducible copy must accompany the original submissions. Discussion is limited to recent reports (not more than 2 years old) and may be in either English or French. Every effort is made to include both Discussion and Reply in the same issue. Current Research is published in January and July. Submissions should be sent to the Chief Scientific Editor, Geological Survey of Canada, 601 Booth Street, Ottawa K1A 0E8 Canada.

AVIS AUX AUTEURS D'ARTICLES

Nous encourageons tant le personnel de la Commission géologique que le grand public à nous faire parvenir des articles destinés à la section discussion de la publication Recherches en cours. Le texte doit comprendre au plus six pages dactylographiées à double interligne (environ 1500 mots), texte qui peut faire l'objet d'un réexamen par le rédacteur scientifique en chef. Les discussions doivent se limiter au contenu scientifique des rapports de la Commission géologique. Les discussions générales sur le Secteur ou les politiques gouvernementales ne seront pas acceptées. Le texte doit être soumis à un traitement de texte informatisé par un système IBM compatible et enregistré sur disquette WordPerfect. Les illustrations ne seront acceptées que dans la mesure où, selon l'opinion du rédacteur, elles seront considérées comme essentielles. Aucune retouche ne sera faite au texte et dans tous les cas, une copie qui puisse être reproduite doit accompagner le texte original. Les discussions en français ou en anglais doivent se limiter aux rapports récents (au plus de 2 ans). On s'efforcera de faire coïncider les articles destinés aux rubriques discussions et réponses dans le même numéro. La publication Recherches en cours paraît en janvier et en juillet. Les articles doivent être envoyés au rédacteur en chef scientifique, Commission géologique du Canada, 601, rue Booth, Ottawa K1A 0E8 Canada.

Geological Survey of Canada Current Research, is released twice a year, in January and July. The four parts published in January 1996 (Current Research 1996-A to D) are listed below and can be purchased separately.

Recherches en cours, une publication de la Commission géologique du Canada, est publiée deux fois par année, en janvier et en juillet. Les quatre parties publiées en janvier 1996 (Recherches en cours 1996-A à D) sont énumérées ci-dessous et sont vendues séparément.

Part A: Cordillera and Pacific Margin
Partie A : Cordillère et marge du Pacifique

Part B: Interior Plains and Arctic Canada
Partie B : Plaines intérieures et région arctique du Canada

Part C: Canadian Shield
Partie C : Bouclier canadien

Part D: Eastern Canada and national and general programs
Partie D : Est du Canada et programmes nationaux et généraux

Part E: (this volume)
Partie E: (ce volume)